ZEBRAFISH IN DEVELOPMENT AND DISEASE

EDITED BY: Gokhan Dalgin, Rebecca Ann Wingert and Ryan M. Anderson
PUBLISHED IN: Frontiers in Cell and Developmental Biology and
Frontiers in Genetics

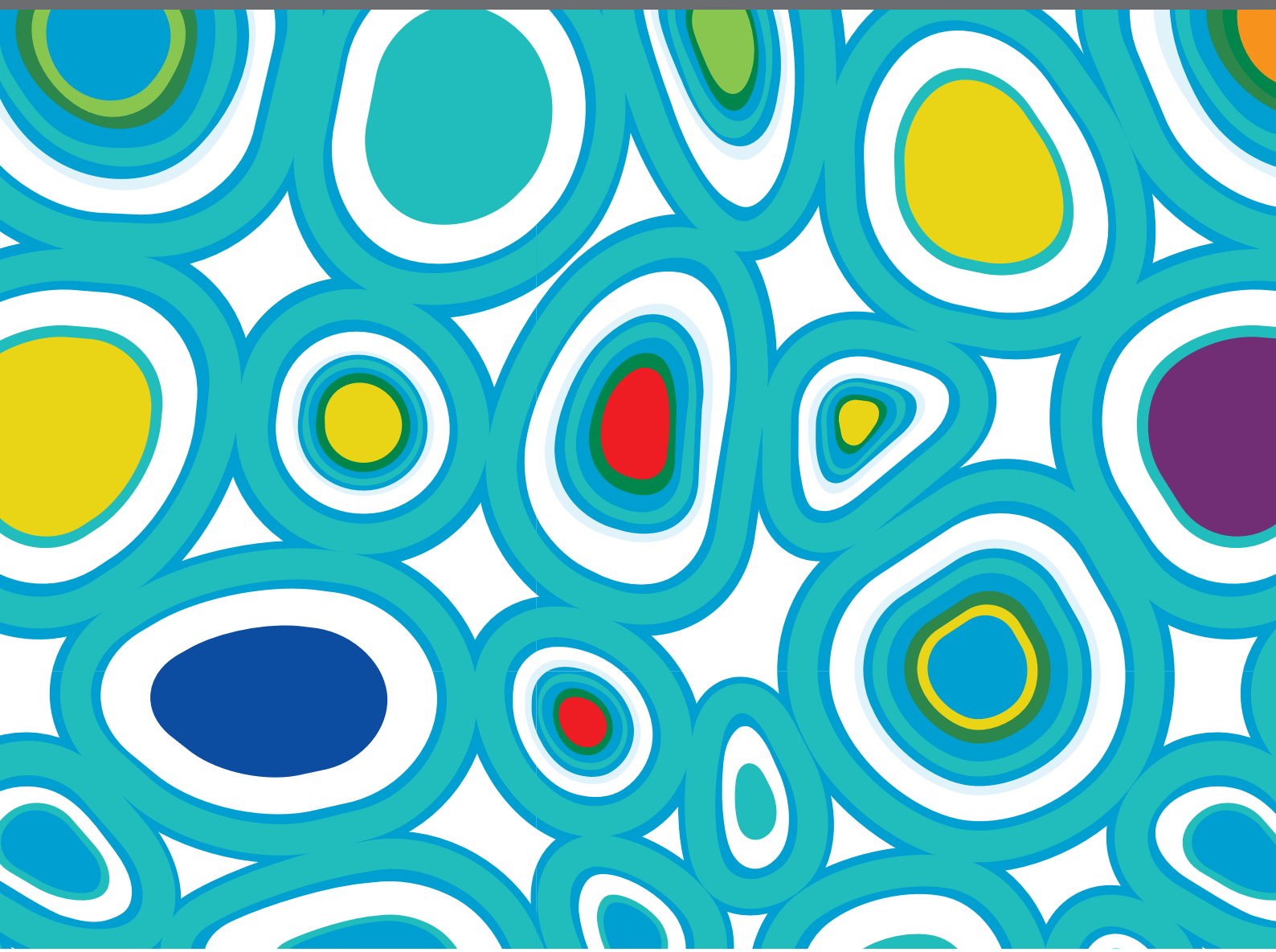

frontiers Research Topics

frontiers

ISSN 1664-8714
ISBN 978-2-88963-248-0
DOI 10.3389/978-2-88963-248-0

About Frontiers

Frontiers is more than just an open-access publisher of scholarly articles: it is a pioneering approach to the world of academia, radically improving the way scholarly research is managed. The grand vision of Frontiers is a world where all people have an equal opportunity to seek, share and generate knowledge. Frontiers provides immediate and permanent online open access to all its publications, but this alone is not enough to realize our grand goals.

Frontiers Journal Series

The Frontiers Journal Series is a multi-tier and interdisciplinary set of open-access, online journals, promising a paradigm shift from the current review, selection and dissemination processes in academic publishing. All Frontiers journals are driven by researchers for researchers; therefore, they constitute a service to the scholarly community. At the same time, the Frontiers Journal Series operates on a revolutionary invention, the tiered publishing system, initially addressing specific communities of scholars, and gradually climbing up to broader public understanding, thus serving the interests of the lay society, too.

Dedication to Quality

Each Frontiers article is a landmark of the highest quality, thanks to genuinely collaborative interactions between authors and review editors, who include some of the world's best academicians. Research must be certified by peers before entering a stream of knowledge that may eventually reach the public - and shape society; therefore, Frontiers only applies the most rigorous and unbiased reviews.
Frontiers revolutionizes research publishing by freely delivering the most outstanding research, evaluated with no bias from both the academic and social point of view. By applying the most advanced information technologies, Frontiers is catapulting scholarly publishing into a new generation.

What are Frontiers Research Topics?

Frontiers Research Topics are very popular trademarks of the Frontiers Journals Series: they are collections of at least ten articles, all centered on a particular subject. With their unique mix of varied contributions from Original Research to Review Articles, Frontiers Research Topics unify the most influential researchers, the latest key findings and historical advances in a hot research area! Find out more on how to host your own Frontiers Research Topic or contribute to one as an author by contacting the Frontiers Editorial Office: researchtopics@frontiersin.org

ZEBRAFISH IN DEVELOPMENT AND DISEASE

Topic Editors:
Gokhan Dalgin, University of Chicago, United States
Rebecca Ann Wingert, University of Notre Dame, United States
Ryan M. Anderson, Indiana University, Purdue University Indianapolis, United States

There are only a few vertebrate systems that can be used to model human diseases for biomedical discovery. The zebrafish model provides key advantages over existing models. Their externally developing embryos provide high-throughput non-invasive imaging, chemical screening, forward and reverse genetics, and their regeneration capacity make zebrafish a valuable system for novel discovery.

Developmental studies using zebrafish has influenced discoveries in many human health-related conditions. This Research Topic covers all aspects of zebrafish studies, providing developmental mechanisms to human health conditions. The aim of the Research Topic was to foster a platform to bring all levels of zebrafish research including but not limited to development, disease, regeneration, drug screening, bioinformatics and Omics studies.

Citation: Dalgin, G., Wingert, R. A., Anderson, R. M., eds. (2019). Zebrafish in Development and Disease. Lausanne: Frontiers Media SA.
doi: 10.3389/978-2-88963-248-0

Table of Contents

frontiers in Cell and Developmental Biology

REVIEW
published: 16 July 2018
doi: 10.3389/fcell.2018.00070

Problems in Fish-to-Tetrapod Transition: Genetic Expeditions Into Old Specimens

*Thomas W. P. Wood and Tetsuya Nakamura**

Department of Genetics, Rutgers, The State University of New Jersey, Piscataway, NJ, United States

The fish-to-tetrapod transition is one of the fundamental problems in evolutionary biology. A significant amount of paleontological data has revealed the morphological trajectories of skeletons, such as those of the skull, vertebrae, and appendages in vertebrate history. Shifts in bone differentiation, from dermal to endochondral bones, are key to explaining skeletal transformations during the transition from water to land. However, the genetic underpinnings underlying the evolution of dermal and endochondral bones are largely missing. Recent genetic approaches utilizing model organisms—zebrafish, frogs, chickens, and mice—reveal the molecular mechanisms underlying vertebrate skeletal development and provide new insights for how the skeletal system has evolved. Currently, our experimental horizons to test evolutionary hypotheses are being expanded to non-model organisms with state-of-the-art techniques in molecular biology and imaging. An integration of functional genomics, developmental genetics, and high-resolution CT scanning into evolutionary inquiries allows us to reevaluate our understanding of old specimens. Here, we summarize the current perspectives in genetic programs underlying the development and evolution of the dermal skull roof, shoulder girdle, and appendages. The ratio shifts of dermal and endochondral bones, and its underlying mechanisms, during the fish-to-tetrapod transition are particularly emphasized. Recent studies have suggested the novel cell origins of dermal bones, and the interchangeability between dermal and endochondral bones, obscuring the ontogenetic distinction of these two types of bones. Assimilation of ontogenetic knowledge of dermal and endochondral bones from different structures demands revisions of the prevalent consensus in the evolutionary mechanisms of vertebrate skeletal shifts.

Keywords: fish, tetrapods, dermal bones, endochondral bones, skull, girdle, fin

OPEN ACCESS

Edited by:
Gokhan Dalgin,
University of Chicago, United States

Reviewed by:
Raman Chandrasekar,
Kansas State University, United States
Randall Dahn,
University of Wisconsin-Madison, United States

***Correspondence:**
Tetsuya Nakamura
nakamura@dls.rutgers.edu

Specialty section:
This article was submitted to Molecular Medicine, a section of the journal Frontiers in Cell and Developmental Biology

Received: *30 March 2018*
Accepted: *15 June 2018*
Published: *16 July 2018*

Citation:
Wood TWP and Nakamura T (2018) Problems in Fish-to-Tetrapod Transition: Genetic Expeditions Into Old Specimens. Front. Cell Dev. Biol. 6:70. doi: 10.3389/fcell.2018.00070

INTRODUCTION

The fish-to-tetrapod transition during the Devonian is one of the prominent events in vertebrate evolution. The invasion of the land from the water necessitated the evolution of the novel structures in skeletons, musculatures, innervations, visceral organs, and respiratory systems in order to adapt to a terrestrial life (Romer, 1949; Clack, 2012; Dial et al., 2015). Robust appendage skeletons with associated musculatures evolved to support body weight against gravitational force and to aid with movement on land (Coates, 1996; Shubin et al., 2006). To facilitate respiration in air, gill breathing had transformed to lung breathing through morphological innovations (Zheng et al., 2011; Sagai et al., 2017).

Sensory systems have been dramatically reconstructed, and the lateral line that sensed physical movement of water was simply lost due to a lack of necessity on land (Piotrowski and Baker, 2014). The function of the kidney shifted from osmoregulation to the excretion of nitrogen in the form of urine or uric acid paste (Mahasen, 2016).

Among the many evolutionary novelties associated with terrestriality, the evolution of the skeleton has attracted much interest from evolutionary biologists. This is mainly because of the ability to trace its evolutionary history through relatively well-preserved structures in the fossil record. Skeletal shifts in the fish-to-tetrapod transition have been understood through the so-called dermal-to-endochondral transition (Westoll et al., 1977; Shubin et al., 2006; Hirasawa and Kuratani, 2015). A fish possesses a significant amount of dermal bones: the dermatocranium, shoulder girdle, jaw, teeth, scales, and fin rays. As lobe-finned fish (sarcopterygians) invaded land, the necessities of these dermal bones for survival fitness largely changed and dermal bones had been reorganized. The dermatocranium of fish skulls, that consists of multiple dermal plates, has experienced major reorganizations in its morphology and composition during the evolution into tetrapods (Coates, 1996; Daeschler et al., 2006). The cranial dermal bones articulate with the shoulder girdle at its posterior end, but, the tetrapod skull has lost several posterior bones, resulting in the dissociation of the skull from the shoulder girdle—the origin of the neck. Dorsal and anal fins are indispensable to stabilize the fish-body for fast swimming in water. However, they are a hindrance on land and have been lost in the tetrapod lineage. Scales that serve as osmotic controls and as protection of the body in an aquatic habitat were also lost during landing. With this concomitant loss of dermal bones, the relative ratio of endochondral bones in vertebrae, girdle, and fins increased in early tetrapods. The endochondral bones in the pectoral girdle enlarged and evolved into the scapula of modern tetrapods (Shubin et al., 2006). In accompaniment with the loss of dermal fin rays in paired fins that propel and balance their bodies, early tetrapods evolved endochondral digits and wrists/ankles (Clack, 2009a; Schneider and Shubin, 2013; Pieretti et al., 2015), helping them to acquire diverse locomotory abilities and extensive maneuverability.

Dermal and endochondral bones are histologically and ontogenetically distinct (Hall, 2005). Dermal bones develop directly from the mesenchyme without a pre-formed cartilaginous model (intramembranous ossification), whereas endochondral bones develop by converting cartilage to bone. The dermoskeleton appears to have originated in the teeth of agnathans such as conodonts and diversified into the dermal skull roof, scales, or fin rays during fish evolution, though evolutionary trajectories of dermal bones are under debate (Donoghue and Sansom, 2002; Sire and Huysseune, 2003; Hirasawa and Kuratani, 2015). Endochondral ossification is hypothesized to have arose much later, in Osteoichthyes (Hirasawa and Kuratani, 2015). Even though a large number of dermal bones have been lost in the transition from fish, tetrapods still possess comparable developmental pathways of dermal bones, which grow calvaria and clavicle bones. The vestiges of the dermal-to-endochondral transition in the developmental programs of vertebrate skeleton cause multiple types of congenital and postnatal skeletal diseases in humans (Gilbert, 2000; Hall, 2005; Wagner and Aspenberg, 2011), such as Progressive Osseous Heteroplasia (POH) or Albright Hereditary Osteodystrophy (AHO) (Regard et al., 2013; Pignolo et al., 2015), which both develop heterotopic dermal bones.

Regardless of the central roles of dermal and endochondral bones in skeletal evolution and clinical cases, scrutiny of the genetic mechanisms that differentiate these distinct types of bones is not enough. With the advent of new technology in molecular biology and paleontology, these problems are now becoming more amenable. The invention of novel sequencing methods promotes comparative genomics with high-throughput output across a diverse range of species (Braasch et al., 2016; Smith et al., 2018). Rapid advancements of genetic manipulation techniques opens a new window to observe functioning of target genes in model and non-model organisms that hold prominent positions in vertebrate evolution (Parker et al., 2014). Furthermore, high-resolution CT scanning is revealing fine details of fossil records and living taxa (Giles et al., 2017; Pardo et al., 2017). These advancements of technology fill in the gaps of understanding evolutionary mechanisms of vertebrates by involving model and non-model organisms into lab-level experiments.

In this article, we summarize the current understanding and problems in the developmental processes and evolutionary shifts of dermal and endochondral bones. First, we review the evolution of cranial dermal bones and the underlying developmental mechanisms. Then, we discuss the skeletal shift from dermal to endochondral bones in the shoulder girdle and current perspectives of the underlying mechanisms. Third, we highlight the approaches that integrate developmental mechanisms into comparative anatomy to answer the fin-to-limb conundrum. Assimilating current knowledge about the molecular mechanisms underlying skeletal shifts of distinct structures would take us one step closer to elucidating the fish-to-tetrapod transition.

REARRANGEMENTS OF SKULL DERMAL BONES

The dermal skull roof is one of the remarkable exemplars for continuous modifications of skeletons during the fish-to-tetrapod transition. The skull roof of sarcopterygians that led to the tetrapod lineage consists of multiple dermal units: such as nasal, parietal (or frontal), temporal, intratemporal, or opercular (**Figure 1A**). These dermal bones encase endochondral cranial components and protect the primary operative unit of the central nervous system—the brain. The comparative studies of skull morphology between fish and tetrapods highlight apparent distinctions of their broad proportions: the snout is relatively longer, the orbits are located more dorsally, and the skull is flatter in tetrapods. The functional reasons for these skeletal modifications are obscure, but they are likely to be linked with sensory and feeding requirements, and also size of the otic capsules (Clack, 1989). The proportional shifts of skulls from

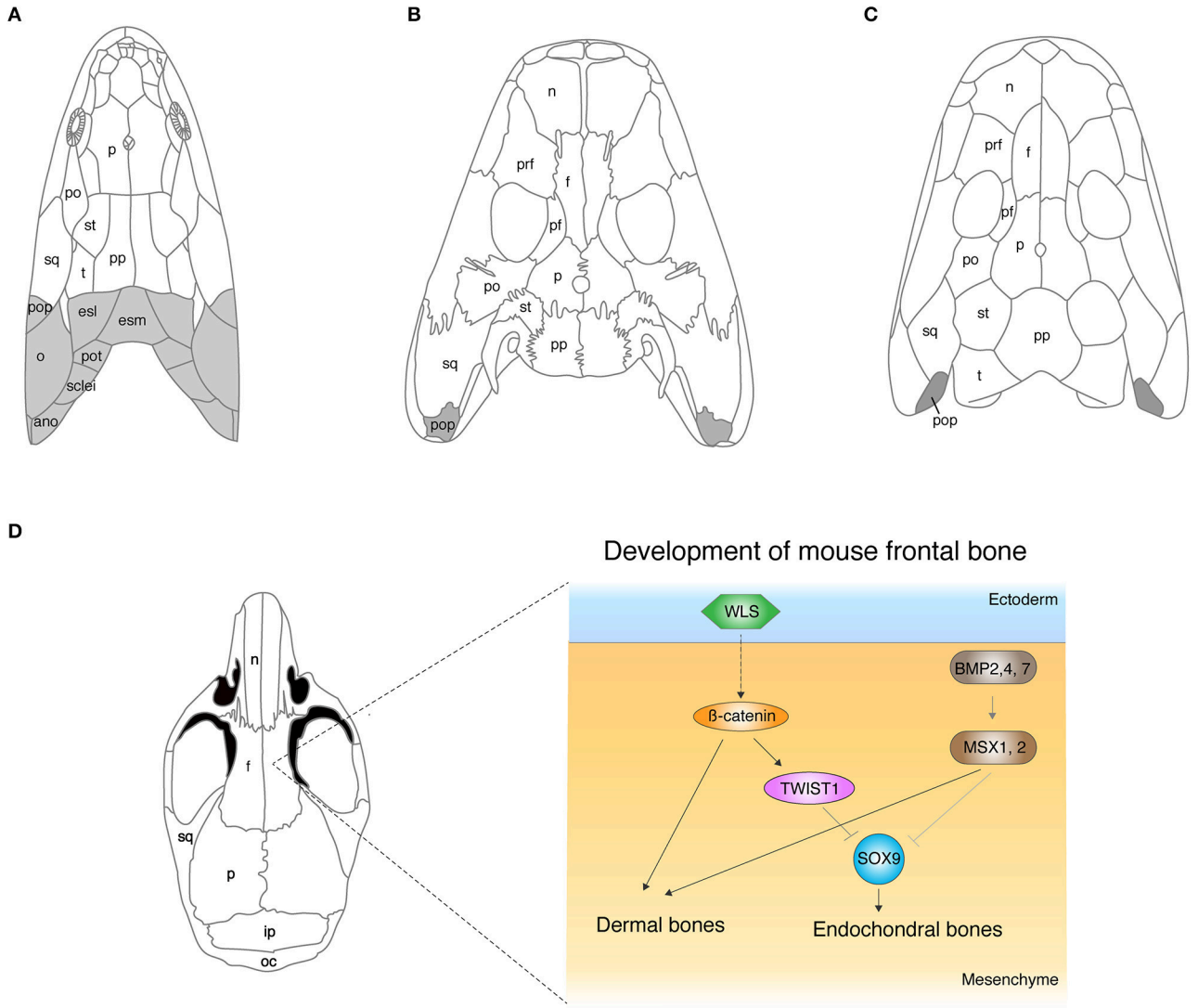

FIGURE 1 | The evolution of cranial dermal bones and the developmental mechanisms. **(A–C)** The skull roof of *Eusthenopteron* **(A)**, *Acanthostega* **(B)**, *Ichthyostega* **(C)**. **(D)** The developmental mechanisms of the frontal bone in mice. The molecules that initiate dermal differentiation from the ectoderm to the mesenchyme have not been identified yet, though the WNT signaling pathway is suggested to be involved (Goodnough et al., 2014). ano, anocleithrum; esl, lateral extrascapular; esm, medial extrascapular; f, frontal; ip, interparietal; n, nasal; o, opercular; oc, occipital; p, parietal; pf, postfrontal; po, postorbital; pop, preopercular; pot, post-temporal; pp, postparietal; prf, prefrontal; st, supratemporal; sq, squamosal; sclei, supracleithrum; t, tabular. Illustrations in **(A–D)** are redrawn with permissions from Clack (2012), Jarvik (1980), and White et al. (2016).

fish to tetrapods are direct consequences of the remodeling of dermal and endochondral bone morphologies, and also simple reductions of dermal bones. *Eusthenopteron* is one of the rhipidistians that lived in shallow freshwater during the late Paleozoic (Andrews and Westoll, 1970). The dermal skull roof of *Eusthenopteron* consists of remarkably large parietals (referred to as "frontals" in actinopterygians) and postparietals (Moy-Thomas and Miles, 1971). Orbits are located at more front of the skull compared with that of tetrapods (**Figure 1**). *Panderichthys* shares multiple unique features with tetrapods: flat skull, medially located eyes, and no dorsal and anal fins (Schultze and Arsenault, 1985; Boisvert et al., 2008). However, the shape of the four median pairs of cranial dermal bones—nasals, frontals, parietals, and postparietal bones—are rather similar to those of fish. The skull of *Tiktaalik* is also flat with large frontals and postfrontals, which bridges the gap of skull morphology between fish and tetrapods (Daeschler et al., 2006). *Acanthostega,* which has limbs with digits, further fills the gap in our understanding of the difference in the skull roof morphology between fish and tetrapods with its intermediate features—large nasals and frontals, and also the relatively small parietal and postparietal bones (Coates, 1996). In the early tetrapod *Ichtyostega*, nasals and frontals are long, and parietals and postparietals are rather short compared to its early fossil relatives (Jarvik, 1980). Due to these

remodeling of dermal bones, the orbits have shifted to a further posterodorsal position—one of the shared features with early tetrapods.

On the lateral side of the skull, gills of osteichthyan fish are covered externally by an opercular series that consists of four dermal bones: the preopercular, opercular, subopercular, and the interopercular. A group of sarcopterygians had adapted to terrestrial life and evolved lungs instead of gills with the gradual loss of opercular series from the skull (**Figure 1**). Rhipidistians (including *Eusthenopteron*) and *Panderichthys* have operculars and suboperculars on the back of their cheek bones (**Figure 1A**), whereas *Acanthostega* and *Tiktaalik* barely possess the opercular bone series, but have a rather small preopercular (Coates, 1996; Daeschler et al., 2006; **Figure 1B**). The skull of *Ichthyostega* also shows a vestige of a preopercular at the back of the squamosals and qudratojugal without any sign of other opercular bone series (Jarvik, 1980; **Figure 1C**). It remains elusive how much of the function of these preoperculars is for gill breathing or whether they are necessary for other physiological activities in these vertebrates.

Extrascapular series connect the skull to the shoulder bones at the most posterior parts of the skull, and they are another example for the loss of dermal bones in the water-to-land transition (**Figure 1**). Rhipidistians retain extrascapular series—medial extrascapular and lateral extrascapular—at the posterior of postparietal and tarbular (Andrews and Westoll, 1970). Supracleithrum (girdle bone) articulates to these extrascapular bones via the post-temporal from the posterior side of the skull (Andrews and Westoll, 1970; **Figure 1A**). However, *Acanthostega* and *Tiktaalik* have lost extrascapular series, resulting in a dissociation of the skull and girdle which led to terrestrial locomotion (Coates, 1996; Daeschler et al., 2006; **Figure 1B**).

Although completing the details of the skeletal shifts from fish to tetrapods is formidable, the remodeling of the dermal skull roof, and loss of extrascapular and opercular series are general trends with alteration of their habitats across vertebrate phylogeny (Clack, 2012). Of particular note, actinopterygians, including zebrafish which is one of the well-established model organisms, possess comparable opercular and girdle bones to those of the rhipidistians, though genetic programs in teleosts underlying development of these bones might be derived compared with rhipidistians.

DEVELOPMENTAL BASIS FOR CRANIAL DERMAL BONES

Along with the extraordinary discoveries of the transitional specimens from water to land, the molecular mechanisms underlying development of cranial dermal bones have been vigorously studied in teeth, operculum, calvaria, mandibule, and other bones (Tucker and Sharpe, 2004; Huycke et al., 2012; Rasch et al., 2016). The dawn of the description of cranial dermal bone development in fish dates back to the early nineteenth century (Pehrson, 1940, 1944, 1958; Aumonier, 1941; Kapoor, 1970; De Beer, 1985; Cubbage and Mabee, 1996). High-resolution histological approaches, including Scanning Electron Microscopy and Transmission Electron Microscopy, have highlighted the developmental process of dermal bones and disparities of structures between dermal and endochondral bones of extinct and living taxa (Verreijdt et al., 2002; Sire and Huysseune, 2003; Witzmann, 2009; Keating and Donoghue, 2016). However, in spite of the continuous efforts (Sire and Huysseune, 2003), the understanding of the development and the evolution of dermal bones still remains poor. Since the changes of cell origins in cranial dermal bone development across species are summarized in previous studies (Piekarski et al., 2014; Hirasawa and Kuratani, 2015; Maddin et al., 2016), we review current perspectives about molecular pathways that are responsible for cranial dermal bone development with the significant emphasis on interchangeability of dermal and endochondral bones.

Dermal bones retain three layers: for example, dentine tubercles are at the outermost surface, middle spongy layer, and basal laminated layer in agnathans (Donoghue and Sansom, 2002). The middle spongy layer is highly vascularized and transports oxygen, proteins, and hormones to support osteogenesis and homeostasis (Percival and Richtsmeier, 2013). Although the details of structures have been modified in different species, the three-layer structure is conserved in vertebrate evolution. The development of dermal bones begins with mesenchymal cell condensations under epithelial layers at their early stages. The aggregated cells directly differentiate into osteoblasts that express osteoblast markers, such as *Runx2* (Abzhanov et al., 2007). In many cases, the epithelial-mesenchyme interaction plays a central role in the initiation of dermal ossification (Sire and Huysseune, 2003). Due to this specific developmental process and the thin structures of dermal bones, surface bones of the fish body consist of dermal bones, not endochondral bones such as scales or spines. Osteoblasts, in turn, induce mineralization around them and differentiate into osteocytes. Distinct from dermal bones, endochondral bones develop from a cartilage template (Long and Ornitz, 2013). The first step of endochondral development is also forming mesenchymal cell condensations, but aggregated mesenchymal cells subsequently differentiate into chondrocytes that express a cartilage marker, *Sox9*. Chondrocytes further differentiate into hypertrophic chondrocytes that induce invasions of blood vessels into developing bones. Chondrocytes are replaced by osteoblasts at the center of long bones, but they do not differentiate into osteoblasts at peripheral regions but rather continue to stimulate cell proliferation and bone growth by Indian Hedgehog (Kronenberg, 2003).

Due to the entrenched idea that dermal bones develop from neural crest cells whereas endochondral bones originate from mesenchymal cells (Smith and Hall, 1990; Sire and Akimenko, 2004), their developmental processes have been hypothesized to be completely distinct. To gain a deeper understanding into the developmental process of dermal bones, Abzhanov and colleagues extensively investigated the gene expression profiles in developing dermal dentary bones of chicken and mouse embryos (Abzhanov et al., 2007). Expanding the previous knowledge of the similarity in some gene expression pattern in dermal and endochondral development including *Runx2*, they discovered that dermal dentary bone expresses some endochondral genes,

which had been regarded as specific markers for chondrocytes, *Collagen type 2* and *9*. Moreover, Abzhanov et al. performed fluorescent double *in situ* hybridization that stained different combinations of osteoblast markers and identified four distinct stages in dermal-bone development, including "chondrocyte-like" osteoblasts in the developmental process of dermal dentary bone. These data suggest that the developmental programs of dermal and endochondral bones are in part similar at least in terms of gene expression profiles.

The developmental process of the dermal skull roof (calvaria) has attracted a large amount of attention due to the significance not only in the evolutionary history of vertebrates (Hanken and Hall, 1993; Janvier, 1996), but also in clinical aspects (Tubbs et al., 2012), resulting in rapid advancements of understanding in the developmental mechanisms of cranial dermal bones. Mouse research has considerably contributed to the elucidation of molecular pathways that regulate calvaria development, such as Bone Morphogenetic Protein (BMP), Fibroblast Growth Factor (FGF), Wingless type MMTV integration site family (WNT), Growth and Differentiation Factor (GDF), TWIST, Engrailed 1, Foxc1, and others (Ishii et al., 2015). *Bmp2*, *4*, and *7* are expressed in cranial neural crest cells and are one of main factors that develop the calvaria. Conditional knockout of *Bmp2, Bmp4, and Bmp7* in cranial neural crest cells during mouse embryonic development by using the *Wnt-Cre* transgenic mice line resulted in the enlarged frontal fontanelle (Bonilla-Claudio et al., 2012). The conditional double knockout mouse of *Msx1* and *Msx2*, downstream targets of the BMP signal pathway, in cranial neural crest cells, also exhibited severe reduction of frontals, and unexpectedly, newly synthesized cartilage compensated the lack of dermal frontals in the mutant mouse (Roybal et al., 2010). Roybal and colleagues identified the cell source of this ectopic cartilage, which indeed developed from a part of the neural crest cells that do not contribute to dermal bones under normal conditions (Roybal et al., 2010). This data implies a dual role of MSXs in calvaria development—an inducer of dermal bones and suppressor of cartilage bones (**Figure 1D**). Thus, the level of BMP signaling is likely to be one of main factors that controls the ratio of dermal and endochondral bones through SMAD1/5/8 and MSX which, in turn, induce downstream target genes in cranial bones (Bonilla-Claudio et al., 2012). Abzhanov and colleagues showed that mis-expression of *Bmp4* by virus infection replaces dermal bones by cartilage in chicken frontal bone (Abzhanov et al., 2007), though the result is intuitively opposite to that of the *Msx* conditional knockout mouse. In either scenario, BMP signaling is likely to regulate dermal and endochondral bone differentiation in the concentration-dependent manner. We do not possess any evidence to substantiate the necessities of the exchange program between dermal and endochondral differentiation in mutant mice. The interchangeability between dermal and endochondral development in cranial bones could be the compensatory mechanism to ensure the development of skull bones, yet their contribution to development and evolution is unknown.

The WNT signaling pathway is another major regulator that develops cranial dermal bones and is a balancer for the ratio of dermal and endochondral bones as well (**Figure 1D**). The conditional knockout mice for *β-catenin*, an intracellular signal transducer of the WNT signal, in cranial neural crest cells and paraxial mesoderm (PAM) by *Engrailed-Cre* transgenic mouse (Goodnough et al., 2012) did not form calvaria. This conditional knockout mouse rather grew cartilage in the original position of calvaria. The phenotype in which dermal bones are replaced by endochondral bones is reminiscent of the conditional double knockout of *Msx1* and *2* and implies that the BMP and WNT pathways crosstalk in calvaria development. Goodnough and colleagues further discovered that *β-catenin* functions to switch differentiation from chondrocytes to osteoblasts *via* TWIST1, which binds to the 3′ untranslated region of *Sox9* mRNA (Goodnough et al., 2012; **Figure 1D**).

The new study added another key player into the development of cranial bones. Barske et al. identified *Nuclear Receptor 2f* genes (*Nr2fs*) as repressor genes of cartilage development in dermal maxilla in zebrafish (Barske et al., 2018). Expression of *Nr2f* is repressed by *Endothelin-1* in the mandible, resulting in endochondral ossification. Though the function of NRF2 in the limb bud is likely to be different from that of maxilla (Barske et al., 2018), it is fascinating to test NRF2s function in calvaria development. One of the subsequent challenges is elucidating how these distinct signal pathways synergistically or redundantly regulate dermal bone development and how they switch the differentiation between dermal and endochondral bones.

Classical surgical experiments suggested that epithelial-mesenchymal interaction initiates dermal bone development in the mesenchyme, yet the molecular mechanisms had remained elusive for a quarter of a century (Hall, 2005). Goodnough and colleagues deployed a conditional knockout system to answer how the epithelial layer promotes development of dermal bones in the cranial mesenchyme (Goodnough et al., 2014); the conditional deletion of *Wls*, the trafficking regulator of the WNT ligand, by *Crect* (ectodermal Cre) mice showed the entire loss of the calvaria bones. However, the conditional knockout of *Wls* in the underlying mesenchyme by *Dermo1Cre* (*Cre* expression in cranial mesenchyme and meningeal progenitor cells) did not show a comparable dermal phenotype (Goodnough et al., 2014). These data suggest that the WNT signal from the ectoderm, presumably through diffusion of proteins, initiates cranial dermal bone development in the underlying mesenchyme. Because multiple WNT ligands are expressed in the epithelial layer and cranial mesenchyme, it is time-intensive to identify the major WNT ligand that transmits signal from the ectoderm to the mesenchyme (Goodnough et al., 2014). While many genes have been discovered to be responsible for cranial dermal bone development, understanding the initial mechanisms that initiate dermal differentiation—the upstream of the WNT signal in the ectoderm—would be one of next challenges. Further experiments are expected to identify molecules or any other cues that trigger the differentiation of cranial dermal bones at the upstream of the WNT signal pathway.

Along with the discoveries of many genes that develop cranial dermal bones, actual genetic loci that have contributed to vertebrate cranial evolution is still obscure. The BMP

and WNT signals, which are necessary for the development of the mouse calvaria, are also involved in developing and diversifying skull shapes in fish (Albertson et al., 2005). The inhibition of WNT signaling by a chemical agonist or antagonist in cichlids created the diversity of preorbital morphologies, which phenocopy cichlid facial diversity (Parsons et al., 2014). The detection of single nucleotide polymorphism (SNP) in *β-catenin* of cichlids also supports the involvement of the WNT signal in facial diversity (Loh et al., 2008). Further assessments to test the functional roles of the BMP and WNT signal pathways in development of the fish skull would enrich developmental and evolutionary basis of fish skull diversity. During the fish-to-tetrapod transition, many cranial dermal bones are lost or reorganized (Clack, 1989; Daeschler et al., 2006). It is likely that different genetic loci contributed to the modifications of different bones, and/or multiple genetic loci contributed to a rearrangement of a single bone, as we have observed in complex evolutionary traits of other vertebrates (Linnen et al., 2013). To gain complete pictures of the molecular mechanisms underlying the evolution of cranial dermal bones, strategies that comprehensively identify genetic loci which contribute to specific phenotypes are ongoing and are successfully capturing responsible regions (Jones et al., 2012; Parsons and Albertson, 2013; Miller et al., 2014). The contribution of genetic loci, which are identified by these QTL studies in closely related species, to a more long-time scale evolution of vertebrates (i.e., the fish-to-tetrapod transition) remains elusive.

DISCONNECTION OF THE SHOULDER GIRDLE FROM THE SKULL

The pectoral girdle morphologies of fish and tetrapods are spectacularly diverse. Since the girdle links appendicular bones to the body trunk and serves as the base of attachment for muscles of the neck and pectoral appendages, the girdle holds a critical position in the evolution of vertebrate locomotion. Comparison of pectoral girdle morphology across vertebrates highlights the general trend in girdle evolution—the reduction of dermal bones and enlargement of endochondral bones. In fish, the series of pectoral girdle bones mainly consists of dermal bony plates: the supracleithrum, postcleithrum, cleithrum, and the clavicle along the dorsoventral axis (Andrews and Westoll, 1970; **Figure 2A**). The supracleithrum articulates the pectoral girdle series to the post-temporal (**Figure 1A**) and orchestrates movements of the head and paired pectoral appendages. Also, the fish pectoral girdle has the scaupulocoracoid, a relatively small endochondral bone that connects the humerus to the pectoral girdle via the glenoid fossa. To invade land, early vertebrates required a robust skeleton to support their body weight without buoyancy. During the fish-to-tetrapod transition, dermal bones had become reduced and simultaneously the endochondral scapulocoracoid had enlarged (**Figures 2A–C**). The scapulocoracoid had split into the scapula and procoracoid bones, which both develop from different developmental centers. In amniotes, the shoulder girdle has been further modified and it has become three bones: the scapula, the procoracoid, and the coracoid.

The developmental processes of girdle bones (Grandel and Schulte-Merker, 1998; Davis et al., 2004; Sears, 2004; Pomikal and Streicher, 2009; Boisvert et al., 2013; Sears et al., 2013; Dillman and Hilton, 2015; Warth et al., 2017) and the associated muscles (Ericsson et al., 2013; Diogo et al., 2014; Masyuk et al., 2014; Pu et al., 2016) have been described in many taxa, yet the problematic evolutionary history of girdle bones has hampered us from understanding the cellular origins of girdle bones. Kague and colleagues tested whether neural crest cells contribute to girdle bones in zebrafish by using *Wnt1-Cre* transgenic fish and confirmed that neural crest cells do not migrate into dermal girdle bones including the supracleithrum, postcleithrum, cleithrum, and the endochondral scapulocoracoid. This finding raises a possibility that the zebrafish girdle bones originate from the lateral plate mesoderm (LPM) or the PAM, yet these hypotheses have not been tested. The cell origins of girdle bones, particularly the scapula, have been more intensively investigated in tetrapods: salamander, turtle, chicken, and mouse embryos (Burke, 1991; Huang et al., 2000; Malashichev et al., 2008; Valasek et al., 2010; Kague et al., 2012; Nagashima et al., 2016). All of these studies support the ontogenetically conserved pattern across tetrapods. The tetrapod scapula has, at the very least, a dual origin—the LPM and somites. Piekarski and Olsson transplanted GFP-labeled somites to wild-type axolotl and demonstrated the somitic contribution to the suprascapular (Piekarski and Olsson, 2011). Burke performed the removal of somites adjacent to the fore limb region of turtle embryos, which resulted in scapular defects (Burke, 1991). Huang and colleagues performed chick-quail chimeric analyses and revealed that the head and neck of the scapula originates from the LPM, but the scapula blade develops from the dermomyotome of somite 17–24 (Huang et al., 2000). Intriguingly, the cells maintain their topology of original somites in the developing scapular such that muscles attach to a specific position of the scapula blade that originate from same somites. The developmental logic underlying the dual origin of scapular cells is explained by Piekarski's non-canonical "position-dependent" hypothesis that proposes that the scapula develops from its most adjacent tissue, either somite or LPM (Piekarski and Olsson, 2011). Mouse studies also showed that the mouse scapula originates from somites by using *Pax3-Cre* transgenic mice (Valasek et al., 2010). In addition, Matsuoka et al. showed that neural crest cells contribute to the scapular spine, coracoid, and acromion by using *Wnt1-Cre* lineage trace system in mice (Matsuoka et al., 2005). Further research could test the contribution of neural crest cells into the girdle bones of primitive actinopterygian or elasmobranchs; whether non-neural crest origin of zebrafish girdle is an evolutionary conserved pattern in fish lineage.

Knowledge about the developmental programs of fish girdle bones is still fragmented. *Syu* homozygous zebrafish that have a mutation in the *Sonic hedgehog a* coding sequence showed a severe defect in cleithrum and pectoral fin development (Neumann et al., 1999). The morpholino knockout of T-box gene, *Tbx5,* also affected the pectoral fin module; with the loss

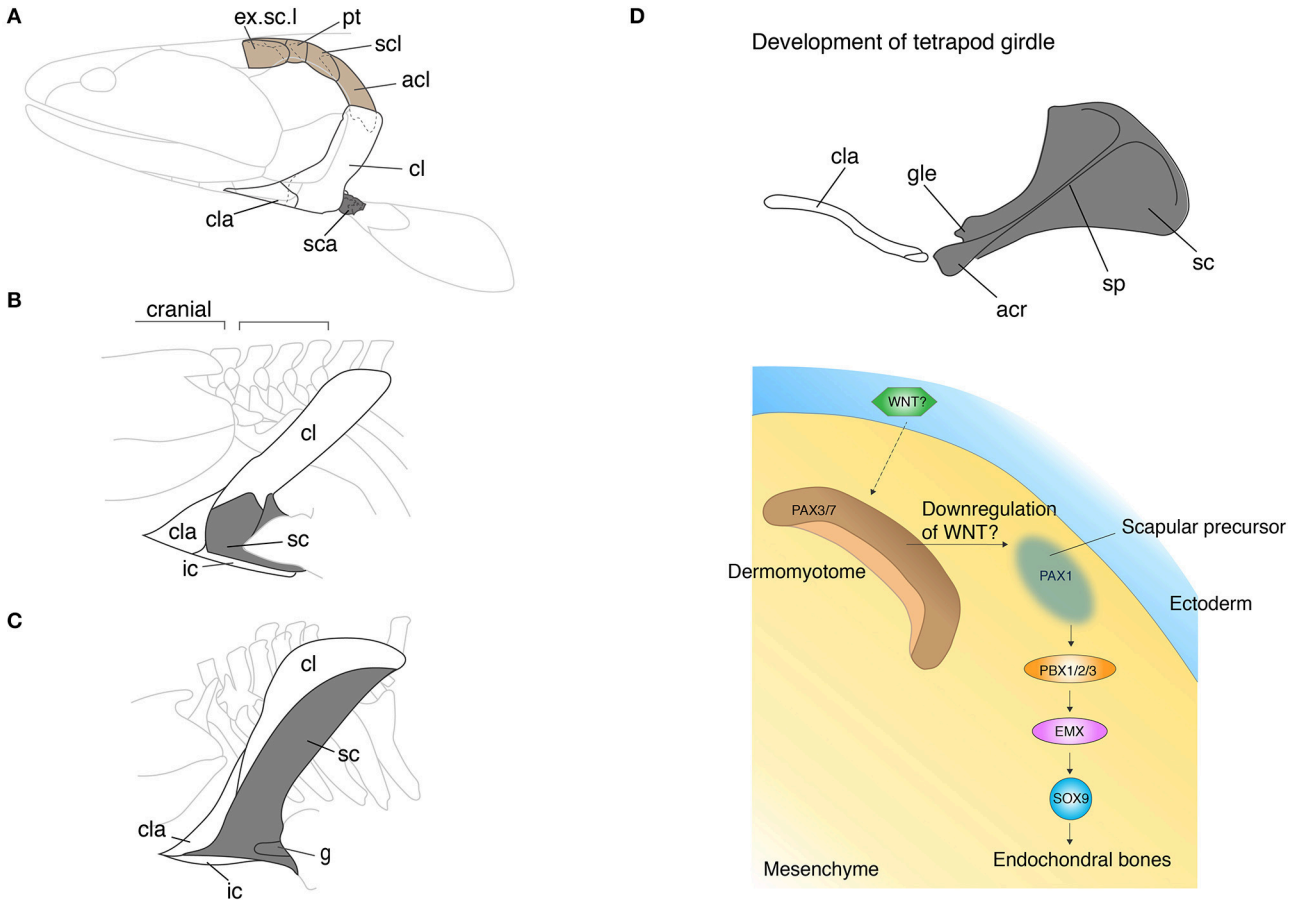

FIGURE 2 | The skeletal shift from dermal to endochondral bones in the pectoral shoulder girdles. **(A–C)** The pectoral girdles of *Eusthenopteron* **(A)**, *Ichthyostega* **(B)**, *Eryops* **(C)**. Brown shaded bones (extrascapular, post-temporal, supracleithrum, and anocleithrum) in **(A)** have been lost during the fish-to-tetrapod transition. Shaded bones depict endochondral bones. Note that the endochondral bones have enlarged with the concomitant decrease of the dermal bones. In **(B,C)**, the spaces between the skull and pectoral girdle demonstrate the origin of the neck. **(D)** The developmental mechanisms of the scapula in mouse and chicken embryos. The epithelial-mesenchymal transition produces prospective scapular cells from the dermomyotome. The understanding of developmental programs underlying the dermal bone development is still poor (see text). acl, anocleithrum; acr, acromion; cl, cleithrum; cla, clavicle; g, glenoid fossa; ic, interclavicle; sc, scapula; sca, scapulocoracoid; scl, supracleithrum; sp, spine; Illustrations in **(A–C)** are redrawn with permissions form Andrews and Westoll (1970), Jarvik (1980), and Gregory (1951). The illustration of the mouse scapula is adapted with permission from Kuijper et al. (2005).

of pectoral fins, the scapulocoracoid, postcoracoid process, and the cleithrum were also severely affected (Ahn et al., 2002). Further, *Dlx5a* and *Dlx6a* morpholino-mediated knockdown in zebrafish disrupted not only the pectoral fin, but also girdle bone development (Heude et al., 2014). These findings indicated that the development of fins and girdles, either dermal or endochondral, are interlinked by the same genes and cannot be simply separated because of their close topology in the developing body.

In tetrapods, especially in chickens and mice, more genes have been uncovered in scapula and clavicle development (Huang et al., 2006; **Figure 2D**). The cranial part of the pectoral girdle, including the acromion, coracoid process, and the glenoid fossa, develops from the LPM. The developmental programs of the anterior scapular bone shares the same set of genes with the limb bud as we have seen in the development of the zebrafish pectoral girdle; *Dlx* (Heude et al., 2014), *Islet1* (Itou et al., 2012), *Tbx5* (Valasek et al., 2011), and *Twist1* (Krawchuk et al., 2010; Loebel et al., 2012) affect both girdle and limb development. Contrary to the canonical hypothesis, the scapular blade develops from dermomyotome, not sclerotome, which goes through the epithelial-mesenchymal transition (EMT) (**Figure 2D**). Several transplantation studies in chicken embryos showed that signals from the ectoderm to dermomyotome are necessary for this EMT (Malashichev et al., 2005). The molecules that induce EMT in the dermomyotome from the ectoderm have not been identified, yet the attenuation of the WNT signal is likely to be involved. Moeller and colleagues ectopically expressed Carboxypeptidase Z (CPZ), which possesses a WNT binding domain, in somites of chicken embryos and discovered that the WNT signal downregulates *Pax1* expression that is necessary for scapular development and promotes *Pax3/7* expression

that is necessary for limb muscle development (Moeller et al., 2003). WNT6 in the ectoderm was suggested as a primary diffusible ligand to maintain *Pax3/7* expression, nevertheless further experiments to verify its function in the EMT are imperative (Schmidt et al., 2004). Once the EMT produces prospective scapular cells with *Pax1* expression, *Pbx* family genes become key players to regulate and pattern scapular development (**Figure 2D**). PBX1/2/3 are expressed in the proximal limb bud and promote cartilaginous condensation through binding with EMX2 (Capellini et al., 2010, 2011). In parallel with developing cell condensation, PBX and BMP (Hofmann et al., 1998; Capdevila et al., 1999) regulate *Hoxa5* and *Pax1* (Timmons et al., 1994; Hofmann et al., 1998; Aubin et al., 2002) to pattern the acromion and the scapular head. The patterning of posterior scapula is established by *Alx1* (Capellini et al., 2010), *Tbx15*, and *Gli3* (Kuijper et al., 2005) that are also downstream of PBX1.

Despite of the discovery of a number of genes for scapular development, little is known about the molecular mechanisms underlying the development of the dermal clavicle in the shoulder girdle. Kuijper and colleagues investigated the girdle phenotype of triple knockout mice of *Alx4*, *Cart1,* and *Tbx15* and discovered that the clavicle showed a severe phenotype while the scapula showed a minorly affected morphology in these mutant mice (Kuijper et al., 2005). These data suggest that these genes may regulate more or less specifically dermal bone development in the shoulder girdle, but the precise mechanisms are unknown.

Fish girdle bones are almost all dermal bones, which may utilize epithelial-mesenchymal interaction or ossify by themselves without any input from epithelial tissue. The ectodermal signal in the scapular development of tetrapods is most likely important to differentiate the competent cell population for the prospective shoulder girdle, not to trigger the bone developmental program itself. As reviewed above, in the shoulder girdle, the developmental programs of dermal and endochondral bones are presumably intermingled; the genes affecting endochondral bone development also affect dermal bone development in most cases. This data implies that the cell sources and developmental programs for these two types of bones in the shoulder girdle are not obviously separated due to their complicated evolutionary history—between the skull and body trunk. It is compelling to test how the epithelial-dermomyotome interaction is conserved in the development of the scapulocoracoid, and dermal bones of fish.

FINS INTO LIMBS

The evolution of tetrapod limbs from fish fins is one of the most remarkable transitions in vertebrate history (Clack, 2009a,b). Whereas fish fins consist of endochondral bones in a proximal domain and dermal fin rays in a distal domain, tetrapod limbs are exclusively composed of endochondral bones. In *Eusthenopteron*, the scapulocoracoid articulates with the humerus that further connects to the ulna and the radius (Andrews and Westoll, 1970; **Figure 3A**). The distal ends of the ulna and the radius attach to the preaxial radials, which are followed by the lepidotrichia. The pectoral fin of *Tiktaalik* presents an intermediate structure between fish and tetrapods with regards to its morphology and function. The *Tiktaalik* fin possesses elaborated distal endochondral bones; their morphology and mobility is reminiscent of distal appendages of tetrapods (Shubin et al., 2006; **Figure 3B**). In contrast to the extension of endochondral domain toward the distal direction, the dermal fin rays of *Tiktaalik* are much reduced compared with that of fish. A further transition from fins into limbs is observed in *Acanthostega*. The paired appendages of *Acanthostega* retain comparable digits to those of tetrapods with a stout humerus, ulna, and radius, but without any evidence of fin rays (Coates, 1996; **Figure 3C**). The number of digits is eight in the fore limb of *Acanthostega*, but *Ichthyostega* shows a reduction of digit number toward five, which is the shared feature with later tetrapods—pentadactylism (Jarvik, 1980). The reduction of dermal bones and the increase of endochondral bones in the evolution of paired appendages is a similar trend such as when shoulder girdle bones evolved and this trend is significantly associated with the functional importance of the endochondral appendage in terrestrial life. However, it is not understood whether underlying molecular mechanisms of shoulder and limb evolution are common, or if they employ distinct mechanisms.

Since fish lepidotrichia, one of the major components of fin rays, directly ossifies without a cartilage model, the cell origin of fin rays had been assumed to be neural crest cells like other dermal bones, such as scales. However, the recent genetic labeling of the specific cell population in zebrafish revealed the other cell origins of fin rays. Lee and colleagues used *Tbx6 promoter-Cre* transgenic fish to trace the derivatives of PAM and discovered that the PAM solely contributes to the development of fin rays in the caudal fin (Lee et al., 2013). Another line of evidence from medaka also supported this conclusion (Shimada et al., 2013). Shimada and colleagues transplanted somite cells of transgenic fish that ubiquitously expresses DsRed into that of wild-type fish and confirmed that these red fluorescent cells contribute to median fin rays. In parallel with this transplantation experiment, they proved the contribution of the PAM to median fin rays by "IR-LEGO" in which *Cre-loxP* system irreversibly marks target cells with heat shock stimulus. Deploying the same labeling system, they discovered that the LPM, not neural crest cells, contributes to lepidotrichia formation in the pectoral fin (Yano et al., 2012; Shimada et al., 2013). Therefore, model organisms, zebrafish and medaka, provide us the ability to perform genetic experiments to test our hypotheses, yet, another compelling experiment is to test the evolutionary synapomorphy with primitive actinopterygians. Tulenko and colleagues injected DiI into the LPM shortly after gastrulation and confirmed that DiI-labeled LPM cells contribute to pectoral fin fold (Tulenko et al., 2017). The distinct cell origins of lepidotrichia (PAM or LPM) in unpaired and paired fins refuels the discussion of the origin of paired fins, which share same *Shh* cis module with unpaired fins (Freitas et al., 2006; Letelier et al., 2018). Mice and chicken studies have provided us with comparable knowledge of the cellular origins of the limb bud to that of fish. Gros and Tabin

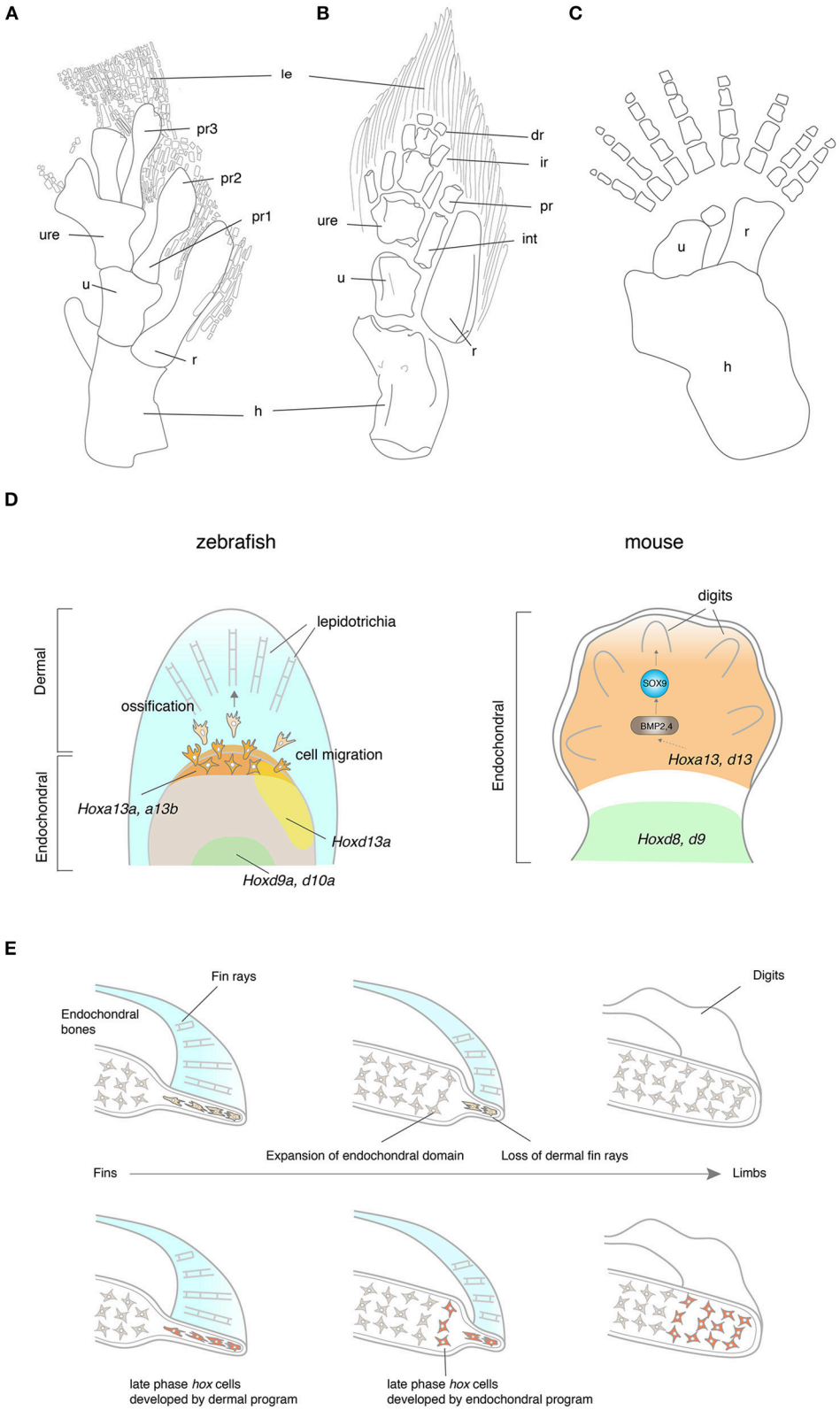

FIGURE 3 | The fin-to-limb transition and their developmental basis. **(A–C)** The pectoral fins and limbs of *Eusthenopteron* **(A)**, *Tiktaalik* **(B)**, and *Acanthostega* **(C)**. Note that *Eusthenopteron* and *Tiktaalik* possess distal fin rays with the endochondral skeletons. **(D)** The developmental mechanisms of fin rays and digits. In zebrafish, *(Continued)*

FIGURE 3 | *hox13* genes are expressed in a distal domain of the endochondral disk. The cells that experienced the late phase *hox* activity migrate out from the distal endochondral disk into the fin fold, that differentiate into the lepidotrichia. In mice, *Hox13* genes are expressed in the autopod, which develop digits at a later stage. HOXA13 is suggested to bind the regulatory region of *Bmp2* and *4* by ChIP experiments (Knosp et al., 2004). While many of the downstream genes of HOX13 have been explored in mice, genes regulated by HOX13 in fish have not been identified. Note that the ossification of lepidotrichia and digits takes place at a later stage than the expression of *Hox13* genes. **(E)** Hypotheses for the fin-to-limb transition. The fin rays (cells shaded by light orange) have degenerated and the endochondral domain (cells shaded by light gray) expanded during the appendage evolution (top). This hypothesis supports that digits and wrists are novel domains that have been acquired as fish have evolved to tetrapods. Another hypothesis claims that the fish fin has an antecedent of digits and wrists (bottom). The cell histories between fish fin rays and tetrapod digits are comparable in terms of their *hox* expression pattern during the embryonic development (cells shaded by orange). In this hypothesis, the cell differentiation program of fin rays might have changed to become endochondral bones, resulting in the acquisition of digits and the wrist. dr, distal radials; hu, humerus; int, intermedium; ir, intermediate radials, le, lepidotrichia; po, postaxial process, pr, preaxial radials; pro, proximal radials; ra, radius; ul,ulna, uln, ulnae; Illustrations of **(A–C)** are redrawn with permissions from Andrews and Westoll (1970), Shubin et al. (2006), and Coates (1996).

demonstrated that the epithelial cells of the somatopleural LPM contribute to the limb bud mesenchyme through EMT (Gros and Tabin, 2014). Further, the genetically labeled mesenchymal cells which expressed *HoxA13* exclusively contribute to digits and wrist bones (Scotti et al., 2015). This evidence collectively suggests that LPM-derived cells express *HoxA13* and contribute to endochondral bones, yet no scrutiny of cell origins of *HoxA13* cells have been conducted to date.

The genetic underpinnings of the development of paired appendages have been profoundly investigated in the embryonic limbs of chickens and mice (Zeller et al., 2009). *Hox* genes—Homeodomain-containing transcription factors—play pivotal roles in body patterning during embryonic development and are expressed in the limb bud (Zakany and Duboule, 2007). In early development of the limb bud, the genes in *HoxA* and *HoxD* clusters are expressed in a nested manner from the posterior to anterior limb bud; expressions from "anterior" genes (3′ side genes of *Hox* clusters. e.g., *Hoxa1* or *Hoxa2*) of *HoxA* and *HoxD* clusters are relatively broader than that of "posterior" genes (5′ side genes of *Hox* clusters. e.g., *Hoxa13* or *Hoxd12*) to the anterior domains of the limb bud. According to this nested expression pattern, *Hox* genes produce positional information along the anteroposterior axis inside the limb bud. *Sonic Hedgehog* is expressed at the Zone of Polarizing Activity (ZPA) and constitutes a positive feedback loop with *Hox* genes, resulting in cell proliferation and also providing positional information with *Hox* genes (Zeller et al., 2009) in the mesenchyme. At later developmental stages, anterior *HoxA* and *D* expression is limited in a proximal domain of the limb bud, while posterior *HoxA* and *D* genes gain a new expression domain in the autopod (**Figure 3D**). The functional roles of these site-specific *Hox* expressions were tested in knockout mice. The *Hoxa13* and *d13* combinatorial knockout mice lost the entire autopod (Fromental-Ramain et al., 1996b), while the *Hoxa9* and *d9* knockout mice eliminated the humerus without affecting autopod development (Fromental-Ramain et al., 1996a). Recent studies revealed genomic underpinnings of the two-phase *Hox* expression; the long-range contacts of the regulatory regions to *HoxA* and *D* clusters from centromeric side or telomeric side establish 3D chromatin loop structures (Topologically Associating Domain, TAD) (Montavon et al., 2011; Andrey et al., 2013) and assure physical proximity of the enhancers to *Hox* genes. These large chromatin structures regulate a group of target gene expression in a time- and site- specific manner and develop two distinct domains in the limb bud—the proximal limb (the humerus, ulna and the radius) and the distal limb (digits).

Hox genes are expressed in a nested manner in the endochondral disk of pectoral fins of fish as well (Ahn and Ho, 2008). At early stages, expression of "posterior" *hoxa* and *d* genes are more restricted to a posterior domain of the fin bud compared with that of "anterior" genes. At later stages, expression from posterior *hoxa11-13* and *d11-13* is restricted to a distal domain of the fin bud as "posterior genes" of mice in the limb bud (**Figure 3D**). Woltering et al. and Gehrke et al. revealed that the chromosomal topologies underlying these two-phase *hox* expression patterns are the shared feature with that of mouse by 4C-sequencing, suggesting that fish fins already retain a dual TAD system in paired fins before evolving digit and wrist (Woltering et al., 2014; Gehrke et al., 2015). Other major genetic networks for the development of paired appendages are also peculiarly conserved between the endochondral disk of fish and limb bud of tetrapods: *Tbx5* (Ahn et al., 2002; Adachi et al., 2016), *Shh* (Neumann et al., 1999), *Fgf8* (Jovelin et al., 2007), *Bmp2* (Laforest et al., 1998), and others. During the fin fold development, the LPM migrates from the proximal fin bud into the distal fin fold, and the cell configuration becomes flat and thin in the distal domain (Thorogood, 1991; Yano et al., 2012). Concomitant with physical cell migration, *hoxa13a* expression also migrates out from the endochondral disk to the proximal fin fold (Ahn and Ho, 2008; Nakamura et al., 2016; Tulenko et al., 2016). Surprisingly, during the late development of fin fold, the gene expression profile of the fin fold in paddlefish and of the autopod in mice is rather similar despite their distinct histological structures (Tulenko et al., 2017). *Shh* is expressed at the posterior edge of the pectoral fin fold, and *Fgf10* and *hoxa13* is in the broad domain of the fin fold, all of which are reminiscent of gene expression patterns of the mesenchyme in the mouse limb bud (Tulenko et al., 2017).

The shared developmental programs between the fin fold and the autopod inevitably drive further questions. For example, how do these two appendage primordia develop into distinct dermal or endochondral bones from the conserved gene expression patterns? The signaling pathways underlying the development of dermal fin rays has been vigorously studied in normal development and also in the regeneration process after amputations of fins (Wehner and Weidinger, 2015). As the fin fold develops, actinotrichia form at a distal tip and leads lepidotrichia development at its proximal part (Wood and

Thorogood, 1984; Durán et al., 2011). *Actinodin* (*And*) *1* and *2* serve as non-collagenous components of actinotrichia in fin development, but they had been lost from the genome of the tetrapod lineage (Zhang et al., 2010; **Figure 3D**). Zhang and colleagues tested their function in zebrafish by morpholino-mediated knockdown, resulting in the loss of fin rays from the pectoral fin. Given that these genes were lost from the tetrapod genome, they posited that the loss of *And* genes from the fish genome is likely to have promoted the fin-to-limb transition through the loss of lepidotrichia (Zhang et al., 2010; Lalonde et al., 2016). Currently, the analysis of regulatory mechanisms of *And1* expression is ongoing (Lalonde et al., 2016). With the developmental pathways of fin rays, the mechanisms that initiate dermal fin ray differentiation in the fin fold remain enigmatic. The WNT and SHH signal from the epithelial cells stimulates cell differentiation during the regeneration of fin rays, but the genetic mechanisms that induce the differentiation of dermal bones in normal fin rays remain unknown (Quint et al., 2002; Wehner and Weidinger, 2015). Harris et al. screened *eda* (ectodysplasin) mutant fish, which show the drastic loss of dermal fin rays from paired and unpaired fins as well as the phenotypes of other dermal bones such as the loss of scales (Harris et al., 2008). Since *eda* is expressed in the epidermal placode and *edar* (ectodysplasin receptor) is in the basal cells of the forming placode in scale development, the EDA signaling pathway is likely to also be involved in fin ray development through epithelial-mesenchymal interaction. Though it is a widely shared consensus that the apical fold [AF-the epithelial structure that forms after Apical Ectodermal Ridge (AER)] plays a critical role in fin fold development (Yano et al., 2012), little is known about how the AF interacts with the underlying mesenchyme and induces dermal ossification.

Due to the apparent loss of the autopod domain in *Hoxa13* and *Hoxd13* double knockout mice (Fromental-Ramain et al., 1996b), the function of HOX13 has been one of main foci in understanding the endochondral development of the limb bud (**Figure 3D**). The overexpression of HOXA13 in the limb bud alternated cell-cell adhesion and affected the size of cartilage condensation (Yokouchi et al., 1995). Knosp et al. identified *Bmp2* and *Bmp7* as direct targets of HOXA13 by using a ChIP assay (Knosp et al., 2004; **Figure 3D**). BMP signaling is well known to play key roles in cartilage and bone development, identities of digits, and interdigital apoptosis during limb development (Suzuki, 2013). Thus, they are likely to be directly involved in the differentiation process of endochondral bones at the downstream of HOXA13. HOXD13 is also suggested to bind the regulatory regions of *Sfrp1*, *Barx1*, and *Fbn1*, all of which are indispensable for normal skeletogenesis (Salsi et al., 2008). Recent advancements of technology in genomics have further accelerated extensive identification of the downstream genes of HOX13 groups. Whole genome tiling arrays and RNA-sequencing explored whole gene expression profile including non-coding RNA in wild-type and *Hox*9-11 mutant mice (Gyurján et al., 2011; Raines et al., 2015). These experiments successfully identified a number of *Hox* downstream genes, including bone developmental factors such as *Runx*, in the limb development. ChIP-sequencing of HOXA13 and HOXD13 in cultured cells of chicken and mouse limb buds suggested that HOX13 and CTCF co-bind to a number of genomic loci (Beccari et al., 2016; Jerković et al., 2017). Given that the CTCF transcription factor regulates 3D chromatin structures, this finding implies that HOX13 transcription factors not only bind directly to their target sites, but rather regulate chromatin structures broadly with CTCF, which consequently shifts the broad gene expression profile.

In parallel with the elucidation of the developmental programs of dermal fin rays and endochondral bones in fish, the evolutionary mechanisms from fins into limbs have been closely investigated (Sordino et al., 1995; Woltering and Duboule, 2010; Schneider and Shubin, 2013; Yano and Tamura, 2013; Woltering et al., 2014; Onimaru et al., 2015; Tanaka, 2018). Sordino et al. suggested that digits and wrists are novel domains of tetrapods due to a striking difference in the expression pattern of *Hoxa-11* between fish and tetrapods (Sordino et al., 1995). Woltering et al. injected a *tetraodon* BAC vector containing *hoxa13b* region into mice and observed the expression pattern of *hoxa13b,* which is regulated by fish regulatory domains in mouse limbs. They observed that the expression domain of the fish *hoxa13b* is confined to a proximal domain of the limb bud of mice, not in a distal domain like mammal *Hoxa13* (Woltering et al., 2014). Woltering et al. also state that while fish have most of the necessary genes and regulatory architecture indispensable to form digits, 5′ regulatory landscapes in fish cannot specify a distinct digit territory (Woltering et al., 2014). This suggests that distal pectoral fins and distal limb buds are not comparable in a classical sense of homology as there is a lack of a common ancestral structure. Freitas et al. overexpressed *hoxd13a* in order to investigate the function of 5′ *hoxd* expression in fin development and discovered that the overexpression of *hoxd13a* results in the proliferative expansion of chondrogenic tissue distally that is akin to autopod development (Freitas et al., 2012). Leite-Castro et al. also propose possible mechanisms of the fin-to-limb transition, a consequence of various modifications in *HoxA* genes, such as: expansion of polyalanine repeats within the HOXA11 and HOXA13 proteins, an acquisition of novel ncRNA with an inhibitory function of HOXA11 or *cis*-regulatory evolution of *hoxa13* (Leite-Castro et al., 2016).

Contrary to the entrenched idea that dermal bones and endochondral bones are ontogenetically and histologically distinct, recently new evidence has implied a possible ontogenetic interchange between these two types of bones in appendage evolution. First, the development of dermal fin rays is unique; the gene expression profile during their development is at an intermediate state between endochondral and dermal bones in appendage evolution. *Col2a1* and *Col10a1*, which are regarded as specific markers of endochondral bones, are expressed despite the absence of cells stained by cartilage staining in fin rays (Smith et al., 2006). Second, functional analyses of *hox13* genes provide a new insight for development of the fin fold. Lalonde and Akimenko deleted *hoxa13a/hoxd13a* expressing cells and observed the defects in the formation of fin rays (Lalonde and Akimenko, 2018). Double knockout zebrafish of *hoxa13a* and *a13b*, and triple knockout fish of *hoxa13a*, *a13b*, and *d13a* lost dermal fin rays (Nakamura et al., 2016). These data demonstrated

that *hox13* genes are indispensable for fin ray development, whereas *hoxa13* and *d13* are necessary to develop endochondral digits in mice. Third, double knockout zebrafish of *hoxa13a* and *a13b*, and triple knockout fish of *hoxa13a*, *a13b*, and *d13a* increased the number of distal endochondral bones along the proximodistal axis with the loss of dermal fin rays (Nakamura et al., 2016). Also, the repetitive excisions of the AF, which is critical to develop fin rays, from the developing pectoral fin, extended the size of the endochondral disk distally (Yano et al., 2012). Summarizing all data leads us to a novel hypothesis—the developmental program between dermal and endochondral programs are interchangeable and the dermal genetic network has been replaced by the endochondral network in appendage evolution (Nakamura et al., 2016; Tulenko et al., 2016, 2017; Paço and Freitas, 2018; **Figure 3E**). Given that LPM cells contribute to lepidotrichia, LPM cells that express *hoxa13* genes are most likely to differentiate into dermal fin rays in fish, whereas LPM cells that experience *hoxa13* and *d13* develop endochondral digits in tetrapods. Further dissection of the cell origins and fate mapping of *Hoxa13* cells in the fish fins and tetrapod limbs would provide us with more insights for the mechanisms of the fin-to-limb transition.

Though the genetic mechanisms underlying for interchanges between dermal and endochondral bones remain elusive, gradual losses of gene expression that are indispensable for the development of fin rays such as *And1*, are likely to play roles (Zhang et al., 2010). Masselink and colleagues' research would illuminate a path to approach the underlying mechanisms. They discovered that whereas ectodermal cells develop an AER which promotes tissue growth via *Fgf8* and *Wnt3* in tetrapods (Lewandoski et al., 2000; Barrow, 2003; Boulet et al., 2004), somitic cells contribute to the AF development (Masselink et al., 2016). They removed somite-derived cells by a genetically targeted cell ablation system before the AF induction, resulting in the severe disruption of AF development, as well as a lack of actinotrichia deposition. Furthermore, they marked somite-derived cells via the introduction of the photoactive protein Kaede, and induced apoptosis by laser illumination. The removal of the somite-derived cells from the AF significantly decreased the size of the actinotrichia as well as a reduction by 30% in the length of the fin fold. They concluded that the swap of the cell contributions from somitic cells to ectodermal cells in the AF was likely to drive the evolutionary shift from the AF to the AER and, consequently, lead to the fin-to-limb transition. Extensive investigations and comparative studies of the cell lineages that contribute to the AF, AER, fin fold, and the endochondral disk would shed light on the evolutionary trajectories of appendages.

GENETICS AND GENOMICS INTO OLD QUESTIONS

Endless discoveries in paleontology have led to continuing scientific questions in vertebrate evolution. The skeletal shifts between dermal and endochondral bones are examples of major vertebrate transitions from water to land, yet revealing the genetic mechanisms underlying their evolution is a long endeavor in evolutionary biology. Integration of novel techniques in both molecular biology and paleontology would accelerate the understanding in developmental and evolutionary mechanisms of cranial dermal bones, shoulder girdles and appendages during the fish-to-tetrapod transition.

In contrast to the canonical hypotheses, new studies demonstrated that the cell origins of some dermal bones are obviously from the LPM and the PAM, not neural crest cells. Furthermore, developmental programs for dermal bones and endochondral bones are ontogenetically interchangeable in skull development by deploying distinct cell origins. They may be interchangeable even in a single cell population of appendage development, though further assessment is necessary. These new discoveries make our understanding of the border line between dermal and endochondral bones obscure; the two types of bones are more similar in terms of their ontogenetic history and characters than we expected. However, the current data has not been so abundant as to be conclusive. For example, the information of cell origins of dermal and endochondral bones in pectoral fin development are still fragmentary. Complete understanding of the cell lineages with genetic labeling in each ossification in wild-type and genetic mutants would provide us an opportunity to propose a more reliable model for the fin-to-limb transition. The most recent studies have elegantly showed that we are able to track the entire cell lineages of early vertebrate development (Briggs et al., 2018; Farrell et al., 2018; Wagner et al., 2018). Comparative analysis of the cell lineages of appendages between fish and tetrapods by deploying these state-of-the-art techniques would help us better our understanding of cell history in appendage development. Also, explicit understanding of genetic basis of dermal and endochondral interchanges needs a significant amount of future work. Previous studies have revealed molecular mechanisms of dermal and endochondral ossifications, yet, the genetic switches to determine dermal and endochondral is still obscure—one of the most critical questions in this field. The integrative approach of high-throughput comparative sequencing, such as RNA-sequencing or ChIP-sequencing, and subsequent functional tests would be a powerful means to discover the genetic loci that have been responsible for dermal-to-endochondral transitions.

Assimilating knowledge from the different structures would lead us one step closer to understanding the whole picture of the vertebrate skeletal shifts. Though the details of genetic mechanisms that regulate dermal and endochondral bones are disparate in each structure, the principal components in bone differentiation, such as *Bmp*, *Sox9*, *Runx2* are clearly conserved. The distinct developmental programs in the skull, the shoulder, and fins are likely to be explained by genetic modifications or deployment of different molecules through a long journey of ancestral vertebrates. Future elaboration of molecular mechanisms in distinct types of ossification in multiple structures will shed light on the common and derived genetic mechanisms of dermal and endochondral development.

Embedding the knowledge about the developmental programs of bones into the background of paleontology with newly emerging tools, shifts our understanding of vertebrate evolution into a new era. Reevaluation of the mechanisms underlying the major skeletal shifts in vertebrates with genomics, genetics, and imaging techniques will cast a new light on the deep history of our ancestors.

AUTHOR CONTRIBUTIONS

TN served as the main author of the body of the manuscript. He also wrote the figure captions as well as completing parts the figure illustrations. TW drafted and made significant edits to the main content of the text, as well as editing the figure captions. He also contributed to the illustration of the figures.

ACKNOWLEDGMENTS

We would like to thank Gayani Senevirathne and Thomas A. Stewart for constructive comments which improved this manuscript substantially. This work was performed with the institutional support provided by the Rutgers University School of Arts and Sciences and the Human Genetics Institute of New Jersey and with 2016 Grant for Basic Science Research Projects (160335) provided by Sumitomo Foundation.

REFERENCES

Abzhanov, A., Rodda, S. J., McMahon, A. P., and Tabin, C. J. (2007). Regulation of skeletogenic differentiation in cranial dermal bone. *Development* 134, 3133–3144. doi: 10.1242/dev.002709

Adachi, N., Robinson, M., Goolsbee, A., and Shubin, N. H. (2016). Regulatory evolution of *Tbx5* and the origin of paired appendages. *Proc. Natl. Acad. Sci.U.S.A.* 113, 10115–10120. doi: 10.1073/pnas.1609997113

Ahn, D., and Ho, R. K. (2008). Tri-phasic expression of posterior Hox genes during development of pectoral fins in zebrafish: implications for the evolution of vertebrate paired appendages. *Dev. Biol.* 322, 220–233. doi: 10.1016/j.ydbio.2008.06.032

Ahn, D. G., Kourakis, M. J., Rohde, L. A., Silver, L. M., and Ho, R. K. (2002). T-box gene tbx5 is essential for formation of the pectoral limb bud. *Nature* 417, 754–758. doi: 10.1038/nature00814

Albertson, R. C., Streelman, J. T., Kocher, T. D., and Yelick, P. C. (2005). Integration and evolution of the cichlid mandible: the molecular basis of alternate feeding strategies. *Proc. Natl. Acad. Sci. U.S.A.* 102, 16287–16292. doi: 10.1073/pnas.0506649102

Andrews, S. M., and Westoll, T. S. (1970). IX.—The postcranial skeleton of *Ensthenopteron foordi* whiteaves. *Earth Environ. Sci. Trans. R. Soc. Edinburgh* 68, 391–489. doi: 10.1017/S0080456800014800

Andrey, G., Montavon, T., Mascrez, B., Gonzalez, F., Noordermeer, D., Leleu, M., et al. (2013). A switch between topological domains underlies HoxD genes collinearity in mouse limbs. *Science* 340:1234167. doi: 10.1126/science.1234167

Aubin, J., Lemieux, M., Moreau, J., Lapointe, J., and Jeannotte, L. (2002). Cooperation of Hoxa5 and Pax1 genes during formation of the pectoral girdle. *Dev. Biol.* 244, 96–113. doi: 10.1006/dbio.2002.0596

Aumonier, F. J. (1941). Development of the dermal bones in the skull of *Lepidosteus Osseus*. *J. Cell Sci.* s2–83:1–33.

Barrow, J. R. (2003). Ectodermal Wnt3/beta -catenin signaling is required for the establishment and maintenance of the apical ectodermal ridge. *Genes Dev.* 17, 394–409. doi: 10.1101/gad.1044903

Barske, L., Rataud, P., Behizad, K., Del Rio, L., Cox, S. G., and Crump, J. G. (2018). Essential role of Nr2f nuclear receptors in patterning the vertebrate upper jaw. *Dev. Cell* 44, 337.e5–347.e5. doi: 10.1016/j.devcel.2017.12.022

Beccari, L., Yakushiji-Kaminatsui, N., Woltering, J. M., Necsulea, A., Lonfat, N., Rodríguez-Carballo, E., et al. (2016). A role for HOX13 proteins in the regulatory switch between TADs at the HoxD locus. *Genes Dev.* 30, 1172–1186. doi: 10.1101/gad.281055.116

Boisvert, C. A., Joss, J. M., and Ahlberg, P. E. (2013). Comparative pelvic development of the axolotl (*Ambystoma mexicanum*) and the Australian lungfish (*Neoceratodus forsteri*): conservation and innovation across the fish-tetrapod transition. *Evodevo* 4:3. doi: 10.1186/2041-9139-4-3

Boisvert, C. A., Mark-Kurik, E., and Ahlberg, P. E. (2008). The pectoral fin of *Panderichthys* and the origin of digits. *Nature* 456, 636–638. doi: 10.1038/nature07339

Bonilla-Claudio, M., Wang, J., Bai, Y., Klysik, E., Selever, J., Martin, J. F., et al. (2012). Bmp signaling regulates a dose-dependent transcriptional program to control facial skeletal development. *Development* 139, 709–719. doi: 10.1242/dev.073197

Boulet, A. M., Moon, A. M., Arenkiel, B. R., and Capecchi, M. R. (2004). The roles of Fgf4 and Fgf8 in limb bud initiation and outgrowth. *Dev. Biol.* 273, 361–372. doi: 10.1016/j.ydbio.2004.06.012

Braasch, I., Gehrke, A. R., Smith, J. J., Kawasaki, K., Manousaki, T., Pasquier, J., et al. (2016). The spotted gar genome illuminates vertebrate evolution and facilitates human-teleost comparisons. *Nat. Genet.* 48, 427–437. doi: 10.1038/ng.3526

Briggs, J. A., Weinreb, C., Wagner, D. E., Megason, S., Peshkin, L., Kirschner, M. W., et al. (2018). The dynamics of gene expression in vertebrate embryogenesis at single-cell resolution. *Science* 360:eaar5780. doi: 10.1126/science.aar5780

Burke, A. C. (1991). The development and evolution of the turtle body plan: inferring intrinsic aspects of the evolutionary process from experimental embryology. *Am. Zool.* 31, 616–627. doi: 10.1093/icb/31.4.616

Capdevila, J., Tsukui, T., Rodríquez Esteban, C., Zappavigna, V., and Izpisúa Belmonte, JC. (1999). Control of vertebrate limb outgrowth by the proximal factor Meis2 and distal antagonism of BMPs by Gremlin. *Mol. Cell* 4, 839–849. doi: 10.1016/S1097-2765(00)80393-7

Capellini, T. D., Handschuh, K., Quintana, L., Ferretti, E., Di Giacomo, G., Fantini, S., et al. (2011). Control of pelvic girdle development by genes of the Pbx family and Emx2. *Dev. Dyn.* 240, 1173–1189. doi: 10.1002/dvdy.22617

Capellini, T. D., Vaccari, G., Ferretti, E., Fantini, S., He, M., Pellegrini, M., et al. (2010). Scapula development is governed by genetic interactions of Pbx1 with its family members and with Emx2 via their cooperative control of Alx1. *Development* 137, 2559–2569. doi: 10.1242/dev.048819

Clack, J. A. (1989). Discovery of the earliest-known tetrapod stapes. *Nature* 342, 425–427. doi: 10.1038/342425a0

Clack, J. A. (2009a). The fin to limb transition: new data, interpretations, and hypotheses from paleontology and developmental biology. *Annu. Rev. Earth Planet. Sci.* 37, 163–179. doi: 10.1146/annurev.earth.36.031207.124146

Clack, J. A. (2009b). The fish–tetrapod transition: new fossils and interpretations. *Evol. Educ. Outreach* 2, 213–223. doi: 10.1007/s12052-009-0119-2

Clack, J. A. (2012). *Gaining Ground: The Origin and Evolution of Tetrapods*. Bloomington, IN: Indiana University Press.

Coates, M. I. (1996). The Devonian tetrapod *Acanthostega gunnari* Jarvik: postcranial anatomy, basal tetrapod interrelationships and patterns of skeletal evolution. *Trans. R. Soc. Edinb. Earth Sci.* 87, 363–421. doi: 10.1017/S0263593300006787

Cubbage, C. C., and Mabee, P. M. (1996). Development of the cranium and paired fins in the zebrafish *Danio rerio* (Ostariophysi, Cyprinidae). *J. Morphol.* 229, 121–160. doi: 10.1002/(SICI)1097-4687(199608)229:2<121::AID-JMOR1>3.0.CO;2-4

Daeschler, E. B., Shubin, N. H., and Jenkins, F. A. (2006). A Devonian tetrapod-like fish and the evolution of the tetrapod body plan. *Nature* 440, 757–763. doi: 10.1038/nature04639

Davis, M. C., Shubin, N. H., and Force, A. (2004). Pectoral fin and girdle development in the basal actinopterygians *Polyodon spathula* and *Acipenser transmontanus*. *J. Morphol.* 262, 608–628. doi: 10.1002/jmor.10264

De Beer, G. (1985). *The Development of the Vertebrate Skull*. Chicago, IL: University of Chicago Press.

Dial, K. P., Shubin, N., and Brainerd, E. L. (eds). (2015). *Great Transformations in Vertebrate Evolution*. Chicago, IL: University of Chicago Press.

Dillman, C. B., and Hilton, E. J. (2015). Anatomy and early development of the pectoral girdle, fin, and fin spine of sturgeons (Actinopterygii: Acipenseridae). *J. Morphol.* 276, 241–260. doi: 10.1002/jmor.20328

Diogo, R., Molnar, J. L., and Smith, T. D. (2014). The anatomy and ontogeny of the head, neck, pectoral, and upper limb muscles of *Lemur catta* and *Propithecus coquereli* (Primates): discussion on the parallelism between ontogeny and phylogeny and implications for evolutionary and developmental biology. *Anat. Rec.* 297, 1435–1453. doi: 10.1002/ar.22931

Donoghue, P. C. J., and Sansom, I. J. (2002). Origin and early evolution of vertebrate skeletonization. *Microsc. Res. Tech.* 59, 352–372. doi: 10.1002/jemt.10217

Durán, I., Marí-Beffa, M., Santamaría, J. A., Becerra, J., and Santos-Ruiz, L. (2011). Actinotrichia collagens and their role in fin formation. *Dev. Biol.* 354, 160–172. doi: 10.1016/j.ydbio.2011.03.014

Ericsson, R., Knight, R., and Johanson, Z. (2013). Evolution and development of the vertebrate neck. *J. Anat.* 222, 67–78. doi: 10.1111/j.1469-7580.2012.01530.x

Farrell, J. A., Wang, Y., Riesenfeld, S. J., Shekhar, K., Regev, A., and Schier, A. F. (2018). Single-cell reconstruction of developmental trajectories during zebrafish embryogenesis. *Science* 360:eaar3131. doi: 10.1126/science.aar3131

Freitas, R., Gómez-Marín, C., Wilson, J. M., Casares, F., and Gómez-Skarmeta, J. L. (2012). Hoxd13 contribution to the evolution of vertebrate appendages. *Dev. Cell* 23, 1219–1229. doi: 10.1016/j.devcel.2012.10.015

Freitas, R., Zhang, G., and Cohn, M. J. (2006). Evidence that mechanisms of fin development evolved in the midline of early vertebrates. *Nature* 442, 1033–1037. doi: 10.1038/nature04984

Fromental-Ramain, C., Warot, X., Lakkaraju, S., Favier, B., Haack, H., Birling, C., et al. (1996a). Specific and redundant functions of the paralogous Hoxa-9 and Hoxd-9 genes in forelimb and axial skeleton patterning. *Development* 122, 461–472.

Fromental-Ramain, C., Warot, X., Messadecq, N., LeMeur, M., Dollé, P., and Chambon, P. (1996b). Hoxa-13 and Hoxd-13 play a crucial role in the patterning of the limb autopod. *Development* 122, 2997–3011.

Gehrke, A. R., Schneider, I., de la Calle-Mustienes, E., Tena, J. J., Gomez-Marin, C., Chandran, M., et al. (2015). Deep conservation of wrist and digit enhancers in fish. *Proc. Natl. Acad. Sci. U.S.A.* 112, 803–808. doi: 10.1073/pnas.1420208112

Gilbert, S. F. (2000). *Osteogenesis: The Development of Bones (Developmental Biology)*. Sunderland, MA: Sinauer Associates.

Giles, S., Xu, G.-H., Near, T. J., and Friedman, M. (2017). Early members of "living fossil" lineage imply later origin of modern ray-finned fishes. *Nature* 549, 265–268. doi: 10.1038/nature23654

Goodnough, L. H., Chang, A. T., Treloar, C., Yang, J., Scacheri, P. C., Atit, R. P., et al. (2012). Twist1 mediates repression of chondrogenesis by β-catenin to promote cranial bone progenitor specification. *Development* 139, 4428–4438. doi: 10.1242/dev.081679

Goodnough, L. H., DiNuoscio, G. J., Ferguson, J. W., Williams, T., Lang, R. A., and Atit, R. P. (2014). Distinct requirements for cranial ectoderm and mesenchyme-derived wnts in specification and differentiation of osteoblast and dermal progenitors. *PLoS Genet.* 10:e1004152. doi: 10.1371/journal.pgen.1004152

Grandel, H., and Schulte-Merker, S. (1998). The development of the paired fins in the zebrafish (*Danio rerio*). *Mech. Dev.* 79, 99–120. doi: 10.1016/S0925-4773(98)00176-2

Gregory, W. (1951). *Evolution Emerging a Survey of Changing Patterns from Primeval Life to Man*. New York, NY: Simon and Schuster.

Gros, J., and Tabin, C. J. (2014). Vertebrate limb bud formation is initiated by localized epithelial-to-mesenchymal transition. *Science* 343, 1253–1256. doi: 10.1126/science.1248228

Gyurján, I., Sonderegger, B., Naef, F., and Duboule, D. (2011). Analysis of the dynamics of limb transcriptomes during mouse development. *BMC Dev. Biol.* 11:47. doi: 10.1186/1471-213X-11-47

Hall, B. K. (2005). *Bones and Cartilage:Developmental and Evolutionary Skeletal Biology*. Cambridge, MA: Academic Press.

Hanken, J., and Hall, B. K. (1993). *The Skull*. Chicago, IL: University of Chicago Press.

Harris, M. P., Rohner, N., Schwarz, H., Perathoner, S., Konstantinidis, P., and Nüsslein-Volhard, C. (2008). Zebrafish eda and edar mutants reveal conserved and ancestral roles of ectodysplasin signaling in vertebrates. *PLoS Genet.* 4:e1000206. doi: 10.1371/journal.pgen.1000206

Heude, É., Shaikho, S., and Ekker, M. (2014). The dlx5a/dlx6a genes play essential roles in the early development of zebrafish median fin and pectoral structures. *PLoS ONE* 9:e98505. doi: 10.1371/journal.pone.0098505

Hirasawa, T., and Kuratani, S. (2015). Evolution of the vertebrate skeleton: morphology, embryology, and development. *Zool. Lett.* 1:2. doi: 10.1186/s40851-014-0007-7

Hofmann, C., Drossopoulou, G., McMahon, A., Balling, R., and Tickle, C. (1998). Inhibitory action of BMPs onPax1 expression and on shoulder girdle formation during limb development. *Dev. Dyn.* 213, 199–206. doi: 10.1002/(SICI)1097-0177(199810)213:2<199::AID-AJA5>3.0.CO;2-B

Huang, R., Christ, B., and Patel, K. (2006). Regulation of scapula development. *Brain Struct. Funct.* 211, 65–71. doi: 10.1007/s00429-006-0126-9

Huang, R., Zhi, Q., Patel, K., Wilting, J., and Christ, B. (2000). Dual origin and segmental organisation of the avian scapula. *Development* 127, 3789–3794.

Huycke, T. R., Eames, B. F., and Kimmel, C. B. (2012). Hedgehog-dependent proliferation drives modular growth during morphogenesis of a dermal bone. *Development* 139, 2371–2380. doi: 10.1242/dev.079806

Ishii, M., Sun, J., Ting, M.-C., and Maxson, R. E. (2015). The development of the calvarial bones and sutures and the pathophysiology of craniosynostosis. *Curr. Top. Dev. Biol.* 115, 131–156. doi: 10.1016/bs.ctdb.2015.07.004

Itou, J., Kawakami, H., Quach, T., Osterwalder, M., Evans, S. M., Zeller, R., et al. (2012). Islet1 regulates establishment of the posterior hindlimb field upstream of the Hand2-Shh morphoregulatory gene network in mouse embryos. *Development* 139, 1620–1629. doi: 10.1242/dev.073056

Janvier, P. (1996). *Early Vertebrates*. Oxford: Oxford University Press.

Jarvik, E. (1980). *Basic Structure and Evolution of Vertebrates, Vol. 1*. Cambridge, MA: Academic Press.

Jerković, I., Ibrahim, D. M., Andrey, G., Haas, S., Hansen, P., Janetzki, C., et al. (2017). Genome-wide binding of posterior HOXA/D transcription factors reveals subgrouping and association with CTCF. *PLOS Genet.* 13:e1006567. doi: 10.1371/journal.pgen.1006567

Jones, F. C., Grabherr, M. G., Chan, Y. F., Russell, P., Mauceli, E., Johnson, J., et al. (2012). The genomic basis of adaptive evolution in threespine sticklebacks. *Nature* 484, 55–61. doi: 10.1038/nature10944

Jovelin, R., He, X., Amores, A., Yan, Y., Shi, R., Qin, B., et al. (2007). Duplication and divergence offgf8 functions in teleost development and evolution. *J. Exp. Zool. Part B Mol. Dev. Evol.* 308B, 730–743. doi: 10.1002/jez.b.21193

Kague, E., Gallagher, M., Burke, S., Parsons, M., Franz-Odendaal, T., and Fisher, S. (2012). Skeletogenic fate of zebrafish cranial and trunk neural crest. *PLoS ONE* 7:e47394. doi: 10.1371/journal.pone.0047394

Kapoor, A. S. (1970). Development of dermal bones related to sensory canals of the head in the fishes *Ophicephalus punctatus* Bloch (Ophicephalidae) and *Wallugo attu* Bl.&Schn. (Siluridae). *Zool. J. Linn. Soc.* 49, 69–95. doi: 10.1111/j.1096-3642.1970.tb00731.x

Keating, J. N., and Donoghue, P. C. J. (2016). Histology and affinity of anaspids, and the early evolution of the vertebrate dermal skeleton. *Proc. R. Soc. B Biol. Sci.* 283:20152917. doi: 10.1098/rspb.2015.2917

Knosp, W. M., Scott, V., Bächinger, H. P., and Stadler, H. S. (2004). HOXA13 regulates the expression of bone morphogenetic proteins 2 and 7 to control distal limb morphogenesis. *Development* 131, 4581–4592. doi: 10.1242/dev.01327

Krawchuk, D., Weiner, S. J., Chen, Y.-T., Lu, B. C., Costantini, F., Behringer, R. R., et al. (2010). Twist1 activity thresholds define multiple functions in limb development. *Dev. Biol.* 347, 133–146. doi: 10.1016/j.ydbio.2010.08.015

Kronenberg, H. M. (2003). Developmental regulation of the growth plate. *Nature* 423, 332–336. doi: 10.1038/nature01657

Kuijper, S., Beverdam, A., Kroon, C., Brouwer, A., Candille, S., Barsh, G., et al. (2005). Genetics of shoulder girdle formation: roles of Tbx15 and aristaless-like genes. *Development* 132, 1601–1610. doi: 10.1242/dev.01735

Laforest, L., Brown, C. W., Poleo, G., Géraudie, J., Tada, M., Ekker, M., et al. (1998). Involvement of the sonic hedgehog, patched 1 and bmp2 genes in patterning of the zebrafish dermal fin rays. *Development* 125, 4175–4184.

Lalonde, R. L., and Akimenko, M.-A. (2018). Effects of fin fold mesenchyme ablation on fin development in zebrafish. *PLoS ONE* 13:e0192500. doi: 10.1371/journal.pone.0192500

Lalonde, R. L., Moses, D., Zhang, J., Cornell, N., Ekker, M., and Akimenko, M.-A. (2016). Differential actinodin1 regulation in zebrafish and mouse appendages. *Dev. Biol.* 417, 91–103. doi: 10.1016/j.ydbio.2016.05.019

Lee, R. T. H., Thiery, J. P., and Carney, T. J. (2013). Dermal fin rays and scales derive from mesoderm, not neural crest. *Curr. Biol.* 23, R336–R337. doi: 10.1016/j.cub.2013.02.055

Leite-Castro, J., Beviano, V., Rodrigues, P., and Freitas, R. (2016). HoxA genes and the fin-to-limb transition in vertebrates. *J. Dev. Biol.* 4:10. doi: 10.3390/jdb4010010

Letelier, J., Calle-Mustienes, E., Pieretti, J., Naranjo, S., Maeso, I., Nakamura, T., et al. (2018). A conserved Shh cis-regulatory module highlights a common developmental origin of unpaired and paired fins. *Nat. Genet.* 50, 504–509. doi: 10.1038/s41588-018-0080-5

Lewandoski, M., Sun, X., and Martin, G. R. (2000). Fgf8 signalling from the AER is essential for normal limb development. *Nat Genet* 26, 460–463. doi: 10.1038/82609

Linnen, C. R., Poh, Y.-P., Peterson, B. K., Barrett, R. D. H., Larson, J. G., Jensen, J. D., et al. (2013). Adaptive evolution of multiple traits through multiple mutations at a single gene. *Science* 339, 1312–1316. doi: 10.1126/science.1233213

Loebel, D. A. F., Hor, A. C. C., Bildsoe, H., Jones, V., Chen, Y.-T., Behringer, R. R., et al. (2012). Regionalized Twist1 activity in the forelimb bud drives the morphogenesis of the proximal and preaxial skeleton. *Dev. Biol.* 362, 132–140. doi: 10.1016/j.ydbio.2011.11.020

Loh, Y.-H. E., Katz, L. S., Mims, M. C., Kocher, T. D., Yi, S. V., and Streelman, J. T. (2008). Comparative analysis reveals signatures of differentiation amid genomic polymorphism in Lake Malawi cichlids. *Genome Biol.* 9:R113. doi: 10.1186/gb-2008-9-7-r113

Long, F., and Ornitz, D. M. (2013). Development of the endochondral skeleton. *Cold Spring Harb. Perspect. Biol.* 5:a008334. doi: 10.1101/cshperspect.a008334

Maddin, H. C., Piekarski, N., Sefton, E. M., and Hanken, J. (2016). Homology of the cranial vault in birds: new insights based on embryonic fate-mapping and character analysis. *R. Soc. Open Sci.* 3:160356. doi: 10.1098/rsos.160356

Mahasen, L. M. A. (2016). Evolution of the kidney. *Anat. Physiol. Biochem. Int. J.* 1:555554. doi: 10.19080/APBIJ.2016.01.555554

Malashichev, Y., Borkhvardt, V., Christ, B., and Scaal, M. (2005). Differential regulation of avian pelvic girdle development by the limb field ectoderm. *Anat. Embryol.* 210, 187–197. doi: 10.1007/s00429-005-0014-8

Malashichev, Y., Christ, B., and Pröls, F. (2008). Avian pelvis originates from lateral plate mesoderm and its development requires signals from both ectoderm and paraxial mesoderm. *Cell Tissue Res.* 331, 595–604. doi: 10.1007/s00441-007-0556-6

Masselink, W., Cole, N. J., Fenyes, F., Berger, S., Sonntag, C., Wood, A., et al. (2016). A somitic contribution to the apical ectodermal ridge is essential for fin formation. *Nature* 535, 542–546. doi: 10.1038/nature18953

Masyuk, M., Abduelmula, A., Morosan-Puopolo, G., Ödemis, V., Rehimi, R., Khalida, N., et al. (2014). Retrograde migration of pectoral girdle muscle precursors depends on CXCR4/SDF-1 signaling. *Histochem. Cell Biol.* 142, 473–488. doi: 10.1007/s00418-014-1237-7

Matsuoka, T., Ahlberg, P. E., Kessaris, N., Iannarelli, P., Dennehy, U., Richardson, W. D., et al. (2005). Neural crest origins of the neck and shoulder. *Nature* 436, 347–355. doi: 10.1038/nature03837

Miller, C. T., Glazer, A. M., Summers, B. R., Blackman, B. K., Norman, A. R., Shapiro, M. D., et al. (2014). Modular skeletal evolution in sticklebacks is controlled by additive and clustered quantitative trait loci. *Genetics* 197, 405–420. doi: 10.1534/genetics.114.162420

Moeller, C., Swindell, E. C., Kispert, A., and Eichele, G. (2003). Carboxypeptidase Z (CPZ) modulates Wnt signaling and regulates the development of skeletal elements in the chicken. *Development* 130, 5103–5111. doi: 10.1242/dev.00686

Montavon, T., Soshnikova, N., Mascrez, B., Joye, E., Thevenet, L., Splinter, E., et al. (2011). A regulatory archipelago controls hox genes transcription in digits. *Cell* 147, 1132–1145. doi: 10.1016/j.cell.2011.10.023

Moy-Thomas, J. A., and Miles, R. S. (1971). *Palaeozoic Fishes*. Philadelphia, PA: Saunders.

Nagashima, H., Sugahara, F., Watanabe, K., Shibata, M., Chiba, A., and Sato, N. (2016). Developmental origin of the clavicle, and its implications for the evolution of the neck and the paired appendages in vertebrates. *J. Anat.* 229, 536–548. doi: 10.1111/joa.12502

Nakamura, T., Gehrke, A. R., Lemberg, J., Szymaszek, J., and Shubin, N. H. (2016). Digits and fin rays share common developmental histories. *Nature* 8, 225–228. doi: 10.1038/nature19322

Neumann, C. J., Grandel, H., Gaffield, W., Schulte-Merker, S., and Nüsslein-Volhard, C. (1999). Transient establishment of anteroposterior polarity in the zebrafish pectoral fin bud in the absence of sonic hedgehog activity. *Development* 126, 4817–4826.

Onimaru, K., Kuraku, S., Takagi, W., Hyodo, S., Sharpe, J., and Tanaka, M. (2015). A shift in anterior-posterior positional information underlies the fin-to-limb evolution. *Elife* 4:e07048. doi: 10.7554/eLife.07048

Paço, A., and Freitas, R. (2018). Hox D genes and the *fin-to-limb* transition: insights from fish studies. *Genesis* 56:e23069. doi: 10.1002/dvg.23069

Pardo, J. D., Szostakiwskyj, M., Ahlberg, P. E., and Anderson, J. S. (2017). Hidden morphological diversity among early tetrapods. *Nature* 546, 642–645. doi: 10.1038/nature22966

Parker, H. J., Bronner, M. E., and Krumlauf, R. (2014). A Hox regulatory network of hindbrain segmentation is conserved to the base of vertebrates. *Nature* 514, 490–493. doi: 10.1038/nature13723

Parsons, K. J., and Albertson, R. C. (2013). Unifying and generalizing the two strands of evo-devo. *Trends Ecol. Evol.* 28, 584–591. doi: 10.1016/j.tree.2013.06.009

Parsons, K. J., Trent Taylor, A., Powder, K. E., and Albertson, R. C. (2014). Wnt signalling underlies the evolution of new phenotypes and craniofacial variability in Lake Malawi cichlids. *Nat. Commun.* 5:3629. doi: 10.1038/ncomms4629

Pehrson, T. (1940). The development of dermal bones in the skull of *Amia calva*. *Acta Zool.* 21, 1–50. doi: 10.1111/j.1463-6395.1940.tb00338.x

Pehrson, T. (1944). Some observations on the development and morphology of the dermal bones in the skull of acipenser and polyodon. *Acta Zool.* 25, 27–48. doi: 10.1111/j.1463-6395.1944.tb00343.x

Pehrson, T. (1958). The early ontogeny of the sensory lines and the dermal skull in *polypterus*. *Acta Zool.* 39, 241–258. doi: 10.1111/j.1463-6395.1958.tb00387.x

Percival, C. J., and Richtsmeier, J. T. (2013). Angiogenesis and intramembranous osteogenesis. *Dev. Dyn.* 242, 909–922. doi: 10.1002/dvdy.23992

Piekarski, N., and Olsson, L. (2011). A somitic contribution to the pectoral girdle in the axolotl revealed by long-term fate mapping. *Evol. Dev.* 13, 47–57. doi: 10.1111/j.1525-142X.2010.00455.x

Piekarski, N., Gross, J. B., and Hanken, J. (2014). Evolutionary innovation and conservation in the embryonic derivation of the vertebrate skull. *Nat. Commun.* 5:5661. doi: 10.1038/ncomms6661

Pieretti, J., Gehrke, A. R., Schneider, I., Adachi, N., Nakamura, T., and Shubin, N. H. (2015). Organogenesis in deep time: a problem in genomics, development, and paleontology. *Proc. Natl. Acad. Sci. U.S.A.* 112, 4871–4876. doi: 10.1073/pnas.1403665112

Pignolo, R., Ramaswamy, G., Fong, J., Shore, E., and Kaplan, F. (2015). Progressive osseous heteroplasia: diagnosis, treatment, and prognosis. *Appl. Clin. Genet.* 8, 37–48. doi: 10.2147/TACG.S51064

Piotrowski, T., and Baker, C. V. H. (2014). The development of lateral line placodes: taking a broader view. *Dev. Biol.* 389, 68–81. doi: 10.1016/j.ydbio.2014.02.016

Pomikal, C., and Streicher, J. (2009). 4D-analysis of early pelvic girdle development in the mouse (*Mus musculus*). *J. Morphol.* 271, 116–126. doi: 10.1002/jmor.10785

Pu, Q., Huang, R., and Brand-Saberi, B. (2016). Development of the shoulder girdle musculature. *Dev. Dyn.* 245, 342–350. doi: 10.1002/dvdy.24378

Quint, E., Smith, A., Avaron, F., Laforest, L., Miles, J., Gaffield, W., et al. (2002). Bone patterning is altered in the regenerating zebrafish caudal fin after ectopic expression of sonic hedgehog and bmp2b or exposure to cyclopamine. *Proc. Natl. Acad. Sci. U.S.A.* 99, 8713–8718. doi: 10.1073/pnas.122571799

Raines, A. M., Magella, B., Adam, M., and Potter, S. S. (2015). Key pathways regulated by HoxA9,10,11/HoxD9,10,11 during limb development. *BMC Dev. Biol.* 15:28. doi: 10.1186/s12861-015-0078-5

Rasch, L. J., Martin, K. J., Cooper, R. L., Metscher, B. D., Underwood, C. J., and Fraser, G. J. (2016). An ancient dental gene set governs development and continuous regeneration of teeth in sharks. *Dev. Biol.* 415, 347–370. doi: 10.1016/j.ydbio.2016.01.038

Regard, J. B., Malhotra, D., Gvozdenovic-Jeremic, J., Josey, M., Chen, M., Weinstein, L. S., et al. (2013). Activation of Hedgehog signaling by loss of GNAS causes heterotopic ossification. *Nat. Med.* 19, 1505–1512. doi: 10.1038/nm.3314

Romer, A. S. (1949). *The Vertebrate Body*. W.B. Philadelphia, PA: Saunders.

Roybal, P. G., Wu, N. L., Sun, J., Ting, M., Schafer, C. A., and Maxson, R. E. (2010). Inactivation of Msx1 and Msx2 in neural crest reveals an unexpected role in suppressing heterotopic bone formation in the head. *Dev. Biol.* 343, 28–39. doi: 10.1016/j.ydbio.2010.04.007

Sagai, T., Amano, T., Maeno, A., Kimura, T., Nakamoto, M., Takehana, Y., et al. (2017). Evolution of Shh endoderm enhancers during morphological transition from ventral lungs to dorsal gas bladder. *Nat. Commun.* 8:14300. doi: 10.1038/ncomms14300

Salsi, V., Vigano, M. A., Cocchiarella, F., Mantovani, R., and Zappavigna, V. (2008). Hoxd13 binds *in vivo* and regulates the expression of genes acting in key pathways for early limb and skeletal patterning. *Dev. Biol.* 317, 497–507. doi: 10.1016/j.ydbio.2008.02.048

Schmidt, C., Stoeckelhuber, M., McKinnell, I., Putz, R., Christ, B., and Patel, K. (2004). Wnt 6 regulates the epithelialisation process of the segmental plate mesoderm leading to somite formation. *Dev. Biol.* 271, 198–209. doi: 10.1016/j.ydbio.2004.03.016

Schneider, I., and Shubin, N. H. (2013). The origin of the tetrapod limb: from expeditions to enhancers. *Trends Genet.* 29, 419–426. doi: 10.1016/j.tig.2013.01.012

Schultze, H. P., and Arsenault, M. (1985). The panderichthyid fish *Elpistostege*: a close relative of tetrapods? *Paleontology* 28, 293–309.

Scotti, M., Kherdjemil, Y., Roux, M., and Kmita, M. (2015). A Hoxa13:Cre mouse strain for conditional gene manipulation in developing limb, hindgut, and urogenital system. *Genesis* 53, 366–376. doi: 10.1002/dvg.22859

Sears, K. E. (2004). Constraints on the morphological evolution of marsupial shoulder girdles. *Evolution* 58, 2353–2370. doi: 10.1554/03-669

Sears, K. E., Bianchi, C., Powers, L., and Beck, A. L. (2013). Integration of the mammalian shoulder girdle within populations and over evolutionary time. *J. Evol. Biol.* 26, 1536–1548. doi: 10.1111/jeb.12160

Shimada, A., Kawanishi, T., Kaneko, T., Yoshihara, H., Yano, T., Inohaya, K., et al. (2013). Trunk exoskeleton in teleosts is mesodermal in origin. *Nat. Commun.* 4:1639. doi: 10.1038/ncomms2643

Shubin, N. H., Daeschler, E. B., and Jenkins, F. A. (2006). The pectoral fin of *Tiktaalik roseae* and the origin of the tetrapod limb. *Nature* 440, 764–771. doi: 10.1038/nature04637

Sire, J.-Y., and Akimenko, M.-A. (2004). Scale development in fish: a review, with description of sonic hedgehog (shh) expression in the zebrafish (*Danio rerio*). *Int. J. Dev. Biol.* 48, 233–247. doi: 10.1387/ijdb.15272389

Sire, J.-Y., and Huysseune, A. (2003). Formation of dermal skeletal and dental tissues in fish: a comparative and evolutionary approach. *Biol. Rev. Camb. Philos. Soc.* 78, 219–249. doi: 10.1017/S1464793102006073

Smith, A., Avaron, F., Guay, D., Padhi, B. K., and Akimenko, M. A. (2006). Inhibition of BMP signaling during zebrafish fin regeneration disrupts fin growth and scleroblast differentiation and function. *Dev. Biol.* 299, 438–454. doi: 10.1016/j.ydbio.2006.08.016

Smith, J. J., Timoshevskaya, N., Ye, C., Holt, C., Keinath, M. C., Parker, H. J., et al. (2018). The sea lamprey germline genome provides insights into programmed genome rearrangement and vertebrate evolution. *Nat. Genet.* 50, 270–277. doi: 10.1038/s41588-017-0036-1

Smith, M. M., and Hall, B. K. (1990). Development and evolutionary origins of vertebrate skeletogenic and odontogenic tissues. *Biol. Rev. Camb. Philos. Soc.* 65, 277–373. doi: 10.1111/j.1469-185X.1990.tb01427.x

Sordino, P., van der Hoeven, F., and Duboule, D. (1995). Hox gene expression in teleost fins and the origin of vertebrate digits. *Nature* 375, 678–681. doi: 10.1038/375678a0

Suzuki, T. (2013). How is digit identity determined during limb development? *Dev. Growth Differ.* 55, 130–138. doi: 10.1111/dgd.12022

Tanaka, M. (2018). Alterations in anterior-posterior patterning and its accompanying changes along the proximal-distal axis during the fin-to-limb transition. *Genesis* 56:e23053. doi: 10.1002/dvg.23053

Thorogood, P. (1991). "The development of the teleost fin and implications for our understanding of tetrapod limb evolution," in *Developmental Patterning of the Vertebrate Limb. NATO ASI Series (Series A: Life Sciences), Vol. 205*.Developmen. eds J. R. Hinchliffe, J. M. Hurle, and D. Summerbell (Boston, MA: Springer), 347–354.

Timmons, P. M., Wallin, J., Rigby, P. W., and Balling, R. (1994). Expression and function of Pax 1 during development of the pectoral girdle. *Development* 120, 2773–2785.

Tubbs, R. S., Bosmia, A. N., and Cohen-Gadol, A. A. (2012). The human calvaria: a review of embryology, anatomy, pathology, and molecular development. *Child Nerv. Syst.* 28, 23–31. doi: 10.1007/s00381-011-1637-0

Tucker, A., and Sharpe, P. (2004). The cutting-edge of mammalian development; how the embryo makes teeth. *Nat. Rev. Genet.* 5, 499–508. doi: 10.1038/nrg1380

Tulenko, F. J., Augustus, G. J., Massey, J. L., Sims, S. E., Mazan, S., and Davis, M. C. (2016). HoxD expression in the fin-fold compartment of basal gnathostomes and implications for paired appendage evolution. *Sci. Rep.* 6:22720. doi: 10.1038/srep22720

Tulenko, F. J., Massey, J. L., Holmquist, E., Kigundu, G., Thomas, S., Smith, S. M. E., et al. (2017). Fin-fold development in paddlefish and catshark and implications for the evolution of the autopod. *Proc. R. Soc. B Biol. Sci.* 284:20162780. doi: 10.1098/rspb.2016.2780

Valasek, P., Theis, S., DeLaurier, A., Hinits, Y., Luke, G. N., Otto, A. M., et al. (2011). Cellular and molecular investigations into the development of the pectoral girdle. *Dev. Biol.* 357, 108–116. doi: 10.1016/j.ydbio.2011.06.031

Valasek, P., Theis, S., Krejci, E., Grim, M., Maina, F., Shwartz, Y., et al. (2010). Somitic origin of the medial border of the mammalian scapula and its homology to the avian scapula blade. *J. Anat.* 216, 482–488. doi: 10.1111/j.1469-7580.2009.01200.x

Verreijdt, L., Vandervennet, E., Sire, J. Y., and Huysseune, A. (2002). Developmental differences between cranial bones in the zebrafish (*Danio rerio*): some preliminary light and TEM observations. *Connect. Tissue Res.* 43, 109–112. doi: 10.1080/03008200290001087

Wagner, D. E., Weinreb, C., Collins, Z. M., Briggs, J. A., Megason, S. G., and Klein, A. M. (2018). Single-cell mapping of gene expression landscapes and lineage in the zebrafish embryo. *Science* 360, 981–987. doi: 10.1126/science.aar4362

Wagner, D. O., and Aspenberg, P. (2011). Where did bone come from? *Acta Orthop.* 82, 393–398. doi: 10.3109/17453674.2011.588861

Warth, P., Hilton, E. J., Naumann, B., Olsson, L., and Konstantinidis, P. (2017). Development of the skull and pectoral girdle in Siberian sturgeon, *Acipenser baerii*, and Russian sturgeon, *Acipenser gueldenstaedtii* (Acipenseriformes: Acipenseridae). *J. Morphol.* 278, 418–442. doi: 10.1002/jmor.20653

Wehner, D., and Weidinger, G. (2015). Signaling networks organizing regenerative growth of the zebrafish fin. *Trends Genet.* 31, 336–343. doi: 10.1016/j.tig.2015.03.012

Westoll, T. S., Andrews, S. M., Miles, R. S., and Walker, A. D. (1977). *Problems in Vertebrate Evolution : Essays Presented to Professor, T. S. Westoll*. Cambridge, MA: Linnean Society of London by Academic Press.

White, J. J., Lin, T., Brown, A. M., Arancillo, M., Lackey, E. P., Stay, T. L., et al. (2016). An optimized surgical approach for obtaining stable extracellular single-unit recordings from the cerebellum of head-fixed behaving mice. *J. Neurosci. Methods* 262, 21–31. doi: 10.1016/j.jneumeth.2016.01.010

Witzmann, F. (2009). Comparative histology of sculptured dermal bones in basal tetrapods, and the implications for the soft tissue dermis. *Palaeodiversity* 2, 233–270.

Woltering, J. M., and Duboule, D. (2010). The origin of digits: expression patterns versus regulatory mechanisms. *Dev. Cell* 18, 526–532. doi: 10.1016/j.devcel.2010.04.002

Woltering, J. M., Noordermeer, D., Leleu, M., and Duboule, D. (2014). Conservation and divergence of regulatory strategies at hox loci and the origin of tetrapod digits. *PLoS Biol.* 12:e1001773. doi: 10.1371/journal.pbio.1001773

Wood, A., and Thorogood, P. (1984). An analysis of *in vivo* cell migration during teleost fin morphogenesis. *J. Cell Sci.* 66, 205–222.

Yano, T., Abe, G., Yokoyama, H., Kawakami, K., and Tamura, K. (2012). Mechanism of pectoral fin outgrowth in zebrafish development. *Development* 139, 2916–2925. doi: 10.1242/dev.075572

Yano, T., and Tamura, K. (2013). The making of differences between fins and limbs. *J. Anat.* 222, 100–113. doi: 10.1111/j.1469-7580.2012.01491.x

Yokouchi, Y., Nakazato, S., Yamamoto, M., Goto, Y., Kameda, T., Iba, H., et al. (1995). Misexpression of Hoxa-13 induces cartilage homeotic transformation

and changes cell adhesiveness in chick limb buds. *Genes Dev.* 9, 2509–2522. doi: 10.1101/gad.9.20.2509

Zakany, J., and Duboule, D. (2007). The role of Hox genes during vertebrate limb development. *Curr. Opin. Genet. Dev.* 17, 359–366. doi: 10.1016/j.gde.2007.05.011

Zeller, R., Lopez-Rios, J., and Zuniga, A. (2009). Vertebrate limb bud development: moving towards integrative analysis of organogenesis. *Nat Rev Genet* 10, 845–858. doi: 10.1038/nrg2681

Zhang, J., Wagh, P., Guay, D., Sanchez-Pulido, L., Padhi, B. K., Korzh, V., et al. (2010). Loss of fish actinotrichia proteins and the fin-to-limb transition. *Nature* 466, 234–237. doi: 10.1038/nature09137

Zheng, W., Wang, Z., Collins, J. E., Andrews, R. M., Stemple, D., and Gong, Z. (2011). Comparative transcriptome analyses indicate molecular homology of zebrafish swimbladder and mammalian lung. *PLoS ONE* 6:e24019. doi: 10.1371/journal.pone.0024019

Conflict of Interest Statement: The authors declare that the research was conducted in the absence of any commercial or financial relationships that could be construed as a potential conflict of interest.

frontiers in Cell and Developmental Biology

REVIEW
published: 17 August 2018
doi: 10.3389/fcell.2018.00083

Using Zebrafish to Study Collective Cell Migration in Development and Disease

Hannah M. Olson[1,2] *and Alex V. Nechiporuk*[1]*

[1] Department Cell, Developmental & Cancer Biology, The Knight Cancer Institute, Oregon Health & Science University, Portland, OR, United States, [2] Neuroscience Graduate Program, Oregon Health & Science University, Portland, OR, United States

Cellular migration is necessary for proper embryonic development as well as maintenance of adult health. Cells can migrate individually or in groups in a process known as collective cell migration. Collectively migrating cohorts maintain cell-cell contacts, group polarization, and exhibit coordinated behavior. This mode of migration is important during numerous developmental processes including tracheal branching, blood vessel sprouting, neural crest cell migration and others. In the adult, collective cell migration is important for proper wound healing and is often misappropriated during cancer cell invasion. A variety of genetic model systems are used to examine and define the cellular and molecular mechanisms behind collective cell migration including border cell migration and tracheal branching in *Drosophila melanogaster,* neural crest cell migration in chick and *Xenopus* embryos, and posterior lateral line primordium (pLLP) migration in zebrafish. The pLLP is a group of about 100 cells that begins migrating around 22 hours post-fertilization along the lateral aspect of the trunk of the developing embryo. During migration, clusters of cells are deposited from the trailing end of the pLLP; these ultimately differentiate into mechanosensory organs of the lateral line system. As zebrafish embryos are transparent during early development and the pLLP migrates close to the surface of the skin, this system can be easily visualized and manipulated *in vivo*. These advantages together with the amenity to advance genetic methods make the zebrafish pLLP one of the premier model systems for studying collective cell migration. This review will describe the cellular behaviors and signaling mechanisms of the pLLP and compare the pLLP to collective cell migration in other popular model systems. In addition, we will examine how this type of migration is hijacked by collectively invading cancer cells.

Keywords: collective cell migration, posterior lateral line, posterior lateral line primordium, collective cell invasion, cancer

OPEN ACCESS

Edited by:
Gokhan Dalgin,
University of Chicago, United States

Reviewed by:
Isaac Skromne,
University of Richmond, United States
Kandice Tanner,
National Institutes of Health (NIH), United States

***Correspondence:**
Alex V. Nechiporuk
nechipor@ohsu.edu

Specialty section:
This article was submitted to Molecular Medicine, a section of the journal Frontiers in Cell and Developmental Biology

Received: *01 May 2018*
Accepted: *16 July 2018*
Published: *17 August 2018*

Citation:
Olson HM and Nechiporuk AV (2018) Using Zebrafish to Study Collective Cell Migration in Development and Disease. Front. Cell Dev. Biol. 6:83. doi: 10.3389/fcell.2018.00083

INTRODUCTION

Cellular migration is necessary both during development and adulthood and has been widely studied in populations of cells that migrate independently. However, cells can also migrate in groups in a process known as collective cell migration. During collective cell migration, cells maintain cell-cell contacts, exhibit both morphological and behavioral polarization and interact with neighboring cells within the collective to affect each others behavior. This process is important

during the morphogenesis of multiple organ systems, as well as during wound healing in adults. In addition, invading cancer cells exhibit many hallmarks of collective cell migration.

Collectives can be organized in a variety of different forms, including loose chains or strands, tight clusters, tubes, or epithelial sheets (**Figure 1**). Neural crest cell migration is an example of chain migration (**Figure 1A**; Rupp and Kulesa, 2007). During migration, neural crest cells migrate out the neural tube in a chain like manner with the ultimate goal of reaching distant sites and differentiating into numerous cell types (Theveneau and Mayor, 2012). Throughout migration, neural crest cells maintain transient adherens junctions when briefly in contact with each other. Specifically, when two migrating neural crest cells touch, they induce contact inhibition of locomotion (Mayor and Carmona-Fontaine, 2010). This causes the two cells to retract cellular extensions at the site of contact and initiate new extensions on the opposing side of contact of the cell. This behavior restricts protrusions within the interior portion of the chain of migrating cells and promotes protrusive behavior along the edges of the chain, specifically the leading edge (Carmona-Fontaine et al., 2008). This behavior is thought to be important for directional migration and self-organization, and loss of this behavior has been shown in invasive cancer cells (Carmona-Fontaine et al., 2008; Astin et al., 2010).

Collectives can also migrate in a much more cohesive group, often referred to as cluster cell migration (**Figures 1B**, **2**). During migration of this type, cells maintain adherens junctions while migrating, thus remaining tightly connected. Examples of cluster cell migration include pLLP migration in zebrafish (**Figures 2**, **3**), border cell migration in *D.melanogaster* (**Figure 1B**), Kupffer vesicle organogenesis in zebrafish, and movement of invasive clusters of tumor cells (**Figure 6**). During border cell migration a group of cells delaminates from the follicular epithelium of the *D.melanogaster* egg chamber and migrates across the chamber toward the developing oocyte (Montell et al., 1992). During this migratory process, these cells maintain adherens junctions while migrating. Similarly, during Kupffer vesicle organogenesis, a group of around 20-30 cells cluster together and migrate cohesively. Finally, invasive groups of tumor cells often migrate as clusters during the invasion of many epithelial-based tumors (**Figure 6**; Freidl et al., 2004; Christiansen and Rajasekaran, 2006; Alexander et al., 2008). This type of collective invasion is discussed in more detail below.

Collective cell migration also contributes to the process of branching morphogenesis. This cellular behavior drives the formation of highly branched tubular structures including mammalian kidneys, lung, prostate and mammary gland as well as *D.melanogaster* trachea (**Figure 1C**; Sutherland et al., 1996; Ewald et al., 2008; Metzger et al., 2008). During branching morphogenesis, epithelial sheets reorganize into tube-like structures through multiple cellular behaviors, one of which is a specialized type of collective cell migration called invasive branching. During this process, extension of new branches is guided through invasive migratory behavior of a tip cell, which exhibits dynamic protrusive behavior. The cells that lag behind the tip cell are referred to as "stalk cells" and maintain cadherin-mediated adhesion to each other as well as to the tip cell.

In contrast to branching morphogenesis, epithelial sheet migration involves collective movement of a leading cell front, rather than individual cells (**Figure 1D**). Epithelial sheet migration mediates wound healing in the adult, dorsal closure in *D. melanogaster*, and migration of germ layers in some animals (Martin and Parkhurst, 2004; Solnica-Krezel, 2005). This type of collective cell migration is also observed *in vitro* after a scratch wound assay of endothelial and epithelial cells **Figure 1D**. In this assay, a scratch is made across a confluent sheet of cells and sheet migration is observed to "heal" or repair the "wound," as cells migrate as a cohesive front to fill in the space that was created by the scratch. On a cellular level, sheet migration is characterized as a monolayer of migrating cells that maintain strong adherens and tight junctions as well as apico-basal polarity while migrating (Bahri et al., 2010). These junctions restrict movement within the sheet and limit cellular rearrangement (Zallen and Blankenship, 2008). Cells at the leading or "free edge" take on leader cell positions and extend actin-based cellular protrusions (**Figure 1D**; Poujade et al., 2007; Vitorino and Meyer, 2008; Omelchenko et al., 2014). Follower cells also exhibit protrusive behavior through the extension of cryptic lamellipodia, as seen during wound closure in MDCK cells *in vitro* (**Figure 1D**; Fenteany et al., 2000; Farooqui and Fenteany, 2005). These cryptic lamellipodia form at the basal side of the follower cells and protrude under cells in front. These lamellipodia are necessary for generating traction against the basal lamina (Fenteany et al., 2000; Farooqui and Fenteany, 2005).

From these examples, it is clear that collective cell migration is employed during the morphogenesis of multiple organ systems. Despite this diversity, collectives often employ conserved cellular strategies during the migratory process. Our understanding of these mechanisms comes from studying various models including pLLP migration. Here, we will first review the cellular and molecular mechanisms that drive pLLP migration. Then we will briefly review a few other examples of collective cell migration and compare the pLLP to these other forms of collective cell migration. Finally, we will discuss how mechanisms of collective cell migration can be misappropriated during cancer cell invasion.

Zebrafish Posterior Lateral Line Primordium as a Model System to Understand Collective Cell Migration

Over the years a variety of model systems have been used to understand cellular and molecular mechanisms of collective cell migration. These range from the slime mold *Dictyostelium discoideum* to study movement of cell aggregates, to the mouse retina to investigate blood vessel branching. With zebrafish emerging as a genetic model system in the 1980s and 1990s, collective cell migration of the lateral line primordium during embryogenesis became one of the premier model systems to dissect collective cell migration. Lateral line research has a rich

Abbreviations: pLL, posterior Lateral Line; pLLP, posterior Lateral Line Primordium; NM, Neuromast.

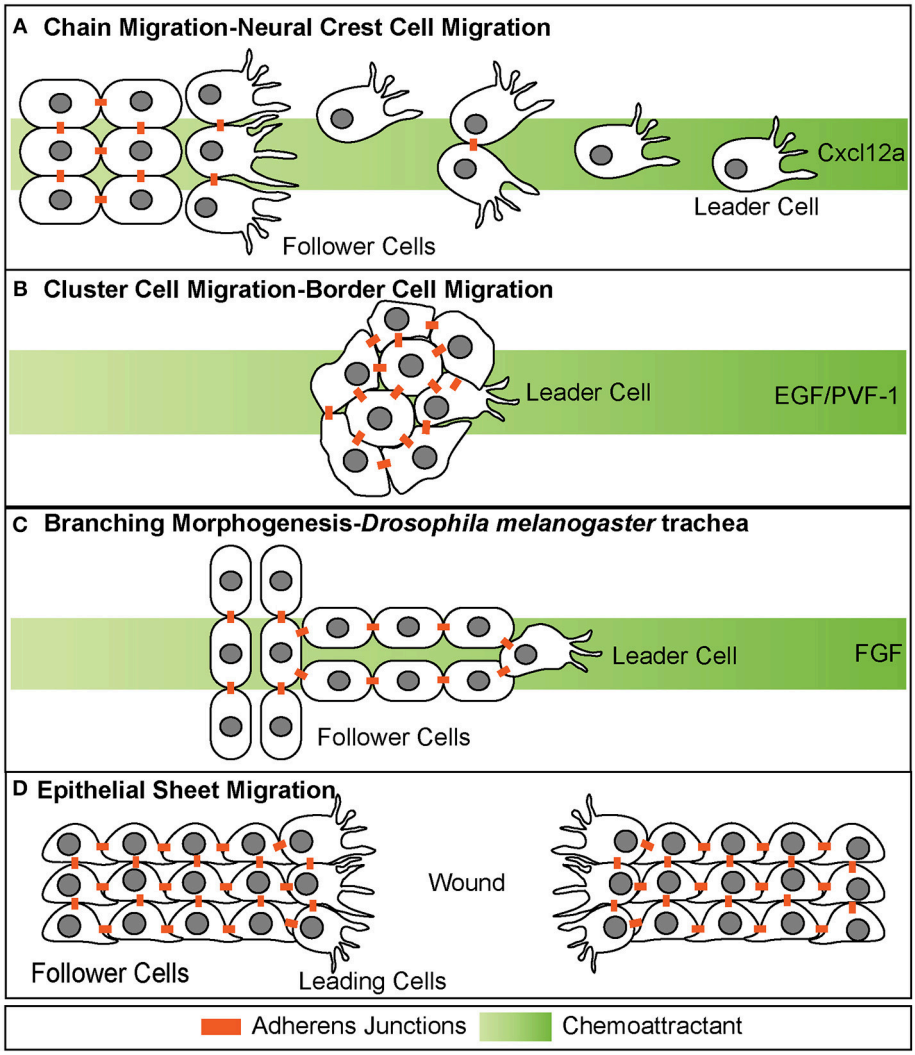

FIGURE 1 | Different modes of collective cell migration. **(A)** Chain migration of neural crest cells. Cells start as a cohesive cluster at the neural plate border and then delaminate away and migrate as chains toward the Cxcl12a source. Cells display transient adherens junctions. **(B)** Cluster cell migration of border cells in *Drosophila melanogaster.* Cells maintain tight adherens junctions while migrating with the leading cell in front exhibiting extensive protrusive behavior. These cells migrate toward the EGF/PVF-1 source. **(C)** Branching morphogenesis of *Drosophila melanogaster* trachea. While the leading cell migrates toward the source of Fgf, trailing cells form tube like structures. **(D)** Epithelial sheet migration-wound healing. Leading cells on either side of the wound migrate toward each other to close the wound. Leading cells extend filopodial protrusions toward each other. Follower cells extend cryptic lamellipodia underneath cells in front of them. Adherens junctions are maintained during migration.

history, as studies examining this system date back to the 1600s, when scholars first discovered that various fish species contain a row of small pores that stretch along the trunk of the fish from the head to the tail. At that time it was believed that this was a glandular system required for the secretion of mucous that covered the fish (Monro, 1785). However, in the 1800's that view was challenged when it discovered that this system is in fact a mechanosensory system, similar to the touch sensory system within the skin (Knox, 1825). Around 1850, Leydig discovered that within the row itself there were actually small sensory organs and in 1870, Schulze postulated that these sensory organs were actually similar to those within the inner ear and that movement of water stimulated their sensory capabilities (Leydig, 1850; Schulze, 1861, 1870). Up until this point however, the majority of research had focused on observing the system but not perturbing it. Fuchs (1894) was one of the first scholars to experimentally test the system and discovered that the lateral line in *Torpedo* only responded to changes in tactile stimulation but not in regards to changes in temperature or chemical stimulation (Fuchs, 1894). Finally, in 1904 Parker took a systematic approach to examine factors that stimulated lateral line sensory organs in eight different species of fish (Parker, 1904). He tested light, heat, salinity, food, oxygen, carbon dioxide, foulness of water, water current, water pressure, high frequency vibrations (hearing), and low frequency vibrations. Interestingly, he found that only vibrations of low frequency were sensed by the lateral line. He

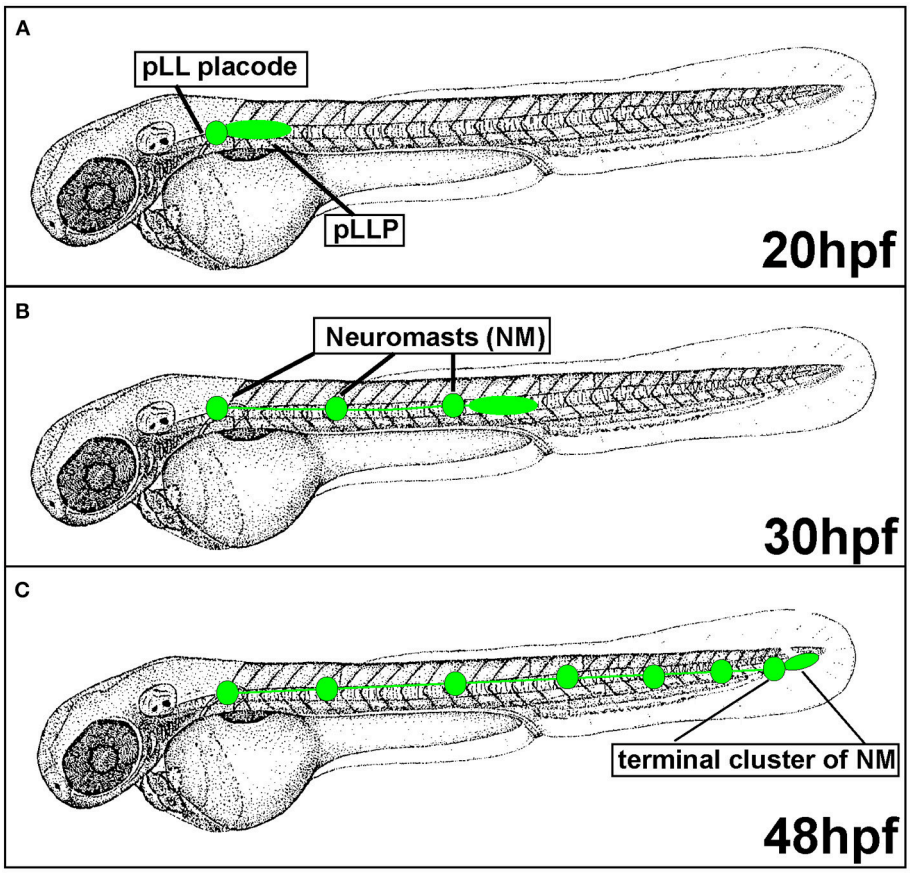

FIGURE 2 | Posterior Lateral Line formation (pLL) and posterior Lateral Line Primordium (pLLP) migration. **(A)** pLLP begins migrating around 20 hours post-fertilization (hpf). **(B)** At 30 hpf the pLLP has migrated about half way down the trunk and deposited 3 neuromasts (NMs). **(C)** pLLP migration is complete at 48 hpf with the deposition of the terminal cluster of NMs.

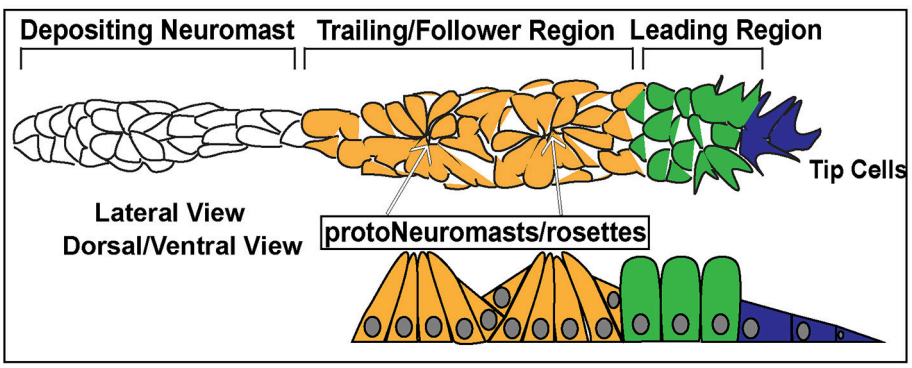

FIGURE 3 | Schematic of the posterior Lateral Line Primordium (pLLP). In blue are the 2–3 leader cells. In green is the leading region. In orange is the trailing region. In white is a depositing neuromast. The top schematic is a lateral view of pLLP cells. The bottom schematic is a dorsal/ventral view. Arrows point to proto-neuromasts/rosettes.

concluded that the lateral line system was a mix of the touch (skin) sensory system and the hearing (ear) sensory system. Further studies confirmed these findings and expanded on them culminating in the conclusion that the lateral line in aquatic vertebrates is a mechanosensory system that detects changes in water current and is necessary for behaviors such as feeding and swimming (Montgomery et al., 2000).

Harrison (1904) was the first to determine that this mechanosensory system develops through the migration of a group of cells that deposits smaller clusters of cells while

migrating (Harrison, 1904). Specifically, Harrison used chimeric frog embryos to study posterior lateral line (pLL) development. In this study Harrison fused the head of a black tadpole to the tail of brown tadpole and observed pLL development. Surprisingly, he witnessed a dark streak (black cells) appear on the brown tadpoles tail and this streak separated into pigmented dots. From this he concluded that the lateral line develops by the concerted migration of a group of cells down the trunk of fish and amphibians. Further research in the 1920s and 1930s identified the origin of this group of cells. Stone (1933) discovered that this group of cells originates from the post auditory placode (Stone, 1933). Specifically, Stone stained salamander embryos with Nile blue sulfate and then grafted the post auditory placode from these stained donor embryos to unstained host embryos. Following transplantation he observed a group of blue stained cells migrating along the trunk of the embryo that deposited small clusters of blue stained cells (presumptive mechanosensory organs—neuromasts). These clusters then differentiated into the sensory organs that form the lateral line. These experiments identified the post auditory placode as the group of cells giving rise to the pLL. As evident from these classical experiments, the close proximity to the surface of the skin makes this an easily tractable system to study mechanisms of mechanosensation and collective cell migration.

Posterior Lateral Line Development and Posterior Lateral Line Primordium Migration

Since the pLLP discovery in the early twentieth century, the migratory behavior of this system has been actively investigated in various aquatic species including zebrafish. In zebrafish, the posterior Lateral Line Primordium (pLLP) is a group of around 100 cells that migrates along the lateral aspect of the trunk of the embryo during embryogenesis (**Figure 2**). The pLLP and sensory neurons of the pLL ganglion are both derived from the pLL placode, a transient thickening of the embryonic ectoderm positioned caudally to the developing otic vesicle (**Figure 2**; Mizoguchi et al., 2011). Surprisingly, little is known about molecular pathways that regulate pLL placode induction and differentiation and this topic has been discussed elsewhere (Sarrazin et al., 2010; McCarroll et al., 2012; Piotrowski and Baker, 2014; Nikaido et al., 2017). At about 22 hours post fertilization (hpf), the distal portion of the pLL placode begins migrating along the lateral aspect of the trunk, whereas the proximal portion, comprised of sensory neurons, stays behind (**Figure 2A**). The pLLP continues migrating along the trunk of the zebrafish until it reaches the tip of the tail at 48 hpf (**Figure 2C**). As the pLLP migrates, it deposits clusters of about 20–30 cells from its trailing (caudal) end; these clusters will differentiate into mechanosensory neuromasts (NMs) (**Figures 2**, **3**). The pLLP also lays down a single line of inter-neuromast cells (**Figure 2**; Metcalfe et al., 1985), which are latent precursors that will differentiate into additional NMs during larval development. Migration of the pLLP is complete with the deposition of the terminal cluster, a group of two to three NMs that are located at the distal region of the trunk (**Figure 2C**). Rapid embryonic development, optical translucence, and genetic tractability make the zebrafish a particularly suitable model system to define cellular and molecular mechanisms of collective cell migration.

How Is the Posterior Lateral Line Primordium Organized?

Cells within the pLLP display differential morphology and different states of differentiation depending on their location and can be generally designated as leader or follower cells. The leading third of the pLLP is comprised of 2–3 tip cells of mesenchymal character and less differentiated epithelial cells (**Figure 3**, Blue, Green). Follower cells within the trailing two-thirds of the pLLP (**Figure 3**, Yellow) form polarized rosettes. Tip cells exhibit flat mesenchymal morphology (**Figure 3**), display active protrusive behavior in their leading edge, and respond to guidance cues that steer the collective. Cells proximal to tip cells in the leading region, exhibit columnar epithelial morphology (**Figure 3**). Cells within the trailing region (last 2/3 of the pLLP) apically constrict to form epithelial rosette structures of the proto-NM (**Figure 3**; Lecaudey et al., 2008). The remaining cells in the trailing region contribute to the inter-neuromast cells and are deposited between the NMs. These cells are positioned on the periphery of the pLLP, surrounding the cells that have formed rosettes (Dalle Nogare et al., 2017).

In addition to differences in morphology, leader and follower cells within the pLLP show differences in their fate. As the pLLP migrates it deposits proto-NMs every 5–7 somites. At the onset of migration the pLLP contains 2 to 3 proto-NMs; however, by the end of migration the pLL consists of 5–6 NMs and the terminal cluster of NMs (**Figure 2**). Thus, new proto-NMs must be generated during pLLP migration. These new proto-NMs are generated by cell proliferation throughout the pLLP (Dalle Nogare et al., 2017). Newly generated cells within the leading region of the pLLP differentiate last and ultimately contribute to the terminal cluster of NMs, while those in the trailing region begin differentiating into cells that will contribute to more proximal NMs and inter-neuromast cells (Dalle Nogare et al., 2017). As a new proto-NM begins differentiating, cells undergo apical constriction to form a rosette-like structure that constitutes the proto-NM (**Figure 3**).

Chemokine Signaling During Posterior Lateral Line Primordium Migration

Similarly to neural crest cell migration, the pLLP uses Cxcl12a as a chemotactic cue. The pLLP migrates along the myoseptum of the zebrafish embryo where *cxcl12a* is uniformly expressed (**Figure 4B**; David et al., 2002; Li et al., 2004; Haas and Gilmour, 2006; Dambly-Chaudiere et al., 2007; Valentin et al., 2007). Loss of Cxcl12a leads to a failure of migration (David et al., 2002; Valentin et al., 2007), whereas ectopic expression of *cxcl12a* results in a redirection of pLLP toward the "new" Cxcl12a source (Li et al., 2004).

While pLLP can migrate toward an ectopic source of the ligand, two recent studies demonstrated that the Cxcl12a does not present as a gradient along the trunk (Donà et al., 2013; Venkiteswaran et al., 2013). Instead, the pLLP produces an

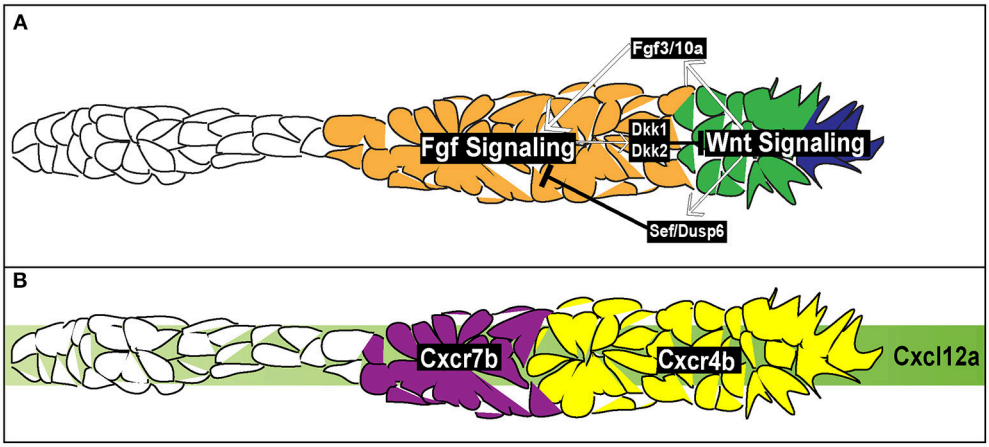

FIGURE 4 | Signaling and chemotactic pathways active during pLLP migration. **(A)** Signaling pathways active during pLLP migration. Wnt signaling is active in the leading region (blue and green cells). Wnt signaling initiates expression of Fgf3/10a in the leading cells. Fgf 3/10a activate Fgf signaling in the trailing region (orange). Wnt signaling initiates expression of *sef*, an inhibitor of Fgf signaling. Fgf signaling initiates expression of *dkk1* and *dkk2*, inhibitors of Wnt signaling. Thus the two signaling regions are maintained through mutual inhibition. **(B)** Chemokine signaling during pLLP migration. Green strip indicates the internal Cxlc12a generated within the pLLP. *cxcr4b* chemokine receptor (yellow) is expressed in the leading 2/3 of the pLLP. *cxcr7b* is expressed in the trailing 1/3 of the pLLP (purple).

internal gradient of Cxcl12a through differential expression of two chemokine receptors, *cxcr4b* and *cxcr7b*. *cxcr4b* is expressed within the leading region whereas *cxcr7b* is expressed within the trailing region (**Figure 4B**; Haas and Gilmour, 2006; Dambly-Chaudiere et al., 2007; Valentin et al., 2007). Loss of either Cxcr4b or Cxcr7b leads to a failure in migration (Haas and Gilmour, 2006; Valentin et al., 2007) indicating the necessity of both receptors to ensure proper pLLP migration. Additionally, wild-type cells transplanted to the leading region of *cxcr4b* mutant pLLP can rescue migratory defects in these mutants (Haas and Gilmour, 2006). This is also true for wild-type cells transplanted to the trailing region of *cxcr7b* mutants (Valentin et al., 2007). However, when wild-type cells are transplanted to the leading region in *cxcr4b* mutants, impaired migration is not rescued. Finally, when *cxcr7b* mutant cells are transplanted into the leading region of *cxcr4b* mutants, migration is rescued (Valentin et al., 2007). Altogether, these transplantation experiments underscore the necessity for region-specific distribution of Cxcr4b and Cxcr7b during pLLP migration. Two recent studies used live imaging to visualize chemokine-receptor internalization to demonstrate that Cxcl12a binds to Cxcr7b and then is internalized with the Cxcr7b receptor (Donà et al., 2013; Venkiteswaran et al., 2013). In doing so, this creates an internal gradient of Cxcl12a, with low levels of Cxcl12a in the trailing region and high levels of Cxcl12a in the leading region. Previous reports support this model as Cxcr7b acts as a ligand sink in other contexts (Dambly-Chaudiere et al., 2007; Boldajipour et al., 2008; Naumann et al., 2010; Mahabaleshwar et al., 2012).

At this point, it is unclear how this region specific expression of *cxcr4b* and *cxcr7b* in the leading and trailing region arises. Aman and Piotrowski (2008) argued that *cxcr7b* expression is downstream of two signaling pathways active within the pLLP, Wnt (leading region) and Fgf (trailing region) signaling (**Figure 4A**). When Wnt was constitutively active or Fgf was inhibited there was a reduction in *cxcr7b* expression. Additionally, while inhibition of Wnt signaling had no effect of *cxcr4b* expression it did lead to an expansion of *cxcr7b* expression into the leading region. However, a separate study did not report any effect on *cxcr4b* or *cxcr7b* expression in the absence of Wnt signaling (Valdivia et al., 2011). It should be also noted that expression of chemokine receptors does not mirror Wnt and Fgf signaling domains, suggesting that these receptors are not directly regulated by these signaling pathways (**Figure 4**). Further experiments are needed to determine how chemokine receptor expression is regulated during pLLP migration.

Signaling Pathways Within the Posterior Lateral Line Primordium

Within the pLLP there are a number of signaling pathways that regulate patterning, maintain migratory behavior, and initiate proto-NM differentiation. Among the main pathways are the canonical Wnt signaling pathway (**Figure 4**; Aman and Piotrowski, 2008), active in the leading region of the pLLP, the Fgf pathway (**Figure 4**; Lecaudey et al., 2008; Nechiporuk and Raible, 2008), active in the trailing region of the pLLP, and the Notch-Delta pathway active in the forming proto-NM in the trailing region (**Figure 5**; Matsuda and Chitnis, 2010). Canonical Wnt signaling maintains proliferation, patterning, and migration of the pLLP. Additionally, canonical Wnt signaling is necessary for initiating expression of *fgf3* and *10a* ligands in the leading cells (Aman and Piotrowski, 2008; Matsuda et al., 2013). These ligands activate Fgf signaling in the trailing region and initiate proto-NM differentiation. Wnt signaling also initiates the expression of *dusp6* and *sef*, which are inhibitors of Fgf signaling, allowing for restriction of the Wnt signaling domain to the leading region (Aman and Piotrowski, 2008). Furthermore, Fgf signaling also induces expression of *dkk1* and *dkk2* (**Figure 3**; Aman and Piotrowski, 2008; McGraw et al.,

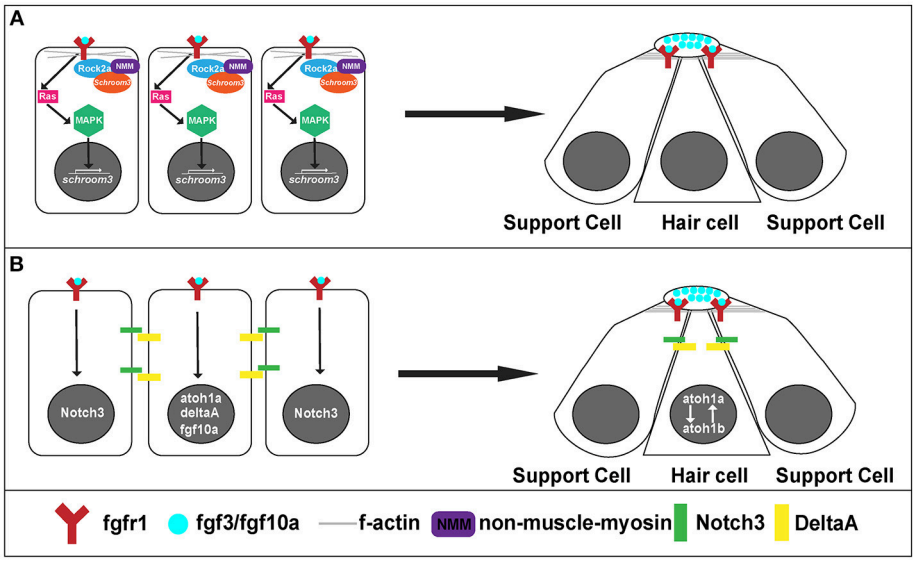

FIGURE 5 | Signaling pathways for rosette formation and proto-NM maturation. **(A)** Hypothesized signaling that initiates apical constriction. Fgf signaling activates Ras and MAPK. This initiates transcription of *schroom3*. Schroom3 interacts with Rock 2a (Rho Kinase) and activates non-muscle myosin at the membrane, which initiates apical constriction of cells through reorganization of the actin cytoskeleton. **(B)** proto-NM maturation signaling. Fgf luminal signaling initiates *atoh1a* and *notch3* expression. Atoh1a induces expression of *deltaA* and *fgf10a*. DeltaA interaction with Notch3 initiates lateral inhibition allowing for *atoh1a* expression to be localized to the central cell (hair cell precursor) and surrounding cells to remain as supporting cells.

2014), both of which are inhibitors of Wnt signaling to restrict Fgf signaling to the trailing region. Thus, both Wnt and Fgf mutually inhibit each other to generate region specific signaling domains (**Figure 4A**).

Canonical Wnt Signaling Is Necessary for Posterior Lateral Line Primordium Migration and Proto-NM Formation

As mentioned above, canonical Wnt signaling is active in the leading third of the pLLP and is necessary for pLLP migration and patterning. Global inactivation of Wnt signaling during pLLP migration causes a loss of proliferation, cell death, and a loss of patterning within the pLLP (Aman and Piotrowski, 2008; McGraw et al., 2011). Additionally, overexpression of Wnt signaling leads to overproliferation and premature termination of the pLLP (Aman and Piotrowski, 2008). Interestingly, exclusive loss of Lef1, a downstream effector of canonical Wnt signaling, causes defects in migration and cellular behavior within the leading region with no effects on cell death or proliferation (McGraw et al., 2011). Specifically, cells in the leading region of the pLLP are prematurely incorporated into NMs and deposited early. This gradual depletion of cells in the leading region ultimately results in a dispersal of the pLLP and an absence of the terminal cluster of NMs (McGraw et al., 2011; Valdivia et al., 2011). In summary, results from many studies highlight the significance of canonical Wnt signaling in regulating multiple cellular behaviors within the pLLP; however, how these behaviors are executed downstream of Wnt is not well understood.

Fgf Signaling Is Necessary for Neuromast Formation and Differentiation

The Fgf signaling pathway functions downstream of Wnt and is necessary for proto-NM formation (**Figure 4A**; Lecaudey et al., 2008; Nechiporuk and Raible, 2008; Chitnis et al., 2012). Blocking or reducing Fgf activity inhibits the formation of rosettes and ultimately halts pLLP migration (Lecaudey et al., 2008; Nechiporuk and Raible, 2008; Chitnis et al., 2012;), whereas ectopic expression of Fgf leads to the formation of additional rosettes (Lecaudey et al., 2008).

On a cellular level, Fgf signaling promotes the shape change of epithelial cells from a columnar to an apically constricted morphology during the formation of rosettes or proto-NMs (**Figures 3**, **4A**; Lecaudey et al., 2008; Nechiporuk and Raible, 2008; Chitnis et al., 2012). Two studies published in the same year presented complimentary findings related to the intracellular pathway that drives apical constriction of pLLP cells. In the first study, researchers found that Fgf signaling activates Ras-MAPK signaling which induces Rock2a localization to the apical portion of cells where it activates myosin regulatory light chain and induces apical constriction (**Figure 5A**; Harding and Nechiporuk, 2012). The second study demonstrated that Fgf signaling transcriptionally regulates Schroom3, a scaffold protein that binds to Rock and has been shown to activate apical constriction in other contexts (**Figure 5A**; Ernst et al., 2012).

Neuromast Maturation

Neuromasts are the sensory organs that comprise the pLL. These sensory organs are composed of hair cells and supporting cells. Hair cells lie within the middle of the neuromast with

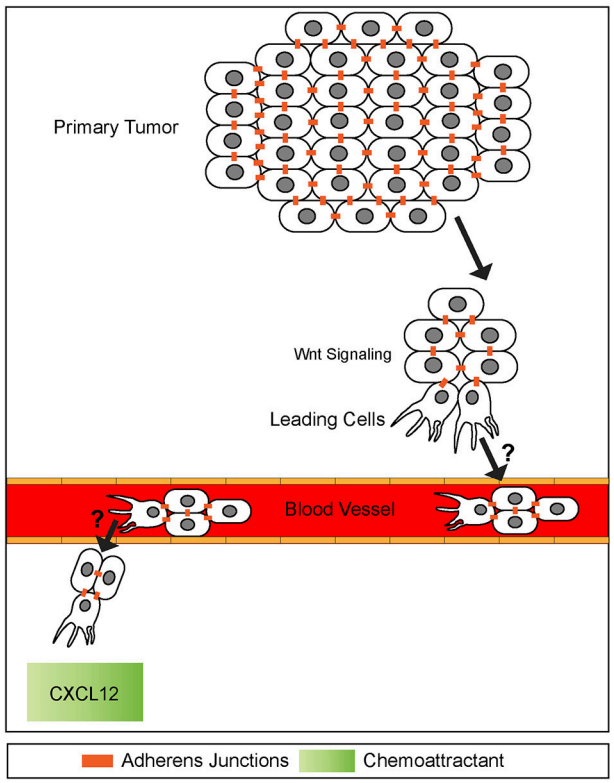

FIGURE 6 | A potential model of collective cell invasion. Small groups of cells high in canonical Wnt signaling break off from the primary tumor, invade surrounding tissue, and enter the blood stream. This cluster then extravisates from the blood stream homing onto to a chemokine source, such as CXCL12. The mechanisms of blood vessel intravisation and extravasation by cell clusters are not known (question marks). It has been speculated that behaviors of such clusters exhibit many similarities to leading front cells present in collective cell migration during embryogenesis. Adherens junctions are maintained throughout invasion process.

support cells surrounding the hair cells. When hair cell bundles are deflected by changes in water current, this information is mechanotransduced through the hair cell and then transmitted back to the brain where it is further processed.

Differentiation into hair and supporting cell precursors occurs during pLLP migration and is driven by Fgf signaling. In addition to its role in apical constriction, Fgf signaling also initiates expression of *atoh1a* (**Figure 5B**), a transcription factor that is a master regulator of hair cell fate and thus its activation initiates a hair cell program in a small subset (1 to 2 cells) of cells within a forming proto-NM (Sarrazin et al., 2006; Nechiporuk and Raible, 2008). *atoh1a* expression and action is limited to a single focus through Notch-Delta lateral inhibition. *atoh1a* expression induces expression of *deltaA,* whereas expression of its receptor *notch3* is induced by Fgf signaling within the forming proto-NM. Therefore, the DeltaA ligand (driven through the Atoh1a transcriptional program) interacts with the Notch3 receptor (driven by Fgf signaling) on neighboring cells within the proto-NM and inhibits expression of *atoh1a,* in neighboring cells therefore specifying them as supporting cells (**Figure 5B**; Itoh and Chitnis, 2001; Matsuda and Chitnis, 2010). If Notch3 is blocked, proto-NMs generate more hair cells at the expense of supporting cells (Matsuda and Chitnis, 2010). Through this mechanism, *atoh1a* expression is restricted to the central cell, inducing hair cell progenitor fate in that cell.

Atoh1a also induces expression of both the *fgf10a* ligand and *atoh1b* (Millimaki et al., 2007; Matsuda and Chitnis, 2010) within the same hair cell precursor. Expression of *fgf10a* from the central hair cell progenitor initiates a new Fgf signaling center within the trailing region that promotes maturation of proto-NMs (**Figure 5B**; Matsuda and Chitnis, 2010). Atoh1b maintains *atoh1a* expression within the central proto-NM and inhibition of Atoh1b results in a reduction in *atoh1a* expression (Millimaki et al., 2007; Matsuda and Chitnis, 2010). Notably, Fgf ligands accumulate in a microlumen at the apical center of the rosette (Durdu et al., 2014). Inhibiting the formation of the microlumen by knockout of Schroom3 results in a reduction of Fgf response in cells that comprise rosettes. This suggests that the microlumen acts to coordinate Fgf signaling among cells of the rosette during migration. In summary, Fgf signaling plays a key role in both the establishment of hair cell precursors as well as maturation of proto-NMs.

Cell-Cell Adhesion and Cytoskeletal Regulation During Posterior Lateral Line Primordium Migration

During pLLP migration cells remain in a close contact as they cohesively migrate along the trunk of the zebrafish. Cells within the cluster are connected by cadherin mediated adherens junctions. Specifically, E-cadherin and N-cadherin are both expressed in the pLLP but show specific localization within the proto-NM. In the proto-NM, N-cadherin is expressed in both the hair cell progenitor cell (central cell of the proto-NM) and supporting cells, whereas E-cadherin is only expressed in the hair cell progenitor cell (Matsuda and Chitnis, 2010). However, Revenu et al., reported in 2014 that E-cadherin and N-cadherin are expressed in all cells within the pLLP as evidenced by antibody staining against both cadherins (Revenu et al., 2014). Revenu et al. also examined the maturation of adherens junctions using a BAC fluorescent reporter of N-cadherin as N-cadherin shows enhanced localization at apical junctions. Specifically, they reported a role for N-cadherin in initiating the change in morphology from mesenchymal in the leading cells to columnar epithelial in more trailing cells. The authors showed that N-cadherin clusters first and then epithelial columnar reorganization follows. Finally, using tandem fluorescent protein timers, a readout of protein turnover, the authors determined that the N-cadherin localized at apical junctions is more stable than N-cadherin localized at the basolateral membrane. Moreover, the apical junctions become progressively more stable from the leading to the trailing region.

Adherens junctions between cells often trigger activation of intracellular signaling pathways via various binding partners such as catenins. Recently, one of the catenins expressed in the pLLP, Catenin Delta 1, was shown to regulate Rac1 signaling in cultured

cells (Mizoguchi et al., 2017). Specifically, mutation of Mib1, an E3 ubiquitin ligase, caused an accumulation of Catenin Delta 1 and hyperactivation of Rac1, which in turn induced ectopic, random non-persistent protrusions and ultimately impaired migration of cultured cells (Mizoguchi et al., 2017). The authors showed that Mib1 is required for pLLP migration and normal protrusive behaviors of pLLP cells. However, it is not clear if Mib1 also regulates Rac1 activity in the pLLP, similar to the *in vitro* model. In fact, not much is known about how Rac1 and other modulators of protrusive activity are regulated during pLLP migration.

Below we will compare mechanisms active during pLLP migration to other examples of collective cell migration and then focus on how collectively invading cancer cells subvert these mechanisms to invade surrounding tissues.

Distribution of Leaders and Followers Within Collectives

Similar to the pLLP, most collectives show division into two different populations of cells, leaders and followers (**Figure 1**). Leaders are the cells that detect and sense chemotactic cues, exhibit active protrusive behavior, and produce molecular or mechanical cues to guide the trailing population to the proper destination. While leader cells exhibit common behaviors, follower cells have diverse functions and fates depending on the context. For example, follower cells contribute to trachea bronchi or blood vessels during branching morphogenesis whereas during pLLP migration follower cells ultimately contribute the sensory organs of the lateral line system. Leaders and followers show differences in morphology with leaders displaying mesenchymal morphology and in some contexts follower cells displaying polarization. Interestingly, the assignment as leader or follower is not always permanent during this migratory process. In border cell migration for example, the leader cell rotates as the cell with the highest levels of RTK/MAPK signaling acquires the leader cell position (Bianco et al., 2007). Another example in which leader cell identity is not maintained throughout migration is during neural crest cell migration (Kuriyama et al., 2014). Whereas it is not exactly clear what determines neural crest cell leader position, leader cells maintain higher levels of RAC1 activity and exhibit greater protrusive behavior than follower cells (Theveneau et al., 2010). Further, during branching morphogenesis of the trachea in *D. melanogaster,* cells that receive the highest level of the breathless (Fgf) signal take on the role of the leader cell (Caussinus et al., 2008; Lebreton and Casanova, 2014).

Although in many examples of collective cell migration, it is not uncommon for cells to switch positions during migration, this is not observed in wild-type pLLPs. In some instances cells within the pLLP can be forced to move into new positions as a result of experimental manipulation. Haas and Gilmour (2006) found that when wild-type cells were transplanted into *cxcr4b* mutant embryos, they often ended up at the leading edge of the pLLP. Live imaging of chimeric pLLP revealed that this resulted from the tumbling behavior exhibited by wild-type cells in *cxcr4b* mutant pLLPs. They suggested that the tumbling behavior exposes wild-type cells to the Cxcl12a signal and "captures" these cells at the leading edge of the pLLP. Once wild-type cells are captured in the leading region, the pLLP commences normal migration and proper deposition of NMs. A similar tumbling behavior was observed in chimeric primordia that contained *lef1* mutant cells (McGraw et al., 2011). When *lef1* mutant cells were too close to the leading edge (a couple of cell diameters), the chimeric pLLP stopped and tumbled until mutant cells were "pushed back" and excluded from this leading region (McGraw et al., 2011). Once this occurred, the pLLP resumed its migration. The reason for this tumbling behavior is not clear and it is unlikely that this results from *lef1* mutant cells being unable to sense the chemokine, as *lef1* mutants still express normal levels of the *cxcr4b* receptor. Although collectives determine leading and following positions differently, the division of collectives into these two populations allows for cohesive migration of these cohorts of cells.

Chemotactic Cues Guide Collectives During Migration

In order for collectives to migrate in a directional manner they must respond to specific chemotactic cues. Usually, these cues appear as a gradient, with the collective migrating to the highest levels of chemokine or secreted ligand. Leading cells sense these cues and in turn change their behavior, morphology, and protrusive behavior to respond to the cue appropriately (Sutherland et al., 1996; Haas and Gilmour, 2006; Prasad and Montell, 2007). This is often achieved by regulating proteins that remodel the cytoskeleton. For example, RAC1 activation in leader cells in response to guidance cues has been observed in numerous examples of collective cell migration including border cell migration, *D.melanogaster* trachea formation, and neural crest cell migration (Murphy and Montell, 1996; Chihara et al., 2003; Theveneau et al., 2010; Scarpa et al., 2015).

Despite differences in organization of collectives and environmental contexts through which they migrate, some collectives utilize common guidance cues during migration. For example both neural crest cells in *Xenopus* and the cells within pLLP respond to Cxcl12a during migration (**Figures 1A**, **4B**; David et al., 2002; Li et al., 2004; Theveneau et al., 2010). Overexpression of Cxcl12a during neural crest cell migration leads to aberrant migration whereas loss of Cxcl12a during pLLP migration results in inhibition of migration (Valentin et al., 2007; Olesnicky Killian et al., 2009). Additionally, in both of these examples Cxcl12a is uniformly expressed and self-generated gradients are produced by the collectives. During neural crest cell migration, neural crest cells migrate toward the epibranchial placodes, the source of the Cxcl12a (Theveneau and Mayor, 2013). Neural crest cells use contact inhibition of locomotion to facilitate proper migratory behavior. Specifically, neural crest cells extend protrusions that interact with the placodes during the onsent of migration. This induces a repulsive response by placodal cells in which focal adhesions are dissassembled and placodal cells migrate away. Neural crest cells then migrate toward the placodal cells again and migration occurs in a "chase and run" manner (Theveneau et al., 2013).

In the case of pLLP migration, Cxcl12a is expressed uniformly throughout the myoseptum of the zebrafish (**Figure 4B**; David et al., 2002; Li et al., 2004). In this case, domain specific expression of Cxcl12a receptors, *cxcr4b* and *cxcr7b*, produces a local gradient within the pLLP. *cxcr4b* is expressed in the leading region, whereas *cxcr7b* is expressed in the trailing region. Cxcr4b acts as the chemoreceptor initiating a G-protein signaling cascade within the leading cells whereas expression of *cxcr7b* in the trailing region acts as a ligand sink creating a gradient within the pLLP itself (Haas and Gilmour, 2006; Dambly-Chaudiere et al., 2007; Valentin et al., 2007). These differences in the ligand binding and ligand-receptor turnover lead to a gradient of Cxcl12a response within the pLLP.

Other examples of different guidance cues used during the migration of collectives include EGF and PVF-1, two molecules within the developing *D. melanogaster* oocyte that are necessary for proper border cell migration (**Figure 1C**). Mutation of either EGFR or PVR results in uncontrolled protrusive behavior and defects in migration (Prasad and Montell, 2007). Finally, Fibroblast Growth Factor (FGF) is used as a chemotactic cue during branching morphogenesis in the trachea, mammary gland, and lung (**Figure 1D**; Sutherland et al., 1996; Ewald et al., 2008; Metzger et al., 2008) as well as in other examples of collective cell migration such as nephric duct migration, wound healing, and endothelial cell migration (Werner et al., 1992; Vitorino and Meyer, 2008; Attia et al., 2015). In summary, collectives recognize a variety of guidance cues and employ diverse strategies as to interpret these cues and maintain their migratory behaviors.

Cell-Cell Junctions and Cell-ECM Interactions During Collective Cell Migration

In order for cells to migrate cohesively as a group during collective cell migration, cells must communicate often through stable or transient cell-cell junctions. These junctions usually consist of cadherins, desmosomes, and tight junction proteins; loss of these structures often leads to improper or failed migration. Cadherin junctions are the most prevalent junctions observed during collective cell migration. For example, cell-cell junctions between migrating border cells and nurse cells are mediated by the transient presence of E-cadherin and loss of E-cadherin results in decreased protrusion formation at the front of the cluster and ultimately impaired migration (Niewiadomska et al., 1999; Geisbrecht and Montell, 2002; Cai et al., 2014). Additionally, during neural crest cell migration in *Xenopus*, Cadherin-11 is necessary for contact inhibition of locomotion, which allows for processive and directed migration of neural crest cells as described above (Becker et al., 2014). Loss of Cadherin-11 results in non-directional migration and impaired adhesive ability (Becker et al., 2014). In addition to cadherin-based cell-cell junctions, desmosomes and tight junctions are also observed during collective cell migration. In wound healing, both desomosomal-junctions and tight junctions are necessary for proper healing (Danjo and Gipson, 1998; Shaw and Martin, 2009). Knockdown of either desomosomal or tight junction proteins leads to decreases in cell migration velocity and ultimately impairment of migration to close the wound (Bazellières et al., 2015). Desomosomal and tight junctions are also observed during mammary gland morphogenesis. Interestingly, these two junctional complexes show differences in cellular localization within the developing mammary gland (Shamir and Ewald, 2015). Tight junctions are only seen at the apical portion of cells that face lumens, whereas desomosomal junctions connect interior portions of cells in the mammary duct (Shamir and Ewald, 2015).

During migration, cells need to generate force to processively migrate toward their destination. To achieve this, cells adhere to the extracellular matrix as well as use supracellular organization to generate force between the leaders and the followers. To connect with the extracellular matrix cells utilize integrins, which link the intracellular cytoskeleton to the extracellular matrix. This allows transduction of mechanical signals as well as force generation through the recruitment of cytoskeletal adaptor proteins, which couple the integrins and their extracellular binding partners (Nobes and Hall, 1999; Zaidel-Bar et al., 2007). During wound healing, integrin-mediated signaling induces cytoskeletal rearrangements that initiate leader cell properties at the wound edge (Etienne-Manneville and Hall, 2001). These leader cells use the integrins α2β1, α5β1, and αvβ3 to generate force on a collagen substrate and initiate movement to close in the wound (Grose et al., 2002). Similarly, β1 integrins are used during angiogenesis to couple the extracellular matrix to the cytoskeleton within the endothelial collective. β1 integrins activate guanine nucleotide exchange factors (GEFs) for Cdc42 and Rac1 as well as kinases such as Src and FAK (Lamalice et al., 2007; Osmani et al., 2010) to promote protrusive behavior at the leading edge of tip cells, which is necessary for appropriate migratory behavior (Scales and Parsons, 2011; Lawson and Burridge, 2014).

In addition to integrin-mediated force generation, collectives also maintain collective movement and force generation through supracellular cytoskeletal organization. Specifically, focal adhesions at the leading front edge associate with actin-myosin cables, which initiate contraction and force generation. These actin-myosin cables ultimately extend through multiple layers of follower cells allowing for force generation throughout the entire collective instead of the first row of cells (Li et al., 2012; Reffay et al., 2014). However, during collective cell migration the largest forces are generated at the leading edge of collectives with a decrease in force strength in back of the collective (du Roure et al., 2005; Trepat et al., 2009; Tambe et al., 2011; Anon et al., 2012; Cai et al., 2014). For example, during border cell migration, tension decreases at the back of the cluster (Cai et al., 2014). A similar distribution of force is observed in wound healing, where the greatest traction forces are exhibited at the leading edge of the monolayer but forces are maintained among follower cells in the collective (du Roure et al., 2005; Trepat et al., 2009; Tambe et al., 2011; Anon et al., 2012).

In addition to adhering to the extracellular matrix for force generation, cells in collectives also remodel the extracellular matrix while migrating. Migrating and/or surrounding cells

deposit new basement membrane to form migrating tracks. The deposition of a new basement membrane forms a smooth surface to promote migration. During neural crest cell migration in both *Xenopus* and chick embryos, neighboring cells deposit fibronectin along neural crest migrating streams to facilitate migration (Alfandari et al., 2003). Similarly, astrocytes underlying the migrating endothelial cells secrete fibronectin during angiogenesis (Stenzel et al., 2011). Fibronectin then induces tip cell filopodia promoting migratory behavior (Stenzel et al., 2011). When fibronectin is specifically deleted from the astrocytes, endothelial cells show defects in migration (Stenzel et al., 2011). In addition, the basement membrane that is produced by endothelial cells and pericytes during angiogenesis helps stabilize the migrating blood vessels (Eming et al., 2007). The deposition of new basement membrane allows for migrating collectives to migrate through the path of least resistance.

How Does Collective Cell Migration Influence Our Understanding of Invasive Cancer?

The dogma surrounding cancer cell invasion for many years was that single cells would detach from cancerous tumors, enter the blood stream and metastasize in other tissues. However, in the last 50 years that viewpoint has been gradually expanded and it is now widely recognized that in many cases clusters of cells can also detach from the primary tumor to initiate metastasis (**Figure 6**).

It was first reported more than half a century ago that cancer cell metastasis could be associated with both single and clusters of tumor cells (presumably detached from the primary tumor) found in blood samples of patients (**Figure 6**) (Zeidman and Buss, 1952). Subsequent research indicated tumor cell clusters were better at initiating metastasis than single cells when intravenously injected into mice (Liotta et al., 1976). Further studies confirmed this observation and revealed that tumor cell clusters are actually 20–30-fold better at initiating metastasis *in vitro* (Cheung et al., 2016) and *in vivo* (Hou et al., 2012; Maddipati and Stanger, 2015; Cheung et al., 2016).

Research over the last two decades strongly suggests that collective cell invasion mediates metastasis in numerous epithelial cancers including prostate, pancreatic, lung, colorectal and breast cancer (Friedl et al., 1995; Nabeshima et al., 2000; Hegerfeldt et al., 2002; Aceto et al., 2014; Gundem et al., 2015; Maddipati and Stanger, 2015; Cheung et al., 2016). However, only recently studies provided most rigorous evidence for collective cell invasion mechanisms in both humans and mouse models. Recent advances in microfluidics and next generation nucleic acid sequencing allowed for isolation and interrogation of a small number of circulating tumor microclusters. In humans, RNA sequencing of circulating cancer cell clusters in comparison to circulating single cancer cells (Aceto et al., 2014) revealed a small subset of differentially expressed genes. One of the transcripts enriched in microclusters was Plakoglobin, a component of desmosomes and adherens junctions. This study revealed that Plakoglobin plays a role in maintaining adherens junctions in cancer cell clusters and thus enhances their metastatic potential. Interestingly, Plakoglobin has been shown to be important in focal adhesions during collective cell migration of mesendoderm in *Xenopus* (Bjerke et al., 2014). Another study investigating breast cancer invasion in a mouse model, found that Keratin14 is upregulated in circulating tumor cell clusters and lung metastasis (Cheung et al., 2016). When Keratin14 was depleted, it disrupted the metastases markers Tenascin C, Jagged 1, and Epiregulin. As Keratin14 is also enriched in desmosomes, this study further emphasizes a critical role for cell-cell adhesions during tumor cluster invasion.

Interestingly, these invasive fronts share molecular similarities to collective cell migration observed during embryonic development. For example, the leading edge of invasive cancer clusters share common molecular properties observed at the leading edges of collectives including cell-cell junctions and cell adhesion receptors (**Figure 6**) (Freidl et al., 2004; Christiansen and Rajasekaran, 2006; Alexander et al., 2008). In addition, collectively invading cancer cells use self-generated gradients to promote migration. Similar to self-generated gradients by border cells and the pLLP, a study examining invasion of melanoma cells identified a mechanism by which tumor cells generated a gradient of lysophosphatidic acid (LPA) (Muinonen-Martin et al., 2014) and used this gradient to promote cancer cell invasion. In this study, tumor cells acted as a ligand sink by breaking down LPA into byproducts. This created a gradient in which LPA was high in surrounding tissues but low within the tumor itself. Melanoma tumors then used this gradient to migrate to higher sources of LPA in the surrounding tissue, initiating metastasis.

Common signaling pathways used during development as well as collective cell migration are often reactivated during collective invasion (Korc and Friesel, 2009; Katoh, 2017; Bach et al., 2018). For example, many downstream components of the canonical Wnt signaling pathway are misregulated in a variety of cancers (hepatocellular, colorectal, orapharyngeal squamous cell carcinoma) and their associated metastasis including Axins, β-catenin, and TCF/Lef1 transcription factors (**Figure 6**) (Lammi et al., 2004; Salahshor and Woodgett, 2005; Marvin et al., 2011; Papagerakis et al., 2012). Notably, Lef1 is active at the leading front of invasive lung and colorectal cancers, similar to canonical Wnt signaling being active within the leading region of the pLLP (Nguyen et al., 2009; Wang et al., 2013). In addition to mutations in canonical Wnt signaling, other signaling pathways active during pLLP migration are also implicated in certain types of metastatic cancer. Mutations in the Notch/Delta pathway have been associated with poor prognosis in colorectal and breast cancer as activation of this pathway is associated with metastasis. Although it is not clear whether this pathway is involved in collective cell invasion (Leong et al., 2007; Wang et al., 2013).

Cancer cells also make use of chemotactic signals during metastases. In particular, numerous invasive cancers show abnormal expression of the chemokine receptors CXCR4 and CXCR7 as well as the ligand CXCL12 both within the tumors and at potential sites of metastases. For example in breast cancer, tumor cells express high levels of CXCR4 and metastatic target tissues (lung, liver, bone) express high levels of the ligand CXCL12 (**Figure 6**) (Wang et al., 2013; Wu et al., 2015). Further, high levels of CXCR4 and CXCR7 are associated

with shorter survival times than those with low levels (Wu et al., 2015). Although, this association does not seem to hold true for other types of cancers. In a pancreatic cancer *in vivo* mouse model, cells producing CXCL12 showed deficits in migration and poor metastatic potential in comparison to control cells producing no CXCL12 (Roy et al., 2014). Based on this evidence it is possible that the CXCL12 chemokine may act differently in various cancer contexts. Despite the known prevalence of mutations within these signaling pathways, the mechanisms by which these mutations induce and promote or inhibit collective invasion and metastases remain unknown. Understanding how these signaling pathways regulate collective cell migration of the pLLP may provide clues as to how these pathways are hijacked during cancer invasion.

Based on the similarities between collective invasion and collective cell migration, we can use models of collective cell migration during development to discern mechanisms used by tumor clusters during metastasis. For example, as Lef1 is upregulated at the invasive fronts of both lung and colorectal invasive cancers and canonical Wnt signaling via Lef1 is active in the leading region of the pLLP we can use the leading region of the pLLP as a model for collective cancer invasion. We can study cellular adhesion, protrusive behavior, and cell-ECM interactions using the pLLP model to identify cellular mechanisms that promote cancer front migration and metastasis. Identification of cellular pathways that act downstream of Lef1 in the pLLP may provide clues as to how these factors are misregulated during invasive cancers that show increased Lef1 expression at their leading edge. Thus, further insights gained through studies of pLLP leading edge behavior could provide insight into how these invasive clusters promote metastasis.

CONCLUSIONS

Collective cell migration is a widely used developmental process that initiates and promotes morphogenesis of many different organ systems. While collectives are organized into a variety of different forms, they often share similar cellular strategies. Collectives are guided by leading cells that sense and respond to the extracellular environment, specifically chemotactic cues. These chemotactic cues are then transmitted through specific signaling pathways to initiate molecular changes that guide migration as well as differentiation. Insights gained from studying mechanisms of collective cell migration can be used to identify mechanisms by which invasive cancers hijack developmental machinery to promote metastasis.

AUTHOR CONTRIBUTIONS

HO wrote the manuscript. AN edited the manuscript.

FUNDING

Research in the AN Laboratory is supported by funds from the National Institutes of Health and Presidential Bridge Funding from Oregon Health and Science University.

REFERENCES

Aceto, N., Bardia, A., Miyamoto, D., Donaldson, M., Wittner, B., Spencer, J., et al. (2014). Circulating tumor cell clusters are oligoclonal precursours of breast cancer metastasis.*Cell* 158, 1110–1122. doi: 10.1016/j.cell.2014.07.013

Alexander, S., Koehl, G. E., Hirschberg, M., Geissler, E. K., and Friedl, P. (2008). Dynamic imaging of cancer growth and invasion: a modified skin-fold chamber model. *Histochem. Cell Biol.* 130, 1147–1154. doi: 10.1007/s00418-008-0529-1

Alfandari, D., Cousin, H., Gaultier, A., Hoffstrom, B. G., and DeSimone, D. W. (2003). Integrin α5β1 supports the migration of Xenopus cranial neural crest on fibronectin. *Dev. Biol.* 260, 449–464. doi: 10.1016/S0012-1606(03)00277-X

Aman, A., and Piotrowski, T. (2008). Wnt/beta-catenin and Fgf signaling control collective cell migration by restricting chemokine receptor expression. *Dev. Cell* 15, 749–761. doi: 10.1016/j.devcel.2008.10.002

Anon, E., Serra-Picamal, X., Hersen, P., Gauthier, N. C., Sheetz, M. P., Trepat, X., et al. (2012). Cell crawling mediates collective cell migration to close undamaged epithelial gaps. *Proc. Natl. Acad. Sci. U.S.A.* 109, 10891–10896. doi: 10.1073/pnas.1117814109

Astin, J. W., Batson, J., Kadir, S., Charlet, J., Persad, R., Gillatt, D., et al. (2010). Competition amongst Eph receptors regulates contact inhibition of locomotion and invasiveness in prostate cancer cells. *Nat. Cell Biol.* 12, 1194–1204. doi: 10.1038/ncb2122

Attia, L., Schneider, J., Yelin, R., and Schultheiss, T. (2015). Collective cell migration of the nephric duct requires FGF signaling. *Dev. Dyn.* 244, 157–167. doi: 10.1002/dvdy.24241

Bach, D. H., Park, H. J., and Lee, S. K. (2018). The dual role of bone morphogenetic proteins in cancer. *Mol. Ther. Oncolytics* 8, 1–13. doi: 10.1016/j.omto.2017.10.002

Bahri, S., Wang, S., Conder, R., Choy, J., Vlachos, S., Dong, K., et al. (2010). The leading edge during dorsal closure as a model for epithelial plasticity: pak is required for recruitment of the Scribble complex and septate junction formation. *Development* 137, 2023–2032. doi: 10.1242/dev.045088

Bazellières, E., Conte, V., Elosegui-Artola, A., Serra-Picamal, X., Bintanel-Morcillo, M., RocaCusachs, P., et al. (2015). Control of cell–cell forces and collective cell dynamics by the intercellular adhesome. *Nat. Cell Biol.* 17, 409–420. doi: 10.1038/ncb3135

Becker, S. F., Mayor, R., and Kashef, J. (2014). Cadherin-11 mediates contact inhibition of locomotion during xenopus neural crest cell migration. *PLoS ONE* 8:e85717.doi: 10.1371/journal.pone.0085717

Bianco, A., Poukkula, M., Cliffe, A., Mathieu, J., Luque, C., Fulga, T., et al. (2007). Two distinct modes of guidance signalling during collective migration of border cells. *Nature* 448, 362–365. doi: 10.1038/nature05965

Bjerke, M. A., Dzamba, B. J., Wang, C., and DeSimone, D.,(2014). FAK is required for tension dependent organization of collective cell movements in Xenopus mesendoderm. *Dev. Biol.* 394, 340–356. doi: 10.1016/j.ydbio.2014.07.023

Boldajipour, B., Mahabaleshwar, H., Kardash, E., Reichman-Fried, M., Blaser, H., Minina, S., et al. (2008). Control of chemokine-guided cell migration by ligand sequestration. *Cell*. 132, 463–473. doi: 10.1016/j.cell.2007.12.034

Cai, D., Chen, S., Prasad, M., He, L., Wang, X., Choesmel-Cadamuro, V., et al. (2014). Mechanical feedback through e-cadherin promotes direction sensing during collective cell migration. *Cell* 157, 1146–1159. doi: 10.1016/j.cell.2014.03.045

Carmona-Fontaine, C., Matthews, H., Kuriyama, S., Moreno, M., Dunn, G., et al. (2008). Contact inhibition of locomotion *in vivo* controls neural crest directional migration. *Nature* 456, 957–961. doi: 10.1038/nature07441

Caussinus, E., Colombelli, J., and Affolter, M. (2008). Tip-cell migration controls stalk-cell intercalation during Drosophila tracheal tube elongation. *Curr. Biol.* 18, 1727–1734. doi: 10.1016/j.cub.2008.10.062

Cheung, K. J., Padmanaban, V., Silvestri, V., Schipper, K., Cohen, J., Fairchild, A. N., et al. (2016). Polyclonal breast cancer metastases arise from collective dissemination of keratin 14 expressing tumor cell clusters. *Proc. Natl. Acad. Sci. U.S.A.* 113, E854–E863. doi: 10.1073/pnas.1508541113

Chihara, T., Kato, K., Taniguchi, M., Ng, J., and Hayashi, S. (2003). Rac promotes epithelial rearrangement during tracheal tubulogenesis in Drosophila. *Development* 130, 1419–1429. doi: 10.1242/dev.00361

Chitnis, A. B., Nogare, D. D., and Matsuda, M. (2012). Building the posterior lateral line system inzebrafish. *Dev. Neurobiol.* 72, 234–255. doi: 10.1002/dneu.20962

Christiansen, J. J., and Rajasekaran, A. K.,(2006). Reassessing epithelial to mesenchymal transition as a prerequisite for carcinoma invasion and metastasis. *Cancer Res.* 66, 8319–8326. doi: 10.1158/0008-5472.CAN-06-0410

Dalle Nogare, D. D., Nikaido, M., Somers, K., Head, J., Piotrowski, T., and Chitinis, A. B. (2017). In toto imaging of the migrating Zebrafish lateral line primordium at single cell resolution. *Dev. Biol.* 422, 14–23. doi: 10.1016/j.ydbio.2016.12.015

Dambly-Chaudiere, C., Cubedo, N., and Ghysen, A. (2007). Control of cell migration in the development of the posterior lateral line: antagonistic interactions between the Feedback through E-Cadherin CXCR4 and CXCR7/RDC1. *BMC Dev. Biol.* 7:23. doi: 10.1186/1471-213X-7-23

Danjo, Y., and Gipson, I. (1998). Actin "purse string" filaments are anchored by E-cadherin mediated adherens junctions at the leading edge of the epithelial wound, providing coordinated cell movement. *J. Cell Sci.* 111, 3323–3332.

David, N. B., Sapède, D., Saint-Etienne, L., Thisse, C., Thisse, B., Dambly-Chaudiere, C., et al. (2002). Molecular basis of cell migration in the fish lateral line: role of the chemokinereceptor CXCR4 and of its ligand, SDF1. *Proc. Natl. Acad. Sci. U.S.A.* 99, 16297–16302. doi: 10.1073/pnas.252339399

Donà, E., Barry, J., Valentin, G., Quirin, C., Khmelinskii, A., Kunze, A., et al. (2013). Directional tissue migration through a self-generated chemokine gradient. *Nature* 503, 285–289. doi: 10.1038/nature12635

du Roure, O., Saez, A., Buguin, A., Austin, R., Chavrier, P., Siberzan, P., et al. (2005). Force mapping in epithelial cell migration. *Proc. Natl. Acad. Sci. U.S.A.* 102, 2390–2395. doi: 10.1073/pnas.0408482102

Durdu, S., Iskar, M., Revenu, C., Schieber, N., Kunze, A., Bork, P., et al. (2014). Luminal signaling links cell communication to tissue architecture during organogenesis. *Nature* 515, 120–124. doi: 10.1038/nature13852

Eming, S. A., Brachvogel, B., Odorisio, T., and Koch, M. (2007). Regulation of angiogenesis: wound healing as a model. *Prog. Histochem. Cytochem.* 42, 115–170. doi: 10.1016/j.proghi.2007.06.001

Ernst, S., Liu, K., Agarwala, S., Moratscheck, N., Avci, M. E., Nogare, D. D., et al. (2012). Shroom3 is required downstream of FGF signalling to mediate proneuromast assembly in zebrafish. *Development* 139, 4571–4581. doi: 10.1242/dev.083253

Etienne-Manneville, S., and Hall, A. (2001). Integrin-mediated activation of Cdc42 controls cell polarity in migrating astrocytes through PKC. *Cell* 106, 489–498. doi: 10.1016/S0092-8674(01)00471-8

Ewald, A. J., Brenot, A., Duong, M., Chan, B. S., and Werb, Z. (2008). Collective epithelial migration and cell rearrangements drive mammary branching morphogenesis. *Dev. Cell.* 14, 570–581. doi: 10.1016/j.devcel.2008.03.003

Farooqui, R., and Fenteany, G. (2005). Multiple rows of cells behind an epithelial wound edge extend cryptic lamellipodia to collectively drive cell-sheet movement. *J. Cell Sci.* 118, 51–63. doi: 10.1242/jcs.01577

Fenteany, G., Janmey, P. A., and Stossel, T. p. (2000). Signaling pathways and cell mechanics involved in wound closure by epithelial cell sheets. *Curr. Biol.* 10, 831–838. doi: 10.1016/S0960-9822(00)00579-0

Freidl, P., Hegerfeldt, Y., and Tusch, M. (2004). Collective cell migration in morphogenesis and cancer. *Int. J. Dev. Biol.* 48, 441–449. doi: 10.1387/ijdb.041821

Friedl, P., Noble, P., Walton, P., Laird, D., Chauvin, P., Tabah, R., et al. (1995). Migration of coordinated cell clusters in mesenchymal and epithelial cancer explants. *Cancer Res.* 55, 4557–4560.

Fuchs, S. (1894). Ueber die Function der unter der Haut liegenden Canalsysteme bei den Seleachiern. *Arch. Gesammte Physiol.* 59, 454–478.

Geisbrecht, E. R., and Montell, D. J. (2002). Myosin VI is required for E-cadherin-mediated border cell migration. *Nat. Cell Biol.* 4, 616–620. doi: 10.1038/ncb830

Grose, R., Hutter, C., Bloch, W., Thorey, I., Watt, F., Fässler, R., et al. (2002). A crucial role of β1integrins for keratinocyte migration *in vitro* and during cutaneous wound repair. *Development* 129, 2303–2315.

Gundem, G., Van Loo, P., Kremeyer, B., Alexandrov, L. B., Tubio, J., Papaemmanuil, E., et al. (2015). The evolutionary history of lethal metastatic prostate cancer. *Nature* 520, 353–357. doi: 10.1038/nature14347

Haas, P., and Gilmour, D. (2006). Chemokine signaling mediates self-organizing tissue migration inthe zebrafish lateral line. *Dev. Cell.* 10, 673–680. doi: 10.1016/j.devcel.2006.02.019

Harding, M., and Nechiporuk, A. (2012). Fgfr-Ras-MAPK signaling is required for apical constriction via apical positioning of Rho-associated kinase during mechanosensory organ formation. *Development* 139, 3130–3135. doi: 10.1242/dev.082271

Harrison, R. (1904). Experimentelle Untersuchung über die Entwicklung der Sinnesorgane der Seitenlinie bei den Amphibien. *Arch. Mikrosk Anat. Entw. Mech.* 63, 35–149.

Hegerfeldt, Y., Tusch, M., Bröcker, E., and Friedl, P. (2002). Collective cell movement in primary melanoma explants. *Cancer Res.* 62, 2125–2130.

Hou, J. M., Krebs, M. G., Lancashire, L., Sloane, R., Backen, A., Swain, R., et al. (2012). Clinical significance and molecular characteristics of circulating tumor cells and circulating tumor microemboli in patients with small-cell lung cancer. *J. Clin. Oncol.* 30, 525–532. doi: 10.1200/JCO.2010.33.3716

Itoh, M., and Chitnis, A. (2001). Expression of proneural and neurogenic genes in the zebrafish lateral line primordium correlates with selection of hair cell fate in neuromasts. *Mech. Dev.* 102, 263–266. doi: 10.1016/S0925-4773(01)00308-2

Katoh, M. (2017). Canonical and non-canonical WNT signaling in cancer stem cells and their niches: cellular heterogeneity, omics reprogramming, targeted therapy and tumor plasticity (Review). *Int. J. Oncol.* 51, 1357–1369. doi: 10.3892/ijo.2017.4129

Knox, R. (1825). On the theory of a sixth sense in fishes; supposed to reside in certain pecular tubular prgans, found immediately under the integuments of the head in sharks and rays. *Ediburgh J. Sci.* 2, 23–16.

Korc, M., and Friesel, R. (2009). The role of fibroblast growth factors in tumor growth. *Curr. Cancer Drug Targets* 9, 639–651. doi: 10.2174/156800909789057006

Kuriyama, S., Theveneau, E., Benedetto, A., Parsons, M., Tanaka, M., Charras, G., et al. (2014). *In vivo* collective cell migration requires an LPAR2-dependent increase in tissue fluidity. *J. Cell Biol.* 206, 113–127. doi: 10.1083/jcb.201402093

Lamalice, L., Le Boeuf, F., and Huot, J. (2007). Endothelial cell migration during angiogenesis. *Circ. Res.* 100, 782–794. doi: 10.1161/01.RES.0000259593.07661.1e

Lammi, L., Arte, S., Somer, M., Järvinen, H., Lahermo, P., Thesleff, I., et al. (2004). Mutations inAXIN2 cause familial tooth agenesis and predispose to colorectal cancer. *Am. J. Hum. Genet.* 74, 1043–1050. doi: 10.1086/386293

Lawson, C. D., and Burridge, K. (2014). The on-off relationship of Rho and Rac during integrin mediated adhesion and cell migration. *Small GTPases* 5:e27958. doi: 10.4161/sgtp.27958

Lebreton, G., and Casanova, J. (2014). Specification of leading and trailing cell features during collective migration in the *Drosophila trachea*. *J. Cell Sci.* 127, 465–474. doi: 10.1242/jcs.142737

Lecaudey, V., Cakan-Akdogan, G., Norton, W., and Gilmour, D. (2008). Dynamic Fgf signaling couples morphogenesis and migration in the zebrafish lateral line primordium. *Development* 135, 2695–2705. doi: 10.1242/dev.025981

Leong, K. G., Niessen, K., Kulic, I., Raouf, A., Eaves, C., Pollet, I., et al. (2007). Jagged1mediated Notch activation induces epithelial-to-mesenchymal transition through Sluginduced repression of E-cadherin. *J. Exp. Med.* 204, 2935–2948. doi: 10.1084/jem.20071082

Leydig, F. (1850). Ueber die Schleimkanäle der Knochenfische. *Mull. Arch. Anat. Physiol.* 170–181.

Li, L., Hartley, R., Reiss, B., Sun, Y., Pu, J., Wu, D., et al. (2012). E-cadherin plays an essential rolein collective directional migration of large epithelial sheets. *Cell. Mol. Life Sci.* 69, 2779–2789. doi: 10.1007/s00018-012-0951-3

Li, Q., Shirabe, K., and Kuwada, J. (2004). Chemokine signaling regulates sensory cell migration in zebrafish. *Dev. Biol.* 269, 123–136. doi: 10.1016/j.ydbio.2004.01.020

Liotta, L. A., Saidel, M. G., and Kleinerman, J. (1976). The significance of hematogenous tumorcell clumps in the metastatic process. *Cancer Res.* 36, 889–894.

Maddipati, R., and Stanger, B. (2015). Pancreatic cancer metastases harbor evidence ofpolyclonality. *Cancer Discov.* 5, 1086–1097. doi: 10.1158/2159-8290.CD-15-0120

Mahabaleshwar, H., Tarbashevich, K., Nowak, M., Brand, M., and Raz, E. (2012). Beta-arrestincontrol of late endosomal sorting facilitates decoy receptor function and chemokine gradient formation. *Development* 139, 2897–2902. doi: 10.1242/dev.080408

Martin, P., and Parkhurst, S. (2004). Parallels between tissue repair and embryo morphogenesis. *Development* 131, 3021–3034. doi: 10.1242/dev.01253

Marvin, M., Mazzoni, S., Herron, C., Edwards, S., Gruber, S., and Petty, E. (2011). AXIN2-associated autosomal dominant ectodermal dysplasia and neoplastic syndrome. *Am. J. Med. Genet. Part A* 155, 898–902. doi: 10.1002/ajmg.a.33927

Matsuda, M., and Chitnis, A. B. (2010). Atoh1a expression must be restricted by Notch signaling foreffective morphogenesis of the posterior lateral line primordium in zebrafish. *Development* 137, 3477–3487. doi: 10.1242/dev.052761

Matsuda, M., Nogare, D., Somers, K., Martin, K., Wang, C., and Chitnis, A. (2013). Lef1 regulatesDusp6 to influence neuromast formation and spacing in the zebrafish posterior lateralline primordium. *Development* 140, 2387–2397. doi: 10.1242/dev.091348

Mayor, R., and Carmona-Fontaine, C. (2010). Keeping in touch with contact inhibition of locomotion. *Trends Cell Biol.* 20, 319–328. doi: 10.1016/j.tcb.2010.03.005

McCarroll, M. N., Lewis, Z. R., Culbertson, M. d., Martin, B., Kimelman, D., and Nechiporuk, A. (2012). Graded levels of Pax2a and Pax8 regulate cell differentiation during sensory placode formation. *Development* 139, 2740–2750. doi: 10.1242/dev.076075

McGraw, H. F., Culbertson, M. D., and Nechiporuk, A. (2014). Kremen1 restricts Dkk activity during posterior lateral line development in zebrafish. *Development* 141, 3212–3221, doi: 10.1242/dev.102541

McGraw, H. F., Drerup, C. M., Culbertson, M. D., Linbo, T., Raible, D., and Nechiporuk, A. (2011). Lef1 is required for progenitor cell identity in the zebrafish lateral line primordium. *Development* 138, 3921–3930. doi: 10.1242/dev.062554

Metcalfe, W. K., Kimmel, C. B., and Schabtach, E. (1985). Anatomy of the posterior lateral line system in young larvae of the zebrafish. *J. Comp. Neurol.* 233, 377–389.

Metzger, R. J., Klein, O. D., Martin, G. R, and Krasnow, M. A. (2008). The branching programme of mouse lung development. *Nature* 453, 745–750. doi: 10.1038/nature0700

Millimaki, B. B., Sweet, E. M., Dhason, M. S., and Riley, B. B. (2007). Zebrafish atoh1 genes: classic proneural activity in the inner ear and regulation by Fgf and Notch. *Development* 134, 295–305. doi: 10.1242/dev.02734

Mizoguchi, T., Ikeda, S., Watanabe, S., Sugawara, M., and Itoh, M. (2017). Mib1 contributes topersistent directional cell migration by regulating the Ctnnd1-Rac1 pathway. *Proc. Natl. Acad. Sci. U.S.A.* 114, E9280–E9289. doi: 10.1073/pnas.171256011

Mizoguchi, T., Togawa, S., Kawakami, K., and Itoh, M. (2011). Neuron and sensory epithelial cellfate is sequentially determined by notch signaling in zebrafish lateral line development. *J. Neurosci.* 31, 15522–15530. doi: 10.1523/JNEUROSCI.3948-11.2011

Monro, A. (1785). *The Structure and Physiology of Fishes Explained and Compared with those of Man and other Animals*. Edinburgh: Charles Elliot.

Montell, D. J., Rorth, P., and Spradling, A. (1992). Slow border cells, a locus required for a developmentally regulated cell migration during oogenesis, encodes Drosophila C/EBP. *Cell* 71, 51–62.

Montgomery, J., Carton, G., Voigt, R., Baker, C., and Diebel, C. (2000). Sensory processing of water currents by fishes. *Philos. Trans. R. Soc. Lond. B. Biol. Sci.* 355, 1325–1327.

Muinonen-Martin, A. J., Susanto, O., Zhang, Q., Smethurst, E., Faller, W., Veltman, D., et al. (2014). Melanoma cells break down LPA to establish local gradients that drive chemotactic dispersal. *PLoS Biol.* 12:e1001966. doi: 10.1371/journal.pbio.1001966

Murphy, A. M., and Montell, D. J. (1996). Cell type-specific roles for Cdc42, Rac, and RhoL in *Drosophila oogenesis*. *J. Cell Biol.* 133, 617–630.

Nabeshima, K., Inoue, T., Shimao, Y., Okada, Y., Itoh, Y., Seiki, M., et al. (2000). Front cell-specific expression of membrane-type 1 matrix metalloproteinase and gelatinase A during cohort migration of colon carcinoma cells induced by hepatocyte growth factor/scatter factor. *Cancer Res.* 60, 3364–3349.

Naumann, U., Cameroni, E., Pruenster, M., Mahabaleshwar, H., Raz, E., Zerwes, H. G., et al. (2010). CXCR7 functions as a scavenger for CXCL12 and CXCL11. *PLoS ONE* 5:e9175. doi: 10.1371/journal.pone.0009175

Nechiporuk, A., and Raible, D. (2008). FGF-dependent mechanosensory organ patterning inzebrafish. *Science* 320, 1774–1777. doi: 10.1126/science.1156547

Nguyen, D. X., Chiang, A., Zhang, X., Kim, J., Kris, M., Ladanyi, M., et al. (2009). WNT/TCF signaling through LEF1 and HOXB9 mediates lung adenocarcinoma metastasis. *Cell* 138, 51–62. doi: 10.1016/j.cell.2009.04.030

Niewiadomska, P., Godt, D., and Tepass, U. (1999). DE-cadherin is required for intercellular motility during drosophila oogenesis. *J. Cell Biol.* 144, 533–547.

Nikaido, M., Navajas Acedo, J., Hatta, K., and Piotrowski, T. (2017). Retonic acid is required and Fgf, Wnt, and Bmp signaling inhibit posterior lateral line placode induction in zebrafish. *Dev. Biol.* 431, 215–225. doi: 10.1016/j.ydbio.2017.09.017

Nobes, C. D., and Hall, A. (1999). Rho GTPases control polarity, protrusion, and adhesion during cell movement. *J. Cell Biol.* 144, 1235–1244.

Olesnicky Killian, E. C., Birkholz, D. A., and Artinger, K. B. (2009). A role for chemokine signaling in neural crest cell migration and craniofacial development. *Dev. Biol.* 333, 161–172. doi: 10.1016/j.ydbio.2009.06.031

Omelchenko, T., Rabadan, M., Hernández-Martínez, R., Grego-Bessa, J., Anderson, K., and Hall, A. (2014). β-Pix directs collective migration of anterior visceral endoderm cells in the early mouse embryo. *Genes Dev.* 28, 2764–2777. doi: 10.1101/gad.251371.114

Osmani, N., Peglion, F., Chavrier, P., and Etienne-Manneville, S. (2010). Cdc42 localization and cell polarity depend on membrane traffic. *J. Cell Biol.* 191, 1261–1269. doi: 10.1083/jcb.201003091

Papagerakis, P., Pannone, G., Shabana, A., Depondt, J., Santoro, A., Ghirtis, K., et al. (2012). Aberrant β-catenin and lef1 expression may predict the clinical outcome for patients with or opharyngeal cancer. *Int. J. Immunopathol. Pharmacol.* 25, 135–146. doi: 10.1177/039463201202500116

Parker, G. (1904). The function of lateral-line organs in fishes. *Dep. Comm. Labor Bureau Fish.* 24, 185–207.

Piotrowski, T., and Baker, C. (2014). The development of lateral line placodes: taking a broader view. *Dev. Biol.* 389, 68–81. doi: 10.1016/j.ydbio.2014.02.016

Poujade, M., Grasland-Mongrain, E., Hertzog, A., Jouanneau, J., Chavrier, P., Ladoux, B., et al. (2007). Collective migration of an epithelial monolayer in response to a model wound. *Proc. Natl. Acad. Sci. U.S.A.* 104, 15988–15993. doi: 10.1073/pnas.0705062104

Prasad, M., and Montell, D. (2007). Cellular and molecular mechanisms of border cell migration analyzed using time-lapse live-cell imaging. *Dev. Cell.* 12, 997–1005. doi: 10.1016/j.devcel.2007.03.021

Reffay, M., Parrini, M. C., Cochet-Escartin, O., Ladoux, B., Buguin, A., Coscoy, S., et al. (2014). Interplay of RhoA and mechanical forces in collective cell migration driven by leader cells. *Nat. Cell Biol.* 16, 217–223. doi: 10.1038/ncb2917

Revenu, C., Streichan, S., Donà, E., Lecaudey, V., Hufnagel, L., and Gilmour, D. (2014). Quantitative cell polarity imaging defines leader-to-follower transitions during collective migration and the key role of microtubule-dependent adherens junction formation. *Development* 141, 1282–1291. doi: 10.1242/dev.101675

Roy, I., Zimmerman, N. P., Mackinnon, A. C., Tsai, S., Evans, D. B., and Dwinell, M. B. (2014). CXCL12 chemokine expression suppresses human pancreatic cancer growth and metastasis. *PLoS ONE* 9:e90400. doi: 10.1371/journal.pone.0090400

Rupp, P. A., and Kulesa, P. M. (2007). A role for rhoa in the two-phase migratory pattern of post oticneural crest cells. *Dev. Biol.* 311, 159–171. doi: 10.1016/j.ydbio.2007.08.027

Salahshor, S., and Woodgett, J. (2005). The links between axin and carcinogenesis. *J. Clin. Pathol.* 58, 225–236. doi: 10.1136/jcp.2003.009506

Sarrazin, A. F., Nuñez, V. A., Sapède, D., Tassin, V., Dambly-Chaudière, C., and Ghysen, A. (2010). Origin and early development of the posterior lateral line system of zebrafish. *J. Neurosci.* 30:8234. doi: 10.1523/jneurosci.5137-09.2010

Sarrazin, A. F., Villablanca, E., Nuñez, V., Sandoval, P., Ghysen, A., and Allende, M. (2006). Proneural gene requirement for hair cell differentiation in the zebrafish lateral line. *Dev. Biol.* 295, 534–545. doi: 10.1016/j.ydbio.2006.03.037

Scales, T. M., and Parsons, M. (2011). Spatial and temporal regulation of integrin signalling during cell migration. *Curr. Opin. Cell Biol.* 23, 562–568. doi: 10.1016/j.ceb.2011.05.008

Scarpa, E., Szabó, A., Bibonne, A., Theveneau, E., Parsons, M., and Mayor, R. (2015). Cadherin switch during EMT in neural crest cells leads to contact inhibition of locomotion via repolarization of forces. *Dev. Cell*. 34, 421–434. doi: 10.1016/j.devcel.2015.06.012

Schulze, F. (1861). Ueber die Nervenendigung in den sogenannten Schleimkanälen der Fische undueber entsprechende Organe der durch Kiemen athmenden Amphibien. *Arch. Anat. Physiol. Lpz* 3, 759–769.

Schulze, F. (1870). Ueber die Sinnesorgane der Seitenlinie bei Fischen und Amphibien. *Arch. Mikrosk Anat*. 6, 62–68. doi: 10.1007/BF02955971

Shamir, E. R., and Ewald, A. J. (2015). Adhesion in mammary development: novel roles for E-cadherin in individual and collective cell migration. *Curr. Top. Dev. Biol.* 112, 353–382. doi: 10.1016/bs.ctdb.2014.12.001

Shaw, T. J., and Martin, P. (2009). Wound repair at a glance. *J. Cell Sci*. 122, 3209–3213. doi: 10.1242/jcs.031187

Solnica-Krezel, L. (2005). Conserved patterns of cell movements during vertebrate gastrulation. *Curr. Biol.* 15, R213–R228. doi: 10.1016/j.cub.2005.03.016

Stenzel, D., Lundkvist, D., Sauvaget, M., Busse, M., Graupera, A., van der Flier, E., et al. (2011). Integrin dependent and -independent functions of astrocytic fibronectin in retinal angiogenesis. *Development* 138, 4451–4463. doi: 10.1242/dev.071381

Stone, L. (1933). The development of lateral-line sense organs in amphibians observed in living and vitally stained preparations. *J. Comp. Neurol.* 57, 507–540.

Sutherland, D., Samakovlis, C., and Krasnow, M. (1996). Branchless encodes a Drosophila FGF homolog that controls tracheal cell migration and the pattern of branching. *Cell* 87, 1091–1101.

Tambe, D. T., Hardin, C. C., Angelini, T. E., Rajendran, K., Park, C., Serra-Picamal, X., et al. (2011). Collective cell guidance by cooperative intercellular forces. *Nat. Mater.* 10, 469–475. doi: 10.1038/nmat3025

Theveneau, E., Marchant, L., Kuriyama, S., Gull, M., Moepps, B., Parsons, M., et al. (2010). Collective chemo taxis requires contact-dependent cell polarity. *Dev. Cell*. 19, 39–53. doi: 10.1016/j.devcel.2010.06.012

Theveneau, E., and Mayor, R. (2012). Collective cell migration of epithelial and mesenchymal Cells. *Cell Mol. Life Sci*. 70, 3481–3492. doi: 10.1007/s00018-012-1251-7

Theveneau, E., and Mayor, R. (2013). Neural crest delamination and migration: from epithelium-to mesenchyme transition to collective cell migration. *Dev. Biol.* 366, 34–54. doi: 10.1016/j.ydbio.2011.12.041

Theveneau, E., Steventon, B., Scarpa, E., Garcia, S., Trepat, X., Streit, A., et al. (2013). Chase-and run between adjacent cell populations promotes directional collective migration. *Nat. Cell Biol.* 15, 763–772. doi: 10.1038/ncb2772

Trepat, X., Wasserman, M., Angelini, T., Millet, E., Weitz, D., Butler, J., et al. (2009). Physical forces during collective cell migration. *Nat. Phys*. 5, 426–430. doi: 10.1038/nphys1269

Valdivia, L., Young, R., Hawkins, T., Stickney, H., Cavodeassi, F., Schwarz, Q., et al. (2011). Lef1 dependent Wnt/β-catenin signaling drives the proliferative engine that maintains tissue homeostasis during lateral line development. *Development* 138, 3931–3941. doi: 10.1242/dev.062695

Valentin, G., Haas, P., and Gilmour, D. (2007). The chemokine SDF1a coordinates tissue migration through the spatially restricted activation of Cxcr7 and Cxcr4b. *Curr. Biol.* 17, 1026–1031. doi: 10.1016/j.cub.2007.05.020

Venkiteswaran, G., Lewellis, S. W., Wang, J., Reynolds, E., Nicholson, C., and Knaut, H. (2013). Generation and dynamics of an endogenous, self-generated signaling gradient across amigrating tissue. *Cell* 155, 674–687. doi: 10.1016/j.cell.2013.09.046

Vitorino, P., and Meyer, T. (2008). Modular control of endothelial sheet migration. *Genes Dev*. 22, 3268–3281. doi: 10.1101/gad.1725808

Wang, W., Yao, Y., Jiang, L., Hu, T., Ma, J., Liao, Z., et al. (2013). Knock down of lymphoid enhancer factor 1 inhibits colon cancer progression *in vitro* and *in vivo*. *PLoS ONE* 8:e76596. doi: 10.1371/journal.pone.0076596

Werner, S., Peters, K. G., Longaker, M. T., Fuller-Pace, F., Banda, M., and Williams, L. T. (1992). Large induction of keratinocyte growth factor expression in the dermis during wound healing. *Proc. Natl. Acad. Sci. U.S.A*. 89, 6896–6900.

Wu, W., Qian, L., Chen, X., and Ding, B. (2015). Prognostic significance of CXCL12, CXCR4, and CXCR7 in patients with breast cancer. *Inter. J. Clin. Exp. Pathol.* 8, 13217–13224.

Zaidel-Bar, R., Itzkovitz, S., Ma'ayan, A., Iyengar, R., and Geiger, B. (2007). Functional atlas of the integrin adhesome. *Nat. Cell Biol*. 9, 858–867. doi: 10.1038/ncb0807-858.

Zallen, J. A., and Blankenship, J. T. (2008). Multicellular dynamics during epithelial elongation. *Sem. Cell Dev. Biol.* 19, 263–270. doi: 10.1016/j.semcdb.2008.01.005

Zeidman, I., and Buss, J. (1952). Trans pulmonary passage of tumor cell emboli. *Cancer Res.* 12, 731–733.

Conflict of Interest Statement: The authors declare that the research was conducted in the absence of any commercial or financial relationships that could be construed as a potential conflict of interest.

frontiers in Cell and Developmental Biology

REVIEW
published: 20 August 2018
doi: 10.3389/fcell.2018.00091

Zebrafish as a Model for Obesity and Diabetes

Liqing Zang[1,2], *Lisette A. Maddison*[3] *and Wenbiao Chen*[1]*

[1] Department of Molecular Physiology and Biophysics, Vanderbilt University School of Medicine, Nashville, TN, United States, [2] Graduate School of Regional Innovation Studies, Mie University, Tsu, Japan, [3] Center for Reproductive Biology, Washington State University, Pullman, WA, United States

Obesity and diabetes now considered global epidemics. The prevalence rates of diabetes are increasing in parallel with the rates of obesity and the strong connection between these two diseases has been coined as "diabesity." The health risks of overweight or obesity include Type 2 diabetes mellitus (T2DM), coronary heart disease and cancer of numerous organs. Both obesity and diabetes are complex diseases that involve the interaction of genetics and environmental factors. The underlying pathogenesis of obesity and diabetes are not well understood and further research is needed for pharmacological and surgical management. Consequently, the use of animal models of obesity and/or diabetes is important for both improving the understanding of these diseases and to identify and develop effective treatments. Zebrafish is an attractive model system for studying metabolic diseases because of the functional conservation in lipid metabolism, adipose biology, pancreas structure, and glucose homeostasis. It is also suited for identification of novel targets associated with the risk and treatment of obesity and diabetes in humans. In this review, we highlight studies using zebrafish to model metabolic diseases, and discuss the advantages and disadvantages of studying pathologies associated with obesity and diabetes in zebrafish.

Keywords: zebrafish, obesity, diabetes, transgenic models, disease models, animal

OPEN ACCESS

Edited by:
Ryan M. Anderson, Indiana University, Purdue University Indianapolis, United States

Reviewed by:
Marta Letizia Hribal, Università Degli Studi Magna Græcia di Catanzaro, Italy
Anne-Francoise Burnol, Institut National de la Santé et de la Recherche Médicale (INSERM), France

***Correspondence:**
Wenbiao Chen
wenbiao.chen@Vanderbilt.Edu

Specialty section:
This article was submitted to Cellular Endocrinology, a section of the journal Frontiers in Cell and Developmental Biology

Received: *02 April 2018*
Accepted: *25 July 2018*
Published: *20 August 2018*

Citation:
Zang L, Maddison LA and Chen W (2018) Zebrafish as a Model for Obesity and Diabetes. Front. Cell Dev. Biol. 6:91. doi: 10.3389/fcell.2018.00091

INTRODUCTION

The prevalence of overweight and obesity has steadily increased worldwide in the past several decades. In 2016, more than 1.9 billion adults were overweight, and of these over 650 million were obese (WHO, 2017). This is primarily due to excess food consumption (Vandevijvere et al., 2015). Overweight and obesity are major risk factors for numerous chronic diseases, including cardiovascular diseases, diabetes, and certain types of cancer (Haslam and James, 2005). In the United States, class III obese individuals (BMI $\geq$ 40 kg/m^2) have a six-fold increase in diabetes risk over normal-weight individuals (Leung et al., 2017) and more than 90% of people with type 2 diabetes mellitus (T2DM) are overweight or obese. The global increase of overweight and obesity largely explains the incidence and prevalence of type 2 diabetes over the past 20 years. Obesity and T2DM can substantially decrease life expectancy, diminish quality of life, and impose a large economic burden to society (Leung et al., 2017).

Both obesity and T2DM have high heritability (Poulsen et al., 2001; Willemsen et al., 2015). Recent genome wide association studies and whole exome sequencing studies have identified a large number of genetic variants that are associated with overweight/obesity and/or T2DM (Lawlor et al., 2017; Loos, 2018). In most cases, however, the causative genes for these linked variants are

uncertain and the mechanism by which these variants contribute to the disease phenotypes is unclear (Loos, 2018). Furthermore, the aggregate effect of all the variants only account for a small fraction of the heritability of these conditions (Fuchsberger et al., 2016). It is likely that more alleles are yet to be discovered to play a role in obesity and T2DM susceptibility.

The wealth of human genetic and epidemiological data on obesity and T2DM provides ample opportunity for mechanistic investigations in animal models. Zebrafish is a well-established model system for developmental biology, human genetics, and human diseases (Dooley and Zon, 2000; Gibert et al., 2013; Freifeld et al., 2017). Several features have propelled zebrafish to its current prominence in developmental biology and disease modeling. It is a vertebrate, having high degree of genetic, anatomical, and physiological similarities to humans. It is fecund, easy to maintain in large number and has a relative short generation time, allowing facile genetic, and chemical genetic screens (Kimmel et al., 1995; MacRae and Peterson, 2015). Its external development affords easy accessibility to embryonic and genetic manipulations (Kimura et al., 2014; Hoshijima et al., 2016; Yin et al., 2016). The optical transparency of its embryos permits time lapse live imaging (Hall et al., 2009; Herrgen et al., 2009; Feierstein et al., 2015). Although traditionally used for developmental biology, zebrafish has recently been used to investigate metabolic diseases. Here, we will review some of the recent studies using zebrafish to model human metabolic diseases, with an emphasis on obesity, and diabetes. We will discuss the advantages and disadvantages of studying pathologies associated with obesity and diabetes in zebrafish.

ZEBRAFISH OBESITY MODELS

Lipid Metabolism and Adipose Biology in Zebrafish

Obesity is a consequence of positive energy balance. Regulation of energy intake and expenditure involves many organ systems including the brain, intestines, skeletal muscle, and adipose tissue (Cai, 2013; Dailey, 2014; Periasamy et al., 2017). Therefore, whole animal models are essential for better understanding of the development and progression of metabolic dysfunction. Zebrafish is an excellent model in which to study metabolic dysfunction because they have the key organs that are important for regulation of energy homeostasis and metabolism in mammals, including digestive organs, adipose tissues, and skeletal muscle (Lieschke and Currie, 2007; Schlegel and Stainier, 2007). The key functions such as appetite regulation, insulin regulation and lipid storage are also well conserved (Elo et al., 2007; Flynn et al., 2009; Nishio et al., 2012). Similar to mammals, excess nutrients in zebrafish cause increased plasma triglyceride levels and hepatic steatosis (Oka et al., 2010). Obese zebrafish also exhibit dysregulation of pathways that control lipid metabolism, including SREBF1, PPARs, NR1H3, and LEP (Oka et al., 2010). The conservation of these metabolic pathways that play key roles in adipocyte differentiation, energy homeostasis (Den Broeder et al., 2015), and cholesterol metabolism (Schlombs et al., 2003) demonstrates zebrafish as a suitable model for human lipid metabolism. However, zebrafish is an ectotherm species and its metabolic rate is not regulated by environmental temperature. Consistent with this, zebrafish does not have brown adipocyte tissues (BAT).

A primary characteristic of obesity is adipose hypertrophy and hyperplasia. Zebrafish have multiple adipose tissue depots and their development has been characterized (Flynn et al., 2009). Neutral lipid droplets first appear in visceral adipocytes and accumulate as zebrafish grow. Similar to mammalian white adipose tissue (WAT), early-stage zebrafish adipocytes contain multiple small lipid droplets while mature zebrafish adipocytes have a single large lipid droplet. As occurs in mammals, the adipocyte lineage expresses *pparg,* and *fabp4* (Flynn et al., 2009). Visceral adiposity is a critical risk factor for T2DM and other metabolic diseases (Ahima and Lazar, 2013). In zebrafish, like in mammals, lipids are stored in visceral, intramuscular and subcutaneous adipocyte depots (Song and Cone, 2007), providing the opportunity to understand the regulation of body fat distribution. The high degree of conservation in distribution and formation of adipose tissue in the zebrafish compared to mammals makes it an appropriate model to study obesity.

Methods to Quantitate Adiposity in Zebrafish

Quantitative measures of adiposity are important to assess the degree of obesity-related metabolic derangements. Body mass index (BMI) and quantitative computed tomography (CT) are widely used measurements of adiposity in humans but are more difficult to apply in zebrafish. Commonly used lipophilic dyes for visualizing lipids in histological sections and cultured cells, including Nile red, Oil red O, and Sudan black B, have been utilized to detect lipids in adult zebrafish sections and fixed zebrafish larvae (Marza et al., 2005; Schlegel and Stainier, 2006). With the optical transparency of zebrafish larvae, live-imaging, and fluorescence based screens have been developed for the study of digestive physiology or lipid metabolism. In particular, Nile red has been used for live imaging and quantification of intracellular neutral lipid droplets (Greenspan et al., 1985) as well as for purification of adipocyte tissues (Jones et al., 2008; Flynn et al., 2009; Oka et al., 2010). In addition, a variety of fluorescent lipid analogs and tracers are available, including BODIPY Fatty Acid Analogs, BODIPY-cholesterol analogs and fluorescence reports like PED6, for tracking the metabolism and distribution of exogenous lipids in live zebrafish (Hölttä-Vuori et al., 2010; Anderson et al., 2011). 3D micro-CT is also available for this small animal and allows volume measurement of total adipocyte tissue as well as different fat depots (Hasumura et al., 2012; **Figure 1**). Recently, Landgraf et al. compared the methodology of quantify zebrafish body fat mass using MR images (MRI) and EchoMRI 4in1 (EchoMRI^{TM}; Landgraf et al., 2017). The body fat mass of 8 adult male zebrafish was measured using the two methods and the two techniques showed high correlation. Overall, these methods provide accurate measurements of zebrafish adiposity and provide means for longitudinal monitoring.

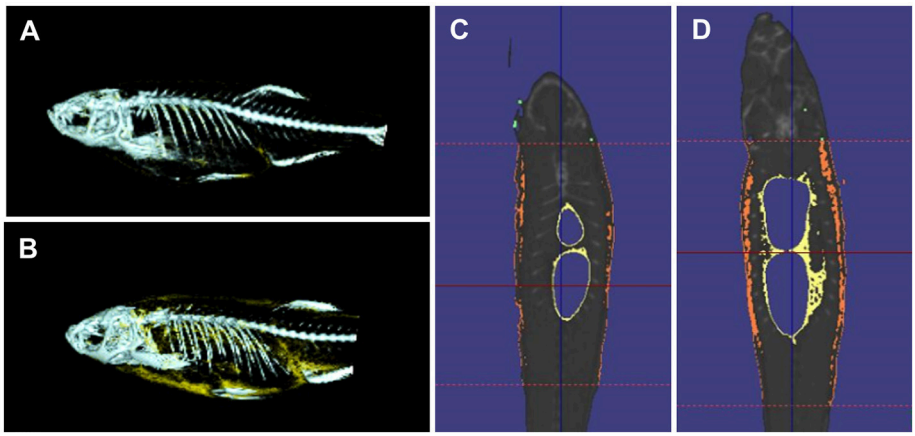

FIGURE 1 | 3D micro-CT analysis in normal fed and diet-included obese zebrafish. **(A)** 3D-images of normal fed zebrafish. Gray color indicates skeleton and yellow color means adipocyte tissue. **(B)** 3D-images obese zebrafish. **(C)** Cross-sectional images of normal fed zebrafish. Yelloe color indicates visceral adipose tissue and orange color indicates subcutaneous adipocyte tissue. **(D)** Cross-sectional images of obese zebrafish.

A number of obesity models have been developed in zebrafish using diet and genetic manipulations (**Table 1**). The next section describes the details of these models.

High-Fat Diet/Over-Nutrition Induced Obesity

A common approach to induce obesity is excess fat intake. Obese zebrafish can be conveniently produced by overfeeding starting from the onset of feeding at 5 dpf (day post fertilization). This is advantageous over rodent models since diet can only be manipulated after weaning, which is at least 3 weeks after birth. Although early larvae have no WAT (Imrie and Sadler, 2010), lipid droplets accumulate in the blood stream and other measures such as whole-larval triacylglycerol level may be used as an indicator for quantifying obesity progression (Schlegel and Stainier, 2006; Tingaud-Sequeira et al., 2011). Although heavy cream has been used (Schlegel and Stainier, 2006), chicken egg yolk solution is the most used high-fat diet for zebrafish larvae and juveniles (Tingaud-Sequeira et al., 2011; Zhou et al., 2015; Kopp et al., 2016; den Broeder et al., 2017). The high fat diet rapidly increases zebrafish adiposity.

Adult zebrafish have also been used as an obesity model. The first diet-induced obese (DIO) zebrafish model was reported in 2010 (Oka et al., 2010) where adult fish (3.5 months of age) were fed with 60 mg or 5 mg of freshly hatched *Artemia* per day for 8 weeks (150 calories vs. 20 calories). The overfed zebrafish exhibited increased BMI, hypertriglyceridemia and hepatosteatosis compared to the normal fed zebrafish. Male and female zebrafish showed similar responses to over-nutrition treatment. Furthermore, comparative transcriptome analysis of visceral adipose tissue among zebrafish, mouse, rat and human revealed that lipid metabolism networks of zebrafish are similar to those of mammals.

Besides overfeeding with *Artemia*, several other methods have been used to generate obese zebrafish. Meguro et al. developed custom high-fat zebrafish diets containing 20% corn oil or lard. They demonstrated that these high-fat diets make zebrafish obese (Meguro et al., 2015). Similarly, overfeeding the combination of a commercial tropical fish flakes (Tetramin) and 20% crude vegetable oil to zebrafish for 256 days triggers cardiovascular overload (Vargas and Vásquez, 2017).

It is interesting to note that obesity induced by overfeeding normal fat diet differs from that induced by high fat diet. Landgraf et al. compared the metabolic phenotype of obesity induced by overfeeding of a normal fat diet (NFD; *Artemia* cysts, 22% fat) to that by high fat diet (HFD; egg yolk powder, 59% fat). Although both increase adiposity, fish with NFD-induced obesity are metabolically healthy. In contrast, fish with HFD-induced obesity are metabolically unhealthy, with glucose intolerance, fatty liver, and preferential increase of visceral fat (Landgraf et al., 2017). This is consistent with the "obesity paradox" observed in humans. Overweight and obesity are not always associated with insulin resistance, the major driver and precursor of T2DM. In fact, overweight has also been paradoxically associated with lower mortality (Kokkinos et al., 2009; Flegal et al., 2013). This is thought to be due to the difference in the fat distribution pattern. In general, the visceral fat mass is a better predictor for insulin resistance and T2DM than BMI (Lebovitz and Banerji, 2005; InterAct et al., 2012). Therefore, the pathophysiological consequences of different fat depots are also conserved in zebrafish.

Genetic Models of Obesity

Obesity is a complex disease that results of an interaction between genetic and environmental factors. Genetically-modified animal models that reflect human obesity pathology are needed for understanding the physiological and genetic basis of obesity and for the development of pharmaceuticals to treat obesity. Genetic models of obesity have been characterized in zebrafish including transgenic lines expressing obesogenic genes or mutants from targeted mutagenesis and genetic screens.

TABLE 1 | Zebrafish obesity models.

	Type of model	Treatment or genetic manipulation	Age	Characteristics	References
Induced models	High-fat diet	Heavy whipping cream	Larvae	Lipid accumulation in intersegmental vessels; increased whole-larval triacylglycerol (TAG) and apolipoprotein B levels	Schlegel and Stainier, 2006
		Chicken egg yolk	Larvae, juvenile, adult	Hyperlipidemia, increased adipose tissue area and TAG	Tingaud-Sequeira et al., 2011; Zhou et al., 2015; Kopp et al., 2016; den Broeder et al., 2017; Landgraf et al., 2017
		Corn oil and lard	Adult	Increased body fat	Meguro et al., 2015
	Over-nutrition	Artemia	Adult	Increased BMI, hypertriglyceridemia and hepatosteatosis	Oka et al., 2010; Tainaka et al., 2011; Hasumura et al., 2012; Hiramitsu et al., 2014; Zang et al., 2014, 2015a; Meguro et al., 2015; Ran et al., 2017; Meguro and Hasumura, 2018
	Over-nutrition and high-fat diet	Tetramin and vegetable oil	Juvenile, adult	Increased weight gain, cardiovascular overload	Vargas and Vásquez, 2017
		Artemia and egg yolk powder	Adult	Increased body weight, adipose tissue mass, adipocyte hypertrophy, hyperglycemia and hepatosteatosis	Landgraf et al., 2017
Transgenic lines	*Tg(b-actin:AgRP)*	Overexpression of *agrp*	All stages	Increased linear growth, adipocyte hypertrophy	Ahima and Lazar, 2013
	Tg(-2.5β-Act:mCherry-miR-27b-SP)	miR-27b depletion	All stages	Hyperlipidemia, hepatic steatosis and increased white adipose tissue mass	Hsu et al., 2017
	Tg(krt4Hsa.myrAkt1)^{cy18}	Overexpression of *akt1*	Adult	Increased BMI, adipocyte hyperplasia, abnormal fat deposition, and glucose intolerance	Chu et al., 2012
Mutant lines	*Foie gras (hi*^{1532B}*)*	Mutation in *trappc11*	Larvae	Hepatomegaly and steatosis	Sadler et al., 2005; DeRossi et al., 2016
	cdipt$^{hi559Tg/+}$ *(hi*^{559}*)*	Mutation in *cdipt*	Larvae	Hepatic steatosis	Thakur et al., 2011
	harvest moon (hmn^{z110}*)*	Mutation in *gfpt1*	Larvae	Increased whole body TAG and hepatic steatosis	Hugo and Schlegel, 2017
	vmp1 (7466^{mu110}*)*	Mutation in *vmp1*	larvae	Hepatic steatosis	Kim et al., 2015
	ducttrip (dtp^{p14nb}*).*	Mutation in *achy*	Larvae	Mitochondrial dysfunction, hepatic steatosis, and disrupted exocrine pancreas	Yee et al., 2005
	red moon (rmn)	Mutation in *slc16a6a*	Larvae	Fasting hepatic steatosis	Hugo et al., 2012
	vizzini	Mutation in *gh1*	Larvae, adult	Decreased somatic growth, increased accumulation of adipose tissue	McMenamin et al., 2013
	cyp2r1 mutants	*cyp2r1* mutations	Adult	Growth retardation, increased adiposity	Peng et al., 2017
	plxnd1^{fov01b}	Mutation in *plxnd1*	Adult	Disproportional SAT, altered body fat distribution after high-fat feeding, protected from insulin resistance	Minchin et al., 2015

Underscoring the conservation of metabolic regulation, genetic manipulation of pathways that control body weight in mammalian systems also causes obesity in zebrafish. Transgenic zebrafish obesity models are often generated by mimicking existing mammalian models. The central melanocortin system (CMS), including peptides derived from proopiomelanocortin (POMC), their receptors (MC3R and MC4R), and Agouti-related peptide (AgRP), regulates energy homeostasis in zebrafish as it does in mammals (Ringholm et al., 2002; Hansen et al., 2003). Suppression of central melanocortin receptors by ectopic expression of the hair follicle restricted *Agouti* due to chromosomal translocations underlies one of the classical obese mouse models, Agouti Yellow (Bultman et al., 1992; Lu et al., 1994). This led to the identification of the endogenous melanocortin antagonist AgRP, whose transgenic overexpression in brain also causes obesity (Ollmann et al., 1997). In the zebrafish a genetic model of obesity has been developed by overexpressing AgRP [*Tg(b-actin:AgRP)*] (Song and Cone, 2007). These transgenic zebrafish exhibit an increase in body weight, linear growth, visceral adipose accumulation,

and total triglycerides in all stages. The increased adiposity results from both hypertrophic and hyperplastic growth of adipocytes (Song and Cone, 2007). This transgenic zebrafish model demonstrates that central regulation of metabolism is conserved. The microRNA miR-27b has been suggested to be a regulatory hub for lipid metabolism by inhibiting the translation of a number of key lipid-metabolism genes (Vickers et al., 2013). Although several lines of evidence from cell culture support a role of miR-27b in lipid metabolism (Karbiener et al., 2009; Kang et al., 2013), there was a lack of *in vivo* supporting evidence. Recently, Hsu et al. generated transgenic zebrafish lines to deplete miR-27b by expressing a miR-27b sponge (*C27bSP*) driven by the ubiquitous beta-actin promoter (*bC27bSP*) or the hepatocyte-specific *fabp10* promoter (*hC27bSP*). They demonstrated that the transgenic fish display hyperlipidemia, hepatic steatosis and increased white adipose tissue mass (Hsu et al., 2017), supporting a role of miR-27b in lipid metabolism *in vivo*. Another obesogenic model, *Tg(krt4Hsa.myrAkt1)*^{cy18}, was initially generated to study skin cancer. However, the transgenic adults were found to be obese, with increased BMI, adipocyte hyperplasia, abnormal fat deposition, and glucose intolerance. These phenotypes likely result from ectopic expression of the constitutively active human AKT1 in several mesenchymal derived tissues (Chu et al., 2012). *Tg(krt4Hsa.myrAkt1)*^{cy18} fish differ from *Tg(b-actin:AgRP)* in two aspects. First, *Tg(krt4Hsa.myrAkt1)*^{cy18} fish do not display adipocyte hypertrophy. Second, *Tg(krt4Hsa.myrAkt1)*^{cy18} fish exhibit ectopic lipoma-like adipose tissue in dorsal muscle, gill arches, and tail bone tissues, whereas *Tg(b-actin:AgRP)* fish show a normal distribution of adipocyte tissues.

Multiple mutant lines have been identified that reveal genes and pathways contributing to lipid metabolism and adipose tissue regulation. These mutants are identified often because they have fatty liver at larval stages. Still other mutants are identified as adults due to increased adiposity. Although these mutants may share a common phenotype, they are due to the disruption of a diverse number of processes. Many mutants have larval hepatic steatosis, or fatty liver due to ER stress. In a "shelf screen" for liver size, *Foie gras*, and *cdipt*$^{hi559Tg/+}$ were identified because they displayed fatty liver by 5 days of age (Sadler et al., 2005; Thakur et al., 2011). The affected gene product in *cdipt*$^{hi559Tg/+}$, Cdipt, is necessary for phosphatidylinositol synthesis and lack of phosphatidylinositol causes ER stress and lipid accumulation in hepatocytes (Thakur et al., 2011). The *Foie gras* mutant results from mutation in transport protein particle 11 (*trappc 11*) that encodes a protein critical for ER to Golgi vesicular transport. As a result, the mutation causes pathogenic ER stress in hepatocytes, leading to fatty liver (DeRossi et al., 2016).

Beyond ER stress, other pathways leading to fatty liver have been identified using staining of never-fed mutant larvae with lipophilic dyes (Schlegel and Stainier, 2006; Kim et al., 2015; Hugo and Schlegel, 2017). One of these mutants, *harvest moon* (*hmn*), results from a mutation in glutamine-fructose-6-phosphate transamidase (*gfpt1*) gene (Hugo and Schlegel, 2017), while another mutant, 7466^{mu110}, is caused by a mutation in vacuole membrane protein 1 (*vmp1*; Kim et al., 2015). These mutants feature lipid accumulation in hepatocytes and increased whole body adiposity and may provide clues to pathogenesis of fatty liver. Another mutant with fatty liver, *ducttrip* (*dtp*), was identified in a screen for mutations affecting the development of exocrine pancreas. The *dtp* mutant stems from a mutation in the gene encoding S-adenosylhomocysteine hydrolase and larvae exhibit mitochondrial dysfunction and liver degeneration in addition to hepatic steatosis and disrupted exocrine pancreas (Yee et al., 2005). While most fatty liver mutants do not survive to adulthood there are exceptions such as *red moon* (*rmn*) where both larvae and adults exhibit increased liver neutral lipids. The mutant is due to a loss-of-function of β-hydroxybutyrate transporter (*slc16a6a*; Hugo et al., 2012) and fatty liver results from the diversion of entrapped ketogenic precursor into lipids. Furthermore, the mutants are less tolerant of starvation. This mutant thus reveals a role of ketone body export in fasting energy homeostasis (Hugo et al., 2012). This diverse group of mutants highlights the complex regulation of lipid metabolism and how disruption at one node can lead to a phenotype of hepatic steatosis.

Other zebrafish mutants have alterations in adipose tissue. The zebrafish *vizzini* mutant exhibits decreased somatic growth and increased subcutaneous and visceral adipose tissues relative to body size. In *vizzini*, the subcutaneous adipose tissue (SAT) lipid droplets are extremely large although the number of lipid droplets in adipocytes is unchanged (McMenamin et al., 2013). This is due to a mutation in growth hormone 1 gene (*gh1*) leading to a premature stop codon. The phenotype is consistent with GH-deficient mice and humans that develop enlarged volume of SAT (Li et al., 1990; Wabitsch et al., 1995). Mutations in *cyp2r1* gene (Peng et al., 2017) also results in growth retardation and increased adiposity. These *cyp2r1* mutants are deficient in $1\alpha,25(OH)_2D_3$, the principal active form of vitamin D3, and 25(OH)D3 treatment rescues the growth and adiposity defects. In mammals, genetic and epidemiological data suggest a role of vitamin D deficiency in obesity, but vitamin D supplement fails to reduce the risk of obesity and associated pathologies (Rosen et al., 2012). These zebrafish mutants support a role of vitamin D in lipid metabolism and distribution. Mechanisms underlying distribution of adipose are critical as visceral fat is a better predictor than BMI of risk for cardiovascular diseases, insulin resistance and T2DM (Lebovitz and Banerji, 2005; InterAct et al., 2012). The loss of *plexin d1* function in zebrafish specifically impacts visceral fat (Minchin et al., 2015). PLEXIN D1 is one of the 67 genes identified in GWAS analyses in humans to be associated with visceral fat mass (Shungin et al., 2015), but the function of PLEXIN D1 in the distribution of fat mass was unknown. In zebrafish *plxnd1* mutants, visceral fat is reduced due to a decrease of lipid droplet size and adipocyte hyperplasia. Consequently, with high fat diet, the mutants preferentially store lipid in subcutaneous adipose tissue and are protected from developing insulin resistance (Minchin et al., 2015).

Taken together, these transgenic and mutant zebrafish lines further demonstrate conserved regulation of lipid metabolism. They also provide models in which to address mechanistic understanding of the underlying phenotypes.

Utilities of Zebrafish Obesity Models

One advantage of zebrafish models is the amenability for quick identification of chemical and genetic modifiers of the phenotype. The diet-induced obesity models have been used to test the effects of some dietary supplements on body fat accumulation. Green tea extract inhibited lipid accumulation (Tainaka et al., 2011; Meguro et al., 2015; Meguro and Hasumura, 2018), by decreasing the visceral adipose tissue volume and altering the expression of lipid catabolism genes (Hasumura et al., 2012). Eriocitrin, an antioxidative flavonoid in lemon, showed lipid-lowering effects in DIO zebrafish similar to that reported in a high-fat diet in rats (Hiramitsu et al., 2014). Oral administration of Yuzu (*Citrus junos* Siebold ex Tanaka) peel to DIO zebrafish exhibited anti-obesity effects by activating hepatic PPARα and adipocyte PPARγ pathways (Zang et al., 2014). Rhamnan sulfate, a sulphated polysaccharide from a marine green alga (*Monostroma nitidum*), also attenuated hepatic steatosis by suppressing lipogenesis (Zang et al., 2015a). Recently, a natural polyphenol, resveratrol, was reported to have anti-obesity effects via regulating lipid metabolism (Ran et al., 2017). Overall, DIO zebrafish is an attractive model system to evaluate the effects of functional foods and compounds on obesity development and treatment.

The diet-induced obesity models have also been used in drug testing. Tingaud-Sequeira et al. assessed the effect of small molecules on the whole-body adiposity after 24-h fasting in larvae previously overfed with egg yolk power (Tingaud-Sequeira et al., 2011). They found that two PPARγ agonists, rosiglitazone and TBT, a biocide found in antifouling paints, increases adiposity by inducing adipocyte hypertrophy and are thus obesogenic. In contrast, a PPARγ antagonist and an α1-adrenergic receptor agonist, known to promote lipolysis, are anti-obesogenic. Zhou et al. also performed proof of principle drug testing experiments using a similar model and found that all the 5 human hypolipidemic drugs exhibit significant hypolipidemic effect in zebrafish as they do in humans (Zhou et al., 2015). These results demonstrate the value of zebrafish obesity model on drug screening.

Genetic zebrafish models of obesity also provide mechanistic insights into the underlying causes. For instance, studies in the *cyp2r1* mutants that show increased adiposity and growth retardation identified *pgc1a* as a direct target for vitamin D receptor. As Pgc1a is a known master regulator of mitochondrial biogenesis, the study further showed that the increased adiposity results from impaired mitochondrial function (Peng et al., 2017). Similarly, using the *plxnd1* mutants, Minchin et al. investigated transcriptional changes in extracellular matrix genes (Minchin et al., 2015). They found that the mRNA and protein product of *col5a1* was increased and the visceral fat in the *plxnd1* mutants had more pronounced fibrillogenesis. Knocking down *col5a1* normalized the defects in visceral fat.

One cautionary note is that not all of the lipid metabolism genes are highly conserved in sequence and function in zebrafish. For example, the leptin protein of zebrafish is only 19% identical to the human protein. In mice and humans, leptin is an adipostatic hormone that regulates adipose mass, and failure of leptin signaling results in hyperphagia and obesity (Myers et al., 2010). Unlike mammals, leptin, and leptin receptor are not expressed in adipose tissue in zebrafish. Leptin receptor-deficient zebrafish primarily have disrupted glucose homeostasis (Michel et al., 2016), which is different from phenotypes observed in mouse models such as severe hyperphagia, hyperlipidemia and morbid obesity (Yen et al., 1976).

These examples illustrate the utility of zebrafish models for mechanistic investigations, drug testing and drug discovery in obesity and lipid metabolism. Thus far, the power these models remain largely untapped. It is anticipated that more mechanistic discoveries will be made from these and other zebrafish obesity models.

ZEBRAFISH DIABETES MODELS

Pancreas Development and Glucose Homeostasis in Zebrafish

The morphogenesis and basic cellular architecture of zebrafish pancreas is similar to mammalian pancreas (Tehrani and Lin, 2011) with both exocrine and endocrine compartments. The endocrine compartment consists of glucagon-secreting α-cells, insulin-producing β-cells, somatostatin-producing δ-cells, ghrelin-producing ε-cells and pancreatic polypeptide producing PP-cells. These cells are arranged in a manner similar to mouse islets (Argenton et al., 1999; Biemar et al., 2001). The signaling pathways and mechanisms of zebrafish endocrine pancreas development are highly homologous to those of mammals (Kinkel and Prince, 2009). In addition to the pancreas, development and function of other organ systems involved in glucose homeostasis, including brain, liver, adipocyte tissue and skeletal muscle, are also conserved (Maddison and Chen, 2017). The conservation of the pancreas structure and glucose homeostasis system make zebrafish useful to identify novel targets in pancreas related diseases such as diabetes.

Tools to Studies Glucose Homeostasis in Zebrafish

Numerous transgenic zebrafish strains with a fluorescent protein expression have been widely used to study pancreas development and glucose homeostasis in a whole living vertebrate (Kinkel and Prince, 2009; Tiso et al., 2009; Prince et al., 2017). For example, *Tg(-1.2ins:EGFP)* transgenic lines, where GFP expression is driven by the zebrafish preproinsulin promoter, provide a convenient fluorescent marker of β-cells (Xu et al., 2010) and insulin-expressing cells of the pancreatic islets can be visualized under a fluorescent microscope. Additionally, a transgenic line, *Tg(gcga:GFP)*, where GFP is driven by zebrafish preproglucagon promotor, marks pancreatic α-cell (Zecchin et al., 2007). Using these cell-specific transgenic lines, the β-cell and α-cell area and total numbers are easily measured to evaluate alterations in cell mass and number, which is a predictor for glucose clearance (Li et al., 2015; Maddison et al., 2015).

Methods for zebrafish pancreas function have been established, including fasting and postprandial glucose measurement, and intraperitoneal glucose tolerance tests as well as techniques for pancreas dissection and islet cell culture (Eames et al., 2010; Eames Nalle et al., 2017). In larvae, blood

collection for glucose measurement is not a viable methodology but free glucose in whole larvae can be measured by a coupled-enzyme fluorescent assay (Jurczyk et al., 2011). For adult zebrafish, the small size (3–4 cm) makes blood collection challenging. Nevertheless, several protocols for blood collection have been developed, such as lateral incision in the region of the dorsal aorta, decapitation and tail ablation although these methods require sacrifice of the animal (Jagadeeswaran et al., 1999; Eames et al., 2010; Velasco-Santamaría et al., 2011). However, a method for repeated blood collection in the same individual adult zebrafish has been developed (Zang et al., 2013, 2015b). Blood glucose can be measured by hand-held glucose-meters (Eames et al., 2010; Zang et al., 2015b). Protocols for glucose tolerance test (GTT) have also been developed in zebrafish (Kinkel et al., 2010; Matsuda et al., 2017; Zang et al., 2017), which is the most used approach to diagnose diabetes mellitus or glucose intolerance in humans.

Measuring insulin and insulin function has presented more of a challenge. As surrogate indicators, *insulin* mRNA levels can be determined directly by qPCR (Michel et al., 2016) and insulin promoter activity may be determined indirectly by measuring EGFP signal intensity in *Tg(−1.0ins:EGFP)*^{sc1} zebrafish (Zang et al., 2017). An insulin antibody for immunostaining both in whole larvae or adult zebrafish histologic sections is also available (Kimmel et al., 2015). Semi-quantitative dot-blot has been used to compare insulin levels in different fish simultaneously (Olsen et al., 2012). But insulin release has yet to be reliably measured in zebrafish. GFP has been used to replace the C-peptide of proinsulin in a transgenic line as one method to measure insulin release (Eames et al., 2013). Phosphorylation of Akt has been used to assess insulin function as a method to investigate early stage insulin resistance (Maddison et al., 2015; Landgraf et al., 2017). Insulin sensitivity can also be assessed by intraperitoneal injection of insulin in hyperglycemic zebrafish (Capiotti et al., 2014; Maddison et al., 2015).

Much of the biology in glucose homeostasis, from genes to organs, is conserved from zebrafish to humans. The application of powerful live imaging in zebrafish, coupled with genetic, and chemical genetic manipulations, will likely yield insights to many outstanding questions in diabetes.

Zebrafish Diabetes Models

Table 2 summaries zebrafish diabetes models developed by diet and genetic manipulations.

Type 1 Diabetes Mellitus Models

Type 1 diabetes mellitus (T1DM) is primarily an autoimmune disease caused by destruction of insulin producing pancreatic β-cells. Although an autoimmune derived T1DM model is lacking in zebrafish, several models have been developed using targeted β-cell damage. Three methods of β-cell destruction have been applied: surgical removal, chemical-dependent ablation, and genetic ablation. Pancreatectomy is feasible under the microscope in transgenic zebrafish with islet specific expression of GFP (Moss et al., 2009; Delaspre et al., 2015). However, this method is technically difficult and is not commonly used in zebrafish. Chemical-induced diabetes is widely used in rodents and also in zebrafish. Intraperitoneal injection of streptozotocin (STZ) is effective at β-cell ablation in adult zebrafish and eventually causes elevated fasting blood glucose and reduced insulin levels (Moss et al., 2009; Olsen et al., 2010; Intine et al., 2013). A total of 6 administrations of STZ within 4 weeks induces stable hyperglycemia and diabetic complications including retinopathy, nephropathy, and impaired fin regeneration. Alloxan can also selectively kill β-cells in zebrafish larvae (Nam et al., 2015; Castañeda et al., 2017). However, these compounds also exhibit other toxicity. Multiple genetic model of T1DM have been reported. Although stable expression of cell-lethal diphtheria toxin A chain (DTA) can eliminate all β-cells, these fish have growth retardation and fail to thrive (Ninov et al., 2013). Therefore, inducible β-cell ablation has been the preferred method for modeling T1DM. Two approaches of inducible β-cell ablation have been reported. In one approach, transgenic zebrafish lines with β-cell specific expression of the bacterial nitroreductase (NTR) enzyme, are exposed to the prodrug metronidazole (MTZ), the NTR substrate, which is converted into a cytotoxic compound that rapidly induces β-cell apoptosis (Curado et al., 2007, 2008; Pisharath et al., 2007; Ye et al., 2015). This NTR/MTZ ablation system is used for β-cell regeneration research as the elimination of β-cell occurs in 18–24 h after MTZ administration and recovers within 3–4 days after MTZ washout. A different approach has been to use a combinatorial, inducible transgene where the insulin promoter drives the expression of a doxycycline/ecdysone-dependent transcription factor and the TetOR-based promoter to express activated human Bid that triggers apoptosis (Li et al., 2014). Ablation models all face the same hurdle in that zebrafish have a remarkable regenerative capacity and β-cell mass is restored once the ablation mechanism is removed.

Type 2 Diabetes Mellitus Models

T2DM is characterized by insulin resistance and β-cell dysfunction. β-cell death may also occur in long standing T2DM. Both nutritional and genetic approaches have been used to generate T2DM models in zebrafish. Immersion of zebrafish in glucose solution is a widely-used method because of its convenience. Immersing adult zebrafish into alternating concentrations of 0 and 2% glucose every other day for 28–30 days, or chronic exposure to 2% glucose solution for 14 days, induces diabetic phenotypes, including elevated blood glucose levels and impaired response to exogenous insulin (Gleeson et al., 2007; Alvarez et al., 2010; Capiotti et al., 2014), similar to mice following 6 weeks of high-galactose diet (Joussen et al., 2009). Young zebrafish (4–11 months) acclimate to glucose exposure better than older zebrafish (1–3 years), but persistent hyperglycemia, can be achieved even in young zebrafish by gradually increasing the glucose concentration (Connaughton et al., 2016).

Obesity is the major risk factor for T2DM. High-fat diet causes both obesity and T2DM in rodent models (Winzell and Ahrén, 2004). In zebrafish, overfeeding with a commercial food quickly caused insulin resistance, elevated fasting blood glucose, and impaired glucose tolerance (Zang et al., 2017). Calorie restriction

TABLE 2 | Zebrafish diabetic models.

Model type		Disease type	Treatment or genetic manipulation	Age	Phenotype	References	Disadvantage
Induced models	Pancreatectomy	T1DM	physical removal of pancreas	Adult	Elevated blood glucose levels	Moss et al., 2009; Delaspre et al., 2015	Technically difficult
	Chemical-ablation of β-cells	T1DM	Intraperitoneal injection of streptozotocin (STZ)	Adult	Hyperglycemia and diabetic complications	Moss et al., 2009; Olsen et al., 2010; Intine et al., 2013	Rapid recovery
		T1DM	Alloxane exposure through incubation or IP injection	Larvae, adult	β-cell necrosis, decreased neuromast number,	Moss et al., 2009; Nam et al., 2015; Castañeda et al., 2017	Rapid recovery
	Glucose immersion	T2DM	Incubation in glucose solution	Adult	Hyperglycaemia, impaired response to inuslin, diabetic retinopathy	Gleeson et al., 2007; Alvarez et al., 2010; Capiotti et al., 2014; Connaughton et al., 2016	Requires frequent solution exchange
	Over-nutrition	T2DM & Obesity	Overfeeding zebrafish with a commercial food	Adult	Hyperglycaemia, glucose intolerance, insulin resistance	Zang et al., 2017	
Targeted genetic ablation	NTR-mediated cell ablation	T1DM	Nitroreductase (NTR) expressing transgenic lines exposed to metronidazole (MTZ) through incubation or IP injection	Larvae, adult	Destroyed islet tissue, increased blood glucose levels	Curado et al., 2007, 2008; Pisharath et al., 2007; Moss et al., 2009; Ninov et al., 2013; Delaspre et al., 2015; Ye et al., 2015	Rapid recovery
	Induction of apoptosis through expression of activated Bid	T1DM	*Tg(1.2ins:htBid^{TE-ON}; LR)* Induced by doxycycline and tebufenozide	Larvae	β-cell ablation, increased free glucose levels	Li et al., 2014	Rapid recovery
Transgenic lines	*Tg(acta1:dnIGF1R-EGFP)*	T2DM	Transgenic expression of a dominant-negative IGF-I receptor (IGF-IR) in skeletal muscle	Adult	Increased fasting blood glucose level	Zang et al., 2017	
	Tg(actb2:cas9; (U6x:sgRNA(insra/b)	T2DM	Liver specific knockdown of the insulin receptor a and b	Larvae	Hyperglycemia, insulin resistance	Yin et al., 2015	
	Tg(C43G-GFP)	MODY 10	Transgenic expression of C43G human proinsulin	Larvae, adult	Normal glucose homeostasis, no loss in β-cell mass	Eames et al., 2013	
Mutant lines	*liger^{s430} (hnf1ba^{s430})*	MODY5	Mutation in *hnf1ba*	Larvae	MODY5-like pancreas hypoplasia, reduced β-cell numbers	Lancman et al., 2013	
	CRISPR induced gene deficiency	MODY6	Mutation in *neurod1*	Larvae	Failed endocrine cell differentiation, increased free glucose levels	Dalgin and Prince, 2015	
	pdx1^{sa280}	MODY4	Mutation in *pdx1*	Larvae, adult	Reduced β-cell numbers, disrupted glucose homeostasis, sensitivity to overnutrition	Kimmel et al., 2015	

and anti-diabetic drugs (metformin and glimepiride) ameliorated the hyperglycemia in the overfed zebrafish. These drugs are both frequently prescribed treatments for T2DM and their effectiveness in the zebrafish model demonstrates conservation in glucose homeostasis pathways.

Insulin resistance is a major driver of T2DM. Our lab has developed two transgenic models of insulin resistance. In one model, skeletal muscle insulin resistance is achieved by transgenic expression of a dominant-negative IGF-I receptor (IGF-IR) in skeletal muscle. The transgenic fish showed impaired Akt phosphorylation postprandially or after insulin administration (Maddison et al., 2015). These fish had significantly increased fasting blood glucose as early as 3-month old compared to wild-type fish and is exacerbated by overfeeding (unpublished data). In the other model, insulin resistance is achieved through liver specific knockdown of the insulin receptors using CRISPR/Cas9 (Yin et al., 2015). Similar to mice and humans, liver insulin resistance causes fasting hypoglycemia and postprandial hyperglycemia. Since muscle and liver insulin resistance are thought to be the major drivers of T2DM, these models will be useful to dissect the progression of T2DM.

Another type of diabetes, MODY (maturity-onset diabetes of the young), is a rare, autosomal dominant, noninsulin-dependent and monogenic form of diabetes resulting from pancreatic β-cell dysfunction with an onset before 25 years of age. Since this disease is caused by mutation in a single gene, with different genes leading to different forms, MODY models can be developed by targeted gene ablation. However, as in mice, the mode of inheritance in MODY gene mutations is usually recessive, not autosomal dominant. MODY5 stems from mutations in hepatocyte nuclear factor 1β (HNF1β). A zebrafish *hnf1ba* mutant line (*hnf1ba*^{s430}) was identified from a zebrafish ENU mutagenesis screen (Lancman et al., 2013). The homozygous mutants exhibit pancreas hypoplasia and reduced β-cell numbers similar to MODY5. MODY6 results from mutations in NEUROD1 (Malecki et al., 1999). In mice, disruption of *NeuroD1* leads to diabetes and premature death (Naya et al., 1997). In zebrafish *neurod1* deficiency led to failed endocrine cell differentiation and increased free glucose levels in larvae (Dalgin and Prince, 2015). MODY4 is a result of PDX1 mutation (Stoffers et al., 1997) and a *pdx1* mutant line exhibited reduced β-cell numbers, disrupted glucose homeostasis, sensitivity to over-nutrition and is responsive to anti-diabetic drug treatment (Kimmel et al., 2015). The adult *pdx1* mutant zebrafish have small body size and decreased viability. MODY10 results from mutations in INS gene (Meur et al., 2010). A transgenic line expressing a mutated preproinsulin protein (C43G) has been developed (Eames et al., 2013). Interestingly, glucose homeostasis and β-cell mass were not altered in these fish, even though excess proinsulin accumulates in endoplasmic reticulum (ER). This could be due to the regenerative capacity of the zebrafish leading to turnover of the dysfunctional β-cells. However, this provides an opportunity to investigate misfolded proinsulin and ER stress in a non-diabetic *in vivo* system. Together, these MODY models develop phenotypes observed in patients, further supporting the utility of zebrafish as a diabetes model.

Although an appropriate model is still lacking for studying the long-term effect of diabetes, there have been approaches to study diabetic complications. For example, long immersion of larval or adult zebrafish in glucose solution has been used to model chronic hyperglycemia (Capiotti et al., 2014; Connaughton et al., 2016). This approach has been used to study diabetic retinopathy (Gleeson et al., 2007; Jung et al., 2016) as well as changes in bone metabolism (Carnovali et al., 2016). Inducing hyperglycemia through repeated STZ treatment in adult fish can impair wound healing (Olsen et al., 2010) and can cause heritable epigenetic changes after normalization of glycemia (Olsen et al., 2012). These studies underscore the lasting consequences of disrupting glucose control in zebrafish.

Overall, zebrafish offers particular advantages to the study of metabolic diseases. Models for studying obesity, pancreas regeneration, hyperglycemia, and diabetic complications have been established and will promote the understanding of the disease mechanisms, and provide new targets for disease therapy.

AUTHOR CONTRIBUTIONS

All authors listed have made a substantial, direct and intellectual contribution to the work, and approved it for publication.

FUNDING

Supported by ADA 1-13-BS-27 and a Vanderbilt DRTC Pilot and Feasibility Grant (WC), R01 DK109407 (WC), and by JSPS KAKENHI Grant Number 15KK0305 (LZ).

REFERENCES

Ahima, R. S., and Lazar, M. A. (2013). Physiology. The health risk of obesity–better metrics imperative. *Science* 341, 856–858. doi: 10.1126/science.1241244

Alvarez, Y., Chen, K., Reynolds, A. L., Waghorne, N., O'Connor, J. J., and Kennedy, B. N. (2010). Predominant cone photoreceptor dysfunction in a hyperglycaemic model of non-proliferative diabetic retinopathy. *Dis. Model. Mech.* 3, 236–245. doi: 10.1242/dmm.003772

Anderson, J. L., Carten, J. D., and Farber, S. A. (2011). Zebrafish lipid metabolism: from mediating early patterning to the metabolism of dietary fat and cholesterol. *Methods Cell Biol.* 101, 111–141. doi: 10.1016/B978-0-12-387036-0.00005-0

Argenton, F., Zecchin, E., and Bortolussi, M. (1999). Early appearance of pancreatic hormone-expressing cells in the zebrafish embryo. *Mech. Dev.* 87, 217–221. doi: 10.1016/S0925-4773(99)00151-3

Biemar, F., Argenton, F., Schmidtke, R., Epperlein, S., Peers, B., and Driever, W. (2001). Pancreas development in zebrafish: early dispersed appearance of endocrine hormone expressing cells and their convergence to form the definitive islet. *Dev. Biol.* 230, 189–203. doi: 10.1006/dbio.2000.0103

Bultman, S. J., Michaud, E. J., and Woychik, R. P. (1992). Molecular characterization of the mouse agouti locus. *Cell* 71, 1195–1204. doi: 10.1016/S0092-8674(05)80067-4

Cai, D. (2013). Neuroinflammation and neurodegeneration in overnutrition-induced diseases. *Trends Endocrin. Met.* 24, 40–47. doi: 10.1016/j.tem.2012.11.003

Capiotti, K. M., Antonioli, R. Jr., Kist, L. W., Bogo, M. R., Bonan, C. D., and Da Silva, R. S. (2014). Persistent impaired glucose metabolism in a zebrafish hyperglycemia model. *Comp. Biochem. Physiol. B Biochem. Mol. Biol.* 171, 58–65. doi: 10.1016/j.cbpb.2014.03.005

Carnovali, M., Luzi, L., Banfi, G., and Mariotti, M. (2016). Chronic hyperglycemia affects bone metabolism in adult zebrafish scale model. *Endocrine* 54, 808–817. doi: 10.1007/s12020-016-1106-3

Castañeda, R., Rodriguez, I., Nam, Y. H., Hong, B. N., and Kang, T. H. (2017). Trigonelline promotes auditory function through nerve growth factor signaling on diabetic animal models. *Phytomedicine* 36, 128–136. doi: 10.1016/j.phymed.2017.09.023

Chu, C. Y., Chen, C. F., Rajendran, R. S., Shen, C. N., Chen, T. H., Yen, C. C., et al. (2012). Overexpression of Akt1 enhances adipogenesis and leads to lipoma formation in zebrafish. *PLoS ONE* 7:e36474. doi: 10.1371/journal.pone.0036474

Connaughton, V. P., Baker, C., Fonde, L., Gerardi, E., and Slack, C. (2016). Alternate immersion in an external glucose solution differentially affects blood sugar values in older versus younger zebrafish adults. *Zebrafish* 13, 87–94. doi: 10.1089/zeb.2015.1155

Curado, S., Anderson, R. M., Jungblut, B., Mumm, J., Schroeter, E., and Stainier, D. Y. (2007). Conditional targeted cell ablation in zebrafish: a new tool for regeneration studies. *Dev. Dyn.* 236, 1025–1035. doi: 10.1002/dvdy.21100

Curado, S., Stainier, D. Y., and Anderson, R. M. (2008). Nitroreductase-mediated cell/tissue ablation in zebrafish: a spatially and temporally controlled ablation method with applications in developmental and regeneration studies. *Nat. Protoc.* 3, 948–954. doi: 10.1038/nprot.2008.58

Dailey, M. J. (2014). Nutrient-induced intestinal adaption and its effect in obesity. *Physiol. Behav.* 136, 74–78. doi: 10.1016/j.physbeh.2014.03.026

Dalgin, G., and Prince, V. E. (2015). Differential levels of Neurod establish zebrafish endocrine pancreas cell fates. *Dev. Biol.* 402, 81–97. doi: 10.1016/j.ydbio.2015.03.007

Delaspre, F., Beer, R. L., Rovira, M., Huang, W., Wang, G., Gee, S., et al. (2015). Centroacinar cells are progenitors that contribute to endocrine pancreas regeneration. *Diabetes* 64, 3499–3509. doi: 10.2337/db15-0153

Den Broeder, M. J., Kopylova, V. A., Kamminga, L. M., and Legler, J. (2015). Zebrafish as a model to study the role of peroxisome proliferating-activated receptors in adipogenesis and obesity. *PPAR Res.* 2015:358029. doi: 10.1155/2015/358029

den Broeder, M. J., Moester, M. J. B., Kamstra, J. H., Cenijn, P. H., Davidoiu, V., Kamminga, L. M., et al. (2017). Altered adipogenesis in zebrafish larvae following high fat diet and chemical exposure is visualised by stimulated raman scattering microscopy. *Int. J. Mol. Sci.* 18:E894. doi: 10.3390/ijms18040894

DeRossi, C., Vacaru, A., Rafiq, R., Cinaroglu, A., Imrie, D., Nayar, S., et al. (2016). Trappc11 is required for protein glycosylation in zebrafish and humans. *Mol. Biol. Cell* 27, 1220–1234. doi: 10.1091/mbc.e15-08-0557

Dooley, K., and Zon, L. I. (2000). Zebrafish: a model system for the study of human disease. *Curr. Opin. Genet. Dev.* 10, 252–256. doi: 10.1016/S0959-437X(00)00074-5

Eames Nalle, S. C., Franse, K. F., and Kinkel, M. D. (2017). Analysis of pancreatic disease in zebrafish. *Method Cell Biol.* 138, 271–295. doi: 10.1016/bs.mcb.2016.08.005

Eames, S. C., Kinkel, M. D., Rajan, S., Prince, V. E., and Philipson, L. H. (2013). Transgenic zebrafish model of the C43G human insulin gene mutation. *J. Diabetes Investig.* 4, 157–167. doi: 10.1111/jdi.12015

Eames, S. C., Philipson, L. H., Prince, V. E., and Kinkel, M. D. (2010). Blood sugar measurement in zebrafish reveals dynamics of glucose homeostasis. *Zebrafish* 7, 205–213. doi: 10.1089/zeb.2009.0640

Elo, B., Villano, C. M., Govorko, D., and White, L. A. (2007). Larval zebrafish as a model for glucose metabolism: expression of phosphoenolpyruvate carboxykinase as a marker for exposure to anti-diabetic compounds. *J. Mol. Endocrinol.* 38, 433–440. doi: 10.1677/JME-06-0037

Feierstein, C. E., Portugues, R., and Orger, M. B. (2015). Seeing the whole picture: a comprehensive imaging approach to functional mapping of circuits in behaving zebrafish. *Neuroscience* 296, 26–38. doi: 10.1016/j.neuroscience.2014.11.046

Flegal, K. M., Kit, B. K., Orpana, H., and Graubard, B. I. (2013). Association of all-cause mortality with overweight and obesity using standard body mass index categories: a systematic review and meta-analysis. *JAMA* 309, 71–82. doi: 10.1001/jama.2012.113905

Flynn, E. J. III, Trent, C. M., and Rawls, J. F. (2009). Ontogeny and nutritional control of adipogenesis in zebrafish (Danio rerio). *J. Lipid Res.* 50, 1641–1652. doi: 10.1194/jlr.M800590-JLR200

Freifeld, L., Odstrcil, I., Förster, D., Ramirez, A., Gagnon, J. A., Randlett, O., et al. (2017). Expansion microscopy of zebrafish for neuroscience and developmental biology studies. *Proc. Natl. Acad. Sci. U.S.A.* 114, E10799–E10808. doi: 10.1073/pnas.1706281114

Fuchsberger, C., Flannick, J., Teslovich, T. M., Mahajan, A., Agarwala, V., Gaulton, K. J., et al. (2016). The genetic architecture of type 2 diabetes. *Nature* 536, 41–47. . doi: 10.1038/nature18642

Gibert, Y., Trengove, M. C., and Ward, A. C. (2013). Zebrafish as a genetic model in pre-clinical drug testing and screening. *Curr. Med. Chem.* 20, 2458–2466. doi: 10.2174/0929867311320190005

Gleeson, M., Connaughton, V., and Arneson, L. S. (2007). Induction of hyperglycaemia in zebrafish (Danio rerio) leads to morphological changes in the retina. *Acta Diabetol.* 44, 157–163. doi: 10.1007/s00592-007-0257-3

Greenspan, P., Mayer, E. P., and Fowler, S. D. (1985). Nile red: a selective fluorescent stain for intracellular lipid droplets. *J. Cell Biol.* 100, 965–973. doi: 10.1083/jcb.100.3.965

Hall, C., Flores, M. V., Crosier, K., and Crosier, P. (2009). Live cell imaging of zebrafish leukocytes. *Methods Mol. Biol.* 546, 255–271. doi: 10.1007/978-1-60327-977-2_16

Hansen, I. A., To, T. T., Wortmann, S., Burmester, T., Winkler, C., Meyer, S. R., et al. (2003). The pro-opiomelanocortin gene of the zebrafish (Danio rerio). *Biochem. Biophys. Res. Commun.* 303, 1121–1128. doi: 10.1016/S0006-291X(03)00475-3

Haslam, D. W., and James, W. P. (2005). Obesity. *Lancet* 366, 1197–1209. doi: 10.1016/S0140-6736(05)67483-1

Hasumura, T., Shimada, Y., Kuroyanagi, J., Nishimura, Y., Meguro, S., Takema, Y., et al. (2012). Green tea extract suppresses adiposity and affects the expression of lipid metabolism genes in diet-induced obese zebrafish. *Nutr. Metab.* 9:73. doi: 10.1186/1743-7075-9-73

Herrgen, L., Schröter, C., Bajard, L., and Oates, A. C. (2009). Multiple embryo time-lapse imaging of zebrafish development. *Methods Mol. Biol.* 546, 243–254. doi: 10.1007/978-1-60327-977-2_15

Hiramitsu, M., Shimada, Y., Kuroyanagi, J., Inoue, T., Katagiri, T., Zang, L., et al. (2014). Eriocitrin ameliorates diet-induced hepatic steatosis with activation of mitochondrial biogenesis. *Sci. Rep.* 4:3708. doi: 10.1038/srep03708

Hölttä-Vuori, M., Salo, V. T., Nyberg, L., Brackmann, C., Enejder, A., Panula, P., et al. (2010). Zebrafish: gaining popularity in lipid research. *Biochem. J.* 429, 235–242. doi: 10.1042/BJ20100293

Hoshijima, K., Jurynec, M. J., and Grunwald, D. J. (2016). Precise editing of the zebrafish genome made simple and efficient. *Dev. Cell* 36, 654–667. doi: 10.1016/j.devcel.2016.02.015

Hsu, C. C., Lai, C. Y., Lin, C. Y., Yeh, K. Y., and Her, G. M. (2017). MicroRNA-27b Depletion Enhances Endotrophic and Intravascular Lipid Accumulation and Induces Adipocyte Hyperplasia in Zebrafish. *Int. J. Mol. Sci.* 19:E93. doi: 10.3390/ijms19010093

Hugo, S. E., Cruz-Garcia, L., Karanth, S., Anderson, R. M., Stainier, D. Y., and Schlegel, A. (2012). A monocarboxylate transporter required for hepatocyte secretion of ketone bodies during fasting. *Genes Dev.* 26, 282–293. doi: 10.1101/gad.180968.111

Hugo, S. E., and Schlegel, A. (2017). A genetic screen for zebrafish mutants with hepatic steatosis identifies a locus required for larval growth. *J. Anat.* 230, 407–413. doi: 10.1111/joa.12570

Imrie, D., and Sadler, K. C. (2010). White adipose tissue development in zebrafish is regulated by both developmental time and fish size. *Dev. Dyn.* 239, 3013–3023. doi: 10.1002/dvdy.22443

InterAct, C., Langenberg, C., Sharp, S. J., Schulze, M. B., Rolandsson, O., Overvad, K., et al. (2012). Long-term risk of incident type 2 diabetes and measures of overall and regional obesity: the EPIC-InterAct case-cohort study. *PLoS Med.* 9:e1001230. doi: 10.1371/journal.pmed.1001230

Intine, R. V., Olsen, A. S., and Sarras, M. P. Jr. (2013). A zebrafish model of diabetes mellitus and metabolic memory. *J. Vis. Exp.* 72:e50232. doi: 10.3791/50232

Jagadeeswaran, P., Sheehan, J. P., Craig, F. E., and Troyer, D. (1999). Identification and characterization of zebrafish thrombocytes. *Br. J. Haematol.* 107, 731–738. doi: 10.1046/j.1365-2141.1999.01763.x

Jones, K. S., Alimov, A. P., Rilo, H. L., Jandacek, R. J., Woollett, L. A., and Penberthy, W. T. (2008). A high throughput live transparent animal bioassay to identify non-toxic small molecules or genes that regulate vertebrate fat metabolism for obesity drug development. *Nutr. Metab.* 5:23. doi: 10.1186/1743-7075-5-23

Joussen, A. M., Doehmen, S., Le, M. L., Koizumi, K., Radetzky, S., Krohne, T. U., et al. (2009). TNF-alpha mediated apoptosis plays an important role in the development of early diabetic retinopathy and long-term histopathological alterations. *Mol. Vis.* 15, 1418–1428.

Jung, S. H., Kim, Y. S., Lee, Y. R., and Kim, J. S. (2016). High glucose-induced changes in hyaloid-retinal vessels during early ocular development of zebrafish: a short-term animal model of diabetic retinopathy. *Br. J. Pharmacol.* 173, 15–26. doi: 10.1111/bph.13279

Jurczyk, A., Roy, N., Bajwa, R., Gut, P., Lipson, K., Yang, C., et al. (2011). Dynamic glucoregulation and mammalian-like responses to metabolic and developmental disruption in zebrafish. *Gen. Comp. Endocrinol.* 170, 334–345. doi: 10.1016/j.ygcen.2010.10.010

Kang, T., Lu, W., Xu, W., Anderson, L., Bacanamwo, M., Thompson, W., et al. (2013). MicroRNA-27 (miR-27) targets prohibitin and impairs adipocyte differentiation and mitochondrial function in human adipose-derived stem cells. *J. Biol. Chem.* 288, 34394–34402. doi: 10.1074/jbc.M113.514372

Karbiener, M., Fischer, C., Nowitsch, S., Opriessnig, P., Papak, C., Ailhaud, G., et al. (2009). microRNA miR-27b impairs human adipocyte differentiation and targets PPARgamma. *Biochem. Biophys. Res. Commun.* 390, 247–251. doi: 10.1016/j.bbrc.2009.09.098

Kim, S. H., Wu, S. Y., Baek, J. I., Choi, S. Y., Su, Y., Flynn, C. R., et al. (2015). A post-developmental genetic screen for zebrafish models of inherited liver disease. *PLoS ONE* 10:e0125980. doi: 10.1371/journal.pone.0125980

Kimmel, C. B., Ballard, W. W., Kimmel, S. R., Ullmann, B., and Schilling, T. F. (1995). Stages of embryonic development of the zebrafish. *Dev. Dyn.* 203, 253–310. doi: 10.1002/aja.1002030302

Kimmel, R. A., Dobler, S., Schmitner, N., Walsen, T., Freudenblum, J., and Meyer, D. (2015). Diabetic pdx1-mutant zebrafish show conserved responses to nutrient overload and anti-glycemic treatment. *Sci. Rep.* 5:14241. doi: 10.1038/srep14241

Kimura, Y., Hisano, Y., Kawahara, A., and Higashijima, S. (2014). Efficient generation of knock-in transgenic zebrafish carrying reporter/driver genes by CRISPR/Cas9-mediated genome engineering. *Sci. Rep.* 4:6545. doi: 10.1038/srep06545

Kinkel, M. D., Eames, S. C., Philipson, L. H., and Prince, V. E. (2010). Intraperitoneal injection into adult zebrafish. *J. Vis. Exp.* 42:2126. doi: 10.3791/2126

Kinkel, M. D., and Prince, V. E. (2009). On the diabetic menu: zebrafish as a model for pancreas development and function. *Bioessays* 31, 139–152. doi: 10.1002/bies.200800123

Kokkinos, P., Myers, J., Nylen, E., Panagiotakos, D. B., Manolis, A., Pittaras, A., et al. (2009). Exercise capacity and all-cause mortality in African American and Caucasian men with type 2 diabetes. *Diabetes Care* 32, 623–628. doi: 10.2337/dc08-1876

Kopp, R., Billecke, N., Legradi, J., den Broeder, M., Parekh, S. H., and Legler, J. (2016). Bringing obesity to light: rev-erbalpha, a central player in light-induced adipogenesis in the zebrafish? *Int. J. Obes.* 40, 824–832. doi: 10.1038/ijo.2015.240

Lancman, J. J., Zvenigorodsky, N., Gates, K. P., Zhang, D., Solomon, K., Humphrey, R. K., et al. (2013). Specification of hepatopancreas progenitors in zebrafish by hnf1ba and wnt2bb. *Development* 140, 2669–2679. doi: 10.1242/dev.090993

Landgraf, K., Schuster, S., Meusel, A., Garten, A., Riemer, T., Schleinitz, D., et al. (2017). Short-term overfeeding of zebrafish with normal or high-fat diet as a model for the development of metabolically healthy versus unhealthy obesity. *BMC Physiol.* 17,4. doi: 10.1186/s12899-017-0031-x

Lawlor, N., Khetan, S., Ucar, D., and Stitzel, M. L. (2017). Genomics of Islet (Dys)function and Type 2 Diabetes. *Trends Genet.* 33, 244–255. doi: 10.1016/j.tig.2017.01.010

Lebovitz, H. E., and Banerji, M. A. (2005). Point: visceral adiposity is causally related to insulin resistance. *Diabetes Care* 28, 2322–2325. doi: 10.2337/diacare.28.9.2322

Leung, M. Y., Carlsson, N. P., Colditz, G. A., and Chang, S. H. (2017). The burden of obesity on diabetes in the united states: medical expenditure panel survey, 2008 to 2012. *Value Health* 20, 77–84. doi: 10.1016/j.jval.2016.08.735

Li, M., Dean, E. D., Zhao, L., Nicholson, W. E., Powers, A. C., and Chen, W. (2015). Glucagon receptor inactivation leads to alpha-cell hyperplasia in zebrafish. *J. Endocrinol.* 227, 93–103. doi: 10.1530/JOE-15-0284

Li, M., Maddison, L. A., Page-McCaw, P., and Chen, W. (2014). Overnutrition induces beta-cell differentiation through prolonged activation of beta-cells in zebrafish larvae. *Am. J. Physiol. Endocrinol. Metab.* 306, E799–E807. doi: 10.1152/ajpendo.00686.2013

Li, S., Crenshaw, E. B. III., Rawson, E. J., Simmons, D. M., Swanson, L. W., and Rosenfeld, M. G. (1990). Dwarf locus mutants lacking three pituitary cell types result from mutations in the POU-domain gene pit-1. *Nature* 347, 528–533. doi: 10.1038/347528a0

Lieschke, G. J., and Currie, P. D. (2007). Animal models of human disease: zebrafish swim into view. *Nat. Rev. Genet.* 8, 353–367. doi: 10.1038/nrg2091

Loos, R. J. (2018). The genetics of adiposity. *Curr. Opin. Genet. Dev.* 50, 86–95. doi: 10.1016/j.gde.2018.02.009

Lu, D., Willard, D., Patel, I. R., Kadwell, S., Overton, L., Kost, T., et al. (1994). Agouti protein is an antagonist of the melanocyte-stimulating-hormone receptor. *Nature* 371, 799–802. doi: 10.1038/371799a0

MacRae, C. A., and Peterson, R. T. (2015). Zebrafish as tools for drug discovery. *Nat. Rev. Drug Discov.* 14, 721–731. doi: 10.1038/nrd4627

Maddison, L. A., and Chen, W. B. (2017). Modeling pancreatic endocrine cell adaptation and diabetes in the zebrafish. *Front Endocrinol.* 8:9. doi: 10.3389/fendo.2017.00009

Maddison, L. A., Joest, K. E., Kammeyer, R. M., and Chen, W. (2015). Skeletal muscle insulin resistance in zebrafish induces alterations in beta-cell number and glucose tolerance in an age- and diet-dependent manner. *Am. J. Physiol. Endocrinol. Metab.* 308, E662–E669. doi: 10.1152/ajpendo.00441.2014

Malecki, M. T., Jhala, U. S., Antonellis, A., Fields, L., Doria, A., Orban, T., et al. (1999). Mutations in NEUROD1 are associated with the development of type 2 diabetes mellitus. *Nat. Genet.* 23, 323–328. doi: 10.1038/15500

Marza, E., Barthe, C., André, M., Villeneuve, L., Hélou, C., and Babin, P. J. (2005). Developmental expression and nutritional regulation of a zebrafish gene homologous to mammalian microsomal triglyceride transfer protein large subunit. *Dev. Dyn.* 232, 506–518. doi: 10.1002/dvdy.20251

Matsuda, H., Mullapudi, S. T., Zhang, Y. X., Hesselson, D., and Stainier, D. Y. R. (2017). Thyroid hormone coordinates pancreatic islet maturation during the zebrafish larval-to-juvenile transition to maintain glucose homeostasis. *Diabetes* 66, 2623–2635. doi: 10.2337/db16-1476

McMenamin, S. K., Minchin, J. E., Gordon, T. N., Rawls, J. F., and Parichy, D. M. (2013). Dwarfism and increased adiposity in the gh1 mutant zebrafish vizzini. *Endocrinology* 154, 1476–1487. doi: 10.1210/en.2012-1734

Meguro, S., and Hasumura, T. (2018). Fish oil suppresses body fat accumulation in zebrafish. *Zebrafish* 15, 27–32. doi: 10.1089/zeb.2017.1475

Meguro, S., Hasumura, T., and Hase, T. (2015). Body fat accumulation in zebrafish is induced by a diet rich in fat and reduced by supplementation with green tea extract. *PLoS ONE* 10:e0120142. doi: 10.1371/journal.pone.0120142

Meur, G., Simon, A., Harun, N., Virally, M., Dechaume, A., Bonnefond, A., et al. (2010). Insulin gene mutations resulting in early-onset diabetes: marked differences in clinical presentation, metabolic status, and pathogenic effect through endoplasmic reticulum retention. *Diabetes* 59, 653–661. doi: 10.2337/db09-1091

Michel, M., Page-McCaw, P. S., Chen, W., and Cone, R. D. (2016). Leptin signaling regulates glucose homeostasis, but not adipostasis, in the zebrafish. *Proc. Natl. Acad. Sci. U.S.A.* 113, 3084–3089. doi: 10.1073/pnas.1513212113

Minchin, J. E., Dahlman, I., Harvey, C. J., Mejhert, N., Singh, M. K., Epstein, J. A., et al. (2015). Plexin D1 determines body fat distribution by regulating the type V collagen microenvironment in visceral adipose tissue. *Proc. Natl. Acad. Sci. U.S.A.* 112, 4363–4368. doi: 10.1073/pnas.1416412112

Moss, J. B., Koustubhan, P., Greenman, M., Parsons, M. J., Walter, I., and Moss, L. G. (2009). Regeneration of the pancreas in adult zebrafish. *Diabetes* 58, 1844–1851. doi: 10.2337/db08-0628

Myers, M. G. Jr., Leibel, R. L., Seeley, R. J., and Schwartz, M. W. (2010). Obesity and leptin resistance: distinguishing cause from effect. *Trends Endocrinol. Metab.* 21, 643–651. doi: 10.1016/j.tem.2010.08.002

Nam, Y. H., Hong, B. N., Rodriguez, I., Ji, M. G., Kim, K., Kim, U. J., et al. (2015). Synergistic potentials of coffee on injured pancreatic islets and insulin action via KATP channel blocking in zebrafish. *J. Agric. Food Chem.* 63, 5612–5621. doi: 10.1021/acs.jafc.5b00027

Naya, F. J., Huang, H. P., Qiu, Y. H., Mutoh, H., DeMayo, F. J., Leiter, A. B., et al. (1997). Diabetes, defective pancreatic morphogenesis, and abnormal enteroendocrine differentiation in BETA2/NeuroD-deficient mice. *Genes Dev.* 11, 2323–2334. doi: 10.1101/gad.11.18.2323

Ninov, N., Hesselson, D., Gut, P., Zhou, A., Fidelin, K., and Stainier, D. Y. (2013). Metabolic regulation of cellular plasticity in the pancreas. *Curr. Biol.* 23, 1242–1250. doi: 10.1016/j.cub.2013.05.037

Nishio, S., Gibert, Y., Berekelya, L., Bernard, L., Brunet, F., Guillot, E., et al. (2012). Fasting induces CART down-regulation in the zebrafish nervous system in a cannabinoid receptor 1-dependent manner. *Mol. Endocrinol.* 26, 1316–1326. doi: 10.1210/me.2011-1180

Oka, T., Nishimura, Y., Zang, L., Hirano, M., Shimada, Y., Wang, Z., et al. (2010). Diet-induced obesity in zebrafish shares common pathophysiological pathways with mammalian obesity. *BMC Physiol.* 10:21. doi: 10.1186/1472-6793-10-21

Ollmann, M. M., Wilson, B. D., Yang, Y. K., Kerns, J. A., Chen, Y., Gantz, I., et al. (1997). Antagonism of central melanocortin receptors *in vitro* and *in vivo* by agouti-related protein. *Science* 278, 135–138. doi: 10.1126/science.278.5335.135

Olsen, A. S., Sarras, M. P. Jr., and Intine, R. V. (2010). Limb regeneration is impaired in an adult zebrafish model of diabetes mellitus. *Wound Repair Regener.* 18, 532–542. doi: 10.1111/j.1524-475X.2010.00613.x

Olsen, A. S., Sarras, M. P. Jr., Leontovich, A., and Intine, R. V. (2012). Heritable transmission of diabetic metabolic memory in zebrafish correlates with DNA hypomethylation and aberrant gene expression. *Diabetes* 61, 485–491. doi: 10.2337/db11-0588

Peng, X., Shang, G., Wang, W., Chen, X., Lou, Q., Zhai, G., et al. (2017). Fatty acid oxidation in zebrafish adipose tissue is promoted by 1alpha,25(OH)2D3. *Cell Rep.* 19, 1444–1455. doi: 10.1016/j.celrep.2017.04.066

Periasamy, M., Herrera, J. L., and Reis, F. C. G. (2017). Skeletal muscle thermogenesis and its role in whole body energy metabolism. *Diabetes Metab. J.* 41, 327–336. doi: 10.4093/dmj.2017.41.5.327

Pisharath, H., Rhee, J. M., Swanson, M. A., Leach, S. D., and Parsons, M. J. (2007). Targeted ablation of beta cells in the embryonic zebrafish pancreas using *E. coli* nitroreductase. *Mech. Dev.* 124, 218–229. doi: 10.1016/j.mod.2006.11.005

Poulsen, P., Vaag, A., Kyvik, K., and Beck-Nielsen, H. (2001). Genetic versus environmental aetiology of the metabolic syndrome among male and female twins. *Diabetologia* 44, 537–543. doi: 10.1007/s001250051659

Prince, V. E., Anderson, R. M., and Dalgin, G. (2017). Zebrafish pancreas development and regeneration: fishing for diabetes therapies. *Curr. Top. Dev. Biol.* 124, 235–276. doi: 10.1016/bs.ctdb.2016.10.005

Ran, G., Ying, L., Li, L., Yan, Q., Yi, W., Ying, C., et al. (2017). Resveratrol ameliorates diet-induced dysregulation of lipid metabolism in zebrafish (Danio rerio). *PLoS ONE* 12:e0180865. doi: 10.1371/journal.pone.0180865

Ringholm, A., Fredriksson, R., Poliakova, N., Yan, Y. L., Postlethwait, J. H., Larhammar, D., et al. (2002). One melanocortin 4 and two melanocortin 5 receptors from zebrafish show remarkable conservation in structure and pharmacology. *J. Neurochem.* 82, 6–18. doi: 10.1046/j.1471-4159.2002.00934.x

Rosen, C. J., Adams, J. S., Bikle, D. D., Black, D. M., Demay, M. B., Manson, J. E., et al. (2012). The nonskeletal effects of vitamin D: an endocrine society scientific statement. *Endocr. Rev.* 33, 456–492. doi: 10.1210/er.2012-1000

Sadler, K. C., Amsterdam, A., Soroka, C., Boyer, J., and Hopkins, N. (2005). A genetic screen in zebrafish identifies the mutants vps18, nf2 and foie gras as models of liver disease. *Development* 132, 3561–3572. doi: 10.1242/dev.01918

Schlegel, A., and Stainier, D. Y. (2006). Microsomal triglyceride transfer protein is required for yolk lipid utilization and absorption of dietary lipids in zebrafish larvae. *Biochemistry* 45, 15179–15187. doi: 10.1021/bi0619268

Schlegel, A., and Stainier, D. Y. (2007). Lessons from "lower" organisms: what worms, flies, and zebrafish can teach us about human energy metabolism. *PLoS Genet.* 3:e199. doi: 10.1371/journal.pgen.0030199

Schlombs, K., Wagner, T., and Scheel, J. (2003). Site-1 protease is required for cartilage development in zebrafish. *Proc. Natl. Acad. Sci. U.S.A.* 100, 14024–14029. doi: 10.1073/pnas.2331794100

Shungin, D., Winkler, T. W., Croteau-Chonka, D. C., Ferreira, T., Locke, A. E., Mägi, R., et al. (2015). New genetic loci link adipose and insulin biology to body fat distribution. *Nature* 518, 187–196. doi: 10.1038/nature14132

Song, Y., and Cone, R. D. (2007). Creation of a genetic model of obesity in a teleost. *FASEB J.* 21, 2042–2049. doi: 10.1096/fj.06-7503com

Stoffers, D. A., Ferrer, J., Clarke, W. L., and Habener, J. F. (1997). Early-onset type-II diabetes mellitus (MODY4) linked to IPF1. *Nat. Genet.* 17, 138–139. doi: 10.1038/ng1097-138

Tainaka, T., Shimada, Y., Kuroyanagi, J., Zang, L., Oka, T., Nishimura, Y., et al. (2011). Transcriptome analysis of anti-fatty liver action by Campari tomato using a zebrafish diet-induced obesity model. *Nutr. Metab.* 8:88. doi: 10.1186/1743-7075-8-88

Tehrani, Z., and Lin, S. (2011). Endocrine pancreas development in zebrafish. *Cell Cycle* 10, 3466–3472. doi: 10.4161/cc.10.20.17764

Thakur, P. C., Stuckenholz, C., Rivera, M. R., Davison, J. M., Yao, J. K., Amsterdam, A., et al. (2011). Lack of de novo phosphatidylinositol synthesis leads to endoplasmic reticulum stress and hepatic steatosis in cdipt-deficient zebrafish. *Hepatology* 54, 452–462. doi: 10.1002/hep.24349

Tingaud-Sequeira, A., Ouadah, N., and Babin, P. J. (2011). Zebrafish obesogenic test: a tool for screening molecules that target adiposity. *J. Lipid Res.* 52, 1765–1772. doi: 10.1194/jlr.D017012

Tiso, N., Moro, E., and Argenton, F. (2009). Zebrafish pancreas development. *Mol. Cell. Endocrinol.* 312, 24–30. doi: 10.1016/j.mce.2009.04.018

Vandevijvere, S., Chow, C. C., Hall, K. D., Umali, E., and Swinburn, B. A. (2015). Increased food energy supply as a major driver of the obesity epidemic: a global analysis. *Bull. World Health Organ.* 93, 446–456. doi: 10.2471/BLT.14.150565

Vargas, R., and Vásquez, I. C. (2017). Effects of overfeeding and high-fat diet on cardiosomatic parameters and cardiac structures in young and adult zebrafish. *Fish. Physiol. Biochem.* 43, 1761–1773. doi: 10.1007/s10695-017-0407-7

Velasco-Santamaría, Y. M., Korsgaard, B., Madsen, S. S., and Bjerregaard, P. (2011). Bezafibrate, a lipid-lowering pharmaceutical, as a potential endocrine disruptor in male zebrafish (Danio rerio). *Aquat. Toxicol.* 105, 107–118. doi: 10.1016/j.aquatox.2011.05.018

Vickers, K. C., Shoucri, B. M., Levin, M. G., Wu, H., Pearson, D. S., Osei-Hwedieh, D., et al. (2013). MicroRNA-27b is a regulatory hub in lipid metabolism and is altered in dyslipidemia. *Hepatology* 57, 533–542. doi: 10.1002/hep.25846

Wabitsch, M., Hauner, H., Heinze, E., and Teller, W. M. (1995). The role of growth hormone/insulin-like growth factors in adipocyte differentiation. *Metab. Clin. Exp.* 44, 45–49. doi: 10.1016/0026-0495(95)90220-1

WHO. (2017). *Obesity and Overweight*. Available online at: http://www.who.int/news-room/fact-sheets/detail/obesity-and-overweight

Willemsen, G., Ward, K. J., Bell, C. G., Christensen, K., Bowden, J., Dalgård, C., et al. (2015). The concordance and heritability of type 2 diabetes in 34,166 twin pairs from international twin registers: the discordant twin (DISCOTWIN) consortium. *Twin Res. Hum. Genet.* 18, 762–771. doi: 10.1017/thg.2015.83

Winzell, M. S., and Ahrén, B. (2004). The high-fat diet-fed mouse: a model for studying mechanisms and treatment of impaired glucose tolerance and type 2 diabetes. *Diabetes* 53 (Suppl. 3), S215–S219. doi: 10.2337/diabetes.53.suppl_3.S215

Xu, P. F., Zhu, K. Y., Jin, Y., Chen, Y., Sun, X. J., Deng, M., et al. (2010). Setdb2 restricts dorsal organizer territory and regulates left-right asymmetry through suppressing fgf8 activity. *Proc. Natl. Acad. Sci. U.S.A.* 107, 2521–2526. doi: 10.1073/pnas.0914396107

Ye, L., Robertson, M. A., Hesselson, D., Stainier, D. Y. R., and Anderson, R. M. (2015). glucagon is essential for alpha cell transdifferentiation and beta cell neogenesis. *Development* 142, 1407–1417. doi: 10.1242/dev.117911

Yee, N. S., Lorent, K., and Pack, M. (2005). Exocrine pancreas development in zebrafish. *Dev. Biol.* 284, 84–101. doi: 10.1016/j.ydbio.2005.04.035

Yen, T. T., Allan, J. A., Yu, P. L., Acton, M. A., and Pearson, D. V. (1976). Triacylglycerol contents and *in vivo* lipogenesis of ob/ob, db/db and Avy/a mice. *Biochim. Biophys. Acta* 441, 213–220. doi: 10.1016/0005-2760(76)90164-8

Yin, L., Maddison, L. A., and Chen, W. (2016). Multiplex conditional mutagenesis in zebrafish using the CRISPR/Cas system. *Methods Cell Biol.* 135, 3–17. doi: 10.1016/bs.mcb.2016.04.018

Yin, L., Maddison, L. A., Li, M., Kara, N., LaFave, M. C., Varshney, G. K., et al. (2015). Multiplex conditional mutagenesis using transgenic expression of Cas9 and sgRNAs. *Genetics* 200, 431–441. doi: 10.1534/genetics.115.176917

Zang, L., Shimada, Y., Kawajiri, J., Tanaka, T., and Nishimura, N. (2014). Effects of Yuzu (Citrus junos Siebold ex Tanaka) peel on the diet-induced obesity in a zebrafish model. *J. Funct. Foods* 10, 499–510. doi: 10.1016/j.jff.2014.08.002

Zang, L., Shimada, Y., and Nishimura, N. (2017). Development of a novel zebrafish model for type 2 diabetes mellitus. *Sci. Rep.* 7:1461 doi: 10.1038/s41598-017-01432-w

Zang, L., Shimada, Y., Nishimura, Y., Tanaka, T., and Nishimura, N. (2013). A novel, reliable method for repeated blood collection from aquarium fish. *Zebrafish* 10, 425–432. doi: 10.1089/zeb.2012.0862

Zang, L., Shimada, Y., Nishimura, Y., Tanaka, T., and Nishimura, N. (2015b). Repeated blood collection for blood tests in adult zebrafish. *Jove J. Vis. Exp.* 102:e53272. doi: 10.3791/53272

Zang, L., Shimada, Y., Tanaka, T., and Nishimura, N. (2015a). Rhamnan sulphate from Monostroma nitidum attenuates hepatic steatosis by suppressing lipogenesis in a diet-induced obesity zebrafish model. *J. Funct. Foods* 17, 364–370. doi: 10.1016/j.jff.2015.05.041

Zecchin, E., Filippi, A., Biemar, F., Tiso, N., Pauls, S., Ellertsdottir, E., et al. (2007). Distinct delta and jagged genes control sequential segregation of pancreatic cell types from precursor pools in zebrafish. *Dev. Biol.* 301, 192–204. doi: 10.1016/j.ydbio.2006.09.041

Zhou, J., Xu, Y. Q., Guo, S. Y., and Li, C. Q. (2015). Rapid analysis of hypolipidemic drugs in a live zebrafish assay. *J. Pharmacol. Toxicol. Methods* 72, 47–52. doi: 10.1016/j.vascn.2014.12.002

Conflict of Interest Statement: The authors declare that the research was conducted in the absence of any commercial or financial relationships that could be construed as a potential conflict of interest.

frontiers in Genetics

MINI REVIEW
published: 31 August 2018
doi: 10.3389/fgene.2018.00348

Rare Genetic Blood Disease Modeling in Zebrafish

*Alberto Rissone and Shawn M. Burgess**

Translational and Functional Genomics Branch, National Human Genome Research Institute, National Institutes of Health, Bethesda, MD, United States

Hematopoiesis results in the correct formation of all the different blood cell types. In mammals, it starts from specific hematopoietic stem and precursor cells residing in the bone marrow. Mature blood cells are responsible for supplying oxygen to every cell of the organism and for the protection against pathogens. Therefore, inherited or *de novo* genetic mutations affecting blood cell formation or the regulation of their activity are responsible for numerous diseases including anemia, immunodeficiency, autoimmunity, hyper- or hypo-inflammation, and cancer. By definition, an animal disease model is an analogous version of a specific clinical condition developed by researchers to gain information about its pathophysiology. Among all the model species used in comparative medicine, mice continue to be the most common and accepted model for biomedical research. However, because of the complexity of human diseases and the intrinsic differences between humans and other species, the use of several models (possibly in distinct species) can often be more helpful and informative than the use of a single model. In recent decades, the zebrafish (*Danio rerio*) has become increasingly popular among researchers, because it represents an inexpensive alternative compared to mammalian models, such as mice. Numerous advantages make it an excellent animal model to be used in genetic studies and in particular in modeling human blood diseases. Comparing zebrafish hematopoiesis to mammals, it is highly conserved with few, significant differences. In addition, the zebrafish model has a high-quality, complete genomic sequence available that shows a high level of evolutionary conservation with the human genome, empowering genetic and genomic approaches. Moreover, the external fertilization, the high fecundity and the transparency of their embryos facilitate rapid, *in vivo* analysis of phenotypes. In addition, the ability to manipulate its genome using the last genome editing technologies, provides powerful tools for developing new disease models and understanding the pathophysiology of human disorders. This review provides an overview of the different approaches and techniques that can be used to model genetic diseases in zebrafish, discussing how this animal model has contributed to the understanding of genetic diseases, with a specific focus on the blood disorders.

Keywords: zebrafish, hematopoiesis, modeling human diseases, SCID, blood, genome editing

OPEN ACCESS

Edited by:
Gokhan Dalgin,
The University of Chicago,
United States

Reviewed by:
Eirini Trompouki,
Max-Planck-Institut für Immunobiologie und Epigenetik,
Germany
Julien Y. Bertrand,
Université de Genève, Switzerland

***Correspondence:**
Shawn M. Burgess
burgess@mail.nih.gov

Specialty section:
This article was submitted to Stem Cell Research, a section of the journal Frontiers in Genetics

Received: *31 May 2018*
Accepted: *09 August 2018*
Published: *31 August 2018*

Citation:
Rissone A and Burgess SM (2018) Rare Genetic Blood Disease Modeling in Zebrafish. Front. Genet. 9:348. doi: 10.3389/fgene.2018.00348

INTRODUCTION

Genetic diseases can be both inherited and acquired. In particular, most of the inherited diseases belong to the category called "orphan diseases" (Strynatka et al., 2018). The term orphan disease can refer to two different types: common diseases neglected by doctors or rare diseases with a variable incidence in the population (Aronson, 2006). Although for different reasons, both have in common minimal scientific research about their genetic causes and molecular mechanisms and a lack of investments by pharmaceutical sector to develop new treatments (Strynatka et al., 2018). The definition of rare disease in not universal and depends on the country. In the United States, for example, a disease is considered rare when affecting fewer than 1 person in 200,000, but in Japan and Australia the numbers are very different: 1/50,000 and 1/2,000, respectively (Lavandeira, 2002).

With the advent of next-generation sequencing technologies and a progressive reduction in sequencing costs, we will begin to see a dramatic increase in the identification of the genes responsible for human genetic disorders. Model organisms played a pivotal role in genotype-to-phenotype studies, in particular when the association is unclear (Strynatka et al., 2018). However, with an estimated total number of Mendelian genetic diseases between 7,000 and 15,000 (Boycott et al., 2013) and only ∼1,500 drugs approved by FDA, most of the genetic diseases still have no effective treatment, indicating a constant need for new experimental animal models.

Animal Models to Study Genetic Diseases

Animal models are fundamental tools in biomedical research because they can fill the gap between basic science and the treatment of human diseases (Zon, 2016). Several different animal models can be used to study the gene function providing new insight into pathophysiology of human disorders (Bier and McGinnis, 2004). Simple models such as *Saccharomyces cerevisiae* (Foury, 1997) and *Dictyostelium discoideum* (Firtel and Chung, 2000; Chung et al., 2001) proved to be very helpful in elucidating the basic mechanisms of eukaryotic cell function, such as the regulation of the cell cycle, the mechanisms of DNA damage and repair, metabolism, and cell signaling. Similarly, invertebrates like *Caenorhabditis elegans* (Aboobaker and Blaxter, 2000; Culetto and Sattelle, 2000) and *Drosophila melanogaster* (Bernards and Hariharan, 2001; Reiter et al., 2001; Chien et al., 2002) represent outstanding models to study genes involved in more complex body plans (Bier and McGinnis, 2004). However, their very high evolutionary distance with a low rate of sequence conservation compared to vertebrates and the huge difference in their anatomy and physiology, limit their use in studying vertebrate-specific embryonic development and in directly modeling human diseases.

Traditionally, among mammals *Mus musculus* (mouse) and *Rattus norvegicus* (rat) are the species most commonly used as a vertebrate model organisms. Particularly the mouse with its small size, genomic resources, genetic tractability, and anatomic and physiologic conservation with humans, elected it as the favored species to model human genetic disorders. Although in the past, mouse models were usually generated using homologous recombination methods in embryonic stem cells (ESCs) it was a laborious, time consuming and not so efficient approach. With the advent of the new genome-editing techniques the overall process has been speed-up and today the generation of new mouse models require just few weeks, instead of the previous 1–2 years (Ott de Bruin et al., 2015). However, the maintenance of large mouse colonies is still expensive reducing its use in large-scale genetic screens and phenotyping studies. In addition, because of the complexity of human diseases and the intrinsic differences between humans and other species, it is often the case that some aspects of the model organisms physiology makes it a poor model for a specific disease, and so multiple model organisms are needed. Based on several features described in detail below, zebrafish represents a good compromise for modeling human diseases, filling the gap between the invertebrate and mammalian model systems.

Zebrafish as an Animal Model

The zebrafish (*Danio rerio*) is a tropical freshwater fish from South-East Asia which has in recent decades gained popularity in the research community. Zebrafish popularity began at the end of the last century (1970s–1980s), when they became a new genetic model for developmental biologists. However, because of the numerous advantages that zebrafish offer, it has rapidly become popular in the study of human disease.

Zebrafish belong to the teleost clade, also known as "bony" fish. The eggs are externally fertilized which allows for simple experimental manipulation of the embryos, and each mating produces a high number (usually >100) of embryos. The embryo development is very fast compared to other vertebrate models such as mice, and a few days after the hatching (48–72 h post fertilization) zebrafish embryos already show all the major organs of the adult animals. Notably, the anatomy and physiology of most of the zebrafish organs are very similar to those of mammals and in terms of hematopoiesis, Teleosts have all the different hematopoietic cellular elements found in mammals (i.e., erythroid, myeloid and lymphoid lineages).

Although under normal conditions zebrafish embryos are not completely transparent, they may be treated with 1-phenyl 2-thiourea (PTU) at ∼24 h post fertilization (hpf) which will inhibit melanin formation resulting in almost transparent embryos that will continue to remain in this condition as long as the PTU treatment is continued (Karlsson et al., 2001). Alternatively, numerous genetic pigmentation mutants with different levels of transparency are available and can permit *in vivo* imaging from the embryo phases to adulthood (White et al., 2008).

The zebrafish is well suited for molecular and genetic analysis of temporal and spatial gene expression using whole mount *in situ* hybridization (WISH) (Thisse and Thisse, 2008); moreover, a very long list of transgenic lines (including inducible models)

are publicly available that allows study of tissue and organ development *in vivo* and in real-time during all the phases of embryo development (Kondrychyn et al., 2011; Ruzicka et al., 2015). For a comprehensive list of transgenic lines helpful in studying zebrafish hematopoiesis see Gore et al. (2018).

Thousands of mutations obtained using large scale mutagenesis screens are available and moreover new mutations can be easily introduced in zebrafish genome using the most recent techniques of site-specific genome editing such as the Clustered Regularly Interspaced Short Palindromic Repeat/CRISPR associated protein 9 (CRISPR/Cas9). The zebrafish genome has been fully sequenced and high-quality assemblies are publically available (Howe et al., 2013). Genomic analysis shows that there is a high degree of sequence conservation and synteny between the zebrafish and human genomes. Zebrafish, especially during its embryonic stages, proved to be very suitable for medium- to large-throughput drug screening, because it is possible to add the different compounds directly into the embryo medium. Moreover, usually zebrafish bioassays are cheaper and faster than the comparable mouse assays. Finally, maintenance costs of zebrafish model are lower than those for mammals. While this review focuses on mutational analysis in early embryos, adult zebrafish are increasingly being used to study some blood diseases as well, particularly blood cancers (Langenau et al., 2003; Alghisi et al., 2013).

Like any other animal model and despite its numerous advantages and unique features, the zebrafish model system is not devoid of disadvantages and/or limitations. One of major limitations is the teleost-specific genome duplication. This event occurred ∼400 millions of years ago and corresponded to a complete duplication of teleost genome (Meyer and Van de Peer, 2005). After the duplication event, the majority of the duplicated genes were lost or became pseudogenes. However, roughly 20% of the genes maintained two functional copies in the genome. As a results, zebrafish and other teleost species have a higher number of protein coding genes (∼26,000) compared to other vertebrates like human, mouse or chicken (∼21,000) (Howe et al., 2013). This information must be taken in consideration during reverse genetic analysis of the duplicated genes as a result of compensatory effects, most of the cases knocking out one copy of the gene is not enough to mimic the effects of a null allele. Another important aspect to take into consideration is that, after gene duplication, each duplicate can functionally diverge from each other through sub-functionalization and/or neo-functionalization events (Ohno, 1970; Postlethwait et al., 2004; Rastogi and Liberles, 2005). Although the modern genome-editing technologies allow the targeting of multiple genes at the same time, somewhat overcoming the problem duplicate genes, neo-functionalization events could have partially changed the gene's function. These phenomena could be responsible for discrepant functional outcomes among models in different species and potentially could limit the use of zebrafish in modeling human diseases. Unfortunately, it is currently not possible to determine *a priori* whether this would be an issue for any given gene duplication.

Zebrafish as a Tool to Study Human Diseases

The recent advent in the zebrafish field of targeted genome editing techniques, such as ZFN, TALEN, and in particular CRISPR/Cas9, has opened up the model to reproduce human pathological conditions of known disease-related genes and to study their effects *in vivo,* with the ultimate goal of identifying new therapeutic targets (Detrich et al., 1999; Langheinrich, 2003; Santoriello and Zon, 2012). Although historically the first successful attempts to use zebrafish for genetic studies were represented by forward genetic approaches using chemical or insertional mutagenesis techniques (Haffter and Nusslein-Volhard, 1996; Golling et al., 2002; Varshney et al., 2013), later on, thanks to the development of knockdown and targeted genome editing techniques, this model system proved that it could be efficiently used in reverse genetic approaches as well.

Knockdown Approach to Study Gene Function

In zebrafish, with the exception of limited cases where RNAi has been used to knockdown specific targets (Oates et al., 2000), the knockdown approach has been performed through the use of morpholinos (MOs) (Nasevicius and Ekker, 2000). Because of their ease of use, MOs represented the first and they are still today one of the most popular approaches to perform reverse genetic analysis in zebrafish (Eisen and Smith, 2008; Bill et al., 2009; Timme-Laragy et al., 2012; Stainier et al., 2017). MOs are modified antisense oligonucleotides (ASOs) that are manually microinjected in the embryos at the first stages of development (1–4 cells maximum). MO oligonucleotides are very stable because they are not targeted by nuclease enzymes and they do not act through an RNaseH mechanism, as in the case of RNA interference (RNAi) technology (Eisen and Smith, 2008). Instead, through the binding to their RNA targets (pre-mRNA or mRNA), MOs induce a transient dose-dependent knockdown effect in the injected embryos (morphants). During embryonic development, MOs concentration is gradually reduced in the cells due to cell divisions and therefore they do not typically stay effective beyond 3–5 days post fertilization (dpf) (Timme-Laragy et al., 2012).

Usually, low doses of MOs are well tolerated by zebrafish embryos, allowing the targeting of more than a single transcript at the same time to study synergistic effects of multiple knockdowns (Rissone et al., 2012). While the report of potential off-target effects mediated by the *tp53* activation following MOs injection (Robu et al., 2007) raised several criticisms to the validity of some results obtained with them (Blum et al., 2015; Kok et al., 2015; Stainier et al., 2015), they have been extensively used to study gene function during embryo development and to confirm the role of candidate genes involved in human diseases. Usually, if used with full knowledge of the potential risks and limitations and with all the essential controls (Eisen and Smith, 2008; Stainier et al., 2015, 2017), MOs represents a good starting point to infer gene function in a fast and inexpensive way and, at least in one case, it has been shown that MOs action can prevent the genetic compensatory effects induced in some mutant animals (Rossi et al., 2015).

Recently, an alternative knockdown approach requiring the injection of RNA–DNA hybrid ASOs (also known as gapmers) has been used to overcome some of the limitations of MOs (Pauli et al., 2015): first, each molecule of a steric-blocking MO will only bind a single target RNA transcript; second, translational MOs, designed to block the ATG codon of mRNAs, do not induce the degradation of the target transcripts impeding the quantification of their knockdown efficiency. In contrast, gapmer ASOs contains a central DNA region, which triggers an RNAse H-mediated degradation of the target RNAs. The molecules also have flanking 2′-modified nucleosides at both ends to protect them from exonucleases activity and to increase the affinity for the targets (Evers et al., 2015). While they have already been used in cell culture (Dimitrova et al., 2014) and other species (Heasman et al., 1994; Zhang et al., 1998; Wheeler et al., 2012), gapmers-mediated knockown represents a relatively unexplored approach in zebrafish. Pauli et al. (2015) tested the feasibility of this approach in zebrafish targeting ∼20 protein-coding and non-coding transcripts with known embryonic loss-of-functions phenotypes and showing that gapmers can represent an effective RNA knockdown alternative. Although representing a promising tool, more studies are required to further confirm their potential utility.

Finally, given the continuous reduction of the costs required to create mutant alleles in zebrafish (Varshney et al., 2015b), in the future the studies involving the use of MOs or other knockown techniques could and should include a comparison of the phenotypes observed in bona fide genetic mutants as a control (Stainier et al., 2017).

Zebrafish Genome Editing Tools

In zebrafish, large-scale genetic screens using random mutagenesis were successfully introduced at the end of the 1990s (Haffter and Nusslein-Volhard, 1996; Haffter et al., 1996). These forward genetic techniques proved to be very helpful in identifying mutants presenting phenotypes typical of several human disorders (North and Zon, 2003; Amsterdam and Hopkins, 2006; Bradford et al., 2017; Howe et al., 2017). However, these approaches were not devoid of limitations; especially in the amount of efforts required to isolate each mutation by positional cloning and they were gradually replaced by the use of reverse genetic approaches. In particular, the advent of the TILLING (or Targeting Induced Local Lesions in Genome) system in early 2000s (Wienholds et al., 2002) allowed the researchers to screen for mutations in specific genes of interest. Later, new and more efficient tools for targeted mutagenesis were developed and they were quickly adopted by the zebrafish community (Doyon et al., 2008; Meng et al., 2008; Huang et al., 2011; Bedell et al., 2012). Briefly, all the major genome editing techniques are based on the coupling of DNA-binding domains or guide RNA molecules to proteins with nuclease activity used to induce double-stranded breaks (DSB) in the target genomic regions. Then inductions of DSBs prompts the activity of two different cellular DNA repair mechanisms: (a) the most common, but highly error–prone non-homologous end joining (NHEJ) and (b) the homology-directed repair (HDR) which is rarer *in vivo* and requires a template DNA to repair the DSB (Symington and Gautier, 2011). The HDR mechanism seems to be particularly challenging in zebrafish and so far, despite numerous efforts of the community to optimize the mutagenic protocol in order to increase its frequency in zebrafish, very few successful cases are described in literature (Hruscha et al., 2013; Hwang et al., 2013a; Auer et al., 2014; Irion et al., 2014; Kimura et al., 2014; Hisano et al., 2015; Li et al., 2015; Armstrong et al., 2016; Hoshijima et al., 2016; Zhang et al., 2016; Moreno-Mateos et al., 2017; Zhang et al., 2018). In contrast, in zebrafish the NHEJ repair mechanism works very efficiently and usually it is associated with loss/gain of small fragments of genomic DNA in the range of 1 bp to ∼40 bps. Selecting frame-shift mutations introduced by NHEJ potentially impairs the structure and/or the functionality of the targeted protein.

The first examples of zebrafish mutants obtained with Zinc Finger Nucleases (ZFNs) and Transcription Activator-Like Effector Nucleases (TALENs) were published in the late 2000s and 2011, respectively (Doyon et al., 2008; Meng et al., 2008; Huang et al., 2011; Sander et al., 2011). They both allowed an easy targeting and recovery of the different mutations introduced in the specific genomic regions, although their major limitations resided in their still high costs and in the efforts necessary to develop the modular DNA-binding motifs responsible for the sequence specificity.

The recent advent of CRISPR/Cas9 system moved the versatility and affordability of the genome editing in zebrafish to a new level, allowing the targeting of multiple regions at the same time (multiplexing) with a consistent reduction of the costs (Hwang et al., 2013b; Jao et al., 2013; Varshney et al., 2015a). In the CRISPR/Cas9 system, the sequence specificity is obtained using an ∼20 base pairs long guide RNA (gRNA), while the DNA double-strand cleavage activity is attained using the Cas9 endonuclease activity. Compared to ZFNs and TALENs, CRISPR/Cas9 system has a similar or better efficiency in targeting genomic DNA, with a higher versatility and simplicity of design. The only limitation in the target design consist in the presence of a protospacer adjacent motif (PAM) directly upstream the target region bound by the gRNA. The PAM sequence depends on the Cas9 protein used, but in most of the cases is the nucleotide sequence NGG (Varshney et al., 2015b). Based on the biological target system used (cells or animal embryos) the gRNA sequence is delivered by transfection of specific gRNA-containing vectors or direct injection of gRNAs generated by *in vitro* transcription. In zebrafish, its intrinsic features such as the external fertilization and the easy manipulation of the embryos, allow the direct co-injection of Cas9 mRNA (or Cas9 protein) and the gRNAs into the embryos during the earliest stages of development (similarly to MOs). One further advantage of the zebrafish embryos is that they can easily tolerate multiple gRNAs at the same time, making possible a multiplexing approach that dramatically increases its versatility. It becomes possible to target multiple genes at the same time or to use specific gRNA directed against different regions of a single gene to maximize the number of mutated allele or to induce the deletion of a large genomic region based on the specific needs of the researchers. Another benefit of a multiplexing approach in zebrafish consists in overcoming the potential compensatory effects due to the duplicated genes, which clearly represents a problem for genetic analysis in this

animal model. In contrast, an obvious downside of a multiplexing approach is represented by the increased probability of off-target activity, which seems to be relatively rare, but detectable (Varshney et al., 2015a). Recently, in order to maximize the specificity of the CRISPR/Cas9 system, different variants of the Cas9 enzyme (Cas9n and Cas9/FokI) were successfully developed and proved to work very well in limiting nuclease activity to specific genomic sites, although reducing at the same time the overall multiplex potential of the system (Ran et al., 2013; Tsai et al., 2014). Many human diseases are due to mutations predicted to cause single or multiple amino acid substitutions that partially inhibit gene activity, instead of completely impairing protein function or mRNA stability. Therefore, in order to better mimicking the mutations found in human patients, the ability to introduce in an animal substitution genetic mutations (in contrast to null alleles) represents one of the current challenges of the genomic editing era. Recently, a new genome editing technique called "base editing" has been developed and tested in mammalian cells and different model species (Komor et al., 2016; Kim et al., 2017). Through the fusion of a cytidine deaminase enzyme to the N-terminal region of a Cas9 nickase (nCas9) protein, this new technology allows direct conversion of one single base in a programmable way bypassing the DSBs. Recently, Zhang et al. (2017) adapted a similar approach to work efficiently in zebrafish, further increasing its versatility as animal model in modeling human diseases.

Zebrafish Hematopoiesis

Usually, during both zebrafish and mammal embryo development, hematopoiesis is obtained in three distinctive, but partially overlapping, processes termed "hematopoietic waves" (Ciau-Uitz et al., 2014). For correct hematopoietic development, both their timing and embryonic localization need to be strictly regulated (for a comprehensive list of the genes expressed and involved in the different phases of zebrafish hematopoiesis see Gore et al., 2018). Based on the type of blood cells originated, the three major hematopoietic waves are distinguished in primitive, prodefinitive (or intermediate) and definitive. In mammals, during the first two hematopoietic waves, red blood cells and macrophages, and erythroid-myeloid precursors are generated extra-embryonically in the yolk sac blood island (Ciau-Uitz et al., 2014). In contrast, the definitive hematopoiesis produces all the major hematopoietic cell types (erythroid, myeloid, and lymphoid) through the creation of hematopoietic stem and precursor cells (HSPCs).

Over the years, several reports pointed out the utility of the zebrafish model to study the different aspects of vertebrate hematopoiesis (Gore et al., 2018). Despite the >400 million years of evolutionary distance (Postlethwait et al., 1999) and the different embryonic territories involved (Ciau-Uitz et al., 2014), zebrafish and mammal species share the same key genetic regulation and mechanisms (Sood and Liu, 2012; Avagyan and Zon, 2016; Gore et al., 2018).

Zebrafish Primitive Hematopoiesis

In zebrafish, primitive hematopoiesis starts around 11 h post fertilization (hpf) during somitogenesis (Davidson and Zon, 2004). Specific cells inside the anterior and posterior lateral mesoderm (ALM and PLM, respectively) start expressing endothelial and hematopoietic markers generating different populations of vascular and hematopoietic precursors. Later, the ALM gives rise to the rostral blood island (RBI) region. The cells in the ALM/RBI region generate primitive myeloid precursors which eventually differentiate into macrophages and neutrophils (Herbomel et al., 1999). Specifically, primitive myeloid precursors start to express the transcription factor *pu.1* and then they leave the RBI spreading on the yolk sac (Galloway et al., 2005; Rhodes et al., 2005; Monteiro et al., 2011). Following *pu.1* activation, different myeloid markers start to be expressed in these migrating cells and finally, with the expression of *irf8*, *cebpa,* and *cebp1* genes, these precursors begin to assume a more restricted myeloid identity (Li et al., 2011; Jin et al., 2012, 2016; Mommaerts et al., 2014; Dai et al., 2016). Precursor cells from RBI are also responsible for the generation of mast cells (Dobson et al., 2008) and microglia, which will eventually colonize the brain (Xu et al., 2015, 2016). In contrast, the future hematopoietic precursors that reside in the PLM migrate, converging to the midline of the embryo body and forming the intermediate cell mass (ICM). The ICM occupies the space between the yolk extension and the notochord and it extends throughout the trunk of the embryos to the end of the yolk extension (Ciau-Uitz et al., 2014). Although the hematopoietic precursors forming the ICM region during development express both erythroid and myeloid markers (such as *gata1a*, and *spi1b* or *mpx*, respectively) this posterior first hematopoietic wave seems to generate mostly primitive erythrocytes that enter the circulation at ∼24 hpf, when the zebrafish heart starts beating (Berman et al., 2003). Primitive erythroid and myeloid cells are then gradually replaced by blood cells produced during the following hematopoietic waves.

Zebrafish Prodefinitive Hematopoiesis

Around 24 hpf, the zebrafish embryos switch from the primitive to the definitive hematopoiesis. This transition occurs concurrently in two different regions of the embryo: the posterior blood island (PBI) and the ventral wall of the dorsal aorta (VDA). From the VDA originates the precursors of HSPCs; while in the PBI, which is the most caudal region of the ICM right after the end of the yolk extension, only erythroid-myeloid progenitors (EMP) begin to differentiate (Bertrand et al., 2007). Because they do not derive from HSPCs, the hematopoietic potential of EMPs is limited to the erythroid and myeloid lineages (Gore et al., 2018). However, a very recent temporally–spatially resolved fate-mapping analysis (Tian et al., 2017) showed that the ventral endothelium in the VDA and PBI regions, gives rise to a transient wave of T lymphopoiesis which does not require HSPCs. Notably, the generated T-cells are mostly CD4 Tαβ cells and are temporally limited to the larval stages of development (Tian et al., 2017).

Zebrafish Definitive and Adult Hematopoiesis

The formation of HSPCs is the characteristic step of definitive hematopoiesis. Compared to previous hematopoietic progenitors generated during primitive hematopoiesis, HSPCs are self-renewable pluripotent stem cells responsible for the formation of

all the hematopoietic lineages during the zebrafish development and the adult phase. In zebrafish the definitive hematopoiesis starts around ∼24 hpf with the formation of the first *runx1* and then *cmyb* positive cells in a specific region of the trunk of the embryos, the VDA which functionally corresponds to the aorta-gonad-mesonephros (AGM) region in mammals. In the VDA, a subset of endothelial cells starts to differentiate in HSPCs and they eventually bud from the aorta and colonize the region between the aorta and the posterior cardinal vein (PCV) (Bertrand et al., 2010; Kissa and Herbomel, 2010). This process is usually indicated as endothelial-hematopoietic transition (EHT) (Kissa and Herbomel, 2010; Bresciani et al., 2014). Then, HSPCs enter the circulation through the PCV and move caudally to colonize by 2 dpf the so called caudal hematopoietic tissue (CHT) which consists of the region where the vascular plexus connecting the dorsal aorta and the cardinal vein resides (Murayama et al., 2006; Bertrand et al., 2010; Kissa and Herbomel, 2010; Sood et al., 2010; Bresciani et al., 2014; Gore et al., 2016; Tian et al., 2017). This region is also indicated as PBI. Due to the reduced blood flow and the presence of specific signals on the surface of HSPCs and endothelial cells of the caudal vein plexus (CVP), HSCPs leave the circulation and extravasate in the PBI region, where they are surrounded by endothelial and perivascular mesenchymal stromal cells that modulates their subsequent proliferative and/or differentiation fate (Murayama et al., 2006; Jin et al., 2007, 2009; Tamplin et al., 2015). The CHT region is the teleost homologous of the mammalian fetal liver and there, part of the HSCPs proliferates and gives rise to erythroid and myeloid cells, and some of them through circulation, move anteriorly to the thymus and to the anterior part of the kidney by 3 and 4 dpf, respectively (Kissa et al., 2008). Like in mammals, the zebrafish thymus is the site of differentiation and maturation of T-lymphocytes (Hess and Boehm, 2012), while the kidney marrow, where HSPCs reside through adulthood, is analogous to mammalian bone marrow (Bertrand and Traver, 2009). Both organs represent the sites where the adult hematopoiesis reside (de Jong and Zon, 2005).

ZEBRAFISH MODELS OF BLOOD DISEASE

Historically, the zebrafish mutant *sauternes* (*sau*), represented the first example of a growing list of zebrafish contributions to the study of human diseases. Isolated during a large zebrafish forward genetic screening, the mutated gene encodes δ-aminolevulinate synthase (ALAS-2), an enzyme involved in the first step of heme biosynthesis (Brownlie et al., 1998). Notably, because mutations in ALAS2 gene are responsible for the congenital sideroblastic anemia (CSA) in humans, zebrafish *sauternes* mutants represented also the first animal model for the disease (Brownlie et al., 1998). Since then, through both forward and reverse genetic analysis, the zebrafish have proven to be instrumental in the study of human blood disorders (Berman et al., 2003; North and Zon, 2003; Forrester et al., 2012; Moore and Langenau, 2012; Santoriello and Zon, 2012; Zhang and Yeh, 2012; Avagyan and Zon, 2016; Robertson et al., 2016; Gore et al., 2018). In the following sections we will discuss a few of these disease models.

Zebrafish Erythroid and Myeloid Models of Disease

Diamond–Blackfan Anemia

Diamond–Blackfan anemia (DBA) is a congenital bone marrow failure syndrome characterized by a complex array of hematopoietic and non-immunological defects. Patients with DBA are generally diagnosed during infancy or early childhood and present erythrocyte aplasia with anemia, macrocytosis, reticulocytopenia, and a paucity of red blood cell precursor cells within a normocellular marrow, associated with growth retardation, and limb, cardiac, and/or craniofacial malformations and have a predisposition to cancer (O'Brien et al., 2017). Other specific features of DBA are an elevated erythrocyte adenosine deaminase (ADA) activity and an elevated fetal hemoglobin concentration (McGowan and Mason, 2011). The primary treatment of DBA is corticosteroids, but ∼40% of patients lose steroid responsiveness, requiring chronic red cell transfusions (O'Brien et al., 2017). The only definitive treatment for DBA consists of hematopoietic stem cell transplantation (HSCT). In the 65% of patients DBA is caused by heterozygous mutations in ribosomal genes; while in the remaining ∼35% the genetics causes are still unknown (O'Brien et al., 2017). While, the most commonly mutated gene in DBA patients is RPS19 (Draptchinskaia et al., 1999; Campagnoli et al., 2008), germ-line mutations in genes encoding both small and large components of the ribosomal subunits (RPS24, RPS17, RPS7, RPS10, RPS26 and RPL35A, RPL5, RPL11, RPL26, respectively) have also been described (Farrar et al., 2011; Gazda et al., 2012).

In mice, homozygous knockout mutants for the rps19 gene presented early embryonic lethality (Matsson et al., 2004). Heterozygous mice did not present hematologic or developmental phenotypes, because of a genetic compensation from the wild-type rps19 locus (Matsson et al., 2006). Another mouse model with a ethylnitrosourea (ENU)-induced missense point mutation in rps19 gene showed a hematopoietic defect that was rescued by p53 knockdown (McGowan et al., 2008; McGowan and Mason, 2011).

To date two independent models of DBA were developed in zebrafish using MOs knockdown approaches against the ribosomal protein S19 (*rps19)* transcripts (Danilova et al., 2008; Uechi et al., 2008). In both cases, *rps19* knockdown recapitulated the phenotypes observed in DBA patients such as the defective erythropoiesis and morphologic abnormalities. A subsequent zebrafish knockdown model of *rpl11*, another ribosomal protein found mutated in DBA patients (Chakraborty et al., 2009), confirmed the central role for p53 activation in the pathophysiology of DBA (Ball, 2011). More recently, the genetic models of *rps19* and *rpl11* deficiency were developed (Zhang et al., 2014). Both models presented a reduction of protein production and in particular of globin proteins in red blood cells, suggesting that the protein reduction could be a key contributing factor to erythroid defects observed in DBA (Zhang

et al., 2014). Finally, Danilova et al. (2018) investigated the role of immune system in DBA. Using *rpl11* mutants and *rps19* morphants, they showed an increased level of interferon network, inflammatory pathways and complement system suggesting that the activation of the innate immune system could contribute to the physiopathology of DBA (Danilova et al., 2018).

Recently, another gene of the rps family, rps29, has been associated with DBA using whole-exome sequencing and functional studies in a zebrafish model of rps29 deficiency (Taylor et al., 2012; Mirabello et al., 2014).

Finally, DBA patients present a high incidence of cancer, with particularly high risks of leukemia, osteosarcoma, myelodysplastic syndrome and colon adenocarcinoma (Vlachos et al., 2012); notably, *rps* and *rpl* heterozygous mutations also cause tumors in zebrafish (Amsterdam et al., 2004; Lai et al., 2009).

Erythropoietic Protoporphyria

The different inherited porphyrias are genetic diseases affecting heme biosynthesis, caused by mutations in specific enzymes of the heme biosynthetic pathway. As a result of these enzymatic deficiencies, the intermediates of the heme biosynthetic pathway (porphyrinogens, porphyrins and their precursors) are produced in excess and accumulate in tissues resulting in neurological, photo-cutaneous symptoms, and hematological disturbances (Richard et al., 2008). Based on which tissue accumulates porphyrin, this group of diseases can be divide into erythropoietic or hepatic. Three different erythropoietic porphyrias have been described: erythropoietic protoporphyria (EPP), which is the most frequent, congenital erythropoietic porphyria (CEP), and the very rare hepatoerythropoietic porphyria (HEP) (Richard et al., 2008). In humans, EPP is associated with inherited defects in the ferrochelatase (FECH) gene which catalyzes the insertion of a ferrous iron into protoporphyrin IX (PPIX) to form heme (Puy et al., 2010). The main clinical manifestation is painful skin inflammation after short exposure to sunlight. However, because the heme formation mainly occurs in the bone marrow and liver, mutations affecting FECH activity lead to PPIX accumulation in the bone marrow, erythrocytes, plasma, and liver and it has been estimated that up to 20% of the EPP patients have liver injury and approximately 2–5% develop serious liver damage or even liver failure (Wang et al., 2018).

After chemical mutagenesis using ENU, a viable autosomal recessive mutation in mouse fech gene was isolated and characterized in the early 1990s (Tutois et al., 1991; Boulechfar et al., 1993). Homozygous null mice present a severe reduction of FECH enzymatic activity and they exhibit jaundice, photosensitivity and dramatic hepatic dysfunction (Tutois et al., 1991).

A zebrafish genetic model of EPP, with mutations in the ferrochelatase (*fech*) gene, was obtained from a large-scale genetic screen (Childs et al., 2000). Zebrafish ferrochelatase mutants (*Dracula*) present a light-dependent lysis of red blood cells and liver disease (Childs et al., 2000).

A zebrafish mutant (ype^{tp61}), which represented the first genetic model of HEP, was obtained in a forward genetic screen (Wang et al., 1998). The mutant presents a mutation in the *uroporphyrinogen decarboxylase* (*urod*) gene. Homozygous embryos die due to photo-ablation of their auto-fluorescent blood cells upon light exposure (Wang et al., 1998) and present clinical similarities to the defects observed in HEP patients.

Systemic Mastocytosis

Mastocytosis refers to a group of hematological disorders characterized by an increase in mast cell production, as well as abnormal morphology with aberrant surface receptor expression of tissue mast cells. These disorders are usually the result of various gain-of-function mutations affecting the tyrosine kinase KIT receptor, leading to increased accumulation and survival of tissue mast cells (Klaiber et al., 2017). Mastocytosis is divided in different subtypes: mastocytoma, urticaria pigmentosa, and systemic mastocytosis (SM), which represents the most severe subtype because mast cells accumulate in multiple organs. In the case of SM, a c-Kit D816V mutation is the most common cause of the disease and it gives rise to a constitutively active form of the protein that activates PI3K, Jak-STAT, and MAPK pathways (Lennartsson and Ronnstrand, 2012). Mouse models of SM using D816V mutation of human (Zappulla et al., 2005) or mouse (Gerbaulet et al., 2011) c-Kit gene have been developed. Similarly, a zebrafish transgenic model ubiquitously expressing the human KIT-D816V mutation has been developed (Balci et al., 2014). Adult transgenic fish demonstrate a myeloproliferative disease phenotype with a strong accumulation of mast cells in the kidney marrow and high expression levels of endopeptidases, consistent with SM defects observed in patients. Moreover, the zebrafish model showed a higher incidence of disease than in the transgenic mice overexpressing the same human mutant gene (Balci et al., 2014).

Zebrafish Models of Primary Immunodeficiencies

Primary immunodeficiencies (PIDs) represent a heterogeneous group of genetic disorders characterized by the partial or complete absence of the immune system or its improper activity (Al-Herz et al., 2011). So far, more than 230 PID-causing genes have been identified and novel gene defects continue to be discovered (Al-Herz et al., 2011). Among PIDs, severe combined immunodeficiencies (SCIDs) are the most severe forms, resulting in a block of the development of T, B and/or NK cells and, consequently, in a high susceptibility to any kind of infection. For the most severe forms of PIDs the HSCT represents the current treatment of choice and, when a histocompatibility leukocyte antigen (HLA)-matched donor is not available, conditioning chemotherapy may be needed to facilitate robust and sustained engraftment of donor cells and improve immune reconstitution (Pai et al., 2014; Ott de Bruin et al., 2015). Some SCIDs have also been successfully treated with gene therapy (Fischer et al., 2013; Mukherjee and Thrasher, 2013). Unfortunately, for many cases of PIDs the genetic causes are still unknown or poorly understood (Shearer et al., 2014). Although current advances in analyzing the genome or exome sequences of patients and their relatives uncover many

sequence polymorphisms (SNPs) possibly affecting the blood disorders, *in vivo* analysis still represent the golden standard to functionally confirm their effects and, from this point of view, the zebrafish can provide a good platform to test the functional consequences of different genetic variants (Iwanami, 2014).

Reticular Dysgenesis

Reticular dysgenesis is one of the most rare and severe forms of SCIDs. The disease is clinically characterized by congenital lymphopenia, lymphoid and thymic hypoplasia with agranulocytosis and sensorineural deafness (Hoenig et al., 2018) and is caused by mutations in adenylate kinase 2 (*ak2*) gene (Lagresle-Peyrou et al., 2009; Pannicke et al., 2009; Six et al., 2015). Ak2 protein is mostly located in the mitochondrial membrane space where it catalyzes the conversion of 1ATP + 1AMP = 2ADP sustaining the mitochondrial oxidative phosphorylation (Dzeja and Terzic, 2003). In mouse *ak2* mutations are embryonically lethal, therefore zebrafish represented an alternative to try to model the disease. The first attempts to model RD in zebrafish consisted of embryonic knockdown with a splicing-MO mimicking one of the mutations found in a patient (Pannicke et al., 2009). Overall, larvae showed a reduction of the *ikaros* signal in the thymus indicating an impairment of leukocyte development during definitive hematopoiesis (Pannicke et al., 2009). Recently, the first knockdown results were independently confirmed using two other different MOs and, more importantly, by two distinct zebrafish genetic models (with a missense point mutation and a frame shift mutation, respectively) and a patient-derived iPSCs model of RD (Rissone et al., 2015). As previously shown *in vitro* in fibroblast of RD patients, ak2-deficiency in zebrafish induces an increased level of oxidative stress resulting in increased apoptosis and cell death of the HSPC population. *In vitro* differentiated iPSCs recapitulate the promyeloid block of their differentiation that has been described in the bone marrow of RD patients (Lagresle-Peyrou et al., 2009; Hoenig et al., 2017). Notably, in zebrafish antioxidant treatments with *N*-acetyl cysteine or Glutathione (GSH) were able to reduce the cellular oxidative stress *in vivo* rescuing the hematopoietic phenotypes; moreover similar results were obtained in the RD-patient derived iPSCs model, where the GSH, but not the all-*trans* retinoic acid (ATRA), treatment was able to significantly increase the differentiation of AK2-deficient iPSCs into mature granulocytes (Rissone et al., 2015). Interestingly, a recent report showed that in ak2-deficiencient hematopoietic progenitors obtained from a different RD-patient derived iPSCs, the intracellular ATP redistribution is impaired with a strong ATP depletion in the nucleus and an altered global transcriptional profile (Oshima et al., 2018).

Wiskott–Aldrich Syndrome

The Wiskott–Aldrich syndrome (WAS) is a rare X-linked recessive disease (with an estimated incidence of less than 1 in 100,000 births) characterized by eczema, bleeding diathesis, and recurrent infections that occurs in boys (Ochs and Thrasher, 2006; Puck and Candotti, 2006). The disease is associated with mutations in a gene on the short arm of the X chromosome (Xp11.23) that was originally termed the WAS gene (Derry et al., 1994). The protein encoded by the WAS gene (WASp) is a major regulator of actin polymerization and it plays a role in the remodeling of the cytoskeleton during the formation of the immunological synapse between T cells and the and antigen-presenting cells. Mutations in WASp can prevent the formation of the immunologic synapse, impairing T-cell function and compromise the locomotion and the adhesion of other immunological cells such as B cells, macrophages, dendritic cells, etc. (Ochs and Thrasher, 2006; Puck and Candotti, 2006). Moreover, constitutively activating mutations of WASp are responsible for the X-linked severe congenital neutropenia (XLN) disorder (Devriendt et al., 2001).

Different knock-out and knock-in murine models of WAS were developed (Leon et al., 2016). The complete inactivation of WASp mimicked the thrombocytopenia although failed to reproduce the microcytosis observed in human patients (Sabri et al., 2006; Marathe et al., 2009). Notably, murine models have been successfully used to conduct preclinical trials evaluating somatic gene therapy as an alternative to transplantation (Dupre et al., 2006; Bosticardo et al., 2011, 2014; Uchiyama et al., 2012).

In zebrafish the *was* gene is duplicated and both present a very similar expression pattern (Cvejic et al., 2008). Morpholino analysis targeting *wasa* or *wasb* showed that they exhibit different levels of disruption to the wound inflammatory response. In particular, *wasa* morphants showed the strongest phenotypes, which consisted of impaired migration of neutrophils and macrophages in a tail wound assays and a thrombosis and/or bleeding phenotype that mirrored the human syndrome (Cvejic et al., 2008). Morpholino studies were then confirmed by two different mutant alleles (Cvejic et al., 2008). More recently, a zebrafish *wasa* null mutant allele modeling WAS and XLN disorders was characterized (Jones et al., 2013). The null mutant showed defects in the wound-induced inflammatory response, due to inefficiency in forming and maintaining new leading pseudopods, and also defects in immune-cell-mediated resistance to bacterial infection, as observed in WAS patients (Jones et al., 2013).

WHIM Syndrome

The warts, hypogammaglobulinemia, infections, and myelokathexis (WHIM) syndrome is caused by dominant mutations in chemokine receptor CXCR4 that induce the truncation of its carboxy-terminal domain. This leads to a defect in the internalization of the CXCR4 receptor after the binding to the sdf1 ligand (which is encoded in humans by CXCL12 gene) and it induces an increased signaling and enhanced migration after stimulation by chemokine (Hernandez et al., 2003). The WHIM syndrome is an inherited immunodeficiency that presents a range of symptoms, including human papillomavirus (HPV)-induced warts, reduced long-term immunoglobulin G (IgG) titers, recurring infections, retention of neutrophils in the bone marrow (myelokathexis), and leukopenia (Kallikourdis et al., 2015). In a mouse model

of the WHIM syndrome, which recapitulates the defects observed in human patients, the expression of the mutant forms of CXCR4 in hematopoietic stem cells blocks the release of neutrophils from the bone marrow, inducing apoptosis in neutrophils and eventually neutropenia (Kawai et al., 2007). A stable transgenic line specifically expressing in neutrophils the homologous CXCR4 receptor truncation mutations found in WHIM patients was generated in zebrafish to model the disorder. As observed in the mouse model and in human patients, the zebrafish model showed neutrophil retention in hematopoietic tissue and an impairment of neutrophil motility and wound recruitment. The neutrophil retention is SDF1 dependent, because depletion of SDF1 using MOs restores neutrophil chemotaxis to wounds (Walters et al., 2010).

Chronic Granulomatous Disease

Chronic granulomatous disease (CGD) is an inherited PID caused by functional impairment of the NADPH oxidase complex in neutrophilic granulocytes and monocytes compromising their ability to produce ROS that are highly toxic to phagocytosed microorganisms. CGD is characterized by recurrent and severe infections, dysregulated inflammation, and autoimmunity, and patients are at increased risk of life-threatening infections with catalase-positive bacteria and fungi and inflammatory complications such as CGD colitis (Arnold and Heimall, 2017). Mutations in any of the five structural subunits of the NADPH oxidase complex result in defective ROS production that are highly toxic to phagocytosed microorganisms.

Although only mouse genetic models of CGD are currently available (Schaffer and Klein, 2013), studies in zebrafish using MOs targeting different components of the PHOX complex successfully demonstrated that phagocyte-mediated killing of *Candida albicans* (Brothers et al., 2011) and *Mycobacterium marinum* (Yang et al., 2012) are dependent on their ability to generate an oxidative burst (Harvie and Huttenlocher, 2015).

Leukocyte Adhesion Deficiency

Leukocyte Adhesion Deficiency (LAD) is a group of disorders characterized by devastating bacterial infections associated with an increased number of circulating neutrophils (neutrophilia) (Burns et al., 2017). So far, four different types of LAD have been described (Burns et al., 2017). The LADs are usually distinguished by Roman numerals, I, II, III, and IV. There are mouse models for each of the four diseases, and additional non-murine animal models for two of them (Hanna and Etzioni, 2012). In particular, LAD IV (also indicated as Rac2-deficiency), is a very rare autosomal recessive disorder in which loss of function Rac2 mutations cause defects of neutrophil F-actin assembly, adhesion and migration (Schaffer and Klein, 2013). Although, because of the additional role of RAC2 in the NADPH complex, the phenotypes of RAC2-deficiency overlap those observed in CGD. Due to RAC2's role in cell adhesion and migration, and other pathways, the phenotypes are more severe than in CGD. Recently, two models of RAC2-deficiency have been developed in zebrafish (Deng et al., 2011) using MOs and expressing in zebrafish neutrophils the human dominant inhibitory Rac2D57N mutation found in patients, respectively. Both models present a failure in wound healing due to impaired neutrophil chemotaxis and in both, the neutrophils fail to respond to a *Pseudomonas aeruginosa* infection (Deng et al., 2011). As observed in patients, LAD fish exhibit neutrophilia from hematopoietic tissue without increased production of neutrophils and a defect in leaving the vasculature to reach the sites of tissue damage. Notably, neutrophil retention in the CHT of WHIM fish is reduced by the expression of Rac2D57N in neutrophils, suggesting that Rac2 signaling is also necessary in CXCR4-mediated neutrophil retention in hematopoietic tissues (Deng et al., 2011).

ZAP70 Deficiency

Zeta-chain (TCR) associated protein kinase, 70 kDa (ZAP70) deficiency is a rare form of SCID characterized by a deficit of mature CD8+ T cells along with a regular number of non-functional circulating CD4+ T cells unable to mount an effective T cell response (Arpaia et al., 1994; Chan et al., 1994; Elder et al., 1994; Hivroz and Fischer, 1994). ZAP70 is an important mediator of T cell activation, proliferation, and differentiation (Wang et al., 2010). Mouse models of the disease present an even more severe block in T cell differentiation phenotypes with a lack of mature T cells (Negishi et al., 1995; Kadlecek et al., 1998), that usually is explained by a compensatory effect induced in humans by spleen tyrosine kinase (SYK) protein (Kadlecek et al., 1998). Although defects in lymphatic or blood endothelial specification have not been reported for ZAP70-deficient mice or humans, a first model in zebrafish using knockdown approaches indicated a role for both *syk* and *zap70* in vascular embryonic development (Christie et al., 2010). However, a more recent zebrafish genetic model, where a frame-shift mutation was introduced using a TALEN targeting exon 2 of the *zap70* gene, failed to show any vascular and/or lymphatic defects (Moore et al., 2016). However, zebrafish *zap70* null mutants presented a reduction of developing thymocytes and mature T cells during embryo development and later they develop a T cell-specific immunodeficiency that cannot be compensated by syk protein, fully confirming the data obtained in mouse models (Moore et al., 2016).

CONCLUSION AND FUTURE PERSPECTIVES

Thanks to the next-generation sequencing techniques, the ability to identify gene defects in small populations or even in single patients with inherited diseases is increased rapidly. More importantly, the overall costs of whole-exome sequencing and whole genome-wide association studies are steadily dropping and, based on all the predictions, they will continue to decrease in the coming years. In this scenario, the use of the latest genome-editing techniques such as CRIPR/Cas9 in association with the numerous unique features of the zebrafish model, will represents a huge boost in the modeling and in the understanding of the physiopathology of human diseases.

AUTHOR CONTRIBUTIONS

All authors listed have made a substantial, direct and intellectual contribution to the work, and approved it for publication.

FUNDING

This research was funded by the Intramural Research Program of the National Human Genome Research Institute; National Institutes of Health (SB: 1ZIAHG000183).

REFERENCES

Aboobaker, A. A., and Blaxter, M. L. (2000). Medical significance of *Caenorhabditis elegans*. *Ann. Med.* 32, 23–30. doi: 10.3109/07853890008995906

Alghisi, E., Distel, M., Malagola, M., Anelli, V., Santoriello, C., Herwig, L., et al. (2013). Targeting oncogene expression to endothelial cells induces proliferation of the myelo-erythroid lineage by repressing the Notch pathway. *Leukemia* 27, 2229–2241. doi: 10.1038/leu.2013.132

Al-Herz, W., Bousfiha, A., Casanova, J. L., Chapel, H., Conley, M. E., Cunningham-Rundles, C., et al. (2011). Primary immunodeficiency diseases: an update on the classification from the international union of immunological societies expert committee for primary immunodeficiency. *Front. Immunol.* 2:54. doi: 10.3389/fimmu.2011.00054

Amsterdam, A., and Hopkins, N. (2006). Mutagenesis strategies in zebrafish for identifying genes involved in development and disease. *Trends Genet.* 22, 473–478. doi: 10.1016/j.tig.2006.06.011

Amsterdam, A., Sadler, K. C., Lai, K., Farrington, S., Bronson, R. T., Lees, J. A., et al. (2004). Many ribosomal protein genes are cancer genes in zebrafish. *PLoS Biol.* 2:E139. doi: 10.1371/journal.pbio.0020139

Armstrong, G. A., Liao, M., You, Z., Lissouba, A., Chen, B. E., and Drapeau, P. (2016). Homology directed knockin of point mutations in the Zebrafish tardbp and fus genes in ALS using the CRISPR/Cas9 system. *PLoS One* 11:e0150188. doi: 10.1371/journal.pone.0150188

Arnold, D. E., and Heimall, J. R. (2017). A review of chronic granulomatous disease. *Adv. Ther.* 34, 2543–2557. doi: 10.1007/s12325-017-0636-2

Aronson, J. K. (2006). Rare diseases and orphan drugs. *Br. J. Clin. Pharmacol.* 61, 243–245. doi: 10.1111/j.1365-2125.2006.02617.x

Arpaia, E., Shahar, M., Dadi, H., Cohen, A., and Roifman, C. M. (1994). Defective T cell receptor signaling and $CD8^+$ thymic selection in humans lacking zap-70 kinase. *Cell* 76, 947–958. doi: 10.1016/0092-8674(94)90368-9

Auer, T. O., Duroure, K., De Cian, A., Concordet, J. P., and Del Bene, F. (2014). Highly efficient CRISPR/Cas9-mediated knock-in in zebrafish by homology-independent DNA repair. *Genome Res.* 24, 142–153. doi: 10.1101/gr.161638.113

Avagyan, S., and Zon, L. I. (2016). Fish to learn: insights into blood development and blood disorders from zebrafish hematopoiesis. *Hum. Gene Ther.* 27, 287–294. doi: 10.1089/hum.2016.024

Balci, T. B., Prykhozhij, S. V., Teh, E. M., Da'as, S. I., McBride, E., Liwski, R., et al. (2014). A transgenic zebrafish model expressing KIT-D816V recapitulates features of aggressive systemic mastocytosis. *Br. J. Haematol.* 167, 48–61. doi: 10.1111/bjh.12999

Ball, S. (2011). Diamond Blackfan anemia. *Hematol. Am. Soc. Hematol. Educ. Program* 2011, 487–491. doi: 10.1182/asheducation-2011.1.487

Bedell, V. M., Wang, Y., Campbell, J. M., Poshusta, T. L., Starker, C. G., Krug, R. G., et al. (2012). In vivo genome editing using a high-efficiency TALEN system. *Nature* 491, 114–118. doi: 10.1038/nature11537

Berman, J., Hsu, K., and Look, A. T. (2003). Zebrafish as a model organism for blood diseases. *Br. J. Haematol.* 123, 568–576. doi: 10.1046/j.1365-2141.2003.04682.x

Bernards, A., and Hariharan, I. K. (2001). Of flies and men–studying human disease in Drosophila. *Curr. Opin. Genet. Dev.* 11, 274–278. doi: 10.1016/S0959-437X(00)00190-8

Bertrand, J. Y., Chi, N. C., Santoso, B., Teng, S., Stainier, D. Y., and Traver, D. (2010). Haematopoietic stem cells derive directly from aortic endothelium during development. *Nature* 464, 108–111. doi: 10.1038/nature08738

Bertrand, J. Y., Kim, A. D., Violette, E. P., Stachura, D. L., Cisson, J. L., and Traver, D. (2007). Definitive hematopoiesis initiates through a committed erythromyeloid progenitor in the zebrafish embryo. *Development* 134, 4147–4156. doi: 10.1242/dev.012385

Bertrand, J. Y., and Traver, D. (2009). Hematopoietic cell development in the zebrafish embryo. *Curr. Opin. Hematol.* 16, 243–248. doi: 10.1097/MOH.0b013e32832c05e4

Bier, E., and McGinnis, W. (2004). "Chapter 3. Model organisms in the study of development and disease," in *Molecular Basis of Inborn Errors of Development*, eds R. P. Erickson and A. J. Wynshaw-Boris (New York, NY: Oxford University Press), 25–45.

Bill, B. R., Petzold, A. M., Clark, K. J., Schimmenti, L. A., and Ekker, S. C. (2009). A primer for morpholino use in zebrafish. *Zebrafish* 6, 69–77. doi: 10.1089/zeb.2008.0555

Blum, M., De Robertis, E. M., Wallingford, J. B., and Niehrs, C. (2015). Morpholinos: antisense and sensibility. *Dev. Cell* 35, 145–149. doi: 10.1016/j.devcel.2015.09.017

Bosticardo, M., Draghici, E., Schena, F., Sauer, A. V., Fontana, E., Castiello, M. C., et al. (2011). Lentiviral-mediated gene therapy leads to improvement of B-cell functionality in a murine model of Wiskott-Aldrich syndrome. *J. Allergy Clin. Immunol.* 127, 1376–U1109. doi: 10.1016/j.jaci.2011.03.030

Bosticardo, M., Ferrua, F., Cavazzana, M., and Aiuti, A. (2014). Gene therapy for Wiskott-Aldrich Syndrome. *Curr. Gene Ther.* 14, 413–421. doi: 10.2174/1566523214666140918103731

Boulechfar, S., Lamoril, J., Montagutelli, X., Guenet, J. L., Deybach, J. C., Nordmann, Y., et al. (1993). Ferrochelatase structural mutant (Fechm1Pas) in the house mouse. *Genomics* 16, 645–648. doi: 10.1006/geno.1993.1242

Boycott, K. M., Vanstone, M. R., Bulman, D. E., and MacKenzie, A. E. (2013). Rare-disease genetics in the era of next-generation sequencing: discovery to translation. *Nat. Rev. Genet.* 14, 681–691. doi: 10.1038/nrg3555

Bradford, Y. M., Toro, S., Ramachandran, S., Ruzicka, L., Howe, D. G., Eagle, A., et al. (2017). Zebrafish models of human disease: gaining insight into human disease at ZFIN. *ILAR J.* 58, 4–16. doi: 10.1093/ilar/ilw040

Bresciani, E., Carrington, B., Wincovitch, S., Jones, M., Gore, A. V., Weinstein, B. M., et al. (2014). CBFbeta and RUNX1 are required at 2 different steps during the development of hematopoietic stem cells in zebrafish. *Blood* 124, 70–78. doi: 10.1182/blood-2013-10-531988

Brothers, K. M., Newman, Z. R., and Wheeler, R. T. (2011). Live imaging of disseminated candidiasis in zebrafish reveals role of phagocyte oxidase in limiting filamentous growth. *Eukaryot. Cell* 10, 932–944. doi: 10.1128/EC.05005-11

Brownlie, A., Donovan, A., Pratt, S. J., Paw, B. H., Oates, A. C., Brugnara, C., et al. (1998). Positional cloning of the zebrafish sauternes gene: a model for congenital sideroblastic anaemia. *Nat. Genet.* 20, 244–250. doi: 10.1038/3049

Burns, S. O., Zarafov, A., and Thrasher, A. J. (2017). Primary immunodeficiencies due to abnormalities of the actin cytoskeleton. *Curr. Opin. Hematol.* 24, 16–22. doi: 10.1097/MOH.0000000000000296

Campagnoli, M. F., Ramenghi, U., Armiraglio, M., Quarello, P., Garelli, E., Carando, A., et al. (2008). RPS19 mutations in patients with Diamond-Blackfan anemia. *Hum. Mutat.* 29, 911–920. doi: 10.1002/humu.20752

Chakraborty, A., Uechi, T., Higa, S., Torihara, H., and Kenmochi, N. (2009). Loss of ribosomal protein L11 affects zebrafish embryonic development through a p53-dependent apoptotic response. *PLoS One* 4:e4152. doi: 10.1371/journal.pone.0004152

Chan, A. C., Kadlecek, T. A., Elder, M. E., Filipovich, A. H., Kuo, W. L., Iwashima, M., et al. (1994). ZAP-70 deficiency in an autosomal recessive form of severe combined immunodeficiency. *Science* 264, 1599–1601. doi: 10.1126/science.8202713

Chien, S., Reiter, L. T., Bier, E., and Gribskov, M. (2002). Homophila: human disease gene cognates in *Drosophila*. *Nucleic Acids Res.* 30, 149–151. doi: 10.1093/nar/30.1.149

Childs, S., Weinstein, B. M., Mohideen, M. A., Donohue, S., Bonkovsky, H., and Fishman, M. C. (2000). Zebrafish dracula encodes ferrochelatase and its

mutation provides a model for erythropoietic protoporphyria. *Curr. Biol.* 10, 1001–1004. doi: 10.1016/S0960-9822(00)00653-9

Christie, T. L., Carter, A., Rollins, E. L., and Childs, S. J. (2010). Syk and Zap-70 function redundantly to promote angioblast migration. *Dev. Biol.* 340, 22–29. doi: 10.1016/j.ydbio.2010.01.011

Chung, C. Y., Funamoto, S., and Firtel, R. A. (2001). Signaling pathways controlling cell polarity and chemotaxis. *Trends Biochem. Sci.* 26, 557–566. doi: 10.1016/S0968-0004(01)01934-X

Ciau-Uitz, A., Monteiro, R., Kirmizitas, A., and Patient, R. (2014). Developmental hematopoiesis: ontogeny, genetic programming and conservation. *Exp. Hematol.* 42, 669–683. doi: 10.1016/j.exphem.2014.06.001

Culetto, E., and Sattelle, D. B. (2000). A role for *Caenorhabditis elegans* in understanding the function and interactions of human disease genes. *Hum. Mol. Genet.* 9, 869–877. doi: 10.1093/hmg/9.6.869

Cvejic, A., Hall, C., Bak-Maier, M., Flores, M. V., Crosier, P., Redd, M. J., et al. (2008). Analysis of WASp function during the wound inflammatory response–live-imaging studies in zebrafish larvae. *J. Cell Sci.* 121(Pt 19), 3196–3206. doi: 10.1242/jcs.032235

Dai, Y. M., Zhu, L., Huang, Z. B., Zhou, M. Y., Jin, W., Liu, W., et al. (2016). Cebp alpha is essential for the embryonic myeloid progenitor and neutrophil maintenance in zebrafish. *J. Genet. Genomics* 43, 593–600. doi: 10.1016/j.jgg.2016.09.001

Danilova, N., Sakamoto, K. M., and Lin, S. (2008). Ribosomal protein S19 deficiency in zebrafish leads to developmental abnormalities and defective erythropoiesis through activation of p53 protein family. *Blood* 112, 5228–5237. doi: 10.1182/blood-2008-01-132290

Danilova, N., Wilkes, M., Bibikova, E., Youn, M. Y., Sakamoto, K. M., and Lin, S. (2018). Innate immune system activation in zebrafish and cellular models of Diamond Blackfan Anemia. *Sci. Rep.* 8:5165. doi: 10.1038/s41598-018-23561-6

Davidson, A. J., and Zon, L. I. (2004). The 'definitive' (and 'primitive') guide to zebrafish hematopoiesis. *Oncogene* 23, 7233–7246. doi: 10.1038/sj.onc.1207943

de Jong, J. L., and Zon, L. I. (2005). Use of the zebrafish system to study primitive and definitive hematopoiesis. *Annu. Rev. Genet.* 39, 481–501. doi: 10.1146/annurev.genet.39.073003.095931

Deng, Q., Yoo, S. K., Cavnar, P. J., Green, J. M., and Huttenlocher, A. (2011). Dual roles for Rac2 in neutrophil motility and active retention in zebrafish hematopoietic tissue. *Dev. Cell* 21, 735–745. doi: 10.1016/j.devcel.2011.07.013

Derry, J. M., Ochs, H. D., and Francke, U. (1994). Isolation of a novel gene mutated in Wiskott-Aldrich syndrome. *Cell* 78, 635–644. doi: 10.1016/0092-8674(94)90528-2

Detrich, H. W. III, Westerfield, M., and Zon, L. I. (1999). Overview of the Zebrafish system. *Methods Cell Biol.* 59, 3–10. doi: 10.1016/S0091-679X(08)61816-6

Devriendt, K., Kim, A. S., Mathijs, G., Frints, S. G., Schwartz, M., Van Den Oord, J. J., et al. (2001). Constitutively activating mutation in WASP causes X-linked severe congenital neutropenia. *Nat. Genet.* 27, 313–317. doi: 10.1038/85886

Dimitrova, N., Zamudio, J. R., Jong, R. M., Soukup, D., Resnick, R., Sarma, K., et al. (2014). LincRNA-p21 activates p21 in cis to promote Polycomb target gene expression and to enforce the G1/S checkpoint. *Mol. Cell.* 54, 777–790. doi: 10.1016/j.molcel.2014.04.025

Dobson, J. T., Seibert, J., Teh, E. M., Da'as, S., Fraser, R. B., Paw, B. H., et al. (2008). Carboxypeptidase A5 identifies a novel mast cell lineage in the zebrafish providing new insight into mast cell fate determination. *Blood* 112, 2969–2972. doi: 10.1182/blood-2008-03-145011

Doyon, Y., McCammon, J. M., Miller, J. C., Faraji, F., Ngo, C., Katibah, G. E., et al. (2008). Heritable targeted gene disruption in zebrafish using designed zinc-finger nucleases. *Nat. Biotechnol.* 26, 702–708. doi: 10.1038/nbt1409

Draptchinskaia, N., Gustavsson, P., Andersson, B., Pettersson, M., Willig, T. N., Dianzani, I., et al. (1999). The gene encoding ribosomal protein S19 is mutated in Diamond-Blackfan anaemia. *Nat. Genet.* 21, 169–175. doi: 10.1038/5951

Dupre, L., Marangoni, F., Scaramuzza, S., Trifari, S., Hernandez, R. J., Aiuti, A., et al. (2006). Efficacy of gene therapy for Wiskott-Aldrich syndrome using a WAS promoter/cDNA-containing lentiviral vector and nonlethal irradiation. *Hum. Gene Ther.* 17, 303–313. doi: 10.1089/hum.2006.17.303

Dzeja, P. P., and Terzic, A. (2003). Phosphotransfer networks and cellular energetics. *J. Exp. Biol.* 206(Pt 12), 2039–2047. doi: 10.1242/jeb.00426

Eisen, J. S., and Smith, J. C. (2008). Controlling morpholino experiments: don't stop making antisense. *Development* 135, 1735–1743. doi: 10.1242/dev.001115

Elder, M. E., Lin, D., Clever, J., Chan, A. C., Hope, T. J., Weiss, A., et al. (1994). Human severe combined immunodeficiency due to a defect in ZAP-70, a T cell tyrosine kinase. *Science* 264, 1596–1599. doi: 10.1126/science.8202712

Evers, M. M., Toonen, L. J. A., and van Roon-Mom, W. M. C. (2015). Antisense oligonucleotides in therapy for neurodegenerative disorders. *Adv. Drug Deliv. Rev.* 87, 90–103. doi: 10.1016/j.addr.2015.03.008

Farrar, J. E., Vlachos, A., Atsidaftos, E., Carlson-Donohoe, H., Markello, T. C., Arceci, R. J., et al. (2011). Ribosomal protein gene deletions in Diamond-Blackfan anemia. *Blood* 118, 6943–6951. doi: 10.1182/blood-2011-08-375170

Firtel, R. A., and Chung, C. Y. (2000). The molecular genetics of chemotaxis: sensing and responding to chemoattractant gradients. *Bioessays* 22, 603–615. doi: 10.1002/1521-1878(200007)22:7<603::AID-BIES3>3.0.CO;2-#

Fischer, A., Hacein-Bey-Abina, S., and Cavazzana-Calvo, M. (2013). Gene therapy of primary T cell immunodeficiencies. *Gene* 525, 170–173. doi: 10.1016/j.gene.2013.03.092

Forrester, A. M., Berman, J. N., and Payne, E. M. (2012). Myelopoiesis and myeloid leukaemogenesis in the zebrafish. *Adv. Hematol.* 2012:358518. doi: 10.1155/2012/358518

Foury, F. (1997). Human genetic diseases: a cross-talk between man and yeast. *Gene* 195, 1–10. doi: 10.1016/S0378-1119(97)00140-6

Galloway, J. L., Wingert, R. A., Thisse, C., Thisse, B., and Zon, L. I. (2005). Loss of gata1 but not gata2 converts erythropoiesis to myelopoiesis in zebrafish embryos. *Dev. Cell* 8, 109–116. doi: 10.1016/j.devcel.2004.12.001

Gazda, H. T., Preti, M., Sheen, M. R., O'Donohue, M. F., Vlachos, A., Davies, S. M., et al. (2012). Frameshift mutation in p53 regulator RPL26 is associated with multiple physical abnormalities and a specific pre-ribosomal RNA processing defect in diamond-blackfan anemia. *Hum. Mutat.* 33, 1037–1044. doi: 10.1002/humu.22081

Gerbaulet, A., Wickenhauser, C., Scholten, J., Peschke, K., Drube, S., Horny, H. P., et al. (2011). Mast cell hyperplasia, B-cell malignancy, and intestinal inflammation in mice with conditional expression of a constitutively active kit. *Blood* 117, 2012–2021. doi: 10.1182/blood-2008-11-189605

Golling, G., Amsterdam, A., Sun, Z., Antonelli, M., Maldonado, E., Chen, W., et al. (2002). Insertional mutagenesis in zebrafish rapidly identifies genes essential for early vertebrate development. *Nat. Genet.* 31, 135–140. doi: 10.1038/ng896

Gore, A. V., Athans, B., Iben, J. R., Johnson, K., Russanova, V., Castranova, D., et al. (2016). Epigenetic regulation of hematopoiesis by DNA methylation. *eLife* 5:e11813. doi: 10.7554/eLife.11813

Gore, A. V., Pillay, L. M., Venero Galanternik, M., and Weinstein, B. M. (2018). The zebrafish: a fintastic model for hematopoietic development and disease. *Wiley Interdiscip. Rev. Dev. Biol.* 7:e312. doi: 10.1002/wdev.312

Haffter, P., Granato, M., Brand, M., Mullins, M. C., Hammerschmidt, M., Kane, D. A., et al. (1996). The identification of genes with unique and essential functions in the development of the zebrafish, *Danio rerio*. *Development* 123, 1–36.

Haffter, P., and Nusslein-Volhard, C. (1996). Large scale genetics in a small vertebrate, the zebrafish. *Int. J. Dev. Biol.* 40, 221–227.

Hanna, S., and Etzioni, A. (2012). Leukocyte adhesion deficiencies. *Year Hum. Med. Genet.* 1250, 50–55. doi: 10.1111/j.1749-6632.2011.06389.x

Harvie, E. A., and Huttenlocher, A. (2015). Neutrophils in host defense: new insights from zebrafish. *J. Leukoc. Biol.* 98, 523–537. doi: 10.1189/jlb.4MR1114-524R

Heasman, J., Ginsberg, D., Geiger, B., Goldstone, K., Pratt, T., Yoshidanoro, C., et al. (1994). A functional test for maternally inherited cadherin in xenopus shows its importance in cell-adhesion at the blastula stage. *Development* 120, 49–57.

Herbomel, P., Thisse, B., and Thisse, C. (1999). Ontogeny and behaviour of early macrophages in the zebrafish embryo. *Development* 126, 3735–3745.

Hernandez, P. A., Gorlin, R. J., Lukens, J. N., Taniuchi, S., Bohinjec, J., Francois, F., et al. (2003). Mutations in the chemokine receptor gene CXCR4 are associated with WHIM syndrome, a combined immunodeficiency disease. *Nat. Genet.* 34, 70–74. doi: 10.1038/ng1149

Hess, I., and Boehm, T. (2012). Intravital imaging of thymopoiesis reveals dynamic lympho-epithelial interactions. *Immunity* 36, 298–309. doi: 10.1016/j.immuni.2011.12.016

Hisano, Y., Sakuma, T., Nakade, S., Ohga, R., Ota, S., Okamoto, H., et al. (2015). Precise in-frame integration of exogenous DNA mediated by CRISPR/Cas9 system in zebrafish. *Sci. Rep.* 5:8841. doi: 10.1038/srep08841

Hivroz, C., and Fischer, A. (1994). Immunodeficiency diseases. Multiple roles for ZAP-70. *Curr. Biol.* 4, 731–733. doi: 10.1016/S0960-9822(00)00162-7

Hoenig, M., Lagresle-Peyrou, C., Pannicke, U., Notarangelo, L. D., Porta, F., Gennery, A. R., et al. (2017). Reticular dysgenesis: international survey on clinical presentation, transplantation, and outcome. *Blood* 129, 2928–2938. doi: 10.1182/blood-2016-11-745638

Hoenig, M., Pannicke, U., Gaspar, H. B., and Schwarz, K. (2018). Recent advances in understanding the pathogenesis and management of reticular dysgenesis. *Br. J. Haematol.* 180, 644–653. doi: 10.1111/bjh.15045

Hoshijima, K., Jurynec, M. J., and Grunwald, D. J. (2016). Precise genome editing by homologous recombination. *Methods Cell Biol.* 135, 121–147. doi: 10.1016/bs.mcb.2016.04.008

Howe, D. G., Bradford, Y. M., Eagle, A., Fashena, D., Frazer, K., Kalita, P., et al. (2017). The zebrafish model organism database: new support for human disease models, mutation details, gene expression phenotypes and searching. *Nucleic Acids Res.* 45, D758–D768. doi: 10.1093/nar/gkw1116

Howe, K., Clark, M. D., Torroja, C. F., Torrance, J., Berthelot, C., Muffato, M., et al. (2013). The zebrafish reference genome sequence and its relationship to the human genome. *Nature* 496, 498–503. doi: 10.1038/nature12111

Hruscha, A., Krawitz, P., Rechenberg, A., Heinrich, V., Hecht, J., Haass, C., et al. (2013). Efficient CRISPR/Cas9 genome editing with low off-target effects in zebrafish. *Development* 140, 4982–4987. doi: 10.1242/dev.099085

Huang, P., Xiao, A., Zhou, M., Zhu, Z., Lin, S., and Zhang, B. (2011). Heritable gene targeting in zebrafish using customized TALENs. *Nat. Biotechnol.* 29, 699–700. doi: 10.1038/nbt.1939

Hwang, W. Y., Fu, Y., Reyon, D., Maeder, M. L., Kaini, P., Sander, J. D., et al. (2013a). Heritable and precise zebrafish genome editing using a CRISPR-Cas system. *PLoS One* 8:e68708. doi: 10.1371/journal.pone.0068708

Hwang, W. Y., Fu, Y., Reyon, D., Maeder, M. L., Tsai, S. Q., Sander, J. D., et al. (2013b). Efficient genome editing in zebrafish using a CRISPR-Cas system. *Nat. Biotechnol.* 31, 227–229. doi: 10.1038/nbt.2501

Irion, U., Krauss, J., and Nusslein-Volhard, C. (2014). Precise and efficient genome editing in zebrafish using the CRISPR/Cas9 system. *Development* 141, 4827–4830. doi: 10.1242/dev.115584

Iwanami, N. (2014). Zebrafish as a model for understanding the evolution of the vertebrate immune system and human primary immunodeficiency. *Exp. Hematol.* 42, 697–706. doi: 10.1016/j.exphem.2014.05.001

Jao, L. E., Wente, S. R., and Chen, W. (2013). Efficient multiplex biallelic zebrafish genome editing using a CRISPR nuclease system. *Proc. Natl. Acad. Sci. U.S.A.* 110, 13904–13909. doi: 10.1073/pnas.1308335110

Jin, H., Huang, Z. B., Chi, Y. L., Wu, M., Zhou, R. Y., Zhao, L. F., et al. (2016). c-Myb acts in parallel and cooperatively with Cebp1 to regulate neutrophil maturation in zebrafish. *Blood* 128, 415–426. doi: 10.1182/blood-2015-12-686147

Jin, H., Li, L., Xu, J., Zhen, F. H., Zhu, L., Liu, P. P., et al. (2012). Runx1 regulates embryonic myeloid fate choice in zebrafish through a negative feedback loop inhibiting Pu.1 expression. *Blood* 119, 5239–5249. doi: 10.1182/blood-2011-12-398362

Jin, H., Sood, R., Xu, J., Zhen, F., English, M. A., Liu, P. P., et al. (2009). Definitive hematopoietic stem/progenitor cells manifest distinct differentiation output in the zebrafish VDA and PBI. *Development* 136, 647–654. doi: 10.1242/dev.029637

Jin, H., Xu, J., and Wen, Z. (2007). Migratory path of definitive hematopoietic stem/progenitor cells during zebrafish development. *Blood* 109, 5208–5214. doi: 10.1182/blood-2007-01-069005

Jones, R. A., Feng, Y., Worth, A. J., Thrasher, A. J., Burns, S. O., and Martin, P. (2013). Modelling of human Wiskott-Aldrich syndrome protein mutants in zebrafish larvae using in vivo live imaging. *J. Cell Sci.* 126(Pt 18), 4077–4084. doi: 10.1242/jcs.128728

Kadlecek, T. A., van Oers, N. S., Lefrancois, L., Olson, S., Finlay, D., Chu, D. H., et al. (1998). Differential requirements for ZAP-70 in TCR signaling and T cell development. *J. Immunol.* 161, 4688–4694.

Kallikourdis, M., Viola, A., and Benvenuti, F. (2015). Human immunodeficiencies related to defective APC/T cell interaction. *Front. Immunol.* 6:433. doi: 10.3389/fimmu.2015.00433

Karlsson, J., von Hofsten, J., and Olsson, P. E. (2001). Generating transparent zebrafish: a refined method to improve detection of gene expression during embryonic development. *Mar. Biotechnol.* 3, 522–527. doi: 10.1007/s1012601-0053-4

Kawai, T., Choi, U., Cardwell, L., DeRavin, S. S., Naumann, N., Whiting-Theobald, N. L., et al. (2007). WHIM syndrome myelokathexis reproduced in the NOD/SCID mouse xenotransplant model engrafted with healthy human stem cells transduced with C-terminus-truncated CXCR4. *Blood* 109, 78–84. doi: 10.1182/blood-2006-05-025296

Kim, K., Ryu, S. M., Kim, S. T., Baek, G., Kim, D., Lim, K., et al. (2017). Highly efficient RNA-guided base editing in mouse embryos. *Nat. Biotechnol.* 35, 435–437. doi: 10.1038/nbt.3816

Kimura, Y., Hisano, Y., Kawahara, A., and Higashijima, S. (2014). Efficient generation of knock-in transgenic zebrafish carrying reporter/driver genes by CRISPR/Cas9-mediated genome engineering. *Sci. Rep.* 4:6545. doi: 10.1038/srep06545

Kissa, K., and Herbomel, P. (2010). Blood stem cells emerge from aortic endothelium by a novel type of cell transition. *Nature* 464, 112–115. doi: 10.1038/nature08761

Kissa, K., Murayama, E., Zapata, A., Cortes, A., Perret, E., Machu, C., et al. (2008). Live imaging of emerging hematopoietic stem cells and early thymus colonization. *Blood* 111, 1147–1156. doi: 10.1182/blood-2007-07-099499

Klaiber, N., Kumar, S., and Irani, A. M. (2017). Mastocytosis in children. *Curr. Allergy Asthma Rep.* 17:80. doi: 10.1007/s11882-017-0748-4

Kok, F. O., Shin, M., Ni, C. W., Gupta, A., Grosse, A. S., van Impel, A., et al. (2015). Reverse genetic screening reveals poor correlation between morpholino-induced and mutant phenotypes in zebrafish. *Dev. Cell* 32, 97–108. doi: 10.1016/j.devcel.2014.11.018

Komor, A. C., Kim, Y. B., Packer, M. S., Zuris, J. A., and Liu, D. R. (2016). Programmable editing of a target base in genomic DNA without double-stranded DNA cleavage. *Nature* 533, 420–424. doi: 10.1038/nature17946

Kondrychyn, I., Teh, C., Garcia-Lecea, M., Guan, Y., Kang, A., and Korzh, V. (2011). Zebrafish Enhancer TRAP transgenic line database ZETRAP 2.0. *Zebrafish* 8, 181–182. doi: 10.1089/zeb.2011.0718

Lagresle-Peyrou, C., Six, E. M., Picard, C., Rieux-Laucat, F., Michel, V., Ditadi, A., et al. (2009). Human adenylate kinase 2 deficiency causes a profound hematopoietic defect associated with sensorineural deafness. *Nat. Genet.* 41, 106–111. doi: 10.1038/ng.278

Lai, K., Amsterdam, A., Farrington, S., Bronson, R. T., Hopkins, N., and Lees, J. A. (2009). Many ribosomal protein mutations are associated with growth impairment and tumor predisposition in zebrafish. *Dev. Dyn.* 238, 76–85. doi: 10.1002/dvdy.21815

Langenau, D. M., Traver, D., Ferrando, A. A., Kutok, J. L., Aster, J. C., Kanki, J. P., et al. (2003). Myc-induced T cell leukemia in transgenic zebrafish. *Science* 299, 887–890. doi: 10.1126/science.1080280

Langheinrich, U. (2003). Zebrafish: a new model on the pharmaceutical catwalk. *Bioessays* 25, 904–912. doi: 10.1002/bies.10326

Lavandeira, A. (2002). Orphan drugs: legal aspects, current situation. *Haemophilia* 8, 194–198. doi: 10.1046/j.1365-2516.2002.00643.x

Lennartsson, J., and Ronnstrand, L. (2012). Stem cell factor receptor/c-Kit: from basic science to clinical implications. *Physiol. Rev.* 92, 1619–1649. doi: 10.1152/physrev.00046.2011

Leon, C., Dupuis, A., Gachet, C., and Lanza, F. (2016). The contribution of mouse models to the understanding of constitutional thrombocytopenia. *Haematologica* 101, 896–908. doi: 10.3324/haematol.2015.139394

Li, J., Zhang, B. B., Ren, Y. G., Gu, S. Y., Xiang, Y. H., Huang, C., et al. (2015). Intron targeting-mediated and endogenous gene integrity-maintaining knockin in zebrafish using the CRISPR/Cas9 system. *Cell Res.* 25, 634–637. doi: 10.1038/cr.2015.43

Li, L., Jin, H., Xu, J., Shi, Y., and Wen, Z. (2011). Irf8 regulates macrophage versus neutrophil fate during zebrafish primitive myelopoiesis. *Blood* 117, 1359–1369. doi: 10.1182/blood-2010-06-290700

Marathe, B. M., Prislovsky, A., Astrakhan, A., Rawlings, D. J., Wan, J. Y., and Strom, T. S. (2009). Antiplatelet antibodies in WASP(-) mice correlate with evidence of increased in vivo platelet consumption. *Exp. Hematol.* 37, 1353–1363. doi: 10.1016/j.exphem.2009.08.007

Matsson, H., Davey, E. J., Draptchinskaia, N., Hamaguchi, I., Ooka, A., Leeven, P., et al. (2004). Targeted disruption of the ribosomal protein S19 gene is lethal prior to implantation. *Mol. Cell. Biol.* 24, 4032–4037. doi: 10.1128/MCB.24.9.4032-4037.2004

Matsson, H., Davey, E. J., Frojmark, A. S., Miyake, K., Utsugisawa, T., Flygare, J., et al. (2006). Erythropoiesis in the Rps19 disrupted mouse: analysis of

erythropoietin response and biochemical markers for Diamond-Blackfan anemia. *Blood Cells Mol. Dis.* 36, 259–264. doi: 10.1016/j.bcmd.2005.12.002

McGowan, K. A., Li, J. Z., Park, C. Y., Beaudry, V., Tabor, H. K., Sabnis, A. J., et al. (2008). Ribosomal mutations cause p53-mediated dark skin and pleiotropic effects. *Nat. Genet.* 40, 963–970. doi: 10.1038/ng.188

McGowan, K. A., and Mason, P. J. (2011). Animal models of Diamond Blackfan anemia. *Semin. Hematol.* 48, 106–116. doi: 10.1053/j.seminhematol.2011.02.001

Meng, X., Noyes, M. B., Zhu, L. J., Lawson, N. D., and Wolfe, S. A. (2008). Targeted gene inactivation in zebrafish using engineered zinc-finger nucleases. *Nat. Biotechnol.* 26, 695–701. doi: 10.1038/nbt1398

Meyer, A., and Van de Peer, Y. (2005). From 2R to 3R: evidence for a fish-specific genome duplication (FSGD). *Bioessays* 27, 937–945. doi: 10.1002/bies.20293

Mirabello, L., Macari, E. R., Jessop, L., Ellis, S. R., Myers, T., Giri, N., et al. (2014). Whole-exome sequencing and functional studies identify RPS29 as a novel gene mutated in multicase Diamond-Blackfan anemia families. *Blood* 124, 24–32. doi: 10.1182/blood-2013-11-540278

Mommaerts, H., Esguerra, C. V., Hartmann, U., Luyten, F. P., and Tylzanowski, P. (2014). Smoc2 modulates embryonic myelopoiesis during zebrafish development. *Dev. Dyn.* 243, 1375–1390. doi: 10.1002/dvdy.24164

Monteiro, R., Pouget, C., and Patient, R. (2011). The gata1/pu.1 lineage fate paradigm varies between blood populations and is modulated by tif1 gamma. *EMBO J.* 30, 1093–1103. doi: 10.1038/emboj.2011.34

Moore, F. E., and Langenau, D. M. (2012). Through the looking glass: visualizing leukemia growth, migration, and engraftment using fluorescent transgenic zebrafish. *Adv. Hematol.* 2012:478164. doi: 10.1155/2012/478164

Moore, J. C., Mulligan, T. S., Torres Yordan, N., Castranova, D., Pham, V. N., Tang, Q., et al. (2016). T cell immune deficiency in *zap70* mutant zebrafish. *Mol. Cell Biol.* [Epub ahead of print]. doi: 10.1128/MCB.00281-16

Moreno-Mateos, M. A., Fernandez, J. P., Rouet, R., Vejnar, C. E., Lane, M. A., Mis, E., et al. (2017). CRISPR-Cpf1 mediates efficient homology-directed repair and temperature-controlled genome editing. *Nat. Commun.* 8:2024. doi: 10.1038/s41467-017-01836-2

Mukherjee, S., and Thrasher, A. J. (2013). Gene therapy for PIDs: progress, pitfalls and prospects. *Gene* 525, 174–181. doi: 10.1016/j.gene.2013.03.098

Murayama, E., Kissa, K., Zapata, A., Mordelet, E., Briolat, V., Lin, H. F., et al. (2006). Tracing hematopoietic precursor migration to successive hematopoietic organs during zebrafish development. *Immunity* 25, 963–975. doi: 10.1016/j.immuni.2006.10.015

Nasevicius, A., and Ekker, S. C. (2000). Effective targeted gene 'knockdown' in zebrafish. *Nat. Genet.* 26, 216–220. doi: 10.1038/79951

Negishi, I., Motoyama, N., Nakayama, K., Nakayama, K., Senju, S., Hatakeyama, S., et al. (1995). Essential role for ZAP-70 in both positive and negative selection of thymocytes. *Nature* 376, 435–438. doi: 10.1038/376435a0

North, T. E., and Zon, L. I. (2003). Modeling human hematopoietic and cardiovascular diseases in zebrafish. *Dev. Dyn.* 228, 568–583. doi: 10.1002/dvdy.10393

Oates, A. C., Bruce, A. E., and Ho, R. K. (2000). Too much interference: injection of double-stranded RNA has nonspecific effects in the zebrafish embryo. *Dev. Biol.* 224, 20–28. doi: 10.1006/dbio.2000.9761

O'Brien, K. A., Farrar, J. E., Vlachos, A., Anderson, S. M., Tsujiura, C. A., Lichtenberg, J., et al. (2017). Molecular convergence in ex vivo models of Diamond-Blackfan anemia. *Blood* 129, 3111–3120. doi: 10.1182/blood-2017-01-760462

Ochs, H. D., and Thrasher, A. J. (2006). The Wiskott-Aldrich syndrome. *J. Allergy Clin. Immunol.* 117, 725–738;quiz739. doi: 10.1016/j.jaci.2006.02.005

Ohno, S. (1970). *Evolution by Gene Duplication*. New York, NY: Springer. doi: 10.1007/978-3-642-86659-3

Oshima, K., Saiki, N., Tanaka, M., Imamura, H., Niwa, A., Tanimura, A., et al. (2018). Human AK2 links intracellular bioenergetic redistribution to the fate of hematopoietic progenitors. *Biochem. Biophys. Res. Commun.* 497, 719–725. doi: 10.1016/j.bbrc.2018.02.139

Ott de Bruin, L. M., Volpi, S., and Musunuru, K. (2015). Novel genome-editing tools to model and correct primary immunodeficiencies. *Front. Immunol.* 6:250. doi: 10.3389/fimmu.2015.00250

Pai, S. Y., Logan, B. R., Griffith, L. M., Buckley, R. H., Parrott, R. E., Dvorak, C. C., et al. (2014). Transplantation outcomes for severe combined immunodeficiency, 2000-2009. *N. Engl. J. Med.* 371, 434–446. doi: 10.1056/NEJMoa1401177

Pannicke, U., Honig, M., Hess, I., Friesen, C., Holzmann, K., Rump, E. M., et al. (2009). Reticular dysgenesis (aleukocytosis) is caused by mutations in the gene encoding mitochondrial adenylate kinase 2. *Nat. Genet.* 41, 101–105. doi: 10.1038/ng.265

Pauli, A., Montague, T. G., Lennox, K. A., Behlke, M. A., and Schier, A. F. (2015). Antisense oligonucleotide-mediated transcript knockdown in zebrafish. *PLoS One* 10:e0139504. doi: 10.1371/journal.pone.0139504

Postlethwait, J., Amores, A., Cresko, W., Singer, A., and Yan, Y. L. (2004). Subfunction partitioning, the teleost radiation and the annotation of the human genome. *Trends Genet.* 20, 481–490. doi: 10.1016/j.tig.2004.08.001

Postlethwait, J., Amores, A., Force, A., and Yan, Y. L. (1999). The zebrafish genome. *Methods Cell Biol.* 60, 149–163. doi: 10.1016/S0091-679X(08)61898-1

Puck, J. M., and Candotti, F. (2006). Lessons from the Wiskott-Aldrich syndrome. *N. Engl. J. Med.* 355, 1759–1761. doi: 10.1056/NEJMp068209

Puy, H., Gouya, L., and Deybach, J. C. (2010). Porphyrias. *Lancet* 375, 924–937. doi: 10.1016/S0140-6736(09)61925-5

Ran, F. A., Hsu, P. D., Lin, C. Y., Gootenberg, J. S., Konermann, S., Trevino, A. E., et al. (2013). Double nicking by RNA-guided CRISPR Cas9 for enhanced genome editing specificity. *Cell* 154, 1380–1389. doi: 10.1016/j.cell.2013.08.021

Rastogi, S., and Liberles, D. A. (2005). Subfunctionalization of duplicated genes as a transition state to neofunctionalization. *BMC Evol. Biol.* 5:28. doi: 10.1186/1471-2148-5-28

Reiter, L. T., Potocki, L., Chien, S., Gribskov, M., and Bier, E. (2001). A systematic analysis of human disease-associated gene sequences in *Drosophila melanogaster*. *Genome Res.* 11, 1114–1125. doi: 10.1101/gr.169101

Rhodes, J., Hagen, A., Hsu, K., Deng, M., Liu, T. X., Look, A. T., et al. (2005). Interplay of pu.1 and gata1 determines myelo-erythroid progenitor cell fate in zebrafish. *Dev. Cell* 8, 97–108. doi: 10.1016/j.devcel.2004.11.014

Richard, E., Robert-Richard, E., Ged, C., Moreau-Gaudry, F., and de Verneuil, H. (2008). Erythropoietic porphyrias: animal models and update in gene-based therapies. *Curr. Gene Ther.* 8, 176–186. doi: 10.2174/156652308784746477

Rissone, A., Foglia, E., Sangiorgio, L., Cermenati, S., Nicoli, S., Cimbro, S., et al. (2012). The synaptic proteins beta-neurexin and neuroligin synergize with extracellular matrix-binding vascular endothelial growth factor a during zebrafish vascular development. *Arterioscler. Thromb. Vasc. Biol.* 32, 1563–1572. doi: 10.1161/ATVBAHA.111.243006

Rissone, A., Weinacht, K. G., la Marca, G., Bishop, K., Giocaliere, E., Jagadeesh, J., et al. (2015). Reticular dysgenesis-associated AK2 protects hematopoietic stem and progenitor cell development from oxidative stress. *J. Exp. Med.* 212, 1185–1202. doi: 10.1084/jem.20141286

Robertson, A. L., Avagyan, S., Gansner, J. M., and Zon, L. I. (2016). Understanding the regulation of vertebrate hematopoiesis and blood disorders - big lessons from a small fish. *FEBS Lett.* 590, 4016–4033. doi: 10.1002/1873-3468.12415

Robu, M. E., Larson, J. D., Nasevicius, A., Beiraghi, S., Brenner, C., Farber, S. A., et al. (2007). p53 activation by knockdown technologies. *PLoS Genet.* 3:e78. doi: 10.1371/journal.pgen.0030078

Rossi, A., Kontarakis, Z., Gerri, C., Nolte, H., Holper, S., Kruger, M., et al. (2015). Genetic compensation induced by deleterious mutations but not gene knockdowns. *Nature* 524, 230–233. doi: 10.1038/nature14580

Ruzicka, L., Bradford, Y. M., Frazer, K., Howe, D. G., Paddock, H., Ramachandran, S., et al. (2015). ZFIN, The zebrafish model organism database: updates and new directions. *Genesis* 53, 498–509. doi: 10.1002/dvg.22868

Sabri, S., Foudi, A., Boukour, S., Franc, B., Charrier, S., Jandrot-Perrus, M., et al. (2006). Deficiency in the Wiskott-Aldrich protein induces premature proplatelet formation and platelet production in the bone marrow compartment. *Blood* 108, 134–140. doi: 10.1182/blood-2005-03-1219

Sander, J. D., Cade, L., Khayter, C., Reyon, D., Peterson, R. T., Joung, J. K., et al. (2011). Targeted gene disruption in somatic zebrafish cells using engineered TALENs. *Nat. Biotechnol.* 29, 697–698. doi: 10.1038/nbt.1934

Santoriello, C., and Zon, L. I. (2012). Hooked! Modeling human disease in zebrafish. *J. Clin. Invest.* 122, 2337–2343. doi: 10.1172/JCI60434

Schaffer, A. A., and Klein, C. (2013). Animal models of human granulocyte diseases. *Hematol. Oncol. Clin. North Am.* 27, 129–148, ix. doi: 10.1016/j.hoc.2012.10.005

Shearer, W. T., Dunn, E., Notarangelo, L. D., Dvorak, C. C., Puck, J. M., Logan, B. R., et al. (2014). Establishing diagnostic criteria for severe combined immunodeficiency disease (SCID), leaky SCID, and Omenn syndrome: the

Primary Immune Deficiency Treatment Consortium experience. *J. Allergy Clin. Immunol.* 133, 1092–1098. doi: 10.1016/j.jaci.2013.09.044

Six, E., Lagresle-Peyrou, C., Susini, S., De Chappedelaine, C., Sigrist, N., Sadek, H., et al. (2015). AK2 deficiency compromises the mitochondrial energy metabolism required for differentiation of human neutrophil and lymphoid lineages. *Cell Death Dis.* 6:e1856. doi: 10.1038/cddis.2015.211

Sood, R., English, M. A., Belele, C. L., Jin, H., Bishop, K., Haskins, R., et al. (2010). Development of multilineage adult hematopoiesis in the zebrafish with a runx1 truncation mutation. *Blood* 115, 2806–2809. doi: 10.1182/blood-2009-08-236729

Sood, R., and Liu, P. (2012). Novel insights into the genetic controls of primitive and definitive hematopoiesis from zebrafish models. *Adv. Hematol.* 2012:830703. doi: 10.1155/2012/830703

Stainier, D. Y., Kontarakis, Z., and Rossi, A. (2015). Making sense of anti-sense data. *Dev. Cell* 32, 7–8. doi: 10.1016/j.devcel.2014.12.012

Stainier, D. Y. R., Raz, E., Lawson, N. D., Ekker, S. C., Burdine, R. D., Eisen, J. S., et al. (2017). Guidelines for morpholino use in zebrafish. *PLoS Genet.* 13:e1007000. doi: 10.1371/journal.pgen.1007000

Strynatka, K. A., Gurrola-Gal, M. C., Berman, J. N., and McMaster, C. R. (2018). How surrogate and chemical genetics in model organisms can suggest therapies for human genetic diseases. *Genetics* 208, 833–851. doi: 10.1534/genetics.117.300124

Symington, L. S., and Gautier, J. (2011). Double-strand break end resection and repair pathway choice. *Annu. Rev. Genet.* 45, 247–271. doi: 10.1146/annurev-genet-110410-132435

Tamplin, O. J., Durand, E. M., Carr, L. A., Childs, S. J., Hagedorn, E. J., Li, P., et al. (2015). Hematopoietic stem cell arrival triggers dynamic remodeling of the perivascular niche. *Cell* 160, 241–252. doi: 10.1016/j.cell.2014.12.032

Taylor, A. M., Humphries, J. M., White, R. M., Murphey, R. D., Burns, C. E., and Zon, L. I. (2012). Hematopoietic defects in rps29 mutant zebrafish depend upon p53 activation. *Exp. Hematol.* 40, 228–237. doi: 10.1016/j.exphem.2011.11.007

Thisse, C., and Thisse, B. (2008). High-resolution in situ hybridization to whole-mount zebrafish embryos. *Nat. Protoc.* 3, 59–69. doi: 10.1038/nprot.2007.514

Tian, Y., Xu, J., Feng, S., He, S., Zhao, S., Zhu, L., et al. (2017). The first wave of T lymphopoiesis in zebrafish arises from aorta endothelium independent of hematopoietic stem cells. *J. Exp. Med.* 214, 3347–3360. doi: 10.1084/jem.20170488

Timme-Laragy, A. R., Karchner, S. I., and Hahn, M. E. (2012). Gene knockdown by morpholino-modified oligonucleotides in the zebrafish (*Danio rerio*) model: applications for developmental toxicology. *Methods Mol. Biol.* 889, 51–71. doi: 10.1007/978-1-61779-867-2_5

Tsai, S. Q., Wyvekens, N., Khayter, C., Foden, J. A., Thapar, V., Reyon, D., et al. (2014). Dimeric CRISPR RNA-guided FokI nucleases for highly specific genome editing. *Nat. Biotechnol.* 32, 569–576. doi: 10.1038/nbt.2908

Tutois, S., Montagutelli, X., Dasilva, V., Jouault, H., Rouyerfessard, P., Leroyviard, K., et al. (1991). Erythropoietic protoporphyria in the house mouse - a recessive inherited ferrochelatase deficiency with anemia, photosensitivity, and liver-disease. *J. Clin. Invest.* 88, 1730–1736. doi: 10.1172/JCI115491

Uchiyama, T., Adriani, M., Jagadeesh, G. J., Paine, A., and Candotti, F. (2012). Foamy virus vector-mediated gene correction of a mouse model of Wiskott-Aldrich syndrome. *Mol. Ther.* 20, 1270–1279. doi: 10.1038/mt.2011.282

Uechi, T., Nakajima, Y., Chakraborty, A., Torihara, H., Higa, S., and Kenmochi, N. (2008). Deficiency of ribosomal protein S19 during early embryogenesis leads to reduction of erythrocytes in a zebrafish model of Diamond-Blackfan anemia. *Hum. Mol. Genet.* 17, 3204–3211. doi: 10.1093/hmg/ddn216

Varshney, G. K., Lu, J., Gildea, D. E., Huang, H., Pei, W., Yang, Z., et al. (2013). A large-scale zebrafish gene knockout resource for the genome-wide study of gene function. *Genome Res.* 23, 727–735. doi: 10.1101/gr.151464.112

Varshney, G. K., Pei, W., LaFave, M. C., Idol, J., Xu, L., Gallardo, V., et al. (2015a). High-throughput gene targeting and phenotyping in zebrafish using CRISPR/Cas9. *Genome Res.* 25, 1030–1042. doi: 10.1101/gr.186379.114

Varshney, G. K., Sood, R., and Burgess, S. M. (2015b). Understanding and editing the zebrafish genome. *Adv. Genet.* 92, 1–52. doi: 10.1016/bs.adgen.2015.09.002

Vlachos, A., Rosenberg, P. S., Atsidaftos, E., Alter, B. P., and Lipton, J. M. (2012). Incidence of neoplasia in Diamond Blackfan anemia: a report from the Diamond Blackfan Anemia Registry. *Blood* 119, 3815–3819. doi: 10.1182/blood-2011-08-375972

Walters, K. B., Green, J. M., Surfus, J. C., Yoo, S. K., and Huttenlocher, A. (2010). Live imaging of neutrophil motility in a zebrafish model of WHIM syndrome. *Blood* 116, 2803–2811. doi: 10.1182/blood-2010-03-276972

Wang, H., Kadlecek, T. A., Au-Yeung, B. B., Goodfellow, H. E., Hsu, L. Y., Freedman, T. S., et al. (2010). ZAP-70: an essential kinase in T-cell signaling. *Cold Spring Harb. Perspect. Biol.* 2:a002279. doi: 10.1101/cshperspect.a002279

Wang, H., Long, Q., Marty, S. D., Sassa, S., and Lin, S. (1998). A zebrafish model for hepatoerythropoietic porphyria. *Nat. Genet.* 20, 239–243. doi: 10.1038/3041

Wang, P., Sachar, M., Guo, G. L., Shehu, A. I., Lu, J., Zhong, X. B., et al. (2018). Liver metabolomics in a mouse model of erythropoietic protoporphyria. *Biochem. Pharmacol.* 154, 474–481. doi: 10.1016/j.bcp.2018.06.011

Wheeler, T. M., Leger, A. J., Pandey, S. K., MacLeod, A. R., Nakamori, M., Cheng, S. H., et al. (2012). Targeting nuclear RNA for *in vivo* correction of myotonic dystrophy. *Nature* 488, 111–115. doi: 10.1038/nature11362

White, R. M., Sessa, A., Burke, C., Bowman, T., LeBlanc, J., Ceol, C., et al. (2008). Transparent adult zebrafish as a tool for in vivo transplantation analysis. *Cell Stem Cell* 2, 183–189. doi: 10.1016/j.stem.2007.11.002

Wienholds, E., Schulte-Merker, S., Walderich, B., and Plasterk, R. H. (2002). Target-selected inactivation of the zebrafish rag1 gene. *Science* 297, 99–102. doi: 10.1126/science.1071762

Xu, J., Wang, T., Wu, Y., Jin, W., and Wen, Z. (2016). Microglia colonization of developing zebrafish midbrain is promoted by apoptotic neuron and lysophosphatidylcholine. *Dev. Cell* 38, 214–222. doi: 10.1016/j.devcel.2016.06.018

Xu, J., Zhu, L., He, S., Wu, Y., Jin, W., Yu, T., et al. (2015). Temporal-spatial resolution fate mapping reveals distinct origins for embryonic and adult microglia in zebrafish. *Dev. Cell* 34, 632–641. doi: 10.1016/j.devcel.2015.08.018

Yang, C. T., Cambier, C. J., Davis, J. M., Hall, C. J., Crosier, P. S., and Ramakrishnan, L. (2012). Neutrophils exert protection in the early tuberculous granuloma by oxidative killing of mycobacteria phagocytosed from infected macrophages. *Cell Host Microbe* 12, 301–312. doi: 10.1016/j.chom.2012.07.009

Zappulla, J. P., Dubreuil, P., Desbois, S., Letard, S., Hamouda, N. B., and Daeron, M. (2005). Mastocytosis in mice expressing human Kit receptor with the activating Asp816Val mutation. *J. Exp. Med.* 202, 1635–1641. doi: 10.1016/j.chom.2012.07.009

Zhang, J., Houston, D. W., King, M. L., Payne, C., Wylie, C., and Heasman, J. (1998). The role of maternal VegT in establishing the primary germ layers in Xenopus embryos. *Cell* 94, 515–524. doi: 10.1016/S0092-8674(00)81592-5

Zhang, Y., Ear, J., Yang, Z., Morimoto, K., Zhang, B., and Lin, S. (2014). Defects of protein production in erythroid cells revealed in a zebrafish Diamond-Blackfan anemia model for mutation in RPS19. *Cell Death Dis.* 5:e1352. doi: 10.1038/cddis.2014.318

Zhang, Y., Huang, H., Zhang, B., and Lin, S. (2016). TALEN- and CRISPR-enhanced DNA homologous recombination for gene editing in zebrafish. *Methods Cell Biol.* 135, 107–120. doi: 10.1016/bs.mcb.2016.03.005

Zhang, Y., Qin, W., Lu, X., Xu, J., Huang, H., Bai, H., et al. (2017). Programmable base editing of zebrafish genome using a modified CRISPR-Cas9 system. *Nat. Commun.* 8:118. doi: 10.1038/s41467-017-00175-6

Zhang, Y., and Yeh, J. R. (2012). In vivo chemical screening for modulators of hematopoiesis and hematological diseases. *Adv. Hematol.* 2012:851674. doi: 10.1155/2012/851674

Zhang, Y., Zhang, Z., and Ge, W. (2018). An efficient platform for generating somatic point mutations with germline transmission in the zebrafish by CRISPR/Cas9-mediated gene editing. *J. Biol. Chem.* 293, 6611–6622. doi: 10.1074/jbc.RA117.001080

Zon, L. (2016). Modeling human diseases: an education in interactions and interdisciplinary approaches. *Dis. Model. Mech.* 9, 597–600. doi: 10.1242/dmm.025882

Conflict of Interest Statement: The authors declare that the research was conducted in the absence of any commercial or financial relationships that could be construed as a potential conflict of interest.

frontiers in Cell and Developmental Biology

REVIEW
published: 11 September 2018
doi: 10.3389/fcell.2018.00114

Transmission Disrupted: Modeling Auditory Synaptopathy in Zebrafish

Katie S. Kindt[1] and Lavinia Sheets[2]**

[1] Section on Sensory Cell Development and Function, NIDCD/National Institutes of Health, Bethesda, MD, United States,
[2] Department of Otolaryngology, Washington University School of Medicine, St. Louis, MO, United States

Sensorineural hearing loss is the most common form of hearing loss in humans, and results from either dysfunction in hair cells, the sensory receptors of sound, or the neurons that innervate hair cells. A specific type of sensorineural hearing loss, referred to as auditory synaptopathy, occurs when hair cells are able to detect sound but fail to transmit sound stimuli at the hair-cell synapse. Auditory synaptopathy can originate from genetic alterations that specifically disrupt hair-cell synapse function. Additionally, environmental factors such as noise exposure can leave hair cells intact but result in loss of hair-cell synapses, and represent an acquired form of auditory synaptopathy. The zebrafish model has emerged as a valuable system for studies of hair-cell function, and specifically hair-cell synaptopathy. In this review, we describe the experimental tools that have been developed to study hair-cell synapses in zebrafish. We discuss how zebrafish genetics has helped identify and define the roles of hair-cell synaptic proteins crucial for hearing in humans, and highlight how studies in zebrafish have contributed to our understanding of hair-cell synapse formation and function. In addition, we also discuss work that has used noise exposure or pharmacological mimic of noise-induced excitotoxicity in zebrafish to define cellular mechanisms underlying noise-induced hair-cell damage and synapse loss. Lastly, we highlight how future studies in zebrafish could enhance our understanding of the pathological processes underlying synapse loss in both genetic and acquired auditory synaptopathy. This knowledge is critical in order to develop therapies that protect or repair auditory synaptic contacts.

Keywords: zebrafish model system, hair cells (HCs), ribbon synapse, deafness/hearing loss, synaptic transmission

OPEN ACCESS

Edited by:
Rebecca Ann Wingert, University of Notre Dame, United States

Reviewed by:
Paola Rizzo, University of Ferrara, Italy
Joachim Berger, Monash University, Australia

****Correspondence:***
Katie S. Kindt
katie.kindt@nih.gov
Lavinia Sheets
sheetsl@wustl.edu

Specialty section:
This article was submitted to Molecular Medicine, a section of the journal Frontiers in Cell and Developmental Biology

Received: *30 April 2018*
Accepted: *23 August 2018*
Published: *11 September 2018*

Citation:
Kindt KS and Sheets L (2018) Transmission Disrupted: Modeling Auditory Synaptopathy in Zebrafish. Front. Cell Dev. Biol. 6:114. doi: 10.3389/fcell.2018.00114

INTRODUCTION

Sensory hair cells in our inner ear must both reliably transduce and transmit auditory and vestibular stimuli (Harris et al., 1970; Eatock and Fay, 2006; **Figures 1A,B**). Hair cells transduce stimuli when apically localized mechanosensitive channels are activated, leading to graded depolarization of the hair-cell membrane (Gillespie and Walker, 2001; **Figure 1C**). Hair-cells transmit stimuli at the hair-cell synapse. At the synapse, hair-cell depolarization opens voltage-gated calcium channels; calcium influx through these channels drives synaptic vesicle fusion and glutamate release onto innervating afferent nerves (Fuchs, 2005; Moser et al., 2006; **Figure 1C**). If either the hair cells or downstream afferent nerves are damaged or dysfunctional, the pathological consequence is sensorineural hearing loss. Sensorineural hearing loss can be caused by genetic factors, infections, toxins, age and excessive noise, and is the most common form of hearing loss in humans (90% of cases) (Eggermont, 2017; World Health Organization, 2018).

One form of sensorineural hearing loss—auditory synaptopathy—results when hair cell transduction is intact, yet synaptic transmission of sound stimuli from hair cells to downstream afferent nerves is disrupted. Auditory synaptopathy can result from genetic alterations that disrupt molecules requires for synapse function. Additionally, auditory synaptopathy and associated hearing loss can also be acquired though noise exposure (Bharadwaj et al., 2014). Both genetic and acquired auditory synaptopathy stem from dysfunction of specialized synapses in hair cells called ribbon synapses. Ribbon synapses have a unique presynaptic specialization called a synaptic ribbon or ribbon body which tethers synaptic vesicles near calcium channels at the presynaptic active zone (**Figure 1C**). Ribbon synapses are required for transmitting stimuli in a fast and sustained manner needed for precise sensory encoding, and are structurally and functionally unique from classic neuronal synapses (Fuchs, 2005; Moser et al., 2006). Understanding the unique properties of hair-cells synapses is an active area of study, and continued research is necessary in order to define the pathologies underlying auditory synaptopathy.

Our current understanding of how hair-cell synapses function, and the underlying causes of auditory synaptopathy, has been built by genetic studies in several model systems. In particular, the zebrafish model has been used to help identify and define the functions of genes important for hair-cell synapse function. Zebrafish hair cells are remarkably similar to mammalian hair cells at the molecular and cellular level (Coffin et al., 2004). Genetic studies have demonstrated that numerous genes required for hearing and balance in zebrafish are also required in mice and humans (Coffin et al., 2004; Nicolson, 2005; Varshney et al., 2016). In addition to genetic conservation, one significant advantage of studying hair cells and their synapses in zebrafish is the ability to study hair cells *in vivo*. In mammals, the inner ear is encased in bone, making it impracticable to study these sensory cells in their native environment. In contrast, larval zebrafish are transparent, and hair cells are optically accessible in whole larvae. In zebrafish larvae, hair cells are present both within the inner ear and the lateral-line system—a sensory organ used to detect the movement of water. The lateral line is made up of clusters of hair cells called neuromasts that are arranged in series along the fish body and head (**Figures 1A,B**). Neuromast

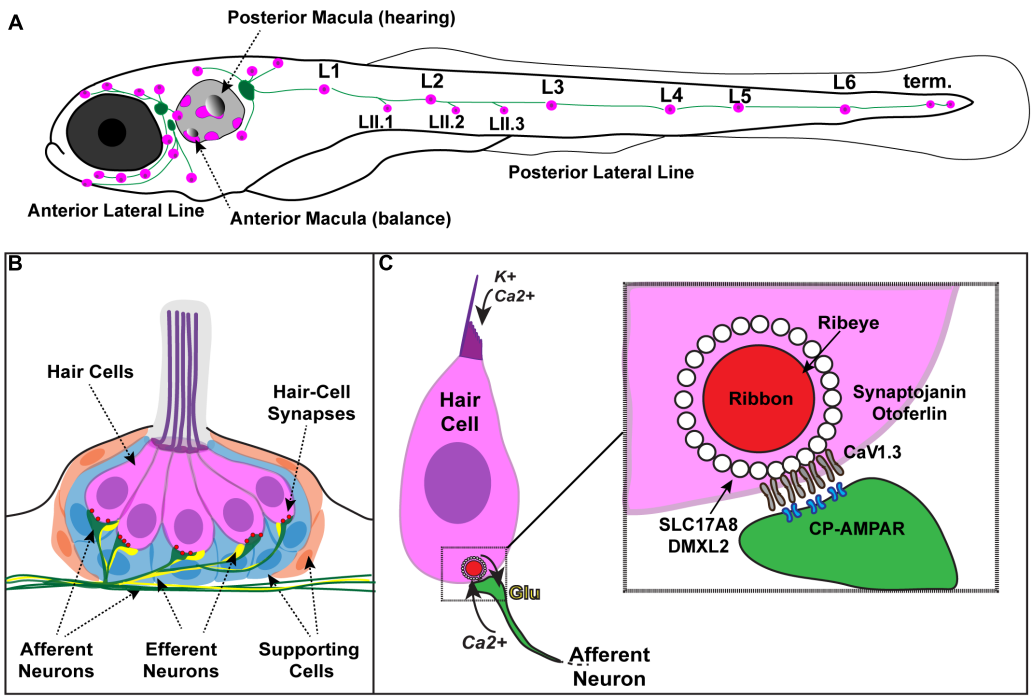

FIGURE 1 | Zebrafish hair cells and ribbons synapses. **(A)** Schematic depicts a larval zebrafish. Pink patches outline the location of hair cells in the inner ear required for hearing and balance, as well as hair cells in the lateral-line system. Green patches represent the location of the anterior and posterior lateral-line ganglia. The cell bodies of neurons in these ganglia project to and innervate hair cells in the lateral line. **(B)** An overview of the anatomy of a single patch of hair cells in the lateral line, referred to as a neuromast. Hair cells (pink) are surrounded by supporting cells (internal, blue and peripheral, orange) and innervated by both afferent (green) and efferent neurons (yellow). Mechanosensory hair bundles (purple) at the apex of hair cells project out into the water to detect local water flow. **(C)** Diagram of a single hair cell. Hair cells are activated when hair bundles are deflected, for example by local water flow. This apical deflection opens mechanosensitive channels allowing in cations including potassium and calcium. This apical activity depolarizes the hair cell, resulting in presynaptic calcium influx and release of glutamate onto the afferent neuron. Inset: magnified view of a hair-cell ribbon synapse. Shown are key evolutionarily conserved synaptic proteins discussed in this review. In hair cells, a presynaptic density called a ribbon (red) helps to recruit synaptic vesicles (white circles) to the synapse near clusters of calcium channels ($Ca_V1.3$). The ribbon is made up primarily of the protein Ribeye. Slc17A8 (Vglut3) and DMXL2 (Rbc3a) colocalize in or near synaptic vesicles. Synaptojanin and Otoferlin are also critical for ribbon-synapse function although their precise localization has not been definitively shown.

hair cells are particularly advantageous for hair-cell assessment because these cells are located superficially just beneath the fish skin, with their apical hair bundles protruding into the aqueous environment. This access makes it relatively straightforward to apply pharmacological agents, to stimulate the hair cells with fluid-flow, and assess hair-cell structure and function *in vivo*. Moreover, relative to mammals where hair cells mature over several weeks (Kraus and Aulbach-Kraus, 1981; Romand and Varela-Nieto, 2003), the hair cells in zebrafish mature rapidly (<24 h; Kindt et al., 2012; Dow et al., 2015), making it possible to study the entirety of hair-cell development in a single imaging session.

In addition to hair-cell accessibility and rapid development, the zebrafish model is valuable for hearing and balance research because, similar to mice, it is genetically tractable model system. Zebrafish are amenable to rapid genetic modification, including transgenic modification to express tissue specific transgenes encoding fluorescent markers or gene products (Kwan et al., 2007). The use of fluorescent markers is especially useful in the transparent larvae where hair-cell structures can easily be visualized *in vivo* and dynamic cellular processes can be imaged in a live, intact preparation.

In this review, we provide an overview of tools and techniques developed in the zebrafish model to examine hair-cell synapse structure and function. We also describe genetic studies in zebrafish that have helped define the roles of key hair-cell synaptic proteins. Given the recent advances in gene-editing technology, we highlight how zebrafish genetics could be applied to further our understanding of the genetic causes of auditory synaptopathy. Lastly, we outline preliminary studies that have explored the potential for using zebrafish to model noise-exposure and its associated excitotoxicity. We conclude with a discussion on how noise exposure studies in zebrafish could be expanded to further our understanding of the specific pathological changes that lead to acquired, noise-induced auditory synaptopathy.

TOOLKIT TO ASSESS HAIR-CELL SYNAPSE FUNCTION AND MORPHOLOGY IN ZEBRAFISH

Over the years, experimental techniques have been developed to study hair cells and hair-cell synapses in zebrafish. These techniques include: optical and ultrastructural analyses to visualize hair-cell synapse morphology, and functional assays to examine how hair cells transduce and transmit sensory stimuli. In the section below, we outline these methods and tools.

Morphological Analysis of Hair-Cell Synapses in Zebrafish

Genetic mutations or environmental insults such as noise exposure can specifically affect the spatial organization of hair-cell synaptic structures (Paquette et al., 2016; Ryan et al., 2016; Song et al., 2016). In the mammalian inner ear, hair-cell synapses are commonly characterized ultrastructurally using transmission electron microscopy (TEM) to examine synapses in either single or serial-sections. In addition, these synapses can be examined using confocal microscopy to visualize immunolabel of hair-cell synaptic proteins (Liberman et al., 2011; Valero et al., 2017; Becker et al., 2018; Jean et al., 2018).

Similar to work in mammals, precise ultrastructural measurements can be obtained from zebrafish hair-cell synapses using TEM (**Figure 2A**). For example, in zebrafish, the synaptic ribbon can be seen clearly in TEM as an electron-dense region that is adjacent to the postsynaptic density on the innervating afferent neuron (**Figure 2A**, ribbon and PSD). TEM is the most accurate way to determine the size of the synaptic ribbon. TEM can also be used to visualize the synaptic vesicles tethered to the synaptic ribbon and near the active zone (**Figure 2A**, SVs). Currently TEM is the only method able to quantify the number and distribution of these synaptic vesicles populations. While these ultrastructural measurements are valuable, preparing, sectioning, imaging and analyzing TEM samples requires considerable time and effort. Moreover, in most cases, TEM is only able to capture a subset of synapses within each hair-cell organ.

In contrast to electron micrographs, quantitative analysis of immunolabeled epithelial whole mounts provide the advantage of being able to examine synaptic features of large numbers of hair cells. This advantage has been used by a number of groups to characterize relative variances in size and morphologies of pre- and postsynaptic components in mammalian and zebrafish hair-cell organs (Wong et al., 2014; Paquette et al., 2016; Suli et al., 2016; Becker et al., 2018; Jean et al., 2018). Further benefits of using the larval zebrafish lateral-line system for quantitative imaging of immunolabeled structures are twofold. First, the relative simplicity; each neuromast contains 10–16 hair cells with ∼3 synapses per cell of similar morphology, making comparative analyses of synapses in numerous lateral-line organs straightforward (Sheets et al., 2012; Suli et al., 2016). This in contrast to mammalian auditory hair cells where the number and size of synapses can vary among individual hair cells depending on location within the Organ of Corti—the sensory organ for hearing (Meyer et al., 2009). Second, the synaptic ribbons in the zebrafish lateral line (TEM, circular 300 nm diameter; Suli et al., 2016) are on average larger compared to those in mammalian auditory hair cells (mouse TEM length (longest axis of the ribbon) ∼120 nm prehearing and ∼170 nm hearing; Wong et al., 2014)). These larger synaptic ribbons are near the resolution of light microscopy (∼200–270 nm) making it relatively straightforward to resolve these structures.

A previous challenge using the zebrafish lateral-line system for analysis of immunolabeled synaptic structures was a scarcity of antibodies that interact with zebrafish hair-cell synaptic proteins. In recent years a number of commercially available antibodies have been identified that label zebrafish synaptic components including synaptic vesicles (**Figure 2F**, CSP), synaptic ribbons (**Figure 2E**, CtBP), postsynaptic densities (**Figure 2E**, MAGUK), afferent (**Figure 2B**, ZN-12) and efferent (**Figure 2C**, Synaptophysin and **Figure 2D**, Vamp2 and TH) lateral-line neurons, and glutamate receptor subunits (Summary of Abs: **Table 1**). Immunolabels can be used in combination with

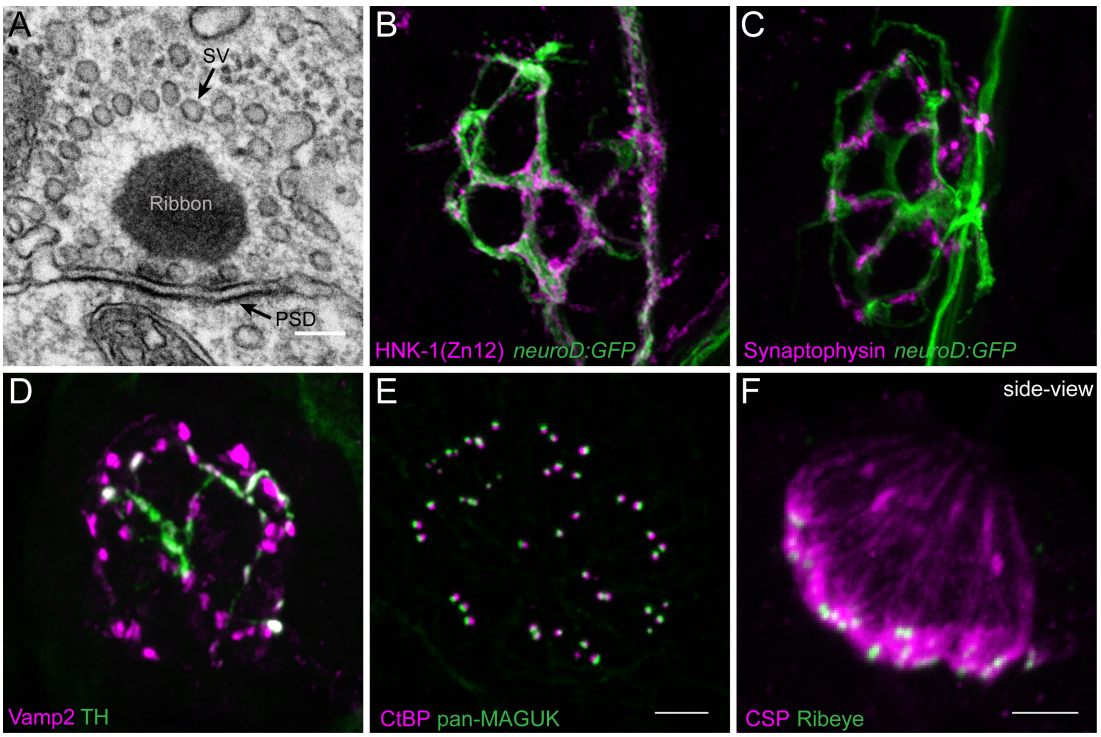

FIGURE 2 | Morphological examination of hair-cell synapses in zebrafish. **(A)** Classically, transmission electron microscopy (TEM) has been used to visualize hair-cell synapses. Shown is a micrograph of a hair-cell synapse from a zebrafish lateral-line hair cell. In this micrograph, the presynaptic ribbon is a dark spherical density. Surrounding the presynaptic ribbon are synaptic vesicles (SV). Beneath the presynaptic ribbon along the plasma membrane is the postsynaptic density (PSD). **(B)** The *neurod:GFP* transgene (green) can be used to label the afferent neurons innervating lateral line (shown in **A,B**), as well as afferents that innervate inner-ear hair cells. Afferent fibers can be labeled with the commercial antibody HNK-1/Zn12 (pink). **(C)** *Neurod:GFP* (green) can be co-labeled with a Synaptophysin antibody (pink) to label both afferent fibers and all efferent synapses respectively. **(D)** Efferent synapses, which can also be labeled with a Vamp2 antibody (pink), can be further sub-classified by a co-label such a tyrosine hydroxylase (TH, green; white overlap indicates dopaminergic synapses). **(E)** Pre- and post-synaptic densities can be labeled with CtBP (pink) and pan-MAGUK (green) antibodies respectively. **(F)** Synaptic vesicles, labeled with cysteine string protein (CSP, pink) are enriched at the basolateral membrane of hair cells near synaptic ribbons labeled with Ribeye antibody (green). Scale bar = 100 nm in **(A)** and 5 μm in **(E)** (for **B–E**) and **(F)**.

transgenic lines that specifically mark cell types of interest such as hair cells, glia-like supporting cells, as well as the innervating neurons (**Figures 2B,C**, *neurod:GFP*; Obholzer et al., 2008; Behra et al., 2012, p. 1; Tabor et al., 2014; Toro et al., 2015).

Transmission electron microscopy and immunostaining provide important information regarding synaptic structure and the localization of proteins at hair-cell synapses. Unfortunately, there are not antibodies for all synaptic proteins, and these approaches do not provide temporal information regarding the dynamics of these proteins within hair cells. Therefore, transgenic fish lines expressing fluorescently tagged synaptic proteins provide a powerful way to determine the localization of these molecules *in vivo* (Trapani et al., 2009; Sheets et al., 2011; Einhorn et al., 2012). For example, transgenic fish expressing fluorescently tagged Ribeye, one of the main structural components of synaptic ribbons, have been used to identify the location of ribbons in developmental analyses and functional imaging experiments (*Tg[myo6b:ribeye-mcherry];* **Figures 3F,G**; Pujol-Martí et al., 2014; Zhang et al., 2018). More recent work has used tagged proteins to investigate the structural dynamics of synaptic ribbons. For example, fish expressing fluorescently tagged Ribeye have been used along with fluorescence recovery after photobleaching (FRAP) to determine the stability and turnover of Ribeye within synaptic ribbons, and the exchange of Ribeye between synaptic ribbons (Graydon et al., 2017; Chen et al., 2018). In the future, the creation of additional zebrafish transgenic lines will provide a valuable resource in this *in vivo* model to study the localization and dynamics of hair-cell synaptic proteins.

Assays for Hair-Cell Mechanotransduction in Zebrafish

Hair-cell function occurs primarily within two main structural domain, the apical hair bundle and the basal ribbon synapse. These structural domains are required for mechanotransduction and neurotransmission respectively. In response to sensory stimuli, apical hair bundles are deflected; this deflection opens mechanosensitive ion channels. This apical activity is essential to initiate hair-cell depolarization, and opening of calcium channels at the synapse, leading to sensory-evoked neurotransmission. Therefore, these two domains are functionally linked and, in order for proper hair-cell synapse function, apical hair bundles must be intact and functional. To

TABLE 1 | Commercially available antibodies labeling zebrafish hair-cell synaptic proteins.

Antigen	Structure Labeled	Host	Antibody type	Dilution	Company/Catalog #	Reference
Acetylated Tubulin	Afferents and hair cells	Mouse	Monoclonal IgG2b	1:5000	Sigma/T7451	Harris et al., 2003; Murakami et al., 2003; Obholzer et al., 2008; Kindt et al., 2012
Calretinin	Afferent processes	Mouse	Monoclonal IgG1	1:1000	Swant/6B3	Pei et al., 2016
Choline Acetyltransferase	Cholinergic efferent terminals	Goat	Polyclonal	1:500	Millipore Sigma/AB144P	Zhang et al., 2018
CtBP (1&2)	Synaptic ribbons	Mouse	Monoclonal IgG2a	1:1000	Santa Cruz/sc-55502	Lv et al., 2016
Cysteine String Protein	Synaptic vesicles	Rabbit	Polyclonal	1:1000	Millipore Sigma/AB1576	Lin et al., 2016
Gria 4	AMPA glutamate receptor subunit	Rabbit	Polyclonal	1:400	Millipore Sigma/AB1508	Sheets, 2017
Grik 2	Kainate glutamate receptor subunit	Rabbit	Polyclonal	1:400	Fitzgerald Industries/70R-1522	Sheets, 2017
Grik 4	Kainate glutamate receptor subunit	Rabbit	Polyclonal	1:400	Genway Biotech Inc./GWB-DA6FF7	Sheets, 2017
Grin 1	NMDA glutamate receptor subunit	Mouse	Monoclonal IgG2b	1:1000	Synaptic Systems/114011	Sheets, 2017
Human Natural Killer-1	Afferent processes	Mouse	Monoclonal IgG1	1:500	Developmental Studies Hybridoma Bank/ Zn-12	Mo and Nicolson, 2011
MAGUK	Postsynaptic densities	Mouse	Monoclonal IgG1	1:500	NeuroMab (UC Davis)/ 75-029	Sheets et al., 2011; Lv et al., 2016
NSF	Hair cells and afferent process	Rabbit	Monoclonal	1:50	Cell Signaling/3924	Mo and Nicolson, 2011
Otoferlin	Hair cells	Mouse	Monoclonal IgG2a	1:500	Developmental Studies Hybridoma Bank/ HCS-1	Faucherre et al., 2009; Goodyear et al., 2010
Rab3	Hair cells and efferent neurons	Mouse	Monoclonal IgG1	1:1000	Synaptic Systems/107011	Einhorn et al., 2012
Synaptophysin 1	Efferent terminals	Mouse	Monoclonal IgG1	1:1000	Synaptic Systems/ 101 011	Toro et al., 2015
Tyrosine Hydroxylase	Dopaminergic efferents	Mouse	Monoclonal IgG2a	1:1000	Vector labs/ VP-T489	Toro et al., 2015
Vamp 2	Efferent terminals	Rabbit	Polyclonal	1:500	Genetex/ GTX132130	Zhang et al., 2018

assay for normal mechanotransduction in zebrafish, microphonic potential measurements and FM 1-43 dye labeling can be used (**Figure 3A**; Nicolson et al., 1998; Seiler et al., 2004). While these measurements are most straightforward in lateral-line hair cells, they have also been adapted to examine hair cells in the zebrafish inner ear (Tanimoto et al., 2011). In the lateral line, microphonic potentials are recorded by placing an extracellular electrode near the apical hair bundles of an individual neuromast. Hair bundles are then deflected with a fluid jet and the flow of current into mechanosensitive ion channels in the bundles of all hair cells within a neuromast can be measured (Trapani and Nicolson, 2010; Olt et al., 2016b). For FM 1-43 analysis, larvae are briefly immersed in the vital dye FM 1-43. This dye rapidly enters hair cells when mechanosensitive ion channels are functional (**Figure 3A**; Seiler and Nicolson, 1999). These combined methods provide a way to ensure that hair-cell mechanotransduction is intact, and represent important assays in the characterization of zebrafish auditory and vestibular mutants. For example, mutants without microphonic potentials or FM 1-43 label can be classified as mechanotransduction mutants. In contrast, mutants with intact microphonic potentials and FM 1-43 label indicate that there is a disruption downstream of mechanotransduction. Importantly, a subset of zebrafish mutants with normal mechanotransduction have been shown to be required for hair-cell synapse function. (See the genetics section below; Nicolson et al., 1998; Sidi et al., 2004; Obholzer et al., 2008; Trapani et al., 2009; Einhorn et al., 2012). Overall, these assays are useful in determining whether specific mutations disrupt components of the transduction apparatus, or potentially affect a process downstream, including hair-cell transmission.

Electrophysiological Approaches to Study Hair-Cell Synapses in Zebrafish

In addition to microphonics and FM 1-43, several additional methods have been established to assay hair-cell function, and specifically hair-cell synapse function in zebrafish. These methods utilize either electrophysiology or imaging-based approaches (Olt et al., 2016b; Zhang et al., 2016). In general, imaging approaches offer superior spatial resolution, while electrophysiological recordings offer greater sensitivity. Both of these methods have proved invaluable in the analysis of molecules required for hair-cell synapse function in zebrafish.

To study presynaptic function, the gold standard in the hair-cell field is whole-cell patch-clamp recordings. Using this approach, stimulatory voltage steps can be applied to electrically isolated individual hair cells in order to obtain important information on synapse function; for example, calcium currents

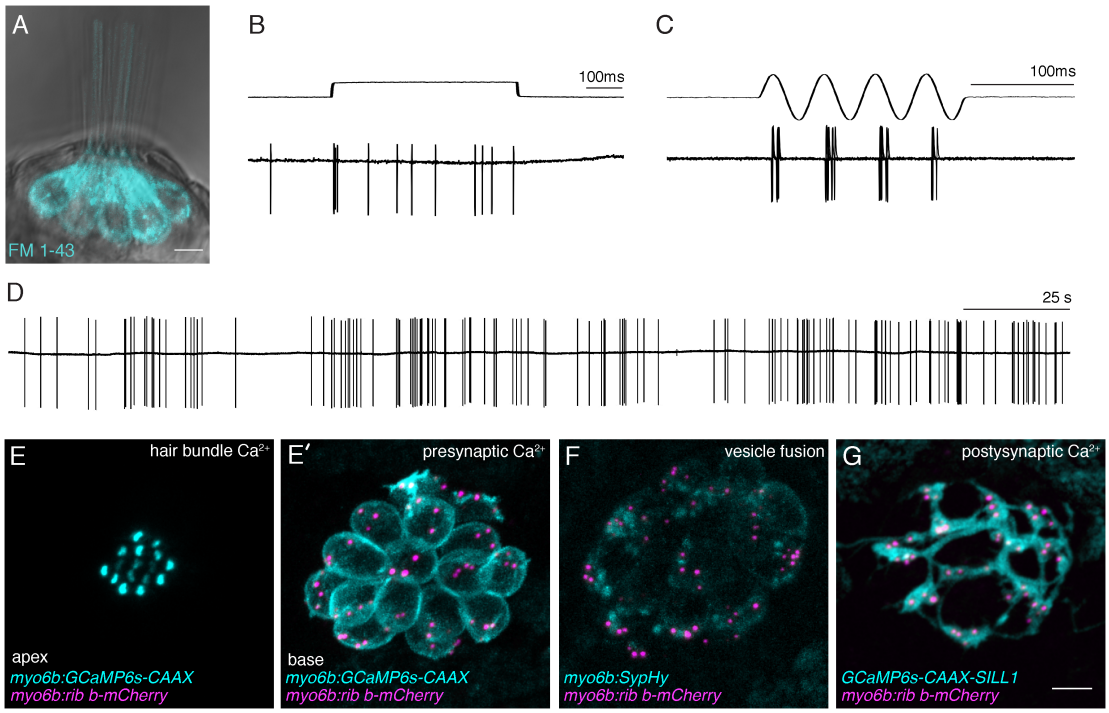

FIGURE 3 | Functional analysis of hair-cell synapses in the zebrafish lateral line. **(A)** In the lateral line, rapid uptake of the vital dye FM 1-43 (cyan), shown in this example, indicates mechanotransduction is intact in these hair cells. **(B–D)** Extracellular recordings from the afferent cell bodies in the posterior lateral-line ganglia can be used as a read-out of synapse function. During these afferent recordings, evoked spikes can be detected when innervated hair cells are stimulated along their axis of sensitivity **(B,C)**. Step stimuli (**B**, anterior step shown) are useful to quantify spike number and the timing of the first spike. Sine stimuli (**C**, anterior-posterior sine stimulus shown) are useful to quantify the precision of spike timing within the waveform. Note that each afferent only responds to one direction of stimuli (for example the anterior but not posterior phase of the sine wave in **C**). Even in the absence of stimuli there is spontaneous spiking in that can be used as a read-out of synaptic function **(D)**. **(E,E')** A transgenic line expressing a membrane-localized calcium indicator GCaMP6s (cyan) can be used to detect mechanotransduction-dependent calcium influx in apical hair bundles **(E)** and calcium influx at synaptic ribbons **(E')** when apical and basal planes are imaged respectively. **(F)** Transgenic fish expressing SypHy, an indicator of vesicle fusion can be used to detect presynaptic vesicle fusion at hair-cell synapses. **(G)** GCaMP6s can also be used to detect postsynaptic calcium activities in the afferent process beneath hair cells. All of the transgenic approaches outlined in **(E–G)** can be used in combination with a transgenic line that marks synaptic ribbons via a Ribeye b-mCherry fusion protein. The scale bar in **(A,G)** = 5 μm.

reliant on presynaptic calcium channels can be isolated and characterized (Brandt et al., 2005; Ricci et al., 2013; Olt et al., 2014). In addition, increases in cell-membrane capacitance that are associated with vesicle fusion can also be measured. These hair-cell recording have been pioneered in zebrafish by several groups (Ricci et al., 2013; Olt et al., 2014). Using this method, both presynaptic calcium currents and capacitance changes have been recorded in larval and juvenile zebrafish lateral-line hair cells (Olt et al., 2014, 2016a).

In addition to hair-cell electrophysiological measurements, recordings from the afferent posterior lateral-line ganglia have also been used to characterize hair-cell synapse function (Trapani and Nicolson, 2010). Within each neuromast there are two populations of hair cells that respond to water flow in two directions along a single axis. Afferent neurons that innervate neuromasts form bouton-like synapses on multiple hair cells that respond to one of these two directions (Nagiel et al., 2008; Faucherre et al., 2009; Sheets et al., 2011; Pujol-Martí et al., 2014). Therefore, electrophysiological recording from afferents represent the summed output of several hair cells within a neuromast.

Afferent recordings in zebrafish have primarily measured extracellular currents from afferent cell bodies in a loose-patch configuration. Initially, a successful afferent recording is identified by detection of spontaneous spiking that results from hair-cell neurotransmission in the absence of stimuli (**Figure 3D**; Trapani and Nicolson, 2011). Spontaneous spike rate on its own has been shown to be an important feature of synaptic-release properties in both zebrafish and mammals (Pfeiffer and Kiang, 1965; Merchan-Perez and Liberman, 1996; Furman et al., 2013; Sheets et al., 2017). After identifying a spiking afferent neuron, a fluid-jet can be used to deflect the hair bundles of each neuromast along its axis of sensitivity in order to identify an afferent neuron and neuromast that are synaptically paired (**Figures 3B,C**). Each afferent will respond to a single direction along the neuromast's axis of sensitivity (**Figures 3B,C**). Once this pairing is identified, many features relevant to hair-cell synapse function can be quantified using these recordings. For example, during fluid-jet stimulation, the timing and number of afferent spikes can be recorded. While spike number can provide important information on vesicle release and replenishment (Trapani et al., 2009; Einhorn et al., 2012; Sheets et al., 2017),

measurements such as first spike latency (time from stimulus to the first spike) can provide important information on the timing of vesicle release (Sheets et al., 2017). Additionally, during a sinusoidal stimulus where the fluid-jet is used to stimulate both populations of hair cells within a neuromast along its axis of sensitivity, phase-locking can be measured (**Figure 3C**). Phase-locking assesses how consistently the afferent neuron spikes during a particular phase of the sine stimulus and reflects the fidelity of neurotransmission. Overall, afferent recordings have been able to resolve subtle yet important differences in zebrafish mutants that alter hair-cell synapse function (Obholzer et al., 2008; Trapani et al., 2009; Einhorn et al., 2012).

Using Functional Imaging to Study Hair-Cell Synapses in Zebrafish

Because the zebrafish model system is genetically tractable, work in the last decade has expanded toward using genetically encoded optical indicators to examine hair-cell function in zebrafish (Kindt et al., 2012; Esterberg et al., 2014; Zhang et al., 2016, 2018; Sheets et al., 2017). These studies have utilized transgenic zebrafish that express functional indicators in either hair cells or afferent neurons using cell-type specific promoters (**Figures 3E–G**). An important advantage of functional imaging over electrophysiogical recordings is the ability to resolve activity spatially among multiple cells and subcellularly within individual cells. In contrast, microphonics or extracellular afferent recordings are the readout of many hair cells within a neuromast, and whole-cell recordings examine activity from one hair cell at a time.

The majority of functional imaging studies have used genetically encoded indicators of calcium because calcium influx is an important feature of both apical mechanotransduction and basal neurotransmission in hair cells (**Figure 1C**). Initial work primarily used genetically encoded calcium indicators localized to the cytosol of lateral-line hair cells. During fluid-jet stimulation, it was shown that calcium signals could be reliably measured in the cytosol (Kindt et al., 2012; Sheets et al., 2012, 2017; Sebe et al., 2017). Disrupting hair-cell mechanotransduction abolished these cytosolic signals indicating that they are mechanically evoked calcium signals. In addition, it was possible to determine the contribution of presynaptic calcium channels to these cytosolic calcium responses by using pharmacology or mutant analysis (Kindt et al., 2012; Sheets et al., 2012, see the genetics section below).

Unfortunately, it is challenging to use a cytosolic calcium indicator to understand the physiological properties of channel activity within hair cells. Therefore, more recent studies have used localized calcium indicators to examine subcellular activity within hair cells (Sheets et al., 2017; Zhang et al., 2018). In particular, membrane-localized calcium indicators have proved advantageous to assess localized calcium influx into the hair-cell bundle and at the hair-cell synapse (Zhang et al., 2018). This approach is particularly useful because both of these measurements can be made within the same cell by using either an apical or basal imaging plane respectively (**Figures 3E,E'**). To determine the location of synaptic ribbons and measure presynaptic calcium signals at sites of release, calcium indicator lines can be combined with an additional transgenic line that marks synaptic ribbons via a Ribeye-mCherry fusion protein (*Tg[myo6b:ribeye-mcherry];* **Figures 3E–G**; Sheets, 2017; Zhang et al., 2018). Similar to work in hair cells, membrane-localized calcium indicators have also been used to assay postsynaptic activity in the afferent process beneath neuromast hair cells (**Figure 3G**). In response to fluid-jet stimulus, afferent calcium signals can be detected at sites adjacent to synaptic ribbons that are marked using a Ribeye-mCherry transgenic line (Zhang et al., 2018).

While calcium indicators have proved useful, other indicators of activity have been utilized to examine hair-cell synapse function in zebrafish. For example, a genetically encoded indictor called SypHy has been used as a readout of vesicle fusion at synaptic ribbons (**Figure 3F**; Zhang et al., 2018). In the future, SypHy may provide valuable information regarding the spatial properties of vesicle fusion at hair-cell synapses. At the postsynapse, instead of a calcium indicator, recent work has used a genetically encoded glutamate sensor to measure postsynaptic activity (Pichler and Lagnado, 2018). Overall, these functional studies highlight that the zebrafish is an excellent model to test the efficacy of using genetically encoded optical indicators, with the hope that they can ultimately be used in both zebrafish and mammalian models to assess hair-cell synapse function. With the advance of functional imaging, it also will be informative to combine electrophysiology and functional imaging in zebrafish to gain a more comprehensive understanding of the temporal and spatial properties underlying hair-cell synapse function.

THE GENETICS OF HEARING LOSS AFFECTING HAIR-CELL SYNAPSES IN MAMMALS AND ZEBRAFISH

To date, numerous genetic studies in zebrafish, mice and humans have uncovered molecules required for hearing and balance (Nicolson, 2005; Safieddine et al., 2012; Pan and Holt, 2015). In zebrafish, mutants with hearing and balance defects were first identified behaviorally in large-scale forward genetic screens (Nicolson et al., 1998; Lin et al., 2016). These fish were initially identified as motility mutants with circling behavior, an indicator of vestibular dysfunction; additional screening showed these fish also lacked acoustic-vibrational startle responses, an indicator of deafness (Nicolson et al., 1998; Tubingen 2000 Screening Consortium). Over the last 20 years considerable work has focused on identifying the lesions underlying deafness in these zebrafish mutants. Concurrent work in mice and humans has revealed, perhaps not surprisingly, that orthologous genes, when mutated, cause deafness in zebrafish and mammals. This body of work supports functional conservation of deafness genes among vertebrates.

During characterization of these genes, zebrafish deafness mutants were classified based on morphological and functional assays. For example, one class of mutations disrupted overall hair-cell morphology while another class specifically affected hair-bundle integrity. In most zebrafish mutants with disrupted

hair-bundle integrity, mechanotransduction was also affected (Ernest et al., 2000; Seiler et al., 2004; Söllner et al., 2004; Gleason et al., 2009). Importantly, a distinct class of zebrafish mutants had normal hair-cell and hair-bundle morphology and intact mechanotransduction, indicating that that the affected genes altered function downstream of hair-bundle function. Further characterization of 6 of these zebrafish mutants revealed molecules that are specifically required for proper hair-cell neurotransmission: $Ca_V1.3$, Vglut3, Nsf, Rabconnectin 3α, Synaptojanin and Wrb (Sidi et al., 2004; Obholzer et al., 2008; Trapani et al., 2009; Mo and Nicolson, 2011; Einhorn et al., 2012; Lin et al., 2016).

In the section below, we outline how studies characterizing zebrafish auditory and vestibular mutants revealed the function of these molecules in hair-cell neurotransmission. Further, we discuss how these mutants have expanded our understanding of each molecule's contribution to hair-cell synaptic development, maintenance and function. To date, mutations in four of the synapse-associated genes identified above have also been associated with human hearing loss (Rodríguez-Ballesteros et al., 2008; Ruel et al., 2008; Baig et al., 2011). This genetic conservation between zebrafish and humans suggests that there is also functional conservation at hair-cell synapses, and further supports that the zebrafish model is useful for studying auditory synaptopathy.

$Ca_V1.3$; Sinoatrial Node Dysfunction and Deafness (SANDD) Syndrome

In humans, loss of function mutations in $Ca_V1.3$ (CACNA1D) results in Sinoatrial Node Dysfunction and Deafness (SANDD), a disorder whereby affected individuals have abnormal heart rhythms and severe deafness (Platzer et al., 2000; Baig et al., 2011). $Ca_V1.3$ channels are the presynaptic calcium channel required for neurotransmission at hair-cell synapses. The requirement for $Ca_V1.3$ channels in hearing is highly conserved; mutations in *$ca_V1.3$* result in profound deafness in human, mice and zebrafish (Sidi et al., 2004; Brandt et al., 2005; Baig et al., 2011).

$Ca_V1.3$ channels are part of the L-type calcium channel family—they are uniquely sensitive to dihydropyridines and have large single channel conductance (Bean, 1989). $Ca_V1.3$ channels also activate with rapid kinetics at low voltages relative to other Ca_V1 channels (Lipscombe et al., 2004) and inactivate slowly in hair cells. These properties make $Ca_V1.3$ channels ideal for mediating rapid and continuous exocytosis. In zebrafish and mice, $Ca_V1.3$ channels cluster tightly at synaptic ribbons (Frank et al., 2009, 2010; Sheets et al., 2011; Wong et al., 2014). Presynaptic clustering of $Ca_V1.3$ channels is thought to be important to tightly couple calcium influx and vesicle release. Precise control of vesicle release is an important feature for reliable sensory encoding in hair cells (Brandt et al., 2003, 2005; Wong et al., 2014).

In addition to its role in hair-cell neurotransmission, $Ca_V1.3$ channels are essential for hair-cell development and synapse maintenance. While *$ca_V1.3$* knockout mice initially form synapses, they progressively lose hair cells and postsynaptic afferents that innervate the remaining hair cells degenerate (Glueckert et al., 2003). In zebrafish *$ca_V1.3a$* mutants, lateral-line hair cells were also shown to initially form synapses, a phenotype that can be assessed in developing hair cells when larvae are 3-days-old, 2 days prior to the onset of lateral-line function (Trapani and Nicolson, 2010; Suli et al., 2016). Nevertheless, in the zebrafish, a progressive loss of juxtaposition between hair-cell pre- and postsynaptic components was observed in functionally mature hair cells of *$ca_V1.3a$* mutants just 2 days later (Sheets et al., 2012). Additionally, this work found hair-cell ribbons were significantly enlarged in both 3- and 5-day-old *$ca_V1.3a$* mutants. The rapid formation (by day 3) and subsequent loss of synaptic juxtaposition (at day 5) in zebrafish *$ca_V1.3a$* mutants is one example of how quickly phenotypic differences in synapse development and maintenance can be assayed in zebrafish. By taking advantage of these distinct developmental time points, this study also found that transiently (1 h.) treating the developing hair cells of 3 day-old zebrafish with dihydropyridine agonists and antagonists was able to rapidly decrease or increase presynaptic-ribbon size respectively (Sheets et al., 2012). In 5 day-old zebrafish, these compounds affected synaptic-ribbon size to a far lesser degree, revealing that calcium influx through $Ca_V1.3$ channels could dramatically influence presynaptic morphology during a critical window of development.

Cumulatively, these results support that functional $Ca_V1.3$ channels are necessary to properly form synaptic ribbons and to maintain pre- and postsynaptic juxtaposition in zebrafish hair cells. Although is it clear that $Ca_V1.3$-dependent presynaptic calcium influx regulates presynaptic size during zebrafish hair-cell development, it is less clear what role these channels play in synapse maintenance. It has been proposed that synapse maintenance could require release of synaptic vesicle contents (Mo and Nicolson, 2011). Consistent with this idea, zebrafish *$ca_V1.3a$* mutants lack evoked and spontaneous synaptic vesicle release (Trapani and Nicolson, 2011). Because formation and maintenance of hair-cell synapses in mutants lacking synaptic glutamate release appear relatively normal (*vglut3*−/−; see next section), it possible that the release of trophic factors from the synapse is required for maintenance of hair-cell synaptic connections (Fritzsch et al., 1997, 2004; Mo and Nicolson, 2011; Kersigo and Fritzsch, 2015). In the future, it may be informative to use zebrafish as a platform to screen for compounds that maintain synaptic juxtaposition in *$ca_V1.3a$* mutants in order to identify factors necessary for hair-cell synapse maintenance.

SLC17A8/vglut3; Autosomal Dominant Deafness-25 (DFNA25)

In human patients, autosomal dominant deafness-25 (DFNA25) is a progressive, high frequency non-syndromic hearing loss caused by a heterozygous mutation in the *SLC17A8* gene encoding Vesicular Glutamate Transporter-3 (VGLUT3) (Ruel et al., 2008). Vglut3—a transporter that packages glutamate into synaptic vesicles—was identified independently in both zebrafish loss-of-function mutants and mouse knockouts as a critical component for hearing and hair-cell neurotransmission (Obholzer et al., 2008; Seal et al., 2008). These studies found that both zebrafish hair cells and mammalian auditory hair cells express *vglut3*. In zebrafish and mice, *vglut3* mutant hair cells

have normal microphonic potentials, suggesting that Vglut3 is not required for mechanotransduction (Obholzer et al., 2008; Ruel et al., 2008). Additionally, *vglut3* mutant mice and zebrafish show normal calcium responses, and in mice exocytosis is not altered. In zebrafish, despite normal mechanotransduction and evoked calcium responses in hair cells, no postsynaptic spikes are detected in the innervating afferent neurons (Obholzer et al., 2008; Sheets et al., 2012). Similarly, in *vglut3* knockout mice, auditory nerves lacked responses to auditory stimuli, despite normal hair-cell calcium currents and exocytosis (Ruel et al., 2008).

In *vglut3* zebrafish mutants, afferent innervation appears relatively normal (Sheets et al., 2012). There does not appear to be any major structural changes in presynaptic ribbon morphology beyond the normal variances in mice and zebrafish (Obholzer et al., 2008; Ruel et al., 2008). Overall, these mild synaptic morphology phenotypes in *vglut3* mutants are quite different compared to $ca_V1.3$ mutants where the synapses ultimately degenerate. Synapses may be preserved due to the presence of normal calcium currents and hair-cell exocytosis despite an absence of glutamate release (Ruel et al., 2008). This supports an important role for exocytosis in the release of other trophic factors in synaptic maintenance. Relatively normal development and maintenance of hair cells in *vglut3* knockout mice have made this deafness model a promising target of virally-mediated gene therapy (Akil et al., 2012).

Notably, there are a few morphological differences observed between Vglut3-deficient zebrafish lateral-line hair cells and Vglut3-deficient mouse auditory hair cells. Zebrafish *vglut3* mutant synaptic ribbons have a reduced number of ribbon-associated vesicles, which is not observed in mouse auditory hair cells. Additionally, there is evidence that the glutamate transporter Vglut1 is also expressed in zebrafish hair cells, yet Vglut1 appears unable to compensate for neurotransmission in the *vglut3* mutant (Obholzer et al., 2008). Further studies in zebrafish are needed to confirm the presence of Vglut1 in hair cells and to define its function in order to understand the unique functional role of Vglut3 in hair-cell neurotransmission.

DMXL2/Rabconnectin 3α; Autosomal Dominant Deafness-71 (DFNA71)

A recent study identified a heterozygous missense variant of *DMXL2* that is associated with dominant, non-syndromic hearing loss in humans (Chen et al., 2017). Notably, this gene had been previously identified in a zebrafish hearing and balance mutant and represents an example of hereditary deafness gene identified in zebrafish prior to mice or humans. *DMXL2* encodes Rabconnectin 3α—the α-subunit of the Rabconnectin protein complex. *Rbc3*α zebrafish mutants, when compared to *vglut3* and $ca_V1.3a$ zebrafish mutants, have relatively mild to moderate auditory and vestibular deficits (Einhorn et al., 2012). Phenotypically, similar to *vglut3* mutants, both pre- and post-synaptic morphology appeared normal in *rbc3*α mutants. Subsequent analysis of Rbc3α localization revealed it was enriched basolaterally and overlapped with Vglut3 in hair cells, suggesting that Rbc3α is localized to synaptic vesicles.

This study found that zebrafish hair cells deficient in Rbc3α impacted Vacuolar-type H^+-ATPase (V-ATPase) localization at the base of hair cells (Einhorn et al., 2012). V-ATPase generates a proton gradient and acidifies subcellular compartments, including synaptic vesicles. This gradient is important for the accumulation of glutamate into synaptic vesicles. These results suggested that *rbc3*α mutants could have deficient synaptic-vesicle acidification. To determine whether vesicles properly acidified, this study pioneered the use of lysotracker in hair cells. Lysotracker is a membrane-permeable vital dye that labels acidic organelles. In combination with a live presynaptic ribbon label (Ribeye-GFP), lysotracker brightly labeled rings around synaptic ribbons that likely correspond to ribbon-associated vesicles. The intensity of lysotracker labeling was dramatically reduced in *rbc3*α mutants, indicating reduced acidification of organelles and vesicles surrounding synaptic ribbons.

To better understand the relationship between Rbc3α and the V-ATPase, this work used the genetic tractability of the zebrafish model to rapidly express tagged proteins in hair cells. Transient expression of either the cytosolic (V1) or the membrane (V0) subunits of the V-ATPase in wild-type and Rbc3α deficient hair cells revealed that Rbc3α is required to traffic or assemble the V1 subunit at the base of hair cells (Einhorn et al., 2012). Therefore, Rbc3α is required for proper V-ATPase localization and ultimately synaptic vesicle acidification. Because synaptic vesicle acidification contributes to vesicular glutamate accumulation, this observation suggests that *rbc3*α mutant synaptic vesicles contain less glutamate. Accordingly, afferent recordings revealed reduced glutamate-dependent evoked release from *rbc3*α mutant hair cells. In addition, *rbc3*α mutants showed loss of fidelity of phase-locked spiking at higher frequencies (20 vs. 60 Hz) (Einhorn et al., 2012). Currently there is no other established model to study *DMXL2*-related human hearing loss. In the future, it will be interesting to test whether expression of the dominant human mutation in zebrafish hair cells also disrupts hearing and balance, which could provide further insight into the pathology underlying this genetic lesion.

Synaptojanin

Proteins in the Synaptojanin family are lipid phosphatases that play an important role in endocytosis and vesicle recovery at synapses (Harris et al., 2000; Song and Zinsmaier, 2003). Although no members of the Synaptojanin family have been associated with hearing loss in humans, mutations that abolish the lipid phosphatase activity of Synaptojanin 2 result in progressive age-related hearing loss in mice without any other accompanying phenotype (Manji et al., 2011). Synaptojanin 2 is expressed in auditory hair cells, and the progressive hearing loss observed in *Synj2* mutants appears to be due to degeneration or loss of hair bundles, and sunken appearance of cell bodies, followed by hair-cell death. These observations support that Synaptojanin 2 plays an important role in hair-cell survival, but the process by which it contributes to cell survival is not understood.

While mice express Synaptojanin 2 in hair cells, zebrafish express Synaptojanin 1 (McDermott et al., 2007; Trapani et al., 2009). *Synj1* zebrafish mutants, similar to *rbc3*α

zebrafish mutants, have moderate auditory and vestibular defects. These behavioral defects were accompanied by morphological disruptions in Synj1-defficient hair cells; specifically, basal membrane protrusions, or blebbing. These protrusions were dependent on functional Cav1.3 channels and were observed in 1/3 of *synj1* mutant hair cells. In contrast to mice *Synj2* mutants, other aspects of hair-cell morphology in zebrafish *synj1* mutants appeared normal. Transmitted electron micrographs revealed fewer vesicles at *synj1* ribbons, indicating vesicle recycling was impaired. Reduced vesicles and basal membrane protrusions in mutant *synj1* hair cells led to deficits in synapse function; afferent recordings in *synj1* mutants revealed a delay in afferent spike timing and impaired phase-locking in response to high-frequency stimuli (Trapani et al., 2009). Speculatively, impaired hair-cell membrane recycling could contribute to a progressive degeneration of hair cells. It will be informative in follow-up studies to examine whether disrupting Synj1 function impacts zebrafish hair-cell maintenance and survival in older larvae.

Otoferlin and WRB (pwi); Autosomal Recessive Deafness-9 (DFNB9)

In human patients, mutations in the Otoferlin gene gives rise to neurosensory non-syndromic recessive deafness DFNB9 (Yasunaga et al., 1999), and is the cause of ∼1.4–5% of the cases of autosomal recessive hearing loss (Santarelli et al., 2015). Otoferlin exists in a long form containing six C2 domains (C2A-F) and a short form containing three C2-domains (Yasunaga et al., 2000). C2 domains are important for membrane localization and bind calcium (Lek et al., 2012). Mutations in nearly any of the C2 domains in the long form (C2B, C, D, E, or F) are linked to deafness in humans and mice (Yasunaga et al., 2000; Ramakrishnan et al., 2009), indicating that the presence of the long form is important for hearing. Knockdown of Otoferlin in zebrafish results in deafness (Chatterjee et al., 2015). Otoferlin is proposed to be an essential regulator of hair-cell neurotransmission, functioning to both couple calcium signaling with vesicle fusion and to regulate vesicle replenishment (Roux et al., 2006; Pangršič et al., 2015; Vogl et al., 2016; Michalski et al., 2017). Otoferlin's sequence identity and protein localization are highly conserved between divergent species (Goodyear et al., 2010). Additionally, Otoferlin's function also appears to be conserved; acoustic startle responses can restored in zebrafish *otof* knockdowns using exogenous mouse Otoferlin (Chatterjee et al., 2015).

A highly conserved role for Otoferlin in hair-cell synapse function is further supported by the identification of a gene important for hearing and vision in a large-scale mutagenesis screen. A null mutation the gene *pinball wizard* (*pwi*) resulted in zebrafish with impaired acoustic startle response, vestibular abnormalities and defective optokinetic response (Lin et al., 2016). *Pwi* encodes tryptophan-rich basic (WRB) protein, a small transmembrane protein found in the endoplasmic reticulum that is a receptor for insertion of tail-anchored (TA) proteins. Disruption of TA-protein membrane insertion would likely result in disruption of TA-protein trafficking, and numerous hair-cell vesicular proteins are TA, including Otoferlin. A subsequent report further examined zebrafish *pwi* mutants, and verified that Wrb is necessary for normal Otoferlin protein levels in hair cells and hearing in zebrafish (Vogl et al., 2016). Additionally, this study showed mutating *wrb* in mice disrupted ER-insertion of Otoferlin into vesicles, which greatly reduced Otoferlin levels in auditory hair cells. A reduction in Otoferlin levels contributed to impaired sustained exocytosis at *Wrb*-deficient hair-cell synapses and disruptions in sound encoding. These observations further support the functional conservation of hair-cell synaptic proteins between zebrafish and mammals. This works also demonstrates the effectiveness of using the zebrafish model to identify novel proteins involved in auditory synaptopathy and to define the molecular functions of these proteins in hair cells.

Ribeye

Ribeye is the main component of synaptic ribbons and is a presynaptic protein that is unique to ribbon synapses (Schmitz et al., 2000). Ribeye is a splice isoform of the transcriptional co-repressor CtBP2. As CtBP2 is a protein that regulates a number of diverse transcriptional targets, knockouts of CtBP2 are embryonic lethal (Hildebrand and Soriano, 2002). Biochemical studies have demonstrated that individual Ribeye subunits self-associate, and this self-association may form synaptic ribbons (Magupalli et al., 2008). There is currently no known mutation in CtBP2/Ribeye that contributes to hearing loss in humans. Nevertheless, studies in zebrafish and mouse models have depleted or knocked out Ribeye expression (while leaving the transcriptional co-repressor CtBP2's function intact) to understand the role of the synaptic ribbon in hair-cells. These genetic studies motivated discussion of Ribeye in this section.

In zebrafish, there are two paralogs of Ribeye and both are found in hair cells. Two main studies have examined the role of these Ribeye paralogs in zebrafish hair cells; one study transiently knocked down Ribeye and the other study created a genetic mutant that permanently eliminated nearly all Ribeye in hair cells. Transient knockdown of both Ribeye transcripts during development resulted in reduced number of hair-cell synaptic ribbons which correlated with reduced afferent innervation and reduced afferent firing (Sheets et al., 2011). By contrast, while *ribeye* mutant zebrafish also eliminated synaptic ribbons, these genetic mutants did not appear to affect afferent innervation nor significantly disrupt lateral-line afferent firing properties (Lv et al., 2016). This latter work suggests that compensatory mechanisms may be engaged when Ribeye is severely and permanently depleted. One additional similarity observed with either transient Ribeye knockdown and *ribeye* mutants was that $Ca_V1.3a$ channels failed to localize and cluster at the synapse. Despite this clustering defect, an enhancement of $Ca_V1.3a$ channel currents was observed in *ribeye* mutants (Lv et al., 2016).

In the mouse knockout of Ribeye, the entire ribbon structure was shown to be absent in hair cells (Maxeiner et al., 2016; Becker et al., 2018; Jean et al., 2018). Yet the absence of synaptic ribbons in knockout mice did not disrupt $Ca_V1.3$ localization at the hair-cell synapse. Instead, Ribeye was shown to be important for presynaptic $Ca_V1.3$ calcium channel organization; without Ribeye there was a preponderance of small $Ca_V1.3$ clusters at each synapse instead of a single organized structure (Jean

et al., 2018). Functionally, Ribeye knockout mice showed minor auditory deficits despite the absence of synaptic ribbons in hair cells (Becker et al., 2018; Jean et al., 2018). Both zebrafish and mouse studies cumulatively revealed that loss of synaptic ribbons via mutation or knockout of Ribeye leads to surprisingly minor deficits hair-cell synapse function and support the idea that compensatory mechanisms exist in both model systems.

In addition to these loss of function models, work in zebrafish has also demonstrated that overexpression of exogenous Ribeye in hair cells can enlarge synaptic ribbons and influence synaptic activity (Sheets et al., 2017). Synaptic ribbons in hair cells overexpressing Ribeye were ∼2 fold larger and transmission electron micrographs showed that these synaptic ribbons had a greater number of synaptic vesicles relative to wild-type siblings. Hair cells containing enlarged synaptic ribbons had less tightly clustered $Ca_V1.3a$ channels yet showed increased $Ca_V1.3a$ channel currents and correspondingly larger ribbon-localized calcium signals. Despite larger calcium signals, there was no change in exocytosis or afferent spike number in response to strong stimulus. Importantly, enlarged synaptic ribbons resulted in a significant reduction in spontaneous afferent activity, and disrupted evoked release at the onset of stimuli. These results indicate that enlarging the synaptic ribbon can influence the activity of innervating afferent neurons and degrade sensory encoding. These observations may have clinical significance; in noise-exposed guinea pig, the synaptic-ribbon size gradient found in auditory hair cells is disrupted (Furman et al., 2013) and synaptic ribbon volume is increased (See section on noise-exposure below, Furman et al., 2013; Song et al., 2016). This increase in synaptic ribbon volume is accompanied by deficits in intensity and temporal coding by auditory nerve fibers (Song et al., 2016). An interesting prospect for future zebrafish work is to determine whether noise can also induce changes in synaptic ribbon size and whether these changes can influence afferent neuron function, and if so by what mechanisms.

THE FUTURE OF USING ZEBRAFISH GENETICS TO STUDY HAIR-CELL SYNAPSES

Action potentials do not drive neurotransmitter release at hair-cell synapses. Instead, in order to convey information about timing and intensity of stimuli, hair-cell neurotransmission is driven by graded depolarizations (Glowatzki and Fuchs, 2002; Trussell, 2002). While hair-cell synapses contain many of the same molecular components as conventional synapses, such as presynaptic calcium channels and postsynaptic glutamate receptors, their specialized function may require synaptic proteins that are unique to hair cells. Indeed, a number of molecules that are required at neuronal synapses are not present in mammalian hair cells, including Munc-13 and CAPS (two important proteins for synaptic vesicle tethering and priming), Synaptotagmins 1 and 2 (calcium sensors for vesicle fusion), Complexins (which regulate vesicle fusion), and Synaptophysins (Safieddine and Wenthold, 1999; Strenzke et al., 2009; Johnson et al., 2010; Uthaiah and Hudspeth, 2010; Vogl et al., 2015). These important synaptic functions are instead thought to be accomplished by specialized hair-cell synaptic proteins. One notable example is Otoferlin which, as highlighted in this review, appears to act in place of Synaptotagmins and functions as a calcium sensor for vesicle fusion (Johnson and Chapman, 2010; Michalski et al., 2017).

Identifying the unique molecular players at ribbon synapses in hair cells has been hampered by the difficultly in acquiring a sufficient amount of material for biochemical and proteomic approaches (Uthaiah and Hudspeth, 2010; Kantardzhieva et al., 2012). Moreover, it is possible that proteins found at both conventional and hair-cell synapses may be present but not be functioning in the same way. For example, SNARE proteins that are required for vesicle fusion at conventional synapses may also be present in hair cells (Uthaiah and Hudspeth, 2010), but do not appear to be required in mouse hair cells for synaptic-vesicle fusion (Nouvian et al., 2011). In future studies, with the advent of CRISPR technology, zebrafish could be used as platform to rapidly and inexpensively identify what synaptic proteins are present in hair cells. Using this approach, it may be possible to identify the molecular equivalents of neuronal molecules that are not present in hair cells, and determine whether neuronal synaptic proteins have specialized functions when they are present in hair cells. In support of this idea, a recent study in zebrafish demonstrated that targeted mutagenesis of protein-coding genes using CRISPR-Cas9 is a powerful and high-throughput way to assess the role of candidate deafness genes identified in humans (Varshney et al., 2015). This work also highlights that the zebrafish model is a useful platform to not only rapidly evaluate the role of both known human deafness genes but also probe for yet unknown molecules that may be required at hair-cell synapses. CRISPR technology, combined with the functional and morphological toolkit outlined in this review, make zebrafish a favorable model to use toward determining the complete molecular composition of hair-cell synapses.

NOISE EXPOSURE, EXCITOXICITY AND ACQUIRED HEARING LOSS IN ZEBRAFISH

In addition to gene mutations that cause hereditary forms of hearing loss, environmental factors such as intense or prolonged noise exposure can result in an acquired form of hearing loss. In humans, intense noise exposure can rapidly lead to profound hearing loss. In other cases following noise exposure, hearing loss is not profound but rather hearing sensitivity is diminished and higher sound pressure levels are needed to perceive a given stimulus (Mills et al., 1979). This diminished hearing sensitivity for a given stimulus is referred to as an elevated shift in hearing threshold.

After noise exposure, hearing loss can either be permanent or temporary depending on the intensity, duration and repetition of the exposure. Cumulatively, studies in mammals have demonstrated that noise exposures can result in damage or loss of hair cells, hair-cell synapses or the innervating afferent neurons (Bohne, 1976; Dinh et al., 2015; Liberman and Kujawa, 2017).

Intense noise exposures that result in permanent hearing loss are accompanied by progressive hair-cell death and loss of afferent neurons (Ryan et al., 2016). Notably in mice, intense impulse noise (i.e., blast) also appeared to result in a significant decrease in the number of hair-cell synapses in surviving hair cells (Cho et al., 2013). This synaptic pathology supports the hypothesis that intense noise exposures contributes to both hair-cell damage, synapse loss and ultimately a permanent, acquired hearing loss.

By contrast, moderate noise exposures are initially accompanied by elevated shifts in hearing threshold, but the thresholds eventually return to normal (Ryan et al., 2016). These noise exposures leave auditory hair cells intact, but contribute to afferent terminal swelling and a subsequent reduction in synaptic contacts, followed by progressive loss of auditory nerves (Kujawa and Liberman, 2009; Lin et al., 2011; Jensen et al., 2015). Currently it is hypothesized that, although clinical hearing thresholds return to normal, there may be subclinical hearing deficits associated with hair-cell synapse loss and afferent nerve degeneration (Bharadwaj et al., 2014). These deficits include difficultly resolving sounds in challenging listening environments such as discerning speech in a noisy room (Moser and Starr, 2016). Afferent-terminal swelling and synapse loss are thought to be a consequence of excess glutamate accumulation in the synaptic cleft during noise over-exposure, resulting in glutamate excitotoxicity (Puel et al., 1994, 1998; Hakuba et al., 2000; Ruel et al., 2005). Similar to genetic lesions that impair hair-cell synapse function, acquired noise-induced hearing loss resulting from a reduction in hair-cell synapses is a form of auditory synaptopathy (Moser and Starr, 2016).

Intense Noise Exposure in Zebrafish

While zebrafish have been used extensively to understand how ototoxic agents, such as aminoglycoside antibiotics and platinum-based cancer therapeutics, damage hair-cell organs (Coffin et al., 2010; Namdaran et al., 2012; Ou et al., 2012), less work has been done to model the toxic effects of noise damage on these organs. Currently there are only a few published studies exploring noise exposure paradigms in zebrafish (Schuck and Smith, 2009; Sun et al., 2011; Uribe et al., 2018). In studies examining auditory over-stimulation, adult zebrafish were exposed to a 100 Hz pure tone at 179 dB for 36 h. After this intense exposure, hair cells in the saccular epithelia (a hair-cell organ in the zebrafish inner ear used to detect sound (Schuck and Smith, 2009)) showed damage or loss of apical mechanosensory structures immediately following noise exposure. The damage was most apparent in the caudal region of the saccule which corresponds to a region sensitive to low frequency tones. Overall, the cellular damage following intense noise exposure was similar to damage that has been observed in mammalian models (Wang et al., 2002). Similar to the regenerative capability that has been demonstrated in the lateral-line system (Coffin et al., 2010; Namdaran et al., 2012; Ou et al., 2012), there was evidence of hair-cell proliferation in the adult zebrafish inner ear just days after noise exposure. Follow up work from this study later revealed that Growth Hormone (GH) may be important for hair-cell proliferation after this level of trauma (Schuck and Smith, 2009; Sun et al., 2011).

The role of GH is intriguing because work in mammals indicates that other hormones and neurotrophins including Thyroid hormone (TH), Neurotrophin-3 (NT-3), Brain-derived neurotrophic factor (BDNF) may be important for the survival and recovery of afferent terminals and synapses (Wan and Corfas, 2015). More specifically, studies in noise-exposed mice suggest NT-3/TrkC signaling promotes synaptic repair and regeneration in auditory hair cells (Wan et al., 2014; Suzuki et al., 2016), while BDNF/TrkB signaling regulates time-dependent noise sensitivity and protects against synapse loss during periods of wakefulness (Meltser et al., 2014). In zebrafish, it has been demonstrated that hair-cell synapse stabilization during normal development requires the protein *N*-ethylmaleimide-sensitive factor (Nsf) in order to release neurotrophic factors including BDNF (Mo and Nicolson, 2011). Future studies in the zebrafish model could provide mechanistic information toward how these trophic factors provide protection or promote repair of hair-cell synapses following noise exposure.

Modeling Noise-Induced Excitotoxicity in Zebrafish

In addition to the few noise exposure studies in zebrafish, recent work has used pharmacology to model glutamate excitotoxicity associated with noise exposure (Sebe et al., 2017; Sheets, 2017). These models are based on the premise that, during noise exposure, excess glutamate accumulates in the synaptic cleft leading to over activation of ionotropic glutamate receptors (iGluR) and subsequent excitotoxic damage. Application of the iGluR agonists α-amino-3-hydroxy-5-methyl-4-isoxazolepropionic acid (AMPA), Kainic acid (KA) and *N*-methyl-D-aspartate (NMDA) to mammalian inner ears or hair-cell explants has also been used to mimic glutamate excitotoxicity associated with noise exposure. In mammals, application of AMPA or KA results in overactivation of the iGluR receptors mediating neurotransmission on postsynaptic afferent terminals (Puel et al., 1994; Zheng et al., 1997; Sun et al., 2001; Sasaki et al., 2012). Subsequently, the afferent terminals swell and, in the case of KA application on auditory hair-cell explants, neurites retract (Wang and Green, 2011). In cases of AMPA administration to inner ears, a small but significant percentage of inner hair cells are also lost 7 days following exposure (Hakuba et al., 2003; Hyodo et al., 2009). Two recent pharmacological studies have used iGluR agonists to mimic noise exposure in zebrafish larvae. These studies took advantage of the accessibility of the larval lateral-line organ to apply iGluR agonists externally, and image hair cells during and after drug exposure (Sebe et al., 2017; Sheets, 2017).

In one study, a single, short application of AMPA (100 or 300 μM AMPA, 15 min) was examined (Sebe et al., 2017). This treatment resulted in swelling of lateral-line afferent nerve terminals. This swelling was similar to what has been reported in mammal auditory system after AMPA exposure (Puel et al., 1994; Hyodo et al., 2009). Functional calcium imaging revealed a loss of activity in afferent nerve terminals after this treatment. Lateral-line hair cells, on the other hand, were not morphologically affected by these treatments and showed normal

mechanotransduction, suggesting glutamate excitotoxicity underlies afferent terminal damage and synaptopathy (Sebe et al., 2017). Importantly, this work demonstrated that the excitotoxic effects of AMPA occurred through calcium-permeable AMPA receptors (CP-AMPARs), as blocking CP-AMPARs prevented postsynaptic swelling and loss-of-function. Furthermore, this study used immunohistochemistry, electrophysiology and pharmacology to demonstrate that CP-AMPARs are present and mediate synaptic currents not only within the postsynapses of lateral-line afferents of the zebrafish lateral line, but also within rat and bullfrog auditory synapses (Sebe et al., 2017). The morphological and functional conservation of CP-AMPARs among species indicates the mechanism underlying glutamate excitotoxicity at hair-cell synapses may also be conserved.

A second study used similar methodology but applied iGluR agonists for longer durations (Sheets, 2017). Here the iGluR agonist NMDA or non-sensitizing AMPA/kainite receptor agonist KA were applied over longer time scales (10–600 μm; 1 h). Similar to what has been demonstrated in the mammalian auditory system after NMDA and KA application (Puel et al., 1994), this study found that NMDA did not cause appreciable swelling in the afferent nerve terminals, while KA was extremely potent and caused swelling and even bursting of afferent nerve terminals. In addition, exposure to either NMDA or KA induced apoptotic hair-cell death in a dose-dependent manner (Sheets, 2017). Remarkably, hair-cell death was independent of damage to post-synaptic terminals—loss of hair cells following NMDA and KA application occurred even in the absence of afferent neurons. Further, this work identified AMPA, Kainate and NMDA receptor subunits that appear to be expressed in hair cells, suggesting that presynaptic iGluR receptors may contribute to hair-cell excitotoxic damage.

THE FUTURE OF NOISE EXPOSURE AND EXCITOTOXICITY RESEARCH IN ZEBRAFISH

Currently there are no published zebrafish studies in adults or larvae using noise exposures to model acquired auditory synaptopathy in the ear. In the future, it will be useful to create protocols to modulate the intensity and duration of noise exposures in order to define the pathological changes in the zebrafish inner ear that are associated with moderate noise exposure. By modulating the intensity and duration of noise exposures in zebrafish, it will be possible to examine the dynamic progression of damage following moderate noise exposure, including loss of afferent fibers and synapses (Kujawa and Liberman, 2009; Shi et al., 2013; Song et al., 2016). In addition to noise damage paradigms to study pathology in the zebrafish inner ear, it will be experimentally worthwhile to develop approaches to directly mechanically over-stimulate the well characterized lateral-line organs. Here, noxious water flow could be used to over-stimulate lateral-line hair cells. Although a previous report outlined a microfluidic device that could be used to confer damage to the lateral-line system in larval zebrafish, no studies have demonstrated the effectiveness of this design (Kwon et al., 2014).

After establishing both moderate and intense noise exposure methods in zebrafish, it will be informative to apply the same tools and assays that have been used to understand the effects ototoxic drugs on hair-cell pathology. For example, the zebrafish lateral line has been used to screen for compounds that protect hair cells or promote hair-cell regeneration during and after ototoxic insult (Coffin et al., 2010; Ou et al., 2012; Esterberg et al., 2014, 2016; Hailey et al., 2017). Based on ototoxicity studies, it is likely that the zebrafish lateral-line system or inner ear could also be used as a screening platform to identify compounds that are protective during noise exposure or lateral-line over-stimulation. Alternatively, zebrafish could be used to identify compounds that promote synaptogenesis after synapse loss and afferent nerve damage.

These studies will be particularly advantageous in larval zebrafish where transgenic lines (**Figure 3**), can be used to image hair cells *in vivo*. Using live imaging, it will be possible to examine the morphology of hair cells, ribbon synapses and afferent nerve terminals during noise exposure, as well as during repair and regeneration. Currently, it is not possible to visualize these changes in the hair-cell organs in living mammals. The ability to visualize morphological changes during and after insults in whole animals is an important advantage to using zebrafish for these studies. These live imaging approaches could reveal the specific pathological changes accompanying both moderate and intense noise exposures. While imaging morphological changes accompanying noise exposure or lateral-line over stimulation will be invaluable, it will also be interesting to explore the functional consequences to the synapse during the noxious insult, as well as during recovery. These studies could be accomplished using electrophysiology and imaging-based methods that have been established in the zebrafish lateral line (**Figure 3**).

Finally, in addition to examining the morphological and functional consequences of noise exposure or lateral-line over stimulation in zebrafish, it will also be worthwhile to explore the downstream molecular mechanisms underlying the observed pathologies, as well as the recovery. In recent years, several models and methods have been developed to profile gene expression changes in specific cell types, including zebrafish hair cells (Steiner et al., 2014; Esterberg et al., 2016; Barta et al., 2018; Matern et al., 2018). It will therefore be beneficial and informative to use these approaches to define the pre- and post-synaptic molecular pathways underlying the pathologies during and recovery after noise damage.

AUTHOR CONTRIBUTIONS

KK and LS wrote the review article and made the figures.

FUNDING

This work was supported by NIH/NIDCD intramural research funds 1ZIADC000085-01 (KK), and NIH/NIDCD Grant R01-DC-016066 (LS).

REFERENCES

Akil, O., Seal, R. P., Burke, K., Wang, C., Alemi, A., During, M., et al. (2012). Restoration of hearing in the VGLUT3 knockout mouse using virally-mediated gene therapy. *Neuron* 75, 283–293. doi: 10.1016/j.neuron.2012.05.019

Baig, S. M., Koschak, A., Lieb, A., Gebhart, M., Dafinger, C., Nürnberg, G., et al. (2011). Loss of Cav1.3 *(CACNA*1D) function in a human channelopathy with bradycardia and congenital deafness. *Nat. Neurosci.* 14, 77–84. doi: 10.1038/nn.2694

Barta, C. L., Liu, H., Chen, L., Giffen, K. P., Li, Y., Kramer, K. L., et al. (2018). RNA-seq transcriptomic analysis of adult zebrafish inner ear hair cells. *Sci. Data* 5:180005. doi: 10.1038/sdata.2018.5

Bean, B. P. (1989). Classes of calcium channels in vertebrate cells. *Annu. Rev. Physiol.* 51, 367–384. doi: 10.1146/annurev.ph.51.030189.002055

Becker, L., Schnee, M. E., Niwa, M., Sun, W., Maxeiner, S., Talaei, S., et al. (2018). The presynaptic ribbon maintains vesicle populations at the hair cell afferent fiber synapse. *eLife* 7:e30241. doi: 10.7554/eLife.30241

Behra, M., Gallardo, V. E., Bradsher, J., Torrado, A., Elkahloun, A., Idol, J., et al. (2012). Transcriptional signature of accessory cells in the lateral line, using the Tnk1bp1:EGFP transgenic zebrafish line. *BMC Dev. Biol.* 12:6. doi: 10.1186/1471-213X-12-6

Bharadwaj, H. M., Verhulst, S., Shaheen, L., Liberman, M. C., and Shinn-Cunningham, B. G. (2014). Cochlear neuropathy and the coding of supra-threshold sound. *Front. Syst. Neurosci.* 8:26. doi: 10.3389/fnsys.2014.00026

Bohne, B. A. (1976). Safe level for noise exposure? *Ann. Otol. Rhinol. Laryngol.* 85, 711–724. doi: 10.1177/000348947608500602

Brandt, A., Khimich, D., and Moser, T. (2005). Few CaV1.3 channels regulate the exocytosis of a synaptic vesicle at the hair cell ribbon synapse. *J. Neurosci. Off J. Soc. Neurosci.* 25, 11577–11585. doi: 10.1523/JNEUROSCI.3411-05.2005

Brandt, A., Striessnig, J., and Moser, T. (2003). CaV1.3 channels are essential for development and presynaptic activity of cochlear inner hair cells. *J. Neurosci. Off. J. Soc. Neurosci.* 23, 10832–10840. doi: 10.1523/JNEUROSCI.23-34-10832.2003

Chatterjee, P., Padmanarayana, M., Abdullah, N., Holman, C. L., LaDu, J., Tanguay, R. L., et al. (2015). Otoferlin deficiency in zebrafish results in defects in balance and hearing: rescue of the balance and hearing phenotype with full-length and truncated forms of mouse otoferlin. *Mol. Cell. Biol.* 35, 1043–1054. doi: 10.1128/MCB.01439-14

Chen, D.-Y., Liu, X.-F., Lin, X.-J., Zhang, D., Chai, Y.-C., Yu, D.-H., et al. (2017). A dominant variant in DMXL2 is linked to nonsyndromic hearing loss. *Genet. Med. Off. J. Am. Coll. Med. Genet.* 19, 553–558. doi: 10.1038/gim.2016.142

Chen, Z., Chou, S. W., and McDermott, B. M. (2018). Ribeye protein is intrinsically dynamic but is stabilized in the context of the ribbon synapse. *J. Physiol.* 596, 409–421. doi: 10.1113/JP271215

Cho, S.-I., Gao, S. S., Xia, A., Wang, R., Salles, F. T., Raphael, P. D., et al. (2013). Mechanisms of hearing loss after blast injury to the ear. *PLoS One* 8:e67618. doi: 10.1371/journal.pone.0067618

Coffin, A., Kelley, M., Manley, G. A., and Popper, A. N. (2004). "Evolution of sensory hair cells," in *Evolution of the Vertebrate Auditory System*, eds G. A. Manley, R. R. Fay, and A. N. Popper (New York, NY: Springer), 55–94. doi: 10.1007/978-1-4419-8957-4_3

Coffin, A. B., Ou, H., Owens, K. N., Santos, F., Simon, J. A., Rubel, E. W., et al. (2010). Chemical screening for hair cell loss and protection in the zebrafish lateral line. *Zebrafish* 7, 3–11. doi: 10.1089/zeb.2009.0639

Dinh, C. T., Goncalves, S., Bas, E., Van De Water, T. R., and Zine, A. (2015). Molecular regulation of auditory hair cell death and approaches to protect sensory receptor cells and/or stimulate repair following acoustic trauma. *Front. Cell Neurosci.* 9:96. doi: 10.3389/fncel.2015.00096

Dow, E., Siletti, K., and Hudspeth, A. J. (2015). Cellular projections from sensory hair cells form polarity-specific scaffolds during synaptogenesis. *Genes Dev.* 29, 1087–1094. doi: 10.1101/gad.259838.115

Eatock, R., and Fay, R. R. (eds) (2006). *Vertebrate Hair Cells*. New York, NY: Springer-Verlag. doi: 10.1007/0-387-31706-6

Eggermont, J. J. (2017). *Hearing Loss: Causes, Prevention, and Treatment*, 1st Edn. Cambridge, MA: Academic Press.

Einhorn, Z., Trapani, J. G., Liu, Q., and Nicolson, T. (2012). Rabconnectin3α promotes stable activity of the H+ pump on synaptic vesicles in hair cells. *J. Neurosci. Off. J. Soc. Neurosci.* 32, 11144–11156. doi: 10.1523/JNEUROSCI.1705-12.2012

Ernest, S., Rauch, G. J., Haffter, P., Geisler, R., Petit, C., and Nicolson, T. (2000). Mariner is defective in myosin VIIA: a zebrafish model for human hereditary deafness. *Hum. Mol. Genet.* 9, 2189–2196. doi: 10.1093/hmg/9.14.2189

Esterberg, R., Hailey, D. W., Rubel, E. W., and Raible, D. W. (2014). ER–mitochondrial calcium flow underlies vulnerability of mechanosensory hair cells to damage. *J. Neurosci.* 34, 9703–9719. doi: 10.1523/JNEUROSCI.0281-14.2014

Esterberg, R., Linbo, T., Pickett, S. B., Wu, P., Ou, H. C., Rubel, E. W., et al. (2016). Mitochondrial calcium uptake underlies ROS generation during aminoglycoside-induced hair cell death. *J. Clin. Invest.* 126, 3556–3566. doi: 10.1172/JCI84939

Faucherre, A., Pujol-Martí, J., Kawakami, K., and López-Schier, H. (2009). Afferent neurons of the zebrafish lateral line are strict selectors of hair-cell orientation. *PLoS One* 4:e4477. doi: 10.1371/journal.pone.0004477

Frank, T., Khimich, D., Neef, A., and Moser, T. (2009). Mechanisms contributing to synaptic Ca2+ signals and their heterogeneity in hair cells. *Proc. Natl. Acad. Sci. U.S.A.* 106, 4483–4488. doi: 10.1073/pnas.0813213106

Frank, T., Rutherford, M. A., Strenzke, N., Neef, A., Pangršič, T., Khimich, D., et al. (2010). Bassoon and the synaptic ribbon organize Ca2+ channels and vesicles to add release sites and promote refilling. *Neuron* 68, 724–738. doi: 10.1016/j.neuron.2010.10.027

Fritzsch, B., Silos-Santiago, I. I., Bianchi, L. M., and Fariñas, I. I. (1997). Effects of neurotrophin and neurotrophin receptor disruption on the afferent inner ear innervation. *Semin. Cell Dev. Biol.* 8, 277–284. doi: 10.1006/scdb.1997.0144

Fritzsch, B., Tessarollo, L., Coppola, E., and Reichardt, L. F. (2004). Neurotrophins in the ear: their roles in sensory neuron survival and fiber guidance. *Prog. Brain Res.* 146, 265–278. doi: 10.1016/S0079-6123(03)46017-2

Fuchs, P. A. (2005). Time and intensity coding at the hair cell's ribbon synapse. *J. Physiol.* 566, 7–12. doi: 10.1113/jphysiol.2004.082214

Furman, A. C., Kujawa, S. G., and Liberman, M. C. (2013). Noise-induced cochlear neuropathy is selective for fibers with low spontaneous rates. *J. Neurophysiol.* 110, 577–586. doi: 10.1152/jn.00164.2013

Gillespie, P. G., and Walker, R. G. (2001). Molecular basis of mechanosensory transduction. *Nature* 413, 194–202. doi: 10.1038/35093011

Gleason, M. R., Nagiel, A., Jamet, S., Vologodskaia, M., López-Schier, H., and Hudspeth, A. J. (2009). The transmembrane inner ear (Tmie) protein is essential for normal hearing and balance in the zebrafish. *Proc. Natl. Acad. Sci. U.S.A.* 106, 21347–21352. doi: 10.1073/pnas.0911632106

Glowatzki, E., and Fuchs, P. A. (2002). Transmitter release at the hair cell ribbon synapse. *Nat. Neurosci.* 5, 147–154. doi: 10.1038/nn796

Glueckert, R., Wietzorrek, G., Kammen-Jolly, K., Scholtz, A., Stephan, K., Striessnig, J., et al. (2003). Role of class D L-type Ca2+ channels for cochlear morphology. *Hear. Res.* 178, 95–105. doi: 10.1016/S0378-5955(03)00054-6

Goodyear, R. J., Legan, P. K., Christiansen, J. R., Xia, B., Korchagina, J., Gale, J. E., et al. (2010). Identification of the hair cell soma-1 antigen, HCS-1, as otoferlin. *JARO J. Assoc. Res. Otolaryngol.* 11, 573–586. doi: 10.1007/s10162-010-0231-6

Graydon, C. W., Manor, U., and Kindt, K. S. (2017). In vivo ribbon mobility and turnover of ribeye at zebrafish hair cell synapses. *Sci. Rep.* 7:7467. doi: 10.1038/s41598-017-07940-z

Hailey, D. W., Esterberg, R., Linbo, T. H., Rubel, E. W., and Raible, D. W. (2017). Fluorescent aminoglycosides reveal intracellular trafficking routes in mechanosensory hair cells. *J. Clin. Invest.* 127, 472–486. doi: 10.1172/JCI85052

Hakuba, N., Koga, K., Gyo, K., Usami, S. I., and Tanaka, K. (2000). Exacerbation of noise-induced hearing loss in mice lacking the glutamate transporter GLAST. *J. Neurosci. Off. J. Soc. Neurosci.* 20, 8750–8753. doi: 10.1523/JNEUROSCI.20-23-08750.2000

Hakuba, N., Matsubara, A., Hyodo, J., Taniguchi, M., Maetani, T., Shimizu, Y., et al. (2003). AMPA/kainate-type glutamate receptor antagonist reduces progressive inner hair cell loss after transient cochlear ischemia. *Brain Res.* 979, 194–202. doi: 10.1016/S0006-8993(03)02919-6

Harris, G. G., Frishkopf, L. S., and Flock, A. (1970). Receptor potentials from hair cells of the lateral line. *Science* 167, 76–79. doi: 10.1126/science.167.3914.76

Harris, J. A., Cheng, A. G., Cunningham, L. L., MacDonald, G., Raible, D. W., and Rubel, E. W. (2003). Neomycin-induced hair cell death and rapid regeneration

in the lateral line of zebrafish (*Danio rerio*). *J. Assoc. Res. Otolaryngol.* 4, 219–234. doi: 10.1007/s10162-002-3022-x

Harris, T. W., Hartwieg, E., Horvitz, H. R., and Jorgensen, E. M. (2000). Mutations in synaptojanin disrupt synaptic vesicle recycling. *J. Cell Biol.* 150, 589–600. doi: 10.1083/jcb.150.3.589

Hildebrand, J. D., and Soriano, P. (2002). Overlapping and unique roles for C-Terminal binding protein 1 (CtBP1) and CtBP2 during mouse development. *Mol. Cell. Biol.* 22, 5296–5307. doi: 10.1128/MCB.22.15.5296-5307.2002

Hyodo, J., Hakuba, N., Hato, N., Takeda, S., Okada, M., Omotehara, Y., et al. (2009). Glutamate agonist causes irreversible degeneration of inner hair cells. *Neuro Report* 20:1255. doi: 10.1097/WNR.0b013e32833017ce

Jean, P., Morena, D. L., de la Michanski, S., Tobón, L. M. J., Chakrabarti, R., Picher, M. M., et al. (2018). The synaptic ribbon is critical for sound encoding at high rates and with temporal precision. *eLife* 7:e29275. doi: 10.7554/eLife.29275

Jensen, J. B., Lysaght, A. C., Liberman, M. C., Qvortrup, K., and Stankovic, K. M. (2015). Immediate and delayed cochlear neuropathy after noise exposure in pubescent mice. *PLoS One* 10:e0125160. doi: 10.1371/journal.pone.0125160

Johnson, C. P., and Chapman, E. R. (2010). Otoferlin is a calcium sensor that directly regulates SNARE-mediated membrane fusion. *J. Cell Biol.* 191, 187–197. doi: 10.1083/jcb.201002089

Johnson, S. L., Franz, C., Kuhn, S., Furness, D. N., Rüttiger, L., Münkner, S., et al. (2010). Synaptotagmin IV determines the linear Ca2+ dependence of vesicle fusion at auditory ribbon synapses. *Nat. Neurosci.* 13, 45–52. doi: 10.1038/nn.2456

Kantardzhieva, A., Peppi, M., Lane, W. S., and Sewell, W. F. (2012). Protein composition of immunoprecipitated synaptic ribbons. *J. Proteome Res.* 11, 1163–1174. doi: 10.1021/pr2008972

Kersigo, J., and Fritzsch, B. (2015). Inner ear hair cells deteriorate in mice engineered to have no or diminished innervation. *Front. Aging Neurosci.* 7:33. doi: 10.3389/fnagi.2015.00033

Kindt, K. S., Finch, G., and Nicolson, T. (2012). Kinocilia mediate mechanosensitivity in developing zebrafish hair cells. *Dev. Cell* 23, 329–341. doi: 10.1016/j.devcel.2012.05.022

Kraus, H. J., and Aulbach-Kraus, K. (1981). Morphological changes in the cochlea of the mouse after the onset of hearing. *Hear. Res.* 4, 89–102. doi: 10.1016/0378-5955(81)90038-1

Kujawa, S. G., and Liberman, M. C. (2009). Adding insult to injury: cochlear nerve degeneration after "temporary" noise-induced hearing loss. *J. Neurosci. Off. J. Soc. Neurosci.* 29, 14077–14085. doi: 10.1523/JNEUROSCI.2845-09.2009

Kwan, K. M., Fujimoto, E., Grabher, C., Mangum, B. D., Hardy, M. E., Campbell, D. S., et al. (2007). The Tol2kit: a multisite gateway-based construction kit for Tol2 transposon transgenesis constructs. *Dev. Dyn. Off. Publ. Am. Assoc. Anat.* 236, 3088–3099. doi: 10.1002/dvdy.21343

Kwon, H.-J., Xu, Y., Solovitz, S. A., Xue, W., Dimitrov, A. G., Coffin, A. B., et al. (2014). Design of a microfluidic device with a non-traditional flow profile for on-chip damage to zebrafish sensory cells. *J. Micromech. Microeng.* 24, 017001. doi: 10.1088/0960-1317/24/1/017001

Lek, A., Evesson, F. J., Sutton, R. B., North, K. N., and Cooper, S. T. (2012). Ferlins: regulators of vesicle fusion for auditory neurotransmission, receptor trafficking and membrane repair. *Traffic Cph Den.* 13, 185–194. doi: 10.1111/j.1600-0854.2011.01267.x

Liberman, L. D., Wang, H., and Liberman, M. C. (2011). Opposing gradients of ribbon size and AMPA receptor expression underlie sensitivity differences among cochlear-nerve/hair-cell synapses. *J. Neurosci.* 31, 801–808. doi: 10.1523/JNEUROSCI.3389-10.2011

Liberman, M. C., and Kujawa, S. G. (2017). Cochlear synaptopathy in acquired sensorineural hearing loss: manifestations and mechanisms. *Hear. Res.* 349, 138–147. doi: 10.1016/j.heares.2017.01.003

Lin, H. W., Furman, A. C., Kujawa, S. G., and Liberman, M. C. (2011). Primary neural degeneration in the Guinea pig cochlea after reversible noise-induced threshold shift. *J. Assoc. Res. Otolaryngol. JARO* 12, 605–616. doi: 10.1007/s10162-011-0277-0

Lin, S., Vollrath, M. A., Mangosing, S., Shen, J., Cardenas, E., and Corey, D. P. (2016). The zebrafish pinball wizard gene encodes WRB, a tail-anchored-protein receptor essential for inner-ear hair cells and retinal photoreceptors. *J. Physiol.* 594, 895–914. doi: 10.1113/JP271437

Lipscombe, D., Helton, T. D., and Xu, W. (2004). L-type calcium channels: the low down. *J. Neurophysiol.* 92, 2633–2641. doi: 10.1152/jn.00486.2004

Lv, C., Stewart, W. J., Akanyeti, O., Frederick, C., Zhu, J., Santos-Sacchi, J., et al. (2016). Synaptic ribbons require ribeye for electron density, proper synaptic localization, and recruitment of calcium channels. *Cell Rep.* 15, 2784–2795. doi: 10.1016/j.celrep.2016.05.045

Magupalli, V. G., Schwarz, K., Alpadi, K., Natarajan, S., Seigel, G. M., and Schmitz, F. (2008). Multiple RIBEYE-RIBEYE interactions create a dynamic scaffold for the formation of synaptic ribbons. *J. Neurosci. Off. J. Soc. Neurosci.* 28, 7954–7967. doi: 10.1523/JNEUROSCI.1964-08.2008

Manji, S. S. M., Williams, L. H., Miller, K. A., Ooms, L. M., Bahlo, M., Mitchell, C. A., et al. (2011). A mutation in synaptojanin 2 causes progressive hearing loss in the ENU-mutagenised mouse strain Mozart. *PLoS One* 6:e17607. doi: 10.1371/journal.pone.0017607

Matern, M. S., Beirl, A., Ogawa, Y., Song, Y., Paladugu, N., Kindt, K., et al. (2018). Transcriptomic profiling of zebrafish hair cells using RiboTag. *Front. Cell Dev. Biol.* 6:47. doi: 10.3389/fcell.2018.00047

Maxeiner, S., Luo, F., Tan, A., Schmitz, F., and Südhof, T. C. (2016). How to make a synaptic ribbon: RIBEYE deletion abolishes ribbons in retinal synapses and disrupts neurotransmitter release. *EMBO J.* 35, 1098–1114. doi: 10.15252/embj.201592701

McDermott, B. M., Baucom, J. M., and Hudspeth, A. J. (2007). Analysis and functional evaluation of the hair-cell transcriptome. *Proc. Natl. Acad. Sci. U.S.A.* 104, 11820–11825. doi: 10.1073/pnas.0704476104

Meltser, I., Cederroth, C. R., Basinou, V., Savelyev, S., Lundkvist, G. S., and Canlon, B. (2014). TrkB-Mediated protection against circadian sensitivity to noise trauma in the murine cochlea. *Curr. Biol.* 24, 658–663. doi: 10.1016/j.cub.2014.01.047

Merchan-Perez, A., and Liberman, M. C. (1996). Ultrastructural differences among afferent synapses on cochlear hair cells: correlations with spontaneous discharge rate. *J. Comp. Neurol.* 371, 208–221. doi: 10.1002/(SICI)1096-9861(19960722)371:2<208::AID-CNE2>3.0.CO;2-6

Meyer, A. C., Frank, T., Khimich, D., Hoch, G., Riedel, D., Chapochnikov, N. M., et al. (2009). Tuning of synapse number, structure and function in the cochlea. *Nat. Neurosci.* 12, 444–453. doi: 10.1038/nn.2293

Michalski, N., Goutman, J. D., Auclair, S. M., Boutet de Monvel, J., Tertrais, M., Emptoz, A., et al. (2017). Otoferlin acts as a Ca2+ sensor for vesicle fusion and vesicle pool replenishment at auditory hair cell ribbon synapses. *eLife* 6:e31013. doi: 10.7554/eLife.31013

Mills, J. H., Gilbert, R. M., Adkins, W. Y., and Kulish, L. (1979). Temporary threshold shifts produced by 24-h exposures to intermittent noise. *J. Acoust. Soc. Am.* 65, S117–S117. doi: 10.1121/1.382791

Mo, W., and Nicolson, T. (2011). Both pre- and postsynaptic activity of Nsf prevents degeneration of hair-cell synapses. *PLoS One* 6:e27146. doi: 10.1371/journal.pone.0027146

Moser, T., Brandt, A., and Lysakowski, A. (2006). Hair cell ribbon synapses. *Cell Tissue Res.* 326, 347–359. doi: 10.1007/s00441-006-0276-3

Moser, T., and Starr, A. (2016). Auditory neuropathy–neural and synaptic mechanisms. *Nat. Rev. Neurol.* 12, 135–149. doi: 10.1038/nrneurol.2016.10

Murakami, S. L., Cunningham, L. L., Werner, L. A., Bauer, E., Pujol, R., Raible, D. W., et al. (2003). Developmental differences in susceptibility to neomycin-induced hair cell death in the lateral line neuromasts of zebrafish (*Danio rerio*). *Hear. Res.* 186, 47–56. doi: 10.1016/S0378-5955(03)00259-4

Nagiel, A., Andor-Ardó, D., and Hudspeth, A. J. (2008). Specificity of afferent synapses onto plane-polarized hair cells in the posterior lateral line of the zebrafish. *J. Neurosci.* 28, 8442–8453. doi: 10.1523/JNEUROSCI.2425-08.2008

Namdaran, P., Reinhart, K. E., Owens, K. N., Raible, D. W., and Rubel, E. W. (2012). Identification of modulators of hair cell regeneration in the zebrafish lateral line. *J. Neurosci. Off J. Soc. Neurosci.* 32, 3516–3528. doi: 10.1523/JNEUROSCI.3905-11.2012

Nicolson, T. (2005). The genetics of hearing and balance in zebrafish. *Annu. Rev. Genet.* 39, 9–22. doi: 10.1146/annurev.genet.39.073003.105049

Nicolson, T., Rüsch, A., Friedrich, R. W., Granato, M., Ruppersberg, J. P., and Nüsslein-Volhard, C. (1998). Genetic analysis of vertebrate sensory hair cell mechanosensation: the zebrafish circler mutants. *Neuron* 20, 271–283. doi: 10.1016/S0896-6273(00)80455-9

Nouvian, R., Neef, J., Bulankina, A. V., Reisinger, E., Pangršič, T., Frank, T., et al. (2011). Exocytosis at the hair cell ribbon synapse apparently operates without neuronal SNARE proteins. *Nat. Neurosci.* 14, 411–413. doi: 10.1038/nn.2774

Obholzer, N., Wolfson, S., Trapani, J. G., Mo, W., Nechiporuk, A., Busch-Nentwich, E., et al. (2008). Vesicular glutamate transporter 3 is required for synaptic transmission in zebrafish hair cells. *J. Neurosci. Off. J. Soc. Neurosci.* 28, 2110–2118. doi: 10.1523/JNEUROSCI.5230-07.2008

Olt, J., Allen, C. E., and Marcotti, W. (2016a). In vivo physiological recording from the lateral line of juvenile zebrafish. *J. Physiol.* 594, 5427–5438. doi: 10.1113/JP271794

Olt, J., Ordoobadi, A. J., Marcotti, W., and Trapani, J. G. (2016b). Physiological recordings from the zebrafish lateral line. *Methods Cell Biol.* 133, 253–279. doi: 10.1016/bs.mcb.2016.02.004

Olt, J., Johnson, S. L., and Marcotti, W. (2014). In vivo and in vitro biophysical properties of hair cells from the lateral line and inner ear of developing and adult zebrafish. *J. Physiol.* 592, 2041–2058. doi: 10.1113/jphysiol.2013.265108

Ou, H., Simon, J. A., Rubel, E. W., and Raible, D. W. (2012). Screening for chemicals that affect hair cell death and survival in the zebrafish lateral line. *Hear. Res.* 288, 58–66. doi: 10.1016/j.heares.2012.01.009

Pan, B., and Holt, J. R. (2015). The molecules that mediate sensory transduction in the mammalian inner ear. *Curr. Opin. Neurobiol.* 34, 165–171. doi: 10.1016/j.conb.2015.06.013

Pangršič, T., Gabrielaitis, M., Michanski, S., Schwaller, B., Wolf, F., Strenzke, N., et al. (2015). EF-hand protein Ca2+ buffers regulate Ca2+ influx and exocytosis in sensory hair cells. *Proc. Natl. Acad. Sci. U.S.A.* 112, E1028–E1037. doi: 10.1073/pnas.1416424112

Paquette, S. T., Gilels, F., and White, P. M. (2016). Noise exposure modulates cochlear inner hair cell ribbon volumes, correlating with changes in auditory measures in the FVB/nJ mouse. *Sci. Rep.* 6:25056. doi: 10.1038/srep25056

Pei, W., Xu, L., Varshney, G. K., Carrington, B., Bishop, K., Jones, M., et al. (2016). Additive reductions in zebrafish PRPS1 activity result in a spectrum of deficiencies modeling several human PRPS1-associated diseases. *Sci. Rep.* 6:29946. doi: 10.1038/srep29946

Pfeiffer, R. R., and Kiang, N. Y. (1965). Spike discharge patterns of spontaneous and continuously stimulated activity in the cochlear nucleus of anesthetized cats. *Biophys. J.* 5, 301–316. doi: 10.1016/S0006-3495(65)86718-2

Pichler, P., and Lagnado, L. (2018). Hair cells with heterogeneous transfer characteristics encode mechanical stimuli in the lateral line of zebrafish. *bioRxiv* [Preprint]. doi: 10.1101/261669

Platzer, J., Engel, J., Schrott-Fischer, A., Stephan, K., Bova, S., Chen, H., et al. (2000). Congenital deafness and sinoatrial node dysfunction in mice lacking class D L-type Ca2+ channels. *Cell* 102, 89–97. doi: 10.1016/S0092-8674(00)00013-1

Puel, J.-L., Pujol, R., Tribillac, F., Ladrech, S., and Eybalin, M. (1994). Excitatory amino acid antagonists protect cochlear auditory neurons from excitotoxicity. *J. Comp. Neurol.* 341, 241–256. doi: 10.1002/cne.903410209

Puel, J.-L., Ruel, J., d'Aldin, C. G., and Pujol, R. (1998). Excitotoxicity and repair of cochlear synapses after noise-trauma induced hearing loss. *Neuro Rep.* 9:2109. doi: 10.1097/00001756-199806220-00037

Pujol-Martí, J., Faucherre, A., Aziz-Bose, R., Asgharsharghi, A., Colombelli, J., Trapani, J. G., et al. (2014). Converging axons collectively initiate and maintain synaptic selectivity in a constantly remodeling sensory organ. *Curr. Biol.* 24, 2968–2974. doi: 10.1016/j.cub.2014.11.012

Ramakrishnan, N. A., Drescher, M. J., and Drescher, D. G. (2009). Direct interaction of otoferlin with syntaxin 1A, SNAP-25, and the L-type voltage-gated calcium channel Cav1.3. *J. Biol. Chem.* 284, 1364–1372. doi: 10.1074/jbc.M803605200

Ricci, A. J., Bai, J.-P., Song, L., Lv, C., Zenisek, D., and Santos-Sacchi, J. (2013). Patch-clamp recordings from lateral line neuromast hair cells of the living zebrafish. *J. Neurosci. Off. J. Soc. Neurosci.* 33, 3131–3134. doi: 10.1523/JNEUROSCI.4265-12.2013

Rodríguez-Ballesteros, M., Reynoso, R., Olarte, M., Villamar, M., Morera, C., Santarelli, R., et al. (2008). A multicenter study on the prevalence and spectrum of mutations in the otoferlin gene (OTOF) in subjects with nonsyndromic hearing impairment and auditory neuropathy. *Hum. Mutat.* 29, 823–831. doi: 10.1002/humu.20708

Romand, R., and Varela-Nieto, I. (2003). *Development of Auditory and Vestibular Systems-3: Molecular Development of the Inner Ear*. Amsterdam: Elsevier.

Roux, I., Safieddine, S., Nouvian, R., Grati, M., Simmler, M.-C., Bahloul, A., et al. (2006). Otoferlin, defective in a human deafness form, is essential for exocytosis at the auditory ribbon synapse. *Cell* 127, 277–289. doi: 10.1016/j.cell.2006.08.040

Ruel, J., Emery, S., Nouvian, R., Bersot, T., Amilhon, B., Van Rybroek, J. M., et al. (2008). Impairment of SLC17A8 encoding vesicular glutamate transporter-3, VGLUT3, underlies nonsyndromic deafness DFNA25 and inner hair cell dysfunction in null mice. *Am. J. Hum. Genet.* 83, 278–292. doi: 10.1016/j.ajhg.2008.07.008

Ruel, J., Wang, J., Pujol, R., Hameg, A., Dib, M., and Puel, J. L. (2005). Neuroprotective effect of riluzole in acute noise-induced hearing loss. *Neuroreport* 16, 1087–1090. doi: 10.1097/00001756-200507130-00011

Ryan, A. F., Kujawa, S. G., Hammill, T., Le Prell, C., and Kil, J. (2016). Temporary and permanent noise-induced threshold shifts: a review of basic and clinical observations. *Otol. Neurotol. Off. Publ. Am. Otol. Soc. Am. Neurotol. Soc. Eur. Acad. Otol. Neurotol.* 37, e271–e275. doi: 10.1097/MAO.0000000000001071

Safieddine, S., El-Amraoui, A., and Petit, C. (2012). The auditory hair cell ribbon synapse: from assembly to function. *Annu. Rev. Neurosci.* 35, 509–528. doi: 10.1146/annurev-neuro-061010-113705

Safieddine, S., and Wenthold, R. J. (1999). SNARE complex at the ribbon synapses of cochlear hair cells: analysis of synaptic vesicle- and synaptic membrane-associated proteins. *Eur. J. Neurosci.* 11, 803–812. doi: 10.1046/j.1460-9568.1999.00487.x

Santarelli, R., del Castillo, I., Cama, E., Scimemi, P., and Starr, A. (2015). Audibility, speech perception and processing of temporal cues in ribbon synaptic disorders due to OTOF mutations. *Hear Res.* 330, 200–212. doi: 10.1016/j.heares.2015.07.007

Sasaki, A., Matsubara, A., Tabuchi, K., Hara, A., Namba, A., Yamamoto, Y., et al. (2012). Immunoelectron microscopic analysis of neurotoxic effect of glutamate in the vestibular end organs during ischemia. *Acta Otolaryngol. (Stockh)* 132, 686–692. doi: 10.3109/00016489.2012.656322

Schmitz, F., Königstorfer, A., and Südhof, T. C. (2000). RIBEYE, a component of synaptic ribbons: a protein's journey through evolution provides insight into synaptic ribbon function. *Neuron* 28, 857–872. doi: 10.1016/S0896-6273(00)00159-8

Schuck, J. B., and Smith, M. E. (2009). Cell proliferation follows acoustically-induced hair cell bundle loss in the zebrafish saccule. *Hear Res.* 253, 67–76. doi: 10.1016/j.heares.2009.03.008

Seal, R. P., Akil, O., Yi, E., Weber, C. M., Grant, L., Yoo, J., et al. (2008). Sensorineural deafness and seizures in mice lacking vesicular glutamate transporter 3. *Neuron* 57, 263–275. doi: 10.1016/j.neuron.2007.11.032

Sebe, J. Y., Cho, S., Sheets, L., Rutherford, M. A., von Gersdorff, H., and Raible, D. W. (2017). Ca2+-permeable AMPARs mediate glutamatergic transmission and excitotoxic damage at the hair cell ribbon synapse. *J. Neurosci. Off. J. Soc. Neurosci.* 37, 6162–6175. doi: 10.1523/JNEUROSCI.3644-16.2017

Seiler, C., Ben-David, O., Sidi, S., Hendrich, O., Rusch, A., Burnside, B., et al. (2004). Myosin VI is required for structural integrity of the apical surface of sensory hair cells in zebrafish. *Dev. Biol.* 272, 328–338. doi: 10.1016/j.ydbio.2004.05.004

Seiler, C., and Nicolson, T. (1999). Defective calmodulin-dependent rapid apical endocytosis in zebrafish sensory hair cell mutants. *J. Neurobiol.* 41, 424–434. doi: 10.1002/(SICI)1097-4695(19991115)41:3<424::AID-NEU10>3.0.CO;2-G

Sheets, L. (2017). Excessive activation of ionotropic glutamate receptors induces apoptotic hair-cell death independent of afferent and efferent innervation. *Sci. Rep.* 7:41102. doi: 10.1038/srep41102

Sheets, L., He, X. J., Olt, J., Schreck, M., Petralia, R. S., Wang, Y.-X., et al. (2017). Enlargement of ribbons in zebrafish hair cells increases calcium currents but disrupts afferent spontaneous activity and timing of stimulus onset. *J. Neurosci. Off. J. Soc. Neurosci.* 37, 6299–6313. doi: 10.1523/JNEUROSCI.2878-16.2017

Sheets, L., Kindt, K. S., and Nicolson, T. (2012). Presynaptic CaV1.3 channels regulate synaptic ribbon size and are required for synaptic maintenance in sensory hair cells. *J. Neurosci. Off. J. Soc. Neurosci.* 32, 17273–17286. doi: 10.1523/JNEUROSCI.3005-12.2012

Sheets, L., Trapani, J. G., Mo, W., Obholzer, N., and Nicolson, T. (2011). Ribeye is required for presynaptic Ca(V)1.3a channel localization and afferent innervation of sensory hair cells. *Dev. Camb. Engl.* 138, 1309–1319. doi: 10.1242/dev.059451

Shi, L., Liu, L., He, T., Guo, X., Yu, Z., Yin, S., et al. (2013). Ribbon synapse plasticity in the cochleae of guinea pigs after noise-induced silent damage. *PLoS One* 8:e81566. doi: 10.1371/journal.pone.0081566

Sidi, S., Busch-Nentwich, E., Friedrich, R., Schoenberger, U., and Nicolson, T. (2004). Gemini encodes a zebrafish L-type calcium channel that localizes at sensory hair cell ribbon synapses. *J. Neurosci. Off. J. Soc. Neurosci.* 24, 4213–4223. doi: 10.1523/JNEUROSCI.0223-04.2004

Söllner, C., Rauch, G.-J., Siemens, J., Geisler, R., Schuster, S. C., The Tübingen 2000 Screen Consortium, et al. (2004). Mutations in *cadherin* 23 affect tip links in zebrafish sensory hair cells. *Nature* 428, 955–959. doi: 10.1038/nature02484

Song, Q., Shen, P., Li, X., Shi, L., Liu, L., Wang, J., et al. (2016). Coding deficits in hidden hearing loss induced by noise: the nature and impacts. *Sci. Rep.* 6:25200. doi: 10.1038/srep25200

Song, W., and Zinsmaier, K. E. (2003). Endophilin and synaptojanin hook up to promote synaptic vesicle endocytosis. *Neuron* 40, 665–667. doi: 10.1016/S0896-6273(03)00726-8

Steiner, A. B., Kim, T., Cabot, V., and Hudspeth, A. J. (2014). Dynamic gene expression by putative hair-cell progenitors during regeneration in the zebrafish lateral line. *Proc. Natl. Acad. Sci. U.S.A.* 111, E1393–E1401. doi: 10.1073/pnas.1318692111

Strenzke, N., Chanda, S., Kopp-Scheinpflug, C., Khimich, D., Reim, K., Bulankina, A. V., et al. (2009). Complexin-I is required for high-fidelity transmission at the endbulb of held auditory synapse. *J. Neurosci.* 29, 7991–8004. doi: 10.1523/JNEUROSCI.0632-09.2009

Suli, A., Pujol, R., Cunningham, D. E., Hailey, D. W., Prendergast, A., Rubel, E. W., et al. (2016). Innervation regulates synaptic ribbons in lateral line mechanosensory hair cells. *J. Cell Sci.* 129, 2250–2260. doi: 10.1242/jcs.182592

Sun, H., Hashino, E., Ding, D.-L., and Salvi, R. J. (2001). Reversible and irreversible damage to cochlear afferent neurons by kainic acid excitotoxicity. *J. Comp. Neurol.* 430, 172–181. doi: 10.1002/1096-9861(20010205)430:2<172::AID-CNE1023>3.0.CO;2-W

Sun, H., Lin, C.-H., and Smith, M. E. (2011). Growth hormone promotes hair cell regeneration in the zebrafish (*Danio rerio*) inner ear following acoustic trauma. *PLoS One* 6:e28372. doi: 10.1371/journal.pone.0028372

Suzuki, J., Corfas, G., and Liberman, M. C. (2016). Round-window delivery of neurotrophin 3 regenerates cochlear synapses after acoustic overexposure. *Sci. Rep.* 6:24907. doi: 10.1038/srep24907

Tabor, K. M., Bergeron, S. A., Horstick, E. J., Jordan, D. C., Aho, V., Porkka-Heiskanen, T., et al. (2014). Direct activation of the Mauthner cell by electric field pulses drives ultrarapid escape responses. *J. Neurophysiol.* 112, 834–844. doi: 10.1152/jn.00228.2014

Tanimoto, M., Ota, Y., Inoue, M., and Oda, Y. (2011). Origin of inner ear hair cells: morphological and functional differentiation from ciliary cells into hair cells in zebrafish inner ear. *J. Neurosci. Off. J. Soc. Neurosci.* 31, 3784–3794. doi: 10.1523/JNEUROSCI.5554-10.2011

Toro, C., Trapani, J. G., Pacentine, I., Maeda, R., Sheets, L., Mo, W., et al. (2015). Dopamine modulates the activity of sensory hair cells. *J. Neurosci.* 35, 16494–16503. doi: 10.1523/JNEUROSCI.1691-15.2015

Trapani, J. G., and Nicolson, T. (2011). Mechanism of spontaneous activity in afferent neurons of the zebrafish lateral-line organ. *J. Neurosci. Off. J. Soc. Neurosci.* 31, 1614–1623. doi: 10.1523/JNEUROSCI.3369-10.2011

Trapani, J. G., and Nicolson, T (2010) Physiological recordings from zebrafish lateral-line hair cells and afferent neurons. *Methods Cell Biol.* 100, 219–231. doi: 10.1016/B978-0-12-384892-5.00008-6

Trapani, J. G., Obholzer, N., Mo, W., Brockerhoff, S. E., and Nicolson, T. (2009). synaptojanin1 Is required for temporal fidelity of synaptic transmission in hair cells. *PLoS Genet.* 5:e1000480. doi: 10.1371/journal.pgen.1000480

Trussell, L. O. (2002). Transmission at the hair cell synapse. *Nat. Neurosci.* 5, 85–86. doi: 10.1038/nn0202-85

Uribe, P. M., Villapando, B. K., Lawton, K. J., Fang, Z., Gritsenko, D., Bhandiwad, A., et al. (2018). Larval zebrafish lateral line as a model for acoustic trauma. *eNeuro*. doi: 10.1523/ENEURO.0206-18.2018

Uthaiah, R. C., and Hudspeth, A. J. (2010). Molecular anatomy of the hair Cell's ribbon synapse. *J. Neurosci. Off. J. Soc. Neurosci.* 30, 12387–12399. doi: 10.1523/JNEUROSCI.1014-10.2010

Valero, M. D., Burton, J. A., Hauser, S. N., Hackett, T. A., Ramachandran, R., and Liberman, M. C. (2017). Noise-induced cochlear synaptopathy in rhesus monkeys (*Macaca mulatta*). *Hear Res.* 353, 213–223. doi: 10.1016/j.heares.2017.07.003

Varshney, G. K., Pei, W., and Burgess, S. M. (2016). Using zebrafish to study human deafness and hearing regeneration. *Genet. Deaf* 20, 110–131. doi: 10.1159/000444569

Varshney, G. K., Pei, W., LaFave, M. C., Idol, J., Xu, L., Gallardo, V., et al. (2015). High-throughput gene targeting and phenotyping in zebrafish using CRISPR/Cas9. *Genome Res* 25, 1030–1042. doi: 10.1101/gr.186379.114

Vogl, C., Cooper, B. H., Neef, J., Wojcik, S. M., Reim, K., Reisinger, E., et al. (2015). Unconventional molecular regulation of synaptic vesicle replenishment in cochlear inner hair cells. *J. Cell Sci.* 128, 638–644. doi: 10.1242/jcs.162099

Vogl, C., Panou, I., Yamanbaeva, G., Wichmann, C., Mangosing, S. J., Vilardi, F., et al. (2016) Tryptophan-rich basic protein (WRB) mediates insertion of the tail-anchored protein otoferlin and is required for hair cell exocytosis and hearing. *EMBO J.* 35, 2536–2552. doi: 10.15252/embj.201593565

Wan, G., and Corfas, G. (2015). No longer falling on deaf ears: mechanisms of degeneration and regeneration of cochlear ribbon synapses. *Hear Res.* 329, 1–10. doi: 10.1016/j.heares.2015.04.008

Wan, G., Gómez-Casati, M. E., Gigliello, A. R., Liberman, M. C., and Corfas, G. (2014). Neurotrophin-3 regulates ribbon synapse density in the cochlea and induces synapse regeneration after acoustic trauma. *eLife* 3:e03564. doi: 10.7554/eLife.03564

Wang, Q., and Green, S. H. (2011). Functional role of neurotrophin-3 in synapse regeneration by spiral ganglion neurons on inner hair cells after excitotoxic trauma *in vitro*. *J. Neurosci.* 31, 7938–7949. doi: 10.1523/JNEUROSCI.1434-10.2011

Wang, Y., Hirose, K., and Liberman, M. C. (2002). Dynamics of noise-induced cellular injury and repair in the mouse cochlea. *J. Assoc. Res. Otolaryngol. JARO* 3, 248–268. doi: 10.1007/s101620020028

Wong, A. B., Rutherford, M. A., Gabrielaitis, M., Pangršič, T., Göttfert, F., Frank, T., et al. (2014). Developmental refinement of hair cell synapses tightens the coupling of Ca2+ influx to exocytosis. *EMBO J.* 33, 247–264. doi: 10.1002/embj.201387110

World Health Organization (2018) *Deafness and Hearing Loss, Key Facts*. Geneva: World Health Organization. Available at: http://www.who.int/en/news-room/fact-sheets/detail/deafness-and-hearing-loss

Yasunaga, S., Grati, M., Chardenoux, S., Smith, T. N., Friedman, T. B., Lalwani, A. K., et al. (2000). OTOF encodes multiple long and short isoforms: genetic evidence that the long ones underlie recessive deafness DFNB9. *Am. J. Hum. Genet.* 67, 591–600. doi: 10.1086/303049

Yasunaga, S., Grati, M., Cohen-Salmon, M., El-Amraoui, A., Mustapha, M., Salem, N., et al. (1999). A mutation in OTOF, encoding otoferlin, a FER-1-like protein, causes DFNB9, a nonsyndromic form of deafness. *Nat. Genet.* 21, 363–369. doi: 10.1038/7693

Zhang, Q., Li, S., Wong, H.-T. C., He, X. J., Beirl, A., Petralia, R. S., et al. (2018). Synaptically silent sensory hair cells in zebrafish are recruited after damage. *Nat. Commun.* 9:1388. doi: 10.1038/s41467-018-03806-8

Zhang, Q. X., He, X. J., Wong, H. C., and Kindt, K. S. (2016). Functional calcium imaging in zebrafish lateral-line hair cells. *Methods Cell Biol.* 133, 229–252. doi: 10.1016/bs.mcb.2015.12.002

Zheng, X.-Y., Ding, D.-L., McFadden, S. L., and Henderson, D. (1997). Evidence that inner hair cells are the major source of cochlear summating potentials. *Hear Res.* 113, 76–88. doi: 10.1016/S0378-5955(97)00127-5

Conflict of Interest Statement: The authors declare that the research was conducted in the absence of any commercial or financial relationships that could be construed as a potential conflict of interest.

frontiers in Cell and Developmental Biology

REVIEW
published: 19 September 2018
doi: 10.3389/fcell.2018.00110

Leveraging Zebrafish to Study Retinal Degenerations

Juan M. Angueyra[1] and Katie S. Kindt[2]**

[1] Retinal Neurophysiology Section, National Eye Institute, National Institutes of Health, Bethesda, MD, United States,
[2] Section on Sensory Cell Development and Function, National Institute on Deafness and Other Communication Disorders, National Institutes of Health, Bethesda, MD, United States

Retinal degenerations are a heterogeneous group of diseases characterized by death of photoreceptors and progressive loss of vision. Retinal degenerations are a major cause of blindness in developed countries (Bourne et al., 2017; De Bode, 2017) and currently have no cure. In this review, we will briefly review the latest advances in therapies for retinal degenerations, highlighting the current barriers to study and develop therapies that promote photoreceptor regeneration in mammals. In light of these barriers, we present zebrafish as a powerful model to study photoreceptor regeneration and their integration into retinal circuits after regeneration. We outline why zebrafish is well suited for these analyses and summarize the powerful tools available in zebrafish that could be used to further uncover the mechanisms underlying photoreceptor regeneration and rewiring. In particular, we highlight that it is critical to understand how rewiring occurs after regeneration and how it differs from development. Insights derived from photoreceptor regeneration and rewiring in zebrafish may provide leverage to develop therapeutic targets to treat retinal degenerations.

Keywords: zebrafish, retinal degeneration, regeneration, photoreceptor cells, Müller glia, developmental biology, rewiring, retinal circuitry and visual pathways

OPEN ACCESS

Edited by:
Gokhan Dalgin, The University of Chicago, United States

Reviewed by:
Glenn Prazere Lobo, Medical University of South Carolina, United States
Deborah Stenkamp, University of Idaho, United States

****Correspondence:***
Juan M. Angueyra
angueyra@nih.gov
Katie S. Kindt
katie.kindt@nih.gov

Specialty section:
This article was submitted to Molecular Medicine, a section of the journal Frontiers in Cell and Developmental Biology

Received: *28 May 2018*
Accepted: *20 August 2018*
Published: *19 September 2018*

Citation:
Angueyra JM and Kindt KS (2018) Leveraging Zebrafish to Study Retinal Degenerations. Front. Cell Dev. Biol. 6:110. doi: 10.3389/fcell.2018.00110

RETINA AND PHOTORECEPTORS

Similar to many organs, the eye is structurally well-conserved between zebrafish and mammals. For example, the eyes of zebrafish have the same gross structure as human and other mammalian eyes, and contain a cornea, lens, vitreous, retina, pigment epithelium, choroid and sclera (**Figure 1A**). Furthermore, the development of the eye during embryogenesis is also conserved, and complimentary work in zebrafish, mice and other species has helped to delineate the key developmental events in eye morphogenesis across vertebrates (Bibliowicz et al., 2011; Stenkamp, 2015).

Within the eye, the retina is of particular interest because it is the site of sensory detection and damage to the retina results in vision loss. The vertebrate retina is a highly structured neuronal tissue that lines the back of the eye. It is responsible for both the detection and processing of visual information, before it is relayed to higher-order visual centers. To achieve this, the retina is equipped with a variety of neurons that are arranged into three nuclear layers and project into two synaptic layers (**Figures 1B,C**). Within these layers, retinal neurons assemble into multiple, distinct circuits that encode different aspects of the visual information (Gollisch and Meister, 2010). The encoding of visual information starts when light is detected by the *rod* and *cone photoreceptors*. The highly sensitive rods are mainly used during dim-lighting conditions, while the more adaptable but less sensitive cones function from dawn until dusk. The retina of the nocturnal rodents commonly

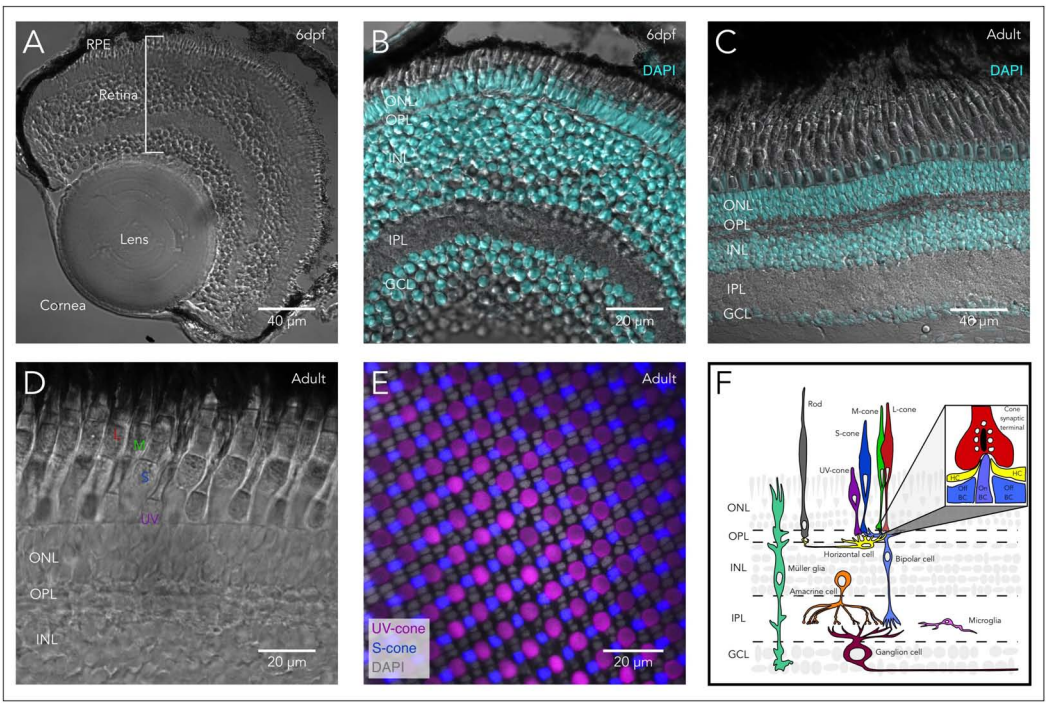

FIGURE 1 | Structure of the zebrafish eye and retina. **(A)** Anatomy of the zebrafish eye: DIC image of a cryosection from a 6 days post-fertilization (6 dpf) larval eye highlighting the main structures of the vertebrate eye including cornea, lens, retina, and retinal pigment epithelium (RPE). **(B)** The larval retina is organized into highly structured layers: Overlay of a DIC image and the fluorescent nuclear marker DAPI of a cryosection from a 6 dpf larva showing the different retinal layers, including the outer nuclear layer (ONL) which contains the cell bodies of photoreceptors (rods and cones). Photoreceptors make synapses in the outer plexiform layer (OPL) with bipolar and horizontal cells. The inner nuclear layer (INL) contains the cell bodies of horizontal, bipolar and amacrine cells, while the ganglion cell layer (GCL) contains the cell bodies of retinal ganglion cells (RGC). Bipolar cells provide excitatory synaptic input to RGC in the inner plexiform layer (IPL), while amacrine cells modulate this input both pre- and post-synaptically. **(C)** The adult retina retains the same layered structure: Overlay of a DIC image and DAPI of a cryosection from an adult zebrafish. **(D)** The zebrafish retina contains 4 subtypes of cones: DIC image of a cryosection from an adult zebrafish showing the short-single or ultraviolet-wavelength sensitive cones (UV-cones), the long-single or short-wavelength sensitive cones (S-cones), and the double cones which correspond to the middle- and long-wavelength sensitive cones (M- and L-cones). **(E)** Mosaic arrangement of zebrafish cone photoreceptors: Confocal image of a whole-mounted retina of a double-reporter transgenic lines to identify UV-cones [*Tg(sws1:GFP)*^{kj9}, magenta] and S-cones [*tg(sws2:mCherry)*^{ua3011}, blue] overlayed with DAPI (gray), allowing the identification of the nuclei of M- and L-cones between the rows of UV- and S-cones. **(F)** Diagram of the vertebrate retina and the retinal cells. Inset highlights the synapse between cones and horizontal and bipolar cells, where the cone synaptic terminal contains synaptic vesicles (white) attached to the synaptic ribbon (black). In close apposition to the ribbon, the dendrites on On-bipolar cells (On-BCs) invaginate into the synaptic terminal and are flanked by two horizontal cell (HC) processes. Off-bipolar cells make more basal contacts in close proximity but not apposed to the synaptic ribbon.

used in research like mice and rats is rod dominated (97% rods and 3% cones) (Carter-Dawson Louvenia and Lavail Matthew, 1979), as is the peripheral human retina. In contrast, zebrafish have a cone-dominated retina (∼40% rods and ∼60% cones) (Fadool, 2003), similar to the central human retina, which provides high-acuity vision, and is essential for most day-to-day visual tasks. Therefore, the zebrafish retina is uniquely positioned to understand the molecular mechanisms relevant to development and regeneration of the photoreceptors that are most relevant for human vision.

The zebrafish retina contains four different cone photoreceptor subtypes (UV-, S-, M-, and L-cones). Each subtype is defined by specific opsin expression that confers a particular wavelength-sensitivity, and morphology (short or long, and single or paired with another cone type) (**Figures 1D,E**). UV-cones express *sws1*, an opsin with peak sensitivity (λ_{max}) in the ultraviolet range (λ_{max} = 354 nm), and are short-single cones morphologically. S-cones express *sws2*, with peak sensitivity at short wavelengths (λ_{max} = 416 nm), and are long-single cones morphologically. M-cones express opsins of the Rh2 class, which have undergone tandem quadruplications (Rh2-1 to Rh2-4), with peak sensitivities at mid wavelengths (λ_{max} = 467 nm, 476 nm, 488 nm, and 505 nm respectively). L-cones express one of two tandemly duplicated opsin genes from the *lws* class, with peak sensitivities at longer wavelengths (λ_{max} = 548 nm and 558 nm). M- and L-cones are morphologically arranged as a double cone, where the L-cone is the long (or principal) member of the pair and the M-cone is the short (or accessory) member (Raymond et al., 1996; Vihtelic et al., 1999; Chinen et al., 2003).

In both rod and cone photoreceptors, light triggers the activation of opsins followed by the rest of the phototransduction cascade. In zebrafish and in mammals, this cascade ultimately leads to changes in photoreceptor membrane potential, and to modulation of neurotransmitter release in the synaptic terminal. Visual information is then directly transmitted from photoreceptors to several subtypes of *horizontal* (inhibitory

interneurons that locally modulate photoreceptor synaptic output) and *bipolar cells* (glutamatergic neurons that transmit light signals into the next processing layer). Information is further processed in the next synaptic layer, where bipolar cells (BC) provide excitation to *ganglion cells* (glutamatergic spiking neurons), while *amacrine cells* (local interneurons) provide modulation pre- and/or post-synaptically. The axons of the retinal ganglion cells (or RGCs) form the optic nerve, and relay the pre-processed visual information to central targets in the brain. Additionally, the retina contains *microglia* (resident immune cells located primarily in the synaptic layers) and two types of true glial cells: *Müller cells* (a type of radial glia) and *astrocytes* (associated with axons of RGCs) (**Figure 1F**). The photoreceptors also closely associate with the *retinal pigment epithelium* (RPE), which provides structural, trophic and metabolic support and is directly involved in the recycling of opsins.

RETINAL DEGENERATIONS

Within the retina, rods and cones are particularly vulnerable to metabolic, genetic or environmental insults; phototransduction and synaptic signaling are demanding processes that require high metabolic rates. Retinal degenerations (RD) are disorders characterized by photoreceptor death and can affect both rods and cones, or each photoreceptor type individually. RD have multiple causes that can be broadly divided based on whether the cause is primary or secondary. In primary RD, photoreceptors are directly affected, for example due to mutations that affect phototransduction proteins. In secondary RD, other cells types, for example the RPE or a single type of photoreceptor degenerates; this can lead to secondary degeneration of other photoreceptors. The main forms of RD in humans are *Age-related Macular Degeneration* (AMD), *Retinitis Pigmentosa* (RP), and *Leber Congenital Amaurosis* (LCA). AMD is a multi-factorial disease that affects the RPE. Advanced RPE dysfunction leads to secondary rod and cone loss. In industrialized countries, AMD is the leading cause of blindness (De Bode, 2017). AMD is associated with age, smoking, nutritional deficiencies, inflammation and mutations or polymorphisms in more than 30 genes, with many more genes still to uncover (Jager et al., 2008; Warwick and Lotery, 2018). RP encompasses a set of complex hereditary diseases that can be caused by a plethora of mutations mapped to more than 70 human genes (Daiger et al., 2013; Farrar et al., 2017)[1]. Most forms of RP in humans are characterized by an initial death of rods, with subsequent secondary cone death. RP presents clinically first with night-blindness, followed by decreases in peripheral visual acuity (tunnel vision) that eventually progresses toward the central areas of the retina. LCA encompasses a group of early-onset and progressive rod and cone dystrophies. Again, 25 genes have already been identified as causes of LCA, and most are expressed either in photoreceptors or in the RPE (Kumaran et al., 2017).

[1]http://www.sph.uth.tmc.edu/retnet

Early forward genetic screens in zebrafish that evaluated defects in the histology of the photoreceptor layer identified many genes that cause RD (Brockerhoff and Fadool, 2011). Most human homologs of these genes have also been shown to cause RD in humans. Subsequent screens in zebrafish assayed for defects in visual function rather than morphological defects. These screens exploited reliable visual behavioral assays in larvae, including the optokinetic response (OKR) (Brockerhoff et al., 1995) or the escape response to moving dark objects (Li and Dowling, 1997) (see below). Together these screens helped, not only to establish additional genetic models for photoreceptor degenerations, but also to identify additional and in some cases novel genes involved in RD. For example, one zebrafish mutant that lacked OKR was linked to a mutation in *pde6c*, a novel cone-specific phototransduction gene. Mutations in *pde6c* cause cone degeneration in zebrafish with secondary rod degeneration (Stearns et al., 2007). The discovery of this mutant was beneficial in two ways. First *pde6c* mutants were used to confirm the existence of rod-specific progenitors in the zebrafish retina (Morris et al., 2008). Second this mutant was used to identify *pde6c* as the causative gene in cone-photoreceptor loss of function 1 (*cpfl1*), a specific type of cone degeneration in mouse and humans (Chang et al., 2009). This is an excellent example of how zebrafish can be used to identify novel genes and pathways involved in RD. More recently, zebrafish models of RD are being leveraged in pharmacological screens, to test or find novel treatments for human RD (Moosajee et al., 2008; Ganzen et al., 2017). Overall these zebrafish genetic screens highlight the conservation of molecules underlying RD between zebrafish and mammals. Given this level of conservation, it is likely similar molecules may be required to regenerate and rewire the zebrafish and mammalian retina after RD.

THERAPIES FOR RD

In humans, photoreceptor loss in RD is permanent (regardless of their diverse causes and speed of progression) and therefore remain largely untreatable and lead to progressive loss of vision and ultimately blindness. In early stages of RD in humans, current treatments include neuroprotective agents (Trifunovic et al., 2012) and antibody therapies in cases where the underlying mutation is well characterized (Lazic and Gabric, 2007). Unfortunately, these treatments only slow down the progression of disease and have variable outcomes (Pardue and Allen, 2018). In addition to these treatments, gene therapy has been used to improve vision in patients with LCA caused by mutations in *RPE65*, an RPE-specific protein involved in the recycling of retinoids (Cideciyan, 2010; Jacobson et al., 2012), but the improvement may not be long-lasting (Jacobson et al., 2015).

In late stages of RD in humans, when there is widespread photoreceptor loss, two distinct approaches for treatment exist. The first seeks to bypass the need for photoreceptors. This can be achieved by either making the surviving retinal bipolar or ganglion cells photosensitive using optogenetics (Busskamp et al., 2010; Yue et al., 2016) or synthetic photo-switchable compounds (Polosukhina et al., 2012; Tochitsky et al., 2017). Additionally,

retinal prostheses capable of stimulating RGCs directly have been developed, attempting to encode visual information directly into these output neurons (da Cruz et al., 2016; Lewis et al., 2016). Of note, the use of retinal prostheses for blindness was approved by the European Union in 2011, and by the FDA in 2013. Use of these prostheses has led to some successful reacquisition of very basic visual functions but only for limited periods of time (Mills et al., 2017). The second and more promising approaches aims to replace the lost photoreceptors by transplantation or by stimulating regeneration. These later approaches have received special attention because they have the capability of renewing the native function of the retina, and could provide a real cure for RD. Due to this potential for complete functional recovery, and because of recent and important developments in the field, transplantation and regeneration will be a focus of this review.

BARRIERS IN PHOTORECEPTOR TRANSPLANTATION AS A THERAPY FOR RD

Just a decade ago, the prospect of producing photoreceptors from stem cells seemed like an overly daunting task (Adler, 2008). Nevertheless, in the last few years, several laboratories have successfully developed protocols to produce eyecup-like structures from induced-pluripotent stem cells (iPSCs) in the span of weeks. Some of these eyecups are able to acquire a layered structure reminiscent of the retina, with photoreceptor-like cells that contain outer segments, express phototransduction proteins (Wahlin et al., 2017), and have some capacity for light responsiveness (Zhong et al., 2014), and vesicular release (Wahlin et al., 2017). The successful development of these eyecups opens the possibility of harvesting cells from an individual to generate iPSCs, and re-differentiate them into photoreceptors that could be then transplanted back into patients with RD. Based on these prospects, recent work in the retinal field has focused on using mice to explore photoreceptor transplantation as a therapy for RD.

Initial transplantation studies in mice attempted to introduce rod photoreceptors, with the best rates of integration (never surpassing a few percent) achieved by transplanting immature rod precursors (MacLaren et al., 2016). Follow-up studies presented equally promising examples of integration, and in some cases demonstrated functional recovery of vision (Santos-Ferreira et al., 2015; Smiley et al., 2016). However, it has recently been discovered that many of these results are due to the exchange of cytoplasmic material (including RNA and/or proteins) between donor cells and the host retina, and *not integration* of transplanted photoreceptors (Pearson et al., 2016; Santos-Ferreira et al., 2016; Singh et al., 2016; Ortin-Martinez et al., 2017). In light of this recent discovery, it will be important to carefully interpret how functional recovery of vision occurred after transplantation/cytoplasmic exchange in degenerated or degenerating retinas (Homma et al., 2013; Singh et al., 2013; Santos-Ferreira et al., 2015). Even if cytoplasmic exchange results in recovery photoreceptor function, it occurs at very low rates (a few percent of host positive cells, for transplantations of tens to hundreds of thousands of donor cells). Such low rates casts doubt on the prospect of leveraging this process as a viable therapeutic strategy, especially in advanced cases of degeneration.

Even with viable evidence for successful photoreceptor transplantation (Waldron et al., 2018), there are additional concerns for this type of therapy. For example, subretinal injection of a mass of cells, the most common transplantation method, causes inflammation and scarring, and inhibits the migration of transplanted cells (Barber et al., 2013). Additionally, it is also unclear if transplanted photoreceptors are capable of rewiring properly into the host retina. This problem is further compounded by our incomplete understanding of how photoreceptors normally wire during development. To date, only a handful of genes are known to be involved in synapse formation between photoreceptors and their postsynaptic targets (Simmons et al., 2017; Zhang et al., 2017; Miller et al., 2018; Sarria et al., 2018; Ueno et al., 2018). Despite this work, we still have little insight on the molecules that drive the initial recognition between these cells, or on the processes that promote, inhibit or refine synapse formation. Unveiling genes involved in photoreceptor synapse formation during normal development in zebrafish could provide direct therapeutic targets to promote rewiring of transplanted photoreceptors.

USING ZEBRAFISH TO EXPLORE RETINAL REGENERATION AS A THERAPY FOR RD

Cumulatively, work on transplantation therapies has highlighted that alternative therapies, such as photoreceptor regeneration, could be a promising alternative. Unfortunately, in mammals there is no regeneration in the retina after damage or RD. In contrast, the zebrafish retina has the innate capacity for regeneration. This capacity may be due to the continued growth of the zebrafish retina into adulthood, as well as the ability of the zebrafish to maintain a population of multipotent stem cells within the retina.

Larval zebrafish form a functional visual system by 4 days post fertilization (4 dpf), and are able to perform complex visual guided behaviors (like prey capture, see below) by 5 dpf (Patterson et al., 2013). This rapid onset of sensory function is critical to survival of the animal. As larvae progress into adulthood, zebrafish continue to grow in size. This growth requires organs like the eye and retina to grow as well. In the retina this growth occurs in the ciliary marginal zone (CMZ). The CMZ maintains a niche of pluripotent cells at the edge of the retina that continually adds neurons in peripheral concentric rings (Centanin et al., 2011). In addition to this continual growth, zebrafish can also regenerate their retinas after injury. In fact, robust retinal regeneration and rewiring have been demonstrated in genetic models of RD and in other models that incur retinal injury. Overall, given that zebrafish is a genetically tractable model with active retinal regeneration, it is poised to uncover the molecular processes that control retinal regeneration and rewiring.

In teleost fish, retinal regeneration after injury has a rich history. It was first reported in goldfish (Lombardo, 1968) and later in cichlids (Johns and Fernald, 1981) and trout (Julian et al., 1998). In zebrafish retinal regeneration is robust after resection (Cameron, 2000), mechanical damage (Fausett and Goldman, 2006), light damage (Bernardos et al., 2007; Thomas et al., 2012), thermal damage (Raymond et al., 2006), pharmacological damage (Fimbel et al., 2007; Sherpa et al., 2008; Nagashima et al., 2013; Tappeiner et al., 2013; Sherpa et al., 2014) and selective ablation of particular cell-types (Montgomery et al., 2010; D'Orazi et al., 2016; Hagerman et al., 2016; Yoshimatsu et al., 2016; White et al., 2017). In teleosts, regeneration can occur from cells generated in the CMZ (Raymond et al., 2006), a dedicated population of progenitors that are committed to a rod fate (Bernardos et al., 2007; Morris et al., 2008), and the Müller glia (Fausett and Goldman, 2006; Bernardos et al., 2007; Fimbel et al., 2007).

Due to its location at the edge of the retina, the CMZ is only involved in regeneration if the injury involves the peripheral retina. During regeneration, the CMZ is capable of giving rise to all retinal neurons except rod photoreceptors (Stenkamp et al., 2001; Raymond et al., 2006). Instead, rods originate from rod-specific progenitors. These progenitors were first identified in goldfish and cichlids (Johns and Fernald, 1981) and were later found in other teleost fish including trout and zebrafish (Julian et al., 1998). Rod-specific progenitors are thought to be important for maintaining the density of rods as the eye grows, and lineage tracing revealed that these rod progenitors derive from Müller cells that slowly and continuously divide in the normal retina (Otteson et al., 2001; Raymond et al., 2006; Bernardos et al., 2007; Nelson et al., 2008). During regeneration, there is an expansion in the number of photoreceptor progenitors, but these mainly derive from actively dividing Müller glia. In fact, in zebrafish the Müller glia are the primary source of regenerated neurons after injury. During regeneration they can act as multipotent stem cells, dividing and differentiating into any retinal cell type (Ramachandran et al., 2010b). In contrast to zebrafish, in humans and other mammals Müller glia do not remain multipotent and therefore cannot readily replace lost neurons in the retina. Because Müller glia are the primary source of regenerated retinal neurons and can regenerate all retinal neurons, considerable work has been dedicated to understanding the differences between the Müller glia of zebrafish and mammals.

A series of studies that investigated the response of zebrafish Müller glia to retinal injury, have unveiled the key transcription factors in a gene regulatory network that controls retinal repair. Shortly after injury, cytokines and growth factors activate the *beta-catenin* and *stat3* pathways (Kassen et al., 2007; Wan et al., 2014). These pathways upregulate the expression of *ascl1* (Fausett et al., 2008), a key transcription factor that (through *lin-28*) leads to the suppression of *let7* microRNA (Ramachandran et al., 2010a). In the uninjured retina, *let7* normally represses the expression of many regeneration-induced genes (including *ascl1* and *lin-28*), closing the loop of a system poised to control Müller glia response to injury (Wan and Goldman, 2016) (**Figure 2A**).

In contrast, mammalian Müller glia does not readily divide (Wan et al., 2008) and responds to retinal injury with an inflammatory response known as *reactive gliosis*, characterized by an increase in size and overproduction of intermediate filaments, and leading to distortion of the architecture of the retina without repair (Dyer and Cepko, 2000; Bringmann et al., 2009; Thomas et al., 2016) (**Figure 2C**). Significant efforts have been devoted to understanding the differences between these species, in the hope of stimulating regeneration in mammals. This work has shown that *ascl1* is not upregulated in mice after retinal injury (Karl et al., 2008), but *ascl1* overexpression in mammalian Müller cells *in vitro* is sufficient to induce production of neurons (Pollak et al., 2013). Moreover, induction of expression of *ascl1* in Müller cells *in vivo,* followed by retinal injury, induces division and production of all classes of retinal neurons, but only in young mice (Ueki et al., 2015). Recently, a successful report of regeneration in adult mice has shown that new bipolar- and amacrine-like cells derived from Müller glia can rewire into the retina. For this work, in addition to overexpression of *ascl1*, inhibition of histone deacetylation was also required (Jorstad et al., 2017). Unfortunately, no other retinal cell types are produced with this protocol (**Figure 2D**). Further insight into retinal regeneration has been gained from studying a related telost, medaka, which shows a restricted capacity for regeneration. In medaka fish, after injury, Müller glia do not readily proliferate, and new retinal progenitors commit almost exclusively to a photoreceptor fate. Comparisons in the Müller glia response to retinal injury in both medaka fish and zebrafish concluded that sustained expression of the transcription factor *sox2* in adult Müller cells is key for maintaining multipotency (Lust and Wittbrodt, 2018) (**Figure 2B**). While it is clear that important strides have been taken to attempt retinal regeneration in mammals, before regeneration can be used as a viable therapy, we need a deeper understanding on the mechanisms that maintain cells with a regenerative potential in zebrafish throughout adulthood.

INSIGHTS FROM ZEBRAFISH ON REWIRING AFTER REGENERATION

Even after successful transplantation or regeneration of photoreceptors, the biggest hurdle in these RD therapies is ensuring that the new photoreceptors rewire into the appropriate retinal circuits so that they are able to restore normal visual function. Once again, zebrafish has offered a unique opportunity to study rewiring after injury and regeneration, in both larvae and adults. Cumulatively, this work has demonstrated that the extent and time course of regeneration and rewiring is determined by lesion-specific differences, in particular the extent of injury and the number of cells that need to be replaced.

Adult teleosts are able to regenerate their retinas even after extensive retinal damage. Early seminal studies in adult goldfish, and later studies in adult zebrafish, showed robust retinal regeneration and rewiring after surgical retinal extirpation (Hitchcock et al., 1992; Cameron, 2000) or pharmacologically induced death of all retinal neurons (Raymond et al., 1988; Sherpa et al., 2008). Under these lesion paradigms, all retinal cell types were regenerated. Importantly, with regards to rewiring, the retinal lamination was reestablished (Raymond et al., 1988;

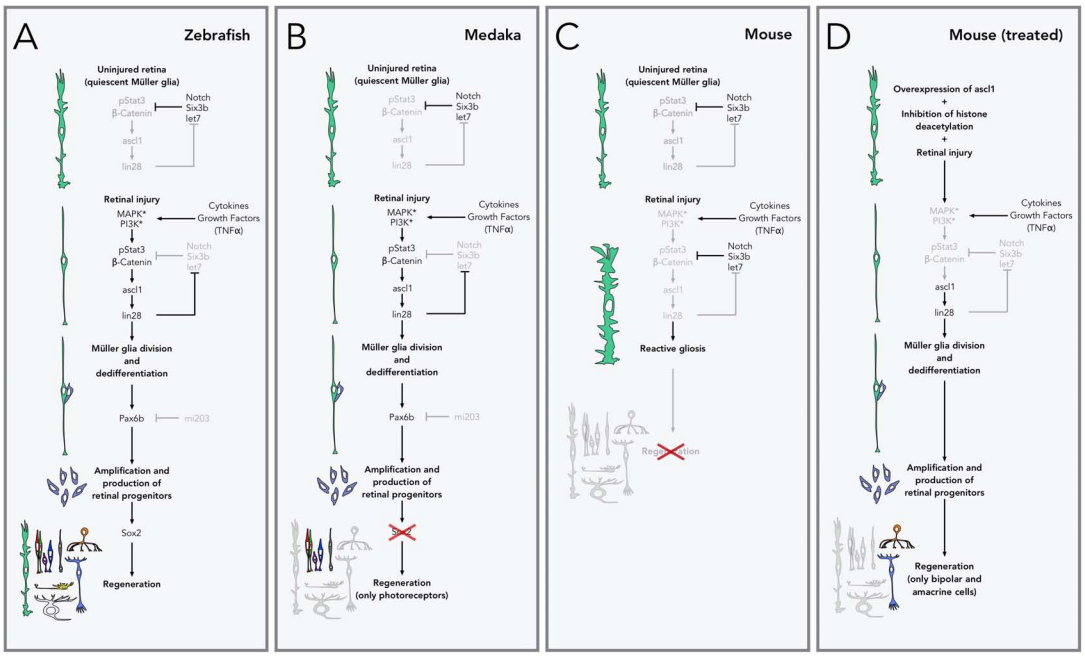

FIGURE 2 | Pathways to retinal regeneration. **(A)** Zebrafish are able to completely regenerate their retina *via* Müller glia. In the uninjured retina, Müller glia is kept quiescent by inhibiting the expression of the genes that control regeneration through Notch signaling and repression by the transcription factor *Six3b* and the microRNA *let7*, amongst others. During *retinal injury*, cell death and inflammation lead to the release of cytokines and growth factors (especially TNFα), which activate receptors and kinases in the Müller glia, leading to activation of β-catenin and phosphorylation of the transcription factor *Stat3*, which in turns leads to the production of the transcription factor *ascl1* and *lin28* microRNA, and the activation of the genes that control Müller glia *division and dedifferentiation*. *lin28* also inhibits the production of *let7*, releasing the inhibition of this pathway. Expression of the transcription factor *Pax6b* (normally inhibited by the microRNA *mi203*), allows the amplification and production of retinal progenitors which are then able to redifferentiate into any retinal neurons or Müller glial cells. **(B)** In medaka fish, lack of production of *Sox2* after the production of retinal progenitors restricts their fate to photoreceptors and does not allow the production of other cell types, including new Müller glia. **(C)** In mice and other mammals, retinal injury does not lead to expression of *ascl1* and the rest of regeneration-related genes. Instead Müller glia activate the production of intermediate filaments and increase their size (*reactive gliosis*) and do not lead to the production of new retinal cells or injury repair. **(D)** Retinal regeneration can be stimulated in mice by artificially overexpressing *ascl1* and inhibiting epigenetic changes (histone deacetylation in particular). With this treatment, Müller glial cells are able to divide and produce retinal progenitors, but their fate is restricted to bipolar and amacrine cells.

Sherpa et al., 2008), and synaptic connections were reformed between retinal neurons (Hitchcock and Cirenza, 1994) and between RGCs and the brain (Stuermer et al., 1985). Parallel work demonstrated that after extensive retinal damage in adult goldfish and zebrafish, visual function is also recovered (Mensinger and Powers, 1999, 2007; Lindsey and Powers, 2007; Sherpa et al., 2008). Nevertheless, because the Müller glia are the main source of regenerated retinal neurons, complete ocular excision prevents regeneration (Mensinger and Powers, 2007).

In adult teleosts, although there is robust regeneration after extensive retinal injury, the time required for regeneration and functional recovery depends on the extent of injury. For example, the differences in regeneration and rewiring were examined after surgical extirpation of ∼25, 50, and 75% of the adult retina. This work found that after surgical extirpation of 25% of the retina, 17 weeks (120 days) are required for regeneration and reestablishment of lamination and 25 weeks (180 days) for functional recovery. Additional extirpation lengthened the time and extent of recovery for both lamination and functional recovery (Mensinger and Powers, 2007). Similar results were observed in adults after pharmacological damage and death of all retinal neurons (induced by high doses of intraocular ouabain). In this study functional recovery started 5 weeks after the injury with further improvement by weeks 7 – 10, albeit with decreased sensitivity (Mensinger and Powers, 1999; Lindsey and Powers, 2007).

In adult zebrafish, the extent and time course of retinal regeneration and rewiring is also dependent on the injury. Extensive pharmacological damage of all retinal layers with ouabain leads to regeneration, and the newly formed cells are capable to reorganize into the three distinct nuclear layers by week 3 after injury. After 14 weeks, the regenerated retinas are well laminated (clear nuclear and plexiform layers), the optic nerve has regrown, and there is functional recovery (Sherpa et al., 2008). Interestingly, with pharmacological damage (using lower doses of ouabain) that spares photoreceptors and Müller glia but still induces a loss of cells in the INL and GCL, regeneration is faster, with significant recovery of function after only 8 weeks (Sherpa et al., 2014; McGinn et al., 2018). In this lesion paradigm, rewiring of a specific (but heterogeneous) subset of regenerated BCs was closely examined. The regenerated BCs had largely normal morphology, and, as a population, were able to reproduce the diversity of connectivity patterns observed in the surviving photoreceptors, with only a few errors in lamination or abnormal

dendritic or axonal arborization, again emphasizing the robust regeneration of zebrafish (McGinn et al., 2018). Nevertheless, in the context of extensive damage, regeneration in adult teleosts is far from perfect. Several structural defects are common including areas with defects in the formation or absence of plexiform layers, disorganization of nuclear layers, presence of cells in the incorrect layer (e.g., RGCs in INL), failure to reestablish the photoreceptor mosaic, formation of photoreceptor rosettes, overproduction of neurons, and the generation of cell types that were not initially damaged (Raymond et al., 1988; Hitchcock et al., 1992; Cameron, 2000; Vihtelic Thomas and Hyde David, 2000; Stenkamp et al., 2001; Stenkamp and Cameron, 2002; Sherpa et al., 2008; Powell et al., 2016).

More recently, the genetic tractability of zebrafish has enabled researchers to damage specific retinal cell types and study their rewiring after regeneration. This work was accomplished by using the recently developed nitroreductase–metronidazole (NTR–MTZ) system. For this method, transgenic zebrafish are created expressing the NTR gene (*nfsb*) under the control of a cell-specific promoter. When these transgenic zebrafish are treated with the compound MTZ, the NTR converts MTZ into a cytotoxic compound. Because this compound does not diffuse to neighboring cells, the resulting ablation is restricted to the NTR-expressing cells. Importantly, this process is reversible, and removal of MTZ solution makes it possible to examine regeneration and rewiring. To date, the NTR-MTZ system has been used to selectively ablate rods, and specific subtypes of cones, bipolar cells and glial cells (Zhao et al., 2009; Ariga et al., 2010; Montgomery et al., 2010; Fraser et al., 2013; D'Orazi et al., 2016; Hagerman et al., 2016; White et al., 2017). Importantly, several of these studies demonstrated that other cells in the retina that did not express NTR were not ablated after MTZ application. In addition, these treatments did not affect the surrounding retinal architecture (Zhao et al., 2009). This highlights the specificity and power of the NTR-MTZ system.

After genetic ablation and removal of MTZ, in each instance the targeted cells regenerated after several days, although the exact time-course varied depending on the ablated cell type and the age of zebrafish treated. For example, after using the NTR–MTZ to completely ablate rods in adult zebrafish, newly generated rods were identified within a week after removal of MTZ, and repopulation of rods attained pre-injury levels within 4 weeks (Montgomery et al., 2010) – a very similar time course required for the regeneration of cones in adults (Raymond et al., 2006; Bernardos et al., 2007). In larvae, the regeneration of cells occurs at a faster timescale. For example, after ablation of rods using the NTR-MTZ system in 5 dpf larvae, newly formed rods attained control levels in just 6 days (White et al., 2017). Similarly, cones ablated between 4 and 6 dpf regenerate in 7 – 10 days (Fraser et al., 2013; Yoshimatsu et al., 2016) and BCs ablated at 7 dpf regenerate in 13 days (D'Orazi et al., 2016).

In the majority of these studies, regeneration was confirmed morphologically. In a subset of studies, after regeneration, the analysis was extended to include behavior or rewiring. For example, in one study, either the UV- or S-cones were ablated (in 7 dpf larvae) and the optomotor response (OMR) (see below) was assayed after ablation and following UV- or S-cone regeneration respectively (Hagerman et al., 2016). The OMR was reduced immediately after ablation of either UV- or S-cones. Surprisingly, while the OMR recovery took 4 days for the UV-cone ablation, the OMR recovered in just 1 day following S-cone ablation, before new S-cones were produced. These differences in behavioral recovery suggest that there may be a capacity for plasticity amongst the remaining cells, used to compensate for the ablated cells during the recovery phase. It is possible that this short-term plasticity relies on activity from other cone subtypes and/or on synaptic remodeling. Evidence for such synaptic remodeling has been reported in a parallel study (Yoshimatsu et al., 2016). In this study, a subtype of horizontal cell (H3) that normally connects preferentially to UV- and S-cones, was able to reconnect to UV-cones after UV-cone specific ablation and regeneration. Nevertheless, if UV-cone regeneration was delayed, the H3 made additional contacts with S-cones and even M- and L-cones, suggesting functional compensation at the level of rewiring. Another recent study examined rewiring after selective loss of a subpopulation of BC using the NTR-MTZ system in 5 dpf larvae (D'Orazi et al., 2016). Thirteen days after the ablation of these BC, the majority of regenerated BC were morphologically normal but the rewiring did not fully recapitulate development, with a relative loss of selectivity for specific cone subtypes. Additionally, BC axons contained significantly more synapses.

As a whole, work in this field proves that retinal regeneration in zebrafish is a robust process, but also suggests that some of the developmental cues required to refine synapse number or proportion of photoreceptor subtypes innervated may not be present during regeneration. In the future, it will be important to further understand what cues are present during development that enable photoreceptors to wire into different retinal circuits. It will be especially important to understand how specific photoreceptor subtypes recognize the different bipolar- and horizontal-cell subtypes, and the factors required for the formation of these synapses. It will also be important to recognize and examine the developmental and environmental differences between larval and adult zebrafish retinas. This knowledge will provide a comprehensive understanding of the differences between development and regeneration, between wiring, rewiring and remodeling, and likely uncover manipulations that could be used to modify or refine rewiring in the context of treatments for RD.

THE ZEBRAFISH TOOLKIT FOR THE STUDY OF RETINAL DEVELOPMENT AND REGENERATION

There are numerous factors that have established zebrafish as a valuable model organism for the study of human disease including rapid development, large clutch sizes, ease of maintenance, genetic conservation, accessibility to genetic manipulations, and optical transparency of embryos. In addition to these advantages, we have described several examples of how zebrafish has been a useful model to investigate retinal development and regeneration. To aid in these studies, multiple tools have been developed that have direct application for the

study of retina in zebrafish. We have summarized *some* of these tools here as a convenient reference.

Imaging Retinal Cells and Their Connectivity

Currently there are established transgenic lines that make it straightforward to visualize each cell subtype within the retina, as well as the lamination and precise wiring of these cells (**Table 1**). For example, taking advantage of the specificity of opsin expression in the different photoreceptor subtypes, promoters from each opsin have been utilized to create transgenic lines that label rods (rods: *rho*) (Fadool, 2003) and each of the four cone subtypes (UV-cones: *opn1sw1*; S-Cones: *opn1sw2*; M-Cones: *opn1mw2*; L-Cones: *opn1lw1)* (Takechi et al., 2003, 2008; Tsujimura et al., 2007, 2010) (**Figures 3A,B**). Additionally, multiple lines exist to label horizontal and BC. Within the retina, horizontal cells can be specifically labeled exploiting the promoter for *connexin 55.5* (Weber et al., 2014; Klaassen et al., 2016), or using an enhancer-trap line that labels a combination of horizontal and amacrine cells (Torvund et al., 2017). BC represent a more diverse cell class. On-BC can be labeled using the promoter for *grm6b*, a metabotropic glutamate receptor that is key for the detection of glutamate release by photoreceptors (Glasauer et al., 2016) (**Figure 3C**), and different subtypes of BC have been labeled with enhancer-trap lines (D'Orazi et al., 2016), or using promoters for transcription factors (Vitorino et al., 2009) or for other bipolar-specific proteins (Schroeter et al., 2006). The promoter for *gfap* (glial fibrillar acidic protein) can be used to label Müller glia (Raymond et al., 2006; Bernardos et al., 2007). Additionally, lines that use the promoter for *mpeg1* label all macrophages (Ellett et al., 2011), allow visualization of the retinal microglia and macrophages in both the normal and regenerating retina (Mitchell et al., 2018).

Most of these lines allow high-resolution imaging of not only the lamination but also the synaptic terminals of these distinct cells types (Noel and Allison, 2018) (**Figure 3D**). For example, in some of these transgenic lines, the connections of photoreceptors have been used to accurately track wiring during development (Yoshimatsu et al., 2016) or rewiring after regeneration (D'Orazi et al., 2016). They can also be adapted for live imaging, allowing connections to be dynamically tracked during circuit formation or during the integration of regenerated neurons into functional retinal circuits (Ariga et al., 2010; Duval et al., 2013). Using the same promoters, several transgenic lines have been developed to express the NTR gene (*nfsb)* and ablate specific subsets of retinal cells (see above, **Table 1**). This approach has enabled the study of regeneration and rewiring after selective ablation (Zhao et al., 2009; D'Orazi et al., 2016; Yoshimatsu et al., 2016; McGinn et al., 2018; Noel and Allison, 2018). Lastly, it is straightforward to perform sparse labeling to capture the fine detail of individual retinal neurons and their contacts during development or regeneration, by using transient expression in larvae (with the same promoters leveraged for transgenic lines) (Klaassen et al., 2016; Yoshimatsu et al., 2016). Alternatively, inorganic fluorescent dyes like DiI can be used in larvae or in adults (**Figures 3E,F**) (Connaughton et al., 2004; Li et al., 2009; Li et al., 2012).

While transgenic lines represent powerful tools to visualize cells and processes within the retina *in situ*, antibodies against specific markers have been identified that can also be exploited to label subsets of retinal cells (**Table 2**). In addition to antibodies, cones can also easily be labeled using fluorescently-tagged *peanut agglutinin* (or PNA), a lectin protein that binds to the cone sheath (Hageman and Johnson, 1986; Shi et al., 2017). In combination with the transgenic lines outlined above, these labels can be used to visualize multiple types of cells simultaneously within the retina (**Figure 3C**). In addition to simply marking specific retinal cell types, antibodies against synaptic markers are of particular usefulness to characterize retinal wiring. In photoreceptors most presynaptic markers label components of the photoreceptor ribbon synapse, like Ribeye or Syntaxin, or adjoining structures like the voltage-gated calcium channels or the synaptic vesicles (Huang et al., 2012; Lv et al., 2012; Daniele et al., 2016). Postsynaptically, photoreceptor synapse markers include: components of the postsynaptic density itself (e.g., MAGUK) and glutamate receptors (*grm6* for ON-bipolars, *gria4* for OFF-bipolars, *gria2* for horizontal cells) (Yazulla and Studholme, 2001) (**Figure 3D**). These synaptic markers are extremely important for understanding the correct development of synapses or the correct rewiring of photoreceptors after regeneration. For example, alterations in the synapses between cones and Off-BC caused by mutations in *pappaa*, a protein recently identified in a behavioral screen, were identified by labeling the photoreceptor synaptic vesicles, but could not be seen by labeling specific cell-types, as retinal lamination was not altered (Miller et al., 2018).

Functional and Behavioral Methods to Assess the Zebrafish Retina

One of the most exploited assays for visual function in humans and many animal models are electroretinograms (ERG). ERG measure bulk electrical signals produced by the whole retina in response to light stimulation and has been adapted to both zebrafish larvae (Nelson and Singla, 2009; Chrispell et al., 2015) and adults (Hughes et al., 1998). Through analysis of the different ERG waves the overall activity of photoreceptors and BC can be evaluated. Using well-designed stimuli or pharmacological agents, other properties like the kinetics of photoreceptor adaptation can also be measured (Korenbrot et al., 2013). Additionally, ERG signals have a spectral signature based on the signals generated by specific subsets of photoreceptor and their downstream partners. These signatures can be utilized to isolate the contributions of each element in different conditions (Nelson and Singla, 2009). ERG measurements have been used in the adult to demonstrate that the retina can recover function after damage and subsequent regeneration (McGinn et al., 2018). In the future ERG could be used both in larvae and adults after NTR-MTZ ablation of specific cells, to assess the functional recovery of retinal processing during regeneration.

While the ERG can provide a powerful readout of retinal activity, functional imaging using genetically encoded calcium

TABLE 1 | Toolkit for the study of retinal development and regeneration: transgenic lines.

Target cell types	Genotype	Description	ZFIN ID	Reference
Reporter lines				
Photoreceptors				
Rods	*Tg(XlRho:EGFP)^{fl1}*	Promoter of rhodopsin from *Xenopus* drives the expression of GFP in rods	ZDB-ALT-080517-1	Fadool, 2003
Rods	*Tg(rho:EGFP)^{kj2}*	Promoter of rhodopsin drives expression of GFP in rods	ZDB-ALT-060830-4	Hamaoka et al. (2002)
Cones (all subtypes)	*Tg(-3.2gnat2:EGFP)^{ucd1}*	Promoter of cone transducin alpha subunit drives the expression of GFP in all cone subtypes	ZDB-ALT-070829-1	Smyth et al., 2008
UV-cones	*Tg(sws1:GFP)^{kj9}*	Promoter of UV-opsin drives the expression of GFP in UV-cones	ZDB-ALT-080227-1	Takechi et al., 2003
S-cones	*Tg(-3.5opn1sw2:EGFP)^{k11}*	Promoter of S-opsin region drives the expression of GFP in S-cones	ZDB-FISH-150901-14019	Takechi et al., 2008
S-cones	*tg(sws2:mCherry)^{ua3011}*	Promoter of S-opsin drives expression of mCherry in S-cones	ZDB-ALT-130819-1	Duval et al., 2013
S-cones	*Tg(opn1sw2:mCherry)^{mi2007}*	Promoter of S-opsin drives expression of mCherry in S-cones	ZDB-ALT-120921-1	Salbreux et al., 2012
M-cones	*Tg(opn1mw2:EGFP)^{kj4}*	Promoter of M-opsin drives the expression of GFP in M-cones	ZDB-ALT-071206-2	Tsujimura et al., 2007
L-cones	*Tg(-0.6opn1lw1-cxxc1:GFP)^{kj19d}*	Promoter of L-opsin genes drives the expression of GFP	ZDB-ALT-110519-13	Tsujimura et al., 2010
L-cones	*Tg(thrb:Tomato)^{q22}*	Promoter of thyroid hormone receptor β drives the expression of tdTomato in L-Cones	ZDB-FISH-150901-15085	Suzuki et al., 2013
Horizontal cells				
All horizontal cells	*Tg(lhx1a:EGFP)^{pt303}*	Promoter of LIM Homeobox 1 drives expression of GFP in horizontal cells	ZDB-ALT-100323-3	Rao et al., 2017
All horizontal cells	*Tg(cx55.5:MA-GFP)^{zf524}*	Promoter of connexin 55.5 drives the expression of GFP in all horizontal cells	ZDB-ALT-150319-1	Weber et al., 2014
All horizontal cells	*Tg(cx55.5:EGFP)^{nhi1}*	Promoter of connexin 55.5 drives the expression of GFP in all horizontal cells	ZDB-ALT-180119-1	Klaassen et al., 2016
Horizontal cell subtype (H4)	*Tg(cx52.7:EGFP)^{nhi2}*	Promoter of connexin 52.7 drives the expression of GFP in H4 horizontal cells	ZDB-ALT-180119-2	Klaassen et al., 2016
Horizontal cell subtype (H1)	*Tg(cx52.9:EGFP)^{nhi3}*	Promoter of connexin 52.9 drives the expression of GFP in H1 horizontal cells	ZDB-ALT-180119-3	Klaassen et al., 2016
Horizontal cell subtypes (H1,H4)	*Tg(cx52.6:EGFP)^{nhi4}*	Promoter of connexin 52.6 drives the expression of GFP in H1 and H4 horizontal cells	ZDB-ALT-180119-2	Klaassen et al., 2016
Horizontal cell subtype	*Tg(hsp70l:EGFP)^{nds1}*	Enhancer trap drives the expression of GFP in horizontal and several subtypes of amacrine cells	ZDB-ALT-170512-1	Torvund et al., 2017
Bipolar cells				
On Bipolar Cells	*Tg(grm6b:EGFP)^{zh1Tg}*	Promoter of metabotropic glutamate receptor 6b drives the expression of GFP in bipolar cells, and subtypes of amacrine and ganglion cells	ZDB-ALT-160819-2	Glasauer et al., 2016
Bipolar cells (subtypes)	*Tg(GAL4-VP16,UAS:EGFP)^{ub43}*	Enhancer trap drives the expression of GFP in subtypes of On- and Off-bipolar cells	ZDB-ALT-100201-1	D'Orazi et al., 2016
Bipolar cells (subtypes)	*Tg(vsx1:GFP)^{nns5}*	Promoter of visual system homeobox 1 drives the expression of GFP in subtypes of bipolar cells	ZDB-ALT-061204-4	Vitorino et al., 2009
Bipolar cells (subtypes)	*Tg(chx10:loxP-dsRed-loxP-GFP)^{nns3}*	Promoter of visual system homeobox 2 drives the expression of GFP in subtypes of bipolar cells, and Müller glia	ZDB-ALT-090116-1	Vitorino et al., 2009
On-bipolar cells (subtypes)	*Tg(nyx:Gal4-VP16)^{q16a}*	Promoter of nyctalopin drives the expression of Gal4 on a subset of On-bipolar cells	ZDB-ALT-071129-2	Schroeter et al., 2006; McGinn et al., 2018
Müller glia				
Müller glia	*Tg(gfap:GFP)^{mi2001}*	Promoter of glial fibrillary acidic protein drives the expression of GFP	ZFIN ID: ZDB-ALT-060623-4	Raymond et al., 2006
Müller glia	*Tg(gfap:nGFP)^{mi2004}*	Promoter of glial fibrillary acidic protein drives the expression of nucleus-localized GFP	ZDB-ALT-070830-1	Bernardos et al., 2007

(Continued)

TABLE 1 | Continued

Target cell types	Genotype	Description	ZFIN ID	Reference
Immune cells				
Microglia and macrophages	*Tg(mpeg1:EGFP)*^{gl22}	Promoter of macrophage-expressed gene 1 drives the expression of GFP	ZDB-ALT-120117-1	Ellett et al., 2011; Mitchell et al., 2018
Microglia and macrophages	*Tg(mpeg1:mCherry)*^{gl23}	Promoter of macrophage-expressed gene 1 drives the expression of mCherry	ZDB-ALT-120117-2	Ellett et al., 2011; Mitchell et al., 2018
Lines for selective ablation (NTR-MTZ)				
Rods	*Tg(zop:nfsb-EGFP)*^{nt19}	Promoter of rhodopsin drives the expression of nitroreductase-GFP fusion in rods	ZDB-ALT-100323-4	Montgomery et al., 2010
UV-cones	*Tg(opn1sw1:KALTA4)*^{ua3139}	Promoter of UV-opsin drives the expression of KalTA4, which binds to a separate transgene and drives expression of a nitroreductase and mCherry fusion protein in UV-cones	ZDB-ALT-160901-14	Hagerman et al., 2016
UV-cones	*Tg(opn1sw1:NTR-mCherry)*^{q28}	Promoter of UV-opsin drives the expression of a nitroreductase and mCherry fusion protein in UV-cones	ZDB-ALT-160425-1	Yoshimatsu et al., 2016
S-cones	*Tg(opn1sw2:NTR-mCherry)*^{q30}	Promoter of S-opsin drives expression of nitroreduactase-mCherry fusion in S-cones	ZDB-ALT-160425-3	D'Orazi et al., 2016; Yoshimatsu et al., 2016
Bipolar cells	*Tg(UAS-E1b:NfsB-mCherry)*^{c264}	Enhancer trap drives the expression of a nitroreductase and mCherry fusion protein in a subset of bipolar cells	ZDB-ALT-070316-1	Zhao et al., 2009; D'Orazi et al., 2016
Lines for functional imaging				
Photoreceptors and Bipolar Cells	*Tg(-1.8ctbp2:Rno.Syp-GCAMP)*^{lmb3}	Promoter of ribeye drives synaptically localized GCaMP2 in photoreceptors and bipolar cells	ZDB-ALT-120320-5	Dreosti et al., 2009
Photoreceptors and Bipolar Cells	*Tg(-1.8ctbp2a:Rno.Syp-GCaMP6)*^{uss1}	Promoter of ribeye drives synaptically localized GCaMP6 in photoreceptors and bipolar cells	ZDB-ALT-161010-18	Johnston et al., 2014
Photoreceptors and Bipolar Cells	*Tg(-1.8ctbp2:SYPHY)*^{lmb2}	Promoter of ribeye drives synaptic phluorin in photoreceptors and bipolar cells	ZDB-ALT-120320-4	Odermatt et al., 2012
Müller glia	*Tg(gfap:Eco.GltL-cpEGFP)*^{cu3313}	Promoter of glial fibrillary acidic protein drives the expression of iGluSnfR	ZDB-ALT-170404-12	MacDonald et al., 2017

sensors has also been developed to measure response in visual centers, especially in the tectum (Förster et al., 2017). Currently these approaches remain challenging in the retina due to the RPE which creates an optical barrier, making it difficult to image directly through the eye. It is possible to use these indicators to image through the lens in adults (Duval et al., 2013). Also, in larvae some transparency can be achieved using PTU to inhibit melanophore production, but this treatment may alter visual function (Antinucci and Hindges, 2016). Better imaging has been achieved with mutant lines that genetically remove the different classes of pigmented cells (White et al., 2008; Antinucci and Hindges, 2016). In the future, additional functional imaging using calcium sensory in photoreceptors along with newly developed neurotransmitter sensors, like iGluSnfR (Marvin et al., 2013), will be an important *in vivo* approach to assess pre- and post-synaptic function with in developing and regenerating retinal circuits. (Zhang et al., 2016; MacDonald et al., 2017).

In addition to electrically or optically recording the activity of cells within the retina, there are many well characterized visual behaviors that can be used to evaluate retinal function. The *optokinetic response* is an extremely robust behavioral assay, where a visual stimulus of moving stripes is tracked by eye movements. This behavior is already present and reliable by 5 dpf and requires minimal equipment to setup (Brockerhoff et al., 1995; Neuhauss et al., 1999; Neuhauss, 2003). In the related *optomotor response*, tracking of moving stripes is followed by swimming in the same direction as the stimulus (Neuhauss et al., 1999; Neuhauss, 2003). This assay has been used to characterize the overall recovery of vision after photoreceptor ablation (Hagerman et al., 2016). At around 5 dpf, larvae also start hunting for small prey using visual cues, another visual behavior that can be quantified (Borla et al., 2002; Gahtan et al., 2005; McElligott and O'Malley, 2005). Larvae also innately exhibit phototaxis and photoavoidance (Brockerhoff et al., 1995; Orger and Baier, 2005; Burgess et al., 2010), and an escape response in response to sudden decreases in illumination (Burgess and Granato, 2007).

Adult zebrafish also exhibit an *escape response* to threatening objects, characterized by rapid turning and swimming away from the threat. The escape response can be elicited by placing fish in a clear tank with a central pole that serves for hiding, and an external rotating drum with a single black stripe to act as a threatening stimulus. Use of this assay allowed to measure behavioral rod and cone thresholds and the time course of photoreceptor adaptation and as part of the screening in a forward-genetic screen for visual mutations (Li and Dowling, 1997; Li and Dowling, 2000). Zebrafish and other teleosts determine their body position using a combination of their sense of balance and the source of illumination, which in their natural environment tends to come from above. Thus, they tend to tilt their bodies such that their backs are turned against the source of illumination (*dorsal light response* or DLR). Tilt can be induced by uneven-illumination between the two eyes (e.g., side illumination) (Silver, 1974; Neuhauss, 2003) or by unilateral

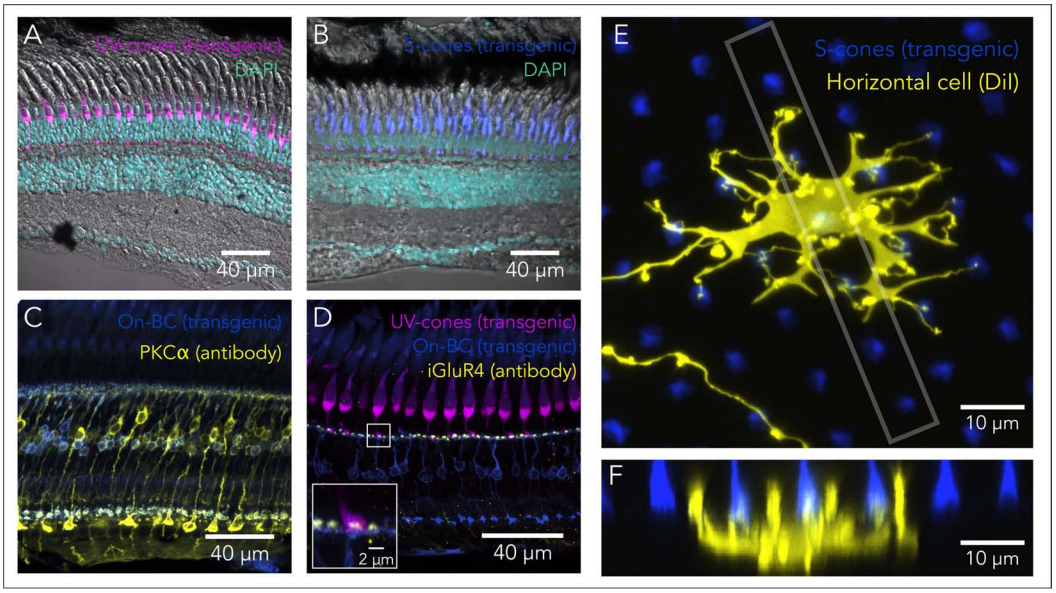

FIGURE 3 | Tools to study retinal circuits. **(A)** Confocal image of the UV-cone reporter line *Tg(sws1:GFP)*^{kj9} retina (magenta), overlaid with DAPI nuclear staining (cyan) and a transmitted DIC image. **(B)** Confocal image of the S-cone reporter line *Tg(-3.5opn1sw2:EGFP)*^{k11} retina (blue), overlaid with DAPI nuclear staining (cyan) and a transmitted DIC image. **(C)** Bipolar cell labeling using PKCα immunolabeling (yellow) and the On-bipolar reporter line *Tg(grm6b:EGFP)*^{zh1} (blue). Rod-contacting bipolar cells are brightly labeled by the PKCα antibody, while another subset of bipolars is more dimly labeled. Some of these are doubly labeled with the transgenic line. **(D)** Immunolabeling of off-bipolar synapses with photoreceptors using an antibody against the inotropic glutamate receptor type 4 (*gria4*), in the background of a double transgenic reporter line *Tg(sws1:GFP)*^{kj9} (magenta) and *Tg(grm6b:EGFP)*^{zh1} (blue). Inset shows that the punctate labeling in the IPL overlaps with the synaptic terminals of cones and the bipolar cell dendrites. **(E)** Sparse labeling of horizontal cells using DiI (yellow) in the background of the S-cone reporter line *Tg(-3.5opn1sw2:EGFP)*^{k11}. Image corresponds to a maximal intensity projection of a confocal stack, where synaptic contacts between the horizontal cell and S-cones are apparent. **(F)** Maximal intensity projection of an orthogonal view restricted to the box gray in **(E)**, highlighting the invaginations of horizontal processes into the cone synaptic terminals. This particular projection is oriented through a row of UV- and S-cones and the bigger horizontal processes most likely correspond to invaginations into UV-cone terminals.

ocular damage, where recovery of a normal tilt is a sign of functional recovery (Mensinger and Powers, 1999; Lindsey and Powers, 2007; Mensinger and Powers, 2007; Sherpa et al., 2014). In zebrafish, information from the vestibular system is capable of overriding visual input, so that the DLR is only apparent when the vestibular system has been damaged (Nicolson et al., 1998) or when fish are placed head down in a tightly fitting tube (Neuhauss, 2003).

In captivity, zebrafish are conditioned to move toward the front of the tank and wait for food whenever a person approaches. This conditioned learning can be exploited to test for visual function (*place preference test*) (Sherpa et al., 2014). A very similar test has been recently used in cichlids to demonstrate their ability to truly discriminate colors (Escobar-Camacho et al., 2017) (**Table 3**).

Interestingly, some of these behaviors seem to rely on only into small subsets of retinal circuits. For example, the OKR seems to be mainly driven by M- and L-cone signals (Orger and Baier, 2005), while the tracking of small dots, at least in goldfish, depends mainly on M-cone signals (Gehres and Neumeyer, 2007). Similarly, photoavoidance is robustly driven by UV-light, and presumably UV-cone signals (Guggiana-Nilo and Engert, 2016). From previous work that has shown fast functional OKR recovery after S-cone ablation even before regeneration and rewiring occur (Hagerman et al., 2016), it is clear that not enough is known about the function, recovery and plasticity of circuits in the retina. Together, behavioral assays along with NTR-mediated ablation of a given cone subtype, could be used to further expand our understanding of these circuits, and the functional consequences of regeneration and rewiring of the different retinal circuits.

Forward and Reverse Genetic Approaches

Zebrafish forward genetic screens are extremely powerful, and have been successfully used to uncover novel genes that are involved in photoreceptor function and RD (Brockerhoff and Fadool, 2011). It is likely that any additional screening that relies on alterations in visual behaviors will continue to uncover new genes that affect photoreceptor function or cause RD. As more causes of RD continue to be unveiled, we now understand that there are limited number of converging pathways that eventually lead to photoreceptor degeneration, including: classic apoptosis, oxidation, activation of proteolytic pathways, misbalance in intracellular levels of cGMP and calcium, and epigenetic regulation (Trifunovic et al., 2012). With this knowledge, reverse-genetic approaches using CRISPR-mediated gene editing to target previously undescribed components within these pathways are likely to be extremely useful in the future. Recent studies in

TABLE 2 | Toolkit for the study of retinal development and regeneration: antibodies and fluorescent labeling.

Labeled cell types or structures	Antibody	Antigen	Manufacturer (Catalog number) Species	ZFIN ID	Reference
Photoreceptors					
Rods	1D4	C-terminus of bovine rhodopsin	Sigma-Aldrich (MAB5356) Abcam (ab5417) Mouse monoclonal	ZDB-ATB-110114-2	Linder et al., 2011
Rods	*gnat1*	Human transducin alpha subunit	ProteinTech (55167-1-AP) Rabbit polyclonal	ZDB-ATB-151005-5	Liu et al., 2015
Cones	Recoverin	Human recoverin	Millipore (AB5585) Rabbit polyclonal	ZDB-ATB-151016-2	Solin et al., 2014
	Peanut agglutinin	Cone extracellular matrix	Molecular Probes (L21409)		Hageman and Johnson, 1986
M- and L-cones	*zpr1*	Arrestin3a	ZIRC (AB_10013803) Mouse Monoclonal	ZDB-ATB-081002-43	Ile et al., 2010
	1D4	C-terminus of bovine rhodopsin	Abcam (ab5417) Mouse monoclonal	ZDB-ATB-121128-10	Yin et al., 2012
Photoreceptor synapses	*ribeyeA*	Ribeye A	Teresa Nicolson Laboratory OHSU Rabbit Polyclonal	ZDB-ATB-120504-2	Randlett et al., 2013
	SV2	Synaptic Vesicle glycoprotein 2	DSHB, Iowa, United States Mouse monoclonal	ZDB-ATB-081201-1	Huang et al., 2012
	syntaxin3	Syntaxin 3	Synaptic Systems (110033) Rabbit polyclonal	ZDB-ATB-160428-2	Lin et al., 2016
Horizontal cells					
	GluR2	Glutamate receptor type 2	Millipore (MAB397) Mouse monoclonal	ZDB-ATB-151118-1	Yazulla and Studholme, 2001
	GAD67	Glutamate decarboxylase 67 kDa isoform	Chemicon International Inc. (AB108) Rabbit Polyclonal	ZDB-ATB-100903-8	Yazulla and Studholme, 2001
Bipolar cells					
Bipolar cells (subset)	PKCα	Protein kinase C alpha subunit	Sigma (P4334) Rabbit polyclonal	ZDB-ATB-090223-3	Yazulla and Studholme, 2001; Moshiri et al., 2008
On-bipolar cell subtype	mGluR1	metabotropic glutamate receptor 1 alpha subunit	Millipore (AB1551) Rabbit polyclonal	ZDB-ATB-100810-1	Yazulla and Studholme, 2001
On- and Off-bipolar cells	anti-GABAa α3	GABA receptor alpha subunit 3	Alomone Labs (#AGA-003) Rabbit polyclonal	ZDB-ATB-100903-6	Yazulla and Studholme, 2001
On Bipolar Cells	PKCβ1 (C-16)	Protein kinase C beta subunit 1	Santa Cruz Biotechnology, sc-209 Rabbit polyclonal	ZDB-ATB-120614-1	Glasauer et al., 2016
On-bipolar cell dendrites	Pan-Maguk	Membrane-associated guanylate kinases	Neuromab (75-029, clone K28/86) Mouse monoclonal	ZDB-ATB-120504-1	Randlett et al., 2013
Off-bipolar cell dendrites	gria4	Ionotropic glutamate receptor type 4	Millipore (AB1508) Rabbit polyclonal	ZDB-ATB-100810-2	Yazulla and Studholme, 2001
Amacrine cells					
Starburst	ChAT	Human placental choline acetyltransferase	Millipore, AB144P, Goat polyclonal	ZDB-ATB-081017-3	Glasauer et al., 2016
GABAergic	GAD65/67	Glutamic acid decarboxylase 65 kDa/67 kDa	Abcam (Ab11070) Rabbit polyclonal	ZDB-ATB-090617-2	Glasauer et al., 2016
Dopaminergic	TH	Tyrosine hydroxylase	Immunostar, Inc. (22941) Mouse monoclonal	ZDB-ATB-081017-8	Glasauer et al., 2016
Müller glia					
	GS	Glutamine Synthase	Millipore (mab302) Mouse monoclonal	ZDB-ATB-081009-5	Randlett et al., 2013
	gfap	Glial Fibrillary Acidic Protein	ZIRC (zrf-1) Mouse monoclonal	ZDB-ATB-081002-46	Solin et al., 2014
	glt1	Glutamate transporter 1 (glial)	Millipore (AB1783) Guinea pig polyclonal	ZDB-ATB-100916-6	Yazulla and Studholme, 2001
Ciliary Marginal Zone	PCNA	Anti-Proliferating Cell Nuclear Antigen	Santa Cruz Biotechnology, sc-56 Mouse monoclonal	ZDB-ATB-081121-4	Inoue and Wittbrodt, 2011
Bipolar, horizontal and amacrine cells	isl1	Islet 1	DSHB, Iowa, United States (40.3A4) Mouse monoclonal	ZDB-ATB-081124-3	Zhang et al., 2012
Bipolar, horizontal, amacrine and ganglion cells	HuC/HuD	ELAV like neuron-specific RNA binding protein 3 and 4	Invitrogen (A-21271) Mouse monoclonal	ZDB-ATB-081003-2	Randlett et al., 2013

TABLE 3 | Toolkit for the study of retinal development and regeneration: electroretinograms and visually guided behaviors.

Visual assay	Description	References
Electroretinogram (ERG)	Measurement of the changes in the bulk electrical activity produced by the retina when stimulated with light. Can be measured in both larvae and adults.	Hughes et al., 1998; Chrispell et al., 2015
Optokinetic reflex (OKR)	Rotational eye movements track moving targets, usually white and black stripes in a rotating drum, are followed by saccades that reset the eye position.	Clark, 1981; Neuhauss et al., 1999; Neuhauss, 2003
Optomotor response (OMR)	Swimming in the direction of a moving stimuli.	Clark, 1981; Neuhauss, 2003
Prey/Small object tracking	Larvae hunt for paramecia by making stereotyped swimming movements to orient themselves before swimming forward to capture their prey	Borla et al., 2002; Gahtan et al., 2005; McElligott and O'Malley, 2005
Phototaxis and Photoavoidance	Swim movements towards or away from light sources	Brockerhoff et al., 1995 Orger and Baier, 2005; Burgess et al., 2010
Escape response to sudden decreases in illumination	Larval zebrafish exhibit escape responses ("O-bends") to sudden decreases in illumination	Miller et al., 2018
Escape response to dark objects	Adult zebrafish avoid moving dark objects by abruptly changing the direction of swimming	Li and Dowling, 1997
Dorsal light reflex (DLR)	Zebrafish tilt their bodies to turn their backs towards the source of illumination by keeping equal input in both eyes, but vestibular information can override this reflex. Reflex can be made apparent by placing fish head down in a tightly fitting tube.	Nicolson et al., 1998; Neuhauss, 2003
Place preference	Captive zebrafish are conditioned by feeding routines to move toward front of the tank when they visually detect a person approaching.	Sherpa et al., 2014

zebrafish have already demonstrated that zebrafish can be used as a platform to rapidly perform genetic screens using CRISPR (Varshney et al., 2015, 2016; Shah et al., 2016). In addition to genetic screens, similar to what has been done in fin and hair-cell regeneration studies (Mathew et al., 2007; Namdaran et al., 2012), pharmacology-based screening could be used to isolate novel compounds with the ability to promote or prevent photoreceptor regeneration. Similar screens could also be accomplished using behavioral assays, evaluating the recovery of visual function after regeneration. Some of the success of such screens in hair cells of the lateral line stems from the fast regeneration times (∼2 days) and the small number of cell types that have to be regenerated. In paradigms of regeneration after extensive damage (surgical of pharmacological) in adults, the long regeneration times (8–14 weeks) and the diversity of cell types that need to be regenerated might present insurmountable hurdles for screens. Nevertheless, photoreceptor regeneration occurs within 4 weeks in adults and in ∼10 days in larvae after cell-specific ablations, opening up the possibility to carry out such screens.

While the majority of regeneration studies in zebrafish have focused on regenerating damaged cells, for functional recovery after regeneration, it is imperative that new cells integrate appropriately into their specific retinal circuits. Our current knowledge on how retinal circuits in the outer retina form during development and after regenerations is limited. Studies into these processes suggest that rewiring after regeneration is not a complete recapitulation of development. First of all, during development retinal cells are derived from retinal progenitors and retinal circuits assemble properly even in the absence of Müller glia (Williams et al., 2010). In contrast, during regeneration, Müller glia are the principal source of new retinal cells. Second, not all the transcription pathways that are active during development are reactivated during regeneration (Veldman et al., 2007; Sherpa et al., 2014). Third, there seems to be more plasticity and a greater capacity for compensation. It appears that during rewiring, at least in larvae, maintaining inputs and outputs is more important than the absolute selectivity of connections (D'Orazi et al., 2016; Yoshimatsu et al., 2016). In adult zebrafish, after pharmacological ablation of bipolar, amacrine and ganglion cells (but survival of photoreceptors) and their subsequent regeneration, various subtypes of BCs seem to be able to recapitulate the diversity of connectivity that is found in uninjured eyes, but as a population, selectivity for photoreceptors seems to be restored (McGinn et al., 2018). Further investigation is required to explain the disagreement between these studies since there are many differences including ablation technique (NTR-MTZ vs. ouabain), age of ablation (larvae vs. adults), time between ablation and assessment of connectivity (1–2 weeks vs. 8 weeks) and subtypes of cells studied. Yet, this raises interesting questions: is the capacity for compensation only present in larvae and lost in the adult? or, is compensation only present in the initial phase after regeneration and normal selectivity of connections reestablished over time?

It is interesting to note that selectivity is not lost during rewiring, it is just more permissive, and it is very likely that the same molecules that allow recognition between retinal cell types are used in both development and regeneration. Only a handful of cell-adhesion and synaptic molecules are known to be necessary for the formation of synaptic contacts between photoreceptors and downstream retinal cells (Zhang et al., 2017; Miller et al., 2018). Some of these molecules are key across all photoreceptors, while others are specific to rods (Cao et al., 2015; Wang et al., 2017) or to cones (Sarria et al., 2018; Ueno et al., 2018). To date, the molecular mechanisms involved in the recognition between specific photoreceptor subtypes and their synaptic partners (horizontal and bipolar cells) are not known. Any of the genetic screening tools mentioned above could be combined with the NTR-MTZ transgenic lines (**Table 1**), to target specific cell subtypes and elucidate the mechanisms that enable rewiring. Research in this front could have a very

significant impact in phenotyping vision loss in RD, and to develop manipulations that could ultimately enable rewiring of transplanted or regenerated photoreceptors into proper retinal circuits.

Gene-Expression Profiling (RNAseq)

During the last decade, advances in the capacity of high-throughput sequencing has allowed to profile the transcriptomes of whole tissues or dissociated single cells. Gene-expression profiling of retinal cells in mice has given great insight in the classification of retinal cells into different (and even novel) subtypes (Macosko et al., 2015), especially for BC, where clear differences in molecules involved in cell-recognition and synapse formation were detected (Shekhar et al., 2016). These techniques can be applied in zebrafish, especially using transgenic lines, as has been recently reported for rods (Sun et al., 2018). RNAseq of zebrafish retinal cells could help unveil the genes that are required for synapse formation between BC and photoreceptors, genes that could be essential to promote rewiring in RD therapies. RNAseq could also be exploited to study the changes in gene expression that occur during degeneration and regeneration. This could be accomplished by profiling single cells in the most relevant time points after photoreceptor death. With a focus on Müller glia, further insights could be gained into the gene networks that allow pluripotent and functional recovery in zebrafish. This knowledge will also be extremely valuable for the treatment of RD and understanding how to initiate regeneration after RD.

CONCLUSION AND OUTLOOK

Our field is developing a deep understanding on many aspects of RD, including risk factors, underlying genetic causes, molecular pathways that lead to photoreceptor death, and the manipulations that could slow down the progression of the disease. During the last decade, we have made significant progress into revolutionary therapies that could, 1 day, cure blindness.

Despite all of the research on RD and regeneration, there are still gaps in our current knowledge that limit our capacity to understand certain aspects of RD and hinder our ability to develop therapies. The zebrafish is an advantageous model to fill in these gaps, especially at a mechanistic level. As a relevant example, we have discussed how zebrafish has been used to delineate molecular pathways within Müller glia that allow regeneration of retinal cells even in the adult zebrafish. This knowledge has been directly applied into the mouse retina and successfully used to generate new and functional bipolar and amacrine cells (Jorstad et al., 2017). Although studies have been able to stimulate retinal regeneration in mice using manipulations derived from the study of zebrafish retinal regeneration, but we do not yet fully understand the pathways required to regenerate each retinal cell type, or how these pathways are regulated to regenerate specific subpopulations. Further studies are required to understand the mechanisms that allow zebrafish Müller glia to not only produce any retinal cell, but also to specifically replace the lost population without overtly producing proliferation of undamaged cell types (D'Orazi et al., 2016; Yoshimatsu et al., 2016; McGinn et al., 2018).

In addition to gaps in knowledge on the role of Müller glia and regeneration, we also have an incomplete grasp on the processes that are involved in recognition between photoreceptors and their postsynaptic targets, with only a handful of molecules known to be involved in the correct formation of synapses. This leaves us with little leverage on manipulations that could promote integration of new photoreceptors into the surviving retinal circuits. Solving these issues and finding viable therapeutic options for RD will certainly require diverse approaches. Research in zebrafish is uniquely poised to make additional key contributions into RD, especially on unveiling the molecular mechanisms involved in photoreceptor regeneration and the processes that guide wiring during development and rewiring after regeneration of photoreceptors into retinal circuits.

AUTHOR CONTRIBUTIONS

JA conceived and carried out the literature review research, designed the figures and diagrams, acquired the images, and wrote the article. KK conceived and carried out the literature review research and wrote the article.

FUNDING

This work was supported by NIH/NIDCD intramural research funds 1ZIADC000085-01 (KK), and NIH/NEI intramural research funds ZIAEY000488-10 (JA).

REFERENCES

Adler, R. (2008). Curing blindness with stem cells: hope, reality, and challenges. *Adv. Exp. Med. Biol.* 613, 3–20. doi: 10.1007/978-0-387-74904-4_1

Antinucci, P., and Hindges, R. (2016). A crystal-clear zebrafish for in vivo imaging. *Sci. Rep.* 6:29490. doi: 10.1038/srep29490

Ariga, J., Walker, S. L., and Mumm, J. S. (2010). Multicolor time-lapse imaging of transgenic zebrafish: visualizing retinal stem cells activated by targeted neuronal cell ablation. *J. Vis. Exp.* 43:2093. doi: 10.3791/2093

Barber, A. C., Hippert, C., Duran, Y., West, E. L., Bainbridge, J. W., Warre-Cornish, K., et al. (2013). Repair of the degenerate retina by photoreceptor transplantation. *Proc. Natl. Acad. Sci. U.S.A.* 110, 354–359. doi: 10.1073/pnas.1212677110

Bernardos, R. L., Barthel, L. K., Meyers, J. R., and Raymond, P. A. (2007). Late-stage neuronal progenitors in the retina are radial Müller glia that function as retinal stem cells. *J. Neurosci.* 27, 7028–7040. doi: 10.1523/JNEUROSCI.1624-07.2007

Bibliowicz, J., Tittle, R. K., and Gross, J. M. (2011). Toward a better understanding of human eye disease insights from the zebrafish, danio rerio. *Prog. Mol. Biol. Transl. Sci.* 100, 287–330. doi: 10.1016/B978-0-12-384878-9.00007-8

Borla, M. A., Palecek, B., Budick, S., and O'Malley, D. M. (2002). Prey capture by larval zebrafish: evidence for fine axial motor control. *Brain Behav. Evol.* 60, 207–229. doi: 10.1159/000066699

Bourne, R. R. A., Flaxman, S. R., Braithwaite, T., Cicinelli, M. V., Das, A., Jonas, J. B., et al. (2017). Magnitude, temporal trends, and projections of the global prevalence of blindness and distance and near vision impairment: a systematic

review and meta-analysis. *Lancet Glob. Health* 5, e888–e897. doi: 10.1016/S2214-109X(17)30293-0

Bringmann, A., Pannicke, T., Biedermann, B., Francke, M., Iandiev, I., Grosche, J., et al. (2009). Role of retinal glial cells in neurotransmitter uptake and metabolism. *Neurochem. Int.* 54, 143–160. doi: 10.1016/j.neuint.2008.10.014

Brockerhoff, S. E., and Fadool, J. M. (2011). Genetics of photoreceptor degeneration and regeneration in zebrafish. *Cell. Mol. Life Sci.* 68, 651–659. doi: 10.1007/s00018-010-0563-8

Brockerhoff, S. E., Hurley, J. B., Janssen-Bienhold, U., Neuhauss, S. C., Driever, W., Dowling, J. E., et al. (1995). A behavioral screen for isolating zebrafish mutants with visual system defects. *Proc. Natl. Acad. Sci. U.S.A.* 92, 10545–10549. doi: 10.1073/pnas.92.23.10545

Burgess, H. A., and Granato, M. (2007). Modulation of locomotor activity in larval zebrafish during light adaptation. *J. Exp. Biol.* 210(Pt 14), 2526–2539. doi: 10.1242/jeb.003939

Burgess, H. A., Schoch, H., and Granato, M. (2010). Distinct retinal pathways drive spatial orientation behaviors in zebrafish navigation. *Curr. Biol.* 20, 381–386. doi: 10.1016/j.cub.2010.01.022

Busskamp, V., Duebel, J., Balya, D., Fradot, M., Viney, T. J., Siegert, S., et al. (2010). Genetic reactivation of cone photoreceptors restores visual responses in retinitis pigmentosa. *Science* 329, 413–417. doi: 10.1126/science.1190897

Cameron, D. A. (2000). Cellular proliferation and neurogenesis in the injured retina of adult zebrafish. *Vis. Neurosci.* 17, 789–797. doi: 10.1017/S0952523800175121

Cao, Y., Sarria, I., Fehlhaber, K. E., Kamasawa, N., Orlandi, C., James, K. N., et al. (2015). Mechanism for selective synaptic wiring of rod photoreceptors into the retinal circuitry and its role in vision. *Neuron* 87, 1248–1260. doi: 10.1016/j.neuron.2015.09.002

Carter-Dawson Louvenia, D., and Lavail Matthew, M. (1979). Rods and cones in the mouse retina. I. Structural analysis using light and electron microscopy. *J. Compar. Neurol.* 188, 245–262. doi: 10.1002/cne.901880204

Centanin, L., Hoeckendorf, B., and Wittbrodt, J. (2011). Fate restriction and multipotency in retinal stem cells. *Cell Stem Cell* 9, 553–562. doi: 10.1016/j.stem.2011.11.004

Chang, B., Grau, T., Dangel, S., Hurd, R., Jurklies, B., Sener, E. C., et al. (2009). A homologous genetic basis of the murine cpfl1 mutant and human achromatopsia linked to mutations in the pde6c gene. *Proc. Natl. Acad. Sci. U.S.A.* 106, 19581–19586. doi: 10.1073/pnas.0907720106

Chinen, A., Hamaoka, T., Yamada, Y., and Kawamura, S. (2003). Gene duplication and spectral diversification of cone visual pigments of zebrafish. *Genetics* 163, 663–675.

Chrispell, J. D., Rebrik, T. I., and Weiss, E. R. (2015). Electroretinogram analysis of the visual response in zebrafish larvae. *J. Vis. Exp.* 97:52662. doi: 10.3791/52662

Cideciyan, A. V. (2010). Leber congenital amaurosis due to rpe65 mutations and its treatment with gene therapy. *Prog. Retin. Eye Res.* 29, 398–427. doi: 10.1016/j.preteyeres.2010.04.002

Clark, D. T. (1981). *Visual Responses in the Developing Zebrafish (Brachydanio rerio)*. Ph.D. thesis, Eugene, OR, University of Oregon.

Connaughton, V. P., Graham, D., and Nelson, R. (2004). Identification and morphological classification of horizontal, bipolar, and amacrine cells within the zebrafish retina. *J. Comp. Neurol.* 477, 371–385. doi: 10.1002/cne.20261

da Cruz, L., Dorn, J. D., Humayun, M. S., Dagnelie, G., Handa, J., Barale, P. O., et al. (2016). Five-year safety and performance results from the argus ii retinal prosthesis system clinical trial. *Ophthalmology* 123, 2248–2254. doi: 10.1016/j.ophtha.2016.06.049

Daiger, S. P., Sullivan, L. S., and Bowne, S. J. (2013). Genes and mutations causing retinitis pigmentosa. *Clin. Genet.* 84, 132–141. doi: 10.1111/cge.12203

Daniele, L. L., Emran, F., Lobo, G. P., Gaivin, R. J., and Perkins, B. D. (2016). Mutation of wrb, a component of the guided entry of tail-anchored protein pathway, disrupts photoreceptor synapse structure and function. *Invest. Ophthalmol. Vis. Sci.* 57, 2942–2954. doi: 10.1167/iovs.15-18996

De Bode, C. (2017). *Blindness and Visual Impairment*. Available at: http://www.who.int/news-room/fact-sheets/detail/blindness-and-visual-impairment [accessed May 28, 2018].

D'Orazi, F. D., Zhao, X. F., Wong, R. O., and Yoshimatsu, T. (2016). Mismatch of synaptic patterns between neurons produced in regeneration and during development of the vertebrate retina. *Curr. Biol.* 26, 2268–2279. doi: 10.1016/j.cub.2016.06.063

Dreosti, E., Odermatt, B., Dorostkar, M. M., and Lagnado, L. (2009). A genetically encoded reporter of synaptic activity *in vivo*. *Nat. Methods* 6, 883–889. doi: 10.1038/nmeth.1399

Duval, M. G., Chung, H., Lehmann, O. J., and Allison, W. T. (2013). Longitudinal fluorescent observation of retinal degeneration and regeneration in zebrafish using fundus lens imaging. *Mol. Vis.* 19, 1082–1095.

Dyer, M. A., and Cepko, C. L. (2000). Control of Müller glial cell proliferation and activation following retinal injury. *Nat. Neurosci.* 3, 873–880. doi: 10.1038/78774

Ellett, F., Pase, L., Hayman, J. W., Andrianopoulos, A., and Lieschke, G. J. (2011). Mpeg1 promoter transgenes direct macrophage-lineage expression in zebrafish. *Blood* 117, e49–e56. doi: 10.1182/blood-2010-10-314120

Escobar-Camacho, D., Marshall, J., and Carleton, K. L. (2017). Behavioral color vision in a cichlid fish: *Metriaclima benetos*. *J. Exp. Biol.* 220, 2887–2899. doi: 10.1242/jeb.160473

Fadool, J. M. (2003). Rod genesis in the teleost retina as a model of neural stem cells. *Exp. Neurol.* 184, 14–19. doi: 10.1016/S0014-4886(03)00309-1

Farrar, G. J., Carrigan, M., Dockery, A., Millington-Ward, S., Palfi, A., Chadderton, N., et al. (2017). Toward an elucidation of the molecular genetics of inherited retinal degenerations. *Hum. Mol. Genet.* 26, R2–R11. doi: 10.1093/hmg/ddx185

Fausett, B. V., and Goldman, D. (2006). A role for α1 tubulin-expressing Müller glia in regeneration of the injured zebrafish retina. *J. Neurosci.* 26, 6303–6313. doi: 10.1523/JNEUROSCI.0332-06.2006

Fausett, B. V., Gumerson, J. D., and Goldman, D. (2008). The proneural basic helix-loop-helix gene ascl1a is required for retina regeneration. *J. Neurosci.* 28, 1109–1117. doi: 10.1523/JNEUROSCI.4853-07.2008

Fimbel, S. M., Montgomery, J. E., Burket, C. T., and Hyde, D. R. (2007). Regeneration of inner retinal neurons after intravitreal injection of ouabain in zebrafish. *J. Neurosci.* 27, 1712–1724. doi: 10.1523/JNEUROSCI.5317-06.2007

Förster, D., Dal Maschio, M., Laurell, E., and Baier, H. (2017). An optogenetic toolbox for unbiased discovery of functionally connected cells in neural circuits. *Nat. Commun.* 8:116. doi: 10.1038/s41467-017-00160-z

Fraser, B., DuVal, M. G., Wang, H., and Allison, W. T. (2013). Regeneration of cone photoreceptors when cell ablation is primarily restricted to a particular cone subtype. *PLoS One* 8:e55410. doi: 10.1371/journal.pone.0055410

Gahtan, E., Tanger, P., and Baier, H. (2005). Visual prey capture in larval zebrafish is controlled by identified reticulospinal neurons downstream of the tectum. *J. Neurosci.* 25, 9294–9303. doi: 10.1523/JNEUROSCI.2678-05.2005

Ganzen, L., Venkatraman, P., Pang, C. P., Leung, Y. F., and Zhang, M. (2017). Utilizing zebrafish visual behaviors in drug screening for retinal degeneration. *Int. J. Mol. Sci.* 18:E1185. doi: 10.3390/ijms18061185

Gehres, M., and Neumeyer, C. (2007). Small field motion detection in goldfish is red-green color blind and mediated by the m-cone type. *Vis. Neurosci.* 24, 399–407. doi: 10.1017/S0952523807070447

Glasauer, S. M., Wager, R., Gesemann, M., and Neuhauss, S. C. (2016). Mglur6b:Egfp transgenic zebrafish suggest novel functions of metabotropic glutamate signaling in retina and other brain regions. *J. Comp. Neurol.* 524, 2363–2378. doi: 10.1002/cne.24029

Gollisch, T., and Meister, M. (2010). Eye smarter than scientists believed: neural computations in circuits of the retina. *Neuron* 65, 150–164. doi: 10.1016/j.neuron.2009.12.009

Guggiana-Nilo, D. A., and Engert, F. (2016). Properties of the visible light phototaxis and uv avoidance behaviors in the larval zebrafish. *Front. Behav. Neurosci.* 10:160. doi: 10.3389/fnbeh.2016.00160

Hageman, G. S., and Johnson, L. V. (1986). Biochemical characterization of the major peanut-agglutinin-binding glycoproteins in vertebrate retinae. *J. Comp. Neurol.* 249, 499–510,482–493. doi: 10.1002/cne.902490406

Hagerman, G. F., Noel, N. C., Cao, S. Y., DuVal, M. G., Oel, A. P., and Allison, W. T. (2016). Rapid recovery of visual function associated with blue cone ablation in zebrafish. *PLoS One* 11:e0166932. doi: 10.1371/journal.pone.0166932

Hamaoka, T., Takechi, M., Chinen, A., Nishiwaki, Y., and Kawamura, S. (2002). Visualization of rod photoreceptor development using gfp-transgenic zebrafish. *Genesis* 34, 215–220. doi: 10.1002/gene.10155

Hitchcock, P. F., and Cirenza, P. (1994). Synaptic organization of regenerated retina in the goldfish. *J. Compar. Neurol.* 343, 609–616. doi: 10.1002/cne.903430410

Hitchcock, P. F., Lindsey Myhr, K. J., Easter, S. S. Jr., Mangione-Smith, R., and Jones, D. D. (1992). Local regeneration in the retina of the goldfish. *J. Neurobiol.* 23, 187–203. doi: 10.1002/neu.480230209

Homma, K., Okamoto, S., Mandai, M., Gotoh, N., Rajasimha, H. K., and Chang, Y. S. (2013). Developing rods transplanted into the degenerating retina of crx-knockout mice exhibit neural activity similar to native photoreceptors. *Stem Cells* 31, 1149–1159. doi: 10.1002/stem.1372

Huang, Y. Y., Haug, M. F., Gesemann, M., and Neuhauss, S. C. (2012). Novel expression patterns of metabotropic glutamate receptor 6 in the zebrafish nervous system. *PLoS One* 7:e35256. doi: 10.1371/journal.pone.0035256

Hughes, A., Saszik, S., Bilotta, J., Demarco, P. J. Jr., and Patterson, W. F. (1998). Cone contributions to the photopic spectral sensitivity of the zebrafish erg. *Vis. Neurosci.* 15, 1029–1037. doi: 10.1017/S095252389815602X

Ile, K. E., Kassen, S., Cao, C., Vihtehlic, T., Shah, S. D., and Mousley, C. J. (2010). Zebrafish class 1 phosphatidylinositol transfer proteins: Pitpβ and double cone cell outer segment integrity in retina. *Traffic* 11, 1151–1167. doi: 10.1111/j.1600-0854.2010.01085.x

Inoue, D., and Wittbrodt, J. (2011). One for all—a highly efficient and versatile method for fluorescent immunostaining in fish embryos. *PLoS One* 6:e19713. doi: 10.1371/journal.pone.0019713

Jacobson, S. G., Cideciyan, A. V., Ratnakaram, R., Heon, E., Schwartz, S. B., Roman, A. J., et al. (2012). Gene therapy for leber congenital amaurosis caused by rpe65 mutations: safety and efficacy in fifteen children and adults followed up to three years. *Arch. Ophthalmol.* 130, 9–24. doi: 10.1001/archophthalmol.2011.298

Jacobson, S. G., Cideciyan, A. V., Roman, A. J., Sumaroka, A., Schwartz, S. B., Heon, E., et al. (2015). Improvement and decline in vision with gene therapy in childhood blindness. *N. Engl. J. Med.* 372, 1920–1926. doi: 10.1056/NEJMoa1412965

Jager, R. D., Mieler, W. F., and Miller, J. W. (2008). Age-related macular degeneration. *N. Engl. J. Med.* 358, 2606–2617. doi: 10.1056/NEJMra0801537

Johns, P. R., and Fernald, R. D. (1981). Genesis of rods in teleost fish retina. *Nature* 293, 141–142. doi: 10.1038/293141a0

Johnston, J., Ding, H., Seibel, S. H., Esposti, F., and Lagnado, L. (2014). Rapid mapping of visual receptive fields by filtered back projection: application to multi-neuronal electrophysiology and imaging. *J. Physiol.* 592, 4839–4854. doi: 10.1113/jphysiol.2014.276642

Jorstad, N. L., Wilken, M. S., Grimes, W. N., Wohl, S. G., VandenBosch, L. S., Yoshimatsu, T. A., et al. (2017). Stimulation of functional neuronal regeneration from Müller glia in adult mice. *Nature* 548, 103–107. doi: 10.1038/nature23283

Julian, D., Ennis, K., and Korenbrot, J. I. (1998). Birth and fate of proliferative cells in the inner nuclear layer of the mature fish retina. *J. Compar. Neurol.* 394, 271–282. doi: 10.1002/(SICI)1096-9861(19980511)394:3<271::AID-CNE1>3.0.CO;2-Z

Karl, M. O., Hayes, S., Nelson, B. R., Tan, K., Buckingham, B., Reh, T. A., et al. (2008). Stimulation of neural regeneration in the mouse retina. *Proc. Natl. Acad. Sci. U.S.A.* 105, 19508–19513. doi: 10.1073/pnas.0807453105

Kassen, S. C., Ramanan, V., Montgomery, J. E., T Burket, C., Liu, C. G., Vihtelic, T. S., et al. (2007). Time course analysis of gene expression during light-induced photoreceptor cell death and regeneration in albino zebrafish. *Dev. Neurobiol.* 67, 1009–1031. doi: 10.1002/dneu.20362

Klaassen, L. J., de Graaff, W., van Asselt, J. B., Klooster, J., and Kamermans, M. (2016). Specific connectivity between photoreceptors and horizontal cells in the zebrafish retina. *J. Neurophysiol.* 116, 2799–2814. doi: 10.1152/jn.00449.2016

Korenbrot, J. I., Mehta, M., Tserentsoodol, N., Postlethwait, J. H., and Rebrik, T. I. (2013). Eml1 (cng-modulin) controls light sensitivity in darkness and under continuous illumination in zebrafish retinal cone photoreceptors. *J. Neurosci.* 33, 17763–17776. doi: 10.1523/JNEUROSCI.2659-13.2013

Kumaran, N., Moore, A. T., Welebe, R. G., and Michaelides, M. (2017). Leber congenital amaurosis/early-onset severe retinal dystrophy: clinical features, molecular genetics and therapeutic interventions. *Br. J. Ophthalmol.* 101, 1147–1154. doi: 10.1136/bjophthalmol-2016-309975

Lazic, R., and Gabric, N. (2007). Verteporfin therapy and intravitreal bevacizumab combined and alone in choroidal neovascularization due to age-related macular degeneration. *Ophthalmology* 114, 1179–1185. doi: 10.1016/j.ophtha.2007.03.006

Lewis, P. M., Ayton, L. N., Guymer, R. H., Lowery, A. J., Blamey, P. J., Allen, P. J., et al. (2016). Advances in implantable bionic devices for blindness: a review. *ANZ J. Surg.* 86, 654–659. doi: 10.1111/ans.13616

Li, L., and Dowling, J. E. (1997). A dominant form of inherited retinal degeneration caused by a non-photoreceptor cell-specific mutation. *Proc. Natl. Acad. Sci. U.S.A.* 94, 11645–11650. doi: 10.1073/pnas.94.21.11645

Li, L., and Dowling, J. E. (2000). Disruption of the olfactoretinal centrifugal pathway may relate to the visual system defect in night blindness b mutant zebrafish. *J. Neurosci.* 20, 1883–1892. doi: 10.1523/JNEUROSCI.20-05-01883.2000

Li, Y. N., Matsui, J. I., and Dowling, J. E. (2009). Specificity of the horizontal cell-photoreceptor connections in the zebrafish (danio rerio) retina. *J. Comp. Neurol.* 516, 442–453. doi: 10.1002/cne.22135

Li, Y. N., Tsujimura, T., Kawamura, S., and Dowling, J. E. (2012). Bipolar cell-photoreceptor connectivity in the zebrafish (danio rerio) retina. *J. Comp. Neurol.* 520, 3786–3802. doi: 10.1002/cne.23168

Lin, S. Y., Vollrath, M. A., Mangosing, S., Shen, J., Cardenas, E., and Corey, D. P. (2016). The zebrafish pinball wizard gene encodes wrb, a tail-anchored-protein receptor essential for inner-ear hair cells and retinal photoreceptors. *J. Physiol.* 594, 895–914. doi: 10.1113/JP271437

Linder, B., Dill, H., Hirmer, A., Brocher, J., Lee, G. P., Mathavan, S., et al. (2011). Systemic splicing factor deficiency causes tissue-specific defects: a zebrafish model for retinitis pigmentosa†. *Hum. Mol. Genet.* 20, 368–377. doi: 10.1093/hmg/ddq473

Lindsey, A. E., and Powers, M. K. (2007). Visual behavior of adult goldfish with regenerating retina. *Vis. Neurosci.* 24, 247–255. doi: 10.1017/S0952523806230207

Liu, F., Chen, J., Yu, S., Raghupathy, R. K., Liu, X., and Qin, Y. (2015). Knockout of rp2 decreases grk1 and rod transducin subunits and leads to photoreceptor degeneration in zebrafish. *Hum. Mol. Genet.* 24, 4648–4659. doi: 10.1093/hmg/ddv197

Lombardo, F. (1968). La rigenerazione della retina negli adulti di un teleosteo. *Accad. Lincei Rend. Commun. Sci. Fish. Mat. Nat.* 45, 631–635.

Lust, K., and Wittbrodt, J. (2018). Activating the regenerative potential of Müller glia cells in a regeneration-deficient retina. *elife* 7:e32319. doi: 10.7554/eLife.32319

Lv, C., Gould, T. J., Bewersdorf, J., and Zenisek, D. (2012). High-resolution optical imaging of zebrafish larval ribbon synapse protein ribeye, rim2, and cav 1.4 by stimulation emission depletion microscopy. *Microsc. Microanal.* 18, 745–752. doi: 10.1017/S1431927612000268

MacDonald, R. B., Kashikar, N. D., Lagnado, L., and Harris, W. A. (2017). A novel tool to measure extracellular glutamate in the zebrafish nervous system in vivo. *Zebrafish* 14, 284–286. doi: 10.1089/zeb.2016.1385

MacLaren, R. E., Bennett, J., and Schwartz, S. D. (2016). Gene therapy and stem cell transplantation in retinal disease: the new frontier. *Ophthalmology* 123, S98–S106. doi: 10.1016/j.ophtha.2016.06.041

Macosko, E. Z., Basu, A., Satija, R., Nemesh, J., Shekhar, K., Goldman, M., et al. (2015). Highly parallel genome-wide expression profiling of individual cells using nanoliter droplets. *Cell* 161, 1202–1214. doi: 10.1016/j.cell.2015.05.002

Marvin, J. S., Borghuis, B. G., Tian, L., Cichon, J., Harnett, M. T., Akerboom, J., et al. (2013). An optimized fluorescent probe for visualizing glutamate neurotransmission. *Nat. Methods* 10, 162–170. doi: 10.1038/nmeth.2333

Mathew, L. K., Sengupta, S., Kawakami, A., Andreasen, E. A., Löhr, C. V., Loynes, C. A., et al. (2007). Unraveling tissue regeneration pathways using chemical genetics. *J. Biol. Chem.* 282, 35202–35210. doi: 10.1074/jbc.M706640200

McElligott, M. B., and O'Malley, D. M. (2005). Prey tracking by larval zebrafish: axial kinematics and visual control. *Brain Behav. Evol.* 66, 177–196. doi: 10.1159/000087158

McGinn, T. E., Mitchell, D. M., Meighan, P. C., Partington, N., Leoni, D. C., Jenkins, C. E., et al. (2018). Restoration of dendritic complexity, functional connectivity, and diversity of regenerated retinal bipolar neurons in adult zebrafish. *J. Neurosci.* 38, 120–136. doi: 10.1523/JNEUROSCI.3444-16.2017

Mensinger, A. F., and Powers, M. K. (1999). Visual function in regenerating teleost retina following cytotoxic lesioning. *Vis. Neurosci.* 16, 241–251. doi: 10.1017/S0952523899162059

Mensinger, A. F., and Powers, M. K. (2007). Visual function in regenerating teleost retina following surgical lesioning. *Vis. Neurosci.* 24, 299–307. doi: 10.1017/S0952523807070265

Miller, A. H., Howe, H. B., Krause, B. M., Friedle, S. A., Banks, M. I., Perkins, B. D., et al. (2018). Pregnancy associated plasma protein-aa (pappaa) regulates photoreceptor synaptic development to mediate visually guided behavior. *J. Neurosci.* 38, 5220–5236. doi: 10.1523/JNEUROSCI.0061-18.2018

Mills, J. O., Jalil, A., and Stanga, P. E. (2017). Electronic retinal implants and artificial vision: journey and present. *Eye* 31, 1383–1398. doi: 10.1038/eye.2017.65

Mitchell, D. M., Lovel, A. G., and Stenkamp, D. L. (2018). Dynamic changes in microglial and macrophage characteristics during degeneration and regeneration of the zebrafish retina. *J. Neuroinflammation* 15:163. doi: 10.1186/s12974-018-1185-6

Montgomery, J. E., Parsons, M. J., and Hyde, D. R. (2010). A novel model of retinal ablation demonstrates that the extent of rod cell death regulates the origin of the regenerated zebrafish rod photoreceptors. *J. Comp. Neurol.* 518, 800–814. doi: 10.1002/cne.22243

Moosajee, M., Gregory-Evans, K., Ellis, C. D., Seabra, M. C., and Gregory-Evans, C. Y. (2008). Translational bypass of nonsense mutations in zebrafish rep1, pax2.1 and lamb1 highlights a viable therapeutic option for untreatable genetic eye disease. *Hum. Mol. Genet.* 17, 3987–4000. doi: 10.1093/hmg/ddn302

Morris, A. C., Scholz, T. L., Brockerhoff, S. E., and Fadool, J. M. (2008). Genetic dissection reveals two separate pathways for rod and cone regeneration in the teleost retina. *Dev. Neurobiol.* 68, 605–619. doi: 10.1002/dneu.20610

Moshiri, A., Gonzalez, E., Tagawa, K., Maeda, H., Wang, M., Frishman, L. J., et al. (2008). Near complete loss of retinal ganglion cells in the math5/brn3b double knockout elicits severe reductions of other cell types during retinal development. *Dev. Biol.* 316, 214–227. doi: 10.1016/j.ydbio.2008.01.015

Nagashima, M., Barthel, L. K., and Raymond, P. A. (2013). A self-renewing division of zebrafish Müller glial cells generates neuronal progenitors that require n-cadherin to regenerate retinal neurons. *Development* 140, 4510–4521. doi: 10.1242/dev.090738

Namdaran, P., Reinhart, K. E., Owens, K. N., Raible, D. W., and Rubel, E. W. (2012). Identification of modulators of hair cell regeneration in the zebrafish lateral line. *J. Neurosci.* 32, 3516–3528. doi: 10.1523/JNEUROSCI.3905-11.2012

Nelson, R., and Singla, N. (2009). A spectral model for signal elements isolated from zebrafish photopic electroretinogram. *Vis. Neurosci.* 26, 349–363. doi: 10.1017/S0952523809990113

Nelson, S. M., Frey, R. A., Wardwell, S. L., and Stenkamp, D. L. (2008). The developmental sequence of gene expression within the rod photoreceptor lineage in embryonic zebrafish. *Dev. Dyn.* 237, 2903–2917. doi: 10.1002/dvdy.21721

Neuhauss, S. C. (2003). Behavioral genetic approaches to visual system development and function in zebrafish. *J. Neurobiol.* 54, 148–160. doi: 10.1002/neu.10165

Neuhauss, S. C., Biehlmaier, O., Seeliger, M. W., Das, T., Kohler, K., Harris, W. A., et al. (1999). Genetic disorders of vision revealed by a behavioral screen of 400 essential loci in zebrafish. *J. Neurosci.* 19, 8603–8615. doi: 10.1523/JNEUROSCI.19-19-08603.1999

Nicolson, T., Rüsch, A., Friedrich, R. W., Granato, M., Ruppersberg, J. P., Nüsslein-Volhard, C., et al. (1998). Genetic analysis of vertebrate sensory hair cell mechanosensation: the zebrafish circler mutants. *Neuron* 20, 271–283. doi: 10.1016/S0896-6273(00)80455-9

Noel, N. C. L., and Allison, W. T. (2018). Connectivity of cone photoreceptor telodendria in the zebrafish retina. *J. Comp. Neurol.* 526, 609–625. doi: 10.1002/cne.24354

Odermatt, B., Nikolaev, A., and Lagnado, L. (2012). Encoding of luminance and contrast by linear and nonlinear synapses in the retina. *Neuron* 73, 758–773. doi: 10.1016/j.neuron.2011.12.023

Orger, M. B., and Baier, H. (2005). Channeling of red and green cone inputs to the zebrafish optomotor response. *Vis. Neurosci.* 22, 275–281. doi: 10.1017/S0952523805223039

Ortin-Martinez, A., Tsai, E. L., Nickerson, P. E., Bergeret, M., Lu, Y., Smiley, S., et al. (2017). A reinterpretation of cell transplantation: Gfp transfer from donor to host photoreceptors. *Stem Cells* 35, 932–939. doi: 10.1002/stem.2552

Otteson, D. C., D'Costa, A. R., and Hitchcock, P. F. (2001). Putative stem cells and the lineage of rod photoreceptors in the mature retina of the goldfish. *Dev. Biol.* 232, 62–76. doi: 10.1006/dbio.2001.0163

Pardue, M. T., and Allen, R. S. (2018). Neuroprotective strategies for retinal disease. *Prog. Retin. Eye Res.* 65, 50–76. doi: 10.1016/j.preteyeres.2018.02.002

Patterson, B. W., Abraham, A. O., MacIver, M. A., and McLean, D. L. (2013). Visually guided gradation of prey capture movements in larval zebrafish. *J. Exp. Biol.* 216(Pt 16), 3071–3083. doi: 10.1242/jeb.087742

Pearson, R. A., Gonzalez-Cordero, A., West, E. L., Ribeiro, J. R., Aghaizu, N., Goh, D., et al. (2016). Donor and host photoreceptors engage in material transfer following transplantation of post-mitotic photoreceptor precursors. *Nat. Commun.* 7:13029. doi: 10.1038/ncomms13029

Pollak, J., Wilken, M. S., Ueki, Y., Cox, K. E., Sullivan, J. M., Taylor, R. J., et al. (2013). Ascl1 reprograms mouse Müller glia into neurogenic retinal progenitors. *Development* 140, 2619–2631. doi: 10.1242/dev.091355

Polosukhina, A., Litt, J., Tochitsky, I., Nemargut, J., Sychev, Y., De Kouchkovsky, I., et al. (2012). Photochemical restoration of visual responses in blind mice. *Neuron* 75, 271–282. doi: 10.1016/j.neuron.2012.05.022

Powell, C., Cornblath, E., Elsaeidi, F., Wan, J., and Goldman, D. (2016). Zebrafish Müller glia-derived progenitors are multipotent, exhibit proliferative biases and regenerate excess neurons. *Sci. Rep.* 6:24851. doi: 10.1038/srep24851

Ramachandran, R., Fausett, B. V., and Goldman, D. (2010a). Ascl1a regulates Müller glia dedifferentiation and retinal regeneration through a lin-28-dependent, let-7 microRNA signalling pathway. *Nat. Cell Biol.* 12, 1101–1107. doi: 10.1038/ncb2115

Ramachandran, R., Reifler, A., Parent, J. M., and Goldman, D. (2010b). Conditional gene expression and lineage tracing of tuba1a expressing cells during zebrafish development and retina regeneration. *J. Comp. Neurol.* 518, 4196–4212. doi: 10.1002/cne.22448

Randlett, O., MacDonald, R. B., Yoshimatsu, T., Almeida, A. D., Suzuki, S. C., Wong, R. O., et al. (2013). Cellular requirements for building a retinal neuropil. *Cell Rep.* 3, 282–290. doi: 10.1016/j.celrep.2013.01.020

Rao, M. B., Didiano, D., and Patton, J. G. (2017). Neurotransmitter-regulated regeneration in the zebrafish retina. *Stem Cell Rep.* 8, 831–842. doi: 10.1016/j.stemcr.2017.02.007

Raymond, P. A., Barthel, L. K., Bernardos, R. L., and Perkowski, J. J. (2006). Molecular characterization of retinal stem cells and their niches in adult zebrafish. *BMC Dev. Biol.* 6:36. doi: 10.1186/1471-213X-6-36

Raymond, P. A., Barthel, L. K., and Stenkam, D. L. (1996). The zebrafish ultraviolet cone opsin reported previously is expressed in rods. *Invest. Ophthalmol. Vis. Sci.* 37, 948–950.

Raymond, P. A., Reifler, M. J., and Rivlin, P. K. (1988). Regeneration of goldfish retina: rod precursors are a likely source of regenerated cells. *J. Neurobiol.* 19, 431–463. doi: 10.1002/neu.480190504

Salbreux, G., Barthel, L. K., Raymond, P. A., and Lubensky, D. K. (2012). Coupling mechanical deformations and planar cell polarity to create regular patterns in the zebrafish retina. *PLoS Comput. Biol.* 8:e1002618. doi: 10.1371/journal.pcbi.1002618

Santos-Ferreira, T., Llonch, S., Borsch, O., Postel, K., Haas, J., Ader, M., et al. (2016). Retinal transplantation of photoreceptors results in donor-host cytoplasmic exchange. *Nat. Commun.* 7:13028. doi: 10.1038/ncomms13028

Santos-Ferreira, T., Postel, K., Stutzki, H., Kurth, T., Zeck, G., and Ader, M. (2015). Daylight vision repair by cell transplantation. *Stem Cells* 33, 79–90. doi: 10.1002/stem.1824

Sarria, I., Cao, Y., Stutzki, H., Kurth, T., Zeck, G., Ader, M., et al. (2018). Lrit1 modulates adaptive changes in synaptic communication of cone photoreceptors. *Cell Rep.* 22, 3562–3573. doi: 10.1016/j.celrep.2018.03.008

Schroeter, E. H., Wong, R. O. L., and Gregg, R. G. (2006). In vivo development of retinal on-bipolar cell axonal terminals visualized in nyx::Myfp transgenic zebrafish. *Vis. Neurosci.* 23, 833–843. doi: 10.1017/S0952523806230219

Shah, A. N., Davey, C. F., Whitebirch, A. C., Miller, A. C., and Moens, C. B. (2016). Rapid reverse genetic screening using CRISPR in zebrafish. *Zebrafish* 13, 152–153. doi: 10.1089/zeb.2015.29000.sha

Shekhar, K., Lapan, S. W., Whitney, I. E., Tran, N. M., Macosko, E. Z., Kowalczyk, M., et al. (2016). Comprehensive classification of retinal bipolar neurons by single-cell transcriptomics. *Cell* 166, 1308–1323.e30. doi: 10.1016/j.cell.2016.07.054

Sherpa, T., Fimbel, S. M., Mallory, D. E., Maaswinkel, H., Spritzer, S. D., Sand, J. A., et al. (2008). Ganglion cell regeneration following whole-retina destruction in zebrafish. *Dev. Neurobiol.* 68, 166–181. doi: 10.1002/dneu.20568

Sherpa, T., Lankford, T., McGinn, T. E., Hunter, S. S., Frey, R. A., Sun, C., et al. (2014). Retinal regeneration is facilitated by the presence of surviving neurons. *Dev. Neurobiol.* 74, 851–876. doi: 10.1002/dneu.22167

Shi, Y., Obert, E., Rahman, B., Rohrer, B., and Lobo, G. P. (2017). The retinol binding protein receptor 2 (rbpr2) is required for photoreceptor outer segment morphogenesis and visual function in zebrafish. *Sci. Rep.* 7:16207. doi: 10.1038/s41598-017-16498-9

Silver, P. H. (1974). Photopic spectral sensitivity of the neon tetra [*Paracheirodon innesi* (Myers)] found by the use of a dorsal light reaction. *Vis. Res.* 14, 329–334. doi: 10.1016/0042-6989(74)90091-1

Simmons, A. B., Bloomsburg, S. J., Sukeena, J. M., Miller, C. J., Ortega-Burgos, Y., Borghuis, B. G., et al. (2017). DSCAM-mediated control of dendritic and axonal arbor outgrowth enforces tiling and inhibits synaptic plasticity. *Proc. Natl. Acad. Sci. U.S.A.* 114, E10224–E10233. doi: 10.1073/pnas.1713548114

Singh, M. S., Balmer, J., Barnard, A. R., Aslam, S. A., Moralli, D., Green, C. M., et al. (2016). Transplanted photoreceptor precursors transfer proteins to host photoreceptors by a mechanism of cytoplasmic fusion. *Nat. Commun.* 7:13537. doi: 10.1038/ncomms13537

Singh, M. S., Charbel Issa, P., Butler, R., Martin, C., Lipinski, D. M., Sekaran, S., et al. (2013). Reversal of end-stage retinal degeneration and restoration of visual function by photoreceptor transplantation. *Proc. Natl. Acad. Sci. U.S.A.* 110, 1101–1106. doi: 10.1073/pnas.1119416110

Smiley, S., Nickerson, P. E., Comanita, L., Daftarian, N., El-Sehemy, A., Tsai, E. L., et al. (2016). Establishment of a cone photoreceptor transplantation platform based on a novel cone-gfp reporter mouse line. *Sci. Rep.* 6:22867. doi: 10.1038/srep22867

Smyth, V. A., Di Lorenzo, D., and Kennedy, B. N. (2008). A novel, evolutionarily conserved enhancer of cone photoreceptor-specific expression. *J. Biol. Chem.* 283, 10881–10891. doi: 10.1074/jbc.M710454200

Solin, S. L., Wang, Y., Mauldin, J., Schultz, L. E., Lincow, D. E., Brodskiy, P. A., et al. (2014). Molecular and cellular characterization of a zebrafish optic pathway tumor line implicates glia-derived progenitors in tumorigenesis. *PLoS One* 9:e114888. doi: 10.1371/journal.pone.0114888

Stearns, G., Evangelista, M., Fadool, J. M., and Brockerhoff, S. E. (2007). A mutation in the cone-specific pde6 gene causes rapid cone photoreceptor degeneration in zebrafish. *J. Neurosci.* 27, 13866–13874. doi: 10.1523/JNEUROSCI.3136-07.2007

Stenkamp, D. L. (2015). Development of the vertebrate eye and retina. *Prog. Mol. Biol. Transl. Sci.* 134, 397–414. doi: 10.1016/bs.pmbts.2015.06.006

Stenkamp, D. L., and Cameron, D. A. (2002). Cellular pattern formation in the retina: retinal regeneration as a model system. *Mol. Vis.* 8, 280–293.

Stenkamp, D. L., Powers, M. K., Carney, L. H., and Cameron, D. A. (2001). Evidence for two distinct mechanisms of neurogenesis and cellular pattern formation in regenerated goldfish retinas. *J. Comp. Neurol.* 431, 363–381. doi: 10.1002/1096-9861(20010319)431:4<363::AID-CNE1076>3.0.CO;2-7

Stuermer, C. A. O., Niepenberg, A., and Wolburg, H. (1985). Aberrant axonal paths in regenerated goldfish retina and tectum opticum following intraocular injection of ouabain. *Neurosci. Lett.* 58, 333–338. doi: 10.1016/0304-3940(85)90076-X

Sun, C., Galicia, C., and Stenkamp, D. L. (2018). Transcripts within rod photoreceptors of the zebrafish retina. *BMC Genomics* 19:127. doi: 10.1186/s12864-018-4499-y

Suzuki, S. C., Bleckert, A., Williams, P. R., Takechi, M., Kawamura, S., Wong, R. O., et al. (2013). Cone photoreceptor types in zebrafish are generated by symmetric terminal divisions of dedicated precursors. *Proc. Natl. Acad. Sci. U.S.A.* 110, 15109–15114. doi: 10.1073/pnas.1303551110

Takechi, M., Hamaoka, T., and Kawamura, S. (2003). Fluorescence visualization of ultraviolet-sensitive cone photoreceptor development in living zebrafish. *FEBS Lett.* 553, 90–94. doi: 10.1016/S0014-5793(03)00977-3

Takechi, M., Seno, S., and Kawamura, S. (2008). Identification of cis-acting elements repressing blue opsin expression in zebrafish uv cones and pineal cells. *J. Biol. Chem.* 283, 31625–31632. doi: 10.1074/jbc.M806226200

Tappeiner, C., Balmer, J., Iglicki, M., Schuerch, K., Jazwinska, A., Enzmann, V., et al. (2013). Characteristics of rod regeneration in a novel zebrafish retinal degeneration model using n-methyl-n-nitrosourea (mnu). *PLoS One* 8:e71064. doi: 10.1371/journal.pone.0071064

Thomas, J. L., Nelson, C. M., Luo, X., Hyde, D. R., and Thummel, R. (2012). Characterization of multiple light damage paradigms reveals regional differences in photoreceptor loss. *Exp. Eye Res.* 97, 105–116. doi: 10.1016/j.exer.2012.02.004

Thomas, J. L., Ranski, A. H., Morgan, G. W., and Thummel, R. (2016). Reactive gliosis in the adult zebrafish retina. *Exp. Eye Res.* 143, 98–109. doi: 10.1016/j.exer.2015.09.017

Tochitsky, I., Trautman, J., Gallerani, N., Malis, J. G., and Kramer, R. H. (2017). Restoring visual function to the blind retina with a potent, safe and long-lasting photoswitch. *Sci. Rep.* 7:45487. doi: 10.1038/srep45487

Torvund, M. M., Ma, T. S., Connaughton, V. P., Ono, F., and Nelson, R. F. (2017). Cone signals in monostratified and bistratified amacrine cells of adult zebrafish retina. *J. Comp. Neurol.* 525, 2800–2801. doi: 10.1002/cne.24227

Trifunovic, D., Sahaboglu, A., Kaur, J., Mencl, S., Zrenner, E., Ueffing, M., et al. (2012). Neuroprotective strategies for the treatment of inherited photoreceptor degeneration. *Curr. Mol. Med.* 12, 598–612. doi: 10.2174/156652412800620048

Tsujimura, T., Chinen, A., and Kawamura, S. (2007). Identification of a locus control region for quadruplicated green-sensitive opsin genes in zebrafish. *Proc. Natl. Acad. Sci. U.S.A.* 104, 12813–12818. doi: 10.1073/pnas.0704061104

Tsujimura, T., Hosoya, T., and Kawamura, S. (2010). A single enhancer regulating the differential expression of duplicated red-sensitive opsin genes in zebrafish. *PLoS Genet.* 6:e1001245. doi: 10.1371/journal.pgen.1001245

Ueki, Y., Wilken, M. S., Cox, K. E., Chipman, L., Jorstad, N., Sternhagen, K., et al. (2015). Transgenic expression of the proneural transcription factor ascl1 in Müller glia stimulates retinal regeneration in young mice. *Proc. Natl. Acad. Sci. U.S.A.* 112, 13717–13722. doi: 10.1073/pnas.1510595112

Ueno, A., Omori, Y., Sugita, Y., Watanabe, S., Chaya, T., Kozuka, T., et al. (2018). Lrit1, a retinal transmembrane protein, regulates selective synapse formation in cone photoreceptor cells and visual acuity. *Cell Rep.* 22, 3548–3561. doi: 10.1016/j.celrep.2018.03.007

Varshney, G. K., Carrington, B., Pei, W., Bishop, K., Chen, Z., Fan, C., et al. (2016). A high-throughput functional genomics workflow based on crispr/cas9-mediated targeted mutagenesis in zebrafish. *Nat. Protoc.* 11, 2357–2375. doi: 10.1038/nprot.2016.141

Varshney, G. K., Pei, W., LaFave, M. C., Idol, J., Xu, L., Gallardo, V., et al. (2015). High-throughput gene targeting and phenotyping in zebrafish using crispr/cas9. *Genome Res.* 25, 1030–1042. doi: 10.1101/gr.186379.114

Veldman, M. B., Bemben, M. A., Thompson, R. C., and Goldman, D. (2007). Gene expression analysis of zebrafish retinal ganglion cells during optic nerve regeneration identifies klf6a and klf7a as important regulators of axon regeneration. *Dev. Biol.* 312, 596–612. doi: 10.1016/j.ydbio.2007.09.019

Vihtelic, T. S., Doro, C. J., and Hyde, D. R. (1999). Cloning and characterization of six zebrafish photoreceptor opsin cDNAS and immunolocalization of their corresponding proteins. *Vis. Neurosci.* 16, 571–585. doi: 10.1017/S0952523899163168

Vihtelic Thomas, S., and Hyde David, R. (2000). Light-induced rod and cone cell death and regeneration in the adult albino zebrafish (danio rerio) retina. *J. Neurobiol.* 44, 289–307. doi: 10.1002/1097-4695(20000905)44:3<289::AID-NEU1>3.0.CO;2-H

Vitorino, M., Jusuf, P. R., Maurus, D., Kimura, Y., Higashijima, S.-I., and Harri, W. A. (2009). Vsx2 in the zebrafish retina: restricted lineages through derepression. *Neural Dev.* 4:14. doi: 10.1186/1749-8104-4-14

Wahlin, K. J., Maruotti, J. A., Maurus, D., Kimura, Y., Higashijima, S., and Harris, W. A. (2017). Photoreceptor outer segment-like structures in long-term 3d retinas from human pluripotent stem cells. *Sci. Rep.* 7:766. doi: 10.1038/s41598-017-00774-9

Waldron, P. V., Di Marco, F., Kruczek, K., Ribeiro, J., Graca, A. B., Hippert, C., et al. (2018). Transplanted donor- or stem cell-derived cone photoreceptors can both integrate and undergo material transfer in an environment-dependent manner. *Stem Cell Rep.* 10, 406–421. doi: 10.1016/j.stemcr.2017.12.008

Wan, J., and Goldman, D. (2016). Retina regeneration in zebrafish. *Curr. Opin. Genet. Dev.* 40, 41–47. doi: 10.1016/j.gde.2016.05.009

Wan, J., Zhao, X.-F., Vojtek, A., and Goldman, D. (2014). Retinal injury, growth factors and cytokines converge on β-catenin and pstat3 signaling to stimulate retina regeneration. *Cell Rep.* 9, 285–297. doi: 10.1016/j.celrep.2014.08.048

Wan, J., Zheng, H., Chen, Z. L., Xiao, H. L., Shen, Z. J., Zhou, G. M., et al. (2008). Preferential regeneration of photoreceptor from Müller glia after retinal degeneration in adult rat. *Vis. Res.* 48, 223–234. doi: 10.1016/j.visres.2007.11.002

Wang, Y., Fehlhaber, K. E., Sarria, I., Cao, Y., Ingram, N. T., Guerrero-Given, D., et al. (2017). The auxiliary calcium channel subunit alpha2delta4 is required for axonal elaboration, synaptic transmission, and wiring of rod photoreceptors. *Neuron* 93, 1359–1374.e6. doi: 10.1016/j.neuron.2017.02.021

Warwick, A., and Lotery, A. (2018). Genetics and genetic testing for age-related macular degeneration. *Eye* 32, 849–857. doi: 10.1038/eye.2017.245

Weber, I. P., Ramos, A. P., Strzyz, P. J., Leung, L. C., Young, S., and Norden, C. (2014). Mitotic position and morphology of committed precursor cells in the zebrafish retina adapt to architectural changes upon tissue maturation. *Cell Rep.* 7, 386–397. doi: 10.1016/j.celrep.2014.03.014

White, D. T., Sengupta, S., Saxena, M. T., Xu, Q., Hanes, J., Ding, D., et al. (2017). Immunomodulation-accelerated neuronal regeneration following selective rod photoreceptor cell ablation in the zebrafish retina. *Proc. Natl. Acad. Sci. U.S.A.* 114, E3719–E3728. doi: 10.1073/pnas.1617721114

White, R. M., Sessa, A., Burke, C., Bowman, T., LeBlanc, J., Ceol, C., et al. (2008). Transparent adult zebrafish as a tool for in vivo transplantation analysis. *Cell Stem Cell* 2, 183–189. doi: 10.1016/j.stem.2007.11.002

Williams, P. R., Suzuki, S. C., Yoshimatsu, T., Lawrence, O. T., Waldron, S. J., Parsons, M. J., et al. (2010). In vivo development of outer retinal synapses in the absence of glial contact. *J. Neurosci.* 30, 11951–11961. doi: 10.1523/JNEUROSCI.3391-10.2010

Yazulla, S., and Studholme, K. M. (2001). Neurochemical anatomy of the zebrafish retina as determined by immunocytochemistry. *J. Neurocytol.* 30, 551–592. doi: 10.1023/A:1016512617484

Yin, J., Brocher, J., Linder, B., Hirmer, A., Sundaramurthi, H., Fischer, U., et al. (2012). The 1d4 antibody labels outer segments of long double cone but not rod photoreceptors in zebrafish. *Invest. Ophthalmol. Vis. Sci.* 53, 4943–4951. doi: 10.1167/iovs.12-9511

Yoshimatsu, T., D'Orazi, F. D., Gamlin, C. R., Suzuki, S. C., Suli, A., Kimelman, D., et al. (2016). Presynaptic partner selection during retinal circuit reassembly varies with timing of neuronal regeneration in vivo. *Nat. Commun.* 7:10590. doi: 10.1038/ncomms10590

Yue, L., Weiland, J. D., Roska, B., and Humayun, M. S. (2016). Retinal stimulation strategies to restore vision: fundamentals and systems. *Prog. Retin. Eye Res.* 53, 21–47. doi: 10.1016/j.preteyeres.2016.05.002

Zhang, C., Kolodkin, A. L., Wong, R. O., and James, R. E. (2017). Establishing wiring specificity in visual system circuits: from the retina to the brain. *Annu. Rev. Neurosci.* 40, 395–424. doi: 10.1146/annurev-neuro-072116-031607

Zhang, Q. X., He, X. J., Wong, H. C., and Kindt, K. S. (2016). Functional calcium imaging in zebrafish lateral-line hair cells. *Methods Cell. Biol.* 133, 229–252. doi: 10.1016/bs.mcb.2015.12.002

Zhang, Y., Yang, Y., Trujillo, C., Zhong, W., and Leung, Y. F. (2012). The expression of irx7 in the inner nuclear layer of zebrafish retina is essential for a proper retinal development and lamination. *PLoS One* 7:e36145. doi: 10.1371/journal.pone.0036145

Zhao, X. F., Ellingsen, S., and Fjose, A. (2009). Labelling and targeted ablation of specific bipolar cell types in the zebrafish retina. *BMC Neurosci.* 10:107. doi: 10.1186/1471-2202-10-107

Zhong, X., Gutierrez, C., Xue, T., Hampton, C., Vergara, M. N., Cao, L. H., et al. (2014). Generation of three dimensional retinal tissue with functional photoreceptors from human ipscs. *Nat. Commun.* 5:4047. doi: 10.1038/ncomms5047

Conflict of Interest Statement: The authors declare that the research was conducted in the absence of any commercial or financial relationships that could be construed as a potential conflict of interest.

frontiers in Cell and Developmental Biology

REVIEW
published: 20 September 2018
doi: 10.3389/fcell.2018.00115

Genetic Models of Leukemia in Zebrafish

*Jeremy T. Baeten and Jill L. O. de Jong**

Department of Pediatrics, University of Chicago, Chicago, IL, United States

The zebrafish animal model is gaining increasing popularity as a tool for studying human disease. Over the past 15 years, many models of leukemia and other hematological malignancies have been developed in the zebrafish. These confer some significant advantages over similar models in other animals and systems, representing a powerful resource for investigation of the molecular basis of human leukemia. This review discusses the various zebrafish models of lymphoid and myeloid leukemia available, the major discoveries that have been made possible by them, and opportunities for future exploration.

Keywords: zebrafish, leukemia, animal models, ALL, AML, MDS, MPN

OPEN ACCESS

Edited by:
Rebecca Ann Wingert, University of Notre Dame, United States

Reviewed by:
Lasse Dahl Ejby Jensen, Linköping University, Sweden
Eirini Trompouki, Max-Planck-Institut für Immunbiologie und Epigenetik, Germany

***Correspondence:**
Jill L. O. de Jong
jdejong@peds.bsd.uchicago.edu

Specialty section:
This article was submitted to Molecular Medicine, a section of the journal Frontiers in Cell and Developmental Biology

Received: *30 April 2018*
Accepted: *23 August 2018*
Published: *20 September 2018*

Citation:
Baeten JT and de Jong JLO (2018) Genetic Models of Leukemia in Zebrafish. Front. Cell Dev. Biol. 6:115. doi: 10.3389/fcell.2018.00115

INTRODUCTION

Leukemia

Leukemia is a broad designation encompassing hematological malignancies that produce the expansion of blood cells, typically starting in the bone marrow. In 2015, there were over 2.3 million patients suffering from leukemia, resulting in over 350,000 deaths worldwide (GBD 2015 Mortality and causes of death collaborators, 2016). In the United States, an estimated 62,130 new leukemia cases were diagnosed and 24,500 deaths caused by leukemia in 2017, with a 5 years survival rate of ∼63% (NCI SEER Cancer Stat Facts: Leukemia). Although the majority of leukemias affect adults, leukemia is also the most common cancer diagnosis in children.

Leukemias are categorized by two major criteria into four groups. The first criterion relates to the cell of origin: leukemias of lymphoid origin are classified "lymphocytic or lymphoblastic" and those of myeloid origin called "myelogenous or myeloid." The second criterion deems rapidly growing leukemias as "acute" and those with more indolent growth as "chronic." The causes of these different malignancies are varied. Some are directly linked to a chromosomal abnormality, such as the Philadelphia chromosome in chronic myelogenous leukemia (Bartram et al., 1983) or the increased incidence of leukemia in patients with trisomy 21 (down syndrome) (Evans and Steward, 1972). However, the etiology of most leukemias is less straightforward. Some leukemias involve mutations and/or translocations of multiple genes associated with growth, differentiation and survival of blood cells. Others have a normal karyotype and no known genetic mutations, highlighting the need for further studies in animal models to uncover these unknown drivers of hematopoietic malignancy.

Zebrafish as a Model Organism

Danio rerio, commonly known as the zebrafish, is a small tropical fish popular in pet stores and aquariums. Since the 1970's when George Streisinger first began using the zebrafish as a model organism (Walker and Streisinger, 1983), more and more labs have begun utilizing this powerful tool for studying development and disease due to numerous advantages over other model systems (**Figure 1**).

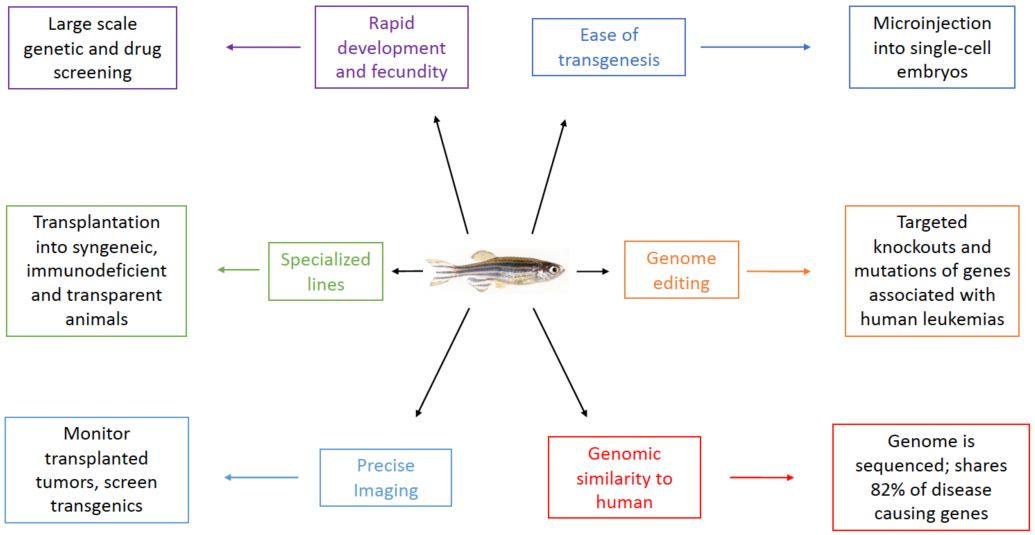

FIGURE 1 | Advantages of the zebrafish model for leukemia research.

Zebrafish fertilization and development occurs externally in optically clear embryos that are easily observed and manipulated. Development is much faster than mammals, with most major organs forming by 2–3 days post-fertilization (dpf). Animals reach sexual maturity by 2–3 months of age (Kimmel et al., 1995) and a single breeding pair produces several hundred embryos weekly. This fecundity coupled with their rapid development makes the zebrafish an excellent model for large-scale screening. Forward and reverse genetic screens as well as toxicity and drug screens in zebrafish have been performed around the world over the past three decades (Ransom et al., 1996; Weinberg et al., 1996; Sood et al., 2006; North et al., 2007; Ridges et al., 2012), including significant work more recently to evaluate therapeutics in zebrafish leukemia models (Mizgirev and Revskoy, 2010; Deveau et al., 2017). Although teleosts (like the zebrafish) and mammals diverged from a common ancestor approximately 340 million years ago, they still share a remarkable amount of their genomes, with a zebrafish ortholog identified for 82% of known disease-causing genes in humans (Howe et al., 2013). Many of these zebrafish genes have already been shown to recapitulate human disease when affected in zebrafish, including several connected to hematopoiesis (Brownlie et al., 1998; Wang et al., 1998) and cancer, as we will discuss in this review.

Several systems have been developed within the zebrafish model to create transgenic and knockout animals. Because the zebrafish embryos are externally developed, it is possible to microinject directly into the single-cell for the first 15–30 min following fertilization. Although, the first transgenic zebrafish were created through injection of naked, linearized DNA (Stuart et al., 1988), more efficient systems of genomic incorporation are now available. The tol2 transposon system creates randomly inserted transgenes that heavily favor single copy insertions (Urasaki et al., 2006) and the I-SceI meganuclease system inserts one or more copies into double-stranded breaks in the genome (Grabher et al., 2004; Ogino et al., 2006). In addition to the ability to integrate transgenes, the advent of CRISPR/Cas9 technology has made it possible to directly edit the zebrafish genome; from creating knockouts to mimicking human mutations to introducing specific SNPs. The use of CRISPR/Cas9 in zebrafish was first described by Keith Joung's lab in 2013 (Hwang et al., 2013), and has since spread throughout the field to become a common tool in many labs' arsenal, just as it has throughout the biomedical community at large (Hruscha et al., 2013; Ablain et al., 2015).

Over the years, the zebrafish community has amassed a large number of inbred, transgenic, knockout, or other specialized lines that have been characterized and maintained for various applications. Important to leukemia models are several lines that allow for transplantation of tumors without the need for pre-transplant immune ablation. Generated by parthenogenesis, the clonal golden lines (CG1 and CG2) allow for syngeneic transplantation within a genetically identical line, similar to transplantation experiments using inbred mice (Mizgireuv and Revskoy, 2006; Smith et al., 2010). The *rag2* (E450fs) mutant line has reduced numbers of functional T- and B-cells, and thus is unable to mount a significant immune response against transplanted cells (Tang et al., 2014). The *c-myb*^{I181N} hypomorphic mutant is another immunocompromised line that has shown promise in xenograft experiments (Hess and Boehm, 2016). These lines allow for immunologically unmatched transplantation from other zebrafish lines as well as xenografts.

A common challenge for many model systems is the ability to visualize and trace the fate of a cancer cell within an animal over time. These issues are often circumvented by euthanizing, sectioning, and staining multiple animals at different timepoints, however, this increases the number of animals required, increases time commitment, and may blur inter-individual variability. In the zebrafish, fluorescently tagged proteins or cells can be clearly imaged from embryo to adulthood in live animals by confocal or lightsheet microscopy (Kaufmann et al., 2012) and at even

greater resolutions in the pigment-less Casper line (White et al., 2008). An excellent example of this utility was described by Kaufman et al. (2016), when they used a *crestin-EGFP* line to show melanoma initiation and progression from a single cell. Also, with the macroscope developed by the Langeneau lab, high-throughput imaging of adult fish is possible for transgenic lines or screening for tumor engraftment in transplantation models (Blackburn et al., 2011).

Hematopoiesis: Zebrafish and Human

Many of the transcription factors and major signaling pathways controlling hematopoietic differentiation are mutated or dysregulated in the transformation and progression of leukemia. Therefore, in addition to the general advantages described above, the zebrafish is an appealing model for studying leukemia because of the close parallels to mammalian hematopoiesis (de Jong and Zon, 2005). Though the locations of hematopoiesis are not perfectly shared between species, the ontogeny of the different hematopoietic cells from progenitors to maturity, as well as the genes and pathways driving differentiation are well conserved (Paik and Zon, 2010). There are two distinct waves of hematopoiesis in all vertebrates; a transient primitive wave supplying necessary macrophages and erythrocytes for early embryonic development, followed by the definitive wave that gives rise to the full complement of blood cells throughout an animal's lifetime. In mammalian development, the primitive hematopoietic stem cells (HSCs) appear within the blood islands in the embryonic yolk sac (Palis and Yoder, 2001). In zebrafish, these limited HSCs instead arise from the intermediate cell mass (ICM) within the ventral mesoderm, and, similarly, produce erythrocytes and other myeloid cells (Detrich et al., 1995). Expression of the transcription factors *scl*, *gata2*, *lmo2*, *tif1*γ, and *fli1* promotes the primitive HSC lineage (Liao et al., 1998; Thompson et al., 1998; Ransom et al., 2004), while *gata1* and *spi1* (also known as *pu.1)* drive their differentiation into the erythroid and myeloid lineages, respectively (Detrich et al., 1995; Lieschke et al., 2002).

The mammalian definitive wave of hematopoiesis begins with true multipotent HSCs emerging from the ventral wall of the dorsal aorta in the aorta-gonad-mesenephros (AGM) region that then migrate to the fetal liver to proliferate and differentiate, and ultimately migrate to seed the bone marrow (Cumano and Godin, 2007). This process is mirrored in the zebrafish with the definitive HSCs also arising from the ventral wall of the dorsal aorta, and migrating to the caudal hematopoietic tissue (CHT) before seeding the kidney marrow, which is the zebrafish adult hematopoietic tissue (Burns et al., 2002; Jin et al., 2007). Definitive HSCs are true multipotent hematopoietic progenitors and are marked by their expression of the transcription factors *runx1*, *c-myb*, *lmo-2*, and *scl* (Thompson et al., 1998; Burns et al., 2002). Similar to primitive hematopoiesis, *gata1* and *tif1*γ drive erythropoiesis (Detrich et al., 1995; Ransom et al., 2004) and *spi1* and *c/ebp1* drive myelopoiesis (Lyons et al., 2001; Lieschke et al., 2002). Unlike the primitive lineages, definitive HSCs also produce lymphoid cells through expression of *rag1*, *rag2*, *ikaros*, *lck*, and *gata3* (Willett et al., 1997, 2001; Langenau et al., 2004). There are several functional and structural differences in the hematopoietic system of zebrafish compared to mammals, namely the location of the marrow, the lack of lymph nodes, and the rapid development and early reliance on the innate immune system (Novoa and Figueras, 2012; Renshaw and Trede, 2012). However, ultimately the blood cells of the zebrafish and human are molecularly very similar and thus have common genetic drivers of leukemia.

The conservation of the genes and pathways regulating hematopoiesis between humans and zebrafish, combined with the significant technical advantages provided by this model animal, make the zebrafish an ideal system for investigating hematological malignancies. In this review, we will examine the many leukemia models that have been developed within the zebrafish, and discuss the major findings made possible by each model that have advanced our understanding of human leukemia.

ZEBRAFISH LEUKEMIA MODELS: LYMPHOID ORIGIN

The first leukemia model in zebrafish was developed over 15 years ago using the lymphocyte-specific *rag2* promoter driving the murine *c-Myc* oncogene to produce T-cell acute lymphoblastic leukemia (T-ALL) (Langenau et al., 2003). The success of that first step has spawned a variety of other models tied to different types of leukemia. Over time, these models have been altered and improved to fit the particular investigations of each project, and there are now multiple similar models available, each with their own strengths and weaknesses (**Table 1**). This section discusses models of lymphoid origin, and the major discoveries made possible by them.

T-cell Acute Lymphoblastic Leukemia (T-ALL)

The majority of lymphoid leukemia models in zebrafish replicate T-ALL, partially due to the success of the *rag2* promoter in driving that particular malignancy. Although *rag2* is expressed in both T- and B-cell precursors in zebrafish (Langenau et al., 2004), only T-cell leukemias were initially identified from models utilizing this promoter. Interestingly, the Langenau lab has recently published a brief communication describing a subset of B-cell derived and bi-phenotypic leukemias produced from a rag2 promoter (Garcia et al., 2018), suggesting some of the research done on these T-ALL models may have unknown contributions from B-ALL as well.

The oncogene *c-Myc* is associated with many cancers and is one of the most frequently affected gene pathways in lymphoid leukemia (La Starza et al., 2014). The first T-ALL model was developed by Langenau et al. by expressing the murine *c-Myc* oncogene under the zebrafish *rag2* promoter, with an EGFP tag for easy monitoring by fluorescent microscopy (Langenau et al., 2003). Tumors were generated in microinjected mosaic F_0 fish at similar rates to *EGFP* expression in control animals injected with *rag2*: *EGFP*, suggesting complete penetrance of tumor induction upon successful integration of the *c-Myc* transgene. These tumors grew rapidly, with a mean latency of 52 days post-fertilization (dpf), extensively infiltrating the entirety of the

TABLE 1 | Zebrafish leukemia models of lymphoid origin.

Model	Gene/pathway; expression	Model features	Major findings
T-ALL			
rag2: EGFP-mMyc	Murine *c-Myc* oncogene (*mMyc*); thymus	Stable transgenesis of GFP-tagged *Myc*, line must be propagated by IVF	First leukemia model in zebrafish, similar disease progression to human T-ALL (Langenau et al., 2003)
Microinjected rag2: EGFP-mMyc		GFP-tagged, microinjected into single-cell embryos	Non-IR transplantation in CG1 line (Smith et al., 2010); undergo clonal evolution, AKT activation increases LSCs and resistance (Blackburn et al., 2014); subset of B-ALL and bi-phenotypic tumors (Garcia et al., 2018)
rag2: Myc-ER;	Tamoxifen-inducible *mMyc*; thymus	4OHT treatment after 5 dpf, induction at ∼35 dpf, not fluorescently labeled	Loss of *Myc* leads to apoptosis, PTEN/AKT-MYC axis (Gutierrez et al., 2011); loss of *bim* promotes *Myc*-independent T-ALL survival (Reynolds et al., 2014)
rag2: loxP-dsRed2-loxP-EGFP-mMyc	Cre-inducible *mMyc*; thymus	Cre-induces *mMyc* transformation and red to green color change; 81% efficient with *hsp70:Cre* and heat shock (Feng et al., 2007)	Progression similar to *rag2: EGFP-mMyc* (Langenau et al., 2005); with *rag2-EGFP-bcl-2*: accelerates T-LBL and autophagy, inhibits T-ALL progression and intravasation (Feng et al., 2010)
rag2: EGFP-ICN1	*notch1* intracellular domain; thymus	High latency (∼11 months), GFP-tagged	Increased expression of Notch targets *her6/9*; cooperation with *rag2-EGFP-bcl-2* increases onset/incidence, survival and resistance to irradiation (Chen et al., 2007); enhances T-ALL progression in combination *with rag2:cMyc,* does not increase LSC frequency, molecularly similar to human disease (Blackburn et al., 2012)
Srk *Hlk* *Otg*	ENU mediated mutagenesis in *Lck:EGFP lines;* thymus	Genes affected not reported; high latency (5–10 months to incidence)	Establishes viability of mutagenesis screen, serially transplanted tumors are increasingly malignant (Frazer et al., 2009)
B-ALL			
β-*actin: EGFP-TEL-AML1*	Human *TEL-AML1* (ETV6-RUNX1) fusion; global	Low incidence (3%), long latency (8–12 months); similar to CD10+ preB-ALL	Only zebrafish model of B-ALL; Likely requires secondary mutation; deregulation of survival genes; *rag2*- driven *TEL-AML* does not produce B-ALL, needs early precursor expression (Sabaawy et al., 2006)
xEf1α:EGFP-TEL-AML1			

fish. Analysis of the expression profiles and T-cell receptor (TCR) rearrangements confirmed that the tumor cells derived from clonal expansion of transformed T lymphocyte precursors and originated in the thymus. Tumor cells could be transplanted into irradiated recipients and quickly grew new tumors that homed to the thymus before spreading throughout the animal. Overall, the tumors progressed, similarly, to human T-ALL, at an accelerated pace. However, most F1 progeny developed advanced disease well before reaching sexual maturity (mean latency 32 dpf), necessitating sperm collection and *in vitro* fertilization (IVF) to continue the stable transgenic line. Subsequent characterization of this model showed that the tumors express *tal1/scl* and *lmo2*, genes associated with a molecular subgroup of *Myc*-induced T-ALL in humans (Langenau et al., 2005).

To circumvent the necessity of IVF, Langenau et al. sought to create an inducible version of their model. They achieved this by inserting a loxP-DsRed2-loxP sequence cassette between the *rag2* promoter and *EGFP-mMyc* oncogene, creating the *rag2:loxP-dsRed2-loxP-EGFP-mMyc* line (*rag2: LDL-Emyc*) (Langenau et al., 2005). This allowed for default red fluorescent expression with a switch to *EGFP-mMyc* expression in the presence of Cre recombinase. The disease in these animals was morphologically similar to that in the *rag2:EGFP-mMyc* model, but with significantly decreased incidence (6.5%) and delayed latency (mean 151 dpf). This was presumed to be due to incomplete recombination of the transgene, as evidenced by the persistence of red fluorescent expression within the tumor. To combat this, they developed a heat shock-inducible Cre line, *hsp70: Cre* (Feng et al., 2007). When combined with their Cre-inducible *rag2: LDL-Emyc* line and subjected embryos to heat shock at 3 dpf, the penetrance (81%) and latency (120 dpf) were closer to those of the original *rag2: EGFP-mMyc* model. This improved model allowed them to explore the molecular events governing the progression of the disease from the localized T-lymphoblastic lymphoma (T-LBL) to disseminated T-ALL. All of the Myc-induced models of T-ALL in zebrafish begin as T-LBL with thymic hyperplasia and localized outgrowth before advancing to T-ALL and expanding

into the circulation and other tissues. The investigation into this transition led them to combine the *rag2:LDL-Emyc; hsp70:Cre* model with a line overexpressing the survival gene *bcl2* (Feng et al., 2010). This combination accelerated T-LBL induction by suppressing Myc-induced apoptosis. However, it also promoted homotypic cell adhesion through *s1p1* and *icam1* that prevented intravasation into the vascular space and restricted the tumor to the thymus. The tumor cells then proliferated until they exhausted their nutrient supply and underwent autophagy. Because AKT-signaling is known to promote T-cell migration and to suppress autophagy (Sotsios and Ward, 2000; Lum et al., 2005), they hypothesized that addition of constitutively active AKT could force progression to T-ALL. Indeed, when their *Myc;Cre;bcl-2* embryos were injected with a myristolated-*akt2* transgene, the resulting tumors rapidly advanced to T-ALL (Feng et al., 2010).

The importance of AKT signaling in zebrafish T-ALL progression is not surprising, given the PTEN-PI3K-AKT pathway is frequently disrupted in human T-ALL (Palomero et al., 2008; Gutierrez et al., 2009). Gutierrez et al. further investigated this connection with the aid of another *Myc*-induced model, the tamoxifen inducible *rag2: Myc-ER* line (Gutierrez et al., 2011). This model allows for conditional expression of the *c-Myc* oncogene only in the presence of 4-hydroxytamoxifen (4-OHT). When continually treated with 4-OHT these fish develop T-ALL, but upon cessation of treatment and loss of *c-Myc* expression, the tumor cells undergo apoptosis and the tumor rapidly regresses. However, when AKT signaling was increased through either loss-of-function mutations in *pten* or constitutively active *akt2*, the tumors lost their dependence on *Myc* expression and were able to continue progression after removal of 4-OHT treatment. Further investigation into the relationship between *Myc* and the AKT pathway revealed that *Myc* drove the expression of the proapoptotic protein *bim*, while the constitutively active myr-*akt2* blocked that induction (Reynolds et al., 2014). Additionally, loss-of-function *bim* mutations allowed for increased persistence of T-ALL after cessation of 4-OHT treatment and *Myc* expression. Overall, these results suggest AKT-signaling enhances *Myc*-induced T-ALL progression via promotion of T-cell migration, suppression of autophagy, and inhibition of apoptosis.

Due to difficulty maintaining stable transgenic lines expressing *c-Myc,* an alternative approach was developed involving co-injection of the *rag2-EGFP* and *rag2-mMyc* transgenes into single-cell embryos (Langenau et al., 2008; Smith et al., 2010). In this model, the two transgenes randomly integrated into the genome to be co-expressed such that GFP expression was observed only in tumors and tumor induction only with GFP+ thymocytes. The resulting tumors followed the same pathology as the stable *Myc*-induced models. Smith et al. (2010) used this method to create tumors in clonal CG1 fish, demonstrating that they could be transplanted into syngeneic recipient CG1 fish without irradiation. This also allowed them to determine the frequency of leukemia stem cells (LSCs) present in these tumors through limit dilution analysis of the transplanted tumors. Each successful engraftment requires at least one LSC, and by transplanting different doses of cells, they were able to determine that 0.1–1.4% of the primary T-ALL tumor cells were LSCs. Transplantation of T-ALLs generated using this co-injection model was further investigated by Blackburn et al. (2014) who demonstrated that serial transplantation of T-ALL tumors led to spontaneous clonal evolution of monoclonal tumor subclones. As tumors were passaged from primary to secondary to tertiary recipients, some subclones evolved increased LSC frequency, growth, and/or resistance to therapy. Subclones with increased LSC frequency also displayed increased AKT phosphorylation, and treatment with an AKT inhibitor dramatically reduced their engraftment after transplant. Co-expression of myr-*akt2* with *Myc* significantly increased proliferation of tumor cells, decreased latency after transplantation, and increased LSC frequency sixfold, and these effects are at least partially due to AKT's induction of *mtorc1* expression. Additionally, the subclones that had evolved glucocorticoid resistance were resensitized to dexamethasone treatment by AKT inhibitors. Altogether, these results provided further evidence of the connection between *Myc* and AKT in T-ALL.

Another major player in the transformation of T-cell precursors to T-ALL is *Notch1*, which has activating mutations in over 65% of T-ALL patients (Weng et al., 2004). To further study the role of *Notch1* in T-ALL, Chen et al. (2007) created a transgenic line expressing *rag2:ICN1-EGFP*, a GFP-tagged *Notch1* intracellular domain which acts as a constitutively active transcription factor to drive Notch target gene expression. This line develops T-ALL, but at a lower incidence (40%) and higher latency (>11 months) than the *Myc*-driven tumors. However, in the presence of bcl2 overexpression, the incidence (60–80%) and latency (40 dpf to induction; 3 months to dissemination) were significantly enhanced and apoptosis was decreased. Blackburn et al. further demonstrated this by combining the *rag2:ICN1-EGFP* and *rag2:cMyc* models which accelerated leukemia onset and incidence (Blackburn et al., 2012). They concluded that Notch signaling expanded pre-leukemic clones that required Myc (or acquired secondary mutations) to transform, and that Notch signaling did not increase the overall frequency of LSCs. They also used this model to make cross-species microarray comparisons with mouse and human T-ALL to identify a common T-ALL gene signature and novel Notch gene expression profile present in humans that is regulated independently of Myc. These two studies suggest that *Notch1* activation alone is not sufficient for induction of T-ALL and requires additional oncogene activation and/or tumor suppressor mutations.

Taking advantage of the ability to perform large-scale forward-genetic screens in zebrafish to identify genetic modifiers of disease, Frazer et al. (2009) developed one such screen for causative mutations in T-ALL using ENU-mediated mutagenesis of an *lck-EGFP* line. This screen identified three mutant lines that developed outgrowth of the GFP-tagged thymus and subsequently T-ALL. Two of these lines, *shrek (srk)* and *hulk (hlk),* contained dominant mutations and one dubbed *Oscar-the-grouch (otg)* contained a recessive mutation. Homozygous fish from all 3 lines had incidences around 50% and time to tumor induction between 6 and 8 months. The mutated genes in these lines have not yet been reported, but the screen demonstrates the potential

for identification of genes driving different leukemias. The lab also developed a chemical screen to identify small molecules capable of eradicating immature T-cells, using the same *lck-EGFP* line (Ridges et al., 2012). They identified Lenaldekar (LDK; 1H-indole-3-carbaldehyde 8-quinolinylhydrazone) as a compound capable of killing both normal and T-ALL blasts in zebrafish, and showed it was effective in mouse xenograft and human primary leukemia cells as well.

B-Cell Acute Lymphoblastic Leukemia (B-ALL)

The *TEL-AML1* (also known as *ETV6-RUNX1*) fusion protein results from t(12;21), the most common translocation in childhood cancer, present in ∼25% of B-cell acute lymphoblastic leukemia (B-ALL) (Romana et al., 1995). However, attempts to produce a model of B-ALL from this fusion gene were unsuccessful in mice (Andreasson et al., 2001). Sabaawy et al. (2006) created multiple lines expressing human *TEL-AML1* from different promoters in zebrafish and were able to produce the only zebrafish model of B-ALL. Three different promoters were tested: the Xenopus *ef1a (Xef1a)* and zebrafish *beta-actin (zba)* for global expression, and zebrafish *rag2* for lymphocyte specific expression. Both of the global promoters produced B-ALL tumors in ∼3% of fish with 8–12 months latency and similar molecular and morphological features to pediatric CD10+ B-ALL. The low incidence likely indicates the need for a secondary mutation for oncogenic transformation. They surmised that the *rag2: TEL-AML1* fish did not develop tumors because the transformation occurs prior to the expression of Rag2 in the common lymphoid progenitor, and instead occurs in an earlier multipotent progenitor or hematopoietic stem cell in the global promoter lines. With the apparent T-cell bias of the *rag2* promoter in zebrafish, it also seems possible that a different promoter of common lymphoid or B-cell progenitors may have more success. However, the recent discovery of B-ALL in the rag2: cMyc fish provides an opportunity for studying B-ALL in a more accessible model, with much shorter latency and higher incidence (Garcia et al., 2018).

ZEBRAFISH LEUKEMIA MODELS: MYELOID ORIGIN

Following the initial success of the zebrafish ALL models, serious efforts began to recapitulate myeloid leukemias including myeloproliferative neoplasms (MPN) and acute myeloid leukemia (AML) in zebrafish. This was done largely through creating transgenic lines that expressed oncogenic fusion genes and mutations commonly found in patients with MPN and AML. This section discusses the features and major findings of the myeloid leukemia models developed to date in zebrafish (**Table 2**).

Acute Myeloid Leukemia (AML) and Myeloproliferative Neoplasms (MPN)

Many hematological malignancies are driven by oncogenic fusion genes created after chromosomal translocations and these fusions can often be expressed in animal models or cell lines to drive transformation and oncogenesis. Zhuravleva et al. were the first to do so with a myeloid malignancy in zebrafish by creating transgenic fish expressing the *MYST3/NCOA2* (*MOZ/TIF2*) fusion product under the *spi-1 (pu.1)* early myeloid promoter (Hsu et al., 2004) along with *EGFP* (Zhuravleva et al., 2008). This fusion protein is the result of the inv(8)(p11q13) chromosome abnormality found in human AML, and fuses two histone acetyltransferases (HATs). A small number of F_0 fish (1.1%) expressing the transgene developed AML after 14–26 months, characterized by expansion of myeloid blast cells and invasion of the kidney. This low incidence and long latency suggest that secondary mutations may be necessary to induce transformation.

Another model using the *NUP98-HOXA9 (NHA9)* fusion gene [t(7;11)(p15;p15)] was developed by Forrester et al. (2011) with an spi-1 promoter driving conditional expression of either *EGFP* or the transgene after heat shock by the *hsp70-Cre* line. This oncogenic fusion product is associated with poor prognosis in AML and chronic myeloid leukemia (CML) (Gough et al., 2011). Following heat shock at 24 hpf, *NUP98-HOXA9;Cre* embryos had perturbed hematopoiesis promoting myeloid fates, and also showed reduced apoptosis and cell cycle arrest in response to irradiation, correlating with increased levels of *bcl2*. 23% of *NUP98-HOXA9;Cre* fish developed myeloid tumors with a latency of 19–23 months. These tumors closely resembled the pathology of the polyclonal MPN found in *NUP98-HOXA9*-transgenic mice (Kroon et al., 2001). Further investigation into the model uncovered an increase in HSCs, as well as a dependency on *meis1*, the prostaglandin/cyclooxygenase pathway, and genome hypermethylation via *dnmt1* for the fusion gene's oncogenic potential (Deveau et al., 2015). This dependency could be exploited through treatment with DNMT or COX inhibitors, or sub-therapeutic doses of either in combination with HDAC inhibitors. This study both revealed mechanistic details of the NHA9 oncogene and demonstrated the potential of zebrafish leukemia models in identification of new treatment combinations.

Because most leukemia oncogenes produce early detectable effects on hematopoiesis, along with the inherent advantages of the zebrafish model, it is possible to develop drug screens in preleukemic embryonic models. One such model was developed by Yeh et al. (2008) using the *AML1(RUNX1)-ETO* fusion oncogene under the heat shock responsive *hsp-70* promoter. After heat shock, embryos accumulated non-circulating immature blast cells, with disruption of definitive hematopoiesis via loss of *runx1* and *cmyb* expression, loss of *gata1*-expressing erythroid cells, and were ultimately driven to a myeloid-granulocytic fate. These effects were all downstream of *AML1-ETO's* suppression of *scl,* and could be reversed with *scl* overexpression. The transcriptional signature of *AML1-ETO*-expressing embryos closely paralleled that of human AML. Using the perturbation of embryonic hematopoiesis and the AML transcriptional signature as a readout of *AML1-ETO* oncogenic activity, they were able to develop a chemical screen for inhibitors that can rescue *AML1-ETO's*

TABLE 2 | Zebrafish leukemia models of myeloid origin.

Model	Gene/pathway; expression	Model features	Major findings
AML and MPN			
spi-1: MYST3/NCOA2-EGFP	Human *MYST3/NCOA2 (MOZ/TIF2)* fusion; Myeloid	EGFP-tagged, low incidence (1%) and high latency (14–26 months) in F_0 fish	First AML model in zebrafish (Zhuravleva et al., 2008)
spi-1: LGL-NUP98-HOXA9; hsp70-Cre	Human *NUP98-HOXA9* fusion; Myeloid	Cre-conditional EGFP or transgene expression. Incidence ∼25%, latency 19–23 months	MPN-like disease, decreased apoptosis and cell cycle arrest in response to irradiation through bcl2 (Forrester et al., 2011); increased HSCs, oncogenesis requires *dnmt1* or *meis1*, epigenetic therapies restore normal hematopoiesis (Deveau et al., 2015)
hsp70: AML1-ETO	Heat shock-inducible human *AML-ETO* fusion; global	Embryonic loss of circulating blood cells, disrupted definitive hematopoiesis	Transcriptional changes mirror human AML, blocks *gata1* to bias granulocytes over erythrocytes (Yeh et al., 2008); embryonic screen of AML-therapeutics, COX and β-catenin are novel hematopoietic regulators/therapeutic targets (Yeh et al., 2009)
CMV/Spi-1: tel-jak2a	Zebrafish *tel-jak2a* mimicking human fusion; Global and myeloid	Embryonic Leukocyte expansion	ALL- and CML-derived fusions bias toward lymphoid or myeloid, respectively (Onnebo et al., 2012)
β-*actin: LGL-KRAS*^{G12D}*; hsp70-Cre*	Cre-inducible Human *KRAS*^{G12D} mutant; global	Multiple different malignancies; MPN incidence higher in non-heat shocked (53%), latency 66 dpf	MPNs are not transplantable past primary, does not confer self-renewal potential to progenitors. MPN can be induced by heat-shock *ex-vivo* (Le et al., 2007)
HSE-MYCN-EGFP	Heat shock inducible Murine *n-Myc*; Global expression	∼75% incidence in F_2 fish, rapid onset (60 dpf), expanded myeloid populations in kidney/spleen	*n-Myc* can promote AML phenotypes, alters hematopoietic transcription factor expression (scl, lmo2, gata1, pu.1, runx1, cmyb) (Shen et al., 2013)
spi1: FLT3-ITD-2A-EGFP	Human *FLT3-ITD* mutant; Myeloid	Myeloid hyperplasia (6 months), AML-like (9 months)	Double mutants develop leukemia by 6 months (Lu et al., 2016)
spi1: *NPM1-Mut-PA*	Human *NPMc+*-cytoplasmic mutant; Myeloid	Normal hematopoietic complement	
mRNA: NPMc+	human Cytoplasmic *NPMc+* mutant; global, transient	Embryonic increase of myeloid lineage	Enhanced myeloid bias in *p53* mutant line, increased apoptosis dependent on p53 (Bolli et al., 2010)
spi-1: CREB-EGFP	*creb*; Myeloid	Incidence 79%, latency 9–14 months; ∼66% monocytic leukemia	Similar expression profile to patients, identified 20 shared *creb* targets, blocks myeloid differentiation through *c/ebpδ,* biases monocytic subtype (Tregnago et al., 2016)
fli1:GAL4-FF; UAS-GFP-HRAS^{G12V}	Human *HRAS*^{G12V} mutant; Endothelial (hemogenic)	Myelo-erythroid proliferative disorder, expansion of CHT and myeloid progenitors	Caused by downregulation of Notch, can be rescued with Notch ICD expression (Alghisi et al., 2013)
LDD731: CBL^{H382T}	*c-cbl*^{H382T} mutant; global	Embryonic expansion of myeloid progenitors, lethal at 14–15 dpf	Increase in progenitors does not correspond with differentiation block, dependent on flt3 (Peng et al., 2015)
irf8Δ57/Δ57	*irf8* knockout; global	Embryonic myeloid expansion, decreased lymphoid, survive to maturity.	*mertk* signaling activated, required for myeloid neoplasia (Zhao et al., 2018)
MDS			
tet-2$^{m/m}$	Enzymatically inactive *tet2*; global	Normal embryonic hematopoiesis, MDS at ∼24 months, myeloid progenitor dysplasia and anemia	Decreased 5hmC only in kidney marrow, redundancy of tet family in other tissues (Gjini et al., 2015)
pu.1^{G242D}	Human *pu.1*^{G242D} *(spi-1)* mutant; global	Embryonic myeloid (granulocyte) expansion, phenotypes resemble MDS by 18 months	Anti-proliferative drug cytrabine, but not apoptosis drug daunorubicin, reduces granulocyte expansion (Sun et al., 2013)
C-myb^{hyper}	Hyperactive *c-myb*; global	Embryonic myeloid (granulocyte) expansion, phenotypes resemble MDS by 1 year	MDS can progress to AML and ALL, are transplantable, and respond to *c-myb* target drug flavopiridol (Liu et al., 2017)

effects (Yeh et al., 2009). This screen identified the COX and β-catenin pathways as vital to the function of *AML1-ETO*.

TEL(ETV6)-JAK2 fusion genes have been identified in both ALL and atypical chronic myelogenous leukemia (aCML), with slightly different translocations driving each, t(9;12)(p24;p13) and t(9;15;12)(p24;q15;p13), respectively (Peeters et al., 1997). Onnebo et al. (2012) created transgenic zebrafish lines expressing these different fusions under *CMV* or *spi-1* promoters to better understand how they drive oncogenesis distinctly. These lines differ from other fusion gene transgenic lines in that the fusion proteins were generated from the zebrafish *tel* and *jak2a* genes combined to mimic two different human translocations found in T-ALL and aCML. Overall, the different genes behaved true to form, with the T-ALL fusion gene disrupting embryonic lymphopoiesis and the aCML fusion gene disrupting myelopoiesis similar to an MPN, driven by either *CMV* or *spi-1*. They were also able to demonstrate subtle differences in activity, with the T-ALL fusion gene showing greater enzymatic activity, but reduced downstream STAT activation and decreased sensitivity to JAK2 inhibition.

Although Zhuravleva et al. were the first to claim production of AML in a zebrafish model, the first myeloid malignancy was created in the Zon lab. Le et al. (2007) generated β-*actin: LGL-KRAS*^{G12D}*; hsp70-Cre* zebrafish, with conditional global expression of an oncogenic KRAS inducible by heat shock. This model produced a variety of tumors following heat shock, including rhabdomyosarcoma, myeloproliferative neoplasm, intestinal hyperplasia, and malignant peripheral nerve sheath tumor. Although the heat-shocked fish had juvenile lethality, they discovered that the non-heat shocked adult fish developed MPN, likely due to the well-known "leakiness" of heat-shock promoters. The MPN-affected fish displayed classic disease characteristics such as expansion of myeloid progenitors, invasion of the marrow (kidney), and depletion of erythroid cells. Interestingly, these MPN cells could engraft after primary transplantation into irradiated recipients, but were unable to engraft after secondary transplantation, suggesting that they lack self-renewal capabilities. Another model utilizing an oncogenic *RAS* mutation was developed by Alghisi et al. (2013) inducing expression in the hemogenic endothelium prior to hematopoietic emergence. This *fli1:GAL4-FF; UAS-GFP-HRAS*^{G12V} line developed an MPN characterized by prominent expansion of the CHT, increased number of immature hematopoietic cells, and a block of myeloid differentiation in the kidney marrow. The Notch pathway was significantly downregulated and overexpression of the active NICD rescued the MPN phenotypes. They used this model to identify candidate genes both downregulated by Notch and upregulated by RAS that could be involved myeloid oncogenesis.

Similar to the connection of *c-Myc* to T-ALL, *n-Myc* is frequently upregulated in AML and is a poor prognostic marker. Shen et al. (2013) created a heat shock responsive zebrafish line expressing murine *n-Myc*, *MYCN:HSE:EGFP*, that simultaneously drives expression of *EGFP*. Following heat shock, *n-Myc* overexpression promoted immature myeloid blast cell expansion and enhanced the repopulating activity of myeloid cells. *N-Myc* enhanced primitive hematopoiesis by upregulating *scl* and *lmo2* expression and promoted myelopoiesis by inhibiting *gata1* expression and inducing *spi1* and *mpo* expression. Many major cancer pathways were upregulated, such as cell cycle, glycolysis/gluconeogenesis, MAPK/Ras, and p53-mediated apoptosis. In contrast, mismatch repair and transforming growth factor β (TGFβ) signaling were downregulated. Overall, the model faithfully recapitulates AML phenotypes with high incidence (∼75%) and rapid onset (∼60 dpf).

Internal tandem duplications of the receptor tyrosine kinase *FLT3 (FLT3-ITD)* is a common mutation in AML and associated with poor prognosis and increased risk of relapse (Takahashi, 2011; Hou et al., 2013). It frequently coincides with mutations to the nucleophosmin *NPM1* that restrict it to the cytoplasm (*NPMc+*). Lu et al. (2016) sought to investigate the interaction of these two mutations in AML by making transgenic lines expressing each under the myeloid spi1 promoter, *spi1:FLT3-ITD-2A-EGFP and spi1:NPM1-Mut-PA*. The *FLT3-ITD* mutant fish alone developed moderate myeloid hyperplasia at 6 months and some of these progressed to leukemia at 9 months. *NPMc+* mutants had grossly normal hematopoietic composition. However, double mutants for both *FLT3-ITD* and *NPMc+* progressed to leukemia by 6 months, demonstrating their synergistic effect in driving AML. In a different model using *NPMc+* mRNA embryonic microinjections, Bolli et al. (2010) saw an increase in *spi1*$^{+}$ early myeloid progenitors, with a more pronounced effect in a *p53* mutant line. *NPMc+* expression resulted in increased erythromyeloid progenitors in the posterior blood island and *c-myb/cd41*$^{+}$ cells in the ventral wall of the aorta. They suggest these results may be relevant to human *NPMc+* AML, where a multilineage expression pattern implies transformation of a multipotent HSPC.

Using a large-scale ENU mutagenesis screen, Peng et al. (2015) identified a line with a significant increase in HSPCs in hematopoietic organs, designated *LDD731:CBL*^{H382T}. They determined the causal mutation was in the *c-cbl* gene, which is found frequently mutated in human MPN and acute leukemias and acts as a tumor suppressor by depressing growth factor and cytokine signals. The mutation was homozygous lethal at ∼15 dpf and led to an expansion of the myeloid/erythroid lineages in definitive hematopoiesis. *Flt3* was necessary for this expansion, consistent with that observed in both mice and humans, suggesting *flt3* signaling promotes HSPC proliferation and is regulated by *c-cbl*.

cAMP response element binding protein (*CREB*) is another frequently overexpressed gene in AML, however, it is unclear whether overactivation alone is sufficient to induce leukemia. Tregnago et al. (2016) generated a zebrafish model overexpressing *creb* with the *spi1* myeloid promoter, which resulted in a disruption of myelopoiesis in 79% of adult fish with 66% progressing to a monocytic leukemia (latency 9–14 months) mirroring the human counterpart. These fish showed a transcriptional signature with 20 differentially expressed genes in common with pediatric AML, including the CCAAT-enhancer-binding protein-δ (*c/ebp*δ). Increased

*c/ebp*δ expression impaired myeloid differentiation which could be reversed through silencing of the *creb-c/ebp*δ axis. Identification of this *creb-c/ebp*δ axis in zebrafish AML led Tregnago et al to classify *C/EBP*δ expression as a new pediatric AML subgroup after validation in publicly available patient databases.

To study the role of interferon regulatory factor 8 (IRF8) in the pathogenesis of myeloid neoplasia, Zhao et al. (2018) created a missense mutation, *irf8*$^{\Delta 57}$ that acted as a functional knockout. IRF8 is a critical transcription regulator for myeloid lineage commitment and closely tied to myeloid leukemia. *irf8* mutants quickly developed MPN with expansion of myeloid precursors, which recurred after transplantation, and invasion of kidney marrow. Myeloid expansion was caused by both increased proliferation and decreased apoptosis. *mertk* expression was increased in irf8 mutants leading to hyperactivation of the ERK pathway. Transgenic *mertk* overexpression recapitulated the myeloid neoplasia and knockdown of *mertk* rescued irf8 mutant myeloid expansion. These results support *mertk* signaling as critical in the *irf8*-mediated regulation of myeloid proliferation and survival.

Myelodysplastic Syndrome

Myelodysplastic syndromes (MDS) are a group of diseases characterized by aberrant hematopoietic differentiation leading to cytopenias and increased blasts, and often splenomegaly and cytogenetic abnormalities (Gangat et al., 2016). Approximately 30% of MDS patients will eventually progress to AML or other leukemias, which are frequently more resistant to conventional therapies.

Somatic loss-of-function mutations of the 10–11 translocation 2 gene *TET2* are frequently observed in patients with MDS. *TET2* encodes a DNA methylcytosine oxidase that converts 5-methylcytosine (5 mC) to 5-hydroxymethylcytosine (5 hmC) to initiate the demethylation (and activation) of DNA. Gjini et al. (2015) created an enzymatically inert *tet2* mutant zebrafish line through genome-editing technology. These fish had normal embryonic hematopoiesis, but developed progressive clonal myelodysplasia as they aged, eventually progressing to MDS by 24 months, with myeloid progenitor cell dysplasia and anemia. Decreased levels of 5 hmC were present in hematopoietic cells of the kidney marrow but not in other cell types, likely a result of compensation in non-hematopoietic tissues by other Tet family members.

The *c-myb* transcription factor is vital to hematopoietic proliferation and differentiation, and is closely associated with an array of hematological disorders. Liu et al. (2017) sought to better define its pathogenic role through characterization of a zebrafish model expressing a GFP-tagged *c-myb* mutant with increased activity, *c-myb*$^{\text{hyper}}$. This hyperactive c-myb resulted in the dysregulation of cell cycle genes and subsequent proliferation of hematopoietic progenitor cells. Abnormal granulocyte expansion began embryonically and was maintained through adulthood, ultimately resulting in MDS. A small number of *c-myb*$^{\text{hyper}}$ fish developed AML or ALL and treatment with *c-myb* target drug flavopiridol relieved the MDS-like symptoms in both embryos and adult fish.

In addition to its previously discussed role in early myeloid progenitors, *spi1 (pu.1)* is an Ets-family transcription factor important in leukemogenesis. It is frequently impaired in AML either through decreased expression or loss-of-function mutations (Mueller et al., 2002; Dakic et al., 2007). Sun et al. (2013) used the Targeting Induced Local Lesions IN Genomes (TILLING) approach to create a hypomorphic *spi1* mutant allele, dubbed *pu.1*$^{\text{G242D}}$. These fish have expanded myelopoiesis by 3 dpf, with increased immature granulocytes within the CHT. By 18 months, immature myeloid cells were increased at the expense of the lymphoid population in both the kidney marrow and peripheral blood, consistent with an MDS or AML-like disorder. The antiproliferative drug cytarabine was able to relieve the myeloid expansion, while apoptosis-inducing daunorubicin could not. This may indicate that spi1-associated neoplasms are more susceptible to drugs limiting their proliferation.

FUTURE DIRECTIONS AND EMERGING METHODS

The discoveries described in this review open numerous avenues for further research. Many of these models require further characterization and could uncover important pathways in leukemia initiation and progression. Drug screens utilizing these models can teach us much about the resistance and response to different therapies depending on the specific genetic drivers of the leukemia. The advent of effective CRISPR-Cas9 protocols has allowed for a rapid advancement in the creation of knockout and transgenic zebrafish investigating various genetic pathways and oncogene fusion products tied to human leukemia. This development will only continue to expand in scope, as ongoing research within the zebrafish field continues to uncover more genes and pathways associated with leukemia, as well as new discoveries made in the clinic that are converted into zebrafish models for further characterization.

One major emerging avenue of research is the identification and characterization of LSCs within hematopoietic malignancies. Cancer stem cells (CSCs), defined by their ability to regrow a tumor from a single cell, are implicated as the cause of cancer evolution, resistance to therapy, and relapse after therapy (Adorno-Cruz et al., 2015). Increased tumor heterogeneity and CSCs have been associated with resistance and relapse for many tumor types, including AML and ALL (Mullighan et al., 2008; Anderson et al., 2011; Notta et al., 2011; Ding et al., 2012). Identification and isolation of these cells is difficult because of a lack of defined surface markers, but there are some promising methods being developed. The side population assay has long been used to isolate normal tissue stem cells by exploiting their ability to export Hoechst dye (Goodell et al., 1996), and has more recently been shown to enrich for CSCs in many cancers (Hu et al., 2010; Britton et al., 2011; Richard et al., 2013). Side populations have also been defined in zebrafish hematopoietic cells and leukemia (Kobayashi et al., 2008; Pruitt et al., 2017), making it possible for LSCs to be further studied in zebrafish

leukemia models. Another similar protocol of enriching for stem cell activity is through the Aldefluor assay, which utilizes the increased aldehyde dehydrogenase (ALDH) activity common in stem cells to produce increased fluorescence from the aldefluor reagent (Storms et al., 1999; Ma et al., 2010). This assay can also be combined with the side population assay to isolate an even greater enrichment of stem cells (Pearce and Bonnet, 2007; Pierre-Louis et al., 2009). Genetic and functional characterization of the combined ALDH^{bright} and side population in zebrafish leukemia models could uncover significant contributors to leukemia resistance and relapse.

Another potential method for defining LSCs within a tumor is through single cell sequencing. Single-cell RNA sequencing techniques are capable of discerning expression profiles of each cell within a population, allowing small subpopulations like LSCs to be characterized within a tumor (Zhang et al., 2016). Multiple microfluidic systems have been developed to produce single-cell expression data, with the Fluidigm system already used by Moore et al. (2016) in a zebrafish T-ALL model to identify a small population with reactivated expression of putative stem cell genes. The DropSeq system is an alternative with much higher throughput that could potentially identify very small subpopulations in tumors with lower LSC frequencies (Macosko et al., 2015). Both systems allow for characterization of the expression profiles of LSCs in the various leukemia models, which opens up exciting possibilities in discovering what drives the LSC subpopulation and their unique functions within the leukemia.

AUTHOR CONTRIBUTIONS

JB wrote the entirety of the review, with significant input from JdJ in the initial outline and also comments and revisions of the final version.

FUNDING

Investigator Award University of Chicago Women's Board Discovering the genetic drivers of leukemia initiating cells in T-cell acute lymphoblastic leukemia. Program Pilot Project Grant University of Chicago Comprehensive Cancer Center Genetic drivers of leukemia initiating cells in the side population of zebrafish T-cell leukemia.

ACKNOWLEDGMENTS

We would like to acknowledge the University of Chicago Women's Board and the University of Chicago Comprehensive Cancer Center for helping to fund our work in this field.

REFERENCES

Ablain, J., Durand, E. M., Yang, S., Zhou, Y., and Zon, L. I. (2015). A CRISPR/Cas9 vector system for tissue-specific gene disruption in zebrafish. *Dev. Cell* 32, 756–764. doi: 10.1016/j.devcel.2015.01.032

Adorno-Cruz, V., Kibria, G., Liu, X., Doherty, M., Junk, D. J., Guan, D., et al. (2015). Cancer stem cells: targeting the roots of cancer, seeds of metastasis, and sources of therapy resistance. *Cancer Res.* 75, 924–929. doi: 10.1158/0008-5472.CAN-14-3225

Alghisi, E., Distel, M., Malagola, M., Anelli, V., Santoriello, C., Herwig, L., et al. (2013). Targeting oncogene expression to endothelial cells induces proliferation of the myelo-erythroid lineage by repressing the Notch pathway. *Leukemia* 27, 2229–2241. doi: 10.1038/leu.2013.132

Anderson, K., Lutz, C., van Delft, F. W., Bateman, C. M., Guo, Y., Colman, S. M., et al. (2011). Genetic variegation of clonal architecture and propagating cells in leukaemia. *Nature* 469, 356–361. doi: 10.1038/nature09650

Andreasson, P., Schwaller, J., Anastasiadou, E., Aster, J., and Gilliland, D. G. (2001). The expression of *ETV6/CBFA2 (TEL/AML1)* is not sufficient for the transformation of hematopoietic cell lines in vitro or the induction of hematologic disease in vivo. *Cancer Genet. Cytogenet.* 130, 93–104. doi: 10.1016/S0165-4608(01)00518-0

Bartram, C. R., de Klein, A., Hagemeijer, A., van Agthoven, T., van Kessel, A. G., Bootsma, D., et al. (1983). Translocation of c-abl oncogene correlates with the presence of a Philadelphia chromosome in chronic myelocytic leukaemia. *Nature* 306, 277–280. doi: 10.1038/306277a0

Blackburn, J. S., Liu, S., Raimondi, A. R., Ignatius, M. S., Salthouse, C. D., and Langenau, D. M. (2011). High-throughput imaging of adult fluorescent zebrafish with an LED fluorescence macroscope. *Nat. Protoc.* 6, 229–241. doi: 10.1038/nprot.2010.170

Blackburn, J. S., Liu, S., Raiser, D. M., Martinez, S. A., Feng, H., Meeker, N. D., et al. (2012). Notch signaling expands a pre-malignant pool of T-cell acute lymphoblastic leukemia clones without affecting leukemia-propagating cell frequency. *Leukemia* 26, 2069–2078. doi: 10.1038/leu.2012.116

Blackburn, J. S., Liu, S., Wilder, J. L., Dobrinski, K. P., Lobbardi, R., Moore, F. E., et al. (2014). Clonal evolution enhances leukemia-propagating cell frequency in T cell acute lymphoblastic leukemia through Akt/mTORC1 pathway activation. *Cancer Cell* 25, 366–378. doi: 10.1016/j.ccr.2014.01.032

Bolli, N., Payne, E. M., Grabher, C., Lee, J. S., Johnston, A. B., Falini, B., et al. (2010). Expression of the cytoplasmic NPM1 mutant (NPMc+) causes the expansion of hematopoietic cells in zebrafish. *Blood* 115, 3329–3340. doi: 10.1182/blood-2009-02-207225

Britton, K. M., Kirby, J. A., Lennard, T. W. J., and Meeson, A. P. (2011). Cancer stem cells and side population cells in breast cancer and metastasis. *Cancers* 3, 2106–2130. doi: 10.3390/cancers3022106

Brownlie, A., Donovan, A., Pratt, S. J., Paw, B. H., Oates, A. C., Brugnara, C., et al. (1998). Positional cloning of the zebrafish sauternes gene: a model for congenital sideroblastic anaemia. *Nat. Genet.* 20, 244–250. doi: 10.1038/3049

Burns, C. E., DeBlasio, T., Zhou, Y., Zhang, J., Zon, L., and Nimer, S. D. (2002). Isolation and characterization of runxa and runxb, zebrafish members of the runt family of transcriptional regulators. *Exp. Hematol.* 30, 1381–1389. doi: 10.1016/S0301-472X(02)00955-4

Chen, J., Jette, C., Kanki, J. P., Aster, J. C., Look, A. T., and Griffin, J. D. (2007). NOTCH1-induced T-cell leukemia in transgenic zebrafish. *Leukemia* 21, 462–471. doi: 10.1038/sj.leu.2404546

Cumano, A., and Godin, I. (2007). Ontogeny of the hematopoietic system. *Annu. Rev. Immunol.* 25, 745–785. doi: 10.1146/annurev.immunol.25.022106.141538

Dakic, A., Wu, L., and Nutt, S. L. (2007). Is PU.1 a dosage-sensitive regulator of haemopoietic lineage commitment and leukaemogenesis?. *Trends Immunol.* 28, 108–114. doi: 10.1016/j.it.2007.01.006

de Jong, J. L., and Zon, L. I. (2005). Use of the zebrafish system to study primitive and definitive hematopoiesis. *Annu. Rev. Genet.* 39, 481–501. doi: 10.1146/annurev.genet.39.073003.095931

Detrich, H. W., Kieran, M. W., Chan, F. Y., Barone, L. M., Yee, K., Rundstadler, J. A., et al. (1995). Intraembryonic hematopoietic cell migration during vertebrate development. *Proc. Natl. Acad. Sci. U.S.A.* 92, 10713–10717. doi: 10.1073/pnas.92.23.10713

Deveau, A. P., Bentley, V. L., and Berman, J. N. (2017). Using zebrafish models of leukemia to streamline drug screening and discovery. *Exp. Hematol.* 45, 1–9. doi: 10.1016/j.exphem.2016.09.012

Deveau, A. P., Forrester, A. M., Coombs, A. J., Wagner, G. S., Grabher, C., Chute, I. C., et al. (2015). Epigenetic therapy restores normal hematopoiesis in a zebrafish model of NUP98–HOXA9-induced myeloid disease. *Leukemia* 29, 2086–2097. doi: 10.1038/leu.2015.126

Ding, L., Ley, T. J., Larson, D. E., Miller, C. A., Koboldt, D. C., Welch, J. S., et al. (2012). Clonal evolution in relapsed acute myeloid leukaemia revealed by whole-genome sequencing. *Nature* 481, 506–510. doi: 10.1038/nature10738

Evans, D. I. K., and Steward, J. K. (1972). Down's syndrome and leukemia. *Lancet* 300:1322. doi: 10.1016/S0140-6736(72)92704-3

Feng, H., Langenau, D. M., Madge, J. A., Quinkertz, A., Gutierrez, A., Neuberg, D. S., et al. (2007). Heat-shock induction of T-cell lymphoma/leukaemia in conditional Cre/lox-regulated transgenic zebrafish. *Br. J. Haematol.* 138, 169–175. doi: 10.1111/j.1365-2141.2007.06625.x

Feng, H., Stachura, D. L., White, R. M., Gutierrez, A., Zhang, L., Sanda, T., et al. (2010). T-lymphoblastic lymphoma cells express high levels of BCL2, S1P1, and ICAM1, leading to a blockade of tumor cell intravasation. *Cancer Cell* 18, 353–366. doi: 10.1016/j.ccr.2010.09.009

Forrester, A. M., Grabher, C., McBride, E. R., Boyd, E. R., Vigerstad, M. H., Edgar, A., et al. (2011). NUP98-HOXA9-transgenic zebrafish develop a myeloproliferative neoplasm and provide new insight into mechanisms of myeloid leukaemogenesis. *Br. J. Haematol.* 155, 167–181. doi: 10.1111/j.1365-2141.2011.08810.x

Frazer, J. K., Meeker, N. D., Rudner, L., Bradley, D. F., Smith, A. C., Demarest, B., et al. (2009). Heritable T-cell malignancy models established in a zebrafish phenotypic screen. *Leukemia* 23, 1825–1835. doi: 10.1038/leu.2009.116

Gangat, N., Patnaik, M. M., and Tefferi, A. (2016). Myelodysplastic syndromes: contemporary review and how we treat. *Am. J. Hematol.* 91, 76–89. doi: 10.1002/ajh.24253

Garcia, E. G., Iyer, S., Garcia, S. P., Loontiens, S., Sadreyev, R. I., Speleman, F., et al. (2018). Cell of origin dictates aggression and stem cell number in acute lymphoblastic leukemia. *Leukemia* doi: 10.1038/s41375-018-0130-0 [Epub ahead of print]. doi: 10.1038/s41375-018-0130-0

GBD 2015 Mortality and causes of death collaborators (2016). Global, regional, and national life expectancy, all-cause mortality, and cause-specific mortality for 249 causes of death, 1980-2015: a systematic analysis for the Global Burden of Disease Study 2015. *Lancet* 388, 1459–1544. doi: 10.1016/S0140-6736(16)31012-1

Gjini, E., Mansour, M. R., Sander, J. D., Moritz, N., Nguyen, A. T., Kesarsing, M., et al. (2015). A zebrafish model of myelodysplastic syndrome produced through tet2 genomic editing. *Mol. Cell. Biol.* 35, 789–804. doi: 10.1128/MCB.00971-14

Goodell, M. A., Brose, K., Paradis, G., Conner, A. S., and Mulligan, R. C. (1996). Isolation and functional properties of murine hematopoietic stem cells that are replicating in vivo. *J. Exp. Med.* 183, 1797–1806. doi: 10.1084/jem.183.4.1797

Gough, S. M., Slape, C. I., and Aplan, P. D. (2011). NUP98 gene fusions and hematopoietic malignancies: common themes and new biologic insights. *Blood* 118, 6247–6257. doi: 10.1182/blood-2011-07-328880

Grabher, C., Joly, J. S., and Wittbrodt, J. (2004). Highly efficient zebrafish transgenesis mediated by the meganuclease I-SceI. *Methods Cell Biol.* 77, 381–401. doi: 10.1016/S0091-679X(04)77021-1

Gutierrez, A., Grebliunaite, R., Feng, H., Kozakewich, E., Zhu, S., Guo, F., et al. (2011). Pten mediates Myc oncogene dependence in a conditional zebrafish model of T cell acute lymphoblastic leukemia. *J. Exp. Med.* 208, 1595–1603. doi: 10.1084/jem.20101691

Gutierrez, A., Sanda, T., Grebliunaite, R., Carracedo, A., Salmena, L., Ahn, Y., et al. (2009). High frequency of PTEN, PI3K, and AKT abnormalities in T-cell acute lymphoblastic leukemia. *Blood* 114, 647–650. doi: 10.1182/blood-2009-02-206722

Hess, I., and Boehm, T. (2016). Stable multilineage xenogeneic replacement of definitive hematopoiesis in adult zebrafish. *Sci. Rep.* 6:19634. doi: 10.1038/srep19634

Hou, H. A., Lin, C. C., Chou, W. C., Liu, C. Y., Chen, C. Y., Tang, J. L., et al. (2013). Integration of cytogenetic and molecular alterations in risk stratification of 318 patients with de novo non-M3 acute myeloid leukemia. *Leukemia* 28, 50–58. doi: 10.1038/leu.2013.236

Howe, K., Clark, M. D., Torroja, C. F., Torrance, J., Berthelot, C., Muffato, M., et al. (2013). The zebrafish reference genome sequence and its relationship to the human genome. *Nature* 496, 498–503. doi: 10.1038/nature12111

Hruscha, A., Krawitz, P., Rechenberg, A., Heinrich, V., Hecht, J., Haass, C., et al. (2013). Efficient CRISPR/Cas9 genome editing with low off-target effects in zebrafish. *Development* 140, 4982–4987. doi: 10.1242/dev.099085

Hsu, K., Traver, D., Kutok, J. L., Hagen, A., Liu, T.-X., Paw, B. H., et al. (2004). The pu.1 promoter drives myeloid gene expression in zebrafish. *Blood* 104, 1291–1297. doi: 10.1182/blood-2003-09-3105

Hu, L., McArthur, C., and Jaffe, R. B. (2010). Ovarian cancer stem-like side-population cells are tumourigenic and chemoresistant. *Br. J. Cancer* 102, 1276. doi: 10.1038/sj.bjc.6605626

Hwang, W. Y., Fu, Y., Reyon, D., Maeder, M. L., Tsai, S. Q., Sander, J. D., et al. (2013). Efficient genome editing in zebrafish using a CRISPR-Cas system. *Nat. Biotechnol.* 31, 227–229. doi: 10.1038/nbt.2501

Jin, H., Xu, J., and Wen, Z. (2007). Migratory path of definitive hematopoietic stem/progenitor cells during zebrafish development. *Blood* 109, 5208–5214. doi: 10.1182/blood-2007-01-069005

Kaufman, C. K., Mosimann, C., Fan, Z. P., Yang, S., Thomas, A., Ablain, J., et al. (2016). A zebrafish melanoma model reveals emergence of neural crest identity during melanoma initiation. *Science* 351, aad2197–aad2197. doi: 10.1126/science.aad2197

Kaufmann, A., Mickoleit, M., Weber, M., and Huisken, J. (2012). Multilayer mounting enables long-term imaging of zebrafish development in a light sheet microscope. *Development* 139, 3242–3247. doi: 10.1242/dev.082586

Kimmel, C. B., Ballard, W. W., Kimmel, S. R., Ullmann, B., and Schilling, T. F. (1995). Stages of embryonic development of the zebrafish. *Dev. Dyn.* 203, 253–310. doi: 10.1002/aja.1002030302

Kobayashi, I., Saito, K., Moritomo, T., Araki, K., Takizawa, F., and Nakanishi, T. (2008). Characterization and localization of side population (SP) cells in zebrafish kidney hematopoietic tissue. *Blood* 111, 1131–1137. doi: 10.1182/blood-2007-08-104299

Kroon, E., Thorsteinsdottir, U., Mayotte, N., Nakamura, T., and Sauvageau, G. (2001). NUP98–HOXA9 expression in hemopoietic stem cells induces chronic and acute myeloid leukemias in mice. *EMBO J.* 20, 350–361. doi: 10.1093/emboj/20.3.350

La Starza, R., Borga, C., Barba, G., Pierini, V., Schwab, C., Matteucci, C., et al. (2014). Genetic profile of T-cell acute lymphoblastic leukemias with MYC translocations. *Blood* 124, 3577–3582. doi: 10.1182/blood-2014-06-578856

Langenau, D. M., Feng, H., Berghmans, S., Kanki, J. P., Kutok, J. L., and Look, A. T. (2005). Cre/lox-regulated transgenic zebrafish model with conditional myc-induced T cell acute lymphoblastic leukemia. *Proc. Natl. Acad. Sci. U.S.A.* 102, 6068–6073. doi: 10.1073/pnas.0408708102

Langenau, D. M., Ferrando, A. A., Traver, D., Kutok, J. L., Hezel, J. P., Kanki, J. P., et al. (2004). In vivo tracking of T cell development, ablation, and engraftment in transgenic zebrafish. *Proc. Natl. Acad. Sci. U.S.A.* 101, 7369–7374. doi: 10.1073/pnas.0402248101

Langenau, D. M., Keefe, M. D., Storer, N. Y., Jette, C. A., Smith, A. C., Ceol, C. J., et al. (2008). Co-injection strategies to modify radiation sensitivity and tumor initiation in transgenic Zebrafish. *Oncogene* 27, 4242–4248. doi: 10.1038/onc.2008.56

Langenau, D. M., Traver, D., Ferrando, A. A., Kutok, J. L., Aster, J. C., Kanki, J. P., et al. (2003). Myc-induced T cell leukemia in transgenic zebrafish. *Science* 299, 887–890. doi: 10.1126/science.1080280

Le, X., Langenau, D. M., Keefe, M. D., Kutok, J. L., Neuberg, D. S., and Zon, L. I. (2007). Heat shock-inducible Cre/Lox approaches to induce diverse types of tumors and hyperplasia in transgenic zebrafish. *Proc. Natl. Acad. Sci. U.S.A.* 104, 9410–9415. doi: 10.1073/pnas.0611302104

Liao, E. C., Paw, B. H., Oates, A. C., Pratt, S. J., Postlethwait, J. H., and Zon, L. I. (1998). SCL/Tal-1 transcription factor acts downstream of cloche to specify hematopoietic and vascular progenitors in?zebrafish. *Genes Dev.* 12, 621–626. doi: 10.1101/gad.12.5.621

Lieschke, G. J., Oates, A. C., Paw, B. H., Thompson, M. A., Hall, N. E., Ward, A. C., et al. (2002). Zebrafish SPI-1 (PU.1*)* marks a site of myeloid development independent of primitive erythropoiesis: implications for axial patterning. *Dev. Biol.* 246, 274–295. doi: 10.1006/dbio.2002.0657

Liu, W., Wu, M., Huang, Z., Lian, J., Chen, J., Wang, T., et al. (2017). c-myb hyperactivity leads to myeloid and lymphoid malignancies in zebrafish. *Leukemia* 31, 222–233. doi: 10.1038/leu.2016.170

Lu, J. W., Hou, H. A., Hsieh, M. S., Tien, H. F., and Lin, L. I. (2016). Overexpression of FLT3-ITD driven by spi-1 results in expanded myelopoiesis with leukemic phenotype in zebrafish. *Leukemia* 30, 2098–2101. doi: 10.1038/leu.2016.132

Lum, J. J., DeBerardinis, R. J., and Thompson, C. B. (2005). Autophagy in metazoans: cell survival in the land of plenty. *Nat. Rev. Mol. Cell Biol.* 6, 439–448. doi: 10.1038/nrm1660

Lyons, S. E., Shue, B. C., Oates, A. C., Zon, L. I., and Liu, P. P. (2001). A novel myeloid-restricted zebrafish CCAAT/enhancer-binding protein with a potent transcriptional activation domain. *Blood* 97, 2611–2617. doi: 10.1182/blood.V97.9.2611

Ma, A. C., Chung, M. I., Liang, R., and Leung, A. Y. (2010). A DEAB-sensitive aldehyde dehydrogenase regulates hematopoietic stem and progenitor cells development during primitive hematopoiesis in zebrafish embryos. *Leukemia* 24, 2090–2099. doi: 10.1038/leu.2010.206

Macosko, E. Z., Basu, A., Satija, R., Nemesh, J., Shekhar, K., Goldman, M., et al. (2015). Highly parallel genome-wide expression profiling of individual cells using nanoliter droplets. *Cell* 161, 1202–1214. doi: 10.1016/j.cell.2015.05.002

Mizgireuv, I. V., and Revskoy, S. Y. (2006). Transplantable tumor lines generated in clonal zebrafish. *Cancer Res.* 66, 3120–3125. doi: 10.1158/0008-5472.Can-05-3800

Mizgirev, I. V., and Revskoy, S. (2010). A new zebrafish model for experimental leukemia therapy. *Cancer Biol. Ther.* 9, 895–902. doi: 10.4161/cbt.9.11.11667

Moore, F. E., Garcia, E. G., Lobbardi, R., Jain, E., Tang, Q., Moore, J. C., et al. (2016). Single-cell transcriptional analysis of normal, aberrant, and malignant hematopoiesis in zebrafish. *J. Exp. Med.* 213, 979–992. doi: 10.1084/jem.20152013

Mueller, B. U., Pabst, T., Osato, M., Asou, N., Johansen, L. M., Minden, M. D., et al. (2002). Heterozygous PU.1 mutations are associated with acute myeloid leukemia. *Blood* 100, 998–1007. doi: 10.1182/blood.V100.3.998

Mullighan, C. G., Phillips, L. A., Su, X., Ma, J., Miller, C. B., Shurtleff, S. A., et al. (2008). Genomic analysis of the clonal origins of relapsed acute lymphoblastic leukemia. *Science* 322, 1377–1380. doi: 10.1126/science.1164266

North, T. E., Goessling, W., Walkley, C. R., Lengerke, C., Kopani, K. R., Lord, A. M., et al. (2007). Prostaglandin E2 regulates vertebrate haematopoietic stem cell homeostasis. *Nature* 447, 1007–1011. doi: 10.1038/nature05883

Notta, F., Mullighan, C. G., Wang, J. C., Poeppl, A., Doulatov, S., Phillips, L. A., et al. (2011). Evolution of human BCR-ABL1 lymphoblastic leukaemia-initiating cells. *Nature* 469, 362–367. doi: 10.1038/nature09733

Novoa, B., and Figueras, A. (2012). "Zebrafish: model for the study of inflammation and the innate immune response to infectious diseases," in *Current Topics in Innate Immunity II*, eds J. D. Lambris and G. Hajishengallis (New York, NY: Springer), 253–275.

Ogino, H., McConnell, W. B., and Grainger, R. M. (2006). High-throughput transgenesis in Xenopus using I-SceI meganuclease. *Nat. Protoc.* 1, 1703–1710. doi: 10.1038/nprot.2006.208

Onnebo, S. M., Rasighaemi, P., Kumar, J., Liongue, C., and Ward, A. C. (2012). Alternative TEL-JAK2 fusions associated with T-cell acute lymphoblastic leukemia and atypical chronic myelogenous leukemia dissected in zebrafish. *Haematologica* 97, 1895–1903. doi: 10.3324/haematol.2012.064659

Paik, E. J., and Zon, L. I. (2010). Hematopoietic development in the zebrafish. *Int. J. Dev. Biol.* 54, 1127–1137. doi: 10.1387/ijdb.093042ep

Palis, J., and Yoder, M. C. (2001). Yolk-sac hematopoiesis: the first blood cells of mouse and man. *Exp. Hematol.* 29, 927–936. doi: 10.1016/S0301-472X(01)00669-5

Palomero, T., Dominguez, M., and Ferrando, A. A. (2008). The role of the PTEN/AKT Pathway in NOTCH1-induced leukemia. *Cell Cycle* 7, 965–970. doi: 10.4161/cc.7.8.5753

Pearce, D. J., and Bonnet, D. (2007). The combined use of Hoechst efflux ability and aldehyde dehydrogenase activity to identify murine and human hematopoietic stem cells. *Exp. Hematol.* 35, 1437–1446. doi: 10.1016/j.exphem.2007.06.002

Peeters, P., Raynaud, S. D., Cools, J., Wlodarska, I., Grosgeorge, J., Philip, P., et al. (1997). Fusion of TEL, the ETS-variant gene 6 (ETV6), to the receptor-associated kinase JAK2 as a result of t(9; 12) in a lymphoid and t(9; 15; 12) in a myeloid leukemia. *Blood* 90, 2535–2540.

Peng, X., Dong, M., Ma, L., Jia, X. E., Mao, J., Jin, C., et al. (2015). A point mutation of zebrafish c-cbl gene in the ring finger domain produces a phenotype mimicking human myeloproliferative disease. *Leukemia* 29, 2355–2365. doi: 10.1038/leu.2015.154

Pierre-Louis, O., Clay, D., Brunet de la Grange, P., Blazsek, I., Desterke, C., Guerton, B., et al. (2009). Dual SP/ALDH functionalities refine the human hematopoietic Lin-CD34+CD38- stem/progenitor cell compartment. *Stem Cells* 27, 2552–2562. doi: 10.1002/stem.186

Pruitt, M. M., Marin, W., Waarts, M. R., and de Jong, J. L. O. (2017). Isolation of the side population in myc-induced T-cell acute lymphoblastic leukemia in zebrafish. *J. Vis. Exp.* 123:e55711. doi: 10.3791/55711

Ransom, D. G., Bahary, N., Niss, K., Traver, D., Burns, C., Trede, N. S., et al. (2004). The zebrafish moonshine gene encodes transcriptional intermediary factor 1γ, an essential regulator of hematopoiesis. *PLoS Biol.* 2:e237. doi: 10.1371/journal.pbio.0020237

Ransom, D. G., Haffter, P., Odenthal, J., Brownlie, A., Vogelsang, E., Kelsh, R. N., et al. (1996). Characterization of zebrafish mutants with defects in embryonic hematopoiesis. *Development* 123, 311–319.

Renshaw, S. A., and Trede, N. S. (2012). A model 450 million years in the making: zebrafish and vertebrate immunity. *Dis. Model. Mech.* 5, 38–47. doi: 10.1242/dmm.007138

Reynolds, C., Roderick, J. E., LaBelle, J. L., Bird, G., Mathieu, R., Bodaar, K., et al. (2014). Repression of BIM mediates survival signaling by MYC and AKT in high-risk T-cell acute lymphoblastic leukemia. *Leukemia* 28, 1819–1827. doi: 10.1038/leu.2014.78

Richard, V., Nair, M. G., Santhosh Kumar, T. R., and Pillai, M. R. (2013). Side population cells as prototype of chemoresistant, tumor-initiating cells. *Biomed Res. Int.* 2013:517237. doi: 10.1155/2013/517237

Ridges, S., Heaton, W. L., Joshi, D., Choi, H., Eiring, A., Batchelor, L., et al. (2012). Zebrafish screen identifies novel compound with selective toxicity against leukemia. *Blood* 119, 5621–5631. doi: 10.1182/blood-2011-12-398818

Romana, S. P., Poirel, H., Leconiat, M., Flexor, M. A., Mauchauffe, M., Jonveaux, P., et al. (1995). High frequency of t(12;21) in childhood B-lineage acute lymphoblastic leukemia. *Blood* 86, 4263–4269.

Sabaawy, H. E., Azuma, M., Embree, L. J., Tsai, H. J., Starost, M. F., and Hickstein, D. D. (2006). TEL-AML1 transgenic zebrafish model of precursor B cell acute lymphoblastic leukemia. *Proc. Natl. Acad. Sci. U.S.A.* 103, 15166–15171. doi: 10.1073/pnas.0603349103

Shen, L.-J., Chen, F.-Y., Zhang, Y., Cao, L.-F., Kuang, Y., Zhong, M., et al. (2013). *MYCN* transgenic zebrafish model with the characterization of acute myeloid leukemia and altered hematopoiesis. *PLoS One* 8:e59070. doi: 10.1371/journal.pone.0059070

Smith, A. C., Raimondi, A. R., Salthouse, C. D., Ignatius, M. S., Blackburn, J. S., Mizgirev, I. V., et al. (2010). High-throughput cell transplantation establishes that tumor-initiating cells are abundant in zebrafish T-cell acute lymphoblastic leukemia. *Blood* 115, 3296–3303. doi: 10.1182/blood-2009-10-246488

Sood, R., English, M. A., Jones, M., Mullikin, J., Wang, D.-M., Anderson, M., et al. (2006). Methods for reverse genetic screening in zebrafish by resequencing and TILLING. *Methods* 39, 220–227. doi: 10.1016/j.ymeth.2006.04.012

Sotsios, Y., and Ward, S. G. (2000). Phosphoinositide 3-kinase: a key biochemical signal for cell migration in response to chemokines. *Immunol. Rev.* 177, 217–235. doi: 10.1034/j.1600-065X.2000.17712.x

Storms, R. W., Trujillo, A. P., Springer, J. B., Shah, L., Colvin, O. M., Ludeman, S. M., et al. (1999). Isolation of primitive human hematopoietic progenitors on the basis of aldehyde dehydrogenase activity. *Proc. Natl. Acad. Sci. U.S.A.* 96, 9118–9123. doi: 10.1073/pnas.96.16.9118

Stuart, G. W., McMurray, J. V., and Westerfield, M. (1988). Replication, integration and stable germ-line transmission of foreign sequences injected into early zebrafish embryos. *Development* 103, 403–412.

Sun, J., Liu, W., Li, L., Chen, J., Wu, M., Zhang, Y., et al. (2013). Suppression of Pu.1 function results in expanded myelopoiesis in zebrafish. *Leukemia* 27, 1913–1917. doi: 10.1038/leu.2013.67

Takahashi, S. (2011). Downstream molecular pathways of FLT3 in the pathogenesis of acute myeloid leukemia: biology and therapeutic implications. *J. Hematol. Oncol.* 4, 13–13. doi: 10.1186/1756-8722-4-13

Tang, Q., Abdelfattah, N. S., Blackburn, J. S., Moore, J. C., Martinez, S. A., Moore, F. E., et al. (2014). Optimized cell transplantation using adult rag2 mutant zebrafish. *Nat. Methods* 11, 821–824. doi: 10.1038/nmeth.3031

Thompson, M. A., Ransom, D. G., Pratt, S. J., MacLennan, H., Kieran, M. W., Detrich, H. W., et al. (1998). Theclocheandspadetailgenes differentially affect hematopoiesis and vasculogenesis. *Dev. Biol.* 197, 248–269. doi: 10.1006/dbio.1998.8887

Tregnago, C., Manara, E., Zampini, M., Bisio, V., Borga, C., Bresolin, S., et al. (2016). CREB engages C/EBPdelta to initiate leukemogenesis. *Leukemia* 30, 1887–1896. doi: 10.1038/leu.2016.98

Urasaki, A., Morvan, G., and Kawakami, K. (2006). Functional dissection of the Tol2 transposable element identified the minimal cis sequence and a highly repetitive sequence in the subterminal region essential for transposition. *Genetics* 174, 639–649. doi: 10.1534/genetics.106.060244

Walker, C., and Streisinger, G. (1983). Induction of mutations by γ-rays in pregonial germ cells of zebrafish embryos. *Genetics* 103, 125–136.

Wang, H., Long, Q., Marty, S. D., Sassa, S., and Lin, S. (1998). A zebrafish model for hepatoerythropoietic porphyria. *Nat. Genet.* 20, 239–243. doi: 10.1038/3041

Weinberg, E. S., Allende, M. L., Kelly, C. S., Abdelhamid, A., Murakami, T., Andermann, P., et al. (1996). Developmental regulation of zebrafish MyoD in wild-type, no tail and spadetail embryos. *Development* 122, 271–280.

Weng, A. P., Ferrando, A. A., Lee, W., Morris, J. P., Silverman, L. B., Sanchez-Irizarry, C., et al. (2004). Activating mutations of NOTCH1 in human T cell acute lymphoblastic leukemia. *Science* 306, 269–271. doi: 10.1126/science.1102160

White, R. M., Sessa, A., Burke, C., Bowman, T., LeBlanc, J., Ceol, C., et al. (2008). Transparent adult zebrafish as a tool for in vivo transplantation analysis. *Cell Stem Cell* 2, 183–189. doi: 10.1016/j.stem.2007.11.002

Willett, C. E., Cherry, J. J., and Steiner, L. A. (1997). Characterization and expression of the recombination activating genes (rag1 and rag2) of zebrafish. *Immunogenetics* 45, 394–404. doi: 10.1007/s002510050221

Willett, C. E., Kawasaki, H., Amemiya, C. T., Lin, S., and Steiner, L. A. (2001). Ikaros expression as a marker for lymphoid progenitors during zebrafish development. *Dev. Dyn.* 222, 694–698. doi: 10.1002/dvdy.1223

Yeh, J. R., Munson, K. M., Chao, Y. L., Peterson, Q. P., Macrae, C. A., and Peterson, R. T. (2008). AML1-ETO reprograms hematopoietic cell fate by downregulating scl expression. *Development* 135, 401–410. doi: 10.1242/dev.008904

Yeh, J. R., Munson, K. M., Elagib, K. E., Goldfarb, A. N., Sweetser, D. A., and Peterson, R. T. (2009). Discovering chemical modifiers of oncogene-regulated hematopoietic differentiation. *Nat. Chem. Biol.* 5, 236–243. doi: 10.1038/nchembio.147

Zhang, X., Marjani, S. L., Hu, Z., Weissman, S. M., Pan, X., and Wu, S. (2016). Single-cell sequencing for precise cancer research: progress and prospects. *Cancer Res.* 76, 1305–1312. doi: 10.1158/0008-5472.CAN-15-1907

Zhao, F., Shi, Y., Huang, Y., Zhan, Y., Zhou, L., Li, Y., et al. (2018). Irf8 regulates the progression of myeloproliferative neoplasm-like syndrome via Mertk signaling in zebrafish. *Leukemia* 32, 149–158. doi: 10.1038/leu.2017.189

Zhuravleva, J., Paggetti, J., Martin, L., Hammann, A., Solary, E., Bastie, J.-N., et al. (2008). MOZ/TIF2-induced acute myeloid leukaemia in transgenic fish. *Br. J. Haematol.* 143, 378–382. doi: 10.1111/j.1365-2141.2008.07362.x

Conflict of Interest Statement: The authors declare that the research was conducted in the absence of any commercial or financial relationships that could be construed as a potential conflict of interest.

frontiers in Cell and Developmental Biology

ORIGINAL RESEARCH
published: 28 September 2018
doi: 10.3389/fcell.2018.00126

Mga Modulates Bmpr1a Activity by Antagonizing Bs69 in Zebrafish

Xiaoyun Sun[1], Ji Chen[1], Yanyong Zhang[1], Mumingjiang Munisha[2], Scott Dougan[2] and Yuhua Sun[1]**

[1] Institute of Hydrobiology, Chinese Academy of Sciences, Wuhan, China, [2] Department of Cellular Biology, University of Georgia, Athens, GA, United States

MAX giant associated protein (MGA) is a dual transcriptional factor containing both T-box and bHLHzip DNA binding domains. *In vitro* studies have shown that MGA functions as a transcriptional repressor or activator to regulate transcription of promotors containing either E-box or T-box binding sites. BS69 (ZMYND11), a multidomain-containing (i.e., PHD, BROMO, PWWP, and MYND) protein, has been shown to selectively recognizes histone variant H3.3 lysine 36 trimethylation (H3.3K36me3), modulates RNA Polymerase II elongation, and functions as RNA splicing regulator. Mutations in MGA or BS69 have been linked to multiple cancers or neural developmental disorders. Here, by TALEN and CRISPR/Cas9-mediated loss of gene function assays, we show that zebrafish Mga and Bs69 are required to maintain proper Bmp signaling during early embryogenesis. We found that Mga protein localized in the cytoplasm modulates Bmpr1a activity by physical association with Zmynd11/Bs69. The Mynd domain of Bs69 specifically binds the kinase domain of Bmpr1a and interferes with its phosphorylation and activation of Smad1/5/8. Mga acts to antagonize Bs69 and facilitate the Bmp signaling pathway by disrupting the Bs69–Bmpr1a association. Functionally, Bmp signaling under control of Mga and Bs69 is required for properly specifying the ventral tailfin cell fate.

Keywords: Mga, Bmp signaling, Zmynd11, Bs69, Bmpr1a, ventral tailfin

OPEN ACCESS

Edited by:
Ryan M. Anderson,
Indiana University–Purdue University Indianapolis, United States

Reviewed by:
Saurabh Chattopadhyay,
University of Toledo, United States
Vasudevan Seshadri,
National Centre for Cell Science (NCCS), India

****Correspondence:***
Scott Dougan
dougan@uga.edu
Yuhua Sun
sunyh@ihb.ac.cn

Specialty section:
This article was submitted to Molecular Medicine, a section of the journal Frontiers in Cell and Developmental Biology

Received: *29 April 2018*
Accepted: *10 September 2018*
Published: *28 September 2018*

Citation:
Sun X, Chen J, Zhang Y, Munisha M, Dougan S and Sun Y (2018) Mga Modulates Bmpr1a Activity by Antagonizing Bs69 in Zebrafish. Front. Cell Dev. Biol. 6:126. doi: 10.3389/fcell.2018.00126

INTRODUCTION

Bone morphogenetic proteins (BMPs) comprise a subgroup of the TGF-beta family of secreted signaling molecules. They transduce their signal by extracellular binding to membrane protein complex consisting of a type I receptor (BMPRI) and a type II receptor (BMPRII). Type I BMP receptor (BMPRI) activation leads to the phosphorylation and activation of Smad1/5/8. The pSmad1/5/8 form complex with SMAD4 and translocate to the nucleus to regulate transcription of downstream target genes. BMP signaling is known to control multiple important biological events, ranging from dorsal-ventral patterning, stem cell maintenance and differentiation to tissue homeostasis (Katagiri and Watabe, 2016). Given its importance in development and homeostasis, Bmp signaling is tightly regulated at the extra- and intracellular levels, by numerous factors such as Noggin, Chordin, Smad7, and Fkbp1A (Wang et al., 2014).MAX's giant associated protein (MGA) was first identified as a MAX interacting protein by a yeast two hybrid assay in a mouse embryonic day e9.5 and e10.5 cDNA library (Hurlin et al., 1999). Like other Myc family of transcriptional factors, MGA has a basic helix-loop-helix zipper (bHLHZip) domain that mediates dimerization with MAX, which is required for their specific DNA binding to E-box sequences. In addition to the bHLHZip domain, MGA contains a second

DNA-binding domain, the T-box or T-domain. *In vitro* studies suggested that MGA could regulate transcription of promotors containing either E-box or T-box binding sites (Hurlin et al., 1999). MGA is thus proposed to function as a dual-specificity transcription factor that could regulate the expression of both the MAX-network and the T-box gene family genes. MGA:MAX heterodimers were often found as part of a large transcription-silencing complex E2F6-com.1 or as part of polycomb repressive complex 1 (PRC1) that catalyzes the monoubiquitylation of histone H2A (Ogawa et al., 2002; Gao et al., 2012). MGA:MAX were shown to repress developmental genes in somatic or embryonic stem cells by recruiting PRC1.6 complex to gene promotors (Endoh et al., 2017; Suzuki et al., 2017). Consistently, MGA depletion leads to the death of proliferating pluripotent ICM cells *in vivo* and *in vitro*, and the loss of self-renewal and pluripotency of embryonic stem cells (Washkowitz et al., 2015). Moreover, Mga mutation in somatic cells is associated with a variety of tumor or cancers, including aggressive lymphoma called Richter's Syndrome, which occurs in a minority of patients with chronic lymphocytic leukemia (De Paoli et al., 2013; The Cancer Genome Atlas Research Network, 2014; Jo et al., 2016). Together, these studies suggest that MGA functions as a tumor suppressor in normal tissues, presumably by antagonizing Myc oncogene or by recruiting PRC1 to target genes.

Because Mga deficient mice are embryonic lethal, the role of MGA in vertebrate embryogenesis and disease remains unclear. To overcome this issue, we and others took advantage of the zebrafish model system, which is useful for developmental biology studies because of its transparent embryo during early embryogenesis and it is also highly amenable for genetic studies. By Morpholino-mediated gene knockdown, Rikin and Evans (2010) showed that Mga plays essential role in organogenesis by regulating gata4 expression. We recently reported that Mga together with Smad4 and Max are required for the dorsal ventral patterning of zebrafish embryos by transcriptionally regulating Bmp2 expression in the extra embryonic tissue, yolk syncytial layer (YSL) (Sun et al., 2014). This was the first report showing that Mga is involved in the regulation of Bmp signaling in a vertebrate. Unlike other Myc family of transcriptional factors, Mga is predominantly localized in the cytoplasm throughout early zebrafish embryogenesis. This observation implies that Mga has important roles in the cytoplasm, and it may also regulate Bmp signaling independent of its transcriptional activities.

BS69 (ZMYND11) is a multidomain-containing (i.e., PHD, BROMO, PWWP, and MYND) protein that was originally identified as an adenoviral early region 1A-interacting protein (Ansieau and Leutz, 2002; Harter et al., 2016). Through its PHD–BROMO–PWWP domains, BS69 selectively recognizes histone variant H3.3 lysine 36 trimethylation (H3.3K36me3), modulates RNA Polymerase II elongation, and functions as RNA splicing regulator for intron retention (Guo et al., 2014; Wen et al., 2014). The MYND domain of BS69 seems to act as an important protein–protein interaction surface, through which BS69 interacts with a variety of chromatin regulators, including MGA (Velasco et al., 2006). Recently, a growing body of research has shown that BS69 localized in the cytoplasm or cytoplasmic membrane is involved in mediating multiple signaling pathways. For instances, BS69 physically interacts with LMP1 and negatively regulates LMP1-mediated JNK and Nf-κB activation (Hateboer et al., 1995; Chung et al., 2002; Wan et al., 2006; Ikeda et al., 2009). BS69 associates with lymphotoxin beta receptor (LTβR) and inhibits LTβR-mediated signaling transduction (Liu et al., 2011). It has been shown that BRAM1, an alternatively spliced form of BS69, may inhibit Bmp signaling by interacting with the type I BMP receptor 1A (Kurozumi et al., 1998; Morita et al., 2001; Wu et al., 2006). However, BRAM1 was thought likely to be an artificial product that generated from the library construction (Velasco et al., 2006). Therefore, it remains unclear whether BS69 is involved in the regulation of Bmp signaling.

Using zebrafish as a model, we revealed a cytoplasmic role for Mga in the regulation of Bmp signaling. We showed that Mga protein localized in the cytoplasm acts to antagonize Bs69 to facilitate the Bmp signaling pathway. Mechanistically, Mga binds to Bs69 and disrupts the Bs69–Bmpr1a association, thereby maintaining proper Bmp signaling that is required to properly specify zebrafish ventral tail fin.

MATERIALS AND METHODS

Zebrafish Maintenance

Zebrafish (*Danio rerio*) were maintained at 28.5°C on a 12 h light/12 h dark cycle. All procedures were performed with the approval of the Institute of Hydrobiology, Chinese Academy of Sciences, Wuhan, China.

Generation of *mga* and *bs69* Mutants Using TALEN or CRISPR/Cas9

Mga mutants (GenBank accession numbers MH853640-853641) were generated by TALEN technology as described (Chen et al., 2016). We identified potential TALEN-target sites in the coding sequence of zebrafish *mga* gene (NM_001170739.1) using ZiFit 3.0[1]. The *mga* TALEN recognition sequences are: left TALEN 5′-CCATTGCAGCCCAGCCTG-3′ and right TALEN 5′-GAATGAGACGAACAGTT-3′. Between the two binding sites is an 16-bp spacer (GAGGATGTCGAAGGTC). Genotyping was conducted using PCR followed by restriction enzyme digestion. The primers used were 5′-TTCTGACAACAGTATTTCCA-3′ and 5′-CTCGTTCTAAACTCGGTTGACT-3′. *Bs69* mutants (GenBank accession numbers MH853642-853643) were generated by CRISPR/Cas9 technology. gRNA was designed to target a site 5′-GGCTGATGTGGAACAGCTGT-3′ in exon 15 of *bs69* gene. Genotyping was conducted using PCR followed by restriction enzyme digest. The primers were 5′-CCCTTACAGTCTCCTCCTGTAT-3′ and 5′-TGTTCTCCGC CTTCATCATTT-3′. Mutagenized F0 males were crossed to wild-type females to obtain F1 fish. The F1 heterozygous females were then crossed with wild type males to derive the F2 heterozygous. The F2 heterozygous fish were randomly intercrossed, yielding F3-offspring.

[1]http://zifit.partners.org/ZiFiT/

Plasmid Constructions and Microinjections

To make PCS2- version of constructs used in this work, cDNAs encoding zebrafish Mga, Bs69 and their mutants were generated by RT-PCR from cDNA libraries made from 8 hpf zebrafish embryos, and then cloned into the pCS2+ vector using the In-fusion HD Cloning kit (Clontech). The primers used are shown in **Table 1**. *Mga*, *bs69* and *bmpr1aa* and mutant mRNAs were made using mMESSAGE mMACHINE® Kit (Ambion, TX, United States). mRNAs were injected to the zebrafish embryos at one-cell-stage by a microinjector (WPI, United States).

Cell Culture and Transfection

HEK293 or HEK293T cells were cultured with DMEM (BI) containing 10% fetal bovine serum (FBS, Gibco). Cell transfection was performed with Lipofectamine 2000 (Invitrogen) according to the manufacturer's instructions. Briefly, cells (about 10^6 viable cells) were seeded in 6-well plates without antibiotics in DMEM medium containing 10% FBS. Then the constructs expressing the tagged protein of interest or empty pCS2+ vector were transiently transfected into HEK293 cells. 48 h later, the cells were harvested for co-immunoprecipitation and Western blot analysis.

Luciferase Assay

The BRE-luc reporter was kindly provided by Prof. Zongbin Cui. pTK-Renilla was kindly provided by Dr. Xing Liu (Liu et al., 2015). HEK293 or C2C12 cells (about 10^5 viable cells) were seeded in 24-well plates in DMEM medium containing 10% FBS for 24 h. The cells were then transiently transfected with indicated luciferase reporters using Lipofectamine 2000 (Invitrogen). pTK-Renilla was used as an internal control. After transfection, the cells were treated with BMP4 (10 ng/ml) or control for 16 h. The luciferase activity was measured with the Dual-luciferase Reporter Assay system (Promega).

Co-immunoprecipitation and Western Blot Analysis

The protocols for the co-immunoprecipitation and WB analysis were described (Sun et al., 2011). For pSmad1/5/9 WB analysis, the phosphatase inhibitor (Thermo, A32957) was used. For *in vivo* co-immunoprecipitation assay, whole cell lysates were prepared with the TEN buffer (50 mM Tris-HCL, 150 mM NaCl, 5 mM EDTA, 1% Triton X-100, 0.5% Na-deoxycholate, and ROCHE protease inhibitor cocktail). The cytoplasmic and nuclear fractions were prepared with a ProteinExt® Mammalian Nuclear and Cytoplasmic Protein Extraction Kit (TransGen, DE201-01). 1.5 mg Dynabeads protein G was conjugated with 10 μg anti-Mga antibodies, 10 μg anti-Bs69 antibody, 10 μg anti-FLAG antibody, 10 μg anti-HA antibody, or 10 μg IgG. The cell lysates and the antibody-conjugated Dynabeads were incubated overnight at 4°C. After extensive washing, the beads-protein complex were boiled and the supernatant was loaded on a 8% PAGE gel for electrophoresis. The proteins were transferred to a PVDF membrane, followed by blocking with 5% (w/v) non-fat milk for 2-h at room temperature. Then the membrane was incubated overnight at 4°C with the primary antibodies. Anti-MgaN (STTPSENLPADAR); anti-MgaI (EHSADKNTLKSSDQN); anti-MgaC (SPDSKDEIDIPPK) were made by Genscript (China). Anti-FLAG(1B10) and anti-HA (4F6) were purchased from Abbkine (China). Anti-pSmad1/5/9 (D5B10) was purchased from the Cell Signaling Technology. HRP-conjugated goat anti-rabbit IgG (GtxRb-003-E3EUR) was purchased from ImmunoReagents. Anti-mouse IgG, HRP-linked antibody (#7076s) was purchased from Cell Signaling Technology.

Protein–Protein Interaction Assay Using Rabbit Reticulocyte Lysate System

FLAG or HA tagged Mga, Bs69 or Bmpr1a proteins were synthesized using the TnT coupled reticulocyte lysate system according to the manual (L5020, Promega, United States). Briefly, 1 μg of circular PCS2- version of plasmid were added directly to the TnT Lysate and incubated in a 50 μl reaction for 1.5 h at 30°C. To evaluate the quality or quantity of the synthesized protein, 1 μl of the reaction products were subjected to WB assay.

For protein–protein interaction assay, 5–10 μl of the synthesized HA or FLAG tagged proteins were mixed in a 1.5 ml tube with the TEN buffer, and the mixture was shaken for 30 min at room temperature. Next, Co-IP or pull-down assay was performed using Dynabeads protein G coupled with FLAG or HA antibodies as described above (Sun et al., 2014).

Immunofluorescence Assay

Six to eight hpf zebrafish embryos were collected and fixed with 4% paraformaldehyde (PFA) overnight at 4°C. Embryos were washed with PBST (0.1% Triton X-100) and then permeabilized

TABLE 1 | Primer used for amplifying the indicated cDNAs.

Name	*Forward sequence (5′–3′)*	*Reverse sequence (5′–3′)*
FLAG-Bs69	*ATGGATTACAAGGATGACGACGATAAGTTGGAACTGGCCACGATGTC*	*TACCCAATAGCGTGTCTCGTG*
FLAG-Bs69Δ	*ATGGATTACAAGGATGACGACGATAAGTTGGAACTGGCCACGATGTC*	*TCACCACTGCTTCTTCTTGGTC*
HA-Bs69-Mynd	*ATGTACCCATACGATGTTCCAGATTACGCTGAGCCCGAGATGGAAGCAG*	*TACCCAATAGCGTGTCTCGTG*
Bmpr1a-FLAG	*ACAATGCGTCAGCTTTTGTTCATCAC*	*TCACTTATCGTCGTCATCCTTGTAA TCGATTTTAATGTCTTGAGATTCCAC*
Bmpr1a-kinase-FLAG	*ATGATCGGAAAAGGACGATATGG*	*TCACTTATCGTCGTCATCCTTGTAATC GATTTTAATGTCTTGAGATTCCAC*
FLAG-Mga-Cter	*ATGGATTACAAGGATGACGACGATAAGATGAATCTGCTCGACGTCACACTG*	*TCACATTTGTGGTGTATCTTGCTC*
FLAG-MgaΔ	*ATGGATTACAAGGATGACGACGATAAGATGAATCTGCTCGACGTCACACTG*	*TCAAGGCCGCCATGTCACACTG*

with acetone for 7 min at −20°C. The embryos were rinsed with PBST, followed by 1 h blocking with solution (0.1% Triton X-100, 1% BSA, and 1% DMSO in PBS). Then the embryos were incubated with primary antibodies overnight rocking at 4°C. After washing with the blocking solution, embryos were incubated with the secondary antibodies for 2 h at room temperature, followed by extensively washing. Nuclei was stained with DAPI. Primary antibodies diluted with blocking solution were anti-pSmad1/5/9 (1:300), anti-FLAG (1:300), and anti-HA (1:300). Secondary antibodies diluted with blocking solution were goat anti-mouse IgG(H+L) Alexa Fluor 555 (1:500, Molecular Probes), goat anti-rabbit IgG(H+L) Alexa Fluor 488 (1:500, Molecular Probes). The embryos were transferred to a Glass Bottom (NEST) and submerged with 75% glycerol. The images were taken under a Leica SP8 confocal microscope (Germany).

Whole-Mount *in situ* Hybridization

Whole-mount *in situ* hybridization (WISH) was performed as described previously (Sun et al., 2011). The DIG-labeled probes were generated with DIG RNA Labeling Kit (SP6/T7) (Roche) and Fluorescein-labeled RNA probes were made with Fluorescein RNA Labeling Mix, 10x conc. (Roche). *Mga, chordin,* and *eve1* RNA *in situ* probes were described before (Sun et al., 2014). Zebrafish embryos were collected at different development stages and fixed with 4% PFA overnight at 4°C. Following the WISH, the embryos were transferred to 6-well plates and submerged by 100% glycerol for imaging.

RESULTS

Mga Positively Regulates Bmp Signaling

To establish a genetic model to explore the developmental function of Mga, and avoid potential off-target effects of Morpholino Oligos, we generated *mga* mutant zebrafish by using TALEN technology (**Figure 1A**). Out of 12 potential founders, we identified two fish in which *mga* gene was mutated at the TALEN cleavage site in the exon 2. The identity of each mutation was confirmed by genotyping (**Figure 1B**).

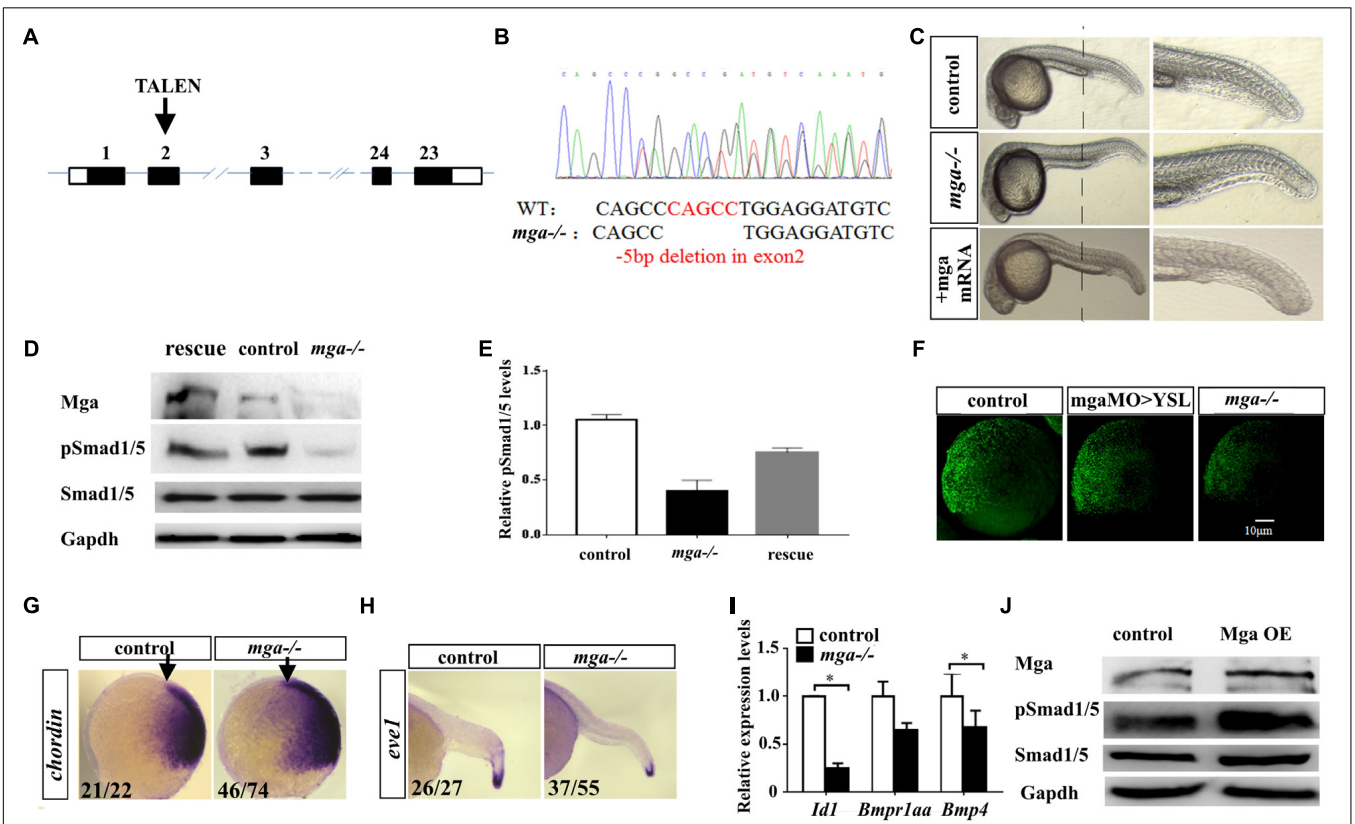

FIGURE 1 | Mga mutant embryos exhibited mild dorsalized phenotype. **(A)** Schematic representation of the zebrafish *mga* gene, depicting the location of the TALEN targeting site. **(B)** Sequences around the TALEN targeting site, showing the TALEN-induced 5-bp deletion in *mga* (in red). **(C)** Phenotypes of 1 dpf wild type, *mga* mutant, and *mga* mutant embryos injected with 50 pg *mga* mRNA at one-cell-stage. The reduction of ventral tail fin was restored by injecting 50 pg *mga* mRNA into one-cell-stage of mga mutant embryos. Lateral view. **(D)** Immunoblot analysis of Mga and pSmad1/5 levels of lysates from 7 hpf control, mutant and *mga* mRNA restored embryos. **(E)** Quantification of pSmad1/5 levels of panel D based on three independent experiments. **(F)** pSmad1/5 gradient of wild type, mga > YSL morphants, and *mga* mutant embryos at 7 hpf. Dorsal to the right. **(G)** *Chordin* expression in *mga* mutant and control embryos at shield stage. Lateral view, and dorsal to the right. **(H)** *eve1* expression in *mga* mutant and control embryos at 22 hpf. Lateral view, and dorsal to the right. **(I)** qRT-PCR transcript analysis of the indicated Bmp target genes in control and *mga* mutant embryos at 8 hpf. **(J)** Immunoblot analysis of pSmad1/5 levels of lysates from 8 hpf control and Mga overexpressing (OE) embryos. All experiments were performed in technical triplicate and are representative of multiple experiments. *$p < 0.05$.

Each mutation results in an open reading frame-shift that leads to a premature stop codon. Western blotting was used to detect Mga protein in lysates from homozygous mutant and control embryos at 8 hpf, using Mga specific antibodies (Sun et al., 2014). As seen in **Figure 1D**, the band around 250 kDa was detected in lysates from control embryos, but was barely detected in lysates from mutant embryos. These results indicate that our mutant alleles are functional nulls. One mutation line with a 5 bp deletion in exon 2 of the *mga* gene, was used for most of the subsequent studies (**Figure 1B**).

The mutant embryos at 1 dpf appear largely normal except the loss or reduction of the ventral tail fin defect (**Figure 1C**). Because *mga* mutant embryos at 1 dpf exhibited the loss of ventral tailfin defect that resembled our previously characterized *mga* > YSL morphants, we went on to confirm that Bmp signaling was compromised in *mga* mutant embryos (Sun et al., 2014). Nuclear phosphorylated Smad1/5/8 is a direct intracellular readout of Bmp signaling. As expected, pSmad1/5 levels were indeed reduced in mutant embryos. Importantly, pSmad1/5 levels could be rescued by injecting 100 pg *mga* mRNA, demonstrating the specificity of observed phenotype (**Figures 1D,E**). A low but detectable level of phospho-Smad1/5 was still present in lysates of mutant embryos, suggesting that Mga is only required for higher Bmp activity. This was in accordance with the notion that the ventral tail fin formation is most sensitive to the reduction of Bmp signaling (Schumacher et al., 2011). We also compared the pSmad1/5 gradient among 7 hpf *mga* > YSL morphants, *mga* mutant and control embryos by immunofluorescence assay using anti-pSmad1/5/9 antibody. As seen from **Figure 1F**, *mga* mutant embryos and *mga* > YSL morphants both exhibited reduced pSmad1/5 gradient when compared with the control embryos. However, the pSmad1/5 gradient in *mga* mutant embryos was reduced to a greater extent than *mga* > YSL morphants (**Figure 1F**), suggesting that Mga cell autonomously regulates Bmp signaling in embryos in addition to its role in YSL (Sun et al., 2014). To further confirm that Bmp activity was reduced in *mga* mutants, whole mount *in situ* hybridization was performed to examine the expression pattern of dorsal marker *chordin* and the ventral marker *eve1*. As expected, *chordin* expression was slightly expanded in mutant embryos at shield stage, whereas *eve1* expression was slightly reduced in mutant embryos at 22 hpf compared with the controls (**Figures 1G,H**). Moreover, the expression of well-known Smad-dependent Bmp target genes *Id1* and *bmp4* was down-regulated in *mga* mutant embryos (**Figure 1I**).

On the other hand, we overexpressed Mga by injecting 200 pg *mga* mRNA into one-cell-stage wild-type embryos. Beta-gal overexpressing embryos were used as controls. As seen in **Figure 1J**, pSmad1/5 levels were slightly elevated in Mga overexpressing embryos compared with control embryos, which further supports that Mga positively regulates Bmp signaling.

Taken together, we concluded that Mga is cell autonomously required for proper Bmp signaling that is important for specifying the ventral tailfin cell fate during zebrafish embryogenesis.

Mga Interacts With Bs69 in Zebrafish Embryos

Our yeast two hybrid experiments have identified multiple Mga interacting proteins, including Smad1, Smad4, and type I Bmp receptors, suggesting that Mga could regulate Bmp signaling by physical association with the core components of Bmp signaling pathway (Sun et al., 2014). Type I Bmp receptor 1a (Bmpr1a) was of particular interest to us because previous studies have shown that *bmpr1a* mutant embryos at 1 dpf exhibited the loss or reduction of ventral tailfin defect that closely resembled our *mga* mutant embryos (Smith et al., 2011), and also that wild type embryos injected with mRNA encoding dominant negative Bmpr1a (dnBmpr1a) at one-cell-stage had defects in the ventral tailfin formation at 1 dpf (Pyati et al., 2005) (**Supplementary Figure S1A**). Wild type embryos treated with 0.05 μM dorsomorphin or LDN193189, which are known potent Bmpr1a inhibitors, exhibited the loss or reduction of ventral tail fin defect at 1 dpf (**Supplementary Figure S1A**). Furthermore and most importantly, injection lower dose (25 pg) constitutive active *bmpr1a* (*caBmpr1a*) mRNA into one-cell-stage *mga* mutant embryos rescued the loss or reduction of the ventral tailfin phenotype (Nikaido et al., 1999) (**Supplementary Figure S1B**). Altogether these previous studies, along with our observations, strongly suggested a functional link between Mga and Bmpr1a. Unfortunately, we failed to detect reproducible interaction between Mga and Bmpr1a (data not shown). Transcriptional regulation of *bmpr1a* gene by Mga was ruled out, as *bmpr1a* transcript levels in *mga* mutant embryos were comparable to control embryos (**Figure 1I**).

It has been previously shown that mammalian MGA directly interacts with BS69, and that BRAM1, a possible spliced form of BS69, may be involved in the regulation of BMPR1A activity (Kurozumi et al., 1998; Ansieau and Leutz, 2002; Velasco et al., 2006; Wu et al., 2006). Therefore, we speculated that Mga may modulate Bmpr1a activity through Bs69 in zebrafish. To test these hypothesis, we firstly examined the gene expression pattern of *mga*, *bs69*, and *bmpr1a* during zebrafish early embryogenesis. The three genes have similar expression patterns from blastula to late organogenesis as reported (Wu et al., 2006; Rikin and Evans, 2010; Smith et al., 2011). During gastrulation, both *bmpr1aa* and *mga* transcription levels are high, whereas *bs69* transcript levels are relatively low. During early somitogenesis stage, *mga* and *bmpr1aa* are strongly expressed in the trunk and tail region, whereas *bs69* expression domain seems to be more restricted to the ventral region of the trunk. During organogenesis, all three genes are strongly expressed in the head and gut regions (**Supplementary Figure S1C**). The contrasting expression patterns between *mga* and *bs69* genes imply that Mga may act to antagonize Bs69 to modulate Bmpr1a activity.

To investigate whether Mga regulates Bmpr1a activity through Bs69, we determined whether Mga associates with Bs69 in physiological conditions in zebrafish embryos. The cellular co-localization of Bs69 and Mga was examined in 7 hpf embryos

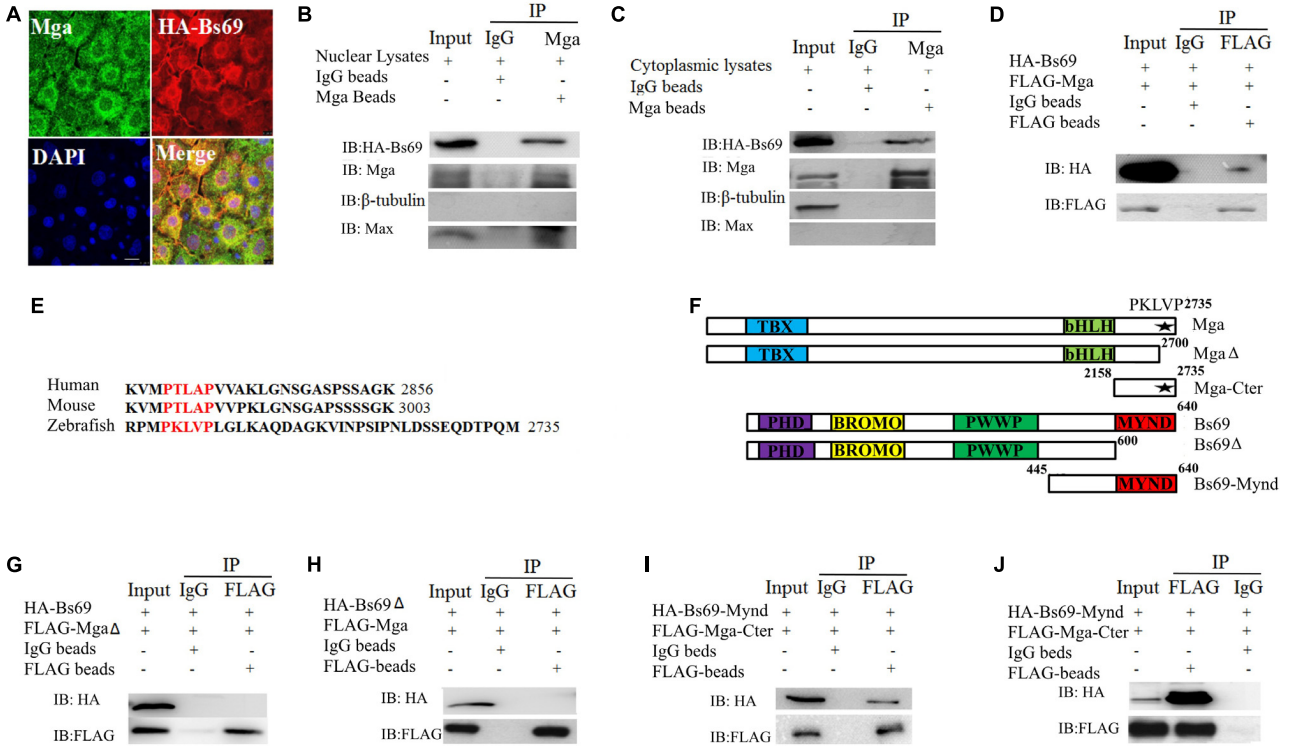

FIGURE 2 | Mga interacts with Bs69. **(A)** Confocal images of Mga and HA-Bs69 proteins in 7 hpf embryos. Scale bar 10 μm. **(B)** Co-immunoprecipitation of Mga and HA-Bs69 in nuclear lysates from 8 hpf embryos. **(C)** Co-immunoprecipitation of Mga and HA-Bs69 in cytoplasmic lysates from 8 hpf embryos. **(D)** Co-immunoprecipitation of HA-Bs69 and FLAG-Mga in 293T cells. **(E)** Identification of a conserved PXLXP motif in human, mouse and zebrafish MGAs at the end of the C-terminal region. The PXLXP conserved motif were highlighted in red. **(F)** Schematic representation of the full-length and truncated Mga and Bs69 constructs as indicated. **(G)** FLAG-MgaΔ did not immunoprecipitate with HA-Bs69 in 293T cells. **(H)** FLAG-Mga did not immunoprecipitate with HA-Bs69Δ in 293T cells. **(I)** FLAG-Mga-Cter immunoprecipitated with HA-Bs69-Mynd in 293T cells. **(J)** Co-immunoprecipitation assay of the *in vitro* translated FLAG-Mga-Cter and HA-Bs69-Mynd.

(**Figure 2A** and **Supplementary Figure S2A**). One-cell-stage wild-type embryos were injected with 100 pg HA-tagged *bs69* mRNA, and embryos were collected for co-immunofluorescence assay using Mga and HA antibodies. Our IF data clearly showed that these two proteins were co-localized in both cytoplasm and nucleus. To determine whether Mga interacts with Bs69 in physiological conditions, we performed co-immunoprecipitation (co-IP) assay using Mga and HA antibodies. Cytoplasmic and nuclear fractions of lysates from 7 hpf embryos were prepared using a commercial TransGen kit, and were subjected to co-IP experiments. It was obvious that Mga interacts with HA-Bs69 in both cytoplasm and nucleus (**Figures 2B,C**).

Next, we mapped the interacting domain between Mga and Bs69 in 293T cells. We first confirmed that FLAG-Mga and HA-Bs69 interact with each other (**Figure 2D**). It was previously reported that the PXLXP motif of mammalian MGA binds to the MYND domain of BS69 (Ansieau and Leutz, 2002). We identified a conserved PXLXP motif (PKLVP) within the C-terminal region (amino acid 2702-2706) of zebrafish Mga protein (**Figure 2E**). Deletion of this PXLXP motif (FLAG-MgaΔ) abrogated Mga binding to HA-Bs69 (**Figure 2G**). Truncated Bs69 lacking the Mynd domain (HA-Bs69Δ) did not co-immunoprecipitate with the FLAG-tagged Mga (**Figure 2H**). However, FLAG-tagged C-terminal fragment of Mga (FLAG-Mga-Cter) containing the PXLXP motif was sufficient to bind the Mynd domain of Bs69 (HA-Bs69-Mynd) (**Figure 2I**). To determine whether this interaction was direct or not, we used a reticulate lysate system to synthesize FLAG-Mga-Cter and HA-Bs69-Mynd. When they were mixed together, the anti-FLAG antibody readily pull-downed HA-Bs69-Mynd (**Figure 2J**).

Taken together, we concluded that zebrafish Mga physically associates with Bs69 in the physiological condition and this interaction is mediated by the PXLXP motif of Mga and the Mynd domain of Bs69.

Bs69 Negatively Regulates Bmp Signaling

To understand the function of Bs69, we generated *bs69* mutant zebrafish by CRISPR/Cas9 technology (**Figure 3A**). We designed gRNAs targeting exon 2 or 15 of bs69. Out of eight potential founders, we identified two fish in which *bs69* gene was mutated around the CRISPR targeting site of exon 2. Both mutations result in an open reading frame-shift that leads to a premature stop codon. Out of nine potential founders, we identified two fish in which *bs69* gene was mutated around the CRISPR targeting site

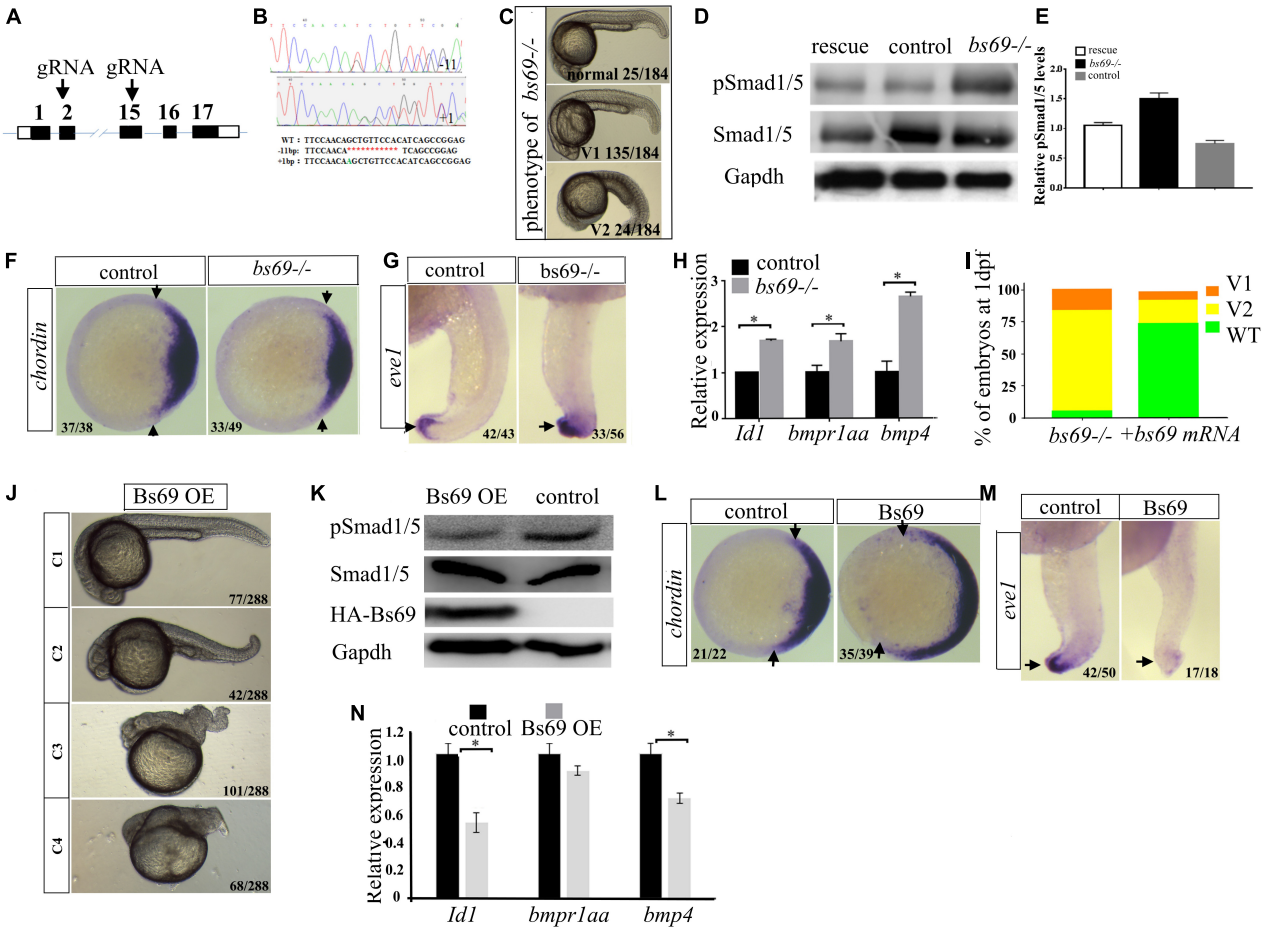

FIGURE 3 | Bs69 negatively regulates Bmp signaling. **(A)** Schematic representation of *bs69* gene, showing the CRISPR/Cas9 targeting site in exon 15. **(B)** Sequences of the two *bs69* mutants at the CRISPR targeting site. CRISPR-induced 11 bp deletion is highlighted in red; CRISPR-induced 1 bp insertion is highlighted in green. **(C)** The phenotypes of *bs69* mutant embryos at 1 dpf. V1: V1 ventralized phenotype; and V2: V2 ventralized phenotype, according to the DV patterning index (Kishimoto et al., 1997). **(D)** Immunoblot analysis of pSmad1/5 levels in lysates from 8 hpf control, *bs69* mutant, and Bs69 restored embryos. **(E)** Quantification of pSmad1/5 levels from panel D. **(F)** *Chordin* expression in *bs69* mutant and control embryos at shield stage. Animal view, and dorsal to the right. **(G)** *eve1* expression in *bs69* mutant and control embryos at 22 hpf. lateral view, and dorsal to the right. **(H)** qRT-PCR analysis of the Bmp target genes in 8 hpf *bs69* mutant and control embryos. **(I)** One-cell-stage *bs69* mutant embryos were injected with 50 pg bs69 mRNA, and the injected embryo at 30 hpf were scored and phenotyped according to the dorsal-ventral patterning index. **(J)** The phenotypes of Bs69 overexpressing embryos at 2 dpf. C1-4 dorsalized phenotypes according to DV patterning index. **(K)** Immunoblot analysis of pSmad1/5 levels of lysates from 8 hpf control and Bs69 overexpressing embryos. **(L)** *Chordin* expression in Bs69 overexpressing embryos at shield stage. Animal view, and dorsal to the right. **(M)** *eve1* expression in BS69 overexpressing embryos at 22 hpf. Lateral view, and dorsal to the right. **(N)** qRT-PCR transcript analysis of the indicated Bmp target genes in 8 hpf control and Bs69 overexpressing embryos. All experiments were performed in technical triplicate and are representative of multiple experiments. $^*p < 0.05$.

of exon 15. Both mutations result in an open reading frame-shift that leads to a truncated Bs69 protein that lack the entire Mynd domain. One mutant causes 1-bp insertion within the CRISPR targeting site, resulting in a ∼475aa truncated protein. Another mutant has 11-bp deletion within the CRISPR targeting site, resulting in a ∼480aa truncated BS69 protein (**Figure 3B**). The F3 zygotic *bs69* mutants are viable and can be raised up to adulthood. When F3 female and male adults were intercrossed, maternal zygotic *bs69* mutant embryos were obtained for further analysis.

The majority of *bs69* mutant embryos at 1 dpf exhibited mild V1 ventralized phenotype, characterized by slightly reduced head region. Some of the *bs69* mutant embryos at 1 dpf displayed missing notochord, and enlarged ventral cell types, indicating a V2 ventralized phenotype (Kishimoto et al., 1997) (**Figure 3C**). Smad1/5 phosphorylation was increased in 8 hpf *bs69* mutants compared with controls, and this could be rescued by injecting *bs69* mRNA into one-cell-stage mutant embryos (**Figures 3D,E**). To confirm that *bs69* mutants had the ventralized phenotype, whole mount *in situ* hybridization was performed to examine the expression pattern of dorsal marker *chordin* and the ventral marker *eve1*. As expected, the *chordin* expression domain was decreased in mutant embryos at shield stage, while *eve1* expression domain was expanded in mutant embryos at 22 hpf compared with control embryos (**Figures 3F,G**). Moreover, the expression of the known Bmp target genes *Id1* and *bmp4* was

examined in *bs69* mutant and control embryos. As seen in **Figure 3H**, the expression of these genes was up-regulated in *bs69* mutant embryos. Injection of 50 pg *bs69* mRNA into one-cell-stage *bs69* mutant embryos largely rescued the ventralized phenotypes (**Figure 3I**).

Next, we overexpressed Bs69 by injecting *bs69* mRNA into one-cell-stage wild-type embryos. Beta-gal overexpressing embryos were used as controls. The Bs69 overexpressing embryos at 24 hpf exhibited dorsalized phenotypes ranging from C1 to C4 dorsalization depending on the injected mRNA dose (**Figure 3J**). Smad1/5 phosphorylation was decreased in Bs69 overexpressing embryos (**Figure 3K**). Importantly, the DV patterning phenotype of Bs69 overexpressing embryos was similar to those of *bmpr1a* mutants or dnBmpr1a overexpressing embryos (Smith et al., 2011). To further confirm that Bs69 overexpressing embryos had dorsalized phenotypes, whole mount *in situ* hybridization was performed to examine the expression pattern of dorsal marker *chordin* and the ventral marker *eve1*. As expected, *chordin* expression domain was expanded in Bs69 overexpressing embryos at shield stage, while *eve1* expression domain was reduced in Bs69 overexpressing embryos at 22 hpf, compared to controls (**Figures 3L,M**). Moreover, the expression of *Id1* and *bmp4* genes was down-regulated in Bs69 overexpressing embryos, which was similar to that of *mga* mutant embryos (**Figure 3N**). Taken together, we concluded that Bs69 is required for the dorsal ventral patterning of zebrafish embryos, and functions as a negative regulator of Bmp signaling.

Bs69 Regulates Bmp Signaling by Association With Bmpr1a

Next, we investigated the mechanism by which Bs69 negatively regulates Bmp signaling. We hypothesized that Bs69 may regulate Bmp signaling through Bmpr1a in zebrafish. We therefore examined whether Bs69 interacts with Bmpr1a *in vivo*. We injected mRNAs encoding HA-Bs69 and Bmpr1a-FLAG into one-cell-stage *bs69* mutant or wild type embryos, and performed co-immunofluorescence and co-immunoprecipitation assays for 7 hpf embryos. Co-immunofluorescence data clearly showed that HA-Bs69 was co-localized with Bmpr1a-FLAG, and co-immunoprecipitation data demonstrated that HA-Bs69 interacts with Bmpr1a-FLAG (**Figure 4A**). Importantly, HA-Bs69 interacts with Bmpr1a-FLAG in the cytoplasmic fraction of embryonic lysate (**Figure 4B**).

Next, we mapped the interacting domain between Bs69 and Bmpr1a. pCS2-HA-Bs69 or pCS2-HA-Bs69-Mynd and PCS2-Bmpr1a-kinase-FLAG were transiently co-transfected into 293T cells, and co-IP experiments were performed using HA and FLAG antibodies **Figure 4C**. The Mynd domain of Bs69 was sufficient to interact with the kinase domain of Bmpr1a (**Figure 4D**). In contrast, Bs69Δ lacking the Mynd domain did not immunoprecipitate with Bmpr1a, and Bmpr1aΔ lacking the kinase domain did not immunoprecipitate with Bs69 (**Figures 4E,F**).

The association of Bs69 and Bmpr1a in physiological conditions strongly suggested that Bs69 modulates Bmpr1a activity. Like its mammalian counterpart, zebrafish Bs69 also has these three conserved chromatin reader domains (**Figure 2F**). It is possible that zebrafish Bs69 regulates Bmp signaling by modulating chromatin or functioning as a transcriptional co-factor. To investigate the significance of Bs69–Bmpr1a association for the regulation of Bmp signaling, we took advantage of the truncated form of Bs69 (BS69-Mynd) lacking all the chromatin reader domains but containing the intact Mynd domain that was still able to interact with Bmpr1a. By overexpressing Bs69-Mynd or HA-Bs69Δ, we were able to determine whether Bs69 regulates Bmp signaling by physical association with Bmpr1a. To this end, we injected 100 pg mRNAs encoding HA-tagged Bs69-Mynd or HA-Bs69Δ into one-cell-stage wild-type embryos, and collected embryos at 7 hpf or 24 hpf for subsequent assays. HA-Bs69-Mynd was localized in both nuclei and cytoplasm which was similar to HA-Bs69 (**Supplementary Figures S2A–C**). HA-Bs69-Mynd overexpressing embryos displayed dorsalized phenotypes that were similar to HA-Bs69 overexpressing embryos at 1 dpf (**Supplementary Figures S3A,B**). In contrast, HA-Bs69Δ overexpression did not cause obvious dorsalization of the embryos (data not shown). Next, we investigated whether Bs69-Mynd could rescue the DV patterning phenotype of *bs69* mutant embryos. Injection of 50 pg *bs69-mynd* or *bs69* mRNA into one-cell-stage *bs69* mutant embryos largely rescued the ventralized phenotypes at 1 dpf (**Supplementary Figure S3C**). In contrast, injection of 50 pg *bs69*Δ mRNA into one-cell-stage *bs69* mutant embryos had no effect on the DV patterning.

Phosphorylation of Smad1/5/8 at the C-terminal SXS motif by Bmp type I receptor is one of the most critical events in the transduction of Bmp signaling. We hypothesized that Bs69 may negatively regulate Bmp signaling through suppressing Bmpr1a activity by interfering its phosphorylation and activation of Smad1/5. If this is the case, loss of Bs69 function should cause increased Bmp signaling, indicated by elevated pSmad1/5 activity; whereas overexpressing Bs69 should cause decreased Bmp signaling, indicated by diminished pSmad1/5 activity. Indeed, Western blot analyses of Smad1/5 phosphorylation indeed supported this hypothesis (**Figures 3D,J**). Overexpressing HA-Bs69Δ had no obvious effect on the Smad1/5 phosphorylation (data not shown).

Taken together, we concluded that Bs69 negatively regulates Bmp signaling by physical association with Bmpr1a, which interferes with its phosphorylation and activation of Smad1/5.

Mga Binding to Bs69 Disrupts the Bs69–Bmpr1a Interaction

Because both Mga and Bmpr1a interact with Bs69 through its Mynd domain, we hypothesized that Mga modulates Bmpr1a activity through Bs69. To explore this, we examined the relationship between Mga–Bs69 and Bmpr1a–Bs69 interactions. We performed competitive protein-binding assay. The amount of HA-Bs69 co-immunoprecipitated with Bmpr1a-FLAG became reduced by the increased addition of Mga (**Figure 5A**), and the amount of HA-Bs69 co-immunoprecipitated with Mga became reduced by the increased addition of Bmpr1a-FLAG (**Figure 5B**).

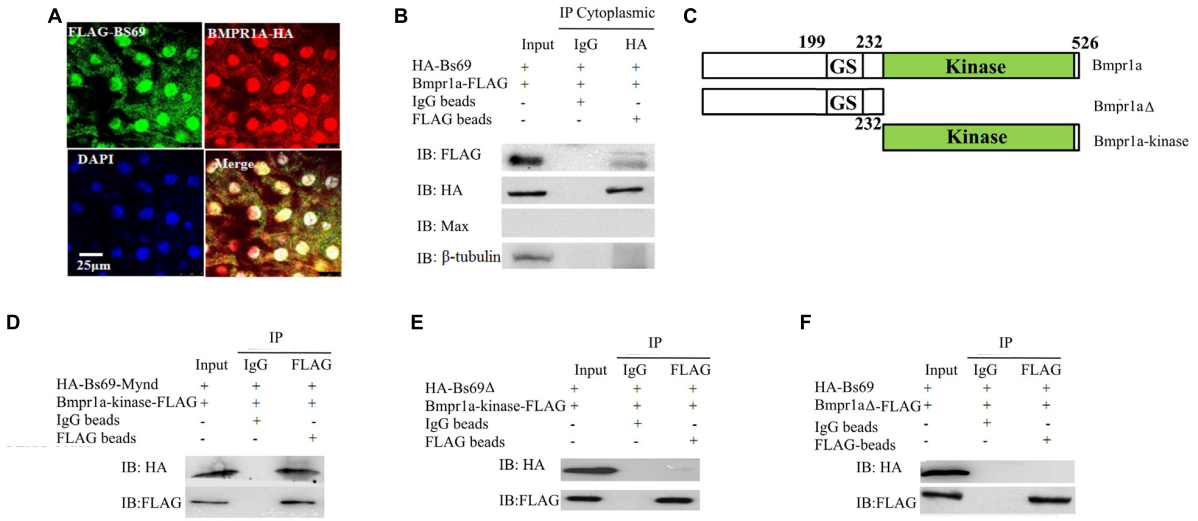

FIGURE 4 | Bs69 associates with Bmpr1a in zebrafish embryos. **(A)** Cellular co-localization of FLAG-Bs69 and Bmpr1a-HA in 7 hpf zebrafish embryos. Scale bar 25 μm. **(B)** Co-immunoprecipitation of HA-Bs69 and Bmpr1a-FLAG in cytoplasmic lysates from 7 hpf embryos. **(C)** Schematic representation of the full-length and truncated Bmpr1a as indicated. **(D)** Co-immunoprecipitation of HA-Bs69-Mynd and Bmpr1a-kinase-FLAG in 293T cells. **(E)** Bmpr1a-kinase-FLAG did not immunoprecipitate with HA-Bs69Δ in 293T cells. **(F)** Bmpr1aΔ-FLAG did not immunoprecipitate with HA-Bs69 in 293T cells.

These data suggested that Mga and Bmpr1a compete for the binding to Bs69.

Since Mga and Bmpr1a compete for the binding to Bs69, we speculated that Mga functions to maintain or enhance Bmp signaling by antagonizing Bs69 in physiological conditions. We injected into one-cell-stage wild-type embryos with 50 pg mRNA encoding HA-Bs69 or mixture of mRNAs encoding both HA-Bs69 and mouse or zebrafish MGAs. Embryos injected with 50 pg *beta-gal* mRNA were used for controls. Phosphorylation of Smad1/5 was detected by Western immunoblotting of lysates from 8 hpf embryos. As seen in **Figure 5C**, the pSmad1/5 levels in HA-Bs69 overexpressing embryos were reduced compared with control embryos. The pSmad1/5 levels were restored and even enhanced by simultaneously expressing either zebrafish or mouse MGAs, but not by MgaΔ that is unable to interact with Bs69 (**Figures 5C,D**). Accordingly, zebrafish or mouse MGAs rescued the loss of ventral tailfin phenotype in Bs69 overexpressing embryos at 1 dpf, supporting that Bmp signaling under control of Mga and bs69 is required for specifying the ventral tailfin cell fate (**Figure 5E**).

That Mga co-localizes and interacts with Bs69 in the cytoplasm strongly suggested that Mga localized in the cytoplasm functions to maintain Bmp signaling through Bs69–Bmpr1a axis. To test this hypothesis, we went on to generate completely nuclear or cytoplasmic version of Mga mutants. Using the NetNES or NLStradamus servers (la Cour et al., 2004; Nguyen et al., 2009), three putative nuclear localization sequences (NLSs) and two putative nuclear export sequences (NESs) were identified for Mga (**Figure 6A**). We injected mRNA encoding FLAG-MgaΔNES or FLAG-Mga-Cter into one-cell stage *mga* mutant zebrafish embryos, and collected 7 hpf embryos for assays described below. Our immunofluorescence assay showed that FLAG-MgaΔNES was strictly localized in the nuclei, whereas FLAG-Mga-Cter was found to be localized only in the cytoplasm (**Figures 6B,C**). These data indicated that we have successfully generated nuclear or cytosolic version of Mga protein. If it was Mga in the cytoplasm that regulates Bmp signaling through Bs69–Bmpr1a axis, then only cytosolic but not nuclear version of Mga protein could rescue the DV patterning defect of *mga* mutant. Indeed, we found that FLAG-Mga-Cter but not FLAG-MgaΔNES rescued the reduced ventral tailfin phenotype of 2 dpf *mga* mutant embryos (**Figure 6D**). Consistently, Smad1/5 phosphorylation was increased in 7 hpf *mga* mutant embryos by overexpressing FLAG-Mga-Cter but not by FLAG-MgaΔNES (**Figure 6E**). Finally, FLAG-Mga-Cter but not FLAG-MgaΔNES rescued the loss of ventral tailfin phenotype in Bs69 overexpressing embryos (data not shown). Together, these data strongly indicated that the role of Mga in the regulation Bmp signaling is mainly acting in the cytoplasm separately from its role as a DNA binding protein.

To further determine how Mga–Bs69 interaction affects Bmp signaling, luciferase activity assays were performed with a Bmp-responsive luciferase reporter BRE-luc. C2C12 cells were co-transfected overnight with pCS2-Mga, PCS2-Bs69, and BRE-luc, followed by 12 h serum starvation, and treated with BMP4 or left untreated for 16 h. As seen from **Figure 6F**, BMP4 treatment remarkably stimulated the Bmp-responsive BRE-luc activity and Bs69 inhibited it. When Mga and Bs69 were co-expressed, Mga substantially antagonized the inhibitory effect of Bs69 on the luciferase activity.

If Mga regulates Bmp signaling through Bs69–Bmpr1a axis, embryos simultaneously depleted of both Mga and Bs69 should have similar DV patterning phenotype to bs69 mutant embryos. To test this hypotheses, we depleted Mga by injecting 4–5 ng *mga* morpholino (mgaMO) into one-cell stage of *bs69* mutant embryos. 4–5 ng mgaMO was shown to cause a reduction of ventral tailfin phenotype in wild-type embryos (Sun et al., 2014).

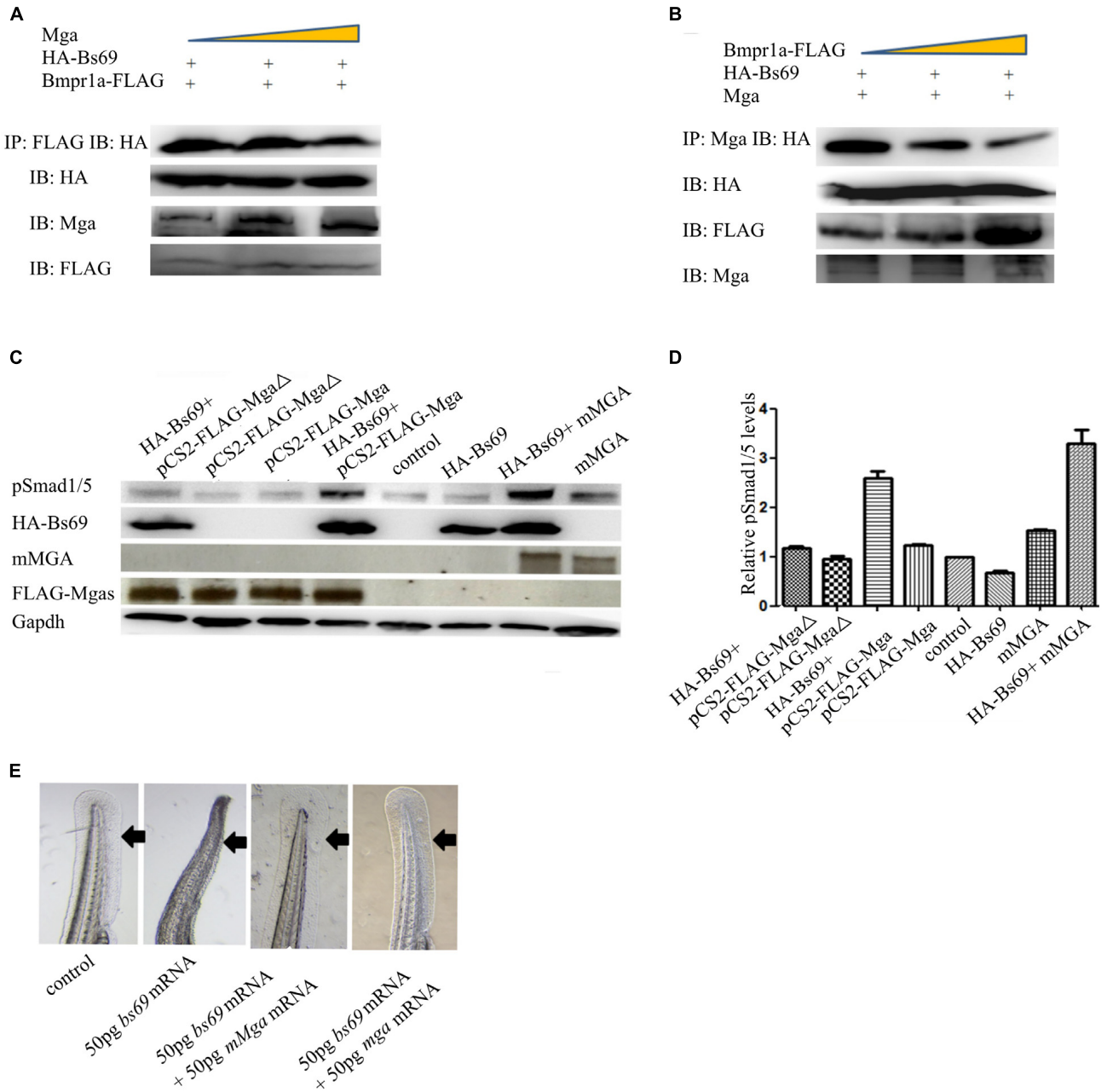

FIGURE 5 | Mga binds to Bs69 and disrupts the Bs69–Bmpr1a interaction. **(A)** Increasing dose of pCS2-Mga (1, 2, 3 μg) along with 1 μg pCS2-HA-Bs69, 1 μg pCS2-Bmpr1a-FLAG were transiently co-transfected into 293T cells, and co-immunoprecipitation of HA-Bs69 and Bmpr1a-FLAG was analyzed. **(B)** Increasing dose of pCS2-Bmpr1a-FLAG (1, 2, 3 μg) along with 1 μg pCS2-HA-Bs69, 1 μg pCS2-Mga were transiently co-transfected into 293T cells, and co-immunoprecipitation of HA-Bs69 and Mga was analyzed. **(C)** One-cell-stage wild-type embryos injected with 50 pg mRNA encoding HA-Bs69 or mixture of mRNAs encoding both HA-Bs69 and mouse MGA, or co-injected with 50 pg mRNA encoding HA-Bs69 with 100ng pCS2-FLAG-Mga or pCS2-FLAG-MgaΔ. Immunoblot analysis of pSmad1/5 levels was performed with lysates from the injected embryos at 8 hpf. **(D)** Relative quantification of pSmad1/5 levels of panel C. **(E)** One-cell-stage wild-type embryos injected with 50 pg mRNA encoding HA-Bs69 or mixture of mRNAs encoding both HA-Bs69 and mouse or zebrafish MGAs, and the ventral tail fin phenotypes of these embryos at 48 hpf were shown.

We found that mgaMO had no obvious effect on DV patterning phenotype of 1 dpf *bs69* mutants (**Supplementary Figure S4**).

Together, our data suggested that Mga antagonizes Bs69 to enhance the phosphorylation and activation of Smad1/5/8 both *in vitro* and *in vivo*.

Previous work showed that there are cardiac laterality defects in *bmpr1a* mutant embryos (Smith et al., 2011). If Mga regulates Bmp signaling through Bs69–Bmpr1a axis, *mga* mutant or Bs69 overexpressing embryos should exhibit similar laterality phenotypes as *bmpr1a* mutant embryos. We therefore

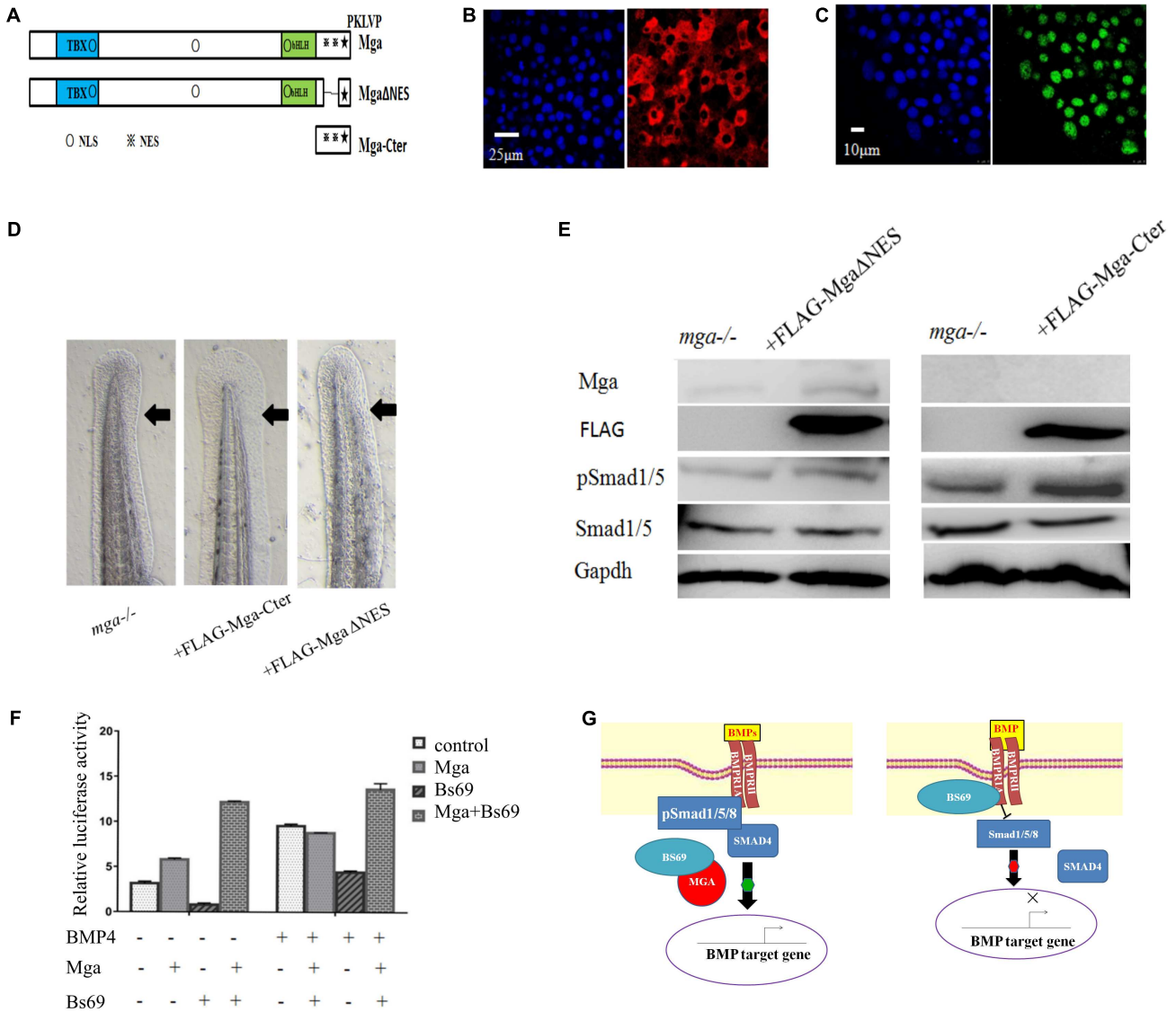

FIGURE 6 | Mga localized in the cytoplasm regulates Bmp signaling. **(A)** Diagram showing the location of putative NLS and ENS in Mga protein. ■: NLS, ■: NES. **(B)** IF showing the cytoplasmic localization of FLAG-Mga-Cter in 7 hpf embryos. **(C)** IF showing the nuclear localization of FLAG-MgaΔNES in 7 hpf embryos. **(D)** FLAG-Mga-Cter but not FLAG-MgaΔNES rescued the reduced ventral tailfin phenotype of *mga* mutant embryos at 2 dpf. **(E)** pSmad1/5 levels were increased in 7 hpf *mga* mutant embryos injected with 100 pg FLAG-Mga-Cter but not FLAG-MgaΔNES. **(F)** The BRE-luc activity assay for Mga and Bs69 in C2C12 cells. **(G)** Cartoon model of how Mga regulates Bmp signaling. Left: Mga localized in the cytoplasm associates with Bs69 which allow Bmpr1a to phosphorylate and activate Smad1/5/8. The pSmad1/5/8 form complex with Smad4 and translocate into nuclei to regulate Bmp target gene expression. Right: In the absence of Mga, Bs69 associates with Bmpr1a and interferes with its phosphorylation and activation of Smad1/5/8 which caused reduced Bmp signaling. All experiments were performed in technical triplicate and are representative of multiple experiments.

investigated whether *mga* mutant or Bs69 overexpressing embryos had the cardiac laterality defects. Whole mount *in situ* hybridization was performed to examine the expression of a set of laterality genes, including *spaw*, *lefty2* and *cmcl2*. Embryos treated with 0.05 μM dorsomorphin or LDN193189 were used as positive controls. A small percentage of *mga* mutant or Bs69 overexpressing embryos indeed displayed the left-right patterning defects similar to *bmpr1a* mutants or dorsomorphin treated embryos (**Supplementary Figures S5A,B**) (Smith et al., 2011). Importantly, Mga or Mga-Cter but not MgaΔ partially rescued the laterality defects of *mga* mutant or Bs69 overexpressing embryos (**Supplementary Figure S5C**).

DISCUSSION

In this work, we demonstrated that Mga protein localized in the cytoplasm regulates Bmp signaling at least partly by physically interacting with and antagonizing Bs69. We provided genetic and biochemical evidence that Bs69 is a negative regulator of

Bmp signaling. The Mynd domain of Bs69 binds to the kinase domain of Bmpr1a which interferes with its phosphorylation and activation of Smad1/5. Mga binds to Bs69 and disrupts the Bs69–Bmpr1a interaction which allows Smad1/5 to be phosphorylated, and proper Bmp signaling to be maintained. Functionally, the Bmp signaling under control of Mga is important for specifying the ventral tailfin cell fate in zebrafish embryos (**Figure 6G**).

Bs69 Functions as a Negative Regulator of Bmp Signaling by Association With Bmpr1a

BRAM1, previously thought as an alternatively spliced product of BS69, was first identified by a yeast two hybrid screen using BMPR1A as a bait in human cells (Kurozumi et al., 1998). However, based on the analysis of genomic sequences and *Bs69* gene product, Velasco et al. (2006) argued that the BRAM1 cDNA is in fact an artificial chimeric product between *Anks1* and *Bs69* sequences that happened from a recombination event during the cDNA library construction. Zebrafish Bram1 cDNA, isolated from a cDNA library by RACE technique, is merely a C-terminal part of the full length Bs69 cDNA, as the proposed zebrafish *bram1* gene encodes a peptide lacks the featured MLLEPPSPVPW sequences like its mammalian counterparts. Moreover, we failed to amplify any Bram1-like cDNAs from our zebrafish cDNA libraries. Thus, we think that no Bram1 type exists in zebrafish. In this context, we are the first to dissect the developmental function of Bs69 using zebrafish as a model. In this work, by loss of function and overexpression assays, we demonstrated that zebrafish Bs69 is a negative regulator of Bmp signaling by physically interacting with Bmpr1a. The Mynd domain of Bs69 is indispensible for this function as it mediates Bs69 binding to the kinase domain of Bmpr1a.

The majority of studies so far proposed that BS69 function as co-factor for transcriptional or chromatin regulation in the nucleus (Hateboer et al., 1995; Guo et al., 2014; Wen et al., 2014). In recent years, however, a growing body of work have demonstrated that BS69 has important roles in the regulation of signaling pathways in the cytoplasmic membrane. For instances, BS69 was shown to interact with multiple *trans*-membrane proteins, including LMP1, LTβR, and BMPR1A (Kurozumi et al., 1998; Liu et al., 2011; this study). BS69 is also constitutively co-localized in the membrane lipid rafts in mammalian cells (Wan et al., 2006). Lipid rafts were proposed to function in membrane protein sorting and in the formation of signaling complexes, as well as in endocytic trafficking (Hartung et al., 2006). It is possible that Bs69 is localized in membrane lipid rafts in zebrafish cells and may be involved in the endocytosis of Bmp receptors or the formation of ligand-receptor complex. In the future, it will be interesting to look into this possibility.

Mga Interacts With Bs69 to Regulate Bmp Signaling

MAX giant associated protein is a transcriptional factor containing both T-box and bHLH domains, and was proposed to regulate the expression of both Max-network or T-box family genes (Hurlin et al., 1999). The Myc family of transcriptional factors are known for their role in the control of cell cycle progression, cellular growth and proliferation (Gallant, 2006). The T-box family of transcriptional factors play key role in mesendoderm formation in vertebrate embryogenesis (Papaioannou, 2014). Surprisingly, our *mga* mutant zebrafish are viable, and can grow up to adult without obvious morphological defects, except the loss or reduction of ventral tailfin. This fact indicates that Mga is not critically required for cell cycle progression and cell proliferation in zebrafish, and that Mga has limited function as the member of the T-box family of transcriptional factors. Alternatively, there are certain compensation mechanisms to allow normal zebrafish development in the absence of Mga. In this context, our work revealed a different requirement of MGA for zebrafish and mice embryonic development.

Our previous work suggested that Mga:Max could transcriptionally regulate bmp2b expression by binding to its promotor or enhancer in YSL in zebrafish. Now, we show that Mga localized in the cytoplasm directly interacts with and antagonizes Bs69 to modulate Bmpr1a-mediated Bmp signaling. This surprising role of Mga protein is executed in the cytoplasm, does not require dimerization with Max, and is independent of its transcriptional or chromatin remodeling activities. This is consistent with the observation that Mga is predominantly localized in the cytoplasm throughout zebrafish early embryogenesis. Indeed, mouse MGA is also predominantly localized in the cytoplasm (data not shown), suggesting that similar mechanism for the regulation of Bmp signaling occurs in mammals. We found that zebrafish Mga physically associates with Bs69 in the physiological conditions and this interaction is mediated by the PXLXP motif of Mga and the Mynd domain of Bs69. Mga-Cter binding to Bs69 disrupts the Bs69–Bmpr1a association which allows proper Bmp signaling to be maintained. By applying mga morpholino, we depleted Mga in *bs69* mutant background. And we found that embryos depleted of both proteins had a similar DV patterning phenotype to bs69 mutant animals. This data further supported our hypotheses that Mga regulates Bmp signaling through Bs69–Bmpr1a axis.

Our previous work showed that Mga-Cter also binds to Smad4 and Smad1, two core components of Bmp signaling pathway (Sun et al., 2014). It is possible that Mga, Bs69, and Smad4 could form a triplex or Bs69 competes with Smad4 for binding to Mga. In any case, Mga binding to Bs69 could even enhance Bmp signaling by simultaneously antagonizing Bs69 and promoting the formation of Smad4: pSmad1/5/8 complex at the cytoplasmic membrane via releasing or bringing Mga bound Smad4 or Smad1 to Bmpr1a. This may explain why expressing both Bs69 and Mga had significantly stronger effect on Bmp activity than expressing Mga only (**Figures 5D**, **6F**). Altogether, these data indicate that Mga functions to control Bmp signaling pathways in different cellular compartments, at different levels and through different mechanisms. To our knowledge, this is the first report showing that certain member of the Myc or T-box

family of transcriptional factors regulates signaling pathways in the cytoplasm. Nevertheless, *mga* mutant embryos at 1 dpf displayed mild DV patterning defects, suggesting that Mga acts to fine-tune Bmp signaling in zebrafish.

In addition to the regulation of Bmp signaling, both Bs69 and Mga are known chromatin readers and remodelers, raising an interesting question whether Mga and Bs69 could link Bmp signaling to chromatin structure regulation or transcriptional elongation (Velasco et al., 2006; Guo et al., 2014). Answering this question will help us to understand how signal transduction pathways directly communicate with chromatin to change the epigenetic landscape or gene expression. With *mga* and *bs69* mutant zebrafish in hand, this question is under investigation in our lab.

ETHICS STATEMENT

This study was carried out in accordance with the recommendations of ethical approval had been obtained from Animal ethical committee of Institute of hydrobiology for the approval of animal experiments. The protocol was approved by the "Animal Ethical Committee."

AUTHOR CONTRIBUTIONS

YS and SD designed the experiments. XS, JC, YZ, and MM performed the experiments. YS wrote the manuscript.

FUNDING

This work was supported by National Key Research and Development Program (2016YFA0101100), National Natural Science Foundation of China (31671526), and Hundred-Talent Program (CAS and IHB) (Y623041501).

ACKNOWLEDGMENTS

We thank Dr. Amar Singh from Molecular Medicine Center of UGA for critical comments of the manuscript, Gang Ouyang and Huan Xiong for excellent technical support, and Prof. Xiao Wuhan and Prof. Cui Zongbin from Institute of Hydrobiology for providing BRE-luc and SBE-luc reporter plasmids.

SUPPLEMENTARY MATERIAL

The Supplementary Material for this article can be found online at: https://www.frontiersin.org/articles/10.3389/fcell.2018.00126/full#supplementary-material

FIGURE S1 | (A) The phenotypes of 1 dpf wild type embryos treated with 0.05 μM DMSO, or 0.05 μM dorsomorphin or 0.05 μM LDN193189 starting at one-cell stage, or injected with 50 pg *dnBmpr1a* mRNA at one-cell-stage. **(B)** 50 pg *caBmpr1a* mRNA rescued the loss of ventral tail fin phenotype of *mga* mutant embryos. Shown are representative embryos at 2 dpf. **(C)** WISH for 72 hpf embryos using *mga*, *bs69*, and *bmpr1aa* probes. *mga* and *bs69* probes are DIG-labeled, whereas *bmpr1aa* probe is fluorescein-labeled.

FIGURE S2 | (A) The co-localization of Mga and HA-Bs69-Mynd in 7 hpf embryos. **(B)** The co-localization of zebrafish Mga and HA-Bs69 in 293T cells. **(C)** The co-localization of zebrafish Mga and HA-Bs69-Mynd in 293T cells.

FIGURE S3 | (A) Dorsalized phenotypes of HA-Bs69-Mynd overexpressing embryos at 2 dpf. C1-4 classification according to DV patterning index. **(B)** Western blot analysis of lysates from 8 hpf HA-Bs69-Mynd overexpressing or control embryos. **(C)** Tail region of 2 dpf *bs69* mutant embryos injected at one-cell-stage with 50 pg mRNAs encoding HA-Bs69-Mynd or β-Gal.

FIGURE S4 | (A) DV patterning phenotypes of $bs69^{-/-}$ mutant embryos at 1 dpf injected with 4 ng mgamisMO or mgaMO. V1-2 classification according to DV patterning index. **(B)** Quantification of **(A)** based on three independent experiments.

FIGURE S5 | (A) The cardiac laterality defects of *mga* mutant or Bs69 overexpressing embryos at 1 dpf revealed by WISH using *spaw*, *lefty2*, and *cmlc2* probes. **(B)** Percentage of embryos that exhibited cardiac laterality defects. L, left; M, middle; R, right. **(C)** 50 pg mouse *mga* mRNA partially rescued the cardiac laterality defects of *mga* mutants at 1 dpf; 50 pg *caBmpr1a* mRNA partially rescued the cardiac laterality defects of Bs69 overexpressing embryos at 1 dpf.

REFERENCES

Ansieau, S., and Leutz, A. (2002). The conserved Mynd domain of BS69 binds cellular and oncoviral proteins through a common PXLXP motif. *J. Biol. Chem.* 277, 4906–4910. doi: 10.1074/jbc.M110078200

Chen, J., Cui, X. J., Jia, S. T., Luo, D. J., Cao, M. X., Zhang, Y. S., et al. (2016). Disruption of dmc1 produces abnormal sperm in medaka (*Oryzias latipes*). *Sci. Rep.* 6:30912. doi: 10.1038/srep30912

Chung, P. J., Chang, Y. S., Liang, C. L., and Meng, C. L. (2002). BRAM1 functions by the bone morphogenetic protein receptor IA-binding protein, negative regulation of epstein-barr virus latent membrane protein 1-mediated. *Biol. Chem.* 277, 39850–39857. doi: 10.1074/jbc.M206736200

De Paoli, L., Cerri, M., Monti, S., Rasi, S., Spina, V., Bruscaggin, A., et al. (2013). MGA, a suppressor of MYC, is recurrently inactivated in high risk chronic lymphocytic leukemia. *Leukemia Lymphoma* 54, 1087–1090. doi: 10.3109/10428194.2012.723706

Endoh, M., Endo, T., Shinga, J., Hayashi, K., Farcas, A., Ma, K. W., et al. (2017). PCGF6-PRC1 suppresses premature differentiation of mouse embryonic stem cells by regulating germ cell-related genes. *eLife* 6:e21064. doi: 10.7554/eLife.21064

Gallant, P. (2006). Myc/Max/Mad in invertebrates: the evolution of the max network. *Curr. Top. Microbiol. Immunol.* 302, 235–253.

Gao, Z. H., Zhang, J., Bonasio, R., Strino, F., Sawai, A., Parisi, F., et al. (2012). PCGF homologs, CBX proteins, and RYBP define functionally distinct PRC1 family complexes. *Mol. Cell* 45, 344–356. doi: 10.1016/j.molcel.2012.01.002

Guo, R., Zheng, L. J., Park, J. W., Lv, R., Chen, H., Jiao, F. F., et al. (2014). BS69/ZMYND11 reads and connects histone H3.3 lysine 36 trimethylation-decorated chromatin to regulated pre-mRNA processing. *Mol. Cell* 56, 298–310. doi: 10.1016/j.molcel.2014.08.022

Harter, M. R., Liu, C. D., Shen, C. L., Gonzalez-Hurtado, E., Zhang, Z. M., and Xu, M. (2016). BS69/ZMYND11 C-terminal domains bind and inhibit EBNA2. *PLoS Pathog.* 12:e1005414. doi: 10.1371/journal.ppat.1005414

Hartung, A., Bitton-Worms, K., Rechtman, M. M., Wenzel, V., Boergermann, J. H., Hassel, S., et al. (2006). Different routes of bone morphogenic protein (BMP) receptor endocytosis influence BMP signaling. *Mol. Cell. Biol.* 26, 7791–7805. doi: 10.1128/MCB.00022-06

Hateboer, G., Gennissen, A., Ramos, Y. F., Kerkhoven, R. M., Sonntag-Buckl, V., Stunnenberg, H. G., et al. (1995). BS69, a novel adenovirus ElA-associated protein that inhibits EIA transactivation. *EMBO J.* 14, 3159–3169. doi: 10.1002/j.1460-2075.1995.tb07318.x

Hurlin, P. J., Steingrı msson, E., Copeland, N. G., Jenkins, N. A., and Eisenman, R. N. (1999). Mga, a dual-specificity transcription factor that interacts with Max and contains a T-domain DNA-binding motif. *EMBO J.* 18, 7019–7028. doi: 10.1093/emboj/18.24.7019

Ikeda, O., Sekine, Y., Mizushima, A., Oritani, K., Yasui, T., Fujimuro, M., et al. (2009). BS69 negatively regulates the canonical NF-jB activation induced by epstein–barr virus-derived LMP1. *FEBS Lett.* 583, 1567–1574. doi: 10.1016/j.febslet.2009.04.022

Jo, Y. S., Kim, M. S., Yoo, N. J., and Lee, S. H. (2016). Somatic mutation of a candidate tumour suppressor MGA gene and its mutational heterogeneity in colorectal cancers. *Pathology* 48, 525–527. doi: 10.1016/j.pathol.2016.04.010

Katagiri, T., and Watabe, T. (2016). Bone Morphogenetic Proteins. *Cold Spring Harbor Perspect. Biol.* 22, 233–241. doi: 10.1101/cshperspect.a021899

Kishimoto, Y., Lee, K. H., Zon, L., Hammerschmidt, M., and Schulte-Merker, S. (1997). The molecular nature of zebrafish swirl: BMP2 function is essential during early dorsoventral patterning. *Development* 124, 4457–4466.

Kurozumi, K., Nishita, M., Yamaguchi, K., Fujita, T., Ueno, N., and Shibuya, H. (1998). BRAM1, a BMP receptor-associated molecule involved in BMP signaling. *Genes Cells* 3, 257–264. doi: 10.1046/j.1365-2443.1998.00186.x

la Cour, T., Kiemer, L., Mølgaard, A., Gupta, R., Skriver, K., and Brunak, S. (2004). Analysis and prediction of leucine-rich nuclear export signals. *Protein Eng. Des. Sel.* 17, 527–536. doi: 10.1093/protein/gzh062

Liu, H. P., Chung, P. J., Liang, C. L., and Chang, Y. S. (2011). The MYND domain-containing protein BRAM1 inhibits lymphotoxin beta receptor-mediated signaling through affecting receptor oligomerization. *Cell. Signal.* 23, 80–88. doi: 10.1016/j.cellsig.2010.08.006

Liu, X., Chen, Z., Xu, C. X., Leng, X. Q., Cao, H., Ouyang, G., et al. (2015). Repression of hypoxia-inducible factor α signaling by set7-mediated methylation. *Nucleic Acids Res.* 43, 5081–5098. doi: 10.1093/nar/gkv379

Morita, K., Shimizu, M., Shibuya, H., and Ueno, N. (2001). A DAF-1-binding protein BRA-1 is a negative regulator of DAF-7 TGF-b signaling. *PNAS* 98, 6284–6288. doi: 10.1073/pnas.111409798

Nguyen, B., Pogoutse, A., Provart, N., and Moses, A. (2009). NLStradamus: a simple Hidden Markov Model for nuclear localization signal prediction. *BMC Bioinformatics* 10:202. doi: 10.1186/1471-2105-10-202

Nikaido, M., Tada, M., Takeda, H., Kuroiwa, A., and Ueno, N. (1999). In vivo analysis using variants of zebrafish BMPR-IA: range of action and involvement of BMP in ectoderm patterning. *Development* 126, 181–190.

Ogawa, H., Ishiguro, K., Gaubatz, S., Livingston, D. M., and Nakatani, Y. (2002). A complex with chromatin modifiers that occupies E2F- and Myc-responsive genes in G0 cells. *Science* 296, 1132–1136. doi: 10.1126/science.1069861

Papaioannou, V. E. (2014). The T-box gene family: emerging roles in development, stem cells and cancer. *Development* 141, 3819–3833. doi: 10.1242/dev.104471

Pyati, U. J., Webb, A. E., and Kimelman, D. (2005). Transgenic zebrafish reveal stage-specific roles for Bmp signaling in ventral and posterior mesoderm development. *Development.* 132, 2333–2343. doi: 10.1242/dev.01806

Rikin, A., and Evans, T. (2010). The tbx/bHLH transcription factor Mga regulates gata4 and organogenesis. *Dev. Dyn.* 239, 535–547. doi: 10.1002/dvdy.22197

Schumacher, J. A., Hashiguchi, M., Nguyen, V. H., and Mullins, M. C. (2011). An intermediate level of BMP signaling directly specifies cranial neural crest progenitor cells in zebrafish. *PLoS One* 6:e27403. doi: 10.1371/journal.pone.0027403

Smith, K. A., Noel, E., Thurlings, I., Rehmann, H., Chocron, S., and Bakkers, J. (2011). Bmp and Nodal independently regulate lefty1 expression to maintain unilateral Nodal activity during left-right axis specification in zebrafish. *PLoS Genet.* 7:e1002289. doi: 10.1371/journal.pgen.1002289

Sun, Y. H., Tseng, W. C., Ball, R., and Dougan, S. (2014). Extra-embryonic signals under the control of Mga, Max and Smad4 are required for dorsoventral patterning. *Dev. Cell* 28, 322–334. doi: 10.1016/j.devcel.2014.01.003

Sun, Y. H., Wloga, D., and Dougan, S. (2011). Embryological manipulations in zebrafish. *Methods Mol. Biol.* 770, 139–184. doi: 10.1007/978-1-61779-210-6_6

Suzuki, A., Hirasaki, M., Hishida, T., Wu, J., and Okamura, D. (2017). Loss of MAX results in meiotic entry in mouse embryonic and germline stem cells. *Nat. Commun.* 7:11056. doi: 10.1038/ncomms11056

The Cancer Genome Atlas Research Network (2014). Comprehensive molecular profiling of lung adenocarcinoma. *Nature* 511, 543–550. doi: 10.1038/nature13385

Velasco, G., Grkovic, S., and Ansieau, S. (2006). New insights into BS69 functions. *J. Biol. Chem.* 281, 16546–16550. doi: 10.1074/jbc.M600573200

Wan, J., Zhang, W., Wu, L., Bai, T., Zhang, M., Lo, K. W., et al. (2006). BS69, a specific adaptor in the latent membrane protein 1-mediated c-Jun N-terminal kinase pathway. *Mol. Cell. Biol.* 26, 448–456. doi: 10.1128/MCB.26.2.448-456.2006

Wang, R. N., Green, J., Wang, Z. L., Deng, Y. L., Qiao, M., Peabody, M., et al. (2014). Bone morphogenetic protein (BMP) signaling in development and human diseases. *Genes Dis.* 1, 87–105. doi: 10.1016/j.gendis.2014.07.005

Washkowitz, A. J., Schall, C., Zhang, K., Wurst, W., Floss, T., Mager, J., et al. (2015). Papaioannou. Mga is essential for the survival of pluripotent cells during peri-implantation development. *Development* 142, 31–40. doi: 10.1242/dev.111104

Wen, H., Li, Y. Y., Xi, Y. X., Jiang, S. M., Stratton, S., Peng, D., et al. (2014). ZMYND11 links histoneH3.3K36me3 to transcription elongation and tumour suppression. *Nature* 508, 263–268. doi: 10.1038/nature13045

Wu, K. M., Huang, C. J., Hwang, S. P., and Chang, Y. S. (2006). Molecular cloning, expression and characterization of the zebrafish bram1 gene, a BMP receptor-associated molecule. *J. Biomed. Sci.* 13, 345–355. doi: 10.1007/s11373-005-9066-2

Conflict of Interest Statement: The authors declare that the research was conducted in the absence of any commercial or financial relationships that could be construed as a potential conflict of interest.

frontiers in Cell and Developmental Biology

METHODS
published: 25 October 2018
doi: 10.3389/fcell.2018.00144

Analyzing Neuronal Mitochondria *in vivo* Using Fluorescent Reporters in Zebrafish

*Amrita Mandal, Katherine Pinter and Catherine M. Drerup**

Unit on Neuronal Cell Biology, NICHD, National Institutes of Health, Bethesda, MD, United States

Despite their importance for cellular viability, the actual life history and properties of mitochondria in neurons are still unclear. These organelles are distributed throughout the entirety of the neuron and serve many functions, including: energy production (ATP), iron homeostasis and processing, calcium buffering, and metabolite production, as well as many other lesser known activities. Given their importance, understanding how these organelles are positioned and how their health and function is maintained is critical for many aspects of cell biology. This is best illustrated by the diverse disease literature which demonstrates that abnormal mitochondrial movement, localization, size, or function often correlates with neural pathology. In the following methods article, we will describe the techniques and tools we have optimized to directly visualize mitochondria and analyze mitochondrial lifetime, health, and function in neurons *in vivo* using fluorescent reporters in the zebrafish. The zebrafish system is ideal for *in vivo* studies of mitochondrial biology as: (1) neuronal circuits develop rapidly, within days; (2) it is genetically accessible; and (3) embryos and larvae are translucent allowing imaging in a completely intact vertebrate nervous system. Using these tools and techniques, the field is poised to answer questions of mitochondrial biology in the context of neuronal health and function in normal and disease states.

Keywords: mitochondria, neuron, dynein, kinesin, zebrafish, axonal transport

OPEN ACCESS

Edited by:
Gokhan Dalgin,
University of Chicago, United States

Reviewed by:
Ross F. Collery,
Medical College of Wisconsin, United States
Rachel Elizabeth Moore,
King's College London, United Kingdom

****Correspondence:***
Catherine M. Drerup
katie.drerup@nih.gov

Specialty section:
This article was submitted to Molecular Medicine, a section of the journal Frontiers in Cell and Developmental Biology

Received: *19 July 2018*
Accepted: *08 October 2018*
Published: *25 October 2018*

Citation:
Mandal A, Pinter K and Drerup CM (2018) Analyzing Neuronal Mitochondria in vivo Using Fluorescent Reporters in Zebrafish. Front. Cell Dev. Biol. 6:144. doi: 10.3389/fcell.2018.00144

INTRODUCTION

Mitochondria and the eukaryotic cells in which they reside are considered symbiotes. This now critical organelle is thought to have originally entered into existence as a bacteria that took up residence in another cell, likely a eukaryote. From that time until now, co-evolution of mitochondria and the cells of plants and animals have given rise to a situation in which each depends upon the other for survival. During this co-evolution, mitochondria have taken on many responsibilities in the cell. In addition to their well-known role in Adenosine Tri-Phosphate (ATP) synthesis, mitochondria function to buffer and store calcium, produce essential metabolites, synthesize signaling molecules, and regulate iron and iron processing. Despite these essential functions, we have only a minimal understanding of mitochondrial life history in cells. In particular, our knowledge of mitochondrial properties in neurons is specifically lacking. We will describe the tools developed by our lab and others that utilize zebrafish to study mitochondrial health, function, movement, and turnover *in vivo*, in order to understand mitochondrial life history in neurons.

Mitochondrial Structure and Function

Mitochondria are double membrane-bound organelles. The canonical structure, starting from the outside, includes an outer membrane, inner membrane space, inner membrane and matrix. The curvature of the inner membrane creates the observed cristae. The most well-characterized function of mitochondria is producing ATP, the primary source of energy for cellular activities. This process occurs within the mitochondrial cristae. In neurons, the demand for ATP is incredibly high due to their high metabolic rate even at resting states. It is estimated that average activity in rodent gray matter, for example, uses ∼30 μmol ATP/g/min (Attwell and Laughlin, 2001). Since an average rat brain is ∼2 g, this means that every hour a rat brain is burning 3.6 mmol of ATP.

The generation of ATP in mitochondria occurs through the conversion of the pyruvate generated from glycolysis to acetyl CoA (the first step of the Kreb cycle; localized to the mitochondrial matrix). Acetyl CoA is then used to generate the carbon dioxide necessary to produce NADH/$FADH_2$, the substrates of oxidative phosphorylation, i.e., ATP production. For this process to proceed, an oxidative potential must be maintained across the inner membrane. To create an oxidative potential, the inner membrane space is maintained at high hydrogen ion concentrations compared to the matrix, this creates a pH and charge gradient within mitochondria. Maintenance of mitochondrial matrix potential is tightly linked to mitochondrial health and several methods have been developed to monitor this aspect of mitochondrial biology. The most common method is the cationic dye tetramethylrhodamine ethyl ester (TMRE). This vital dye accumulates in the mitochondrial matrix due to its negative charge. Consequently, the fluorescence intensity of the mitochondrial TMRE is a readout of matrix potential and health. Though commonly used in cultured cells, the ability to measure matrix potential *in vivo* has, to date, been lacking. The maintenance of mitochondrial matrix potential is accomplished by a complex array of proteins intricately arranged in specific compartments within the organelle. Of particular importance are the respiratory chain complexes I-IV. These complexes maintain the proton and pH gradients across the inner membrane that are critical to ultimately power ATP synthase, generating ATP. Interestingly, a subset of the main components of the electron transport chain in mitochondria are encoded by the mitochondrial DNA, while the rest of the Complex I-IV components and the majority of the proteins that form and maintain the mitochondria are synthesized externally from nuclear DNA.

In addition to generating ATP, mitochondria serve as a calcium buffer and reservoir in cells. Calcium enters mitochondria through the largely unselective Voltage Dependent-Anion Channel (VDAC) (Gincel et al., 2001). Once in the inner membrane space, calcium is transported to the mitochondrial matrix by the mitochondrial calcium uniporter (MCU). For calcium release back to the cytoplasm, mitochondria utilize both sodium-dependent and independent calcium channels. Mitochondrial calcium levels are highly regulated and thought to rely on the cytoplasmic calcium concentration, in addition to other signals (Kirichok et al., 2004). Consequently, high calcium levels in the local microenvironment can result in rapid uptake of calcium into the mitochondrial matrix. In the mitochondria, calcium levels regulate mitochondrial functions as well as signaling molecules associated with cell death and cell survival (reviewed in Pivovarova and Andrews, 2010). Thus, calcium levels must be tightly regulated in mitochondria to ensure organelle function and cell viability are maintained.

Calcium regulation by mitochondria is especially critical in neurons. High cytosolic calcium levels have been linked to axonal and neural degeneration. This is likely due to the fact that mitochondria harbor cell death genes whose release regulates apoptosis. When calcium levels remain elevated in this organelle, mitochondria release these proteins and induce apoptosis, leading to loss of neural tissue. While high calcium levels on a prolonged basis lead to cell death, regulated elevation of calcium levels in mitochondria stimulates ATP synthesis (McCormack and Denton, 1989). Transient increases in cytoplasmic and consequently mitochondrial calcium levels commonly occur in neurons, particularly at synapses. Action potentials triggered by circuit activity lead to the activation of presynaptic calcium channels and calcium influx. Following calcium store release, this ion must be rapidly removed from the cytosol to regulate synaptic release. Both the endoplasmic reticulum (ER) and the mitochondria have been proposed to serve as intracellular stores that can rapidly buffer calcium after neuronal activity, though their relative contribution is still a source of active research and debate. It is likely that these organelles actually function in concert to regulate calcium ion levels as they are tightly coupled at regions of ER-contact sights shown to influence mitochondrial activity and signaling (Boehning et al., 2004; Cárdenas et al., 2010; Raturi et al., 2016). However, the role of mitochondria in calcium homeostasis has been difficult to address *in vivo*. We have optimized approaches to use genetically encoded calcium indicators (GECIs) to assay cytoplasmic and mitochondrial calcium levels *in vivo*. GECIs are commonly used to measure transient increases in intracellular calcium in neurons as an indicator of neuronal activity. These indicators typically consist of a calcium binding domain fused to one or two fluorescent proteins. The binding of calcium changes the fluorescence intensity of the signal. Common GECIs include GCaMP variants and GECOs. Particularly useful are the GECO color variants, including the red indicator R-GECO1, which has been used previously to study hair cell responses to mechanical stimulation (Maeda et al., 2014). The combination of calcium indicators with different spectral properties allows monitoring of whole cell calcium levels and subcellular compartments simultaneously as described below. As calcium serves to regulate neuronal activity, neuronal maintenance, and has a critical role in regulating mitochondrial movement, understanding the dynamics of mitochondrial-cytoplasmic calcium flux *in vivo* is of significant importance.

Finally, mitochondria can also act as signaling centers in cells. During the process of oxidative phosphorylation, mitochondria produce metabolites including NADH, FADH, succinate, reactive oxygen species (ROS), and many others. These molecules, sometimes thought of as byproducts, have been shown to induce cellular responses (Chandel et al., 1998; Sena and Chandel,

2012; Weinberg and Chandel, 2015; Weinberg et al., 2015). For instance, evidence in cancer cell lines has demonstrated that mitochondrial metabolites can in fact signal to regulate the growth and movement of these cells, making this organelle a target for cancer therapy (Wang et al., 2011; Weinberg and Chandel, 2015). In addition, work in neurons has demonstrated that mitochondrial positioning can regulate the localization of axon branching (Courchet et al., 2013; Spillane et al., 2013). While this could be attributed to the higher levels ATP in the microenvironment surrounding this organelle, it is entirely possible that the signaling molecules produced locally could regulate subcellular dynamics necessary for axon branching to initiate as well. With the incredible potential of mitochondrial metabolites to influence the local microenvironment, the maintenance and regulation of mitochondrial health and positioning within the neuron is of obvious importance. To date, it has been difficult to measure mitochondrial metabolite production *in vivo*. We have developed a protocol to use transient transgenic animals that express an indicator of chronic ROS production in neurons. This protein, Timer, is oxidation sensitive, switching its fluorescence spectrum based on oxidation state (Hernandez et al., 2013; Laker et al., 2014). With this new tool, we have the ability to assay chronic ROS in various neuronal compartments in normal states and with manipulation.

Mitochondrial Dynamics

Mitochondria are not static, but are rather quite dynamic organelles. One activity of particular importance for mitochondrial maintenance is the active interchange of mitochondrial components, known as mitochondrial dynamics. The term mitochondrial dynamics describes the fusion events that bring two mitochondria together as well as the fission events which produce two daughter mitochondria from a single parental organelle. Work on mitochondrial dynamics has shown a clear role for fusion in the maintenance of mitochondrial health. Studies in which mitochondrial fusion has been disrupted have shown that this leads to loss of mitochondrial DNA and subsequent mitophagy (Chen et al., 2005, 2010; Chen and Chan, 2009). Several mitochondrial proteins have been identified as necessary for mitochondrial fusion, including Mitofusin and OPA1 (Optic Atrophy 1; Alexander et al., 2000; Delettre et al., 2000; Zuchner et al., 2004). Loss of either protein results in highly fragmented mitochondria, degradation of these organelles, and subsequent neuronal cell death. The necessity of fusion is thought to be due to in its ability to replenish proteins and mitochondrial DNA quality and quantity, maintaining the organelle's health and function. Of similar importance is the process of mitochondrial fission. During fission, receptors on the mitochondrial outer membrane, such as Fis1 and Mff, recruit the dynamin-related protein Drp1 to mitochondria. Drp1 oligomerizes, resulting in a constricted point that then cleaves to generate two independent organelles. While the process of fission is clearly important for the maintenance of a healthy mitochondrial pool (Parone et al., 2008; Twig et al., 2008; Ban-Ishihara et al., 2013), the underlying mechanistic reasons for its necessity, particularly in neurons, are somewhat unknown. A subset of literature suggests that fission may be a way for the "unhealthy" parts of the organelle to be targeted for degradation. Evidence to support this includes the lower membrane potential observed in one of the two daughter mitochondria following division; however, the fate of the daughter mitochondria after fission is not clear. Therefore, the actual function of mitochondrial fission in the maintenance of a healthy mitochondrial pool in neurons is still an active area of investigation.

Mitochondrial Transport

A process intricately related to mitochondrial dynamics is mitochondrial transport. Active transport of this organelle occurs in all cell types, but neurons are perhaps most keenly sensitive to the precise regulation of this process due to their large size and high metabolic demand. Neurons, unlike many cell types, have large processes which can stretch up to a meter away from their cell bodies in humans, as is the case for a subset of axons that make up the sciatic nerve. This means that their axon length to cell body diameter ratio is roughly 100,000 to 1. In order to form and maintain this enormous structure, proteins and organelles must be actively transported through the cell body and processes using molecular motors and their microtubule tracks. These tracks are unipolar in axons, with their plus or fast-growing end situated toward axon terminals. The directionality of these tracks governs the direction of movement by microtubule-based motor proteins. Anterograde axonal transport (away from the cell body/toward microtubule plus ends) utilizes a superfamily of Kinesin motors proteins (Pilling et al., 2006). Conversely, retrograde axonal transport (cell body-directed/toward microtubule minus ends) is primarily accomplished by a single motor protein complex, Cytoplasmic Dynein (Schnapp and Reese, 1989). The mechanics and regulatory mechanisms that control how and when these motors attach to and move mitochondria through axons is tightly regulated and a subject of intense investigation.

Anterograde mitochondrial movement is largely accomplished by the Kinesin-1 molecular motor. To bind to mitochondria, Kinesin-1 elicits the help of adaptor proteins Miro (a Rho GTPase) and Milton (also known as Trak1/2). Originally discovered in Drosophila, these proteins are essential for movement of mitochondria from the neuronal cell body into axons via anterograde transport (Stowers et al., 2002; Glater et al., 2006; Russo et al., 2009). A key discovery in the regulation of mitochondrial movement came due to the study of the structure of Miro in particular. Miro is a small Rho GTPase that contains EF hand structural domains. These EF hand domains bind calcium which elicits a conformational change in the protein that changes the propensity for the Kinesin motor to interact with microtubules, which is necessary for processive mitochondrial movement (Wang and Schwarz, 2009). It is likely that Miro and Milton have a role in retrograde transport of mitochondria as well as loss of either effects transport in both directions. In support of this, elevated calcium levels stop all mitochondrial movement (Russo et al., 2009; van Spronsen et al., 2013). Therefore, an understanding of how direction of mitochondrial transport is actively controlled is still lacking.

A step toward understanding how mitochondria move in either the anterograde or retrograde direction came recently as a result of a forward genetic screen in zebrafish. This genetic approach identified the protein Actr10 as essential for mitochondrial attachment to the retrograde motor protein complex (Drerup et al., 2017). Actr10 is a member of the dynein accessory complex dynactin. It is situated in the so called pointed-end complex of dynactin, in an ideal place for cargo binding. Loss of this protein in zebrafish caused mitochondrial accumulation at microtubule plus ends due to failed mitochondrial retrograde transport (Drerup et al., 2017). Anterograde mitochondrial transport is not affected by loss of Actr10, further suggesting the importance of this protein specifically for regulation of retrograde mitochondrial movement. Below we describe the tools we have developed that allowed us to characterize the retrograde transport defect in this line. We also present the subsequent technologies we have adapted for use in this system which are allowing us to define the ultimate function of retrograde mitochondrial transport in neurons.

METHODOLOGY AND RESULTS

Using Zebrafish to Discover the Mechanisms and Function of Retrograde Mitochondrial Transport

Zebrafish larvae are an ideal system to identify and characterize the mechanisms that regulate axonal transport *in vivo*, as we and others have shown (Drerup and Nechiporuk, 2013, 2016; O'Donnell et al., 2013; Campbell et al., 2014; Paquet et al., 2014; Drerup et al., 2017). Embryos develop rapidly with primary neural circuits developed by 4 days post-fertilization (dpf). Zebrafish are also translucent through these stages, allowing visualization of cellular and sub-cellular phenomena *in vivo*. In addition, zebrafish are a genetically tractable system: they are amenable to forward and reverse genetic screens, transient and stable transgenic animals are easily generated, and a wealth of transgenic and mutant lines are available through community databases. Finally, zebrafish have well-characterized neural circuits for analysis of the functional implications of transport disruption. One well-characterized circuit is the afferent axons of the posterior lateral line (pLL) mechanosensory system.

The pLL is a sensory system in aquatic vertebrates that allows the animal to detect movement in the water around them (Dijkgraaf, 1963). This system is composed of clusters of sensory hair cells situated in neuromasts that are distributed along the flanks and throughout the head. The hair cells themselves have apical protrusions that bend in response to water movement. The mechanical force due to this bending activates hair cells and ultimately leads to the release of glutamate at the synaptic contact they make with the pLL afferent axon terminals (Obholzer et al., 2008). For our purposes, the pLL axons are ideal for studies of both the molecular regulation of mitochondrial transport and the impact that disruption of this process has on the function of the circuit. The pLL forms in the first several days of development with initial axon extension completed by 2 dpf (days post-fertilization) and functional circuits by 4 dpf (**Figure 1**; Metcalfe, 1985; Metcalfe et al., 1985). The axons of the pLL nerve extend from the cell bodies of the pLL ganglion, located behind the ear, and to the tip of the tail in the longest cases. These axons are just under the skin and are largely planar, making visualization easy and reliable. Finally, unlike other sensory neurons, the axons of pLL neurons have stereotyped projections and well-defined axon terminals which allows rapid detection of any abnormalities in structure and function (Faucherre et al., 2009; Sarrazin et al., 2010; Dow et al., 2018). Because of the ease of visualization, mitochondrial transport can be imaged *in vivo* without removing neurons from their natural environment. In this way, neurons, myelinating glia, pre- and post-synaptic components, extracellular structural proteins and molecules, and growth factor support, as well as other more amorphous factors found in the surrounding tissue can be studied in an intact system. As neural circuit activity, growth factors, and myelination have all been proposed to effect mitochondrial transport (Chada and Hollenbeck, 2004; Kiryu-Seo et al., 2010; Ohno et al., 2011), the zebrafish pLL axons are highly suited for understanding the cellular mechanisms that regulate the movement of this organelle *in vivo*.

A critical question in the field of mitochondrial transport is the relevance of retrograde movement to mitochondrial health and neural circuit function. While anterograde mitochondrial transport is necessary to populate the axon and facilitates axon outgrowth (Morris and Hollenbeck, 1993; Han et al., 2016; Zhou et al., 2016), the precise function of retrograde mitochondrial transport is less clear. Evidence from cultured mammalian neurons has demonstrated that mitochondria with lower oxidative potential, thought to be a sign of failing health, are more likely to be transported in the retrograde direction (Miller and Sheetz, 2004; Lin et al., 2017). This work has been used to suggest that the main role of mitochondrial retrograde transport is to remove damaged organelles from the axon; however, there are conflicting reports that indicate that oxidative potential may not influence direction of mitochondrial movement (Suzuki et al., 2018). In addition to understanding the exact relevance of mitochondrial retrograde transport, there are several unexplored questions that are fundamental to axonal mitochondrial transport, health, lifetime, and function. First, how often do mitochondria move in axons? Second, does movement change with development? Third, does mitochondrial health and function differ between different regions of the cell? Finally, do mitochondria serve to regulate calcium levels differentially in subcellular compartments? Below, we will describe the tools we have developed to address these questions.

Analyzing Mitochondrial Transport in the pLL

Two primary systems exist to analyze mitochondrial movement in axons *in vivo* in the zebrafish (O'Donnell et al., 2013; Paquet et al., 2014; Drerup and Nechiporuk, 2016; Drerup et al., 2017). Both use sensory axons and mark these organelles with fluorescent proteins to then monitor their active movement. The method developed independently by the Sagasti and Misgeld groups utilizes a GAL4:UAS system to drive expression of mitochondrial markers in axons of Rohon-Beard cells, a type of cutaneous sensory neuron in the early embryo (O'Donnell

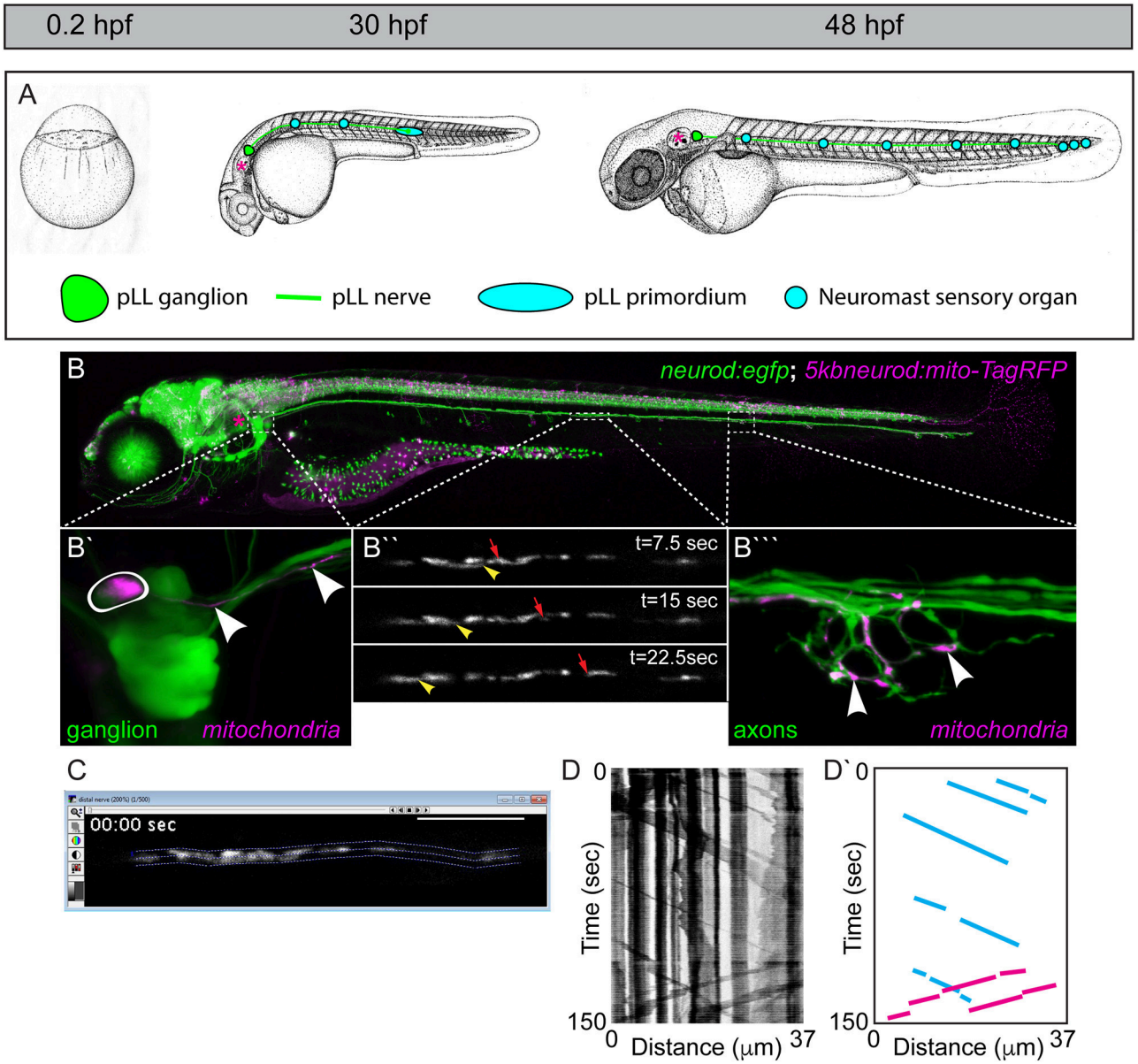

FIGURE 1 | The zebrafish posterior lateral line (pLL): a circuit for addressing mitochondrial transport, health, and function. **(A)** The zebrafish develops rapidly from a single cell stage zygote to a hatched larvae by 48 h post-fertilization (hpf). During that time, the primary pLL also develops. Derived from a single ectodermal placode, the pLL primordium (blue oval) migrates from just behind the ear (asterisk) to the tip of the tail, completing its migration by 48 hpf. Along the way, the pLL primordium deposits approximately five nascent neuromasts which will develop into the sensory organs of the pLL. As it migrates, the pLL primordium guides the axons of the pLL nerve to the tail. The axons stretch from the pLL ganglion (green; contains pLL cell bodies) which remains behind the ear (asterisk) to the terminal cluster neuromasts in the tail in the longest of cases. Images modified from Kimmel et al. (1995). Permissions to use these images were obtained from the copyright holder, John Wiley & Sons, Inc. **(B)** By 5 days post-fertilization (dpf; bottom) the zebrafish larva is freely swimming and feeding. This image is of a live transgenic zebrafish larvae at 5 dpf which carries the stable *TgBAC(neurod:egfp)*^{nl1} transgene (hereafter referred to as *neurod:egfp*) that labels all pLL neurons with cytoplasmic green fluorescent protein (GFP). This larva is also a *5kbneurod:mito-TagRFP* transient transgenic, which expresses mitochondrially-localized TagRFP (shown in magenta) in the mitochondrial inner membrane space in neurons. Transient transgenics are chimeras, with only a subset of neurons expressing this construct. **(B′)** Transient expression of *mito-TagRFP* in a single pLL ganglion neuron (outlined) and the axon extending from it (arrowheads). **(B″)** Mosaic expression allows imaging of a mitochondrial movement in a single axon of the pLL nerve. Yellow arrowhead points to a mitochondria moving in the retrograde direction. Red arrow indicates an anterogradely moving mitochondria (see **Movie 1**). **(B‴)** This single axon forms a basket-like axon terminal that innervates half of the hair cells in this neuromast. Arrowheads point to individual mitochondria in the terminal innervating sensory cells which are not shown. **(C)** Screenshot of an imaging analysis session in MetaMorph. The dotted lines outline the axonal region analyzed. **(D)** Kymograph of this imaging session. Mitochondrial movement is represented by the sloped black lines. Vertical lines show pauses in movement. **(D′)** Schematic of this kymograph with representative anterograde movement bouts (blue lines) and retrograde movement bouts (pink) traced.

et al., 2013; Paquet et al., 2014). Because these axons arborize across the skin, mitochondrial localization and movement can be easily imaged in single axons *in vivo*. However, the precise synaptic targets of these cells are less clear and systems are not in place to monitor synaptic activity, complicating analyses of circuit structure and function. As an alternative system, we have optimized the pLL sensory system for interrogation of mitochondrial transport regulation and function in zebrafish axons. As described above, this system has stereotyped synapses and analysis of circuit function is routine (Zhang et al., 2016). Finally, several reagents, as outlined below, have been generated that allow targeting of mitochondria in single axons in the pLL nerve, allowing analysis of mitochondrial movement *in vivo*.

To visualize mitochondrial transport, we have optimized the system that we used previously to analyze lysosome and dynein movement in pLL axons (Drerup and Nechiporuk, 2013, 2016; Drerup et al., 2017). In this system, zebrafish zygotes can be injected with a plasmid encoding a mitochondrial targeting sequence derived from Cytochrome C Oxidase fused to an open reading frame encoding a fluorescent reporter. Expression is driven in neurons using a five kilobase portion of the *neurod* promotor (*5kbneurod*; Mo and Nicolson, 2011). As zebrafish embryos and larvae develop they exhibit mosaic expression of the reporter in pLL neurons (**Figure 1B**). At the stage of interest, the zebrafish are screened, and those with expression of the mitochondrial marker in one to two neurons of the pLL ganglion are selected for analysis. Individuals are then mounted on a coverslip in 1.5% low melt agarose and imaged at high magnification on a confocal microscope (e.g., a 63X, NA1.2 objective with a 100 × 100 μm field of view on an LSM800 microscope). To capture mitochondrial dynamics, imaging is done in a single *z*-plane, in a 30–100 μm length of axon, three to five times a second, as per Nyquist sampling requirements. The region imaged for analysis is chosen based on the ability to follow a single organelle through the region of interest, ensuring the visualized axon (∼1 μm diameter) is kept in a single *z* plane (±0.44 μm; **Figure 1C**; **Movie 1**). Axonal transport of mitochondria can be imaged in various regions of the expressing pLL axon using this set up, with a consistent area chosen between related experiments. Typically, this imaging is done in the middle portion of the trunk, between neuromasts two and four (see **Figure 1B**), near the end of the yolk sac extension after 2 dpf. For imaging during axon extension, we image a region approximately two thirds of the distance between the neuronal cell body and growth cone of the extending axon. Mitochondrial transport distance, velocity, and direction can then be assayed directly from these image sequences (Drerup and Nechiporuk, 2016; Drerup et al., 2017).

Mitochondrial transport parameters are measured using kymograph analysis in MetaMorph (BioVision). The transport session is analyzed to ensure that individual organelles can be tracked through the length of the region of interest analyzed and the axon region to be analyzed is identified in the program (**Figure 1C**). Kymographs of the fluorescent signal are then generated using MetaMorph (**Figure 1D**). These line traces represent the organelles imaged with longer organelles generating thicker traces. Each individual movement bout, represented by a slanted line that can be followed from beginning to end, is traced (**Figure 1D′**). The distance and time of a single movement bout are identified as the change in X and Y, respectively, on the associated kymograph. The slope then translates to the velocity of movement. Finally, the number of mitochondria moving or stationary is manually counted. While kymographs can be used to estimate these values, we have found that manual assessment is more consistent.

Using this general imaging scheme, we have analyzed mitochondrial transport parameters across development in zebrafish embryos and larvae. After injection of the mitochondrial reporter construct, embryos were raised to 30 hpf, 2, 4, or 5 dpf prior to mounting and imaging. These time-points were chosen specifically to match up with critical developmental stages in the pLL circuit. At 30 hpf, pLL axons are mid-extension and have active growth cone dynamics (Metcalfe, 1985). By 48 hpf, extension of the longest "pioneer" axons of the pLL is complete, but pLL axon terminals synapses are not yet formed with target hair cells (Metcalfe et al., 1985). By 4 dpf the pLL neural circuit is complete. At pLL axon terminals, there are synapses formed with hair cells and active neurotransmission can be observed between pLL axons and their hair cell targets (Zhang et al., 2018). Finally, at 5 dpf myelinating glia are present on the pLL nerve and have wrapped the axons, though compression of the myelin sheath is not yet complete (Monk et al., 2009). When we analyzed mitochondrial transport parameters across these developmental stages we found that the distance and time of anterograde and retrograde movement was maintained at a steady state from 30 hpf to 4 dpf. At 5 dpf there were slight but significant increases in both the time and distance of anterograde and retrograde movement bouts compared to other time-points (**Figures 2A,B**; ANOVA with *post-hoc* contrasts). At all developmental stages, the velocity of mitochondrial movement remained constant at ∼0.83 μm/s and ∼1.14 μm/s for anterograde and retrograde movement, respectively (**Figure 2C**). These values fall within the large window of reported mitochondrial axonal transport velocities among various systems (MacAskill and Kittler, 2010) and align closely with velocities observed *in vivo* in mouse sciatic nerve studies (Misgeld et al., 2007). The underlying reason for the enhanced bi-directional transport at 5 dpf is not clear but could rely on the establishment of stabilized microtubules, the addition of microtubule modifying proteins, or perhaps the expression of adaptor proteins necessary for long-distance transport.

When we focused our developmental analysis on the direction of mitochondrial movement, among all stages, we found no significant change in the proportion of mitochondria that were moving in the anterograde or retrograde direction. Additionally, during development, there was no change in the proportion of mitochondria that were stationary in these axons (**Figure 2D**; ANOVA with *post-hoc* contrasts). This is somewhat contradictory to literature analyzing mitochondrial transport in cultured neurons where days *in vitro* correlated with decreased mitochondrial movement (Kang et al., 2008). The precise reason for these differences is not entirely clear but could be due to a number of reasons. One possibility is the nature of the larval zebrafish. While the primary pLL is fully developed by 5 dpf, the fish continues to grow. This could mean that the axons are not in an entirely mature state by this time-point and do not express

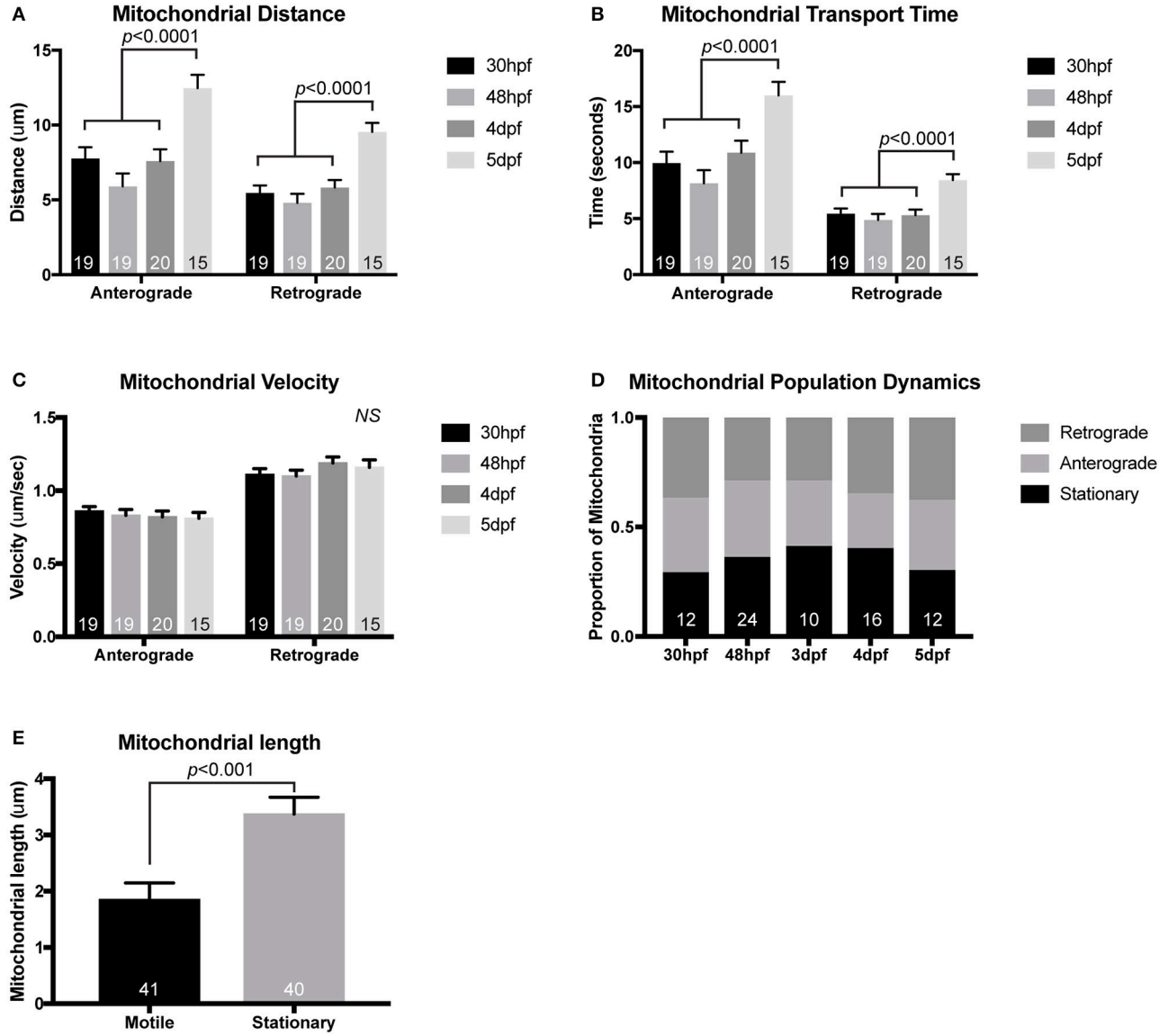

FIGURE 2 | Mitochondrial transport during and after initial pLL development. While mitochondrial transport is fairly consistent during (30 hpf) and after initial axon extension (48 hpf), distance of mitochondrial movement in single bouts of transport **(A)** and the time that the mitochondria can move without stopping **(B)** is increased by 5 dpf (ANOVA with *post-hoc* contrasts). **(C)** Velocity of mitochondrial movement is constant at all ages analyzed. **(D)** Similarly, the proportion of mitochondria moving in either the anterograde or retrograde direction and the proportion that are stationary is not changed across developmental stages (ANOVA with *post-hoc* contrasts). **(E)** Stationary mitochondria are larger than those moving in either direction (ANOVA). *NS*, not significant. In **(A–D),** the number of larvae analyzed is indicated on the graph. In **(E),** the number of individual mitochondria analyzed from eight individual larvae is shown.

all of the docking proteins required to decrease mitochondrial movement (Kang et al., 2008). Another factor that could account for the consistent mitochondrial population dynamics in the pLL axons is the *in vivo* nature of this analysis. Previous work on mitochondrial transport frequency has largely been done on *in vitro* culture systems or in the sciatic nerve of a mouse after removal of surrounding tissues. It is possible that disruption of the neuron's *in vivo* environment alters intracellular transport dynamics, particularly over long periods of time. Future work on adult neurons in zebrafish could allow us to differentiate between these possibilities but technically this is not feasible in the short-term.

Measuring Mitochondrial Lifetime in Axon Terminals

Mitochondria can be long-lived organelles, undergoing dynamic rearrangement to sustain themselves and their viability. Work *in vitro* in cultured Drosophila and chick neurons as well as *in vivo* imaging of mitochondria in the exposed sciatic nerve of mice has shown that these organelles largely exist in two

pools; a stationary pool comprised of longer mitochondria and a smaller, actively moving mitochondrial pool (Miller and Sheetz, 2004; Misgeld et al., 2007; Narayanareddy et al., 2014). This is recapitulated in the zebrafish pLL axons, where stationary mitochondria (∼3.5 μm) are longer than motile mitochondria (<2 μm; **Figure 2E**). This demonstrates that there is consistency between experimental systems. Overall, analyses of mitochondrial transport dynamics have given us a substantial amount of information about the acute nature of mitochondrial movement. Unfortunately the majority of experiments analyzing stationary verses mobile mitochondrial pool have largely been done on time periods that span minutes. Therefore, little is known regarding how the properties of individual mitochondria within axons change over longer periods of time. In addition is not clear whether there are subtypes of mitochondria restricted within the cell body, axon, or axon terminal. To begin to address these questions, we have developed a stable transgenic line to express a photoconvertible protein, mEos (McKinney et al., 2009), in neuronal mitochondria [*Tg(5kbneurod:mito-mEos)*^{y586}]. mEos was originally discovered in coral and is known for its ability to be stably photoconverted from green to red using 405 nm illumination. It is widely used in developmental biology to label independent cells to determine the origin of various tissues and is now used to follow the persistence of intracellular structures as well (Lam et al., 2015). We have utilized it similarly to track the localization and persistence of mitochondria in neuronal compartments. For this work, we engineered a transgenic fish in which mitochondrially targeted mEos (mito-mEos) is expressed in neurons using the *5kbneurod* promotor (Mo and Nicolson, 2011) and the mitochondrial targeting sequence from Cytochrome C Oxidase (Fang et al., 2012). We have previously used this signal sequence to transiently tag mitochondria with red fluorescent protein successfully (Drerup et al., 2017 and **Figure 1**). Analysis of our transgenic line indicates that mitochondria are efficiently tagged with mEos in this line and can be visualized in pLL axon terminals (**Figure 3A**).

In order to analyze mitochondrial lifetime in the pLL sensory axons, we examined larvae at 4 dpf, after pLL axons have formed stable synapses. For conversion and analysis, larvae were mounted in 0.8% low melt agarose for imaging with a 40X, NA1.0 dipping objective on a LSM800 confocal microscope (Zeiss). Pre-conversion, mitochondria were easily visualized with 488 nm excitation (green), indicating unconverted mEos. After short stimulation with 405 nm light, mitochondria were now visualized with 568 nm excitation (red), confirming mEos photoconversion (**Figures 3A,B**). To examine mitochondrial lifetime, imaging was done immediately after photoconversion and again 24 h later in axon terminals. Analysis of red to green fluorescence intensity revealed that immediately after photoconversion the mEos signal was dominated by red fluorescence (**Figure 3B**). In contrast, after 24 h there was an almost complete loss of the converted (red) mEos relative to green in axon terminals, indicating that there are high levels of mitochondrial turnover at this site (**Figures 3A,B**). Next, we analyzed the timeline of mitochondrial turnover using time-lapse imaging following photoconversion at 4 dpf. With both 10 and 3 min intervals, we found relative old (red) to new (green) mitochondria in axon terminals plateaued by ∼3 h post-conversion (**Figures 3C,D**). This data implies a rapid turnover of mitochondria, within hours, in axon terminals.

Turnover could be due to either converted mitochondria moving out of the terminals, mitophagy in the axon terminal, or, perhaps, new (unconverted) mitochondria moving into the terminal, increasing the "green" signal. To differentiate between these possibilities, we analyzed the change in mean green and red fluorescence intensity immediately after photoconversion and compared it to the intensities after 24 h. We found that 24 h after photoconversion, there was an increase in green mEos labeled mitochondria, indicating ample addition of new organelles at the axon terminal. Simultaneously, there was a strong decrease in mean red fluorescence intensity, bringing the values back down to pre-conversion levels, representing loss of all if not almost all photoconverted organelles by 24 h post-conversion (**Figure 3E**). We then wanted to more precisely determine the temporal dynamics of mitochondrial gain and loss from axon terminals. For this analysis, we used timelapse imaging again to monitor the green and red mEos intensity at 3 min intervals immediately after the photoconversion described above. Strikingly, there was a sharp increase in green mEos within 3 h after photoconversion with a concomitant decrease in red fluorescence intensity (**Figure 3F**). This indicates both addition of new mitochondria and loss of old occurs within this time period and both contribute to the ratiometric changes shown in **Figure 3**. The lower fold change in the red channel in **Figure 3F** is likely due to incomplete photoconversion (see **Figure 3A′**) Together, our data support rapid turnover of mitochondria in pLL axon terminals, with addition of new organelles (green) and loss of photoconverted (red/old) organelles on the span of hours. This high level of mitochondrial loss from axon terminals was surprising as previous studies in cultured neurons demonstrated large stationary pools of mitochondria, anticipated to remain in place for extended periods of time (Kang et al., 2008). Our data argues instead that these organelles are very dynamic in the axon *in vivo*, with rapid exchange over a few hours. One still open question is the ultimate fate of the axonal mitochondria lost from axon terminals. Subsequent work using this line will address the relative contribution of mitophagy verses mitochondrial transport in the turnover of mitochondrial axon terminal populations. Additionally, we plan to explore the relative lifetime of mitochondria in other regions of the neurons, including the cell body, to identify any changes in mitochondrial population dynamics related to cellular compartment. Together, this work will shed light on the lifetime and turnover of mitochondria in neuronal compartments *in vivo*.

Measuring Mitochondrial Health and Productivity *in vivo*

Mitochondrial health is often assessed by analyzing the potential/pH across the inner membrane. Indeed, if the mitochondrial machinery that maintains this hydrogen gradient is not maintained, mitochondria fail to function normally and are subject to degradation. The most common way to analyze mitochondrial membrane potential is the vital dye TMRE

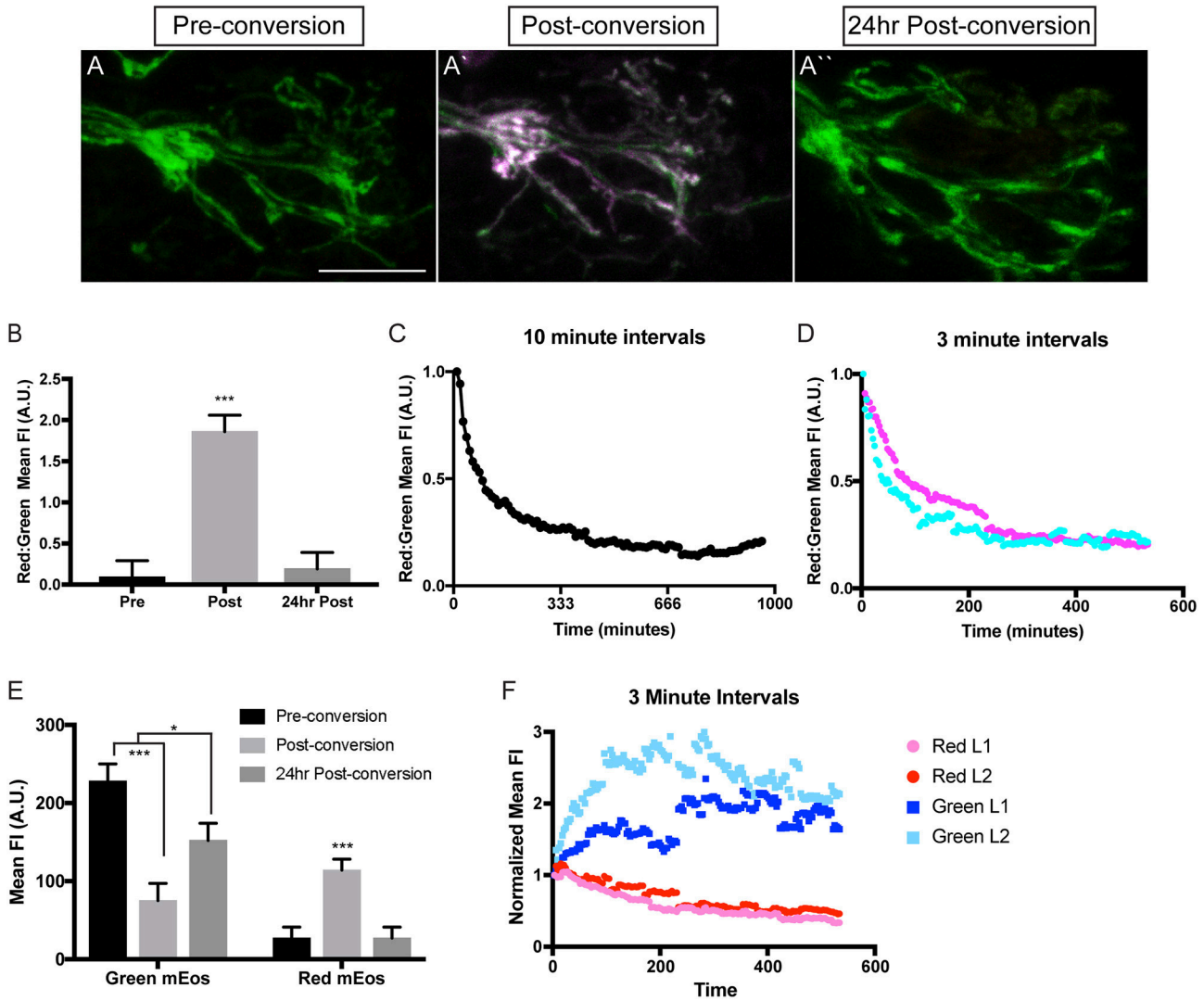

FIGURE 3 | Analysis of mitochondrial lifetime in axons. **(A)** Expression of mitochondrially-localized mEos in the posterior lateral line of a 4 dpf *5kbneurod:mito-mEos* transgenic larvae. For our analysis we used *5kbneurod:mito-mEos* homozygotes to maximize mitochondria-localized mEos expression. This approach provides strong labeling of mitochondria in axon terminals. **(A′)** Illumination with 405 nm light converts mEos from green to red (shown in magenta). **(A″)** Twenty-four hours post-conversion, minimal converted (red) mEos remains in the axon terminal. **(B)** The relative converted to unconverted mito-mEos illustrates an almost complete loss of converted mitochondria from axon terminals by 24 h post-conversion (ANOVA with *post-hoc* contrasts; $^{***}p < 0.0001$; $n = 15$). **(C,D)** Time-lapse analysis of red to green *mito-mEos* in axon terminals after photoconversion shows a rapid turnover of mitochondria from the axon terminal, with most converted (red) mitochondria lost by 3 h post-conversion ($n = 1$ for **C**; $n = 2$ for **D**). **(E)** Quantification of the mean unconverted (green) and converted (red) mito-mEos in axon terminals shows both addition of new mitochondria and loss of converted mitochondria over a 24 h period (ANOVA with *post-hoc* contrasts; $^{***}p < 0.0001$; $^{*}p < 0.01$; $n = 15$). **(F)** Time-lapse analysis of green and red mEos mean fluorescence intensity (normalized to post-conversion values) immediately after photoconversion in two larvae (L) demonstrates increased green and decreased red mEos over time. Timelapse data from two larvae normalized to post-conversion values. Scale bar = 10 μm.

(tetramethylrhodamine ethyl ester). This positively charged dye is highly attracted to the negative charge in the mitochondrial matrix, making it a marker of "healthy" mitochondria. We adapted a TMRE protocol used previously in the zebrafish pLL hair cells (Esterberg et al., 2014) for use in pLL sensory axons. For this experiment, we incubated zebrafish larvae at 4 dpf in 25 μM TMRE in embryo media with 0.1% DMSO (dimethyl sulfoxide) for an hour in the dark. Larvae were subsequently washed three times in embryo media prior to being mounted in 1.5% low melt agarose and imaged with a 63X, NA1.4 objective on a confocal microscope (Zeiss LSM800). For analysis, mitochondrial TMRE was measured in axon terminals and the pLL ganglion after subtraction of nonneural tissue using the ImageJ *Image Calculator* function. This revealed a consistent elevation in TMRE mean fluorescence in axon terminals compared to cell body mitochondria (**Figures 4A,B,E**). As TMRE recruitment is proportional to negative change in the matrix, this could mean that axon terminal mitochondria have a stronger oxidative

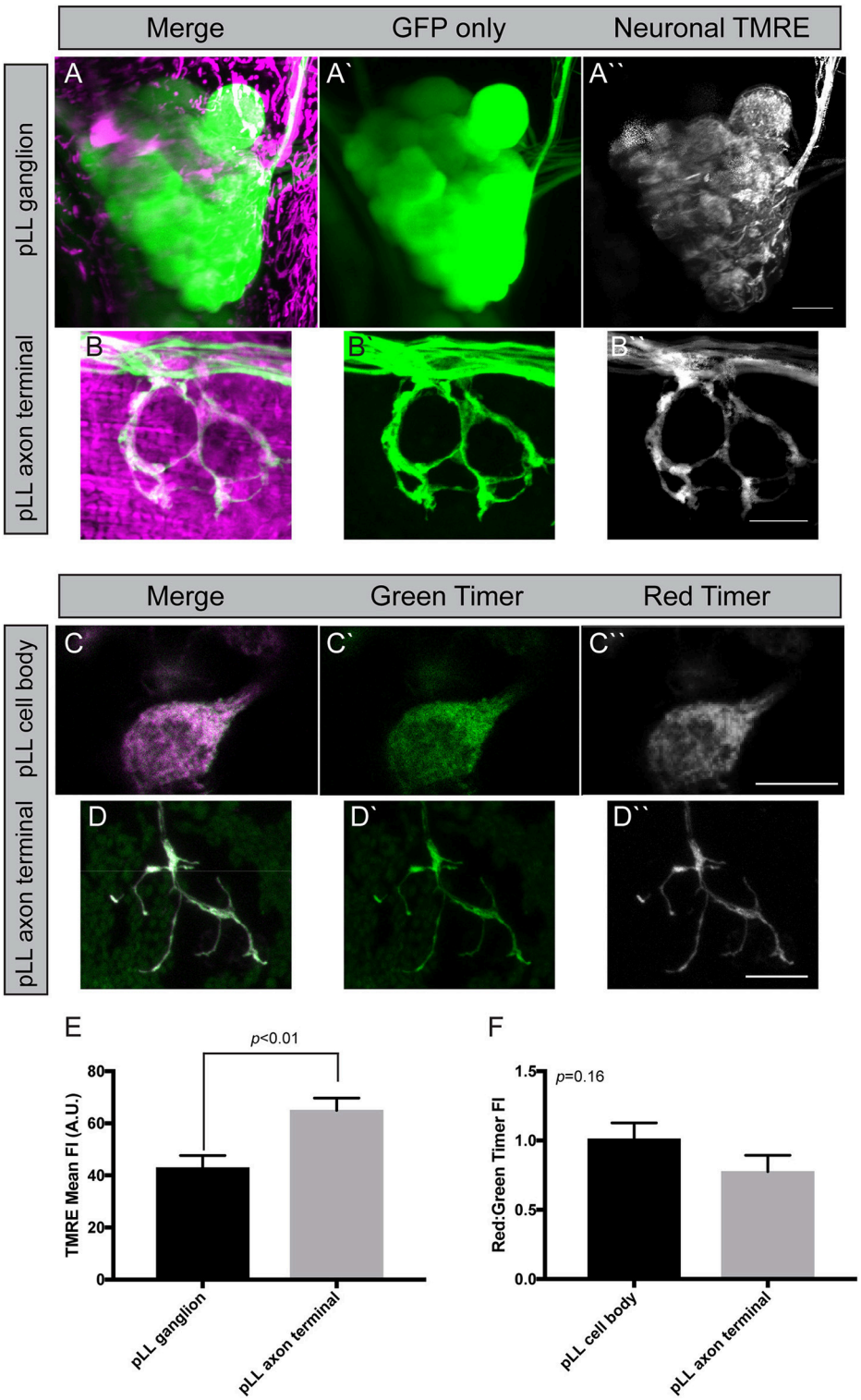

FIGURE 4 | Measuring mitochondrial health in neurons. **(A,B)** Incubation of zebrafish larvae at 4 dpf with 25 μM TMRE results in strong labeling in pLL ganglia and axon terminals (shown in magenta). Cytoplasmic GFP marks the axons. Image subtraction in ImageJ allows analysis of TMRE labeling in neurons (identified by *neurod:egfp* transgene expression). **(C,D)** Transient transgenesis using a *5kbneurod:mito-Timer* construct allows imaging of the oxidation-sensitive protein Timer in individual pLL neurons and axon terminals in larval zebrafish at 4 dpf. Green Timer is native while red Timer (shown in magenta) is oxidized. **(E)** Quantification of TMRE fluorescence intensity shows elevated TMRE labeling in axon terminals compared to cell bodies, an indicator of higher matrix potential (ANOVA; $n = 7$ larvae). **(F)** The red:green Timer ratio is slightly, but not significantly reduced in axon terminals (ANOVA; $n = 16$ larvae). Scale bar = 10 μm.

gradient compared to those in the cell body. Alternatively, dye permeability or light scatter during imaging due to differences in tissue thickness could underlie this difference between pLL ganglion cell bodies and axon terminals. Therefore, we attempted to address the question of mitochodondrial health in another way, using the genetically encoded sensor, Timer (Laker et al., 2014).

Timer is a protein that fluoresces in the green spectrum when in its native conformation but switches to red upon oxidation (Laker et al., 2014). Therefore, the red (568 nm excitation) to green (488 nm excitation) ratio of Timer can be used to assess ROS production, an indicator of mitochondrial health. Excess ROS production is an indicator of oxidative stress and a failing mitochondrion prone to degradation. To express Timer in mitochondria, we used the mitochondrial targeting sequence described above to target it to the inner membrane space and expression was again driven using the minimal *5kbneurod* promotor sequence. Similar to what we described above, injection of the *5kbneurod:mito-Timer* construct resulted in mosaic expression of Timer in pLL neurons. Injected larvae were raised to 4 dpf, and we selected larvae with expression of Timer in a subset of pLL ganglion neurons. These larvae were mounted for imaging as described for TMRE. This analysis revealed no significant difference in the red to green Timer ratio in axon terminals verses the cell body; however, there was a trend toward lower red to green ratios, a potential indicator of lower oxidative stress, in axons terminals (**Figures 4C,D,F**; ANOVA $p = 0.16$). One important point to clarify, however, is that Timer does not just become oxidized based on elevated ROS in unhealthy mitochondria. ROS is a natural biproduct of oxidative phosphorylation. As mitochondrially localized Timer ages, it will naturally become oxidized as well, making the relative contribution of age verses increased oxidative stress difficult to fully distinguish without secondary methods, such as TMRE (Hernandez et al., 2013; Laker et al., 2014). Therefore, it is important to take the results of our mitochondrial turnover assays, TMRE staining, and mito-Timer analyses together. In combination, our work suggests that mitochondria in axon

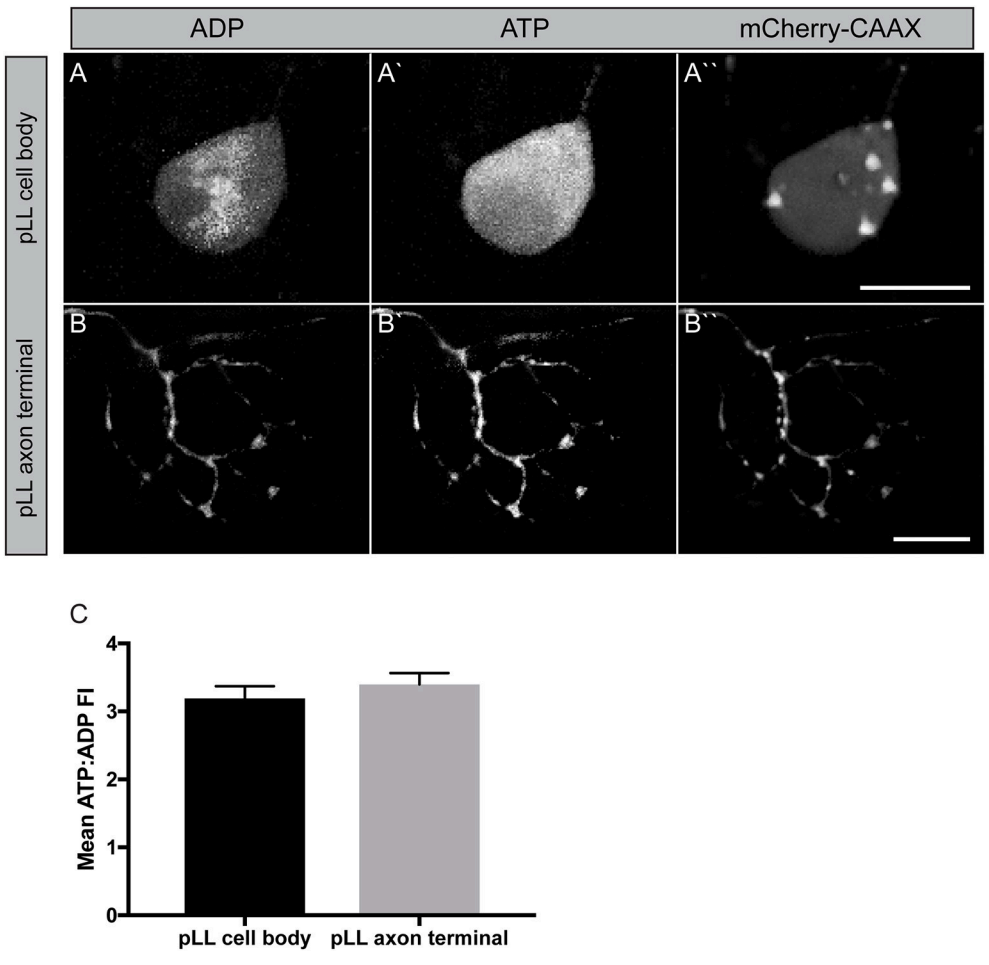

FIGURE 5 | Measuring mitochondrial productivity *in vivo*. **(A,B)** Transient *5kbneurod:PercevalHRp2amCherry-CAAX* expression in a pLL neuron **(A)** and pLL axon terminal **(B)** allows imaging of ADP with 420 nm excitation **(A,B)** and ATP with 500 nm excitation **(A′,B′)**. mCherry expression used to identify the neuron. **(C)** Quantification of the ATP: ADP ratio showed similar levels of mitochondrial productivity in these regions (ANOVA; $n = 21$ larvae). Scale bar = 10 μm.

terminals are rapidly turned over, have a higher potential across their inner membrane, and perhaps have lower ROS production than those in the cell body. This, in turn, would allow axon terminal mitochondria to have increased ATP production relative to those in the cell body.

The next question we wanted to address was in regard to the actual productivity of mitochondria in the cell body and axon terminal of pLL sensory axons. For this, we used the ATP:ADP dual ratiometric sensor PercevalHR (Tantama et al., 2013). PercevalHR was developed as an improved version of the original Perceval: a chimeric protein, composed of the ATP-binding pocket of the bacterial protein GlnK1 and a mutated form of the yellow fluorescent protein mVenus (Berg et al., 2009). This protein can be competitively bound by both ADP and ATP with differential excitation peaks (420 vs. 500 nm, respectively) making it a ratiometric sensor. We made a DNA construct to transiently express PercevalHR in neurons, with a p2a cleavable peptide sequence linking it to mCherry-CAAX (membrane localized red fluorescent protein) to visualize the neuron. This *5kbneurod:PercevalHRp2amCherry-CAAX* construct, when injected into zebrafish zygotes, results in mosaic neuronal expression of the sensor in larval zebrafish. Quantification of the ATP:ADP ratio demonstrated consistent ATP:ADP ratios in axon terminals and the cell body of these neurons (**Figure 5**). Due to the somewhat variable nature of this transient transgenic approach, statistical comparisons between the cell body and axon terminals were challenging; however, as this sensor is ratiometric, our data imply that mitochondria in

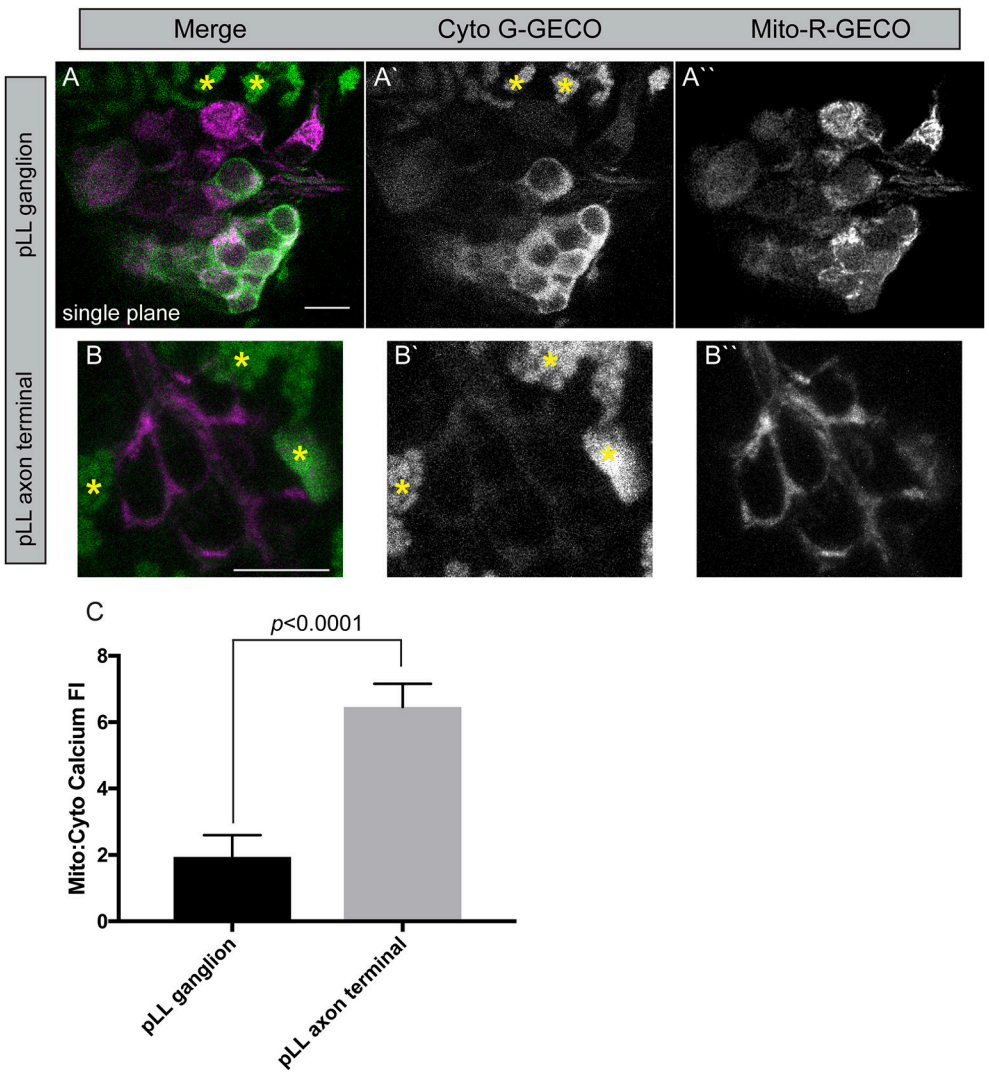

FIGURE 6 | Mitochondrial calcium buffering in neurons. **(A,B)** Stable *5kbneurod:mito-R-GECO1* and *5kbneurod:G-GECO1* transgenics were crossed to generate trans-heterozygotes expressing cytoplasmic G-GECO (green) and mitochondrially localized R-GECO (magenta) in neurons. Asterisks indicate pigment cells that autofluorescence in the G-GECO channel. **(C)** Quantification of the mitochondrial to cytoplasmic GECO signals in the pLL ganglion and axon terminals demonstrates a strong bias toward mitochondrial calcium in axon terminals (ANOVA; $n = 19$ larvae). Scale bar = 10 μm.

these distinct cellular compartments are adequately converting ADP to ATP. The generation of a stable transgenic line expressing this sensor in neurons, which is currently in progress, will allow comparative studies on mitochondrial productivity in various cellular compartments in the near future.

Mitochondrial Calcium Buffering in Neurons

The mitochondrial outer and inner membranes have calcium channels to rapidly take up this ion from the microenvironment surrounding this organelle. It has been proposed that this ability to locally modulate or buffer calcium could be of great importance to neurons, particularly at synapses (reviewed in Devine and Kittler, 2018). Synaptic activity requires active release of calcium from intracellular pools to facilitate neurotransmitter release. After activity, the calcium must then be sequestered to modulate the activity of the synapse. One method of calcium sequestration would be through mitochondrial uptake. In addition to calcium buffering, calcium entry into the mitochondria is also thought to stimulate mitochondrial productivity with elevated calcium levels increasing ATP synthesis; however, the mitochondrial calcium load must be properly regulated as prolonged elevation of mitochondrial calcium stimulates the release of pro-apoptotic factors and initiates cell death (reviewed in Strasser et al., 2000). Therefore, proper regulation of calcium by and in mitochondria is absolutely essential for mitochondrial and neuronal health.

To begin to study the relationship between cytoplasmic and mitochondrial calcium in neurons, we engineered two new transgenic lines. These lines are stable transgenics which express a green calcium indicator [G-GECO1; *Tg(5kbneurod:G-GECO)*^{nl19}] in neuronal cytoplasm and a red calcium indicator [R-GECO1; *Tg(5kbneurod:mito-R-GECO)*^{nl20}] in the mitochondrial inner membrane space (Zhao et al., 2011). Using confocal imaging as described for TMRE analysis, we can image chronic and acute changes in calcium ion abundance in and around mitochondria in these lines. This analysis revealed a striking difference between the neuronal cell body and axon terminals of the pLL sensory neurons. The mitochondria (red) to cytoplasmic (green) GECO ratio is increased in axon terminals compared to the cell body, indicating a higher calcium load in mitochondria compared to the surrounding environment in this compartment of the neuron (**Figure 6**). Together with the increased TMRE/lower Timer signal and rapid turnover, our data indicate that the axon terminal has an extremely dynamic population of mitochondria, that may be necessary to support synaptic activity and signal transduction.

In summary, our work has developed a collection of novel tools to interrogate the lifetime, health, productivity and function of mitochondria in neurons *in vivo* in the embryonic and larval zebrafish pLL sensory system. Our data to date illustrate the importance of considering all compartments when analyzing mitochondrial activity and transport, particularly the differences between organelles residing in the cell body verses those in the synaptically active regions of the axon terminal. Future work using these and other tools developed by the community will allow us to come to a better understanding of the symbiotic relationship between this former prokaryote and the eurkaryotic cell it calls home.

ETHICS STATEMENT

This study was carried out in accordance with the recommendations of NICHD Animal Care and Use Committee. The protocol (ASP 15-039) was approved by the NICHD ACUC.

AUTHOR CONTRIBUTIONS

KP and AM contributed experimental design, data generation, and data analysis to this work. CD designed, conducted, and analyzed experiments and wrote the manuscript.

FUNDING

Funding for this work from the National Institute of Child Health & Human Development.

ACKNOWLEDGMENTS

We would like to thank Wesley Schnapp and Dane Kawano for thoughtful discussions on this work and Dr. Katie Kindt for feedback on this manuscript. We would also like to acknowledge Dr. Alex Nechiporuk who provided thoughtful comments on the development of this project and support during its initial stages.

SUPPLEMENTARY MATERIAL

The Supplementary Material for this article can be found online at: https://www.frontiersin.org/articles/10.3389/fcell.2018.00144/full#supplementary-material

Movie 1 | Mitochondrial transport in a pLL axon. Mitochondria (labeled with TagRFP) are visualized moving in the anterograde (left to right) and retrograde (right to left) direction in a single pLL axon (see **Figure 1**). Scale bar = 10 μm.

REFERENCES

Alexander, C., Votruba, M., Pesch, U. E., Thiselton, D. L., Mayer, S., Moore, A., et al. (2000). OPA1, encoding a dynamin-related GTPase, is mutated in autosomal dominant optic atrophy linked to chromosome 3q28. *Nat. Genet.* 26, 211–215. doi: 10.1038/79944

Attwell, D., and Laughlin, S. B. (2001). An energy budget for signaling in the grey matter of the brain. *J. Cereb. Blood Flow. Metab.* 21, 1133–1145. doi: 10.1097/00004647-200110000-00001

Ban-Ishihara, R., Ishihara, T., Sasaki, N., Mihara, K., and Ishihara, N. (2013). Dynamics of nucleoid structure regulated by mitochondrial fission contributes to cristae reformation and release of cytochrome c. *Proc. Natl. Acad. Sci. U.S.A.* 110, 11863–11868. doi: 10.1073/pnas.1301951110

Berg, J., Hung, Y. P., and Yellen, G. (2009). A genetically encoded fluorescent reporter of ATP:ADP ratio. *Nat. Methods* 6, 161–166. doi: 10.1038/nmeth.1288

Boehning, D., Patterson, R. L., and Snyder, S. H. (2004). Apoptosis and calcium: new roles for cytochrome c and inositol 1,4,5-trisphosphate. *Cell Cycle* 3, 252–254. doi: 10.4161/cc.3.3.705

Campbell, P. D., Shen, K., Sapio, M. R., Glenn, T. D., Talbot, W. S., and Marlow, F. L. (2014). Unique function of Kinesin Kif5A in localization of mitochondria in axons. *J. Neurosci.* 34, 14717–14732. doi: 10.1523/JNEUROSCI.2770-14.2014

Cárdenas, C., Miller, R. A., Smith, I., Bui, T., Molgó J, Müller, M., et al. (2010). Essential regulation of cell bioenergetics by constitutive InsP3 receptor Ca2+ transfer to mitochondria. *Cell* 142, 270–283. doi: 10.1016/j.cell.2010.06.007

Chada, S. R., and Hollenbeck, P. J. (2004). Nerve growth factor signaling regulates motility and docking of axonal mitochondria. *Curr. Biol.* 14, 1272–1276. doi: 10.1016/j.cub.2004.07.027

Chandel, N. S., Maltepe, E., Goldwasser, E., Mathieu, C. E., Simon, M. C., and Schumacker, P. T. (1998). Mitochondrial reactive oxygen species trigger hypoxia-induced transcription. *Proc. Natl. Acad. Sci. U.S.A.* 95, 11715–11720. doi: 10.1073/pnas.95.20.11715

Chen, H., and Chan, D. C. (2009). Mitochondrial dynamics–fusion, fission, movement, and mitophagy–in neurodegenerative diseases. *Hum. Mol. Genet.* 18, R169–R176. doi: 10.1093/hmg/ddp326

Chen, H., Chomyn, A., and Chan, D. C. (2005). Disruption of fusion results in mitochondrial heterogeneity and dysfunction. *J. Biol. Chem.* 280, 26185–26192. doi: 10.1074/jbc.M503062200

Chen, H., Vermulst, M., Wang, Y. E., Chomyn, A., Prolla, T. A., McCaffery, J. M., et al. (2010). Mitochondrial fusion is required for mtDNA stability in skeletal muscle and tolerance of mtDNA mutations. *Cell* 141, 280–289. doi: 10.1016/j.cell.2010.02.026

Courchet, J., Lewis, T. L. Jr., Lee, S., Courchet, V., Liou, D. Y., Aizawa, S., et al. (2013). Terminal axon branching is regulated by the LKB1-NUAK1 kinase pathway via presynaptic mitochondrial capture. *Cell* 153, 1510–1525. doi: 10.1016/j.cell.2013.05.021

Delettre, C., Lenaers, G., Griffoin, J. M., Gigarel, N., Lorenzo, C., Belenguer, P., et al. (2000). Nuclear gene OPA1, encoding a mitochondrial dynamin-related protein, is mutated in dominant optic atrophy. *Nat. Genet.* 26, 207–210. doi: 10.1038/79936

Devine, M. J., and Kittler, J. T. (2018). Mitochondria at the neuronal presynapse in health and disease. *Nat. Rev. Neurosci.* 19, 63–80. doi: 10.1038/nrn.2017.170

Dijkgraaf, S. (1963). The functioning and significance of the lateral-line organs. *Biol. Rev. Camb. Philos. Soc.* 38, 51–105. doi: 10.1111/j.1469-185X.1963.tb00654.x

Dow, E., Jacobo, A., Hossain, S., Siletti, K., and Hudspeth, A. J. (2018). Connectomics of the zebrafish's lateral-line neuromast reveals wiring and miswiring in a simple microcircuit. *Elife* 7:e33988. doi: 10.7554/eLife.33988

Drerup, C. M., Herbert, A. L., Monk, K. R., and Nechiporuk, A. V. (2017). Regulation of mitochondria-dynactin interaction and mitochondrial retrograde transport in axons. *Elife* 6:e22234. doi: 10.7554/eLife.22234

Drerup, C. M., and Nechiporuk, A. V. (2013). JNK-interacting protein 3 mediates the retrograde transport of activated c-Jun N-terminal kinase and lysosomes. *PLoS Genet.* 9:e1003303. doi: 10.1371/journal.pgen.1003303

Drerup, C. M., and Nechiporuk, A. V. (2016). *In vivo* analysis of axonal transport in zebrafish. *Methods Cell Biol.* 131, 311–329. doi: 10.1016/bs.mcb.2015.06.007

Esterberg, R., Hailey, D. W., Rubel, E. W., and Raible, D. W. (2014). ER-mitochondrial calcium flow underlies vulnerability of mechanosensory hair cells to damage. *J. Neurosci.* 34, 9703–9719. doi: 10.1523/JNEUROSCI.0281-14.2014

Fang, C., Bourdette, D., and Banker, G. (2012). Oxidative stress inhibits axonal transport: implications for neurodegenerative diseases. *Mol. Neurodegener.* 7:29. doi: 10.1186/1750-1326-7-29

Faucherre, A., Pujol-Martí, J., Kawakami, K., and López-Schier, H. (2009). Afferent neurons of the zebrafish lateral line are strict selectors of hair-cell orientation. *PLoS ONE.* 4:e4477. doi: 10.1371/journal.pone.0004477

Gincel, D., Zaid, H., and Shoshan-Barmatz, V. (2001). Calcium binding and translocation by the voltage-dependent anion channel: a possible regulatory mechanism in mitochondrial function. *Biochem. J.* 358, 147–155. doi: 10.1042/bj3580147

Glater, E. E., Megeath, L. J., Stowers, R. S., and Schwarz, T. L. (2006). Axonal transport of mitochondria requires milton to recruit kinesin heavy chain and is light chain independent. *J. Cell Biol.* 173, 545–557. doi: 10.1083/jcb.200601067

Han, S. M., Baig, H. S., and Hammarlund, M. (2016). Mitochondria localize to injured axons to support regeneration. *Neuron* 92, 1308–1323. doi: 10.1016/j.neuron.2016.11.025

Hernandez, G., Thornton, C., Stotland, A., Lui, D., Sin, J., Ramil, J., et al. (2013). MitoTimer: a novel tool for monitoring mitochondrial turnover. *Autophagy* 9, 1852–1861. doi: 10.4161/auto.26501

Kang, J. S., Tian, J. H., Pan, P. Y., Zald, P., Li, C., Deng, C., et al. (2008). Docking of axonal mitochondria by syntaphilin controls their mobility and affects short-term facilitation. *Cell* 132, 137–148. doi: 10.1016/j.cell.2007.11.024

Kimmel, C. B., Ballard, W. W., Kimmel, S. R., Ullmann, B., and Schilling, T. F. (1995). Stages of embryonic development of the zebrafish. *Dev. Dyn.* 203, 253–310. doi: 10.1002/aja.1002030302

Kirichok, Y., Krapivinsky, G., and Clapham, D. E. (2004). The mitochondrial calcium uniporter is a highly selective ion channel. *Nature* 427, 360–364. doi: 10.1038/nature02246

Kiryu-Seo, S., Ohno, N., Kidd, G. J., Komuro, H., and Trapp, B. D. (2010). Demyelination increases axonal stationary mitochondrial size and the speed of axonal mitochondrial transport. *J. Neurosci.* 30, 6658–6666. doi: 10.1523/JNEUROSCI.5265-09.2010

Laker, R. C., Xu, P., Ryall, K. A., Sujkowski, A., Kenwood, B. M., Chain, K. H., et al. (2014). A novel mitotimer reporter gene for mitochondrial content, structure, stress, and damage *in vivo*. *J. Biol. Chem.* 289, 12005–12015. doi: 10.1074/jbc.M113.530527

Lam, P. Y., Mangos, S., Green, J. M., Reiser, J., and Huttenlocher, A. (2015). *In vivo* imaging and characterization of actin microridges. *PLoS ONE* 10:e0115639. doi: 10.1371/journal.pone.0115639

Lin, M. Y., Cheng, X. T., Tammineni, P., Xie, Y., Zhou, B., Cai, Q., et al. (2017). Releasing syntaphilin removes stressed mitochondria from axons independent of mitophagy under pathophysiological conditions. *Neuron* 94, 595 e6–610 e6. doi: 10.1016/j.neuron.2017.04.004

MacAskill, A. F., and Kittler, J. T. (2010). Control of mitochondrial transport and localization in neurons. *Trends Cell Biol.* 20, 102–112. doi: 10.1016/j.tcb.2009.11.002

Maeda, R., Kindt, K. S., Mo, W., Morgan, C. P., Erickson, T., Zhao, H., et al. (2014). Tip-link protein protocadherin 15 interacts with transmembrane channel-like proteins TMC1 and TMC2. *Proc. Natl. Acad. Sci. U.S.A.* 111, 12907–12912. doi: 10.1073/pnas.1402152111

McCormack, J. G., and Denton, R. M. (1989). The role of Ca2+ ions in the regulation of intramitochondrial metabolism and energy production in rat heart. *Mol. Cell. Biochem.* 89, 121–125. doi: 10.1007/BF00220763

McKinney, S. A., Murphy, C. S., Hazelwood, K. L., Davidson, M. W., and Looger, L. L. (2009). A bright and photostable photoconvertible fluorescent protein. *Nat. Methods* 6, 131–133. doi: 10.1038/nmeth.1296

Metcalfe, W. K. (1985). Sensory neuron growth cones comigrate with posterior lateral line primordial cells in zebrafish. *J. Comp. Neurol.* 238, 218–224. doi: 10.1002/cne.902380208

Metcalfe, W. K., Kimmel, C. B., and Schabtach, E. (1985). Anatomy of the posterior lateral line system in young larvae of the zebrafish. *J. Comp. Neurol.* 233, 377–389. doi: 10.1002/cne.902330307

Miller, K. E., and Sheetz, M. P. (2004). Axonal mitochondrial transport and potential are correlated. *J. Cell Sci.* 117, 2791–2804. doi: 10.1242/jcs.01130

Misgeld, T., Kerschensteiner, M., Bareyre, F. M., Burgess, R. W., and Lichtman, J. W. (2007). Imaging axonal transport of mitochondria *in vivo*. *Nat. Methods* 4, 559–561. doi: 10.1038/nmeth1055

Mo, W., and Nicolson, T. (2011). Both pre- and postsynaptic activity of Nsf prevents degeneration of hair-cell synapses. *PLoS ONE* 6:e27146. doi: 10.1371/journal.pone.0027146

Monk, K. R., Naylor, S. G., Glenn, T. D., Mercurio, S., Perlin, J. R., Dominguez, C., et al. (2009). A G protein-coupled receptor is essential for Schwann cells to initiate myelination. *Science* 325, 1402–1405. doi: 10.1126/science.1173474

Morris, R. L., and Hollenbeck, P. J. (1993). The regulation of bidirectional mitochondrial transport is coordinated with axonal outgrowth. *J. Cell Sci.* 104 (Pt 3), 917–927.

Narayanareddy, B. R., Vartiainen, S., Hariri, N., O'Dowd, D. K., and Gross, S. P. (2014). A biophysical analysis of mitochondrial movement: differences between transport in neuronal cell bodies versus processes. *Traffic* 15, 762–771. doi: 10.1111/tra.12171

Obholzer, N., Wolfson, S., Trapani, J. G., Mo, W., Nechiporuk, A., Busch-Nentwich, E., et al. (2008). Vesicular glutamate transporter 3 is required for synaptic transmission in zebrafish hair cells. *J. Neurosci.* 28, 2110–2118. doi: 10.1523/JNEUROSCI.5230-07.2008

O'Donnell, K. C., Vargas, M. E., and Sagasti, A. (2013). WldS and PGC-1alpha regulate mitochondrial transport and oxidation state after axonal injury. *J. Neurosci.* 33, 14778–14790. doi: 10.1523/JNEUROSCI.1331-13.2013

Ohno, N., Kidd, G. J., Mahad, D., Kiryu-Seo, S., Avishai, A., Komuro, H., et al. (2011). Myelination and axonal electrical activity modulate the distribution and motility of mitochondria at CNS nodes of Ranvier. *J. Neurosci.* 31, 7249–7258. doi: 10.1523/JNEUROSCI.0095-11.2011

Paquet, D., Plucinska, G., and Misgeld, T. (2014). *In vivo* imaging of mitochondria in intact zebrafish larvae. *Methods Enzymol.* 547, 151–164. doi: 10.1016/B978-0-12-801415-8.00009-6

Parone, P. A., Da Cruz, S., Tondera, D., Mattenberger, Y., James, D. I., Maechler, P., et al. (2008). Preventing mitochondrial fission impairs mitochondrial function and leads to loss of mitochondrial DNA. *PLoS ONE* 3:e3257. doi: 10.1371/journal.pone.0003257

Pilling, A. D., Horiuchi, D., Lively, C. M., and Saxton, W. M. (2006). Kinesin-1 and Dynein are the primary motors for fast transport of mitochondria in Drosophila motor axons. *Mol. Biol. Cell.* 17, 2057–2068. doi: 10.1091/mbc.e05-06-0526

Pivovarova, N. B., and Andrews, S. B. (2010). Calcium-dependent mitochondrial function and dysfunction in neurons. *FEBS J.* 277, 3622–3636. doi: 10.1111/j.1742-4658.2010.07754.x

Raturi, A., Gutiérrez, T., Ortiz-Sandoval, C., Ruangkittisakul, A., Herrera-Cruz, M. S., Rockley, J. P., et al. (2016). TMX1 determines cancer cell metabolism as a thiol-based modulator of ER-mitochondria Ca2+ flux. *J. Cell Biol.* 214, 433–444. doi: 10.1083/jcb.201512077

Russo, G. J., Louie, K., Wellington, A., Macleod, G. T., Hu, F., Panchumarthi, S., et al. (2009). Drosophila Miro is required for both anterograde and retrograde axonal mitochondrial transport. *J. Neurosci.* 29, 5443–5455. doi: 10.1523/JNEUROSCI.5417-08.2009

Sarrazin, A. F., Nuñez, V. A., Sapède, D., Tassin, V., Dambly-Chaudière, C., and Ghysen, A. (2010). Origin and early development of the posterior lateral line system of zebrafish. *J. Neurosci.* 30, 8234–8244. doi: 10.1523/JNEUROSCI.5137-09.2010

Schnapp, B. J., and Reese, T. S. (1989). Dynein is the motor for retrograde axonal transport of organelles. *Proc. Natl. Acad. Sci. U.S.A.* 86, 1548–1552. doi: 10.1073/pnas.86.5.1548

Sena, L. A., and Chandel, N. S. (2012). Physiological roles of mitochondrial reactive oxygen species. *Mol. Cell* 48, 158–167. doi: 10.1016/j.molcel.2012.09.025

Spillane, M., Ketschek, A., Merianda, T. T., Twiss, J. L., and Gallo, G. (2013). Mitochondria coordinate sites of axon branching through localized intra-axonal protein synthesis. *Cell Rep.* 5, 1564–1575. doi: 10.1016/j.celrep.2013.11.022

Stowers, R. S., Megeath, L. J., Górska-Andrzejak, J., Meinertzhagen, I. A., and Schwarz, T. L. (2002). Axonal transport of mitochondria to synapses depends on milton, a novel Drosophila protein. *Neuron* 36, 1063–1077. doi: 10.1016/S0896-6273(02)01094-2

Strasser, A., O'Connor, L., and Dixit, V. M. (2000). Apoptosis signaling. *Annu. Rev. Biochem.* 69, 217–245. doi: 10.1146/annurev.biochem.69.1.217

Suzuki, R., Hotta, K., and Oka, K. (2018). Transitional correlation between inner-membrane potential and ATP levels of neuronal mitochondria. *Sci. Rep.* 8:2993. doi: 10.1038/s41598-018-21109-2

Tantama, M., Martínez-François, J. R., Mongeon, R., and Yellen, G. (2013). Imaging energy status in live cells with a fluorescent biosensor of the intracellular ATP-to-ADP ratio. *Nat. Commun.* 4:2550. doi: 10.1038/ncomms3550

Twig, G., Elorza, A., Molina, A. J., Mohamed, H., Wikstrom, J. D., Walzer, G., et al. (2008). Fission and selective fusion govern mitochondrial segregation and elimination by autophagy. *EMBO J.* 27, 433–446. doi: 10.1038/sj.emboj.7601963

van Spronsen, M., Mikhaylova, M., Lipka, J., Schlager, M. A., van den Heuvel, D. J., Kuijpers, M., et al. (2013). TRAK/Milton motor-adaptor proteins steer mitochondrial trafficking to axons and dendrites. *Neuron* 77, 485–502. doi: 10.1016/j.neuron.2012.11.027

Wang, X., and Schwarz, T. L. (2009). The mechanism of Ca2+-dependent regulation of kinesin-mediated mitochondrial motility. *Cell* 136, 163–174. doi: 10.1016/j.cell.2008.11.046

Wang, Y., Zang, Q. S., Liu, Z., Wu, Q., Maass, D., Dulan, G., et al. (2011). Regulation of VEGF-induced endothelial cell migration by mitochondrial reactive oxygen species. *Am. J. Physiol. Cell Physiol.* 301, C695–C704. doi: 10.1152/ajpcell.00322.2010

Weinberg, S. E., and Chandel, N. S. (2015). Targeting mitochondria metabolism for cancer therapy. *Nat. Chem. Biol.* 11, 9–15. doi: 10.1038/nchembio.1712

Weinberg, S. E., Sena, L. A., and Chandel, N. S. (2015). Mitochondria in the regulation of innate and adaptive immunity. *Immunity* 42, 406–417. doi: 10.1016/j.immuni.2015.02.002

Zhang, Q., Li, S., Wong, H. C., He, X. J., Beirl, A., Petralia, R. S., et al. (2018). Synaptically silent sensory hair cells in zebrafish are recruited after damage. *Nat. Commun.* 9:1388. doi: 10.1038/s41467-018-03806-8

Zhang, Q. X., He, X. J., Wong, H. C., and Kindt, K. S. (2016). Functional calcium imaging in zebrafish lateral-line hair cells. *Methods Cell Biol.* 133, 229–252. doi: 10.1016/bs.mcb.2015.12.002

Zhao, Y., Araki, S., Wu, J., Teramoto, T., Chang, Y. F., Nakano, M., et al. (2011). An expanded palette of genetically encoded Ca(2)(+) indicators. *Science* 333, 1888–1891. doi: 10.1126/science.1208592

Zhou, B., Yu, P., Lin, M. Y., Sun, T., Chen, Y., and Sheng, Z. H. (2016). Facilitation of axon regeneration by enhancing mitochondrial transport and rescuing energy deficits. *J. Cell Biol.* 214, 103–119. doi: 10.1083/jcb.201605101

Zuchner, S., Mersiyanova, I. V., Muglia, M., Bissar-Tadmouri, N., Rochelle, J., Dadali, E. L., et al. (2004). Mutations in the mitochondrial GTPase mitofusin 2 cause Charcot-Marie-Tooth neuropathy type 2A. *Nat. Genet.* 36, 449–451. doi: 10.1038/ng1341

Conflict of Interest Statement: The authors declare that the research was conducted in the absence of any commercial or financial relationships that could be construed as a potential conflict of interest.

frontiers in Cell and Developmental Biology

REVIEW
published: 04 March 2019
doi: 10.3389/fcell.2019.00013

Expanding the CRISPR Toolbox in Zebrafish for Studying Development and Disease

*Kaili Liu, Cassidy Petree, Teresa Requena, Pratishtha Varshney and Gaurav K. Varshney**

Functional and Chemical Genomics Research Program, Oklahoma Medical Research Foundation, Oklahoma City, OK, United States

The study of model organisms has revolutionized our understanding of the mechanisms underlying normal development, adult homeostasis, and human disease. Much of what we know about gene function in model organisms (and its application to humans) has come from gene knockouts: the ability to show analogous phenotypes upon gene inactivation in animal models. The zebrafish (*Danio rerio*) has become a popular model organism for many reasons, including the fact that it is amenable to various forms of genetic manipulation. The RNA-guided CRISPR/Cas9-mediated targeted mutagenesis approaches have provided powerful tools to manipulate the genome toward developing new disease models and understanding the pathophysiology of human diseases. CRISPR-based approaches are being used for the generation of both knockout and knock-in alleles, and also for applications including transcriptional modulation, epigenome editing, live imaging of the genome, and lineage tracing. Currently, substantial effort is being made to improve the specificity of Cas9, and to expand the target coverage of the Cas9 enzymes. Novel types of naturally occurring CRISPR systems [Cas12a (Cpf1); engineered variants of Cas9, such as xCas9 and SpCas9-NG], are being studied and applied to genome editing. Since the majority of pathogenic mutations are single point mutations, development of base editors to convert C:G to T:A or A:T to G:C has further strengthened the CRISPR toolbox. In this review, we provide an overview of the increasing number of novel CRISPR-based tools and approaches, including lineage tracing and base editing.

Keywords: Cas12a (Cpf1), lineage tracing, base editors, zebrafish, disease models, CRISPR/Cas9

OPEN ACCESS

Edited by:
Gokhan Dalgin,
The University of Chicago, United States

Reviewed by:
Mingyu Li,
Xiamen University, China
Máté Varga,
Eötvös Loránd University, Hungary

***Correspondence:**
Gaurav K. Varshney
gaurav-varshney@omrf.org

Specialty section:
This article was submitted to Molecular Medicine, a section of the journal Frontiers in Cell and Developmental Biology

Received: *22 November 2018*
Accepted: *24 January 2019*
Published: *04 March 2019*

Citation:
Liu K, Petree C, Requena T, Varshney P and Varshney GK (2019) Expanding the CRISPR Toolbox in Zebrafish for Studying Development and Disease. Front. Cell Dev. Biol. 7:13. doi: 10.3389/fcell.2019.00013

INTRODUCTION

Information gained from the study of model organisms is essential to our understanding of human development and disease. Replication of a mutant phenotype in a gene knockout (inactivation of a gene in an animal model) is considered to be the gold standard approach to support candidate gene predictions in humans. Zebrafish (*Danio rerio*) is uniquely suited to this approach and has become one of the fastest growing model organisms, useful for both basic and translational research (Bradford et al., 2017).

Zebrafish are an attractive alternative to mouse models because they give rise to a large number of progeny and are amenable to high-throughput mutagenesis and drug screening approaches (Kettleborough et al., 2013; Varshney et al., 2013; Varshney and Burgess, 2014; Gallardo et al., 2015). In addition, zebrafish fertilization is external, and their transparent larvae can be monitored throughout embryogenesis, providing unique accessibility to embryonic lethal mutations.

The process of gene targeting in zebrafish is not as laborious as it is in mice, and the maintenance costs are 10X cheaper per animal (Varshney and Burgess, 2014). Importantly, zebrafish overcome an emerging technical issue in modeling disease pathology: many of the diseases studied today are multigenic, so disruption of a single gene may not produce a disease phenotype in any model system. However, combining genetic variants is straightforward in zebrafish, making it an ideal organism in which to model the functional consequences of multiple mutations. In addition, complementation studies in fish are relatively simple and allow for the direct testing of specific variants (not just knockouts) in a vertebrate system. The utility of zebrafish was further increased upon completion of the zebrafish genome-sequencing project (Howe et al., 2013); zebrafish and mammalian genes are highly conserved, and 70% of human disease genes have an ortholog in zebrafish (Howe et al., 2013). In zebrafish, many large-scale forward and reverse genetic screens have been performed using random mutagenesis methods - ENU or insertional mutagenesis (retroviral, Tol2, DS) - and the number of different genetic and molecular tools rapidly increased once the genome was sequenced (Amsterdam et al., 2011; Marquart et al., 2015; Quach et al., 2015; Seiler et al., 2015; Vrljicak et al., 2016). For decades, targeted gene knockouts were not possible in zebrafish, and its utility for validation studies of candidate genes was limited. This challenge was recently eliminated with the development of novel gene targeting approaches including ZFNs, TALENs, and CRISPR/Cas9 (Bedell et al., 2012; Jinek et al., 2012; Mali et al., 2013; Hsu et al., 2014; Varshney et al., 2015b); other techniques such as Structure Guided Nucleases (SGNs) have been shown to work for gene targeting in zebrafish but have not been adopted widely (Varshney and Burgess, 2016; Xu et al., 2016). With the transformative CRISPR/Cas9 approach, it is now possible to target any number of genes in an efficient and high-throughput manner (Gagnon et al., 2014; Shah et al., 2015; Varshney et al., 2015a). It is also possible to target multiple genes simultaneously; given that part of the zebrafish genome is duplicated, it is very useful in targeting 2 paralogs simultaneously (Jao et al., 2013).

CRISPR/Cas9 and other enzymes are not only being used to generate knockouts, introduce specific changes in the genome and repair mutant alleles, but are also being repurposed in other applications including transcriptional regulation, *in vivo* chromatin imaging, epigenome modulation, genome-wide knockout screens, etc. There are many reviews discussing the use of CRISPR-based approaches and the various technological developments in zebrafish (Varshney et al., 2015b; Li et al., 2016; Demarest and Brooks-Kayal, 2018). In this review we will focus on the latest development in expanding targeting coverage of gene targeting, base editing, transcriptional regulation, epigenome modulation, and lineage tracing.

CRISPR-MEDIATED TARGETED MUTAGENESIS IN ZEBRAFISH

In 2012, a joint team from Jennifer Doudna and Emmanuel Charpentier's lab, and an independent team from Virginijus Siksnys's lab demonstrated that Cas9 from *Streptococcus pyogenes* or *Streptococcus thermophilus* together with CRISPR RNA (crRNA) can be guided to a target site to cleave DNA *in vitro*. Early the following year, George Church and Feng Zhang's labs utilized Cas9 from *Streptococcus pyogenes* and/or *Streptococcus thermophilus* to edit the genome in mammalian cells: they showed that single guide RNA (sgRNAs) can direct Cas9 to the target site to induce a double stranded break, which can then be repaired by either the non-homologous end joining (NHEJ) or homology-directed repair (HDR) pathways. An alternative repair pathway, microhomology-mediated end joining (aka Alt-EJ) (MMEJ; an error-prone repair mechanism that uses microhomologous sequences 5–25 bp in length) has also been shown to be activated by the double-stranded break induced by Cas9 (McVey and Lee, 2008; Ata et al., 2018). In the last 5–6 years, CRISPR-based genome editing tools have been used for many applications in a variety of cells, organisms and plants (Hsu et al., 2014). The use of simple and programmable CRISPR/Cas9 technology has completely transformed reverse genetics in zebrafish.

Zebrafish was the first vertebrate model used to demonstrate that CRISPR/Cas9 can efficiently edit the genome *in vivo* (Hwang et al., 2013) with up to 50% targeting efficiency. Another report demonstrated that CRISPR/Cas9 can be used to generate biallelic mutations in *gata5* and *etsrp*, and the observed phenotypes in injected embryos can phenocopy genetic mutants (Chang et al., 2013). Using a codon optimized version of Cas9 with nuclear localization signals, Jao et al. (2013) showed that Cas9 can efficiently induce biallelic mutations when Cas9 mRNA and sgRNA are injected into one-cell stage embryos. The authors further showed that up to five genes can be targeted simultaneously, and all showed phenotypes associated with each gene (Jao et al., 2013). It is evident from these initial reports that CRISPR/Cas9 is so efficient at inducing biallelic mutations that it allows for the generation of phenotypes in injected embryos similar to antisense morpholinos. Several strategies have been used to screen for phenotypes in the F_0 generation in injected embryos; one such strategy used multiplexing to target multiple genes simultaneously and screen for phenotypes in F_0. This approach was used to screen 48 genes and identify two novel genes involved in electrical-synapse formation (Shah et al., 2015). A similar strategy used a pool of four sgRNAs together with Cas9 protein to identify transcriptional regulators in cardiomyocytes; 50 candidate genes were screened and the role of *zbtb16a* in cardiac development was identified (Wu et al., 2018). Burger et al. (2016) demonstrated that the use of *in vitro* assembled Cas9 mCherry or EGFP fusion protein, and sgRNA together as a ribonucleoprotein complex can provide a visual readout for efficient microinjections for the analysis of mutant phenotypes in F_0 generation. These mutants were termed CRISPR-mediated mutants or crispants (akin to morphants; Burger et al., 2016). While these approaches to screen candidate genes by analyzing the expected phenotypes in injected embryos are efficient, in most cases a stable mutant is required for phenotypic analysis of gene function. Data from Shawn Burgess's lab targeting 89 genes show that genetic mutants can be generated with ∼28% germline transmission rates at a 99% success rate. This high germline transmission rate is four–fivefold higher than

that of other targeting approaches such as ZFNs, and TALENs (Varshney et al., 2015a).

Many groups have developed a streamlined workflow for generating mutants using CRISPR/Cas9 in a high-throughput manner (Gagnon et al., 2014; Varshney et al., 2015a, 2016a). The Burgess Lab addressed a few challenges in developing this workflow: First they developed a strategy to synthesize sgRNA by annealing two oligonucleotides that served as a template for *in vitro* transcription; this allowed for the synthesis of sgRNA in few hours with relatively low cost and is similar to the strategy was used by Gagnon et al. (2014). Secondly, the zebrafish genome is highly polymorphic, and it was predicted that this might cause multiple mismatches in the target sequence and prevent the sgRNA from binding efficiently. To address this, they sequenced the genome of the NHGRI-1 lab strain and identified more than 14 million variants. This data is available through UCSC genome browser track; while designing sgRNAs or PCR primers, variant regions of the genome can be avoided to maximize the success rate (LaFave et al., 2014). The third challenge they encountered was the identification of mutant alleles in a high-throughput manner. Several methods are currently used for the identification of mutants in zebrafish including DNA mismatch nuclease assays (Chang et al., 2013; Jao et al., 2013), restriction fragment length polymorphism (Hruscha et al., 2013) and sequencing (Gagnon et al., 2014; Varshney et al., 2015a; Burger et al., 2016), but none are amenable to high-throughput application. A method to determine the size of amplicons by fluorescent PCR was optimized to identify indels (Sood et al., 2013). This method uses three primers (gene-specific forward and reverse primers and a FAM-labeled primer) to amplify the regions around the target sites and resulting fluorescently labeled amplicons are mixed with a size standard (e.g., Rox400) to determine the amplicon size on ABI sequencing platform. This method can be applied in a high-throughput manner, and has resolution up to 1 bp (**Figure 1**) (Carrington et al., 2015; Varshney et al., 2015a).

Adopting CRISPR/Cas9 technology in a high-throughput manner for targeted mutagenesis has enabled geneticists to screen for large-numbers of genes with relatively modest resources, and generate disease models for ever-increasing candidate disease genes. The approaches have been widely applied: Pei et al. (2018) screened more than 200 candidate genes to identify genes involved in hair cell regeneration, and screens related to retinal regeneration or degeneration (Unal Eroglu et al., 2018) and several disease models including Niemman-Pick disease type C1;(Tseng et al., 2018), hearing disorders (Varshney et al., 2015a), congenital sideroblastic anemia with immunodeficiency, fevers and developmental delay (SIFD; (Giannelou et al., 2018), Mucolipidosis type IV (Li et al., 2017) have been performed. In zebrafish, phenotypes are generally studied in the F_2 generation where homozygous embryos are generated by breeding two heterozygous (F_1) lines over ∼6–7 months. It has been shown that phenotypes can be screened in the F_1 generation in a non-Mendelian manner by inbreeding two founders, thus eliminating a generation and saving time (Varshney et al., 2015a). This could be an important strategy that may speed up the phenotypic screening of a large number of candidate disease genes. To generate knockouts, Cas9 is transiently expressed ubiquitously in one-cell stage embryos thus generating global knockouts, two independent studies have shown that Cas9 can also be expressed in a tissue-specific manner thus it is possible to inactivate genes in a specific tissues (Ablain et al., 2015; Yin et al., 2015). Yin et al. (2015) demonstrated that by using a heat-shock inducible and tissue specific promoters, the expression of Cas9 can be controlled both temporally and spatially [reviewed in (Li et al., 2016)]. They further characterized five U6 promoters to drive the expression of multiple guides thus adopting this approach for multiplex genome editing (Yin et al., 2015).

While CRISPR/Cas9 is an effective and simple tool for genetic manipulations, there are several concerns over its specificity as it has been shown to bind and edit unintended targets (e.g., Off targets) including inducing large deletions (Adikusuma et al., 2018). In zebrafish genetics, off-targets can easily be outcrossed away and a genotype-phenotype linkage must be established thus losing on-target activity by using Cas9 variants to achieve specificity should be considered. There are fewer studies in zebrafish that have tested the off-target effect in zebrafish. One such study detected off-target mutagenesis in only 1/25 off target sites in germline, another study showed off-target mutation rates from 1.1 to 2.5% (Hruscha et al., 2013; Varshney et al., 2015a). Many Cas9 variants such as Cas9-HF1, eSpCas9, evoCas9, HypaCas9, and others have been developed to increase the specificity of the Cas9 enzyme and thus reduce the off targets, however, these variant might also affect the on-target activities (Jamal et al., 2018).

We have summarized important CRISPR-based genome editing tools in **Table 1**. While SpCas9 can target multiple sites in the coding regions of the genome that is GC-rich, efforts are being made to expand target coverage by employing either orthologous Cas9 or evolving SpCas9 to identify different Protoacceptor Adjacent Motif (PAM) sequences.

ENGINEERED AND NOVEL NUCLEASES TO EXPAND THE TARGETING COVERAGE

Cas9 from *Streptococcus pyogenes* (spCas9) is the most popular and effective genome editing tool, and the sequences recognized by *SpCas9* are limited by the specific and simple PAM (5′-NGG-3′) requirement (Jinek et al., 2012). However, this specific PAM sequence may not be available near the target of interest. To expand the targeting coverage, researchers have identified additional, naturally occurring CRISPR nucleases that may have different PAM requirements. Additionally, spCas9 was engineered to recognize other PAM sequences, expanding the targeting coverage and allowing them to be used in orthogonal applications. These newly identified CRISPR nucleases may also address the challenge of delivering the large size of spCas9 (1,368 aa) as they may be smaller; they may also provide a homology template for *in vivo* therapeutic applications (Mout et al., 2017).

Orthologous Cas9

Many of the smaller-sized Cas9 nucleases discovered in different species can recognize different PAM sequences and varied lengths

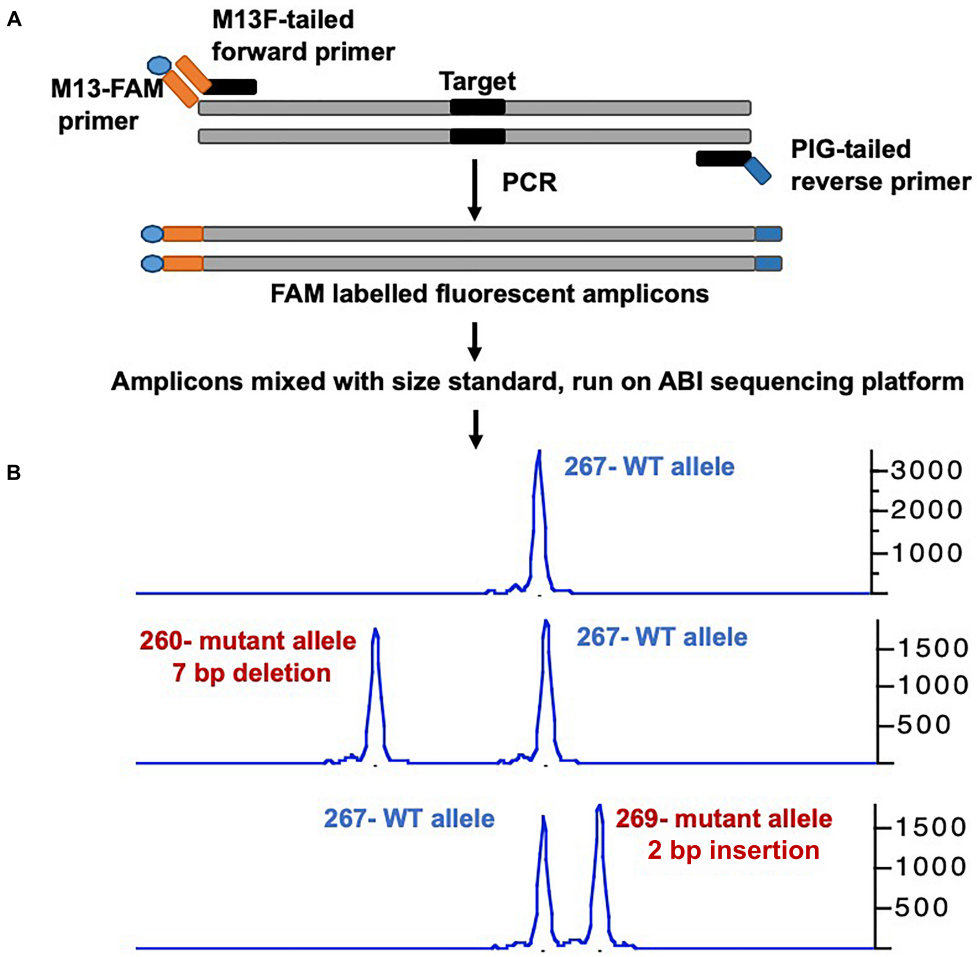

FIGURE 1 | Overview of mutant identification method using fragment analysis approach. **(A)** Gene specific primers are designed covering the target site (amplicon size ranging 200–300 bp). Gene-specific forward primer contains M13F sequence at the 5′, and reverse primer has PIG-tail sequence at 5′ end. PCR is performed using gene specific primer set, and a third primer with M13F sequence labeled with FAM, resulting amplicons are fluorescently labeled. **(B)** Fluorescently labeled primers are mixed with size standard (e.g., ROX-400), and run on ABI capillary sequencer, and data is analyzed using gene mapper software. The output will have the size of amplicon, wild type allele will have only one size, while mutant allele will have two different sizes. The indel size can be determined by comparing the size of two alleles (WT vs. mutant).

of target sequences for *in vivo* genome editing (**Table 2**): the *Staphylococcus aureus* Cas9 (SaCas9, 1053 aa) is not only small in size, but also uses a different complex PAM (NNGRRT; (Muller et al., 2016). Many other Cas9 nucleases from different bacterial species are being used for *in vivo* genome editing: Cas9 from *Neisseria meningitidis* (NmCas9) requires NNAGAAW PAM; Cas9 from *Streptococcus thermophilus* (St1Cas9, 1121 aa and St3Cas9, 1388 aa) require NNAGAAW and NGGNG PAMs, respectively; Cas9 nuclease from *Campylobacter jejuni* (CjCas9, 984 aa) recognizes a 22-nt target sequence with NNNVRYAC and NNNNRYAC PAM (Kim E. et al., 2017).

Engineered Cas9 Variants

Most of the orthologous Cas9 nucleases have long and complex PAM requirements that will limit the targeting range because they will occur less frequently in genomes. An alternative strategy to expand PAM specificity would be to engineer the SpCas9 to recognize other PAMs. Kleinstiver et al. (2015b) engineered SpCas9 based on the crystal structure of the enzyme, and the mutated Cas9 was tested for its ability to recognize different PAM sites. Engineered SpCas9 variants VRER (D1135V/G1218R/R1335E/T1337R) recognizing NGCG PAM, VQR (D1135V/R1335Q/T1337R) recognizing NGAN or NGNG PAM, and EQR (D1135E/R1335Q/T1337R) variants recognizing NGAG PAM were generated. All of these SpCas9 variants were able to target sequences that were not targetable by wild-type SpCas9 in human cells, but only the VQR variant was able to target sites with NGAG PAMs (20–43% efficiency in zebrafish; (Kleinstiver et al., 2015b). The efficiency of the VQR was further validated by showing its ability to target *tyr* and *EGFP* loci with 50 and 70% efficiency, respectively. Zebrafish codon-optimized versions of VQR and EQR SpCas9 generated by Shawn Burgess' lab are also available from Addgene (Varshney et al., 2016a).

TABLE 1 | Commonly used tools for CRISPR-mediated genome editing.

Name	Description	URL	Reference
CRISPRScan	Tool to design Cas9/Cas12a targets.	http://www.crisprscan.org	Moreno-Mateos et al., 2015
CHOPCHOP	Tool to design Cas9, Cas9 variants, Cas12a targets, and genotyping primers. A custom PAM can also be selected.	http://chopchop.cbu.uib.no	Labun et al., 2016
ccTop	Target prediction tool for multiple Cas9 and Cas12a.	https://crispr.cos.uni-heidelberg.de	Stemmer et al., 2017
Cas-Designer	The most comprehensive tool to design Ca9, Cas9 variants, and Cas12a targets.	http://www.rgenome.net/cas-designer	Park et al., 2015
MENTHU	MENTHU (Microhomology-mediated End joining kNockout Target Heuristic Utility) is a tool for designing targets with microhomologies, to induce microhomology-mediated end-joining (MMEJ) deletions.	http://genesculpt.org/menthu	Ata et al., 2018
CRISPR-ERA	Cas9 target design tool for genome editing, repression, and activation	http://crispr-era.stanford.edu	Liu et al., 2015
CRISPResso 2	Webtool to analyze indels and base editing from the high-throughput sequencing data	http://crispresso.pinellolab.partners.org/	Clement et al., 2018
Cas-Analyzer	Online tool for analyzing indels from high-throughput sequencing data	http://www.rgenome.net/cas-analyzer/#!	Park et al., 2017
CRISPR-GA	CRISPR Genome Analyzer is a tool to identify indels from the next-generation sequencing data	http://crispr-ga.net/	Guell et al., 2014
CRISPRz	Database of validated sgRNA sequences in zebrafish	https://research.nhgri.nih.gov/CRISPRz/	Varshney et al., 2016b
inDelphi	Tool to predicts the indels resulting from microhomology-mediated end-joining (MMEJ) and non-homologous end-joining (NHEJ) repair.	https://www.crisprindelphi.design	Shen et al., 2018
FORECasT	Tool to predicts the indels generated by Cas9	https://partslab.sanger.ac.uk/FORECasT	Allen et al., 2018

As described above, the majority of the Cas9 orthologs or variants have complex PAM requirements, and the frequency of these targets in the genome is limited. To circumvent this challenge, David Liu's lab used phage-assisted continuous evolution (PACE) to isolate 14 evolved SpCas9 variants (xCas9 3.0–3.13); one such variant (xCas9 3.7) was able to recognize a broad range of PAM, including NG, NNG, CAA, GAT, and GAA (Hu et al., 2018). The xCas9 3.7 variant was able to cleave multiple PAMs at much higher frequency than wild-type SpCas9: GAA and GAT PAM showed ∼5-fold, NGT ∼4.5-fold and NGC 2.1-fold efficiencies. Another variant, xCas9 3.6, showed the second-best editing efficiencies at fewer PAMs (Hu et al., 2018). SpCas9 was further engineered to generate a variant called SpCas9-NG that has a relaxed preference for the third nucleobases in the NGG PAM (Nishimasu et al., 2018). This variant had seven residues mutated (R1335V/L1111R/D1135V/G1218R/E1219F/A1322R/T1337R) in SpCas9; was capable of cleaving NGA, NGT, and NGG PAMs with more than 20% editing efficiency; and showed lower activity at NGC PAM. A comparison of editing efficiencies showed that spCas9-NG had higher editing efficiencies at NGA, NGT, and NGG sites, and xCas9 failed to edit NGC PAM targets (Nishimasu et al., 2018).

Similarly, *Staphylococcus aureus* Cas9 (SaCas9) was also modified using a molecular evolution strategy to recognize NNNRRT PAMs. This variant of SaCas9 is known as KKH SaCas9 (variant E782K/N968K, R1015H) and can further increase the SaCas9 targeting range by two–fourfold (Kleinstiver et al., 2015a). The KKH SaCas9 variant was able to recognize five independent targets in different genes with 10–90% efficiency, thus expanding targeting coverage further in zebrafish (Feng et al., 2016).

The Cas9 nuclease from *Francisella novocida* (FnCas9) is one of the largest nucleases identified thus far (1629 aa) and recognizes NGG PAM similar to SpCas9, but has failed to generate indels in mammalian cells. It is possible that microinjecting mouse zygotes with FnCas9 protein and a guide RNA ribonucleoprotein complex may induce target-specific indels; a variant of FnCas9 (E1369R/E1449H/R1556A) called RHA FnCas9 could recognize YG PAM (Hirano et al., 2016).

Recently, a homolog of *SpCas9* in *Streptococcus macacae* (*SmacCas9*) has been described to recognize the 5′-NAAN-3′ PAM. A variant of *SmacCas9* (iSpy-macCas9) was engineered to maintain its specificity for adenine dinucleotide PAM while showing higher genome editing efficiency *in vivo* (Jakimo et al., 2018). An orthologous Cas9 protein from *Streptococcus canis* (ScCas9) with 89.2% sequence similarity to wild-type SpCas9 has also been characterized and shown to prefer a more minimal NNG (Chatterjee et al., 2018). An engineered version of ScCas9 (ΔLoop ΔKQ) not only cleaves NGG PAM but also recognizes and edits NNGA PAM at a comparable rate, but it edits other NNGN PAMs with reduced efficiency. All of these engineered and orthologous Cas9 proteins have significantly expanded the targeted coverage.

CRISPR/Cas12a (Cpf1)

The majority of class 2 and type II nucleases and their engineered versions described earlier have preference for GC-rich PAMs that limits the targeting of AT-rich sequences, for example most of the non-coding genome in zebrafish is AT-rich (Howe et al., 2013). Another class 2 and type V family of nucleases, originally described as Cpf1 and later renamed Cas12a (Shmakov et al., 2017), was discovered as an alternative effective genome-editing tool (Zetsche et al., 2015). Cas12a is different from SpCas9 in many ways (**Figure 2**): (i) Cas12a recognizes T-rich PAM located at the 5′ end of the target DNA sequence, (ii) Cas12a is guided by a single CRISPR RNA (crRNA) that is shorter than that of SpCas9 and does not require *trans*-acting crRNA (tracrRNA), (iii) Cas12a

TABLE 2 | Summary of Cas orthologs and variants.

CRISPR Cas orthologs or variants	Recognized PAM	Target length	Use in zebrafish	Reference
Streptococcus pyogenes Cas9 (SpCas9)	NGG	19 or 20 nt	Yes	Jinek et al., 2012; Cong et al., 2013
Streptococcus pyogenes Cas9 Variant VQR *(SpCas9 VQR)*	NGAN, NGNG	19 or 20 nt	Yes	Kleinstiver et al., 2015b
Streptococcus pyogenes Cas9 Variant EQR *(SpCas9 EQR)*	NGAG	19 or 20 nt	Yes	Kleinstiver et al., 2015b
Streptococcus pyogenes Cas9 Variant VRER *(SpCas9 VRER)*	NGCG	20 nt	Yes	Kleinstiver et al., 2015b
Streptococcus pyogenes Cas9 Variant D1135E *(SpCas9 DE)*	NAG	20 nt	Not tested	Kleinstiver et al., 2015b
Streptococcus pyogenes Cas9 Variant QQR1 (SpCas9 QQR1)	NAAG	20 nt	Not tested	Anders et al., 2016
*Streptococcus pyogenes variant TLIKDIV (x*Cas9 3.7)	NG, NNG, CAA, GAT, GAA	20 nt	Not tested	Hu et al., 2018
Streptococcus pyogenes NG variant (SpCas9NG)	NGA, NGT, NG	20 nt	Not tested	Nishimasu et al., 2018
Staphylococcus aureus Cas9 (SaCas9)	NNGRRT	20–24 nt	Not tested	Ran et al., 2015
Staphylococcus aureus KKH Cas9 variant (SaCas9 KKH)	NNNRRT	21 nt	Yes	Kleinstiver et al., 2015a
Streptococcus thermophilus 1 Cas9 (St1Cas9)	NNAGAAW (W = A or T)	20 nt	Not tested	Muller et al., 2016
*Streptococcus thermophilus*3 Cas9 (St3Cas9)	NGGNG	20 nt	Not tested	Glemzaite et al., 2015
Neisseria meningitidis Cas9 (Nm or NmeCas9)	NNNNGMTT (M = A or C)	23–24 nt	Not tested	Hou et al., 2013; Fonfara et al., 2014
Campylobacter jejuni Cas9 *(CjCas9)*	NNNVRYAC NNNNRYAC NNNVRYM (R = A or G) (Y = C or T) (M = A or C)	22 nt	Not tested	Kim E. et al., 2017; Yamada et al., 2017
Francisella novicida Cas9	NGG	22 nt	Not tested	Fonfara et al., 2014; Hirano et al., 2016
Francisella novicida Cas9 RHA variant	YG (Y = C or T)	22 nt	Not tested	Hirano et al., 2016
Treponema denticola Cas9 *(TdCas9)*	NAAAAN	20 nt	Not tested	Esvelt et al., 2013
Streptococcus macacae Cas9 (SmacCas9)	NAAN	20 nt	Not tested	Jakimo et al., 2018
Streptococcus canis (ScCas9)	NNG	20 nt	Not tested	Chatterjee et al., 2018
Streptococcus canis (ScCas9) ΔLoopΔKQ variant	NNGA, NGG	20 nt	Not tested	Chatterjee et al., 2018
Acidaminococcus Cas12a (AsCas12a/Cpf1)	TTTV (V = A or C)	23 or 24 nt	Yes	Zetsche et al., 2015
Lachnospiraceae Cas12a (LbCas12a/Cpf1)	TTTV (V = A or C)	23 or 24 nt	Yes	Zetsche et al., 2015
Francisella Cas12a (FnCas12a/Cpf1)	TTN, KYTV (K = G or T) (Y = C or T) (V = A or C)	23 or 24 nt	Yes	Zetsche et al., 2015; Tu et al., 2017
Moraxella Cas12a (MbCas12a/Cpf1)	TTN	23 or 24 nt	Not tested	Zetsche et al., 2017
AsCas12a, LbCas12a, FnCas12a, and MbCas12a RR variants	TYCV, TWTV (W = A or T) (V = A or C) (Y = C or T)	23 or 24 nt	Not tested	Gao et al., 2017; Nishimasu et al., 2017; Toth et al., 2018
AsCas12a, LbCas12a, FnCas12a, and MbCas12a RVR variant	TATV (V = A or C)	23 or 24 nt	Not tested	Gao et al., 2017; Nishimasu et al., 2017; Toth et al., 2018

uses an ∼23 nt target sequence, (iv) Cas12a induces a double-stranded break in the target sequence via a staggered cut and ∼18 nt distal to PAM, generating a 4–5 nt 5′ overhang, and (v) Cas12a has both DNAse and RNase activity; therefore it is capable of processing its own CRISPR array (Fonfara et al., 2016). As of now, 32 Cas12a orthologs have been described, and their genome-editing potential was screened. Cas12a from *Francisella novicida* (FnCas12a), *Acidaminococcus* sp. BV3L6 (AsCas12a), and *Lachnospiraceae* bacterial ND2006 (LbCas12a) exhibited robust editing in human cells, plants and many other model organisms, including zebrafish (Zetsche et al., 2015). Additionally, four other Cas12a orthologs [*Thiomicrospira* sp. Xs5 (TsCas12a), *Moraxella bovoculi* AAX08_00205 (Mb2Cas12a), *Moraxella bovoculi* AAX11_00205 (Mb3Cas12a), and *Butyrivibrio* sp. NC3005 (BsCas12a)] have been shown to induce indels in human cells, although only Mb3Cas12a was able to induce indels at a

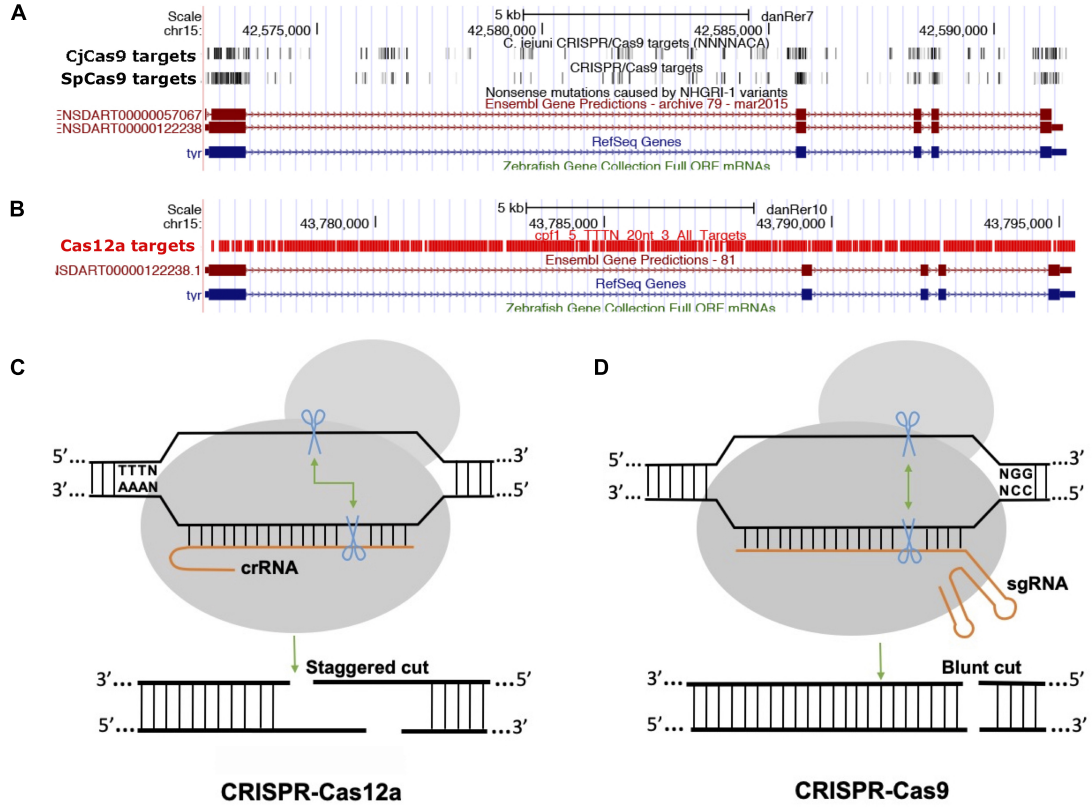

FIGURE 2 | Comparison between Cas9 and Cas12a. **(A)** Screenshot of UCSC genome browser tracks showing predicted target sequences in *tyr* gene for CjCas9, and SpCas9. The targets for both Cas9 nucleases are enriched in coding exons, **(B)** while Cas12 target sequences are enriched mostly in intronic sequences. **(C,D)** Comparison of Cas12a and Cas9, Cas12 a generates a staggered cut, Cas9 induces a blunt end cut.

rate comparable to AsCas12a and LbCas12a (Zetsche et al., 2017). AsCas12a and LbCas12a use TTTV PAM, while FnCas12a and Mb3Cas12a recognize the less-restrictive TTN and NTTN PAMs, respectively. FnCas12a also has been show to target sequences with KYTV PAM preference in mammalian cells (Tu et al., 2017). The Cas12a nucleases were further engineered by introducing mutations S542R/K607R and S542R/K548V/N552R to generate AsCas12aRR and AsCas12RVR variants, and G532R/K592R and G5323R/K538V/Y542R to generate LbCas12a RR or RVR variants, which can recognize non-canonical PAMs such as TYCV, TWTV, and TATV PAMs. Use of Cas12a in editing the zebrafish genome is not as straightforward as editing using SpCas9. Cas12a mRNA and crRNA targeting the *tyr* locus do not induce any indels in zebrafish at optimal temperature (28°C) (Watkins-Chow et al., 2017). Further optimization revealed that Cas12a crRNAs are degraded rapidly after injection in one-cell stage embryos; however, LbCas12a-crRNA ribonucleoprotein (RNP) complex can protect crRNA from degradation and can efficiently induce indels at a rate comparable to that of SpCas9 in zebrafish (Moreno-Mateos et al., 2017). LbCas12a is more effective in inducing indels than AsCas12a, and AsCas12a activity is temperature dependent in zebrafish. Heat shocking embryos after injection for 4 h at 34°C significantly increased the mutagenic activities for AsCas12a and LbCas12a nucleases. (Moreno-Mateos et al., 2017) LbCas12a has been shown to achieve higher homology-directed repair compared to SpCas9. LbCas12a-mediated HDR is most efficient when an ssDNA donor template that is complementary to the target strand is provided (SpCas9 favors the non-target strand). Cas12a nucleases have expanded the targeted coverage many fold, which will help target non-coding regions that are AT rich in zebrafish (Moreno-Mateos et al., 2017).

Base Editing Tools

The majority of genetic diseases are caused by point mutations (single or multiple) that result in amino acid substitutions which generate non- or partially functional proteins. Studying these mutations in a model organism using gene knockout technology may not completely mimic the mutations found in human patients. Creating these mutations in zebrafish has been challenging: a targeted knock-in mutant is achieved via homologous recombination by delivering sgRNA and Cas9 together with either a single-stranded oligonucleotide or a donor plasmid containing the left and right homologous arms. Several strategies have been developed for introducing specific changes using knock-in technologies (Prykhozhij et al., 2018; Tessadori et al., 2018; Zhang et al., 2018), and reviewed in many publications (Albadri et al., 2017).

However, the success rate of homology-directed repair (HDR) is extremely low, so introducing specific changes in the genome has been difficult because repair machinery tends to favor non-homologous end joining repair. Moreover, HDR requires the delivery of donor template to the target cells and precise repair of the genomic sequence. Recently, Jeffery Essner's lab described an optimized targeted knock-in strategy, called GeneWeld, in which they developed a series of donor plasmids for gene tagging [pGTag-plasmids for Gene Tagging (58)]. This strategy is based on the targeting of multiple genomic loci using donor plasmids with short homology arms (24–48 bp), and can be used to integrate cargos up to 2 kb in zebrafish with high efficiency [up to 50% germline transmission (58)]. This technology should allow for maximal integration of fluorescent tags.

For introducing point mutations, recent progress in CRISPR-mediated base editing allows for the introduction of point mutations (conversion of G-C base pairs to A-T base pairs or vice-versa) without inducing a double-stranded break (**Figure 3**; Komor et al., 2016; Gaudelli et al., 2017).

The first-generation CRISPR base editor (BE1) uses catalytically inactive Cas9 (dCas9) fused with cytidine deaminase enzyme encoded by the rat APOBEC1 gene (Komor et al., 2016). The cytidine deaminase enzyme converts cytosine bases into uridine, which are then read as thymine during replication. The result is a conversion of cytosine to thymine that occurs within the five-nucleotide window. The second-generation base editor (BE2) is fused with a uracil glycosylase inhibitor (UGI) that prevents excision of uracil during repair; BE2 has marginally higher activity compared to BE1 but does induce indel formation because it contains dCas9not. To further improve editing efficiency, the catalytic His residue at position 840 (which nicks the non-edited strand to mimic newly synthesized DNA) was restored to create BE3, the most widely used base editor. BE3 is the most efficient of the three base editors, and may also induce indels due to its nicking capabilities (Komor et al., 2016).

A new version of BE3 – HF-BE3 – was developed by incorporating mutations in Cas9 known to increase specificity and decrease off-target editing; in practice HF-BE3 appears to have lower on-target editing efficiency (Rees et al., 2017). Delivering the BE3- ribonucleoprotein complex (RNP) results in more robust editing than using plasmid-mediated delivery. This efficiency of BE3 RNP was further tested in zebrafish to generate specific point mutations targeting the tyrosinase locus: two of the three BE3:sgRNA RNP complexes were able to induce substantial point mutations *in vivo*, with 4–5% editing efficiency (Rees et al., 2017).

David Liu's group continued their effort toward refining and improving the base editors. They engineered the next generation base editors (BE4) to increase the base conversion efficiency by 50%. BE4 editors have extended (32 aa) rAPOBEC1-Cas9n and Cas9n-UGI linker (9 aa), and fusion of an additional UGI to the C terminus with another 9-amino acid linker. The BE4 base editor was further refined by adding the bacteriophage Mu protein Gam, which binds to double-stranded breaks and reduces indel formation to less than 1.5%; this modified base editor is called BE4-Gam (Komor et al., 2017). To increase APOBEC1 expression, ancestral sequence reconstruction using 468 homologs of APOBEC1 was performed, and two ancestors (Anc689 and Anc687) were selected (Koblan et al., 2018). Codon-optimized bipartite NLS were added at the N- and C-termini, similar to BE4max, to create the AncBE4max variant that showed improved editing at multiple loci (Koblan et al., 2018).

In zebrafish, cytidine deaminase fused with Cas9 nickase was able to induce sequence-specific single base mutations from ∼9 to 28% efficiency at multiple loci with a low number of indels (Zhang et al., 2017). Authors targeted *tyr* gene causal gene for human ocular albinism (OA) and oculocutaneous albinism (OCA). A mutation p.P301L in the *tyr* gene has been identified in OCA patients. While they were not able to convert proline to leucine, proline was converted to three other amino acids: serine, alanine or threonine. Edited embryos showed the loss

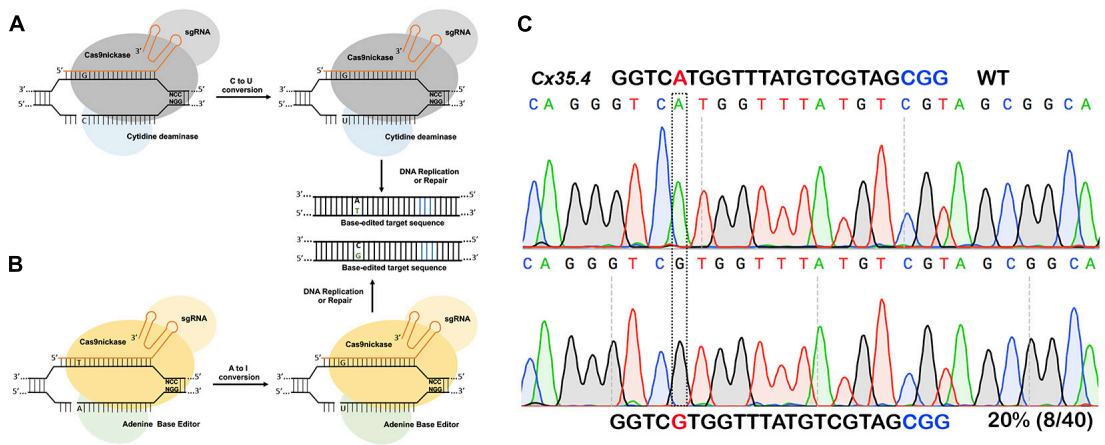

FIGURE 3 | Single nucleotide substitution using base editors. **(A)** Cytidine deaminase fused to nickase Cas9 converts cytosine to thymine to guanine to adenine within a targeting window. **(B)** Adenine base editor converts adenine to inosine that is recognized as guanine during DNA replication or repair thus converting A to G or C to T. **(C)** *In vivo* substitution of adenine to guanine using ABE7.10 base editor in zebrafish. sgRNA targeting cx35.4 gene was injected in 1-cell stage zebrafish embryos, DNA from a pool of four injected embryos was sequenced, and 20% of the clones carrying the desired A to G substitution.

of pigmentation in the eyes of injected embryos. Five other targets tested also converted cytosine to thymine with varying efficiency (Zhang et al., 2017). While the BE system works in zebrafish, the efficiency is low compared to knockouts, and further optimization is required to improve editing efficiency.

Similar to the BE system, the "Target-AID system" was developed by Japanese researchers. The Target-AID system is composed of nuclease-dead Cas9 or Cas9 nickase fused with activation-induced cytidine deaminase (AID) encoded by the PmcDA1 gene from sea lamprey. Target-AID can also induce cytosine to thymine conversion within a five-nucleotide window. The target-AID system was used in zebrafish to introduce premature stop codons (TAG or TAA) by converting cytosine to thymine. Two genes, chordin (*chd*) and one-eyed pinhead (*oep*) were targeted using this strategy, and the introduction of premature stop codons phenocopies the known genetic mutants (Tanaka et al., 2018).

Recently, another base editor (eA3A-BE3) fused with an engineered human APOBEC3A (eA3A) domain was shown to deaminate cytidines in a more controlled manner, and function according to a TCR > TCY > VCN (V = G, A, C, Y = C, T) hierarchy (Gehrke et al., 2018). The new base editor variant has shown comparable activities on cytidines in TC motifs, with reduced or no significant editing on cytidines in other motifs. Furthermore, eA3A-BE3 has shown low undesirable bystander mutations compared to other versions (Gehrke et al., 2018).

Existing cytosine deaminase base editors can target bases located between the 4th and 8th position in the target sequence. To expand the targeting window, a new base editor for programming larger C to U (T) scope (BE-PLUS) was developed. This new editor utilizes the SunTag system (Jiang et al., 2018); SunTag contains multiple copies of GCN4 peptide (each consisting of 19 residues) which is recognized by a single chain variable (scFV) antibody. BE-PLUS contains three components: nickase Cas9 fused at the C-terminus to 10 copies of GCN4 peptide (SunTag), scFv-APOBEC-UGI-GB1, and sgRNA. BE-PLUS induced fewer C-T conversions at positions 4–8, but converted C-T at 9–16 positions more efficiently. However, at positions 4–8, BE-PLUS was as efficient as the previously described BE3 (Jiang et al., 2018).

Third- and fourth-generation base editors (BE3 and BE4Gam) were further optimized by codon optimizing Cas9, as well as by adding a FLAG tag and NLS at the N-terminus. These modified base editors were shown to improve C-T conversion up to 50-fold compared with the original BE3 or BE4 base editors (Zafra et al., 2018). A novel method - CRISPR-SKIP - has been shown to program exon skipping by mutating splice acceptor sites using cytidine deaminase (Gapinske et al., 2018). The CRISPR-SKIP webtool can identify exons that can be skipped using this method, and it currently supports BE3, VQR-BE3, VRER-BE3, and SaKKH-BE3 variants (Gapinske et al., 2018). Michael Bassik's lab developed a novel base editor CRISPR-X, which uses an RNA aptamer (MS2) fused to sgRNA to recruit the cytidine deaminase to the target site and induce somatic hypermutation within a 100 bp window. This is a powerful approach for protein engineering because it can generate a diverse population of alleles that could be useful for directed evolution (Hess et al., 2016).

Adenine Base Editors

Cytidine deaminase-based base editors convert C-T or G-A; there are no natural enzymes that can convert A-G or T-C. To address this problem, David Lius' lab developed an adenine base editor (ABE) to modify adenine bases. The existing adenosine deaminase TadA/ADAR enzymes do not act on double-stranded DNA. Using phage-assisted continuous evolution (PACE), multiple rounds of directed evolution led to the identification of *Escherichia coli* TadA that can use DNA as a substrate. The ABE consists of a nickase Cas9 fused with a heterodimer of wild-type TadA and engineered TadA enzymes, guided by sgRNA to the target site. Engineered TadA converts adenine (A) to inosine (I) on the DNA target; inosine is recognized as guanine during DNA repair or replication, thus converting adenine (A) to guanine (G) or thymine (T) to cytosine (C). Of the Liu lab's multiple versions from ABE 0.1 to ABE 7, ABE7.10 has been shown to convert AT to GC with approximately 50% efficiency in mammalian cells. The ABE7.10 variant converts bases at position 4 to 7, and ABE7.8 or ABE7.9 variants convert bases at positions 4–9. The ABE7.10 variant was further optimized to generate a new variant, ABEmax, by replacing SV40NLS to codon-optimized bipartite NLS at both the N- and C-termini. Modified ABEmax increases the base substitution rate from ∼1.5- to 2-fold without changing the editing window; however, the rate of indels slightly increased.

Both cytidine deaminase and adenine deaminase enzymes are further fused with different variants such as VQR, VRER, SaCas9KKH, and newly evolved Cas9 such as xCas9, iSpy-macCas9, and SpCas9-NG (Kim Y. B. et al., 2017; Hu et al., 2018). Thus, both types of base editors will provide coverage to change all four bases in a targeted manner. As the new variants and new orthologs of nucleases evolve the targeting coverage will further expand covering all of the pathogenic variants. **Tables 3**, **4** summarizes the different base editing resources, targeting range of each base editors mentioned above, respectively.

TRANSCRIPTIONAL MODULATION AND EPIGENOME EDITING

CRISPR/Cas9 has also been repurposed to modulate transcription and manipulate the epigenome. In order to apply the CRISPR system beyond inducing a double stranded break, the DNA cleavage activity of Cas9 nuclease must be inactivated. Cas9 from *Streptococcus pyogenes* (SpCas9) contains two nuclease domains – a RuvC-like domain and a HNH domain – both of which are required to induce a double stranded break (Jinek et al., 2012). Introducing mutations in the catalytic residues of both nuclease domains (D10A, H840A) will create a catalytically inactive version of the Cas9 (dCas9; Qi et al., 2013). Using sgRNA, dCas9 can be recruited to a specific target without inducing a DNA break. To modulate transcription, dCas9 was first fused with transcriptional activators (VP64, a synthetic tetramer of the Herpes Simplex Viral Protein or p65 a transcription factor activation domain) or transcriptional repressors [KRAB, a Kruppel-associated box and the transcriptional repressor of Kox1, or 4X mSin Interaction Domain (SID; Konermann et al., 2015)]. These fusion proteins

TABLE 3 | Resources for base editing.

Resource	Description	URL	Reference
BE-Analyzer	NGS data analysis tool to identify based editing induced events.	http://www.rgenome.net/be-analyzer/	Hwang et al., 2018
BE-Designer	Guide-RNA design tool for base editing.	http://www.rgenome.net/be-designer/	Hwang et al., 2018
BEEP	Command line program to assess CRISPR-mediated base editing efficiency from Sanger sequencing ab1 files.	https://github.com/mitmedialab/BEEP	Chatterjee et al., 2018
CRISPR-SKIP	A tool to design induce exon skipping by base editing.	http://song.igb.illinois.edu/crispr-skip/	Gapinske et al., 2018
CRISPResso 2	Tool to analyze base editing events from next generation sequencing data.	http://crispresso.pinellolab.partners.org/	Clement et al., 2018
EditR	Tool to estimate base editing by Sanger sequencing.	http://baseeditr.com/	Kluesner et al., 2018
iSTOP	Database of sgRNAs for generating STOP codons using base editing.	http://www.ciccialab-database.com/istop	Billon et al., 2017
Beditor	Tool to design genome-wide sgRNA for base editing.	https://github.com/rraadd88/beditor	Dandage et al., 2018

result in transcriptional activation (CRISPRa) or repression (CRISPRi) when targeted to the regulatory or coding regions of the gene.

Both CRISPRa and CRISPRi have been shown to work in modulating transcription of the target genes in zebrafish (Long et al., 2015). Two genes required for otic placode induction (*fgf8a* and *foxi1*) were targeted to demonstrate the utility of CRISPRa and CRISPRi in zebrafish. When sgRNAs targeting *fgf8a* coding regions were co-injected with dCas9-KRAB (CRISPRi) fusion protein, the expression of *fgf8a* was reduced at 11 hpf, and smaller otic vesicles were observed at 32 hpf (Long et al., 2015). Similarly, when dCas9-VP160 (CRISPRa) together with either sgRNAs targeting *fgf8a* or *foxi1* were injected in one-cell stage embryos, the expression of *fgf8a* and *foxi1* was increased and the resulting animals showed enlarged otic vesicles.

The dCas9 was also fused with putative Eve repressor domain of zebrafish *Evx1*, and the resulting dCas9-Eve fusion together with three sgRNAs targeting sequences upstream of all zinc finger transcription factors (*zfnl1s*) were used to inhibit the transcription of the *znfl1* in zebrafish (Dong et al., 2017). Decreased expression of *znfl1* disrupts the formation of the posterior neuroectoderm in zebrafish gastrula, and the phenotype perfectly phenocopies that generated by the anti-sense morpholino (Dong et al., 2017).

In zebrafish it has been shown that mutants generated by targeting mutagenesis techniques, genetic compensation or transcriptional adaptation could all trigger the upregulation of related genes and compensate for the loss of the targeted gene. Such upregulation and compensation were not observed when antisense morpholinos were used, suggesting that downregulation of target genes using CRISPRi could be an alternate tool to study gene function.

Additionally, catalytically inactive Cas9 has been fused to various epigenetic effectors such as the catalytic core of the human acetyltransferase p300 which catalyzes acetylation of histone H3 lysine 27 (Hilton et al., 2015), histone demethylase (Kearns et al., 2015), histone deacetylase (HDAC) (Kwon et al., 2017) and many others (reviewed in Lau and Suh, 2018).

TABLE 4 | Summary of editing windows by base editors.

Base editor (s)	Editing window	Use in zebrafish	Reference
Cytosine deaminase			
SpCas9-BE1, SpCas9-BE2, SpCas9-BE3, SpCas9-BE4 SpCas9-BE4max, and SpCas9-BE4-Gam	4–8	Yes	Komor et al., 2016, 2017; Kim Y. B. et al., 2017
SpCas9VQR-BE3	4–11	Yes	Kim Y. B. et al., 2017
SpCas9VRER-BE3	3–10	Not tested	Kim Y. B. et al., 2017
SpCas9YE1-BE3	4–7	Not tested	Kim Y. B. et al., 2017
SpCas9YE2-BE3, SpCas9YEE-BE3, SpCas9YEE-BE3	5–6	Not tested	Kim Y. B. et al., 2017
SaCas9-BE3, SaCas9-BE4, SaCas9KKH-BE3	3–12	Not tested	Kim Y. B. et al., 2017
xCas9-BE3	4–8	Not tested	Hu et al., 2018
SpCas9 Target-AID	2–4	Yes	Nishida et al., 2016
SpCas9-NG Target-AID	2–4	Not tested	Nishimasu et al., 2018
SpCas9-BE-Plus	4–16	Not tested	Jiang et al., 2018
SpCas9 eA3A-BE3, A3A-BE3	4–8	Not tested	Gehrke et al., 2018
CRISPR-X	−50 bp to +50 bp relative to PAM	Not tested	Hess et al., 2016
Cas12a (Cpf1)-BE	8–13	Not tested	Li et al., 2018
Adenine base editors			
ABE7.9	4–9	Not tested	Gaudelli et al., 2017
ABE7.10	4–8	Not tested	Gaudelli et al., 2017
xCas9 ABE	4–8	Not tested	Hu et al., 2018
SpCas9-VQR ABE	4–8	Not tested	Yang et al., 2018
SaCas9-KKH ABE	6–12	Not tested	Yang et al., 2018
ScCas9-ABE7.10	4–8	Not tested	Chatterjee et al., 2018

LINEAGE TRACING USING CRISPR/Cas9

A fundamental goal in developmental biology is to determine the origin of different cell types and tissues, and to establish their relationship in complex organisms. Lineage tracing is one method employed by developmental biologists to study the origin of cell types: techniques include dye based markers, nucleotide pulse-chase analysis, transplantation, sequencing somatic mutations, Cre-Lox and FLP-FRT based methods (reviewed in Kretzschmar and Watt, 2012). These methods can efficiently label cells at a single time-point to study large numbers of clonal populations in a complex animal, however, a detailed

lineage tree over time cannot be reconstructed; understanding how cells change over the time will help determine the mechanisms of disease progression. Recently, the CRISPR/Cas9 mediated genome editing technique was used to generate genetic scars (indels) in the genome which serve as genetic barcodes for use in the reconstruction of cell lineages in developing animals or adults. Using this principle, many innovative approaches have been developed including genome editing of synthetic target arrays for lineage tracing (GESTALT; McKenna et al., 2016), lineage tracing by nuclease-activated editing of ubiquitous sequences (LINNAEUS; Spanjaard et al., 2018), ScarTrace (Alemany et al., 2018), and memory by engineered mutagenesis with optical *in situ* readout (MEMOIR; Frieda et al., 2017). CRISPR based lineage tracing is being adopted in multiple model organisms including zebrafish (Schmidt et al., 2017; Kalhor et al., 2018; Raj et al., 2018; Spanjaard et al., 2018). GESTALT, first applied to the understanding of the origin of organ development in zebrafish, was developed in the labs of Jay Shendure and Alex Schier. The Schier Lab engineered 10 different target sequences (unique barcodes in the 3′ UTR of DsRed) that are not found in the zebrafish genome to avoid any interreference with normal development. A transgenic line that drives the expression of DsRed under the ubiquitin promoter was generated. Ten sgRNAs that target the 10 unique sequences present in the transgenic lines were injected together with Cas9 protein in one-cell stage zebrafish embryos. Embryos were collected at different time points, and target regions were amplified using primers containing unique molecular identifier (UMI) to add UMI barcodes in the amplicons. (The process of UMI tagging helps in assigning individual sequencing reads back to the cell of origin). Sequencing confirmed the *in vivo* allelic diversity, and the recovered alleles were used to reconstruct the lineage tree. To investigate whether these barcodes can also be recovered in adult animals, several organs (brain, eyes, intestine, gills, heart, and blood) were collected and subjected to DNA sequencing to recover barcode information. It was concluded that most cells in different adult organs were derived from fewer embryonic progenitors; more than 98% of circulating blood in an adult zebrafish contains five common alleles, suggesting a highly clonal origin of the blood system in zebrafish. The GESTALT method was further modified by combining single-cell RNA sequencing to develop scGESTALT [single cell Genome Editing of Synthetic Target Arrays for Lineage Tracing; (Raj et al., 2018)]. The workflow for the cell lineage tracing and scRNA-seq experiment involves the introduction of sgRNAs to target exogenous sequences and the isolation of single cells at appropriate time points. This is followed by mRNA isolation, reverse transcription and cDNA amplification, library preparation, and sequencing both DNA and RNA; this method has been used to identify more than 100 different cell types during brain development. The scGESTALT method also allows barcodes to be recorded at post gastrulation stages by employing temporal control of Cas9 using a heat shock promoter and constitutively expressing sgRNA from the U6 promoter (Raj et al., 2018).

Unlike GESTALT, LINNAEUS, and ScarTrace approaches take advantage of existing transgenic lines carrying multiple integrations of a transgene – green fluorescent protein (GFP) or mCherry. Both LINNEAUS and ScarTrace combine lineage tracing with identification of cell types by single-cell transcriptomics. ScarTrace uses a zebrafish line carrying eight in-tandem copies of a histone–GFP transgene. sgRNA targeting the GFP with Cas9 protein is injected into one-cell stage embryos. Cas9 induces double-stranded breaks that when repaired by non-homologous end joining leave insertions or deletions (scars). During embryonic development, cells accumulate these scars and pass them on to future generations. When the scars are then sequenced, any adult cells containing identical scars must originate from a common progenitor cell. This method also defines cell types based on their transcriptome, thus cataloging both cell type and progenitor for each organ type. ScarTrace revealed that hematopoietic cells in the kidney marrow originated from fewer embryonic progenitors, and multiple progenitors give rise to specific cell types in the brain and eye. It was further revealed that a common progenitor produces both epidermal and mesenchymal cells of the caudal fin. Interestingly, this technique also showed how a progenitor cell commits to produce a left or right eye in zebrafish.

The LINNAEUS approach is similar to ScarTrace, however, LINNAEUS uses a zebrafish line carrying an RFP transgene with 16–32 independent integrations in the genome. The presence of independent integrations in different loci protect the scars from being removed or overwritten by Cas9. sgRNA targeting RFP and Cas9 were together injected into one-cell stage embryos; since RFP-targeting sgRNA generates indels (scars) and leave RFP non-functional, loss of RFP was used as a quality control to monitor the efficiency of editing and scar formation. At later time points, embryos were dissociated into single cells and RFP transcripts were sequenced to quantify the scar formation and the transcriptome from the same cell was sequenced by scRANA-seq. Spanjaard and colleagues applied this approach to identify many different cell types from dissected adult organs including heart, liver, primary pancreatic islets and telencephalon. They found that immune cells from different organs can be grouped together in the lineage tree: analysis of cardiac and pancreatic cell types showed the early separation of myocardial and endocardial lineages.

MEMOIR method uses two different tools: Sequential single molecule Fluorescence *In Situ* Hybridization (smFISH) that reveals which specific genes are active in a particular cell, and CRISPR/Cas9 that generates indels (Frieda et al., 2017). MEMOIR uses bipartite genetic recording elements called barcoded scratchpads. Each scratchpad contains 10 repeat units, and sgRNAs and Cas9 targeting scratchpads induces indels. There is also a barcode adjacent to each scratchpad which can be identified by smFISH and allows for the recording of each lineage. This method has so far only been used *in vitro* to record the cellular history of mouse embryonic stem cells through multiple generations (Frieda et al., 2017).

The methods described above generate complex lineage trees using scarring accumulated over several hours, and each method has a limited number of scars. To overcome this limitation, a self-targeting homing guide RNA (hgRNA) system was developed that can induce scarring over a longer time period and further

increase complexity (Perli et al., 2016; Kalhor et al., 2018). Lineage tracing in mammals has been challenging compared to that in zebrafish. Kalhor et al. (2018) used hgRNAs to generate a mouse model for the study of cell lineages during early mouse development; hgRNA containing a targeting sequence with PAM was attached to a scaffold and allowed Cas9 to target the expression cassette. For *in vivo* cell lineage tracing, a transgenic mouse harboring 41 different homing guide RNA expression cassettes was created. This transgenic mouse was bred with a Cas9 expressing mouse strain to induce indels (barcodes). These barcodes can be used to track cells temporally and spatially (Kalhor et al., 2018).

These proof-of-principle studies have developed elegant lineage tracing strategies to establish lineage relationships and understand the fundamental mechanisms of cell differentiation under normal and pathological conditions (e.g., cancer metastasis) in complex model organisms including zebrafish. The development of CRISPR based lineage tracing methods is well-timed and complementary to the efforts toward building the human cell atlas (Regev et al., 2017). These approaches will have significant impact on our understanding of the origin of each cell type and how the adult body is developed from a single cell.

CONCLUSION AND FUTURE PERSPECTIVES

As described above the focus of recent research has been on developing strategies to improve Cas9 function, targeting coverage, and on-target efficiencies by reducing off target editing. CRISPR-based genome editing technologies have revolutionized biological research; CRISPR-related nucleases have been repurposed in many applications, and recent developments in base editing and lineage tracing have further increased their utility in studying development and human diseases. New and inexpensive sequencing technologies are accelerating the discovery of candidate disease genes and pathogenic variants. CRISPR has provided a variety of tools to precisely modify the genome in a targeted manner for a variety of applications including functional gene knockouts, targeted induction or correction of single point mutations, and epigenome editing. Recent work has been focused on refining the specificity and expanding the target coverage of Cas9; directed evolution has led to the discovery of multiple Cas9 variants that will significantly expand the targeting coverage. Furthermore, development of base-editing techniques is an important milestone in the study of pathogenic variants in animal models; they will not only accelerate the functional validation of candidate disease genes in a model organism, but also accelerate the development of therapeutic tools for the treatment of a wide range of human diseases. Development of CRISPR-based lineage tracing methods are revealing information that could have been challenging to uncover using traditional approaches including the discovery of novel cell types and the origin of cells in different organs and tissues in complex model organisms.

AUTHOR CONTRIBUTIONS

KL, CP, TR, PV, and GV researched the data. GV wrote the article. All authors read the article and approved it for publication.

FUNDING

This research was supported by a grant from NIH/COBRE GM103636 (Project 3 to GV).

REFERENCES

Ablain, J., Durand, E. M., Yang, S., Zhou, Y., and Zon, L. I. (2015). A CRISPR/Cas9 vector system for tissue-specific gene disruption in zebrafish. *Dev. Cell* 32, 756–764. doi: 10.1016/j.devcel.2015.01.032

Adikusuma, F., Piltz, S., Corbett, M. A., Turvey, M., Mccoll, S. R., Helbig, K. J., et al. (2018). Large deletions induced by Cas9 cleavage. *Nature* 560, E8–E9. doi: 10.1038/s41586-018-0380-z

Albadri, S., Del Bene, F., and Revenu, C. (2017). Genome editing using CRISPR/Cas9-based knock-in approaches in zebrafish. *Methods* 12, 77–85. doi: 10.1016/j.ymeth.2017.03.005

Alemany, A., Florescu, M., Baron, C. S., Peterson-Maduro, J., and Van Oudenaarden, A. (2018). Whole-organism clone tracing using single-cell sequencing. *Nature* 556, 108–112. doi: 10.1038/nature25969

Allen, F., Crepaldi, L., Alsinet, C., Strong, A. J., Kleshchevnikov, V., De Angeli, P., et al. (2018). Predicting the mutations generated by repair of Cas9-induced double-strand breaks. *Nat. Biotechnol.* 37, 64–72. doi: 10.1038/nbt.4317

Amsterdam, A., Varshney, G. K., and Burgess, S. M. (2011). Retroviral-mediated insertional mutagenesis in zebrafish. *Methods Cell Biol.* 104, 59–82. doi: 10.1016/B978-0-12-374814-0.00004-5

Anders, C., Bargsten, K., and Jinek, M. (2016). Structural plasticity of PAM recognition by engineered variants of the RNA-guided endonuclease Cas9. *Mol. Cell* 61, 895–902. doi: 10.1016/j.molcel.2016.02.020

Ata, H., Ekstrom, T. L., Martinez-Galvez, G., Mann, C. M., Dvornikov, A. V., Schaefbauer, K. J., et al. (2018). Robust activation of microhomology-mediated end joining for precision gene editing applications. *PLoS Genet.* 14:e1007652. doi: 10.1371/journal.pgen.1007652

Bedell, V. M., Wang, Y., Campbell, J. M., Poshusta, T. L., Starker, C. G., Krug, R. G., et al. (2012). In vivo genome editing using a high-efficiency TALEN system. *Nature* 491, 114–118. doi: 10.1038/nature11537

Billon, P., Bryant, E. E., Joseph, S. A., Nambiar, T. S., Hayward, S. B., Rothstein, R., et al. (2017). CRISPR-mediated base editing enables efficient disruption of eukaryotic genes through induction of STOP codons. *Mol. Cell* 67:e1064. doi: 10.1016/j.molcel.2017.08.008

Bradford, Y. M., Toro, S., Ramachandran, S., Ruzicka, L., Howe, D. G., Eagle, A., et al. (2017). Zebrafish models of human disease: gaining insight into human disease at ZFIN. *ILAR J.* 58, 4–16. doi: 10.1093/ilar/ilw040

Burger, A., Lindsay, H., Felker, A., Hess, C., Anders, C., Chiavacci, E., et al. (2016). Maximizing mutagenesis with solubilized CRISPR-Cas9 ribonucleoprotein complexes. *Development* 143, 2025–2037. doi: 10.1242/dev.134809

Carrington, B., Varshney, G. K., Burgess, S. M., and Sood, R. (2015). CRISPR-STAT: an easy and reliable PCR-based method to evaluate target-specific sgRNA activity. *Nucleic Acids Res.* 43:e157. doi: 10.1093/nar/gkv802

Chang, N., Sun, C., Gao, L., Zhu, D., Xu, X., Zhu, X., et al. (2013). Genome editing with RNA-guided Cas9 nuclease in zebrafish embryos. *Cell Res.* 23, 465–472. doi: 10.1038/cr.2013.45

Chatterjee, P., Jakimo, N., and Jacobson, J. M. (2018). Minimal PAM specificity of a highly similar SpCas9 ortholog. *Sci. Adv.* 4:eaau0766.

Clement, K., Rees, H., Canver, M., Gehrke, J., Farouni, R., Hsu, J., et al. (2018). Analysis and comparison of genome editing using CRISPResso2. *bioRxiv* [Preprint]. doi: 10.1101/392217

Cong, L., Ran, F. A., Cox, D., Lin, S., Barretto, R., Habib, N., et al. (2013). Multiplex genome engineering using CRISPR/Cas systems. *Science* 339, 819–823. doi: 10.1126/science.1231143

Dandage, R., Despres, P. C., Yachie, N., and Landry, C. R. (2018). beditor: A computational workflow for designing libraries of guide RNAs for CRISPR-mediated base editing. *bioRxiv* [Preprint]. doi: 10.1101/426973

Demarest, S. T., and Brooks-Kayal, A. (2018). From molecules to medicines: the dawn of targeted therapies for genetic epilepsies. *Nat. Rev. Neurol.* 14, 735–745. doi: 10.1038/s41582-018-0099-3

Dong, X., Li, J., He, L., Gu, C., Jia, W., Yue, Y., et al. (2017). Zebrafish Znfl1 proteins control the expression of hoxb1b gene in the posterior neuroectoderm by acting upstream of pou5f3 and sall4 genes. *J. Biol. Chem.* 292, 13045–13055. doi: 10.1074/jbc.M117.777094

Esvelt, K. M., Mali, P., Braff, J. L., Moosburner, M., Yaung, S. J., and Church, G. M. (2013). Orthogonal Cas9 proteins for RNA-guided gene regulation and editing. *Nat. Methods* 10, 1116–1121. doi: 10.1038/nmeth.2681

Feng, Y., Chen, C., Han, Y., Chen, Z., Lu, X., Liang, F., et al. (2016). Expanding CRISPR/Cas9 genome editing capacity in zebrafish using SaCas9. *G3 (Bethesda)* 6, 2517–2521. doi: 10.1534/g3.116.031914

Fonfara, I., Le Rhun, A., Chylinski, K., Makarova, K. S., Lecrivain, A. L., Bzdrenga, J., et al. (2014). Phylogeny of Cas9 determines functional exchangeability of dual-RNA and Cas9 among orthologous type II CRISPR-cas systems. *Nucleic Acids Res.* 42, 2577–2590. doi: 10.1093/nar/gkt1074

Fonfara, I., Richter, H., Bratovič, M., Le Rhun, A., and Charpentier, E. (2016). The CRISPR-associated DNA-cleaving enzyme Cpf1 also processes precursor CRISPR RNA. *Nature* 532:517. doi: 10.1038/nature17945

Frieda, K. L., Linton, J. M., Hormoz, S., Choi, J., Chow, K. K., Singer, Z. S., et al. (2017). Synthetic recording and in situ readout of lineage information in single cells. *Nature* 541, 107–111. doi: 10.1038/nature20777

Gagnon, J. A., Valen, E., Thyme, S. B., Huang, P., Ahkmetova, L., Pauli, A., et al. (2014). Efficient mutagenesis by Cas9 protein-mediated oligonucleotide insertion and large-scale assessment of single-guide RNAs. *PLoS One* 9:e98186. doi: 10.1371/journal.pone.0098186

Gallardo, V. E., Varshney, G. K., Lee, M., Bupp, S., Xu, L., Shinn, P., et al. (2015). Phenotype-driven chemical screening in zebrafish for compounds that inhibit collective cell migration identifies multiple pathways potentially involved in metastatic invasion. *Dis. Model Mech.* 8, 565–576. doi: 10.1242/dmm.018689

Gao, L., Cox, D. B. T., Yan, W. X., Manteiga, J. C., Schneider, M. W., Yamano, T., et al. (2017). Engineered Cpf1 variants with altered PAM specificities. *Nat. Biotechnol.* 35, 789–792. doi: 10.1038/nbt.3900

Gapinske, M., Luu, A., Winter, J., Woods, W. S., Kostan, K. A., Shiva, N., et al. (2018). CRISPR-SKIP: programmable gene splicing with single base editors. *Genome Biol.* 19:107. doi: 10.1186/s13059-018-1482-5

Gaudelli, N. M., Komor, A. C., Rees, H. A., Packer, M. S., Badran, A. H., Bryson, D. I., et al. (2017). Programmable base editing of A · T to G · C in genomic DNA without DNA cleavage. *Nature* 551:464. doi: 10.1038/nature24644

Gehrke, J. M., Cervantes, O., Clement, M. K., Wu, Y., Zeng, J., Bauer, D. E., et al. (2018). An APOBEC3A-Cas9 base editor with minimized bystander and off-target activities. *Nat. Biotechnol.* 36, 977–982. doi: 10.1038/nbt.4199

Giannelou, A., Wang, H., Zhou, Q., Park, Y. H., Abu-Asab, M. S., Ylaya, K., et al. (2018). Aberrant tRNA processing causes an autoinflammatory syndrome responsive to TNF inhibitors. *Ann. Rheum. Dis.* 77, 612–619. doi: 10.1136/annrheumdis-2017-212401

Glemzaite, M., Balciunaite, E., Karvelis, T., Gasiunas, G., Grusyte, M. M., Alzbutas, G., et al. (2015). Targeted gene editing by transfection of in vitro reconstituted *Streptococcus thermophilus* Cas9 nuclease complex. *RNA Biol.* 12, 1–4. doi: 10.1080/15476286.2015.1017209

Guell, M., Yang, L., and Church, G. M. (2014). Genome editing assessment using CRISPR genome analyzer (CRISPR-GA). *Bioinformatics* 30, 2968–2970. doi: 10.1093/bioinformatics/btu427

Hess, G. T., Fresard, L., Han, K., Lee, C. H., Li, A., Cimprich, K. A., et al. (2016). Directed evolution using dCas9-targeted somatic hypermutation in mammalian cells. *Nat. Methods* 13, 1036–1042. doi: 10.1038/nmeth.4038

Hilton, I. B., D'ippolito, A. M., Vockley, C. M., Thakore, P. I., Crawford, G. E., Reddy, T. E., et al. (2015). Epigenome editing by a CRISPR-Cas9-based acetyltransferase activates genes from promoters and enhancers. *Nat. Biotechnol.* 33, 510–517. doi: 10.1038/nbt.3199

Hirano, H., Gootenberg, J. S., Horii, T., Abudayyeh, O. O., Kimura, M., Hsu, P. D., et al. (2016). Structure and engineering of *Francisella novicida* Cas9. *Cell* 164, 950–961. doi: 10.1016/j.cell.2016.01.039

Hou, Z., Zhang, Y., Propson, N. E., Howden, S. E., Chu, L. F., Sontheimer, E. J., et al. (2013). Efficient genome engineering in human pluripotent stem cells using Cas9 from *Neisseria meningitidis*. *Proc. Natl. Acad. Sci. U.S.A.* 110, 15644–15649. doi: 10.1073/pnas.1313587110

Howe, K., Clark, M. D., Torroja, C. F., Torrance, J., Berthelot, C., Muffato, M., et al. (2013). The zebrafish reference genome sequence and its relationship to the human genome. *Nature* 496, 498–503. doi: 10.1038/nature12111

Hruscha, A., Krawitz, P., Rechenberg, A., Heinrich, V., Hecht, J., Haass, C., et al. (2013). Efficient CRISPR/Cas9 genome editing with low off-target effects in zebrafish. *Development* 140, 4982–4987. doi: 10.1242/dev.099085

Hsu, P. D., Lander, E. S., and Zhang, F. (2014). Development and applications of CRISPR-Cas9 for genome engineering. *Cell* 157, 1262–1278. doi: 10.1016/j.cell.2014.05.010

Hu, J. H., Miller, S. M., Geurts, M. H., Tang, W., Chen, L., Sun, N., et al. (2018). Evolved Cas9 variants with broad PAM compatibility and high DNA specificity. *Nature* 556, 57–63. doi: 10.1038/nature26155

Hwang, G.-H., Park, J., Lim, K., Kim, S., Yu, J., Kim, S.-T., et al. (2018). Web-based design and analysis tools for CRISPR base editing. *BMC Bioinformatics* 19:542. doi: 10.1186/s12859-018-2585-4

Hwang, W. Y., Fu, Y., Reyon, D., Maeder, M. L., Tsai, S. Q., Sander, J. D., et al. (2013). Efficient genome editing in zebrafish using a CRISPR-Cas system. *Nat. Biotechnol.* 31, 227–229. doi: 10.1038/nbt.2501

Jakimo, N., Chatterjee, P., Nip, L., and Jacobson, J. M. (2018). A Cas9 with complete PAM recognition for adenine dinucleotides. *bioRxiv* [Preprint]. doi: 10.1101/429654

Jamal, M., Ullah, A., Ahsan, M., Tyagi, R., Habib, Z., and Rehman, K. (2018). Improving CRISPR-Cas9 on-target specificity. *Curr. Issues Mol. Biol.* 26, 65–80. doi: 10.21775/cimb.026.065

Jao, L. E., Wente, S. R., and Chen, W. (2013). Efficient multiplex biallelic zebrafish genome editing using a CRISPR nuclease system. *Proc. Natl. Acad. Sci. U.S.A.* 110, 13904–13909. doi: 10.1073/pnas.1308335110

Jiang, W., Feng, S., Huang, S., Yu, W., Li, G., Yang, G., et al. (2018). BE-PLUS: a new base editing tool with broadened editing window and enhanced fidelity. *Cell Res.* 28, 855–861. doi: 10.1038/s41422-018-0052-4

Jinek, M., Chylinski, K., Fonfara, I., Hauer, M., Doudna, J. A., and Charpentier, E. (2012). A programmable dual-RNA-guided DNA endonuclease in adaptive bacterial immunity. *Science* 337, 816–821. doi: 10.1126/science.1225829

Kalhor, R., Kalhor, K., Mejia, L., Leeper, K., Graveline, A., Mali, P., et al. (2018). Developmental barcoding of whole mouse via homing CRISPR. *Science* 361:eaat9804.

Kearns, N. A., Pham, H., Tabak, B., Genga, R. M., Silverstein, N. J., Garber, M., et al. (2015). Functional annotation of native enhancers with a Cas9-histone demethylase fusion. *Nat. Methods* 12, 401–403. doi: 10.1038/nmeth.3325

Kettleborough, R. N., Busch-Nentwich, E. M., Harvey, S. A., Dooley, C. M., De Bruijn, E., Van Eeden, F., et al. (2013). A systematic genome-wide analysis of zebrafish protein-coding gene function. *Nature* 496, 494–497. doi: 10.1038/nature11992

Kim, E., Koo, T., Park, S. W., Kim, D., Kim, K., Cho, H. Y., et al. (2017). In vivo genome editing with a small Cas9 orthologue derived from *Campylobacter jejuni*. *Nat. Commun.* 8:14500. doi: 10.1038/ncomms14500

Kim, Y. B., Komor, A. C., Levy, J. M., Packer, M. S., Zhao, K. T., and Liu, D. R. (2017). Increasing the genome-targeting scope and precision of base editing with engineered Cas9-cytidine deaminase fusions. *Nat. Biotechnol.* 35, 371–376. doi: 10.1038/nbt.3803

Kleinstiver, B. P., Prew, M. S., Tsai, S. Q., Nguyen, N. T., Topkar, V. V., Zheng, Z., et al. (2015a). Broadening the targeting range of *Staphylococcus aureus* CRISPR-Cas9 by modifying PAM recognition. *Nat. Biotechnol.* 33, 1293–1298. doi: 10.1038/nbt.3404

Kleinstiver, B. P., Prew, M. S., Tsai, S. Q., Topkar, V. V., Nguyen, N. T., Zheng, Z., et al. (2015b). Engineered CRISPR-Cas9 nucleases with altered PAM specificities. *Nature* 523, 481–485. doi: 10.1038/nature14592

Kluesner, M. G., Nedveck, D. A., Lahr, W. S., Garbe, J. R., Abrahante, J. E., Webber, B. R., et al. (2018). EditR: A Method to Quantify Base

Editing from Sanger Sequencing. *CRISPR J.* 1, 239–250. doi: 10.1089/crispr.2018.0014

Koblan, L. W., Doman, J. L., Wilson, C., Levy, J. M., Tay, T., Newby, G. A., et al. (2018). Improving cytidine and adenine base editors by expression optimization and ancestral reconstruction. *Nat. Biotechnol.* 36, 843–846. doi: 10.1038/nbt.4172

Komor, A. C., Kim, Y. B., Packer, M. S., Zuris, J. A., and Liu, D. R. (2016). Programmable editing of a target base in genomic DNA without double-stranded DNA cleavage. *Nature* 533, 420–424. doi: 10.1038/nature17946

Komor, A. C., Zhao, K. T., Packer, M. S., Gaudelli, N. M., Waterbury, A. L., Koblan, L. W., et al. (2017). Improved base excision repair inhibition and bacteriophage Mu Gam protein yields C:G-to-T:A base editors with higher efficiency and product purity. *Sci. Adv.* 3:eaao4774.

Konermann, S., Brigham, M. D., Trevino, A. E., Joung, J., Abudayyeh, O. O., Barcena, C., et al. (2015). Genome-scale transcriptional activation by an engineered CRISPR-Cas9 complex. *Nature* 517, 583–588. doi: 10.1038/nature14136

Kretzschmar, K., and Watt, F. M. (2012). Lineage tracing. *Cell* 148, 33–45. doi: 10.1016/j.cell.2012.01.002

Kwon, D. Y., Zhao, Y. T., Lamonica, J. M., and Zhou, Z. (2017). Locus-specific histone deacetylation using a synthetic CRISPR-Cas9-based HDAC. *Nat. Commun.* 8:15315. doi: 10.1038/ncomms15315

Labun, K., Montague, T. G., Gagnon, J. A., Thyme, S. B., and Valen, E. (2016). CHOPCHOP v2: a web tool for the next generation of CRISPR genome engineering. *Nucleic Acids Res.* 44, W272–W276. doi: 10.1093/nar/gkw398

LaFave, M. C., Varshney, G. K., Vemulapalli, M., Mullikin, J. C., and Burgess, S. M. (2014). A defined zebrafish line for high-throughput genetics and genomics: NHGRI-1. *Genetics* 198, 167–170. doi: 10.1534/genetics.114.166769

Lau, C. H., and Suh, Y. (2018). In vivo epigenome editing and transcriptional modulation using CRISPR technology. *Transgenic Res.* 27, 489–509. doi: 10.1007/s11248-018-0096-8

Li, H., Pei, W., Vergarajauregui, S., Zerfas, P. M., Raben, N., Burgess, S. M., et al. (2017). Novel degenerative and developmental defects in a zebrafish model of mucolipidosis type IV. *Hum. Mol. Genet.* 26, 2701–2718. doi: 10.1093/hmg/ddx158

Li, M., Zhao, L., Page-Mccaw, P. S., and Chen, W. (2016). Zebrafish genome engineering using the CRISPR-Cas9 system. *Trends Genet.* 32, 815–827. doi: 10.1016/j.tig.2016.10.005

Li, X., Wang, Y., Liu, Y., Yang, B., Wang, X., Wei, J., et al. (2018). Base editing with a Cpf1-cytidine deaminase fusion. *Nat. Biotechnol.* 36, 324–327. doi: 10.1038/nbt.4102

Liu, H., Wei, Z., Dominguez, A., Li, Y., Wang, X., and Qi, L. S. (2015). CRISPR-ERA: a comprehensive design tool for CRISPR-mediated gene editing, repression and activation. *Bioinformatics* 31, 3676–3678. doi: 10.1093/bioinformatics/btv423

Long, L., Guo, H., Yao, D., Xiong, K., Li, Y., Liu, P., et al. (2015). Regulation of transcriptionally active genes via the catalytically inactive Cas9 in *C. elegans* and *D. rerio*. *Cell Res.* 25, 638–641. doi: 10.1038/cr.2015.35

Mali, P., Yang, L., Esvelt, K. M., Aach, J., Guell, M., Dicarlo, J. E., et al. (2013). RNA-guided human genome engineering via Cas9. *Science* 339, 823–826. doi: 10.1126/science.1232033

Marquart, G. D., Tabor, K. M., Brown, M., Strykowski, J. L., Varshney, G. K., Lafave, M. C., et al. (2015). A 3D searchable database of transgenic zebrafish Gal4 and Cre lines for functional neuroanatomy studies. *Front. Neural Circ.* 9:78. doi: 10.3389/fncir.2015.00078

McKenna, A., Findlay, G. M., Gagnon, J. A., Horwitz, M. S., Schier, A. F., and Shendure, J. (2016). Whole-organism lineage tracing by combinatorial and cumulative genome editing. *Science* 353:aaf7907. doi: 10.1126/science.aaf7907

McVey, M., and Lee, S. E. (2008). MMEJ repair of double-strand breaks (director's cut): deleted sequences and alternative endings. *Trends Genet.* 24, 529–538. doi: 10.1016/j.tig.2008.08.007

Moreno-Mateos, M. A., Fernandez, J. P., Rouet, R., Vejnar, C. E., Lane, M. A., Mis, E., et al. (2017). CRISPR-Cpf1 mediates efficient homology-directed repair and temperature-controlled genome editing. *Nat. Commun.* 8:2024. doi: 10.1038/s41467-017-01836-2

Moreno-Mateos, M. A., Vejnar, C. E., Beaudoin, J. D., Fernandez, J. P., Mis, E. K., Khokha, M. K., et al. (2015). CRISPRscan: designing highly efficient sgRNAs for CRISPR-Cas9 targeting in vivo. *Nat. Methods* 12, 982–988. doi: 10.1038/nmeth.3543

Mout, R., Ray, M., Lee, Y. W., Scaletti, F., and Rotello, V. M. (2017). In Vivo delivery of CRISPR/Cas9 for therapeutic gene editing: progress and challenges. *Bioconjug Chem.* 28, 880–884. doi: 10.1021/acs.bioconjchem.7b00057

Muller, M., Lee, C. M., Gasiunas, G., Davis, T. H., Cradick, T. J., Siksnys, V., et al. (2016). *Streptococcus thermophilus* CRISPR-Cas9 systems enable specific editing of the human genome. *Mol. Ther.* 24, 636–644. doi: 10.1038/mt.2015.218

Nishida, K., Arazoe, T., Yachie, N., Banno, S., Kakimoto, M., Tabata, M., et al. (2016). Targeted nucleotide editing using hybrid prokaryotic and vertebrate adaptive immune systems. *Science* 353:aaf8729. doi: 10.1126/science.aaf8729

Nishimasu, H., Shi, X., Ishiguro, S., Gao, L., Hirano, S., Okazaki, S., et al. (2018). Engineered CRISPR-Cas9 nuclease with expanded targeting space. *Science* 361, 1259–1262. doi: 10.1126/science.aas9129

Nishimasu, H., Yamano, T., Gao, L., Zhang, F., Ishitani, R., and Nureki, O. (2017). Structural basis for the altered PAM recognition by engineered CRISPR-Cpf1. *Mol. Cell* 67:e132. doi: 10.1016/j.molcel.2017.04.019

Park, J., Bae, S., and Kim, J. S. (2015). Cas-designer: a web-based tool for choice of CRISPR-Cas9 target sites. *Bioinformatics* 31, 4014–4016. doi: 10.1093/bioinformatics/btv537

Park, J., Lim, K., Kim, J. S., and Bae, S. (2017). Cas-analyzer: an online tool for assessing genome editing results using NGS data. *Bioinformatics* 33, 286–288. doi: 10.1093/bioinformatics/btw561

Pei, W., Xu, L., Huang, S. C., Pettie, K., Idol, J., Rissone, A., et al. (2018). Guided genetic screen to identify genes essential in the regeneration of hair cells and other tissues. *NPJ Regen. Med.* 3:11. doi: 10.1038/s41536-018-0050-7

Perli, S. D., Cui, C. H., and Lu, T. K. (2016). Continuous genetic recording with self-targeting CRISPR-Cas in human cells. *Science* 353:aag0511. doi: 10.1126/science.aag0511

Prykhozhij, S. V., Fuller, C., Steele, S. L., Veinotte, C. J., Razaghi, B., Robitaille, J. M., et al. (2018). Optimized knock-in of point mutations in zebrafish using CRISPR/Cas9. *Nucleic Acids Res.* 46, 9252. doi: 10.1093/nar/gky674

Qi, L. S., Larson, M. H., Gilbert, L. A., Doudna, J. A., Weissman, J. S., Arkin, A. P., et al. (2013). Repurposing CRISPR as an RNA-guided platform for sequence-specific control of gene expression. *Cell* 152, 1173–1183. doi: 10.1016/j.cell.2013.02.022

Quach, H. N., Tao, S., Vrljicak, P., Joshi, A., Ruan, H., Sukumaran, R., et al. (2015). A Multifunctional mutagenesis system for analysis of gene function in zebrafish. *G3 (Bethesda)* 5, 1283–1299. doi: 10.1534/g3.114.015842

Raj, B., Wagner, D. E., Mckenna, A., Pandey, S., Klein, A. M., Shendure, J., et al. (2018). Simultaneous single-cell profiling of lineages and cell types in the vertebrate brain. *Nat. Biotechnol.* 36, 442–450. doi: 10.1038/nbt.4103

Ran, F. A., Cong, L., Yan, W. X., Scott, D. A., Gootenberg, J. S., Kriz, A. J., et al. (2015). In vivo genome editing using *Staphylococcus aureus* Cas9. *Nature* 520, 186–191. doi: 10.1038/nature14299

Rees, H. A., Komor, A. C., Yeh, W. H., Caetano-Lopes, J., Warman, M., Edge, A. S. B., et al. (2017). Improving the DNA specificity and applicability of base editing through protein engineering and protein delivery. *Nat. Commun.* 8:15790. doi: 10.1038/ncomms15790

Regev, A., Teichmann, S. A., Lander, E. S., Amit, I., Benoist, C., Birney, E., et al. (2017). The human cell atlas. *Elife* 6:e27041. doi: 10.7554/eLife.27041

Schmidt, S. T., Zimmerman, S. M., Wang, J., Kim, S. K., and Quake, S. R. (2017). Quantitative analysis of synthetic cell lineage tracing using nuclease barcoding. *ACS Synth. Biol.* 6, 936–942. doi: 10.1021/acssynbio.6b00309

Seiler, C., Gebhart, N., Zhang, Y., Shinton, S. A., Li, Y. S., Ross, N. L., et al. (2015). Mutagenesis screen identifies agtpbp1 and eps15L1 as essential for T lymphocyte development in zebrafish. *PLoS One* 10:e0131908. doi: 10.1371/journal.pone.0131908

Shah, A. N., Davey, C. F., Whitebirch, A. C., Miller, A. C., and Moens, C. B. (2015). Rapid reverse genetic screening using CRISPR in zebrafish. *Nat. Methods* 12, 535–540. doi: 10.1038/nmeth.3360

Shen, M. W., Arbab, M., Hsu, J. Y., Worstell, D., Culbertson, S. J., Krabbe, O., et al. (2018). Predictable and precise template-free CRISPR editing of pathogenic variants. *Nature* 563, 646–651. doi: 10.1038/s41586-018-0686-x

Shmakov, S., Smargon, A., Scott, D., Cox, D., Pyzocha, N., Yan, W., et al. (2017). Diversity and evolution of class 2 CRISPR-Cas systems. *Nat. Rev. Microbiol.* 15:169. doi: 10.1038/nrmicro.2016.184

Sood, R., Carrington, B., Bishop, K., Jones, M., Rissone, A., Candotti, F., et al. (2013). Efficient methods for targeted mutagenesis in zebrafish using zinc-finger nucleases: data from targeting of nine genes using CompoZr or CoDA ZFNs. *PLoS One* 8:e57239. doi: 10.1371/journal.pone.0057239

Spanjaard, B., Hu, B., Mitic, N., Olivares-Chauvet, P., Janjuha, S., Ninov, N., et al. (2018). Simultaneous lineage tracing and cell-type identification using CRISPR-Cas9-induced genetic scars. *Nat. Biotechnol.* 36, 469–473. doi: 10.1038/nbt.4124

Stemmer, M., Thumberger, T., Del Sol, Keyer, M., Wittbrodt, J., and Mateo, J. L. (2017). Correction: CCTop: an intuitive, flexible and reliable CRISPR/Cas9 target prediction tool. *PLoS One* 12:e0176619. doi: 10.1371/journal.pone.0124633

Tanaka, S., Yoshioka, S., Nishida, K., Hosokawa, H., Kakizuka, A., and Maegawa, S. (2018). In vivo targeted single-nucleotide editing in zebrafish. *Sci. Rep.* 8:11423. doi: 10.1038/s41598-018-29794-9

Tessadori, F., Roessler, H. I., Savelberg, S. M. C., Chocron, S., Kamel, S. M., Duran, K. J., et al. (2018). Effective CRISPR/Cas9-based nucleotide editing in zebrafish to model human genetic cardiovascular disorders. *Dis. Model Mech.* 11:dmm035469. doi: 10.1242/dmm.035469

Toth, E., Czene, B. C., Kulcsar, P. I., Krausz, S. L., Talas, A., Nyeste, A., et al. (2018). Mb- and FnCpf1 nucleases are active in mammalian cells: activities and PAM preferences of four wild-type Cpf1 nucleases and of their altered PAM specificity variants. *Nucleic Acids Res.* 46, 10272–10285. doi: 10.1093/nar/gky815

Tseng, W. C., Loeb, H. E., Pei, W., Tsai-Morris, C. H., Xu, L., Cluzeau, C. V., et al. (2018). Modeling niemann-pick disease type C1 in zebrafish: a robust platform for in vivo screening of candidate therapeutic compounds. *Dis. Model Mech.* 11:dmm034165. doi: 10.1242/dmm.034165

Tu, M., Lin, L., Cheng, Y., He, X., Sun, H., Xie, H., et al. (2017). A 'new lease of life': FnCpf1 possesses DNA cleavage activity for genome editing in human cells. *Nucleic Acids Res.* 45, 11295–11304. doi: 10.1093/nar/gkx783

Unal Eroglu, A., Mulligan, T. S., Zhang, L., White, D. T., Sengupta, S., Nie, C., et al. (2018). Multiplexed CRISPR/Cas9 targeting of genes implicated in retinal regeneration and degeneration. *Front. Cell. Dev. Biol.* 6:88. doi: 10.3389/fcell.2018.00088

Varshney, G. K., and Burgess, S. M. (2014). Mutagenesis and phenotyping resources in zebrafish for studying development and human disease. *Brief Funct. Genomics* 13, 82–94. doi: 10.1093/bfgp/elt042

Varshney, G. K., and Burgess, S. M. (2016). DNA-guided genome editing using structure-guided endonucleases. *Genome Biol.* 17:187. doi: 10.1186/s13059-016-1055-4

Varshney, G. K., Carrington, B., Pei, W., Bishop, K., Chen, Z., Fan, C., et al. (2016a). A high-throughput functional genomics workflow based on CRISPR/Cas9-mediated targeted mutagenesis in zebrafish. *Nat. Protoc.* 11, 2357–2375. doi: 10.1038/nprot.2016.141

Varshney, G. K., Zhang, S., Pei, W., Adomako-Ankomah, A., Fohtung, J., Schaffer, K., et al. (2016b). CRISPRz: a database of zebrafish validated sgRNAs. *Nucleic Acids Res.* 44, D822–D826. doi: 10.1093/nar/gkv998

Varshney, G. K., Lu, J., Gildea, D. E., Huang, H., Pei, W., Yang, Z., et al. (2013). A large-scale zebrafish gene knockout resource for the genome-wide study of gene function. *Genome Res.* 23, 727–735. doi: 10.1101/gr.151464.112

Varshney, G. K., Pei, W., Lafave, M. C., Idol, J., Xu, L., Gallardo, V., et al. (2015a). High-throughput gene targeting and phenotyping in zebrafish using CRISPR/Cas9. *Genome Res.* 25, 1030–1042. doi: 10.1101/gr.186379.114

Varshney, G. K., Sood, R., and Burgess, S. M. (2015b). Understanding and editing the zebrafish genome. *Adv. Genet.* 92, 1–52. doi: 10.1016/bs.adgen.2015.09.002

Vrljicak, P., Tao, S., Varshney, G. K., Quach, H. N., Joshi, A., Lafave, M. C., et al. (2016). Genome-wide analysis of transposon and retroviral insertions reveals preferential integrations in regions of DNA flexibility. *G3 (Bethesda)* 6, 805–817. doi: 10.1534/g3.115.026849

Watkins-Chow, D. E., Varshney, G. K., Garrett, L. J., Chen, Z., Jimenez, E. A., Rivas, C., et al. (2017). Highly efficient Cpf1-mediated gene targeting in mice following high concentration pronuclear injection. *G3 (Bethesda)* 7, 719–722. doi: 10.1534/g3.116.038091

Wu, R. S., Lam, I. I., Clay, H., Duong, D. N., Deo, R. C., Coughlin, S. R., et al. (2018). A rapid method for directed gene knockout for screening in G0 zebrafish. *Dev. Cell* 46:e114. doi: 10.1016/j.devcel.2018.06.003

Xu, S., Cao, S., Zou, B., Yue, Y., Gu, C., Chen, X., et al. (2016). An alternative novel tool for DNA editing without target sequence limitation: the structure-guided nuclease. *Genome Biol.* 17:186. doi: 10.1186/s13059-016-1038-5

Yamada, M., Watanabe, Y., Gootenberg, J. S., Hirano, H., Ran, F. A., Nakane, T., et al. (2017). Crystal structure of the minimal Cas9 from *Campylobacter jejuni* reveals the molecular diversity in the CRISPR-Cas9 systems. *Mol. Cell* 65:e1103. doi: 10.1016/j.molcel.2017.02.007

Yang, L., Zhang, X., Wang, L., Yin, S., Zhu, B., Xie, L., et al. (2018). Increasing targeting scope of adenosine base editors in mouse and rat embryos through fusion of TadA deaminase with Cas9 variants. *Protein Cell* 9, 814–819. doi: 10.1007/s13238-018-0568-x

Yin, L., Maddison, L. A., Li, M., Kara, N., Lafave, M. C., Varshney, G. K., et al. (2015). Multiplex conditional mutagenesis using transgenic expression of Cas9 and sgRNAs. *Genetics* 200, 431–441. doi: 10.1534/genetics.115.176917

Zafra, M. P., Schatoff, E. M., Katti, A., Foronda, M., Breinig, M., Schweitzer, A. Y., et al. (2018). Optimized base editors enable efficient editing in cells, organoids and mice. *Nat. Biotechnol.* 36, 888–893. doi: 10.1038/nbt.4194

Zetsche, B., Gootenberg, J. S., Abudayyeh, O. O., Slaymaker, I. M., Makarova, K. S., Essletzbichler, P., et al. (2015). Cpf1 is a single RNA-guided endonuclease of a class 2 CRISPR-Cas system. *Cell* 163, 759–771. doi: 10.1016/j.cell.2015.09.038

Zetsche, B., Strecker, J., Abudayyeh, O. O., Gootenberg, J. S., Scott, D. A., and Zhang, F. (2017). A survey of genome editing activity for 16 Cpf1 orthologs. *bioRxiv* [Preprint]. doi: 10.1101/134015

Zhang, Y., Qin, W., Lu, X., Xu, J., Huang, H., Bai, H., et al. (2017). Programmable base editing of zebrafish genome using a modified CRISPR-Cas9 system. *Nat. Commun.* 8:118. doi: 10.1038/s41467-017-00175-6

Zhang, Y., Zhang, Z., and Ge, W. (2018). An efficient platform for generating somatic point mutations with germline transmission in the zebrafish by CRISPR/Cas9-mediated gene editing. *J. Biol. Chem.* 293, 6611–6622. doi: 10.1074/jbc.RA117.001080

Conflict of Interest Statement: The authors declare that the research was conducted in the absence of any commercial or financial relationships that could be construed as a potential conflict of interest.

Advantages of publishing in Frontiers

OPEN ACCESS
Articles are free to read for greatest visibility and readership

FAST PUBLICATION
Around 90 days from submission to decision

HIGH QUALITY PEER-REVIEW
Rigorous, collaborative, and constructive peer-review

TRANSPARENT PEER-REVIEW
Editors and reviewers acknowledged by name on published articles

Frontiers
Avenue du Tribunal-Fédéral 34
1005 Lausanne | Switzerland

Visit us: www.frontiersin.org
Contact us: info@frontiersin.org | +41 21 510 17 00

REPRODUCIBILITY OF RESEARCH
Support open data and methods to enhance research reproducibility

DIGITAL PUBLISHING
Articles designed for optimal readership across devices

FOLLOW US
@frontiersin

IMPACT METRICS
Advanced article metrics track visibility across digital media

EXTENSIVE PROMOTION
Marketing and promotion of impactful research

LOOP RESEARCH NETWORK
Our network increases your article's readership